

2. SITE 397

Shipboard Scientific Party¹

SITE DATA

Date Occupied:

Hole 397: 0005Z, 21 March 1976
Hole 397A: 1900Z, 29 March 1976

Date Departed:

Hole 397: 1900Z, 29 March 1976
Hole 397A: 0330Z, 7 April 1976

Time on Hole:

Hole 397: 8 days, 18 hours, 55 minutes
Hole 397A: 8 days, 8 hours, 30 minutes

Position: 26°50.7'N; 15°10.8'W**Water Depth (sea level):** 2900 corrected meters, echo sounding**Water Depth (rig floor):** 2910 corrected meters, echo sounding**Bottom Felt at:** 2914 meters, drill pipe**Penetration:**

Hole 397: 1000.0 meters
Hole 397A: 1453.0 meters

Number of Holes: 2**Number of Cores:**

Hole 397: 104
Hole 397A: 52

Total Length of Cored Section:

Hole 397: 981.0 meters
Hole 397A: 467.0 meters

Total Core Recovered:

Hole 397: 584.83 meters
Hole 397A: 242.66 meters

Percentage Core Recovery:

Hole 397: 60 per cent
Hole 397A: 52 per cent

Oldest Sediment Cored:

Depth sub-bottom:
Hole 397: 1000 meters
Hole 397A: 1453 meters

Nature:

Hole 397: Pebbly muddy sandstone
Hole 397A: Quartzose mudstone with siderite layers

Age:

Hole 397: Early Miocene (NN 3)
Hole 397A: Late Hauterivian

Basement:

Depth sub-bottom: Not reached
Nature: N/A
Velocity range: N/A

Principal Results: Holes 397 and 397A, located on the uppermost rise off Cape Bojador (Figure 1), were drilled and near-continuously cored down to a sub-bottom depth of 1453 meters. The holes penetrated a 1300-meter-thick Quaternary to lower Miocene section and passed directly into the Lower Cretaceous (upper Hauterivian). This 100-m.y. hiatus, shown as a major angular unconformity on some seismic profiles, was generated by one or more mass-wasting events which cut 1 to 2 km deep into a thick, former Mesozoic, marginal wedge. Five prominent lithologic units are recognized.

Unit 1 (from 0 to 313 m sub-bottom) comprises Quaternary to early Pliocene, more or less siliceous, marly nannofossil oozes deposited under conditions of high fertility and good ventilation.

Unit 2 (313 to 545 m sub-bottom) comprises late Miocene to early Pliocene marly nannofossil chalks and marl oozes. Fluctuating carbonate concentrations might reflect dissolution cycles. Several airborne volcanic ash layers of phonolitic and rhyolitic composition were deposited from the middle Miocene to Quaternary (14 to 0.3 m.y.B.P.).

Unit 3 (545 to 752 m sub-bottom), deposited during the middle to early-late Miocene, contains many slump zones of laminated chalks only slightly older than the autochthonous sediments. A detailed magnetostratigraphy, correlated with biostratigraphy, revealed an alternating sequence of normal and reversed polarity intervals from the Brunhes Epoch down to Epoch 7. Sedimentation rates in Units 1 to 3 range from 80 to 30 m/m.y. Periodic changes in the intensity of upwelling, input of sand and clay-sized terrigenous material, reworked shelf carbonate detritus, and dissolution can be related to climatic cycles, as inferred from coarse-fraction and X-ray mineralogical studies.

Unit 4 (752 to 1297 sub-bottom) consists of mudstones, pebbly mudstones, and sandy mudstones. This unit is characterized by many debris flow and slump deposits trans-

¹Ulrich von Rad, Bundesanstalt für Geowissenschaften und Rohstoffe, Hannover, Federal Republic of Germany (co-chief scientist); William B. F. Ryan, Lamont-Doherty Geological Observatory, Palisades, New York (co-chief scientist); Michael A. Arthur, Princeton University, Princeton, New Jersey (present address: Deep Sea Drilling Project, Scripps Institution of Oceanography, La Jolla, California); Boris Lopatin, Research Institute of Arctic Geology, Leningrad, USSR; Oscar E. Weser, Deep Sea Drilling Project, Scripps Institution of Oceanography, La Jolla, California; Michael Sarnthein, University of Kiel, Kiel, Federal Republic of Germany; Floyd McCoy, Lamont-Doherty Geological Observatory, Palisades, New York; Maria B. Cita, University of Milan, Milan, Italy; Gerhard F. Lutze, University of Kiel, Kiel, Federal Republic of Germany; Norman Hamilton, Southampton University, Southampton, England; Pavel Čepěk, Bundesanstalt für Geowissenschaften und Rohstoffe, Hannover, Federal Republic of Germany; Frank H. Wind, Florida State University, Tallahassee, Florida; Gregory Mountain, Lamont-Doherty Geological Observatory, Palisades, New York; Jean K. Whelan, Woods Hole Oceanographic Institution, Woods Hole, Massachusetts; and Christopher Cornford, Programmgruppe für Erdöl und organische Geochemie, Jülich, Federal Republic of Germany.

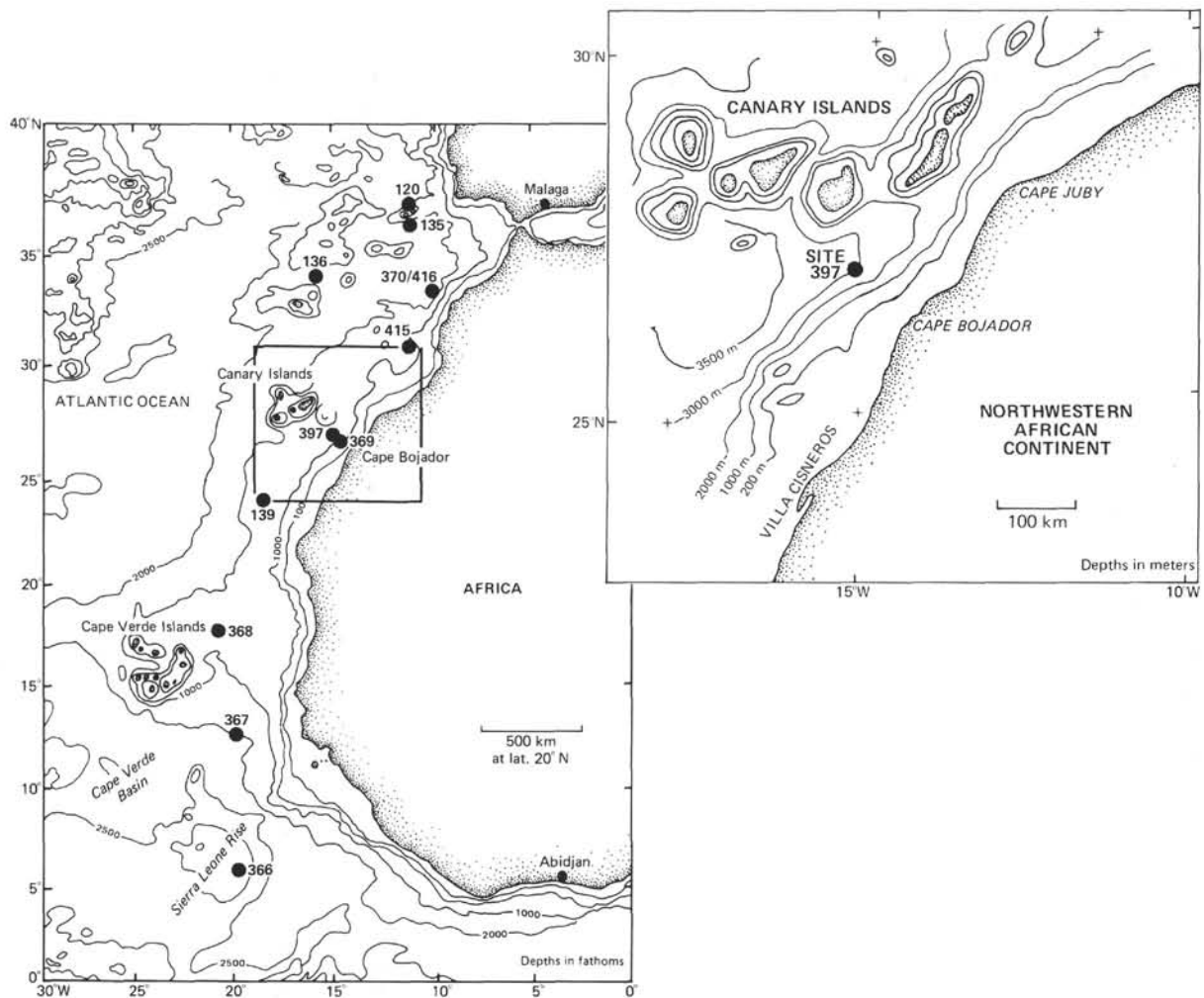


Figure 1. Location map for Site 397.

ported by downslope creep, debris avalanching, and gravity-driven suspension currents (sedimentation rate: 110 to 200 m/m.y.). About 90 per cent of the section is displaced material, derived from the lower and upper slope, gullies, canyons, and the shelf. The autochthonous, hemipelagic, highly burrowed nannofossil marlstones are only slightly younger than the reworked sandstones, siltstones, and pebbly mudstones.

Thick volcanoclastic (tuffaceous) sandstones and altered hyaloclastites (17 to 15.8 m.y.B.P.), rich in alkali basalt and palagonite tuff (respectively), were transported by debris flows from the adjacent Canary Province. They predate the earliest shield-building phase, known from Gran Canaria, and might be derived from Fuerteventura during an early submarine to subaerial shield-building stage. African-derived components include stained and frosted desert-derived and current-reworked quartz, dark olive-green organic-rich mudstones from the slope, and shelf faunas (benthic foraminifers, solitary corals, mollusks, bryozoans, etc.). Preservation of calcitic and aragonitic tests is much better in displaced mudstone pebbles than in the burrowed host sediments.

Unit 5 (1297 to 1453 m sub-bottom) consists of a Lower Cretaceous (early-late Hauterivian), partly massive, partly

laminated silty claystone sequence with numerous thin siderite and a few thin siltstone intercalations. The mudstones are rich in quartz, mica, pyrite, fish debris, and plant remains. The presence of some aragonitic fossils (ammonites and pelecypods) and a sparse low-diversity benthic foraminiferal assemblage, and the absence of bioturbation suggest an oxygen-deficient distal prodelta environment (upper bathyal water depth). Sedimentation rates probably reached 75-150 m/m.y.

All five lithologic units have generated *in-situ* hydrocarbon gases by poorly understood low-temperature diagenetic processes. Lateral preferential migration of the lighter C₁ and C₂ hydrocarbons in respect to the C₃, C₄, and C₅ gases, occurred in more porous sediments. The sediments are all immature with respect to petroleum genesis.

The temperature gradient of the upper 400 meters is about 4°C/100 meters, indicating a heat flow of 1.3 to 1.5 μcal/cm² s.

Seismic reflectors are correlated with lithologic, organic geochemical, and bulk property discontinuities. Certain acoustic horizons correspond to biostratigraphically recognized hiatuses which can be compared with those occurring upslope at DSDP Site 369 and in Aaiun Basin commercial wells.

BACKGROUND AND OBJECTIVES

Introduction

Within the framework of the International Phase of Ocean Drilling (IPOD), Leg 47A was the first of a series of legs selected by the JOIDES Passive Ocean Margin Panel to concentrate on the stratigraphy and evolution of the mature and starved passive continental margins of the eastern Atlantic Ocean between northwestern Africa and the Norwegian Sea. The geology of the coastal basins on land and under the present shelf is relatively well known from seismic results, outcrops, and commercial wells, and the outer continental margins have now been occupied by several DSDP sites. However, the continental slope and uppermost rise of the Atlantic had been drilled only three times (Site 108 with 75 m penetration, 10 m recovery; Site 369 with 489 m penetration, 386 m recovery; Site 392 with 349 m penetration, 38 m recovery). This environment is extremely important for a better understanding of the structure and evolution of passive continental margins, and for appreciation of their hydrocarbon potential as well as the erosional and depositional processes active in the transitional domain between the continental and oceanic realms.

Physiographic Setting

The tectonically stable shelf off Cape Bojador, about 30 km wide, grades at 110 meters water depth into a complex, 70-km-wide slope with an average gradient of about 2-4° (fig. 1 in Arthur et al., this volume). Over a distance of 250 km, 25 submarine canyons deeply incise (200 to 1000 m) into the lower slope in a water depth between 1500 and 3000 meters (see fig. 2 in Arthur et al., this volume). Only the larger canyons have their point of origin on the uppermost slope. Most canyons are V-shaped and unfilled; below 2600 to 2900 meters water depth, however, some canyons are U-shaped with a fill of up to 300 meters of younger sediments. In addition to these deep valleys, the relatively rough topography of the slope results from minor incisions or gullies, and from slumping. Slumping occurs with moderate frequency, especially on parts of the intermediate (Site 369) and lowermost slope and along some steep canyon walls (cf. von Rad et al., 1979).

At about 2700 to 3100 meters water depth, the slope merges with the continental rise (gradient of about 0.2°) which is characterized by leveed channels, continental rise swells (sedimentary ridges, low bottom undulations with hyperbolic reflections), and debris flows derived from large low-angle slides (Uchupi et al., 1976; Jacobi et al., 1975; Embley, 1976). The rise is a broad physiographic province extending nearly 800 km seaward, until it merges either with the Cape Verde-Madeira Abyssal Plain or with the abyssal hill topography east of the Mid-Atlantic Ridge.

Structural Setting

The continental margin off Cape Bojador is the seaward continuation of the Aaiun-Tarfaya coastal basin ("marginal geosyncline"), filled by a thick se-

quence of (mainly Jurassic and Cretaceous) sediments. Gradually, they thin both seaward from a depocenter beneath the present outer shelf and slope, and landwards toward the Precambrian Requibat High. Basement is 12 to 15 km below sea level under the present lower slope and uppermost rise (von Rad and Einsele, in press; also see Frontispiece, this volume).

The key features of the area investigated are two major unconformities and an "anticlinal" structure underneath the lower continental slope detected by shallow-penetration seismic records (Hinz et al., 1974; Seibold and Hinz, 1974). This "slope anticline" had been discovered in 1971 by the cruise of *Meteor-25*, and its extent was traced during the 1975 cruises. However, multichannel seismic profiles later revealed a sequence of horizontal to landward-dipping layers underneath the anticlinal structure (see Frontispiece, this volume; von Rad et al., 1979). Present information points to a 3 to 5 km thick deltaic Early Cretaceous "basin" with gravity tectonics (Beck and Lehner, 1974) under the present upper slope. Hinz et al. (1974) interpreted the two reflectors as Cenomanian ("D₁") and Oligocene/early Miocene ("D₂") unconformities by seaward extrapolation of Spanish Sahara well data. It is, however, extremely difficult to trace reflectors across the slope, where older layers pinch out and younger ones are onlapping farther downslope. Sometimes stratigraphically important events, such as unconformities, are not evident on the seismic records, whereas strong reflectors may depict acoustic impedance and facies changes within continuous lithostratigraphic units. A reinterpretation of the 1971 *Meteor-25* Cruise, Profile A-2, published by Hinz et al. (1974, their fig. 2) is given in Hinz (this volume) and Wissmann (this volume).

The important changes in the interpretation of the Cape Bojador continental margin between 1974 and 1975/1976, following the drilling of Sites 369 and 397, and discussed in the section of the Site 397 Report entitled "Correlation of Seismic Reflection Profiles with Drilling Results" and in Wissmann (both, this volume). The new picture of the geology and structure of the Cape Bojador continental margin is schematically shown in the Frontispiece and briefly discussed following von Rad et al. (1979). Seismic reflection profiles, refraction seismics, and onshore and offshore well data indicated thick Mesozoic sediments overlaying the metamorphic basement, which is Precambrian (or Hercynian?). However, these stratigraphic relationships were not revealed in single or multichannel profiles.

Refraction and multichannel seismic data suggest that an extremely thick (4 to 6 km) accumulation of Jurassic sediments, possibly neritic carbonates, overlies continental or transitional basement below the present slope and upper rise. During the Early Cretaceous, 3 to 5 km of deltaic clastic sediments ("Wealden facies") were deposited in the vicinity of the present upper slope. Following a major Albian to Turonian transgression, the depocenter migrated landward. Paleogene and Upper Cretaceous sediments form a relatively uniform cover (1 to 3 km thick) below the present shelf; they terminate seaward of Site 369, indicating an erosional

truncation. Following this catastrophic erosional event, possibly during the late Oligocene to earliest Miocene, the center of Neogene sedimentation rapidly switched from the shelf and upper slope to the upper rise (Site 397), whereas the continental slope was covered by only a few hundred meters of Neogene to Quaternary sediments (Site 369).

Status of Pre-Site Survey

Site 369 was drilled during Leg 41 (Lancelot, Seibold, et al., 1978) at a water depth of 1752 meters on the intermediate slope off Cape Bojador. At Site 369, a 488-meter-thick Aptian to Quaternary sediment section was continuously cored. The sedimentological and biostratigraphic results and paleoenvironmental and tectonic interpretations of that site provide us with an important input of well-established geological knowledge for the planned drilling program.

In preparation for further drill sites in that continental margin area, a broad reconnaissance geophysical and geological survey was undertaken in 1975 during Cruises VA-10 of R/V *Valdivia* and M-39 of R/V *Meteor* (Seibold and Hinz, 1976; von Rad et al., 1979).

The West Saharan continental margin between Cape Bojador and Cape Blanc was mapped by seismic reflection profiling to find prospective sites along the lower slope, where Mesozoic rocks and a more-or-less complete Paleogene and Neogene sedimentary sequence could be drilled by single-bit holes during Leg 47A. In addition to 10 slope-crossing and 10 slope-parallel single-channel seismic lines from the BGR (Hannover), one multichannel GSI line and several single-channel lines by WHOI (Uchupi et al., 1976) and L-DGO (R/V *Vema* cruises) were used to define the proposed sites. Most of these lines were also used for the construction of bathymetric and reflector isochrone maps (see "Correlation of Seismic Reflection Profiles with Drilling Results"). Based on the seismic results of the *Valdivia* and of the 1971 M-25 cruises, a number of canyons (deeply incised into the steep lower slope off Cape Bojador) and the precipitous upper slope west-southwest of Vila Cisneros were selected for a detailed dredging and coring program (von Rad et al., 1979).

A piston core (VA10-15KL) from a terrace on the northeast wall of Canyon B (fig. 2 in Arthur et al., this volume) contains olive-gray, semiconsolidated upper Aptian to lower Albian marly nannofossil ooze. A dredge sample from the lowermost wall of a nearby canyon consists of middle Eocene/lower Oligocene radiolarian nannofossil chalk, foraminiferal biomicrites enriched in phosphate and mollusks, and calcareous diatom mudstone. All lithologies are rich in quartz, phosphate, fish remains, and their benthic foraminiferal associations reflect deposition in an outer sublittoral (outer shelf-upper slope) environment. The rocks, which can be tentatively correlated with the Eocene Gueran Member of the Samlat Formation (Ratschiller, 1970), probably represent a slump derived from the upper part of the canyon wall above D₁. Different lithologies were recovered from a strongly reflective terrace below D₁ near the floor of Canyon P (VA10-29/30

KD, 2800 to 2760 m water depth). These consist of Albian to Cenomanian quartzose marlstones, subspherical calcilutite concretions, phosphatized mollusk-rich limestone breccia, quartzose mudstone, and belemnites (*Neohibolites ultimus*). These sediments apparently originated in a carbonate shelf and uppermost slope source environment with negligible terrigenous input, upwelling conditions, and reworking of the underlying clastic Lower Cretaceous (von Rad et al., 1979). During the Paleogene, these rocks were displaced into deeper water by slumping and debris flows.

Selection of Site 397

The originally proposed Site 397 (26°46'N, 15°09.5'W; 2820 m water depth, position slightly changed later) is located near shotpoint 2640 on a processed 24-channel seismic line (A1L), kindly provided by Geophysical Service International Ltd. (GSI) as a site proposal to the JOIDES Passive Ocean Margin and Safety Panels. The site is on the uppermost continental rise, west-northwest of Cape Bojador (a few km seaward of the foot of the slope), in an area where reflector D₁ is about 1.0 s below the sea floor and underlain by more-or-less horizontal (Lower Cretaceous) strata. This position is about 7 km west of a parallel *Meteor* profile (M-25 A-2, single-channel line, BGR Hannover, 29 October 1971, 13:45; Hinz et al., 1974, their fig. 2) which shows great detail in the uppermost one second of sediments. Minor slump features on both profiles were avoided.

Temporal constraints and drilling-recovery success at Site 397 disallowed drilling an additional proposed site for Leg 47A. The proposed site (26°30.0'N, 15°22.0'W; 2100 m water depth) was to be drilled on the northwest flank of the deeply incised Canyon B, in an area already thoroughly studied by means of dredging and coring. The proposed site, together with Sites 397 and 369, would have completed a transect from the uppermost rise to the continental slope, and would have allowed construction of a detailed profile of the continental margin off northwestern Africa.

Anticipated Stratigraphy and Lithology

The following anticipated stratigraphic results for Site 397 are estimates, compiled prior to commencement of drilling (also see Wissmann, this volume).

Two-way Travel Time (s)	Lithologic Interval	Description
	1	Recent to Miocene/Oligocene onlapping, bedded, soft (hemi)pelagic rise sediments (calcareous ± siliceous oozes) and turbidites
0.75	2	Well-developed D ₂ unconformity (?late Eocene/early Miocene)
	3	Paleogene/Upper Cretaceous, more strongly reflective strata (limestones, marlstones, cherts, clastic rocks); between D ₂ and D ₁ , an intermediate un-

Two-Way Travel Time (s)	Lithologic Interval	Description
0.98	4	conformity (D _{2a}) can be observed in some of the seismic records Angular unconformity D ₁ (Middle Cretaceous/?Eocene), dipping about 1 to 2° seaward; weakly reflecting, ± horizontal, Lower Cretaceous (?Neocomian/Barremian?), clastic and carbonate rocks

OBJECTIVES

The major objective of Leg 47A was to decipher the complex Cretaceous and Tertiary history of a mature flexured, passive continental margin, for which the West Saharan margin between the Requibat Uplift (Cape Blanc) and the Canary Islands (Cape Juby) is a good example. The subsiding edge of this margin has experienced major episodes of erosion, non-deposition, and redeposition, especially during two major regressions (mid-Cretaceous and mid-Tertiary). The thick wedge of the uppermost continental rise sediments off northwestern Africa had never been penetrated before beyond the Neogene (Site 139). Site 369, on the continental slope nearby, served as an ideal companion site for rise-slope comparisons. The planned site was expected to allow better reconstructions of the history of uplift and subsidence, transgressions and regressions, mechanics of deposition, and erosion during the Early Cretaceous to Neogene. We anticipated that with deep drilling it should be possible to determine whether (1) the erosion was in response to epeirogenetic movements which maintained the continental edge in a shallow-water environment for long time intervals; (2) the truncation was generated by downward dissection of the continental terrace by slumping, turbidity currents, etc., as a consequence of large eustatic sea-level lowerings; or (3) by the vigorous action of deep-water boundary currents at times of enhanced near ocean-floor circulation.

Specific objectives included:

a) Refinement of biostratigraphy, magnetostratigraphy, and lithostratigraphy in an expanded high-fertility upper Neogene section above the CCD.

b) Comparative facies studies in sediments ranging from shelf to slope and rise environments (in conjunction with Site 369, commercial shelf wells, and land outcrops); allochthonous flysch-type sedimentation.

c) Age, nature, and cause of unconformities from shelf to rise depths (reflectors D₁ and D₂).

d) Neogene paleoceanography and paleoclimatology inferred from high-sedimentation rate, hemipelagic sections, and correlations between North Atlantic and Mediterranean basins.

e) Diagenetic behavior of clayey, carbonate, and siliceous sediments; maturation of organic matter in high sedimentation rate continental margin sections.

f) Hydrocarbon potential of the uppermost continental rise setting within the 10 to 15 km thick "Cape Bojador marginal basin."

OPERATIONS

Site Approach

Site 397 was initially targeted near shotpoint 2640 on GSI seismic line A1L. Due to the stratigraphic pinch-out of seismic reflectors D₂ and D₁ at the base of the continental slope, it was considered prudent that, if there were to be any error in longitudinal positioning, the site should be situated to the east of the GSI line and to the west of Profile M-25 A2, on which the pinch-out could also be detected. Hence, *Glomar Challenger* was directed along a dead-reckoning course which took the vessel approximately equidistant between the two seismic lines (see Figure 2). The longitude control was supplied by a west-to-east *Vema* line V30-05. Latitude control would be generated by comparing the sea-floor topography and sub-bottom reflection geometry on the under-way *Challenger* profile, to that on existing profiles for the vicinity of the targeted drill site.

Site 397 was approached late during the evening of 20 March 1976, at a speed of 6 knots. Satellite fixes were computed for 2230 and 2250 hours. As the later fix was plotted, it was realized that the drilling vessel was already too far upslope for her given latitude if the GSI line was correctly positioned. An agreement between the real-time data and that on the GSI profile could be registered by adjusting the GSI line several miles to the north-northwest. It was certainly clear that the *Challenger* could not drill below reflector D₂ at the 2300-hours position, which placed the vessel upslope of the aforementioned pinch-out.

As soon as this judgment was agreed upon by the Co-Chief Scientists and fellow colleagues, the vessel was directed to turn to starboard onto a reciprocal course to take her back down-dip of the slope anticline and north-northwest to the approximate latitude of the *Vema* line. The intended location had a water depth of approximately 2900 meters and a D₁ depth of 4.85 s.

At 0005 hours on 21 March, dead-reckoning placed the *Challenger* close to the *Vema* line; the under-way seismic profile showed the vessel to be far enough off-structure (with relatively horizontal D₁ and D₂ reflectors) to drop the beacon.

The ship proceeded about one-and-a-half km beyond the beacon drop to continue the seismic profile; after pulling in the towed gear, the *Challenger* then commenced back to a station-keeping position over the beacon.

Electrical problems with a relay in the control circuit for the automatic mode of the dynamic positioning system caused the postponement of "spudding in" until the evening of 21 March.

Drilling Operations, Hole 397

Drilling operations at Hole 397 began with a view toward penetrating approximately 1300 meters of strata. Based on anticipated lithologies, a 10" Smith F-94-CK bit was used. The bottom hole assembly consisted of the drill bit with the transducer of a 12-kHz pinger in place, one core barrel, three 8-¼" drill collars, two bumper subs, two 8-¼" drill collars, one 7-¼" drill collar, and

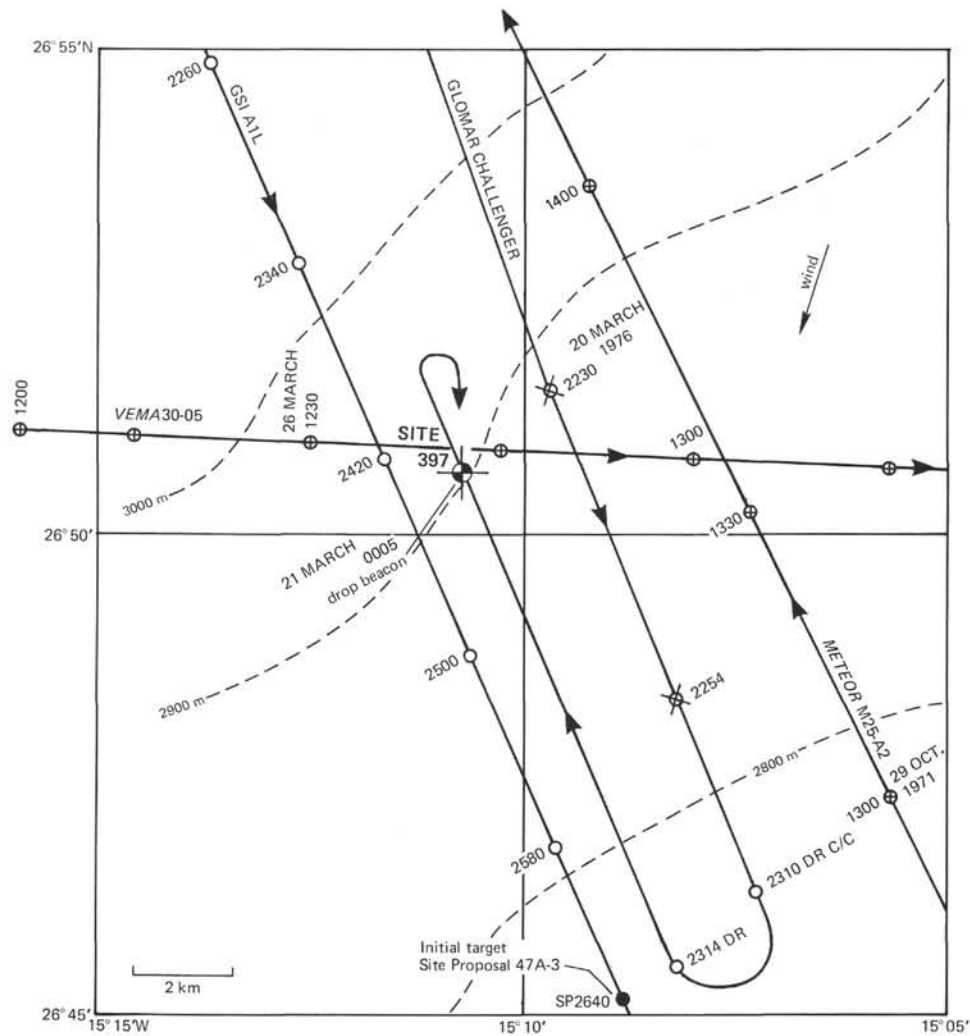


Figure 2. Position of profiler lines in the vicinity of Site 397.

one joint of 5-½" heavy all drill pipe. The heave compensator was not ready to put in to line when drilling operations began. Actual spud-in time was at 2030 hr on 21 March 1976 in a water depth of 2900 meters. The sea floor as measured from the rig floor was 2914 meters (as reported by the drillers) and 2910 meters (as recorded on the PDR).

The drilling plan called for continuous coring, although DSDP allowed for an option of overdrilling (to a penetration of 19 m) for intervals where safety conditions were favorable. The time, depths, and recovery statistics for all cores from Hole 397 are listed in Table 1. Penetration rates (in m/hr), important aspects of the drilling operations, gross lithologic changes, as well as significant acoustostratigraphic units are plotted in Figure 3.

The initial penetration rate of 270 m/hr in hemipelagic strata was slowed irregularly but progressively to about 30 m/hr at a depth of 260 meters. Wide fluctuations within this depth interval were mainly the result of rounding-off the drilling time to the nearest minute on the entry sheet, rather than caused by lithologic variations. At 60 meters, some torque was experienced

on the drill pipe and the driller began rotating at 15 rpm. Rotation was increased to 50 rpm near the bottom of this interval. Circulation was broken for the first time at 240 meters.

From 260 to 290 meters, the decline curve of the penetration rate was offset to higher values of about $80 \pm$ m/hr. The interval of this change occurred approximately where the carbonate content of the hemipelagic sediments showed an increase. It also coincides with the depth at which siliceous fossils decreased to smaller amounts.

From 290 to 700 meters, another irregular but progressive decrease in the penetration rate occurred, beginning with $80 \pm$ m/hr and ending with $15 \pm$ m/hr. The bottom of this interval corresponds to the approximate depth of the D₂ acoustic reflector as well as to the approximate depth ($680 \pm$ m) where appreciable amounts of sands began to appear at the base of the hemipelagic sediments of lithologic Unit 1. Coring within this interval showed a gradual increase in drill-string torque necessitating a slight increase in bit weight. At 313 meters, continuous pumping began which showed an increase in pump pressure of from 50 to 500

TABLE 1
Coring Summary, Hole 397

Core No.	Date (March 1976)	Time	Depth From Drill Floor (m)	Depth Below Sea Floor (m)	Length Cored (m)	Length Recovered (m)	Recovery (%)
1	21	2110	2910.0-2919.0	0.0-9.0	9.0	0.25	3
2	21	2310	2919.0-2928.5	9.0-18.5	9.5	8.25	87
3	22	0030	2928.5-2938.0	18.5-28.0	9.5	8.60	91
4	22	0125	2938.0-2947.5	28.0-37.5	9.5	6.65	70
5	22	0225	2947.5-2957.0	37.5-47.0	9.5	6.77	71
6	22	0325	2957.0-2966.5	47.0-56.5	9.5	7.70	81
7	22	0500	2966.5-2976.0	56.5-66.0	9.5	8.60	91
8	22	0550	2976.0-2985.5	66.0-75.5	9.5	8.75	92
9	22	0705	2985.5-2995.0	75.5-85.0	9.5	6.17	65
10	22	0810	2995.0-3004.5	85.0-94.5	9.5	9.43	99
11	22	0910	3004.5-3014.0	94.5-104.0	9.5	9.69	73
12	22	1010	3014.0-3023.5	104.0-113.5	9.5	9.37	99
13	22	1105	3023.5-3033.0	113.5-123.0	9.5	9.70	102
14	22	1220	3033.0-3042.5	123.0-132.5	9.5	8.32	88
15	22	1320	3042.5-3052.0	132.5-142.0	9.5	9.50	100
16	22	1415	3052.0-3061.5	142.0-151.5	9.5	9.60	101
17	22	1515	3061.5-3071.0	151.5-161.0	9.5	9.60	101
18	22	1630	3071.0-3080.5	161.0-170.5	9.5	9.62	101
19	22	1735	3080.5-3090.0	170.5-180.0	9.5	8.26	87
20	22	1830	3090.0-3099.5	180.0-189.5	9.5	9.65	102
21	22	1950	3099.5-3109.0	189.5-199.0	9.5	9.66	102
22	22	2050	3109.0-3118.5	199.0-208.5	9.5	9.64	101
23	22	2150	3118.5-3128.0	208.5-218.0	9.5	7.25	76
24	22	2250	3128.0-3137.5	218.0-227.5	9.5	9.63	101
25	23	0005	3137.5-3147.0	227.5-237.0	9.5	3.52	37
26	23	0120	3147.0-3156.5	237.0-246.5	9.5	9.62	101
27	23	0250	3156.5-3166.0	246.5-256.0	9.5	7.90	83
28	23	0355	3166.0-3175.5	256.0-265.5	9.5	9.65	102
29	23	0500	3175.5-3185.0	265.5-275.0	9.5	9.58	101
30	23	0605	3185.0-3194.5	275.0-284.5	9.5	9.56	101
31	23	0705	3194.5-3204.0	284.5-294.0	9.5	6.20	65
32	23	0810	3204.0-3213.5	294.0-303.5	9.5	5.81	61
33	23	0920	3213.5-3223.0	303.5-313.0	9.5	6.12	64
34	23	1025	3223.0-3232.5	313.0-322.5	9.5	9.70	102
35	23	1130	3232.5-3242.0	322.5-332.0	9.5	0.70	7
36	23	1230	3242.0-3251.5	332.0-341.5	9.5	3.20	34
37	23	1335	3251.5-3261.0	341.5-351.0	9.5	6.05	64
38	23	1430	3261.0-3270.5	351.0-360.5	9.5	9.47	100
39	23	1650	3270.5-3280.0	360.5-370.0	9.5	7.57	80
40	23	1755	3280.0-3289.5	370.0-379.5	9.5	3.87	41
41	23	1900	3289.5-3299.0	379.5-389.0	9.5	9.56	101
42	23	2015	3299.0-3308.5	389.0-398.5	9.5	2.07	22
43	23	2125	3308.5-3318.0	398.5-408.0	9.5	9.65	102
44	23	2235	3318.0-3327.5	408.0-417.5	9.5	6.91	73
45	23	2355	3327.5-3337.0	417.5-427.0	9.5	7.05	74
46	24	0130	3337.0-3346.5	427.0-436.5	9.5	0.30	3
47	24	0235	3346.5-3356.0	436.5-446.0	9.5	7.53	79
48	24	0345	3356.0-3365.5	446.0-455.5	9.5	3.50	37
49	24	0515	3365.5-3375.0	455.5-465.0	9.5	4.43	47
50	24	0615	3375.0-3384.5	465.0-474.5	9.5	1.28	13
51	24	0805	3394.0-3403.5	484.0-493.5	9.5	0.10	2
52	24	0920	3403.5-3413.0	493.5-503.0	9.5	9.52	100
53	24	1040	3413.0-3422.5	503.0-512.5	9.5	1.56	16
54	24	1155	3422.5-3432.0	512.5-522.0	9.5	8.19	86
55	24	1305	3432.0-3441.5	522.0-531.5	9.5	6.95	73
56	24	1420	3441.5-3451.0	531.5-541.0	9.5	3.95	42
57	24	1545	3451.0-3460.5	541.0-550.5	9.5	7.62	80
58	24	1710	3460.5-3470.0	550.5-560.0	9.5	5.34	56
59	24	1825	3470.0-3479.5	560.0-569.5	9.5	1.70	18
60	24	2000	3479.5-3489.0	569.5-579.0	9.5	8.24	87
61	24	2220	3489.0-3498.5	579.0-588.5	9.5	8.39	88
62	24	2335	3498.5-3508.0	588.5-598.0	9.5	9.13	96
63	25	0110	3508.0-3517.5	598.0-607.5	9.5	2.57	27
64	25	0235	3517.5-3527.0	607.5-617.0	9.5	6.15	65
65	25	0400	3527.0-3536.5	617.0-626.5	9.5	7.70	81
66	25	0540	3536.5-3546.0	626.5-636.0	9.5	9.00	95
67	25	0705	3546.0-3555.5	636.0-645.5	9.5	2.50	26
68	25	0825	3555.5-3565.0	645.5-655.0	9.5	4.92	52

lbs with 35 strokes/minute (SPM) at 700 meters depth. Mud (30 barrels) was first spotted in Hole 397 at 636 meters. At 370 and 587 meters, the heat probe was run. Coring was continuous throughout except for the interval from 474.5 to 484 meters.

From 700 to 750 meters, which represents the remaining portion of the hemipelagic strata of lithologic Unit 2, the penetration rate increased slightly.

Below 750 meters, the penetration rate increased again to an average of $20 \pm$ m/hr. This rate persisted to nearly the bottom of the hole at 1000 meters, a depth which corresponds approximately to the D₁ acoustic reflector. This 250-meter interval represents the upper half of the allochthonous strata of lithologic Unit

TABLE 1 - Continued

Core No.	Date (March 1976)	Time	Depth From Drill Floor (m)	Depth Below Sea Floor (m)	Length Cored (m)	Length Recovered (m)	Recovery (%)
69	25	0950	3565.0-3574.5	655.0-664.5	9.5	6.60	69
70	25	1135	3574.5-3584.0	664.5-674.0	9.5	3.92	41
71	25	1340	3584.0-3593.5	674.0-683.5	9.5	7.40	78
72	25	1615	3593.5-3603.0	683.5-693.0	9.5	9.52	100
73	25	1750	3603.0-3612.5	693.0-702.5	9.5	4.64	49
74	25	1930	3612.5-3622.0	702.5-712.0	9.5	3.57	38
75	25	2110	3622.0-3631.5	712.0-721.5	9.5	3.15	33
76	25	2250	3631.5-3641.0	721.5-731.0	9.5	4.95	52
77	26	0020	3641.0-3650.5	731.0-740.5	9.5	4.35	46
78	26	0200	3650.5-3660.0	740.5-750.0	9.5	5.42	57
79	26	0350	3660.0-3669.5	750.0-759.5	9.5	2.49	26
80	26	0515	3669.5-3679.0	759.5-769.0	9.5	5.00	53
81	26	0645	3679.0-3688.5	769.0-778.5	9.5	0.50	5
82	26	0815	3688.5-3698.0	778.5-788.0	9.5	0.00	0
83	26	1145	3698.0-3707.5	788.0-797.5	9.5	2.68	28
84	26	1430	3707.5-3717.0	797.5-807.0	9.5	4.75	50
85	26	1620	3717.0-3726.5	807.0-816.5	9.5	7.74	81
86	26	1810	3726.5-3736.0	816.5-826.0	9.5	2.15	23
87	26	1945	3736.0-3745.5	826.0-835.5	9.5	4.70	49
88	26	2105	3745.5-3755.0	835.5-845.0	9.5	5.98	63
89	26	2225	3755.0-3764.5	845.0-854.5	9.5	4.63	49
90	27	0155	3764.5-3774.0	854.5-864.0	9.5	3.20	34
91	27	0345	3774.0-3783.5	864.0-873.5	9.5	2.10	22
92	27	0540	3783.5-3793.0	873.5-883.0	9.5	5.33	56
93	27	0710	3793.0-3802.5	883.0-892.5	9.5	3.90	41
94	27	0900	3802.5-3812.0	892.5-902.0	9.5	1.28	13
95	27	1045	3812.0-3821.5	902.0-911.5	9.5	7.70	81
96	27	1200	3821.5-3831.0	911.5-921.0	9.5	1.70	18
97	27	1345	3831.0-3840.5	921.0-930.5	9.5	1.46	15
98	27	1515	3840.5-3850.0	930.5-940.0	9.5	0.00	0
99	27	1645	3850.0-3859.5	940.0-949.5	9.5	0.00	0
100	27	1900	3859.5-3869.0	949.5-959.0	9.5	0.00	0
101	27	2345	3878.5-3888.0	968.5-978.0	9.5	1.56	16
102	28	0210	3888.0-3897.5	978.0-987.5	9.5	0.20	2
103	28	0410	3897.5-3907.0	987.5-997.0	9.5	0.00	0
104	28	0530	3907.0-3916.5	997.0-1006.5	3.0	0.00	0
Total					981.0	584.83	60

2. Highest penetration rates (averaging nearly 35 m/hr) occurred in an interval of shale pebble conglomerate between 820 and 850 meters. Somewhat slower rates took place in the overlying volcanoclastic sandstones and underlying fossiliferous turbidite sediments. Penetration rates varied widely from core to core, reflecting the heterogeneity of this lithologic unit. Pump pressure was increased up to 600 lbs just above the top of this unit and remained high throughout. Fifty barrels of mud were first spotted in the volcanoclastic sands, and further slugs of 50 barrels each were pumped down at regular intervals. For the last core taken at the bottom of the hole, the penetration rate decreased dramatically to 9 m/hr.

Decreasing methane/ethane ratios for the bottom-most cores necessitated short waits on gas analyses before drilling was allowed to continue. Also, near total depth plugging of the bit was experienced and several times a bit breaker was pumped down to clear it. It was further believed that the float valve was not functioning properly. Finally, when it was realized that the bit was plugged, the decision was made to abandon the hole. The hole was then partially filled with 160 barrels of weighted mud which was spotted to 450 meters. Cement was not pumped down because of the probable plugged bit. The drill pipe then was pulled out of the hole.

Drilling Operations, Hole 397A

Following a review among all members of the scientific team as to how the remaining objectives of this leg could best be reached, it was decided to remain at this site. A 16-kHz beacon was then dropped and a new hole was offset about 60 meters from the first one. The same

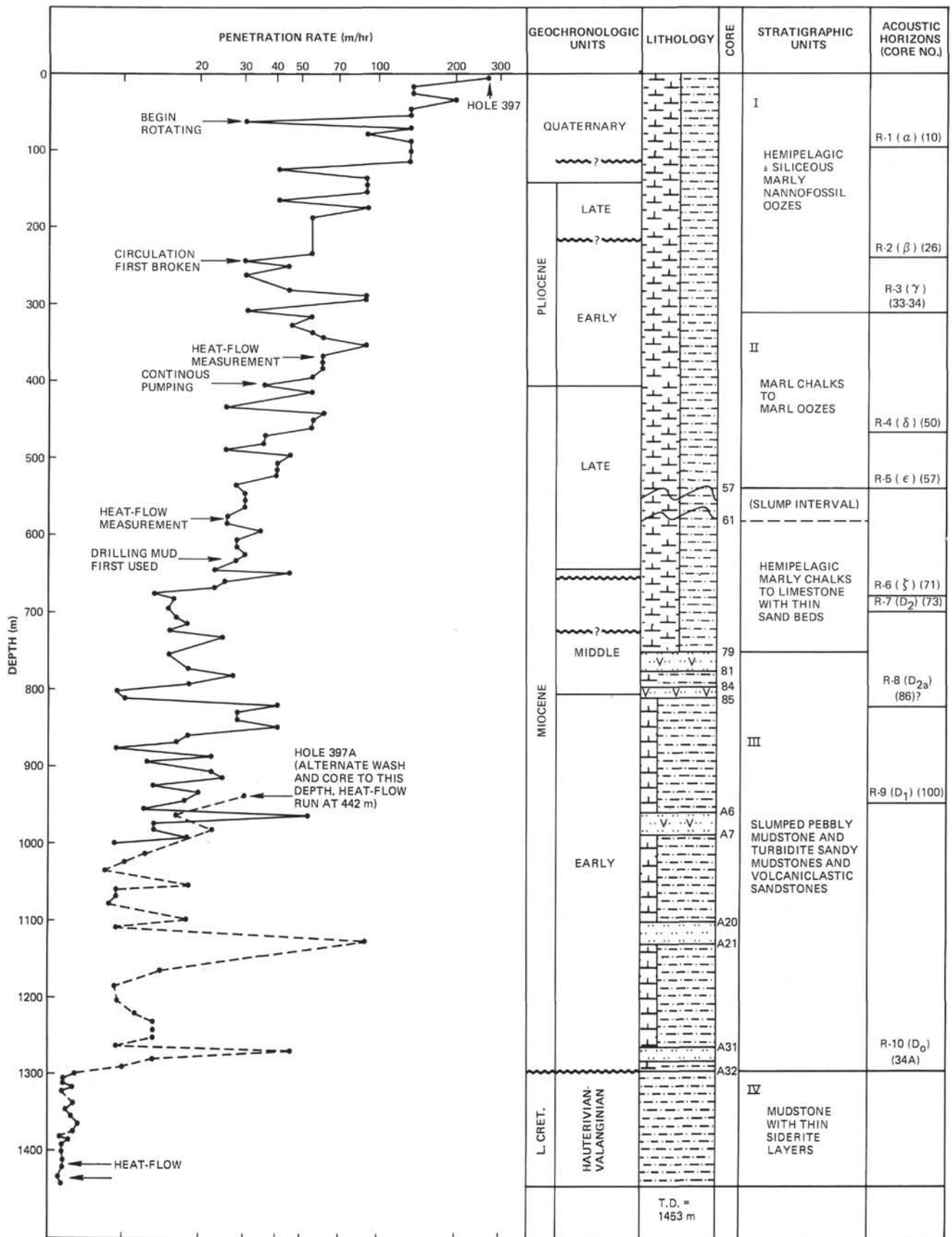


Figure 3. Lithostratigraphy in relation to penetration rate and other drilling operations at Site 397.

bottom hole assembly was used as at Hole 397 except that one less bumper sub was inserted between the two lowest drill collar intervals. At Hole 397A, it was decided to wash ahead without coring as far as possible until the previous bottom hole depth had been reached. This program was interrupted at 450 meters where a heat-flow measurement was taken. At 717 meters, when the drill pipe began sticking, the center bit was retrieved and the core barrel was dropped. Core 1 was then raised after 53 meters had been drilled (see Table 2). Alternate coring and drilling took place down to Core 7 at 982 meters, after which the hole was continuously cored. During the period of intermittent coring and washing, the heave compensator was hooked up for the first time. Penetration rate (see Figure 3) in the interval of coring overlap between the two holes did not differ significantly, which reflects the relatively good condition of the bit when Hole 397 was terminated.

The penetration rate from 1000 to 1300 meters was $12 \pm$ m/hr, with a few high excursions which reflected

TABLE 2
Coring Summary, Hole 397A

Core No.	Date (March 1976)	Time	Depth From Drill Floor (m)	Depth Below Sea Floor (m)	Length Cored (m)	Length Recovered (m)	Recovery (%)
1 ^a	30	0045	3617.0-3670.0	707.0-760.0	9.5	9.65	102
2 ^b	30	0730	3670.0-3794.0	760.0-884.0	9.5	4.25	45
3	30	1045	3794.0-3825.0	884.0-915.0	9.5	5.13	54
4	30	1300	3825.0-3845.0	915.0-935.0	9.5	9.75	103
5	30	1515	3845.0-3873.5	935.0-963.5	9.5	3.34	35
6	30	1740	3873.5-3892.5	963.5-982.5	9.5	3.67	39
7	30	2100	3892.5-3902.0	982.5-992.0	9.5	2.70	28
8	30	2300	3902.0-3911.5	992.0-1001.5	9.5	2.42	25
9	31	0110	3911.5-3921.0	1001.5-1011.0	9.5	0.63	7
10	31	0305	3921.0-3930.5	1011.0-1020.5	9.5	5.64	59
11	31	0500	3930.5-3940.0	1020.5-1030.0	9.5	9.25	97
12	31	0720	3940.0-3949.5	1030.0-1039.5	9.5	4.96	52
13	31	0900	3949.5-3959.0	1039.5-1049.0	9.5	3.80	40
14	31	1050	3959.0-3968.5	1049.0-1058.5	9.5	6.76	71
15	31	1400	3968.5-3978.0	1058.5-1068.0	9.5	9.60	101
16	31	1640	3978.0-3987.5	1068.0-1077.5	9.5	7.81	82
17	31	1900	3987.5-3997.0	1077.5-1087.0	9.5	9.22	97
18	31	2040	3997.0-4006.5	1087.0-1096.5	9.5	6.89	73
19	31	2220	4006.5-4016.0	1096.5-1106.0	9.5	2.92	31
20	April 1	0255	4016.0-4025.5	1106.0-1115.5	9.5	5.61	59
21 ^c		0515	4025.5-4044.5	1115.5-1134.5	9.5	4.42	47
22 ^c	1	0940	4044.5-4063.5	1134.5-1153.5	9.5	3.60	38
23 ^c	1	1345	4063.5-4082.5	1153.5-1172.5	9.5	7.17	75
24 ^c	1	1635	4082.5-4101.5	1172.5-1191.5	9.5	7.95	84
25 ^c	1	1940	4101.5-4120.5	1191.5-1210.5	9.5	2.89	30
26 ^c	1	2230	4120.5-4139.5	1210.5-1229.5	9.5	3.39	36
27	2	0030	4139.5-4149.0	1229.5-1239.0	9.5	2.24	24
28	2	0205	4149.0-4158.5	1239.0-1248.5	9.5	3.20	34
29	2	0410	4158.5-4168.0	1248.5-1258.0	9.5	0.75	8
30	2	0615	4168.0-4177.5	1258.0-1267.5	9.5	3.92	41
31	2	0740	4177.5-4187.0	1267.5-1277.0	9.5	3.43	36
32	2	0935	4187.0-4196.5	1277.0-1286.5	9.5	3.25	34
33	2	1140	4196.5-4206.0	1286.5-1296.0	9.5	1.97	21
34	2	1520	4206.0-4215.5	1296.0-1305.5	9.5	2.55	27
35	2	1950	4215.5-4225.0	1305.5-1315.0	5.5	5.15	94
36	2	2330	4225.0-4234.5	1315.0-1324.5	4.0	6.68	167
37	3	0250	4234.5-4244.0	1324.5-1334.0	9.5	4.59	48
38	3	0730	4244.0-4253.5	1334.0-1343.5	6.0	3.03	51
39	3	1315	4253.5-4263.0	1343.5-1353.0	9.5	2.20	23
40	3	1810	4263.0-4272.5	1353.0-1362.5	9.5	3.44	36
41	3	2250	4272.5-4282.0	1362.5-1372.0	9.5	3.43	36
42	4	0230	4282.0-4291.5	1372.0-1381.5	9.5	2.93	31
43	4	0625	4291.5-4299.5	1381.5-1391.0	9.5	3.25	34
44	4	1020	4299.5-4309.0	1391.0-1400.5	3.0	2.95	98
45	4	1405	4309.0-4318.5	1400.5-1410.0	6.5	3.60	55
46	4	2005	4318.5-4328.0	1410.0-1419.5	9.5	5.73	60
47	5	0150	4328.0-4337.5	1419.5-1429.0	9.5	5.20	55
48	5	0725	4337.5-4347.0	1429.0-1438.5	9.5	2.57	27
49	5	1345	4347.0-4356.5	1438.5-1448.0	9.5	2.90	31
50	6	0345	4356.5-4366.0	1448.0-1457.5	9.5	6.93	73
51	6	1300	4366.0-4375.5	1457.5-1467.0	9.5	8.80	93
52	6	1800	4375.5-4385.0	1467.0-1476.5	5.0	4.55	91
Total					467.0	242.66	52

^aRepresents 53-meter cored interval.

^bRepresents 124-meter cored interval.

^cRepresents 19-meter penetrated interval ("overdrilling" with one 9.5-m core).

the varied facies of the remainder of the allochthonous lithologic Unit 2. Because of this slow rate, six 9.5-meter intervals were washed down. High pump pressures and bit weights were used throughout, and mud was spotted continuously at intervals of 3 to 6 cores. Near a depth of 1300 meters, the heave compensator became passive.

Below 1300 meters to a total depth of 1453 meters, a significant lithologic change occurred and the penetration rate (as seen on Figure 3) was reduced dramatically. Rates were 1.25 to 4 m/hr, with values averaging 2 m/hr occurring in the lower half of this depth interval. The lithology responsible for these low rates was a sticky terrigenous Cretaceous shale which was balling up the intermediate length inserts of the drill bit. The bit became stuck several times in spite of pump pressures above 1000 lbs at 60 spm. At 1439 and 1448 meters, the heat probe was run down the hole. Following the last run, two more cores were taken and when it became apparent that a high sedimentation rate in the Cretaceous shales was a distinct possibility and that minimal stratigraphic information could be recovered during lengthy coring periods. The decision was made to abandon Hole 397A. Following the last core, the hole inclination was measured and found to deviate 28° from the vertical. Then, the hole was filled with 310 barrels of 11.4-lb mud topped with 20 barrels of 12.5-lb cement. The bit (which had 109 hours of rotating time) was examined on deck and, except for a loose bearing, was found to be in good condition.

A review of the penetration rate record at Site 397 (see Figure 3) shows that, although there were irregular plateaus and short fluctuations, a nearly straight line could be drawn through this rate. Indubitably, a re-entry capability and a long tooth bit would have reversed its inexorable decline.

Part of the drilling program at this site was governed by constraints of the JOIDES Safety Panel as well as by gaseous hydrocarbon shows.

LITHOSTRATIGRAPHY

Introduction

A 1453-meter-thick section of sediments and sedimentary rocks on the northwest African continental rise was continuously cored (156 cores) in Holes 397 and 397A. In general, this section represents a sequence rich in terrigenous material of which over half represents allochthonous sediments. Five lithologic units are defined; they are listed in Table 3 and in a large fold-out diagram (see Sediment Summary Chart in the back pocket of this volume), which presents corresponding smear-slide data, carbonate results, and other pertinent information (coarse-fraction data, clay-mineral analyses, etc.).

Description of Lithostratigraphic Units

Unit 1

Age: Early Pliocene-Quaternary.

Major sediment types: Siliceous marl, nannofossil oozes, and marly oozes in the upper portion (Quater-

TABLE 3
Lithologic Unit Summary, Holes 397 and 397A

Unit	Dominant Lithology	Sub-Bottom Depth (m)			Thickness (m)			Core Number		Time-Rock Unit
		397	397A	Total	397	397A	Total	397	397A	
1	Marly nannofossil ooze	0-313.0	—	0-313.0	313.0	—	313.0	1 to 33	—	Quaternary-early Pliocene
A	Siliceous marly nannofossil ooze; marly nannofossil ooze	0-142.0	—	—	142.0	—	142.0	1 to 16 (base 15)	—	Quaternary
B	Slightly siliceous marly nannofossil ooze; marly nannofossil ooze; marly ooze	142.0-313.0	—	—	171.0	—	171.0	16 to 33 (base 32)	—	Pliocene
2	Marly nannofossil ooze/chalk	313.0-544.8	—	313.0-544.8	231.8	—	231.8	33 to 57-3, 80 cm	—	Earliest Pliocene-latest Miocene
3	Marl chalk/limestone; marly nannofossil chalk/limestone	544.8-752.2	707.0-760.0	544.8-752.2	207.4	53.0	207.4	57-3, 80 cm to 79-2, 70 cm	1	Middle-late Miocene
4	Pebbly mudstone; volcaniclastic sandstone and conglomerate; sandy pebbly mudstone; conglomerate; marly limestone	752.2-1000.0	760.0-1296.7	752.2-1296.7	247.8	536.7	544.5	79-2, 70 cm to 104 (base)	2 to 34-1, 70 cm	Middle-early Miocene with reworked Oligocene
5	Quartzose silty claystone and claystone with thin siderite layers	—	1296.7-1453.0	1296.7-1453.0	—	156.3	156.3	—	34-1, 70 cm 52 (base)	Early Cretaceous (late Hauterivian)

nary); slightly siliceous marly nannofossil oozes and marly chalks in the lower (Pliocene) portion.

Minor sediment types: Nannofossil oozes, foraminiferal nannofossil oozes, marly foraminiferal nannofossil oozes, diatom foraminiferal nannofossil oozes, siliceous nannofossil oozes.

Two sub-units: 1A, predominantly siliceous marly ooze; and 1B, predominantly marly nannofossil ooze/chalk.

Sub-bottom depth and core boundaries: Unit 1: 0-313.0 meters, DSDP Cores 397-1 to 397-33; Sub-unit 1A: 0 to 136.0 meters, Cores 397-1 to 397-15-3; Sub-unit 1B: 136 to 313.0 meters (165-m interval), Cores 397-15-3 to 397-33.

Color: Light gray and olive-gray; no color change between sub-units; minor light brown and white intervals.

Carbonate content: 57 per cent average, highly variable throughout unit (25 to 90%); no distinct change in content between sub-units.

Texture: Minor sand-size components (foraminifers and quartz); about one-third silt-sized components and two-thirds clay-sized material.

Organic carbon: About 0.5 per cent average, varies between about 0.3 and 1.2 per cent; strong H₂S smell and gas expansion cracks in some recovered sediments.

Allochthonous intervals: None are apparent; possibly, indistinct turbid layers in Cores 397-22 and 397-23 (Diester-Haass, this volume).

Sedimentary structures: Bioturbation structures; vague bedding in Sub-unit 1A noticeable by slight color changes.

Sedimentary components: Predominantly calcareous nannoplankton and clay minerals, with significant siliceous organisms (Sub-unit 1A), foraminifers, and quartz components. Pyrite is abundant, either as burrow fillings or disseminated in sediments, where gas cracks occur or where there was a strong H₂S smell.

Volcanic material is minor, but persistent (Sub-unit 1A) and disseminated within oozes, partly as distinct ash layers (Schmincke and von Rad, this volume). Minor components are mollusk and ostracode shells, and dolomite.

Basis for unit/sub-unit definition: Lithostratigraphic Unit 1 is defined primarily on the basis of a persistent siliceous biogenic component, and upon a higher organic carbon content than in Unit 2, a fairly constant sand-silt-clay content (which reflects the general absence of allochthonous material) as compared with other lithologic units, a distinctive coarse-fraction assemblage (see Sarnthein in Arthur et al., this volume; and Sediment Summary Chart 1, in back pocket), and a variable clay-mineral content (see Chamley and d'Argoud, this volume). Sub-unit 1A is discernible from Sub-unit 1B because the upper sub-unit has a more variable content of quartz, calcareous nannofossils, and siliceous organisms, with a somewhat higher organic carbon content, and a significant variability in calcium carbonate content. Clay minerals are not as variable in Sub-unit 1A as in Sub-unit 1B (Chamley and d'Argoud, this volume); there is a distinctive change in coarse-fraction constituents between the two sub-units (see Sarnthein in Arthur et al., this volume); textural parameters are not noticeably different between 1A and 1B (see also Cita and Spezzibottiani, this volume).

Unit 2

Age: Late Miocene earliest Pliocene.

Major sediment type: Marly nannofossil ooze/chalk.

Minor sediment types: Marly foraminiferal nannofossil ooze-chalk, zeolitized volcanic ash layers, foraminiferal silt, and sand.

Sub-bottom depth and core boundaries: 313.0 to 544.8 meters (231.8-m interval), Core 397-33 to Sample 397-57-3, 80 cm.

Color: Light gray; minor green-gray, gray, and olive-green intervals.

Carbonate content: 55 per cent average; content is variable but less so than in Unit 1. Between Cores 397-51 and 397-52, there is a distinct decline in CaCO₃ content.

Texture: Minor sand-size component, silt- and clay-sized detritus in approximately the same proportions as in Unit 1; higher sand and/or silt contents do occur and represent either altered volcanic ash layers or sand-silt laminae.

Organic carbon: <5 per cent average values, noticeably lower than in Unit 1; rarely, cracks due to gas release.

Allochthonous intervals: Present as a few sand or silt laminae; coarse-fraction data (Sarnthein in Arthur et al. and Sediment Summary Chart, this volume) suggest some displaced biogenic material (serpulids).

Sedimentary structures: Numerous burrows, particularly in the lower portions of this unit; thin sand-silt laminae show no visually detectable internal structures.

Sedimentary components: Predominantly calcareous nannoplankton and clay minerals, with significant amounts of foraminifers (these form some of the laminae). Three altered volcanic ash layers are identified on the basis of distinct layers containing some glass shards and high amounts of zeolites (mostly phillipsite; see Riech, this volume). Volcanic particles are disseminated in sediments near the upper, middle, and lower portions of the unit. Pyrite ubiquitously occurs in low amounts. Minor components are quartz, siliceous organisms, and dolomite rhombs.

Basis for unit definition: The upper boundary of Unit 2 is the level at which siliceous organisms become rare; the lower boundary (with lithostratigraphic Unit 3) is delineated by contact with slump deposit. Generally, this unit is distinguished from Unit 1 by less variability in clay mineral content (with the exception of changes due to volcanic ash layers), lower amount of biosiliceous material, less variability in calcareous nannoplankton content (with the exception of lower amounts in some of the sand-silt layers), and on the basis of distinct differences in coarse-fraction components.

Unit 3

Age: Middle to late Miocene.

Major sediment types: Marly chalk/limestone, nannofossil marl, chalk/limestone, mudstone.

Minor sediment types: Marly foraminiferal nannofossil chalk, sandy marly foraminiferal nannofossil chalk, nannofossil mudstone, calcareous mudstone, sandy calcareous mudstone, glauconitic sandy mud, pyritic foraminiferal quartz sand, calcareous quartz sand, calcareous quartz-rich sandy mud, quartz-rich foraminiferal sand, calcareous siltstone, calcareous sandstone, quartz sandstone, nannofossil limestone, marly nannofossil limestone, nannofossil foraminiferal limestone, foraminiferal nannofossil limestone, calcite-cemented volcanoclastic quartz sandstone, volcanic ash.

Sub-bottom depth and core boundaries: 544.8 to 752.2 meters (207.4-m interval), Samples 397-57-3, 80

cm to 397-79-2, 70 cm. (Hole 397A: recovery of this unit in Core 397A-1 represents a disturbed section and has not been used for delineating sub-bottom depth range or thickness of unit.)

Color: Highly variable grays, browns, greens, but predominantly light gray.

Carbonate content: 50 per cent average, but highly variable (20 to 85%).

Texture: Highly variable; large fluctuations in sand and silt content correspond to numerous sand and silt layers.

Organic carbon: <0.5 per cent average, with little variability; similar values and trends as noted in lithologic Unit 2.

Allochthonous intervals: Approximately half of this unit is represented by slumps and numerous laminae of sandy and silty sediments. Twenty-six distinct zones of slumping occur, most of which are in the upper two-thirds of this unit and apparently were derived from very nearby. Sand and silt laminae are concentrated near the lower third of the unit. There seems to be a distinct increase in the number of slumping zones towards the Units 3/4 boundary (Arthur et al.; Arthur and von Rad, both, this volume). Allochthonous zones are separated by mudstones in the upper portion of Unit 3, and by marly nannofossil chalks and nannofossil chalks (frequently with worm burrows) in the lower portion of this unit. Over 60 individual sand/silt laminae are present, which have irregular contacts with surrounding sediment. Infrequently, sand layers incorporate clasts of marly chalks.

Sedimentary structures: Soft-sediment deformational structures in slumps include convolute bedding, slump overfolds, hook-shaped and roll-up structures, micro-faults, rip-up clasts, deformed clasts, pull-apart structures, and numerous other types of folds (such as recumbent, isoclinal, overturned, symmetrical, and asymmetrical). Approximately one-third of the sand-silt layers show textural grading; some thin sand layers are disrupted and not horizontally continuous. The basal portion of this lithologic unit is a chaotic mass of deformed sediment clasts, a precursor to the thick section of debris flows in Unit 4.

Sedimentary components: In hemipelagic sediments, there is a predominance of calcareous nannoplankton, foraminifers, clay, and quartz (which increases markedly down-section). Locally high concentrations of volcanic ash occur, associated with the seven volcanic ash layers identified in this unit, zeolites, and unidentified fine-grained carbonate detritus (which becomes more pronounced down-section along with quartz, particularly near the lower boundary of the unit). Displaced shallow-water skeletal debris, pyrite, feldspar, glauconite, heavy minerals, dolomite, and siliceous organisms are present, but in low quantities.

Basis for unit definition: The upper boundary of lithologic Unit 3 is the top of the uppermost zone of slumping; the lower boundary is at the base of the mudstone unit, near the middle Miocene unconformity and immediately above volcanoclastic sandstone. The zones of slump deposits are the outstanding character-

istic of this unit, with corresponding variability in virtually all textural, biogenic, and mineralogical components. Clay mineral composition is, however, not as variable as in Units 1 and 2 (Chamley and d'Argoud, this volume); also, coarse-fraction constituents do not differ significantly from those in the lower portion of Unit 2.

Unit 4

Age: Middle/early Miocene with reworked late Oligocene within allochthonous material (in Cores 397A-17 to 397A-21, and Core 397A-24 to Sample 397A-34-1, 70 cm).

Major sediment types: Pebbly mudstone, sandy pebbly mudstone, conglomerate, volcanoclastic sandstone, volcanoclastic conglomerate, sandstone.

Minor sediment types: Limestone, muddy limestone, marly limestone, silty marly limestone, marly foraminiferal limestone, marly nannofossil limestone, quartz-rich marly limestone, marly dolomite, dolomitic mudstone, quartz mudstone, sandy mudstone, sandy quartz mudstone, calcareous quartz-rich mudstone, calcareous sandy mudstone, calcareous quartz-rich sandy mudstone, calcareous silicified mudstone, volcanoclastic mudstone, sandy silt, siltstone, marly siltstone, silty clay, claystone, calcareous sandstone, marly quartz-rich foraminiferal sandstone, palagonite tuff, volcanic ash (many of these represent matrix material within pebbly mudstones and conglomerates); clasts within allochthonous intervals may be any of the above, as well as silicified mudstone, marly nannofossil chalk, porcellanite, polygranular quartz, and pumice.

Sub-units: Although there are no formal sub-units, the four thick volcanoclastic sequences in the upper portion of Unit 4 have been designated as V₁, V₂, V₃, and V₄ (top to bottom; see also Schmincke and von Rad, this volume).

Sub-bottom depth and core boundaries: Hole 397: 752.2 to 1000.0 meters (247.8-m interval), Samples 397-79-2, 70 cm to 397-104, CC. Hole 397A: 760.0 to 1296.7 meters (536.7-m interval), Core 397A-2 to Sample 397A-34-1, 70 cm. Total: 752.2 to 1296.7 meters (544.5-m interval). Correlations between 397 and 397A for total sub-bottom depth range and thickness of unit are discussed below.

Color: Various shades of dark and light grays with black and olive-green (matrix in pebbly mudstones, calcareous mudstones, calcareous sandstones, volcanoclastic sandstones and conglomerates, and limestones), also dark green-brown and dark brown (mudstones) and some white (calcareous sandstones); clasts within mudstones and conglomerates are similar in color.

Carbonate content: About 20 per cent average, generally decreasing in value (from about 50% in this unit's upper 100 m, to 15% at the base of Unit 4); variation is between 60 and 4 per cent.

Texture: Highly variable; fluctuations in sand and silt content result from poorly sorted matrix material in conglomerates and pebbly mudstones, as well as numerous sand and silt layers.

Organic carbon: Highly variable (0.3 to 3.5%) due to allochthonous material within thin lithologic units.

Allochthonous intervals: Almost the entire portion of this unit represents displaced sediments in the form of thick chaotic debris-flow deposits or thin sand and silt layers (see Arthur and von Rad, this volume). Approximately 50 thin autochthonous intervals of mudstones or marly limestones separate allochthonous portions. These intervals often contain worm burrows or other bioturbation structures that usually have not been distorted by soft-sediment movement. About eighty individual sand or silt layers are also present, particularly in the lower-middle portion. The pebbly mudstones exhibit many sedimentary features (see "Sedimentary structures," below) associated with mass-wasting of a thick sediment pile where a mud matrix has produced either soft-sediment deformational structures or, where more resistant sedimentary pebbles (such as polygranular quartz or porcellanite) are involved, textures suggestive of slow movement with trails of finer debris in their lee. Some episodes of slumping may have become more fluid or detached to produce the graded sand-silt laminae. The numerous intercalated mudstones are marly limestones could mark sole plates or shear zones of downslope movement or intervening zones of (hemi) pelagic sedimentation. Coarse-fraction data (Sarnthein in Arthur et al., this volume; Diester-Haass, this volume) suggest a derivation of some of the sedimentary components (see "Sedimentary components," below) within slumps from shallow water depths.

Sedimentary structures: Volcanoclastic sandstones occur in three sequences in Unit 4 of Site 397. The uppermost sandstone (V₁) is texturally graded near its base with particle sizes varying from pebbles several cm in diameter to silt-sized particles. Volcanoclastic sandstone V₂ is represented by only two large fragments in Core 397-81. The lowermost sandstone (V₃) is a sequence of the following three intervals cited from top to bottom: (1) a black volcanoclastic layer with numerous 1-mm-thick white laminae, four indistinct (1-cm-thick) zones of coarser particles, and a graded basal portion; (2) an intermediate marly nannofossil limestone with burrows overlying a calcareous mudstone (which contains numerous thin darker laminae); and (3) a basal volcanoclastic sandstone also with some fine horizontal veinlets of carbonate near its upper contact and a graded basal unit. Between the two lower intervals within V₃, a thin zone of mudstone clasts (Section 397-85-1) defines a disturbed contact between sedimentation pulses where volcanoclastic sandstones have been injected in each other, possibly disrupting a thin mudstone layer to form clasts. V₄ is a 20 to 30 meter thick mixed sedimentary-volcanoclastic sandstone in Cores 397A-6 and -7 (hyaloclastite; see Arthur and von Rad, this volume).

Calcareous sandstones often occur with deformed mudstone clasts. Frequently, some textural grading is apparent, particularly near the lower contacts; upper portions may contain burrows. One sandstone interbedded between volcanoclastic sequences V₁ and V₂ contains sediment clasts concentrated in at least five distinct

zones. One of these zones (Sections 2 and 3 of Core 397-80) appears to be a mudstone-claystone layer that has been disrupted and pulled apart by downslope movement.

Mudstones, pebbly mudstones, and conglomerates in Unit 4 are typical of deformational structures associated with the episodic mass wasting of a thick sediment pile where soft-sediment deformation has progressed beyond the type of folded structures noted in lithologic Unit 3. Movement has deformed these structures and clasts into an almost migmatitic texture; where more resistant clasts (such as quartzites) are present, these textures either appear to flow around them or are broken behind the clasts forming tails and streaks of finer soft-sediment material. Sedimentary clasts are often so deformed that it is difficult to distinguish them from the matrix, particularly towards the lower central portion of this unit (Cores 397A-15 to 397A-25). Interbedded mudstones often have rip-up clasts from surrounding sediments, smaller clasts where orientation suggests cross-bedding, or concentrations of smaller clasts that form a graded texture. A mudstone layer (Sections 397-80-3 and 397A-2-3) includes lenticular mudstone and claystone clasts producing a boudinage or pull-apart structure surrounded by a claystone matrix with a flow-binding texture; this structural feature is important in correlating cores from Holes 397 and 397A (see below). Of the 80 sand and silt layers in this unit, 32 are texturally graded (a few inversely graded) and are more prevalent immediately above pebbly mudstone sections whose clasts have been intensively deformed by plastic flowage. Within the uppermost part of lithologic Unit 4 (Section 397A-2-2), an 8-cm-thick layer of black and white cross-bedded sands ("climbing ripple" type) suggests vigorous current activity. The black sand layers are reworked volcanic material containing glass shards, while the base of this sand layer and the upper contact with a mudstone has dish structures suggesting dewatering. Non-graded layers are predominantly below or somewhat above those areas, where clasts within pebbly mudstones have been intensively deformed and could represent either thinner slump deposits of coarser detritus or current-winnowed deposits.

Dolomites and limestones often contain numerous thin laminae but rarely bioturbation structures; exceptions are the thick marly limestone beds underlying volcanoclastic sandstone V_3 , which is extensively bioturbated. Infrequently, dolomites and limestones form laminae within mudstone sequences. Stratigraphic dips of 25° occur in the marly limestone underlying the lowermost volcanoclastic sandstone (V_3); between Core 397A-10 and the base of this unit, average dips are about 20° and vary between 5° and 40° .

Sedimentary components: Because of allochthonous intervals in Unit 4, sedimentary components are highly variable. Smear-slide analyses reveal that nannofossil components are significantly less than in the overlying lithostratigraphic Units 1 through 3; average foraminiferal amounts are slightly less than in Unit 3, and similar to amounts in Units 1 and 2. Siliceous organisms are

rare, although poorly preserved and recrystallized diatoms and radiolarians are present in significant quantities within the lower portion of Unit 4 in coarse-fraction separations (Sarnthein; Diester-Haass; and Riech; all, this volume). Quartz content is also variable, but is generally higher than in the upper three lithologic units; quartz grains are subangular to rounded. Coarse-fraction data indicate higher proportions of both stained quartz grains throughout this unit (as also noted for Unit 3) and of frosted quartz in the upper half of this unit. Clay content averages are higher than in preceding lithologic units, but also fluctuate greatly. Zeolites are present in minor quantities, not only as phillipsite within or near volcanic ashes, volcanoclastic sequences, or sediments containing volcanic detritus, but also in the pores of nonvolcanic sediments (mainly clinoptilolite; see Riech, this volume). Dolomite is present, particularly in association with calcareous hemipelagic layers or within the matrix of pebbly mudstones and conglomerates. Unidentified fine-grained carbonate particles are variable but considerably higher than in lithologic Units 1 through 5. Within the pebbly mudstones and conglomerates, calcareous shell debris is present (bivalves, bryozoans, barnacles, calcareous algae, serpulids, ooids, decapods, etc.), indicating transport from shallow-water areas. Clay-mineral composition is distinctively characteristic (Chamley and d'Argoud, this volume), consisting predominantly of smectites.

Basis for unit definition: The upper boundary is delineated by upper contact of volcanoclastic sandstone (V_1) which directly overlies and is in direct contact with the first occurrence of the thick conglomerate-pebbly mudstone sequence. It should be noted that thin sandstones and pebbly mudstones with a few per cent of volcanoclastic material and with plastically deformed clasts of mudstone and limestone are present in the lower portion of lithologic Unit 3 (Schmincke and von Rad, this volume). The lower boundary for Unit 4 has been placed at the unconformity separating lower Miocene debris-flow deposits from the Lower Cretaceous mudstone/dolomite deposits. Lithologic Unit 4 is characterized by the preponderance of allochthonous debris-flow deposits (conglomerates and pebbly mudstone) with distinctive variations in all sedimentary components, high organic carbon content, and clay-mineral assemblage, as well as an upper section of volcanoclastic material.

Correlation between Holes 397 and 397A: Correlation of physical stratigraphic relationships is made difficult by poor recovery in Cores 81 to 83 in Hole 397 (generally, also from Core 90 to 104), as well as coring over longer intervals in the uppermost six cores of Hole 397A. Therefore, comparisons have been based upon overall relationships of distinctive thin interval of claystone containing lenticular mudstone clasts; this distinctive claystone interval occurs at about a 760-meter sub-bottom depth at both sites. We found optimal correlation between Core 397-70/80 and Core 397A-2.

Unit 5

Age: Early Cretaceous (late Hauterivian).

Major sediment types: Quartzose silty claystone, claystone, numerous thin (less than 1 cm) siderite layers.

Minor sediment types: Quartz claystone, calcareous mudstone, nanno marlstone (Cores 397A-46 and -47), thin layers of silt to very fine sandstone.

Sub-bottom depth and core boundaries: 1296.7 to 1453.0 meters (156.3-m interval), Samples 397A-34-1, 70 cm to 397A-52, CC.

Color: Gray, predominantly medium dark gray and olive-gray but also light gray, brown gray, greenish gray, black, and gray-brown; siderite layers are yellowish gray.

Carbonate content: 5 to 10 per cent average, with 1 to 45 per cent variation.

Texture: Variable, higher sand and silt content in thin sandy silt laminae; overall sand-silt variations reflect alternations of siderite layers and host mudstones and claystones.

Organic carbon: About 5 per cent average, with little variability.

Allochthonous intervals: Slumps and associated textures are present only in Cores 397A-39 and 397A-50 to 397-52. Scattered sandy silt layers (with one texturally graded) indicate allochthonous intervals. Other evidence suggestive of displaced portions are sediment clasts (marly limestone in Section 397A-38-1, as well as siderite in Section 397A-46-1 which looks like a graded sequence within a thin siderite layer); a calcareous mudstone (Sample 397A-39, CC) containing pelecypod shell fragments (also an ammonite); and a piece of wood debris found in Sample 397A-49-2, 53 cm (plant debris is an ubiquitous component throughout lithologic Unit 5, as determined by coarse fraction and smear slide analyses).

Sedimentary structures: Most outstanding in this sequence of gray mudstone and claystone are numerous thin layers (<1 cm thickness) siderite (identified as dolomite in smear-slide descriptions). Each of these siderite layers has sharp upper and lower contacts with the host mudstones. At least 265 such layers were identified, excluding those in Core 397A-50 where individual layers were not discernible due to severe deformation. Four sand-silt layers are present in Core 397A-39, one of which appears to be texturally graded. Silty mudstones and claystones in two cores (397A-39 and 397A-46) have small-scale cross-bedding structures. In Hole 397A, Cores 40 to 43 and 45 to 49 display a prevalence of yellowish brown, very thin laminae (0.25 to 0.50 cm thick) in varved-like sequences. These laminae are alternately clay-rich and silt-rich. Within a 12-cm-thick mudstone interval in Core 397A-47, nine such varve couplets were counted. Siltier varves have small Helminthoid burrows which do not disrupt the finely laminated texture. Generally, burrows and bioturbation structures occur in the lower portion of lithologic Unit 5 (Cores 47, 48, and 51 in Hole 397A), although they are also present within shorter sequences elsewhere (e.g., Cores 37 and 41 in Hole 397A).

Towards the base of the unit, slump features in the forms of folds, faults, boudinage type structures, etc., and flow structures have obliterated any original sedimentary structures including individual siderite layers. Stratigraphic dips were between 10° and 30°, averaging about 20°. For a detailed description and discussion of lithostratigraphic Unit 5 see Einsele and von Rad (this volume).

Sedimentary components: Mudstones and claystones are distinctively high in silt-sized quartz (up to 55%) and in their clay-mineral content variation (up to 95%); they share a characteristic assemblage of illite, chlorite, and kaolinite (Chamley and d'Argoud, this volume). Calcareous components generally form 10 per cent or less of sediment, with nanofossils locally higher in abundance within some mudstones and in marly limestones. Feldspar, pyrite, fish remains, and plant debris ubiquitously occur in trace amounts. Pelecypod shell fragments occur in a calcareous mudstone (Core 397A-39) and in a siderite layer (Core 397A-51). Ammonites are present with these shell fragments in Core 397A-39 and in a mudstone in Core 397A-46. Sediment clasts are rare; one of sapropelic mudstone is present in Core 397A-47. The coarse fraction includes fish remains, plant fibers, clastic grains, and pyrite. Siderite layers contain low amounts of quartz, fish debris, clay, pyrite, magnetite, and calcareous material.

Basis for unit definition: The pronounced change in lithology from lower Miocene pebbly mudstones to lower Cretaceous (upper Hauterivian) mudstones with thin siderite layers, marks an unconformity and the upper boundary of lithologic Unit 5. All material recovered at Hole 397A from below this unconformity to where drilling was terminated is part of this lithologic unit.

Summary of Coarse-Fraction Results

A semiquantitative estimate was made of the abundance of particle groups coarser than 63 µm (other than foraminifers) in washed core-catcher samples from Site 397 (Sediment Summary Chart 1, see back pocket, this volume; data from Sarnthein; see also Arthur et al., this volume). A quantitative coarse fraction analysis (>40 µm) has been conducted for samples from Cores 1 to 56 of Hole 397 (Diester-Haass, this volume).

The components distinguished are volcanic grains (glass shards, pumice); ooids; terrigenous sand (unstained, stained, frosted, and unfrosted quartz; mica; feldspar) and glauconite grains; and displaced shells from shallow water including mollusks and serpulids, sponge spicules, radiolarians, diatoms, fish remains, ostracodes, echinoderms, plant fibers, pyrite, and limonite particles. Planktonic foraminifers, benthic foraminifers, and phosphorite grains were also counted during the quantitative investigation.

Lithostratigraphic Units 1 and 2 (upper Miocene to Quaternary)

Variations in the composition of the coarse fraction can be attributed to the influence of the following processes: upwelling, terrigenous sediment input, shal-

low water sediment supply, CaCO_3 dissolution, and volcanism. The influence of upwelling with its increased fertility in the surface waters in apparent from these units (diatoms, radiolarians, sponges), as well as increased benthos (plankton/benthos ratios of foraminifers and an increase in echinoderms and ostracode percentages). Opal is present in Cores 397-1 to 397-26, with higher values in Cores 397-1 to 15 (= Quaternary). Highest opal contents occur in periods with highest terrigenous input and correspond to highest amounts of the various benthic organisms. Pyrite values are lower in the Quaternary sequence (with pronounced upwelling influence) than in the Pliocene less-fertile sequence (except for the core-catcher samples from Cores 397-4 to 397-7). Percentages of fish debris do not show a direct correspondence to opal amounts, but are generally higher in Cores 397-1 to 397-7 than in the interval below.

The terrigenous sediment input in the $> 40 \mu\text{m}$ fraction consists mainly of mica, feldspar, and quartz (stained and unstained). In the upper Miocene, there are strong variations between samples with high terrigenous input ($>40 \mu\text{m}$), corresponding to lower amounts of reddish stained quartz and samples with low terrigenous input having correspondingly higher amounts of red-stained quartz. The lower Pliocene sediments (Cores 397-29 to 397-43) have a consistently low terrigenous fraction ($>40 \mu\text{m}$) and higher amounts of stained quartz in Cores 397-29 to 397-32. The upper Pliocene and lower Quaternary sediments of Cores 397-28 to 397-11 show slight variations in terrigenous proportions and frequently stained-quartz fractions (exceptions are Samples 397-21-23, 80 cm and 397-19-3, 60 cm, as discussed below). In Cores 397-10 to 397-1, the range of the oscillations becomes significantly more pronounced. There is disagreement (see Sarnthein in Arthur et al., Diester-Haass; both, this volume) as to whether increased input of terrigenous sediment and the presence of red-stained desert quartz is related to either humid or arid climate in northwestern Africa. Coarse silt and fine-sand grain sizes are characteristic of lowland rivers, as well as for wind dust proximal to its source. Stained quartz is characteristic of lateritic weathering, but is also found in the dust load of subtropical latitudes (for details of discussion see Lutze et al., Arthur et al., Diester-Haass; all, this volume). Additional coarse terrigenous sediment is supplied by downslope particle-by-particle transport from the shelf controlled by changes in sea level and changes in swell. Sarnthein (in Lutze et al., this volume) favors stained quartz as an indicator of river load or dust load from a lateritic-weathering terrain, while Diester-Haass (this volume) sees this as an indicator of eolian input from an arid desert environment. Diester-Haass also considers the significance of higher opal values, as well as pointing out the relationship between heavier $\delta^{18}\text{O}$ intervals (shown by Shackleton and Cita, this volume; glacial or cooling events) and periods of higher terrigenous input.

Shallow-water sediment supply is indicated by the presence of glauconite, corroded shallow-water shell material ("relict material"), and serpulids, and by

highly increased benthic/planktonic foraminifers ratios (normally 1 to 8, increasing to 25). In the quaternary, an increase in shallow-water particles corresponds to glacial stages and is probably due to lowered sea level, enhancing the supply of shallow-water particles to the slope. In the Pliocene, there are several samples indicating a minor shallow-water (?particle-by-particle) supply. In Samples 397-21-6, 80 cm, 397-22-5, 80 cm, and 397-23-3, 80 cm, there is an increased input of shallow-water particles, possibly caused by turbid layer transport. Also, the late Miocene higher input of benthic foraminifers, glauconite, and serpulids is generally correlated to the cold-climatic phases (Shackleton and Cita, this volume).

Calcium carbonate dissolution has been studied by means of comparing the amount of fragmented tests relative to whole tests of planktonic foraminifers (plotted from Core 397-36 downward in the Sediment Summary Chart 1, back pocket, this volume). Highest fragmentation (up to 75%) is found in the upper Miocene (Core 397-52 and Cores 397-54 to 397-56). It decreases in Core 397-35 and is rather constant in Cores 397-34 to 397-26 (30 to 50%). In Cores 397-1 to 397-26, several cycles of fragmentation can be observed with minima of about 30 per cent and maxima of about 55 per cent. From Cores 397-15 to 397-1 the cycles show decreasing maxima and minima, the lowest fragmentation values being about 20 per cent, comparable to those of upper Quaternary sediments from the same region.

The influence of volcanism is reflected in the sediments by dispersed pumice and glass shards. In the upper Miocene and Pliocene, there are generally low values of about 1 to 10 per cent in the fractions $>40 \mu\text{m}$, except for Core 397-56. The rather constant upper Miocene/Pliocene percentages of dispersed volcanic particles are not correlatable to any major volcanic phase in the Canary Islands and are interpreted as grain-by-grain supply from the Canary Island shelf. Several layers with peak abundances of volcanic material (up to 40% for $>40 \mu\text{m}$ fractions) occur in Cores 13 to 16, 10, 5 to 7, and 2 to 3 in Hole 397, perhaps indicating deposition by eolian ash falls from eruptions on the Canary Islands (see Schmincke and von Rad, this volume).

Lithostratigraphic Units 3 and 4 (lower to lower/upper Miocene)

A semiquantitative coarse-fraction study was conducted for both the allochthonous and the hemipelagic autochthonous sediment portions. Coarse-fraction analyses suggest the following controlling processes: volcanism, significant shallow-water sediment input, terrigenous sediment supply, upwelling enrichment, and CaCO_3 dissolution.

Volcanic glass shards and pumice reflect the early Canary volcanism, starting from Core 397-96 with an early precursor in Core 397A-8 (see Sediment Summary Chart 1, back pocket, this volume). Maxima (90% of coarse fraction) are reached in the giant volcanoclastic grain flows of Cores 89, 86 to 84, and 79 to 80 in Hole 397. Evidence of volcanism (mainly ash layers) continues to Core 397-57. Common euhedral feldspar grains

(albite?) probably indicate continual reworking of volcanic deposits, particularly in Cores 397-71 to 397-58, during the late-middle and early-late Miocene (Arthur et al.; Lopatin; both, this volume).

A significant shallow-water sediment input occurs throughout Units 3 and 4. The main indicative components are coarse-shelled fragments of calcareous algae, shallow-water foraminifers, corals, bryozoans, barnacles, decapods, serpulids, mollusks, and phosphorite, carbonate ooids, and glauconite. Their maximum abundance occurs rather suddenly and parallels that of the Canary volcanic sediment supply in Cores 397-97 and 397A-4 through Core 397-89. A second narrow maximum lies in Cores 397-74 to 397-72 straddling the middle Miocene hiatus. The shallow-water components are dominated by mollusks and barnacles and only few solitary corals, and resemble a warm-temperature shallow-water environment (model of Lees, 1975) in early Miocene which was equal to or only slightly warmer than the present warm stage (Sarnthein, in Arthur et al., this volume).

Terrigenous sediments form a large fraction in the whole section of Units 3 and 4, and are intercalated only with thin intervals of hemipelagic sediments with predominating plankton particles. Phases of wet land climate are inferred from abundant plant fibers and occasional mica in lower Miocene Cores 397A-23 to 397A-16 and 397A-6 to 397-91. Coarse frosted-quartz grains might serve as an indicator of dune formation and more arid climate phases which is represented in the lower and middle Miocene (Hole 397A: Cores 5 to 85, 83, 72, and 73). Stained-quartz persists throughout Units 3 and 4.

An early Miocene phase of upwelling and increased fertility is reflected by abundant radiolarians and some diatoms in Cores 397A-30 to 397A-10. The Miocene occurrence resembles that of the Pleistocene, and pyrite content increases during many of the siliceous pulses. Fish remains are less common in Unit 3 and almost absent in Unit 4. The occurrence of fecal pellets is limited to Cores 397-72 and 397-77 as well as to Cores 397-57 to 397-61, a slumped mass which can be related to the same time-rock interval as Cores 397-72 and 397-73. This might be interpreted as a special high-fertility phase straddling the middle-upper Miocene hiatus.

Calcium carbonate dissolution, as indicated by the fragmentation of planktonic foraminifers, reaches a maximum in upper Unit 3 and continuously decreases to the middle of Unit 4 (i.e., middle-lower Miocene) where good preservation is found.

Lithostratigraphic Unit 5 (upper Hauterivian)

A deltaic or prodeltaic environment of deposition is clearly inferred from abundant fine-grained unstained-quartz, mica, and plant debris in the fine-sand fraction. The abundance of fish remains and echinoderm parts might point to enhanced fertility in the deltaic region. Siderite rhombs are enriched in single sediment laminae partly showing some textural gradation. Aragonitic nacreous shells of gastropods and ammonites indicate optimum conditions of CaCO₃ preservation.

Summary of X-Ray Diffraction Results (clay minerals and authigenic silicates)

The clay mineral associations of all five lithostratigraphic units generally indicate a detrital origin (Chamley and d'Argoud, this volume). Authigenic smectite (frequently associated with phillipsite) could be identified (Riech, this volume) only in some diagenetically altered ashes and volcanoclastic sandstone beds. Part of the smectite matrix of the volcanoclastic sandstones might have been derived from altered fine-grained volcanic debris from The Fuerteventura shelf (Schmincke and von Rad, this volume).

Table 4 shows the X-ray diffraction results of 40 samples selected for studies on silica and carbonate diagenesis. These semiquantitative data supplement the detailed X-ray diffraction results of Chamley and d'Argoud (this volume) and are discussed by Riech (this volume). The large amount of X-ray amorphous matter in Miocene and Lower Cretaceous sediments is possibly due to poorly crystallized phyllosilicates or their precursors.

The Lower Cretaceous Unit 5 is extremely rich in illite with considerable amounts of chlorite, smectite, and mixed-layer clay minerals. In the mainly allochthonous lower Miocene Unit 4, a drastic change to a smectite-dominated association takes place (see Chamley and d'Argoud, this volume; Sediment Summary Chart 1, back pocket, this volume). Apparently, the hinterland was covered by smectite-rich soils formed under a warm climate and seasonally alternating humid and arid conditions (Chamley and d'Argoud, this volume). Units 3 to 1 have a broad assemblage of smectite-illite-chlorite-kaolinite-mixed-layer mineral with trace amounts of palygorskite and sepiolite which might reflect climatic changes (humidity versus aridity) which are discussed in detail by Chamley and d'Argoud (this volume). These interpretations can be correlated with climatological events inferred from coarse-fraction analysis (Chamley and Diester-Haass, this volume).

Volcanoclastic Components

Air-fall ash deposits (probably derived from Gran Canaria or the western Canaries) occur mostly in Units 3 to 1 (14 to 0.3 m.y.B.P.). The fresh ashes consist of colorless individual glass shards, pumice, feldspar phenocrysts, and small felsic rock fragments in distinct layers (0.2 to 5 cm thick; maximum 25 cm). The glass of many ash layers is highly altered to zeolites (mostly phillipsite; see Riech, this volume). Only a few very old (19 m.y.B.P.) altered vitreous tuff layers of trachytic composition (source: Fuerteventura or Lanzarole?) were found in Unit 4 (Section 397A-23-3; see Schmincke and von Rad, this volume).

Two types of volcanoclastic sandstones were identified. A lower 7.8-meter-thick debris flow ("V-3" in Cores 397-84 and 397-85; 397A-2 and 397A-6) consists mainly of altered hyaloclastite (palagonite tuff), probably derived from a submarine shield phase of Fuerteventura. The upper 4.3-meter-thick debris flow ("V-1" in cores 397-79 and 397-80) is a tuffaceous sandstone

TABLE 4
Mineralogical Composition of Selected Samples, Site 397

	Sample (Interval in cm)	Time-Rock Unit	Depth (m)	Lithology	Mineral Composition (XRD)			
					> 25 wt. %	10 to 25 wt. %	< 10 wt. %	
Silicified Sediments	397-96, CC	Early Miocene	915	Pre-Miocene chert pebble	q	am	CT	
	397A-23-5, 90		1160	Porcell. with rad. + foraminifers	CT	am,ca	mtm,q,cli,pal,il	
	397A-26-1, 15		1210	Silicified mudstone with rad. + foraminifers	—	am,CT,ca,q	mtm,ka,il,si,py	
	397A-28-3, CC		1250	Silicified mudstone with radiolarians	—	CT,am,q,mtm,il	ca,ka,f,py	
	397A-29, CC		1260	as 397A-28-3, CC	CT	ca,q,mtm	am,ka	
	397A-33-1, 58		1290		CT	am,mtm,q,ca	il,pal,ka,f,do,py	
Altered Ashes, Tuffs, and Tuffaceous Sandstones	397-34-2, 132*	Early Pliocene	320	Altered vitreous ashes + tuffs	am	mtm,q,f	phi,py,ka,mi	
	397-37-4, 130*		350		am	f,phi,mtm,CT	py,mi,px	
	397-57-3, 87		L. Miocene		550	am,ca	f,q	phi,ka,CT
	397-75-1, 90				710	am	ca	phi
	397-76-4, 28	Middle Miocene	730	—	am,ca,mtm	f		
	397-79-2, 79		750	ca	am,mtm,f,q	ka,py		
	397-79-3, 22		750	mtm	dio,ca	CT,py		
	397-79-4, 38		750	mtm	dio,f	CT,am,ca,do,py,ka		
	397-84-4, 3		800	mtm	—	anal	am,ka,q	
	397-85-3, 58		810	ca	chab,mtm	am,q,py		
	397-85-3, 79*		810	mtm	q,ca	ka,f,phi		
	397A-23-3, 32		E. Miocene	1160	Altered tuffaceous sandstone	mtm	—	q
	Claystones with Aggregate Polarization	397-80, CC	M. Miocene	760	Mudstone with foraminifers	—	ca	q,mtm
		397-95-5, CC	Early Miocene	910	Silty/sandy mudstone	q	—	mtm,f
397A-23-3, 58		1160		Mudstone with siderite rhombs	—	am,si,ca,q,mtm	ka,ml,py,CT,il,f	
397A-46-2, 43		Late Hauterivian	1400	Mudstone	q	—	am,ka,mi,f	
397A-51-3, 90		1440	Mudstone	q	—	am,ka,mtm/il,chl	px,si,ap si,ca	
Zeolite-bearing Non- volcanogenic Sediments	397-76 (mixed)*	Middle Miocene	720	Limestone with foraminifers	cli	—	q,f,CT	
	397-85-3, 138		810	Marly limestone with foraminifers	ca	—	anal	
	397A-11-2, 93*	—	1020	Clayey foraminifer sandstone	CT	—	am,cli,q,ca	
	397A-12-4, CC*		1040	Mudstone with radiolarian casts + foraminifers	—	—	am,mtm,q	
	397A-14-1, 55*		Early Miocene	1050	As 397A-12-4, CC	q	—	am,mtm,f
	397A-14-5, CC			1050	Silty marl with foraminifers	q,ca	—	—
	397A-23-3, 140	1160		Mudstone with radiolarians + foraminifers	am	—	ca,q	
	397A-24-2, 48*	—	1180	Mudstone with foraminifers	am,q	—	cli,CT	
	397A-24-2, 64		1180	q foraminifer sandstone with do. rhombs	am,q,ca	—	cli,do,f	
	Dolomitic and Sideritic Sediments	397-59-1, 146●	L. Miocene	560	Marly chalk with do rhombs	ca,do	—	not determined
397A-5-1, 30		940		Silty dolomitic with foraminifers	do, am	q,ca	mtm,il,f	
397A-10-3, 142		Early Miocene	1020	Limestone with do rhombs	ca	—	do	
397A-11-6, 97●			1030	Mudstone with do/si rhombs	si	—	do	
397A-16-6, CC			1080	Micritic siderite with apatite layers	si	ap,q,am	mtm/il,ka,py	
397A-24, CC			1180	Dolomitic with opal-CT patches	do	am,q,CT	ca,il,chl	
397A-33-2, 12			1290	Micritic siderite	si	—	am	
397A-51-3, 93			L. Hauterivian	1440	Sideritic streaks in mudstone	si,q	am,mu,ka	py,il,q chl,f,ca

Note: Semiquantitative X-ray diffraction analysis by Dr. H. Rösch, Hannover. Explanation of symbols and abbreviations: + = aggregate polarization (uniform extinction of the total matrix under crossed nicols, if polarizer or analyzer are parallel to the bedding plane); * = HCl-residue; ● = heavy liquid separation for dolomite/siderite (> 2.8); am = X-ray amorphous matter, anal = analcime; ap = apatite; ca = calcite; chab = chabazite; chl = chlorite; cli = clinoptilolite; CT = opal-CT; dio = diopside; do = dolomite; f = feldspar; gmel = gmelinite; il = illite; ka = kaolinite; mi = mica; ml = mixed layer; mtm = montmorillonite; mu = muscovite; pal = palygorskite; phi = phillipsite; py = pyrite; px = pyroxene; q = quartz; si = siderite.

to conglomerate which, in addition to biogenic debris, contains sedimentary and metamorphic rock fragments and a montmorillonite-rich matrix, non-vesicular tachylite to fully crystallized basalt and trachyandesite, "micrograbbo" and vesicular pumice shards (now replaced by clay and carbonate). Schmincke and von Rad (this volume) interpret this debris as being derived mainly from subaerially eroded volcanic and sedimentary detritus from Fuerteventura between about 15.5 and 17 m.y.B.P. For a more detailed description and interpretation of the volcanogenic sandstones and inferences on the Neogene evolution of the Canary Island volcanism, see Schmincke and von Rad (this volume).

Depositional Environments and Processes²

Early Cretaceous Sedimentation (lithostratigraphic Unit 5)

The following interrelated sedimentologic and paleo-environmental problems are presented by the enigmatic facies of the late Hauterivian (recovered from Cores 397A-34 to 397A-52: (1) overall depth and environment of deposition, (2) mode of deposition; (3) oxygen levels in bottom water in contact with the sediments; (4) origin

² The interpretations presented include also the paleoenvironmental conclusions derived from the biostratigraphic data discussed later in this Site Report.

of millimeter to centimeter lamination; (5) preservational aspects of calcareous fossils; and (6) origin of siderite beds and nodules. The following paragraphs address each of these problems individually.

At present, evidence is indeterminate for both depth and environment of deposition. Sedimentary structures, rate of sedimentation estimated from biostratigraphic and paleomagnetic evidence (ca 75 to 150 m/m.y.), and composition of the sediments suggest several possibilities. Deposition appears to have taken place in a quiet-water setting (below effective wave base), as evidenced by conspicuous fine parallel lamination (Cores 397A-34 to 397A-48). The paucity of benthic invertebrates and of recognizable burrows (in Cores 397A-41, 397-44, and 397A-47) and the presence of fairly abundant organic matter (up to 1% by weight) suggest low oxygen conditions on the sea floor. No evidence was seen of photosynthetic benthic organisms (such as algae). Therefore, we can estimate a minimum depth of deposition of >100 to 300 meters. None of the features of these sediments seems typical of a shelf or lagoonal setting and a maximum grain size of fine to medium silt lends further support to this argument. Einsele and von Rad (this volume) compare the lithofacies of Site 397 with that of recent prodeltas and Early Cretaceous deltaic sediments in several on- and offshore commercial wells from the Aaiun Basin, and suggest a depth of a few hundred to 1000 meters based on paleogeographic setting and inferred rates of margin subsidence (cf. also Butt, this volume).

Appealing alternative interpretations are an environment under the influence of a pronounced oxygen-minimum zone, either in a slope setting or on a distal prodelta. The latter is favored by Einsele and von Rad (this volume). Abundant organic plant debris, the paucity of recognizable turbidites (only in Section 397A-39-2), and dominance of the clay fraction argues for a distal setting, possibly of a prodelta type (see Einsele and von Rad, their fig. 4). Evidence from more landward sections in the Aaiun Basin points to the existence of an Early Cretaceous deltaic complex. The inferred sedimentation rate at Hole 397A is extremely high for a typical slope setting. Unfortunately, we do not know with confidence the topographic profiles of ancient shelf-slope settings. Evidence for some downslope gradient is seen in Cores 397A-50 through 397A-52, where numerous slump structures and contorted, crinkled laminations occur. These could be due to shear imposed by occasional strong downslope currents, or to instability and downslope creep.

The mode of deposition is also uncertain. Distinct silt-clay lamination is present throughout most of the 156-meter sequence that was cored. Occasional cross-lamination (Section 397A-46-3) may also be seen and some rare slight graded bedding. Deposition may have been accomplished by a combination of turbid layer transport and small grain flows. Lamination is preserved because of the lack of bioturbation, which in turn was caused by oxygen depletion and a high sedimentation rate.

This lamination is important because of its possible implications. Much of the fine, millimeter-scale (varve-like) lamination may indicate annual rhythms. Tentative examination suggests a sedimentation rate on the order of 100 to >200 m/m.y. if the laminations are considered as annual couplets. However, these laminae may also represent longer term climatic variations, storm periods, or internal wave activity in a well-layered ocean.

The fact that fine laminations are preserved, signs of burrowing are scarce, benthic organisms are sparse or absent, and organic contents are relatively high suggests that oxygen-free to oxygen-poor bottom waters were typical during deposition of this sequence. Pyrite is a ubiquitous constituent, which implies that reducing conditions prevailed below the sediment-water interface.

The origin and fate of carbonate constituents is also significant. Nannofossil preservation varies (Wind and Čepék this volume), but is generally good, especially in Cores 397A-46 and 397A-47. Planktonic foraminifers are sparse or absent, which points either to very shallow environments (shelf break), low productivity (low evolutionary level at that time), or dissolution (see also discussion in Butt; Roesler et al.; both, this volume). The small average diameter of benthic foraminifers can be interpreted as indicating either lateral sorting during transport or restricted environmental conditions. Occasional well-preserved ammonites and pelecypods (Sections 397A-39-2, 397A-46-2, 397A-46-4) possessing aragonitic nacreous layers were encountered in the sediment. It is puzzling that relatively solution-susceptible aragonitic fossils would be preserved while planktonic microfossils may be largely dissolved. Thus, it is likely that the depositional environment was above the CCD and that the paucity of planktonic foraminifers is due to low productivity or dilution.

Siderite is also a major constituent of this unit (Einsele and von Rad, this volume), occurring in rhythmically spaced 0.1 to 2-cm-thick layers and nodules. It is probably authigenic, but does not appear to replace nannofossils and other recognizable calcareous constituents (except for possible siderite overgrowths, see Wind and Čepék, this volume). If siderite is wholly authigenic, it indicates that slightly reducing conditions prevailed within the dark mudstones and that dissolved sulfide was exhausted in the interstitial waters, while alkalinity increased. Siderite has been found in other Cretaceous marine organic carbon-rich shales in the North Atlantic in continental margin settings (e.g., Leg 14, Site 144; Leg 47B, Hole 398D) and basinal sites (Leg 11, Site 101).

Neogene Allochthonous Sedimentation and Margin Rebuilding (lithostratigraphic Units 1-4)

As a consequence of continental slope-rise destruction through possible deep-current erosion some time between the late Hauterivian and early Miocene, rapid downslope transverse sedimentation of a complex sequence of slump masses, debris flows, turbidity current deposits, and intercalated hemipelagic "autochtho-

nous" sediments occurred following this margin-sculpturing event or events (see Arthur and von Rad, this volume). Such flysch-type or sedimentary mélange deposits are well known from Alpine settings (fluxoturbidites, pebbly mudstones, turbidites; e.g., Stanley and Unrug, 1974) and are often interpreted as indicating tectonically active margins because of the need to invoke sources for large volumes of coarse debris and high slope gradients to encourage massive downslope movement. The sequences cored at Holes 397 and 397A on the upper continental rise, however, do not necessitate a relationship to tectonic processes. Indeed, they must be related to a cutting back (erosion) of older slope deposits, which stripped away greater thicknesses (>1 to 3 km) of overburden on a local scale (e.g., Cornford et al., Arthur et al.; both, this volume) and oversteepening of gradients on the slope. Sediments subsequently deposited on the slope and upper rise underwent mass-wasting to re-establish an equilibrium gradient from outer shelf to lower rise. Thus, following the rise-slope sculpturing event, the first sediment to appear at the base of the slope consisted of rapidly deposited debris flows. With time, the importance of these flows declined (Arthur and von Rad, this volume) as the gradient was diminished by a combination of upper slope and canyon erosion and the upbuilding and outbuilding of a sedimentary wedge on the rise. Because of slope instability, significant sediment probably did not accumulate on the upper slope (e.g., downslope from Site 369) until sedimentation and erosional processes effectively lowered gradients. The actual rate of stabilization depends on sedimentation rates over the shelf, slope, and rise, i.e., both the availability of terrigenous detritus and of pelagic biogenic material. In a deltaic setting, graded equilibrium could be expected to be rapidly accomplished. In this high fertility region off Cape Bojador, however, biogenic sedimentation is most significant, while terrigenous influx is climatically limited, although Sarnthein (in Arthur et al., this volume) suggests the possibility of an early Miocene deltaic source. Most of the mass wastage consists of pelagic biogenic sediment and dark mudstones with high clay mineral, quartz, and shallow-water calcareous skeletal contents. Due to a combination of special oceanographic conditions (? contour-following currents) and upwelling hemipelagic sedimentation has been effective in draping the rise-lower slope province from the middle Miocene onward; the role of turbidity transport and slumping is presently negligible.

Lithostratigraphic Units 3 and 4

Lithostratigraphic Units 3 and 4 encompass the interval from Cores 397-57 to 397-104, and from Cores 397A-1 to 397A-34 or the time from about 20 to 9 m.y.B.P. The stratigraphic and sedimentary record of these units is extremely complicated because of the interaction of downslope displacement of debris flows (both volcanogenic from the Canary Islands and, more typical, pebbly mudstones from the northwest African margin), turbidity currents, and possible activity of bottom currents.

The site apparently remained in bathyal depths during the deposition of Units 3 and 4: benthic populations consistently yield lower to middle bathyal species (Lutze, in Site Chapter, this volume), both in the autochthonous and allochthonous sediments. Shallow-water forms from the inner shelf, outer shelf, and upper slope are superimposed among the autochthonous benthic populations. A progression in time of reworking and displacement of inner shelf, outer shelf, and slope materials is evidenced by benthic foraminiferal populations present in allochthonous sediments (Lutze; Arthur and von Rad; both, this volume). An early Miocene acme (18-12.5 m.y.; maximum about 16 m.y.B.P.) in stripping of inner and outer shelf and slope sediments, with reworking of Eocene faunal elements, was followed by decreased displacement activity in the late Miocene, affecting the outer shelf and upper slope only.

Sedimentary material derived from the upper slope is consistently dark olive-green to brown-black in color, not strongly bioturbated, and relatively high in organic carbon content. Color is age-independent, and correlates with the color of sediment from piston cores taken on the upper slope from this area, represented by material which is middle Eocene, middle and upper Miocene, Pliocene, and Quaternary (*Vema* cores). Bioturbation is abundant in and above middle Miocene, but absent in lower Miocene laminated sediments which, however, yield an abundance of benthic foraminifers. The populations exhibit low species diversity, which could be the result of relatively oxygen-depleted conditions on this part of the upper rise province (problem of possible expansion of the oxygen-minimum layer).

Corrosive action of carbonate undersaturated bottom waters is evident in the autochthonous sediments of the middle-upper Miocene, whereas older faunas do not show much evidence of dissolution at depth.

Incipient diagenesis was consistently noticed in sediments of the lower Miocene; the foraminiferal tests are recrystallized, filled with tiny calcite crystals, and often deformed and compressed. Incipient diagenesis is limited to the autochthonous, strongly burrowed, light colored biogenic sediments. It is absent in the debris flows, which are allochthonous and penecontemporaneous with the autochthonous deposits. No age difference could be detected between the two in most instances, except in the lowest part of the section where displaced upper Oligocene sediment is intercalated with lower Miocene sediment. Both planktonic and benthic foraminifers from the debris flows are perfectly preserved, with empty tests and no deformation (See Cita, in Site Chapter, this volume).

From the above consideration, it appears that the autochthonous Neogene sediment are readily lithified at burial depths of 400 to 800 meters, because they have higher initial carbonate contents (foraminifers and nanofossils) and thus a higher "diagenetic potential" (cf. degree of CaCO₃ cementation in foraminiferal chambers and sandstones). By contrast, the allochthonous deposits at this burial depth have undergone little or no diagenetic change. The "diagenetic potential" is con-

trolled both by depositional mechanisms and different source areas for carbonate, and by oceanographic circulation events (Schlanger and Douglas, 1974).

The downslope displaced fossils in debris flows include solitary corals, gastropods, and pelecypods possessing aragonitic tests, which do not show any sign of corrosion. The mass transport mechanism (whether slow creep or rapid transport in suspension) and rapid burial protected them from both mechanical and chemical attack.

An enigmatic preservational aspect which deserves further consideration is recorded in Cores 397A-10 and 397A-11. An indurated, dark brown, highly gaseous, porous, marly limestone intercalated with debris flows contains perfectly preserved empty tests of Buliminids (Arthur and von Rad, this volume, plate 7). This association of apparently strong reducing conditions and methane generation with excellent preservation of solution-susceptible calcareous tests is difficult to explain. The following factors may exert some influence:

- 1) Rapid transport and burial from a shelf or slope setting, insulation from carbonate-undersaturated waters.

- 2) Dissolution of other types of soluble shallow-water calcareous organisms quickly saturating the pore waters (e.g., fine hash of pelecypod and gastropod fragments).

- 3) Interstitial water saturated initially (shelf-slope source in density current?).

- 4) High rate of reduction of organic matter by anaerobic organisms and lack of bioturbation led to rapid increase in alkalinity, enhancing preservation (see Berger and Soutar, 1970).

Radiolarians, which are conspicuously absent from the lower Pliocene to middle Miocene, reappear in the lower part of the section (lower Miocene). Their skeletons are mostly replaced by opal-CT (Riech, this volume). They are consistently recorded from Cores 397A-12 to 397A-34 with maximum abundance in Cores 397A-22 and 397A-23.

Siliceous productivity in subtropical belts is usually enhanced at times of known glaciation. However, no record of radiolarians was found at our drill site in correspondence with the late Miocene (Antarctic) glaciation. This must imply a reduced intensity of upwelling, possibly due to changes associated with the uplift of the Canary Islands and consequent readjustment of circulation patterns.

Lithostratigraphic Units 1 and 2

Between the late Miocene and the present (approximately 8 m.y.) pelagic sediments (Cores 57-3 to 1) were deposited which are relatively uniform in color, structure, texture, and biogenic and non-biogenic composition.

Dissolution of calcareous microfossils reaches its maximum at about 8 m.y. in the lowermost part of the upper Miocene, as well as in the immediately preceding time-rock unit (upper-middle Miocene). This may be related to expansion of the Antarctic ice cap (Hayes, Frakes, et al., 1974) and an intensification of ther-

mohaline circulation in the Atlantic Ocean (see also Diester-Haass; Cita and Ryan; Sarnthein in Arthur et al.; all, this volume).

Strong climatic changes are noticed in foraminiferal associations in the youngest part of the Pleistocene (the so-called "glacial" Quaternary). Less-pronounced but noticeable fluctuations are also recorded in the Pliocene; the lower Pliocene seems to reflect cooler conditions with respect to both the overlying upper Pliocene and the underlying upper Miocene, where a higher number of tropical species of planktonic foraminifers is recorded.

The occurrence of siliceous plankton (radiolarians, diatoms, silicoflagellates) in Cores 397-1 to 397-32 (upper Pliocene/Quaternary) indicates siliceous productivity during a period of known glacial expansion, especially during the last 1.8 m.y. (Diester-Haass, this volume). Core 392-25 has an interpolated age of approximately 3 m.y., which corresponds to the onset of Arctic glaciation (DSDP Leg 12).

Generally speaking, the sedimentation rate is high which partially is explainable by high productivity in an area of upwelling (Canary Current) and, in part, by a high input of terrigenous material (particularly in the finer sediment fraction size, although this does not become prominent until Cores 397-19 or 397-20).

Summary

The following sequence of events in the Neogene history of the African margin off Cape Bojador is recognized as a result of Site 397 coring.

Pre-Late Oligocene or Early Miocene Sculpturing Event

Because of the hiatus between Hauterivian and lower Miocene deposits, this event is not well dated; it is thought to be one or more geostrophic current-generated erosional phases with unloading and isostatic uplift establishing high slope relief and instability. Possibly, erosion was accomplished over more than one time period, because several distinct hiatus intervals were noted at Site 369 on the upper slope (Lancelot, Seibold, et al., 1978).

Early to Middle Miocene Initial Sedimentation Phase

After the end of the final erosional phase in the lower Miocene, the first sedimentation consists of pebbly mudstone (F-4A₁; facies notations, e.g., F-1, 2, 3, 4, 5, etc. are discussed in Arthur and von Rad, this volume) transported as debris flows, including detritus from hemipelagic and upper slope carbonaceous mudstone sources (fig. 5 in Arthur and von Rad, this volume). The clasts are typically smeared and flattened by shear and compaction. The debris flows are interbedded with fine-grained, carbonaceous, graded turbidites (F-3). An evolutionary sequence (fig. 3, Arthur and von Rad, this volume) can be followed from (1) predominant debris flows (F-4A type), through (2) poorly sorted debris flows containing few sedimentary clasts but rich in quartz granules and shallow-water calcareous shell debris (F-4C). These are interpreted as grain flows from periodic flushing of canyon head reservoirs at the shelf

edge and into (3) fewer debris flows, more common thin turbidites, and an increasing hemipelagic component. This probably represents the progressive diminishment of the slope-rise gradient. Most turbiditic sands, silts, and clays were probably bypassed to the lower rise during the early Miocene (e.g., to the vicinity of Site 139 and as far as Site 138 (see Berger and von Rad, 1972; Arthur et al., this volume). Those eolian sand turbidites (Sarnthein and Diester-Haass, 1977), etc., were deposited on the upper rise more frequently as the gradient declined. The first and second evolutionary steps (noted above) occur between seismic reflectors R-10 (D₆) and R-8; the third evolutionary step occupies the interval between R-8 and slightly post-R-7 (D₂).

Late-Early to Middle Miocene Canary Islands Uplift Event

Superimposed over the transverse sedimentation processes piling sediment at the base of the slope is evidence of the occurrence (about 16 m.y.B.P.) of a number of debris flows, relatively better sorted than those previously discussed and partly well graded (e.g., Core 397-84), containing primarily volcanic materials of acidic through basic composition (F-4B) along with some pelagic and shallow-water sediment debris (dominant in Cores 397-84 to 397-82). These are interpreted as recording the initiation of significant topographic relief, and possibly subaerial exposure along the Canary Island trend and the establishment of a downslope longitudinal gradient along the rise from the Canaries to at least the location of Site 397 (fig. 5, Arthur and von Rad; Schmincke and von Rad; both, this volume).

The uplift of the Canaries trend and that of the Cape Verde Rise at some time in the early Miocene may also have been responsible for changing oceanographic conditions along the interval of the northwestern African margin between the two island chains, acting as an effective barrier which diverted deep bottom currents which had previously scoured the region, and allowed high rates of sedimentation to persist at the base of slope and upper rise provinces. Only limited evidence for bottom current-produced deposits (e.g., Core 397-73) was found at Site 397 above the lower Miocene, and only minor erosional hiatuses were encountered.

Late Miocene to Recent Hemipelagic Sedimentation Phase

Most of the section above the R-7 (D₂) seismic horizon comprises biogenous hemipelagic sediment deposition along the upper rise. Sedimentation rates of biogenic calcite are extremely high, related to climatically induced upwelling and high fertility. Also, enough bottom-current activity occurs along the foot of the slope to concentrate sedimentation in a wedge at the base of the slope. Terrigenous input is variable, mainly clay-sized particles settled out of nepheloid suspension or a possible eolian contribution. In the lower-upper Miocene (Cores 397-57 to 397-72), downslope creep and slumping of hemipelagic deposits occurred over an interval of about 100 meters, but gradients were apparently not steep enough to encourage complete detachment and formation of debris flows. Thereafter, slope stability was evidently established and rapid upbuilding of the

sediment wedge occurred by hemipelagic depositional processes.

The upbuilding of the upper continental rise sediment drape was interrupted only briefly by four hiatuses: (a) a minor gap at about 15-15.5 m.y.(?); (b) a gap (12.5-10.5 m.y.B.P.) between the middle and late Miocene (also at Site 369, Leg 41), possibly due to slumping; (c) a scouring event (bottom currents) or reduced sedimentation rates during the Pliocene (ca. 3 m.y.B.P.) and (d) another brief intra-Pleistocene (ca. 0.9 m.y. B.P.) scouring event are only based on evidence from physical properties, acoustostratigraphy, magnetostratigraphy, and/or reworking of planktonic foraminifers. The third and fourth hiatuses are both associated with known periods of intensification of northern hemispheric oceanic circulation due to climatic deterioration; three last-mentioned hiatuses are associated with the release of eolian sand turbidites in neighboring DSDP Sites 138, 139, 367, and 370 (Sarnthein and Diester-Haass, 1977; Sarnthein, 1978).

Eustatic sea-level changes have apparently left very little imprint on the upper rise sedimentary record, although variations in amount of the terrigenous component in response to climatic change do occur (Lutze et al.; Diester-Haass; both, this volume). Acoustic stratification especially in the Quaternary section is probably a climatic signature caused by changes in the "diagenetic potential" of deposited biogenic calcareous components (carbonate cycles) related to climate-induced oceanographic events (e.g., Schlanger and Douglas, 1974; Williams and Mountain, this volume; Cita and Ryan, this volume).

The complexity of sedimentation and evolution of the rise prism in Neogene times could not have been deciphered without continuous coring. As a result of this analysis, it is apparent that active tectonism is not required to generate seemingly chaotic sedimentary sequences. The association of sedimentary breccias, conglomerates, and turbidites with volcanogenic debris flows in a passive margin setting suggests that care should be taken in interpreting similar associations in mountain belts.

PHYSICAL PROPERTIES AT SITE 397

Measurements of sound velocity, wet bulk density, porosity, water content, and shear strength were made on samples from Holes 397 and 397A (see Tables 5 and 6, respectively). A brief description of the equipment and techniques used is given in the Explanatory Notes (this volume). Further discussion and evaluation of the data are presented by Williams and Mountain (this volume). Table 14 and Figure 27 show correlations of shipboard sonic velocity measurements with interval velocities between seismic reflectors.

Leg 47A afforded unique opportunities for obtaining information on the effects of the deep burial of marine sediments. All but 70 of the drilled 1453 meters were cored, and reasonably good recovery ensured that the data are representative of the entire section. The uppermost 686 meters penetrated a fairly uniform Neogene section that was deposited nearly continuously at water

TABLE 5
Sound Velocity, Wet Bulk Density, Porosity, Water Content, Shear Strength, and Sand/Silt/Clay Ratios From Hole 397

Core-Section	Velocity (km/s)		Wet Bulk Density (g/cm ³)		Impedance (g/cm ² · s)	Porosity (%)		Water Content Gravimetric	Shear Strength (g/cm ²)	Depth (m)	Grain Size (%)		
	Bedding	⊥ Bedding	Gravimetric	2-min. GRAPE		Gravimetric	2-min. GRAPE				Sand	Silt	Clay
1-1										5	9	33	58
2-1	70-1.74									37	12	34	54
-2										90	6	34	60
-3 ^a	75-1.51		90-1.55 ^c	66-1.79	2.34	90-69.6 ^c	66-56.3	90-44.9 ^c					
-5	100-1.51												
3-1										64	2	19	79
-2 ^a										60	5	16	79
-3	38-1.49		60-1.59 ^c		2.40	60-66.5 ^c		60-41.9 ^c					
-3	123-1.51												
-4 ^a	36-1.55												
-5	18-1.50												
-5	130-1.55												
-6	26-1.46												
-6	86-1.49												
4-1	136-1.48 ^b												
-2 ^a	118-1.48		67-1.62 ^c		2.41	67-66.5 ^c		67-41.4 ^c		66	2	13	85
-3	72-1.50												
-4 ^a	25-1.50												
5-2 ^a										68	3	21	76
										138	2	25	73
-3	27-1.50		90-1.58 ^c		2.37	90-70.8 ^c		90-44.8 ^c	34-35	89	4	32	64
-4 ^a													
6-1	50-1.55									46	4	34	62
-2 ^a	125-1.52												
-3	26-1.53								29-110	44	3	35	62
-4 ^a	80-1.52 ^b												
-5	23-1.50 ^b												
-5	107-1.50 ^b												
7-1	90-1.52												
-2 ^a	80-1.33 ^b		95-1.56 ^c		2.37	95-54.1 ^c		95-34.7 ^c	33-37	95	5	26	69
-3	20-1.51												
-3	55-1.54 ^b												
-4 ^a	96-1.56 ^b												
-5	38-1.54												
-6	34-1.54 ^b												
8-1	50-1.52												
-1	120-1.51 ^b				2.28								
-2 ^a	92-1.53 ^b												
-3			74-1.50 ^c	63-1.62		74-69.1 ^c	63-67.8	74-45.9 ^c	61-64	74	3	34	63
-4 ^a	79-1.51 ^b												
-5	62-1.53 ^b												
9-1	38-1.51												
-1	107-1.55 ^b												
-2 ^a	11-1.53				2.37								
-2	111-1.48 ^b												
-3	53-1.52 ^b		54-1.56 ^c	61-1.68		54-65.9 ^c	61-63.3	54-44.1 ^c	65-74	53	4	30	66
-4 ^a	102-1.52 ^b									56	2	32	66
10-2 ^a													
-3	136-1.53			110-1.52			110-74.0		105-99	106	1	31	68
-4 ^a	92-1.37 ^b												
-5	38-1.54												
-6	76-1.36 ^b												
11-1	37-1.54 ^b												
-2 ^a	37-1.54 ^b												
-3	132-1.53 ^b		126-1.56 ^c	133-1.75	2.40	126-64.9 ^c	133-58.9	126-41.7 ^c	117-151	125	2	28	70
-4 ^a	138-1.53 ^b												
-5	70-1.55 ^b												
12-1 ^a	97-1.48 ^b				2.62				79-107				
-3 ^a			85-1.77 ^c			85-58.5 ^c		85-33.0 ^c		84	3	36	61
13-1	56-1.58												
-2 ^a													
-3	115-1.57 ^b		62-1.63 ^c	67-1.76	2.58	62-60.5 ^c	67-58.6	62-37.2 ^c	72-252 75-219	61	3	32	65
-3													
-5	53-1.59 ^b												
-6				61-1.76				61-58.0					
-7	35-1.48 ^b												
14-1 ^a													
-4	76-1.56 ^b		72-1.65 ^c	80-1.73	2.56	72-71.7 ^c	80-60.3	72-43.5	65-27	71	4	33	63
-6	22-1.53 ^b												
15-1	91-1.42 ^b												
-2 ^a					2.74								
-3			68-1.71 ^c	73-1.81		68-59.8 ^c	78-55.0	68-34.9 ^c	64-179	67	3	36	61
-4	128-1.60												
-5 ^a	132-1.60 ^b												
-6	121-1.60 ^b												

TABLE 5 – Continued

Core-Section	Velocity (km/s)		Wet Bulk Density (g/cm ³)		Impedance (g/cm ² · s)	Porosity (%)		Water Content Gravimetric	Shear Strength (g/cm ²)	Depth (m)	Grain Size (%)		
	Bedding	Bedding	Gravimetric	2-min. GRAPE		Gravimetric	2-min. GRAPE				Sand	Silt	Clay
16-1	107-1.60												
-2a													
-3	16-1.59b		65-1.65 ^c	72-1.68	2.64	65-69.2 ^c	72-63.6	65-42.1 ^c	67-165	65	7	31	62
-4a													
-6	100-1.57b												
17-1	93-1.50b												
-2a													
-3	100-1.60b		100-1.68 ^c	95-1.75	2.67	100-59.2 ^c	95-59.1	100-35.3 ^c	90-293	99	3	30	67
-4a													
-5	89-1.58b												
-6	116-1.63b												
18-2a	125-1.41b												
-3			60-1.70 ^c	35-1.85	2.65	60-59.2 ^c	35-52.3	60-34.9 ^c	57-206	40	3	28	69
-4a	118-1.61b												
-6	145-1.51b												
19-2a	73-1.60												
-3	83-1.59b		92-1.70 ^c	34-1.73	2.72	92-60.0 ^c	34-60.4	92-35.4 ^c	45-316	100	2	36	62
-4a													
-6	58-1.60												
20-1a	104-1.57												
-2	73-1.58												
20-3	83-1.60		92-1.70 ^c	87-1.84	2.69	92-59.3 ^c	87-52.9	92-34.8 ^c	87-234	80	3	36	61
-6	58-1.58												
21-1a	76-1.59												
-3	85-1.31b		90-1.77 ^c	112-1.80	2.87	70-62.6 ^c	112-56.0	90-35.2 ^c	64-174	101	2	36	62
-3													
-4a													
-5	120-1.64												
-7	40-1.47b												
22-1	115-1.55												
-2a													
-3	42-1.43b		121-1.74 ^c	72-1.73	2.76	121-56.3 ^c	72-60.0	121-32.4 ^c	81-170	120	1	39	60
-4a			121-1.75 ^c			58.4		33.4					
-5	28-1.61												
23-2a	80-1.59			97-1.84			97-53.0		04-138	106	2	36	62
-3													
-4a													
-5	87-1.44												
24-1	101-1.56												
-2a													
-3	111-1.62		111-1.72 ^c	96-1.83	2.73	111-59.0 ^c	96-53.8	111-34.2 ^c	98-110	110	3	35	62
-4a	40-1.49b												
-6	39-1.60												
25-5	37-1.60		96-1.81 ^c	69-1.85	2.90	96-55.1 ^c	69-52.5	96-30.4 ^c	62-215	95	2	31	67
26-1	113-1.60												
-2a													
-3									74-192	87	2	28	70
-4a	126-1.70												
27-2a	77-1.60		106-1.86 ^c	129-1.96	2.98	106-46.4 ^c	129-45.0	106-24.9 ^c	06-160	105	2	28	70
-3													
-4a	12-1.64b												
28-2a	57-1.64b												
-3			78-1.89 ^c	67-1.99	3.16	78-49.7 ^c	67-43.3	78-26.2 ^c	73-224	78	1	29	70
-5	49-1.67									77	1	32	67
29-2a	104-1.51												
-3			82-1.87 ^c	56-1.97	2.97	82-51.1 ^c	56-44.7	82-27.3 ^c	73-197	81	1	29	70
-4	82-1.64												
-6a	55-1.60												
30-1a													
-2	111-1.62												
-3			82-1.70 ^c	48-1.79	2.77	82-53.2 ^c	48-56.2	82-31.3 ^c	39-147	81	1	23	76
-4a	36-1.48												
-6	45-1.64												
31-3a	47-1.68		16-1.91 ^c	31-1.96	3.21	16-50.5 ^c	31-45.3	16-26.4 ^c	47-270	15	1	29	70
32-2	97-1.54				2.82								
-3a			33-1.83 ^c	50-1.90		33-55.2 ^c	50-49.4	33-30.1 ^c	79-312	32	2	30	68
33-2a	53-1.61												
-3			83-1.87 ^c	60-1.97	3.01	83-55.2 ^c	60-44.8	83-29.6 ^c	87-142	80	1	28	71
34-1	130-1.60												
-2a													
-3			34-1.76 ^c		2.83	34-49.2 ^c		34-28.0 ^c		33	1	32	67
-4a	32-1.62												

TABLE 5 – Continued

Core-Section	Velocity (km/s)		Wet Bulk Density (g/cm ³)		Impedance (g/cm ² · s)	Porosity (%)		Water Content Gravimetric	Shear Strength (g/cm ²)	Depth (m)	Grain Size (%)		
	Bedding	⊥ Bedding	Gravimetric	2-min. GRAPE		Gravimetric	2-min. GRAPE				Sand	Silt	Clay
36-2	94-1.47 ^b				–					109	1	34	65
37-4	43-1.59				2.70								
-4	131-1.87		130-1.56 ^c			130-62.5		130-39.9					
38-2 ^a													
-3				12-1.92			12-47.5		17-165				
-4 ^a					2.92								
-5	53-1.62												
-6	51-1.34 ^b		85-1.80			85-53.2		85-29.6					
39-2 ^a													
-4 ^a	102-1.66				–								
-5									59 >1051				
-5									79 >416				
40-3	58-1.65		57-1.79		2.95	57-52.8		57-29.4					
41-4	92-1.63												
-5	20-1.64		74-1.86 ^c		3.05	74-54.2 ^c		74-29.1 ^c	103-753	70	1	29	70
-5									124-163				
42-2	49-1.68				–					55	0	24	76
43-2 ^a													
-4	103-1.67				3.16								
-5	91-1.53 ^b		70-1.89 ^c	108-2.00		70-52.2 ^c	108-42.9	70-27.6 ^c	76-188	69	2	31	67
44-2 ^a	140-1.68												
-3			32-1.61 ^{b,c}			32-42.0 ^c		32-26.1 ^c		31	1	24	75
-5	57-1.72				2.74				104-741				
-5									107->416				
45-2	34-1.69												
-4 ^a	63-1.57		77-1.99 ^c		3.23	77-46.5 ^c		77-23.4 ^c	25-359	77	0	29	71
			77-1.97 ^c			77-47.6		77-24.1					
47-2 ^a													
-5			61-1.98 ^c		–	61-46.9 ^c		61-23.7 ^c		60	1	25	74
			61-1.96 ^c			61-46.2 ^c		61-23.6 ^c					
48-2 ^a													
-2			79-1.88			79-49.0		79-26.1		83	1	28	71
			139-1.86			139-47.4		139-25.4					
49-2 ^a													
-3		88-1.62	81-1.59 ^c		2.58	81-43.0 ^c		81-27.0 ^c	43-741	80	1	26	73
50-1		50-1.73	66-1.90		3.29	66-47.5		66-25.0		66	0	29	71
52-3		76-1.71	33-1.87			35-48.7		33-26.0		27	0	22	78
-4 ^a					3.20								
53-1		56-1.66	63-1.89	89-2.04	3.14	63-47.3	89-39.8	63-25.0					
54-2 ^a													
-3			88-1.91			88-47.1		88-24.7		90	0	27	73
54-3	143-1.80	143-1.64			3.13								
-4 ^a													
55-2 ^a													
-3		33-1.66								80	1	28	71
-3			86-1.91	131-2.00	3.17	86-44.1	131-42.9	86-23.1					
-4 ^a													
56-3			38-1.94	34-2.06	–	38-45.7	34-38.5	38-23.5		30	0	24	71
57-4		41-1.75	17-1.91	41-1.98	3.34	17-47.2	41-44.2	17-24.8		12	1	26	73
58-3	127-1.67	127-1.53	17-1.84	101-1.99	2.82	17-46.7	101-43.1	17-25.4		31	2	36	62
59-1		10-1.70	98-2.01		3.42	98-43.2		98-21.5		94	1	43	56
60-3		43-1.66		43-2.03	–		43-40.4			85	1	29	70
61-3		41-1.76	87-1.91	92-2.10	3.36	87-49.6	92-36.3	87-24.2		82	2	36	62
62-4		35-2.00	83-1.93	35-2.04	3.86	83-45.0	35-40.2	83-23.3		87	0	20	80
63-1		58-1.77		58-2.05	3.49		58-39.1						
-2			1-1.97			9-42.8		9-21.7		13	1	29	70
64-3		91-1.66	135-1.93	91-2.06	3.20	135-45.9	91-38.5	135-23.8		138	1	24	75
65-3		44-1.64	91-1.93	44-2.00	3.20	91-45.1	44-42.8	91-23.4		93	3	35	62
		44-1.67											
66-1 ^a													
-3		62-2.06			4.04					92	1	34	65
-3			91-1.96	100-2.07		91-43.1	100-38.2	91-22.0					
67-2		26-1.68	–	26-1.95	–	73-43.7	26-2.62	73-25.8		75	1	29	70
68-2 ^a													
-3			118-1.95		–	118-42.0		118-21.5					
69-3		18-1.84 ^b	72-2.45	18-2.17	–	92-57.8	18-31.8	72-23.6		74	1	39	60
70-1 ^a					–								
-3			20-1.96			20-43.5		20-22.2		31	1	30	69

TABLE 5 – Continued

Core-Section	Velocity (km/s)		Wet Bulk Density (g/cm ³)		Impedance (g/cm ² · s)	Porosity (%)		Water Content Gravimetric	Shear Strength (g/cm ²)	Depth (m)	Grain Size (%)		
	Bedding	⊥ Bedding	Gravimetric	2-min. GRAPE		Gravimetric	2-min. GRAPE				Sand	Silt	Clay
71-3		80-1.50	47-1.97	80-2.09	2.96	47-41.0	80-36.6	47-20.9		92	1	26	73
72-3		136-1.73		127-2.05	(3.43)		124-39.5						
-4 ^a													
-6 ^a													
73-3		70-2.13	47-2.09	70-2.29	[70] 4.45	47-36.7	70-23.7	47-17.6					
74-1		67-2.00	41-2.20	67-2.27	[67] 4.40	41-32.0	67-25.0	41-14.5					
75-1		130-1.91		130-2.03	[130] 4.14		130-40.8						
-2			57-2.17			57-33.8		57-15.5					
76-3		85-2.02	52-1.84	85-2.21	[85] (4.30)	52-50.3	85-29.1	52-27.4					
77-1		127-2.08		127-1.98	[127] 3.81		127-43.6						
-3			69-1.83			69-47.2		69-25.8					
78-3		127-2.17 ^b	52-2.20	127-2.34	(4.90)	52-31.8	127-20.7	52-14.5					
79-2		145-3.02	138-2.28	145-2.40	[145] 6.89	138-25.7	145-16.0	138-11.3					
80-3		48-2.82	48-2.82	48-2.30	[48] (6.26)	48-23.1	48-23.1	129-25.2					
-3		88-2.24		88-2.10	[88] (4.53)	88-36.0							
83-2		21-1.81		21-1.50	–		21-75.2						
84-3		23-2.55	121-2.14	23-2.26	[23] 5.46	121-39.9	23-25.8	121-18.6					
85-2		32-2.49		32-2.09	[32] (5.00)		32-36.9						
-4		149-1.59 ^b		141-2.13	[149] (3.26)		149-34.2						
86-1			105-1.98			105-45.0		105-22.7					
-2		30-1.60	30-1.84	30-2.15	[30] (3.80)		30-32.9						
87-1		66-2.00	66-2.28	66-2.38	[66] 4.61	100-38.3	66-17.4	100-18.9					
		66-2.30	66-2.74										
-3			92-2.02			72-38.3		72-18.9					
88-2		123-1.53	44-2.16	123-2.07	[123] (3.04)	44-24.8	123-37.9	44-11.5					
-4		39-2.90	39-2.58	39-2.52	[39] (6.30)		39-8.8						
		39-2.98											
89-3		123-2.06 ^b	47-2.09	123-2.21	[123] (4.39)	47-23.0	123-29.1	47-10.0					
			89-2.30			89-36.6		89-17.5					
90-2		76-2.13	72-2.21	76-2.35	[96] 4.71	72-34.1	76-19.4	72-15.4					
92-3			135-1.94		–	135-44.3		135-22.8					
93-3		84-2.26	20-1.90		4.29	20-45.0		20-23.6					
95-3		71-2.13	43-2.20	71-2.32	4.69	43-30.4	71-21.8	43-13.8					

Notes: ^aGRAPE scan.
^bUnreliable data.
^cSyringe.

depths above the CCD. These factors contribute to making data from this site ideal for documentation of the change of physical properties with depth without complications of diverse lithologies, large hiatuses, or carbonate dissolution. A 100-million year hiatus was found at 1306 meters and data across this unconformity provide insight into the effects of exhumed and reburied sediments.

Not surprisingly, the physical properties of the sediments reflect the three major lithologic units at Site 397 (lithostratigraphic Units 1 and 2, 3 and 4, 5). This can be seen in a glance at the summary graph of Figure 4. Above 686 meters, gradients are uniform and scatter is relatively small. In the Miocene gravitative sediments below this depth, all values are widely scattered, and there is little indication of vertical gradients. Values are most consistent again in the Lower Cretaceous section below 1300 meters, where there is an appreciable vertical gradient in physical properties. The following discussion is based on data displayed in Figure 4 and is divided into the three intervals just identified.

First Interval: Cores 397-1 to 397-72 (0 to 686 m sub-bottom)

Velocity

Each dot (see Figure 4) in the uppermost 300 meters is the average of one to five measurements made parallel to bedding at different locations through the core liner. Below this depth, measurements were made less frequently, usually at two locations per core. The triangles indicated below 400 meters are values of velocity measured perpendicular to bedding on samples firm enough to be removed from the liner and measured directly. Horizontal lines in Figure 4 connect values measured on the same sample. With the exception of three samples from Site 397, all velocities measured parallel to bedding were higher (average difference of 10 duplications was 0.19 km/s) than those measured perpendicular to the bedding of the same sample.

Values at the top of the hole begin close to that of sea water (1.51 km/s in Core 397-2) and increase with relatively little scatter to roughly 1.70 km/s at the top of

TABLE 6
Sound Velocity, Wet Bulk Density, Porosity, Water Content, and Other Data From Hole 397A

Core-Section	Velocity (km/s)		Wet Bulk Density (g/cm ³)		Impedance (g/cm ² · s)	Porosity (%)		Water Content (%)	Grain Size (%)									
	Bedding	⊥ Bedding	Chunk Gravimetric	2-min. GRAPE		Chunk Gravimetric	2-min. GRAPE	Chunk Gravimetric	Depth (m)	Sand	Silt	Clay						
1-3	10	2.14																
1-3	40	2.36	33	2.25	33	2.28	40	5.31	33	24.3	33	28.7	33	10.8				
1-3	140	2.21	140	2.12	140	2.21	140	4.69	140	35.1	140	24.0	140	16.6				
2-1	30	2.92	40	2.30	30	2.26	30	6.72	40	28.2	30	25.5	40	12.3	123	0	27	73
2-1	90	1.91	90	2.06	90	2.14	90	3.93	90	38.6	90	33.2	90	18.7				
2-1	146	2.76	146	2.05	146	2.15	146	5.66	146	40.0	146	32.6	146	19.4				
3-1	60	2.01 ^a	60	2.09	60	1.98	60	4.20 ^a	60	36.3	60	44.2	60	17.4	36	15	40	45
3-3			55	2.11					55	35.5			55	16.8				
4-1			70	2.19	70	1.61	77	6.11	70	31.3	70	68.3	70	14.3	70	17	35	48
4-1	77	2.79			77	1.69					77	63.1						
5-2			6	1.93					6	41.6			6	21.6				
6-1	37	3.47	33	2.48	37	2.56	37	8.61	33	13.3	37	6.0	33	5.4				
6-2	55	2.54	20	2.28	55	2.23	55	5.79	20	27.0	55	27.3	20	11.9				
7-1	32	2.48			32	2.35			32				32	19.5				
7-1			23	2.25	32	2.38			23	28.9	32	17.5	23	12.8				
7-1	90	2.31	96	2.30	90	2.34	90	5.31	96	24.6	90	20.0	96	20.0				
9-1			36	2.05	41	2.20			36	38.1	41	29.5	36	18.6				
10-2	83	1.94	80	1.88	83	2.00	83	3.65	80	34.3	83	42.6	80	18.3				
11-2	103	2.99	103	1.98	103	2.36	103	5.92	103	18.6	103	19.2	103	9.4				
11-3	118	1.92	129	1.93	118	2.05	118	3.71	129	40.0	118	39.2	129	20.7				
12-3	114	1.67			114	2.06					114	38.8						
13-1	140	1.97	140	2.02	140	2.07	140	3.98	140	34.9	140	38.0	140	17.3				
14-1	85	1.77	80	2.00	85	2.08	85	3.54	80	33.6	85	37.5	80	16.8				
15-4	4	2.05			4	2.07	4	(3.90)			4	37.8						
15-4	72	3.53	75	2.52	72	2.61	72	8.90	75	11.1	72	2.8	75	4.4				
16-3	80	2.31	83	2.21	80	2.29	80	5.08	83	27.7	80	23.9	83	12.5				
16-3			83	2.18					83	30.5			83	14.0				
17-4	65	1.92	60	2.09	65	2.16	65	4.01	60	31.6	65	32.0	60	15.1				
18-1	12	2.04	10	2.06	12	2.20	12	4.20	10	34.4	12	29.4	10	16.7				
18-1			10	2.10					10	36.2			10	17.2				
19-2	2	1.95	4	1.97	2	2.10	2	3.84	4	38.9	2	36.2	4	19.7				
20-2	76	2.19	79	2.19	76	2.28	76	4.80	79	27.4	76	24.5	79	12.5				
21-1	25	2.10			25	2.21					25	29.1						
21-2			112	2.29					112	22.9			112	10.0				
22-2	72	2.09	71	2.03	72	2.23	72	4.24	71	32.0	72	27.6	71	15.8				
22-2	110	1.83	110	2.07	110	2.04	110	3.79	110	31.9	110	39.9	110	15.4				
23-2	52	2.18	51	2.12	52	2.19	52	4.62	51	33.4	52	30.3	51	15.7				
24-2	5	1.76	10	2.00	5	1.98	5	3.52	10	28.5	5	43.7	10	14.3				
26-1	30	2.00	25	2.02	30	2.10	30	4.04	25	31.2	30	36.1	25	15.4				
27-1	60	3.36			60	2.49	60	(8.00)			60	10.7						
27-1	72	2.36			72	2.13	72	4.81			72	12.8						
28-2	140	2.26	140	1.92		140	1.95	140	(4.43)		140	46.1						
29-1	7	2.30			7	2.25	7	(4.99)			7	40.2						
30-2	142	2.07	143	2.21	142	2.16	142	4.57	143	20.9	142	32.5	143	9.4				
31-1			84	2.25	83	2.22			84	24.3	83	28.3	84	10.8				
32-2			85	2.33	70	2.38			85	16.5	70	17.8	85	7.0				
33-1	40	2.45	40	2.08	40	2.23	40	5.10	40	31.8	40	27.4	40	15.3				
34-1	30	1.93	27	2.18	30	2.21	30	4.15	27	28.2	30	28.9	27	12.9				
34-1	68	1.85	78	2.20	68	2.11	68	(3.76)	98	29.9	68	35.2	78	13.6				
35-3			122	2.23	94	2.28	94	3.77 ^a	122	29.1	94	24.3	122	13.0	80	1	46	53
35-3	113	1.98	113	2.63	113	2.56	113	4.60	113	22.6	113	5.6	113	6.9				
36-4	126	3.74	126	3.09	142	2.36	126	11.56	126	12.0	142	18.7	126	3.9				
36-4	142	1.92 ^a	91	2.28	142	2.40	142	4.30	91	26.1	142	16.6	91	11.5				
36-4			114	2.21					114	30.4			114	13.7				
39-1	96	4.99	47	2.18					47	30.8			47	14.1				
41-2	124	1.75	125	2.13	124	2.30	124	3.73	125	35.1	124	22.7	125	16.5				
41-2			118	2.16					118	34.1			118	15.8				
42-2	66	1.74	30	2.12	66	2.36	66	3.71	30	35.6	66	19.0	30	16.8				
43-1			68	2.13					68	33.7			68	15.8				
44-2	1	3.55	102	2.16	85	2.30			102	31.9	85	22.7	102	14.8				
45-2			1	2.93			1	10.40	1	16.7			1	5.7				
46-4			24	2.13					24	30.5			24	13.9				
46-4			62	2.15					62	33.2			62	15.4				
47-1	29	1.84	39	2.17	29	2.31	29	3.78	39	31.3	29	22.4	39	14.4				
47-1			90	2.17	103	2.33	103	4.30	90	31.2	103	21.0	90	14.3				
48-1	3	4.55																
48-2																		
49-2			70	2.26					70	27.4			70	12.1				
50-4			74	2.25					74	28.5			74	12.7				
50-4			149	2.41					149	24.2			149	10.1				
50-5	69	4.81																
51-1	28	2.17	33	2.31	28	2.40	28	4.60	33	25.6	28	16.4	33	11.1				
52-1	118	1.95	118	2.30	118	2.41	118	4.69	118	25.0	118	15.7	118	10.8				

Note: a = unreliable data.

SITE 397 PHYSICAL PROPERTIES SUMMARY CHART

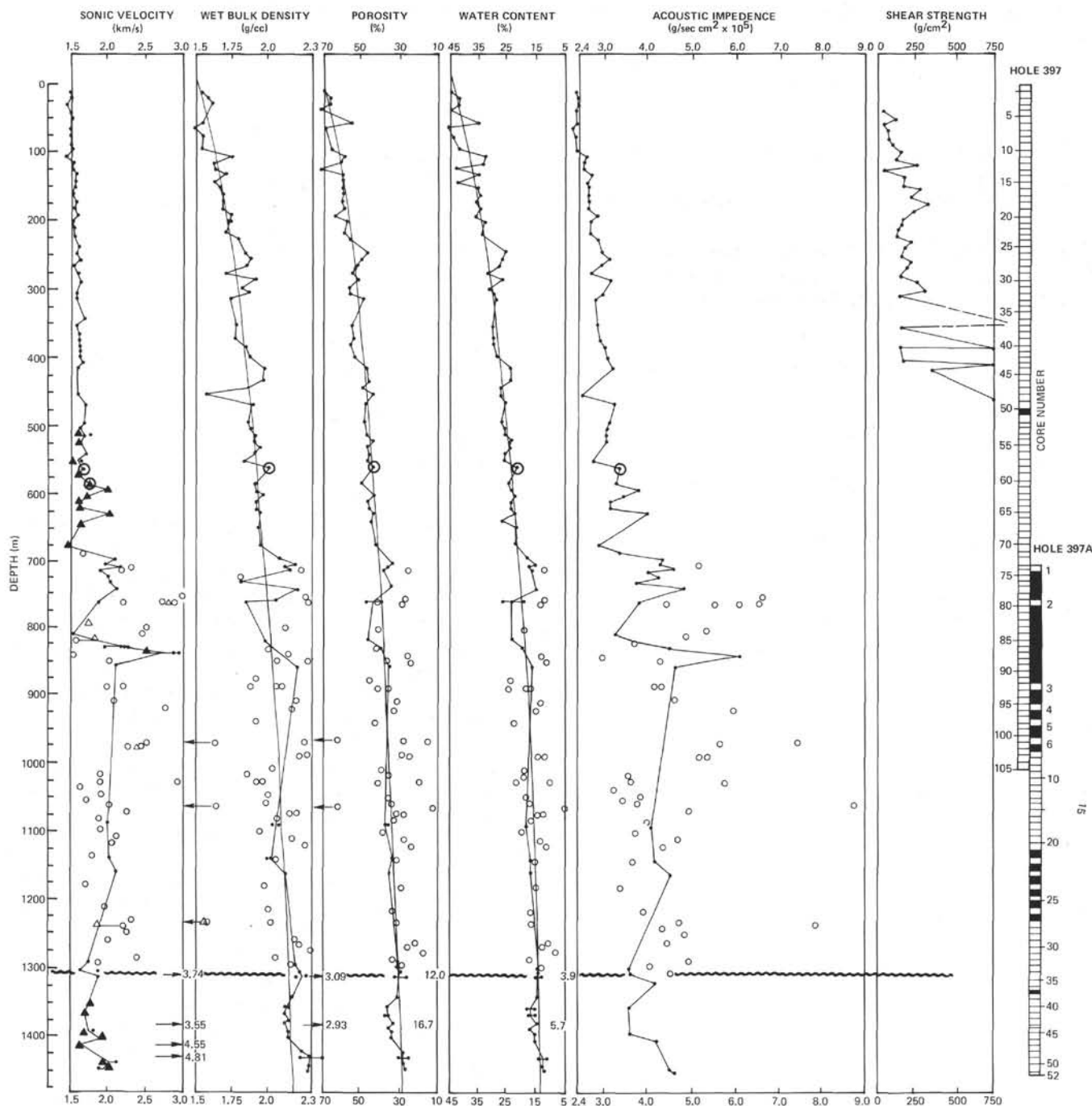


Figure 4. Site 397 physical properties summary chart.

the first slump in Core 397-57. Care was taken to distinguish "slumped" from "in-situ" material; two values from the former are circled. From the similarity of the velocities in these two materials, the mode of deposition does not appear to affect values significantly. However, scatter does seem to increase downwards in the slumped interval. This level is nearly that of the first appearance of chinks and "biscuit" structures, that is, drilling artifacts consisting of alternating hard frag-

ments and soft paste. Though only the hard fragments were measured for sound velocity, they yielded a large range of values, from a low of 1.53 km/s in Core 397-58 to a high of 2.06 km/s in Core 397-66.

In general, a non-linear increase in velocity with depth is implied by the data from the upper 686 meters. This interval is shown on an expanded scale in Figure 5, along with curves derived from laboratory measurements and from sonobuoy refraction measurements at

sea. The former was derived by Laughton (1954) from velocity in compacted globigerina ooze, and is of the form

$$V = V_o + k(h)^{1/2}$$

where

V_o = velocity at one atmosphere = 1.65 km/s

k = constant = 0.44

h = depth below sea floor in km (converted from confining pressure).

The other curve in Figure 5 was derived by Houtz (1974) from 87 seismic refraction measurements along the western North Atlantic continental rise. Rearranging his

equations relating velocity refraction time and interval thickness, the velocity/depth relationship is of the form

$$V = (V_o^2 + 2kh)^{1/2}$$

where

V_o = velocity at the sea floor = 1.58 km/s

k = constant = 1.24

h = depth below sea floor in km.

Shipboard velocities measure considerably below those at equivalent depths on the experimental curves. The curve superimposed on the data is

$$V = V_o + k(h)^{1/2}$$

where V_o is 1.51 km/s and $k = 0.24$.

Raising a deeply buried core from oceanic depths changes its physical properties. But the implication from Figure 5 is that the vertical gradient measured aboard, though lower, is similar in form to the probable "in-situ" gradient.

Bulk Physical Properties

Downhole plots of gravimetric wet bulk density, porosity, and water content are shown in Figure 4. Each dot in the upper 686 meters represents one measurement, usually one per core. Cores 397-22, 397-45, and 397-87 were sampled twice at the same depth; the close agreement in each duplication is clear. For a number of reasons discussed in the later chapter by Williams and Mountain (Part 2 of this volume), the results of the two-minute GRAPE measurements are considered less reliable and are not shown here.

In Cores 397-1 to 397-15, all three bulk properties (wet density, porosity, water content) show downward variations as great as in any interval above 693 meters. Core disturbance in these soft marl oozes was substantial but, as carbonate fluctuations suggest (see Sediment Summary Chart 1, back pocket, this volume), Pleistocene climatic variations may have played a part in causing variations in the physical properties of these sediments.

Downwards from Core 397-15, all bulk physical properties change somewhat more uniformly. Density increases from 1.55 g/cm³ in Core 397-2, to 1.97 in Core 397-71. Porosity in Core 397-2 was 69 per cent, decreasing to 41 per cent in Core 397-71. Through the same interval, water content decreases from 45 to 21 per cent.

Most values plot close to the generalized curves superimposed on the data in Figure 4. The low density, high porosity, and high water content in Core 397-37 (shown as open circles) was measured in a sample of zeolitic mud and ash. Clearly, the coarse grain size and low carbonate content of this sediment accounted for the anomalous physical properties. The very low density recorded for Core 397-49 is not considered reliable. It was the last "syringe" measurement made before the downhole transition from ooze to chalk that made the "chunk" method necessary (see Williams and Mountain, Part 2 of this volume). One sample of slumped material (Core 397-59) was measured and is circled in Figure 4. As was the case for velocity, this value is not

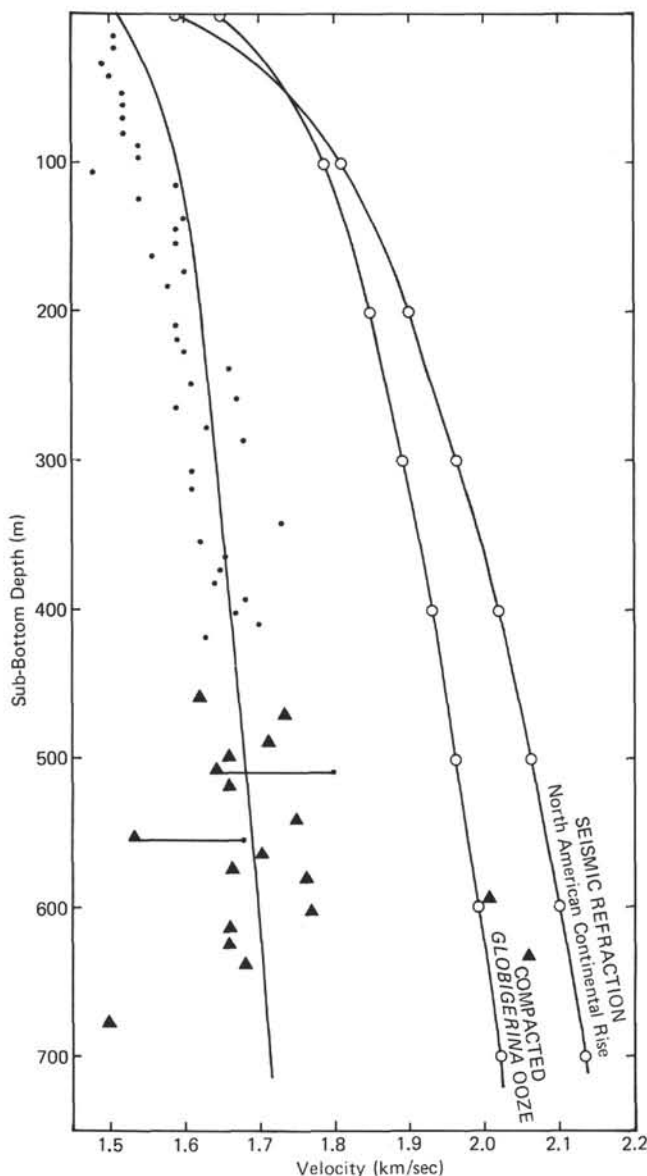


Figure 5. Expanded scale of velocity measurements at Site 397 compared with data on Globigerina oozes (Laughton, 1954) and on refraction measurements at sea (Houtz, 1974).

significantly different from those of the autochthonous sediment.

Two subtle breaks in trend are noteworthy in Figure 4. Many of the bulk properties in the first 11 cores (100 m sub-bottom) fall to the left of the smoothed curves shown. The same is true for sound velocity and density values. Though no lithologic change was detected at this depth, a brief hiatus is suggested by planktonic foraminifers. Paleomagnetic and paleontologic evidence suggests another break between Cores 25 and 26 of Hole 397 (230 m sub-bottom); this depth corresponds with another discontinuity in the physical properties. Figure 4 shows that immediately below Core 397-25, density values are locally high while porosity and water content values are low. A possible explanation for these changes in trend involves post-depositional recrystallization of carbonate. A layer of buried sediment suddenly relieved of overburden due to erosion is likely to expand. With pore spaces made available for mineral-rich pore water, recrystallization could follow, resulting in anomalous density, porosity, and water content values immediately below the erosional unconformity (however, note lack of carbonate cementation in upper 700 m of Site 397, Riech in Sediment Summary Chart 1, back pocket, this volume).

Acoustic Impedance

Acoustic impedance is defined as the product of sound velocity times wet bulk density, and is an indicator of the acoustic reflectivity of sediments. The more distinct the downward change in impedance the greater the probability that it will serve as a sound reflector. Obviously the downward trends of this parameter in Figure 4 follow those of both the velocity and density values already discussed.

Shear Strength

The location of each vane shear measurement was carefully selected in the least-disturbed interval of each of the first 48 cores. However, drilling disturbance was so severe in some intervals that any shear strength values were immediately considered suspect. Values begin at 35 g/cm² in Core 397-6, the shallowest core considered reliable for such measurements. From here downward, values increase to 316 g/cm² in Core 397-19, below which values decrease. Beneath the low value of 110 g/cm² in Core 397-24, shear strength again increases to an immeasurable value in Core 397-37 (741 g/cm³ at Core 397-49). The scattered values below this depth coincide with the ooze/chalk transition. Below Core 397-49, the sediments were too indurated to measure.

Second Interval: Cores 397-72 to 397A-34 (686 to 1306 m sub-bottom)

Velocity

The uniform downward increase of sound velocity in the upper 686 meters ends abruptly in Core 397-72. In the debris flows below this depth, values are extremely variable. As in the overlying interval, the dots in Figure 4 mark values measured parallel to bedding and

triangles mark values measured perpendicular to bedding. Values connected by horizontal lines are duplicate measurements from the same depth. Measurements of autochthonous sediments are connected downhole by a line and are marked by solid symbols. The isolated, open symbols represent measurements of allochthonous material.

At the top of this interval (710 m in Core 397-73) nannofossil chalk measures 2.13 km/s. Induration increases rapidly downwards to nannofossil limestone in Core 397-76, though velocities remain unchanged. Throughout the 620 meters of this interval, most velocities in the autochthonous sediment are considerably above the $V = 1.51 + 0.24(h)^{1/2}$ relationship that fits the overlying interval. This "in-situ" facies actually consists of various lithologies that downhole are progressively less carbonate rich. Limestones at the top give way to marly nannofossil limestones in Cores 397-85, which in turn become calcareous mudstones in Core 397A-18, and finally are mudstones in the top of Core 397A-34, immediately above the unconformity. Velocities from this facies have been grouped in Figure 6 to provide a graphical comparison with values in the displaced material.

In Figure 6, facies designations (see Arthur and von Rad, this volume) are listed at the left; because of their close lithologic similarity, facies 2 and 3 have been grouped together. Measured values of sound velocity and gravimetric wet density, porosity, and water content are displayed graphically. The heavy bars represent mean values, plus and minus one standard deviation unit. The thin lines usually extending beyond the mean value mark the full range of the highest and lowest values measured. The numbers above each bar is the number of measurements represented.

Figure 6 shows that the pelagic sediments of facies 5 have both the lowest mean velocity and the narrowest range: $2.09 \pm .21$ km/s. The highest velocity (3.53 km/s) was found in the calcareous sandstone (facies 1B) of Section 397A-15-4. As a group, facies 4B (volcaniclastic debris) registered the highest mean velocity: $2.73 \pm .41$ km/s.

Bulk Properties

All bulk physical properties in Figure 6 show patterns similar to those of velocity. Where high velocity corresponds with high densities, they correspond as well with low porosities and low water contents. The three values in the sandstone facies 1A and 1B are substantially higher than those of the other facies. Porosity and water content lithofacies 1A and 1B are likewise notably lower than the other, suggesting that secondary recrystallization has progressed further in these sediments. By contrast, mean values of porosity and water content in the pelagic facies 5 ($37.0 \pm 5.5\%$ and $18.0 \pm 3.8\%$, respectively) are higher than those of the displaced material. Perhaps one or more of the following is the cause:

- 1) The allochthonous sediments contained considerable amounts of entrained carbonate material that,

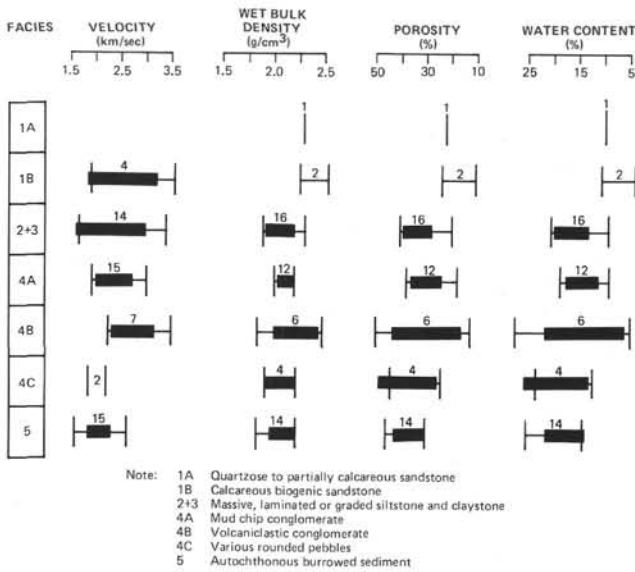


Figure 6. Bulk physical properties measurements on various sediment facies at Site 397.

after burial, supplied ions to the pore water plus carbonate grains on which recrystallization would rapidly occur.

2) Permeability in the allochthonous sediments is greater than it is in the pelagic sediments, and results in more rapid dewatering and compaction.

3) The allochthonous material is slightly older and arrived at the site more consolidated than the autochthonous sediment.

4) There are more uncemented foraminiferal chambers in facies 5 than in facies 2 to 4.

The large range of values in facies 4B might be due to varying degrees of carbonate recrystallization. For example, the sample measured in Section 397-76-3 is a semilithified, nearly pure volcaniclastic sand; porosity is 50.4 per cent. In Section 397-79-2, the sample is a poorly sorted coarse-grained volcanic sandstone with some carbonate clasts, and it shows clear evidence of calcite recrystallization; porosity measures 25.7 per cent. Other factors that could account for the heterogeneity of facies 4B include variable packing, sorting, and grain size.

Third Interval: Cores 397A-34 to 397A-52 (1306 to 1453 m sub-bottom)

The deepest of three major lithologic units at Site 397 is the Lower Cretaceous section found beneath an erosional unconformity at 1296 meters. One of the most striking aspects of these sediments is that they consist of frequent alternations of semilithified, laminated quartz mudstone and hard, massive laminate and lenses of siderite. Despite this marked heterogeneity, physical properties within the mudstones show a remarkably consistent downward pattern. This is apparent in all properties plotted in Figure 4. Values in the siderite are so very different from those of the mudstone that including them on Figure 4 would have overlapped the plots; hence, they are shown as numbers only.

Sound velocity at the top of the interval (Section 397A-1) is 1.85 km/s. Immediately across the unconformity (38 cm higher in the same section) velocity measured 1.93 km/s within Miocene mudstone facies 3. Below Core 397A-34, velocities remain low or even decrease slightly (Core 397A-46 measured 1.74 km/s) and then increase at the bottom of the hole to 2.0 km/s and higher. Anisotropy is marked in these laminated mudstones, but velocities were found both higher and lower than velocities parallel to bedding. Velocities in the siderite reached a high of 4.99 km/s in Core 397-39.

The bulk physical properties in this interval show a pattern similar to that of velocity. While values immediately below the unconformity are close to those in the overlying Miocene mudstones, they change downwards and reach a minimum density and a maximum porosity and water content near Core 397A-42. Below this, the gradients reverse to the bottom of the hole.

In Core 397A-42, density is the lowest of the mudstones, measuring 2.12 g/cm³; Core 397A-52 measures 2.30 g/cm³. Porosity decreases from 34 to 25 per cent in the same interval, and water content decreases from 16 to 11 per cent. By contrast, the values in a siderite laminae of Core 397A-36 are 3.09 g/cm³, 12 and 4 per cent (respectively).

From the above patterns in the Lower Cretaceous section, the following conclusions are drawn. Extrapolating the generalized water content curve downwards from the nearly continuous Neogene section above 686 meters, places it very close to the values measured at the bottom of Hole 397A. Barring the possible effects of secondary recrystallization in the mudstones, this may indicate that the Lower Cretaceous section was at one time buried to a depth comparable to that of today. If so, it is entirely possible that removal of the 1300 meters or more of overburden sometime prior to early Miocene allowed pore spaces to reopen. The local maximum of water content near Core 397A-42 could represent an interval that has not returned to an equilibrium profile. Perhaps this second compaction is hampered by the fact that relatively impermeable siderite laminae formed during the process of relaxing spaces and now inhibit the vertical migration of pore water.

GEOCHEMISTRY

Introduction

A major part of the shipboard geochemical studies on Leg 47 was aimed at evaluating two new rapid methods for monitoring sedimentary hydrocarbon occurrence in time to effect drilling decisions. The two new methods were the gas chromatography measurement of trace C₂ to C₃ hydrocarbons in core liner gas pockets (Whelan, this volume), and a pyrolysis-fluorescence technique, described as a tool for evaluating the generative potential of a sediment and/or identifying migrated heavy hydrocarbons (Heacock and Hood, 1970).

In addition, organic carbon analysis, carbonate content (reported with core data) and organic petrographic (microscopy) studies were conducted on board *Glomar Challenger*. Shipboard pore water analyses were also

made and are discussed in this section together with more detailed shore-based studies by V. Marchig (BGR, Hannover).

More detailed organic geochemical analyses are reported from individual shore-based laboratories later in this volume (Erdman et al.; Deroo et al.; Baker et al.; Kendrick et al.; Whelan; Pearson et al.; Cornford et al.; Johnson et al.; all, this volume) along with a synthesis of all organic geochemical results (Cornford, this volume). The relationship of sediment maturity, source rock potential, and hydrocarbon migration and entrapment in this passive margin setting is discussed in the Sedimentology Synthesis (Arthur et al., this volume).

Organic Geochemistry

C₁ to C₅ Hydrocarbon Analysis

Correlation of the proportions of C₁ to C₅ hydrocarbons in Holes 397 and 397A with seismic, sedimentary, and biostratigraphic data suggests that they may be a useful early indicator of lithologic changes encountered during drilling (see Sediment Summary Chart 1, back pocket, this volume).

Holes 397 and 397A had core liner gas pockets starting at about 80 meters and continuing to 1450 meters, at which depth drilling was terminated. The gas from 80 to 124 meters proved to be mainly air, nitrogen, and carbon dioxide. The odor of H₂S was detected in cores from 9 to 151 meters. At 196 meters, methane became the major hydrocarbon component of the evolved gas (Sediment Summary Chart 1, this volume), although the amounts varied widely from one gas pocket to another. Values of $\delta^{13}\text{C}$ of -60 to -80 indicate that all of the methane was biogenic (Whelan, this volume).

A newly installed gas chromatograph (CG) made possible the shipboard monitoring of exact trace amounts of C₂ to C₅ hydrocarbons and their isomers in these gas samples. This equipment is nearly 1000 times more sensitive for hydrocarbon analysis than the equipment used on previous legs. A similar system was first used to analyze gases from 300 Black Sea gas samples (Leg 42B), which had been collected in Vacutainers and shipped to Woods Hole Oceanographic Institution for C₂ to C₅ hydrocarbon analysis. The most striking feature of the Black Sea results was the way in which the detailed shapes of the logs of the C₂, C₃, C₄, and C₅ hydrocarbon curves were "in phase" throughout Holes 379, 380, 380A, and 381 (Hunt and Whelan, 1978). Similar results were found in top and bottom fine-grained sediment sections of Holes 397 and 397A (see Sediment Summary Chart 1, back pocket, this volume).

Apparently, the C₂ to C₅ hydrocarbons form by some low-temperature (<50°C) process, either staying in place or (more likely) migrating slowly upward together with interstitial water through fine-grained sediments. The exact nature of the generation process is unknown. However, the most reasonable interpretation of the existing data is that the process involved a slow chemical evolution from material associated with bacteria or their remains (Whelan, this volume).

Irrespective of how the C₂ to C₅ hydrocarbons form, the "in phase" behavior correlates remarkably well with lithology. Thus, in fine-grained sediments (from 190 to 350 m, 420 to 530 m, and generally from 840 to 1453 m), the C₂ to C₅ curves travel "in phase" through the fine-grained sediments (Sediment Summary Chart 1, back pocket, this volume), even though the proportions of C₂ to C₅ gases vary widely. In lithostratigraphic Units 3 and 4, containing porous layers of sand and volcanoclastics, especially between 540 and 830 meters, C₁ and C₂ levels generally remains unchanged, while the C₃/C₁, C₄/C₁, and C₅/C₁ ratio curves decrease irregularly. Preferential horizontal movement of the lighter C₁ and C₂ gases (called "diffusion" by petroleum geologists) into these more porous layers could cause such a fractionation.

Shore-based sediment C₁ to C₇ hydrocarbon analyses show substantial differences between lithostratigraphic Units 1 and 2 (0 to 540 m, primarily marly siliceous nanofossil ooze) and the lower Miocene pebbly mudstones of Unit 4. The upper unit shows low levels of C₁-C₅ and limited distribution of C₆ and C₇ compounds. The lower Miocene Unit 4 contains higher levels of C₁-C₅ and a wide spectrum of C₆ and C₇ compounds similar to results at other DSDP sites where organic-rich sediments were encountered. These compounds form from *in-situ* low-temperature chemical reactions similar to those occurring in immature petroleum source rocks (Hunt, 1975).

Organic Carbon

Fifty-seven organic carbon analyses were conducted on board ship as part of a continuous hydrocarbon safety monitoring program. An additional 87 samples were analyzed as part of the routine DSDP shore-based program. The trends established by the shipboard work are essentially confirmed by the shore-based studies, although the absolute values of the shipboard analyses, particularly those of the organic lean sediments (< 0.5% C_{org}), are consistently too high (Table 7). This error could be eliminated by having sediment standards (measured by the DSDP shore-based laboratory) available on board ship. To allow comparison with past and future legs, only the DSDP shore-based data are used in the rest of this discussion.

The downhole variation of organic carbon (see Sediment Summary Chart 1, back pocket, this volume) conforms to the five major lithostratigraphic units (Table 7).

Lithologic Unit 1 is characterized by relatively high (mean value 0.45% C_{org}) and fluctuating carbon values (see Sediment Chart, back pocket, this volume). Such high values in the Pliocene/Pleistocene may be indicative of high bioproductivity in an upwelling area, or a strongly fluctuating terrestrial input.

Lithologic Units 2 and 3 are characterized by low organic carbon values (mean value 0.17% C_{org}) and more typical of previously drilled hemipelagic deep-sea sediments (Figure 7). Lithologic Unit 4 is composed of allochthonous sediments with generally higher C_{org} values (1.39% mean). Sands in this interval have lowest organic values. No highly significant variation of

TABLE 7
Distribution of Mean C_{org} Values in the Five Lithostratigraphic Units of DSDP Site 397 (shipboard and shore-based data)

Lithostratigraphic Unit	Time-Rock Unit	DSDP	Depth (m) of C_{org} Samples	Shore-Based Mean C_{org} (%)	Data Stand. Dev.	N ^a	Ship-board Mean	Data Stand. Dev.	N ^a
1	Pliocene-Recent	397-1 to 397-33	1-313	0.452	0.250	31	0.89	0.71	7
2 and 3	Middle Miocene to Pliocene	397-33 to 397-19	313-752	0.174	0.053	22	0.46	0.15	17
4	Middle-early Miocene	397-87 to 397A-32	752-1297	1.391	1.086	20	1.96	1.29	24
			F1 ^b	—	—	—	0.22	—	3
			F2	0.921	—	1	0.61	—	3
			F3	1.842	1.095	9	2.56	1.10	11
			F4	1.422	0.921	5	2.04	1.06	5
5	Cretaceous	397A-34 to 397A-52	1309-1453	0.559	0.150	18	0.98	0.41	7

^aN = number of determinations.

^bF1 to F5 are lithofacies found in Unit 4: F1 = Coarse-grained calcareous sand; F2 = Lighter green, coarser-grained marl chalk; F3 = Darker green, finer-grained marl chalk; F4 = Clastic gravity flow matrix, flows contain Facies 2 and 3; F5 = Blue-green, fine-grained hemipelagic chalk (see also Lithostratigraphy section and Arthur and von Rad, this volume).

organic carbon content could be found with sediment types F1 to F5 within this unit (Table 7). Values varied widely for any one sediment type. But both the shipboard and shorebased data (Table 7) indicate that the mean organic carbon content increases in the order $F1 < F5 < F2 < F4 < F3$, indicating that in the allochthonous sediments, highest values occur in the fine-grained sediments.

Lithologic Unit 5, the Hauterivian shales with siderite lamellae, shows a mean organic carbon value of 0.56 per cent. There is some indication of an increase with depth. Not included in this mean value is a thin black layer from Sample 397A-47-1, 36 cm?, which is presumed to

be sapropel fragment based on its organic carbon content of 41.5 ± 1.4 per cent (measured at Woods Hole).

Pyrolysis-Fluorescence

This technique provides information on the hydrocarbon generative potential of the sediments by measuring the fluorescent intensity of the lipid soluble sediment distillate. Heacock and Hood (1970) suggest that these data, when taken with organic carbon content, can be used to determine whether a sediment has a hydrocarbon generative potential or contains migrated heavy hydrocarbons. The method has the advantage of speed (about 10 min per analysis) and sensitivity (0.1 g of sediment is required).

Since this was the first time that the pyrolysis-fluorescence technique had been used on board the *Challenger*, a brief outline of the method may be helpful. About 0.1 g of sediment was placed in a "Pyrex" test tube and heated over a colorless gas (propane) flame until red hot (about 20 s). The evolved pyrolysis products condensed on the cool upper parts of the tube wall. After cooling, the pyrolysis products were dissolved in trichloroethane and the solvent decanted into a clean tube. Fluorescence was measured with a Turner Fluorometer after the solution was diluted to give a maximum fluorescence per 3 ml of solvent per 0.1 g of sediment. In spite of the crudeness of the method, measurements were fairly reproducible: a background level of 2 fluorescence units was generally obtained.

Because this was part of the safety monitoring program, the samples submitted for analyses were not representative, but were those felt to have the greatest source rock or reservoir characteristics.

The results of pyrolysis/fluorescence analyses are plotted against shipboard organic carbon values in Figure 8, together with data from other DSDP holes by Hood and co-workers (unpublished results).

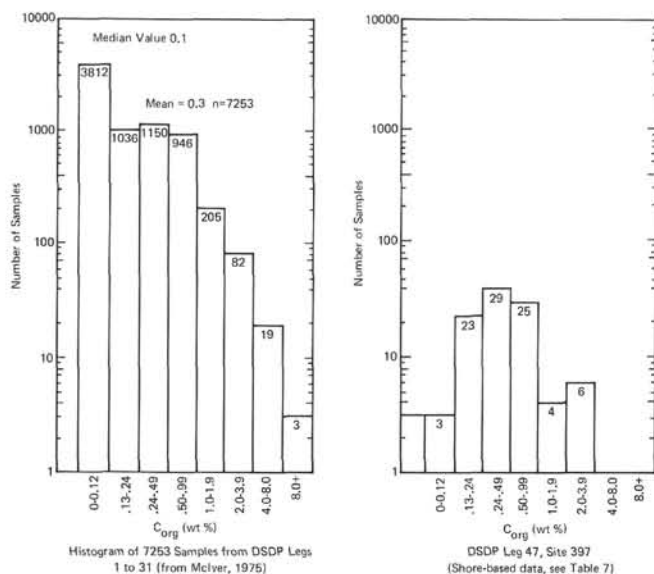


Figure 7. A comparison of Leg 47A organic carbon values with previous DSDP legs (McIver, 1975, unpublished results).

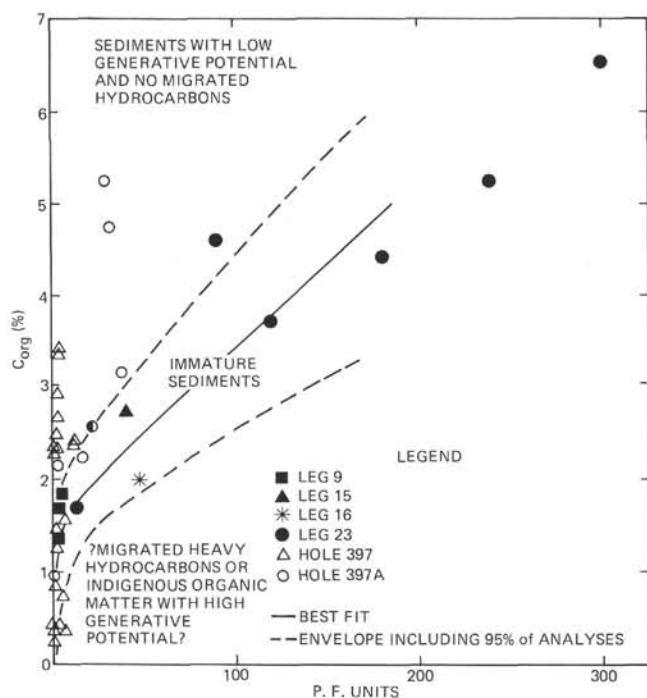


Figure 8. Plot of organic matter versus pyrolysis/fluorescence units for Holes 397 and 397A and for previous DSDP sites (Hood *et al.*, unpublished results).

For interpretation of the data, three areas can be defined in Figure 8 with regard to the presence and/or generative potential of heavy hydrocarbons (Heacock and Hood, 1970). The central area bracketed by the dashed lines may represent an area of immature but potential petroleum-generating sediments. Within this area fall the small number of DSDP samples analyzed previously. Above this area, little fluorescent distillate is produced from a high carbon content. This represents a "safe" area where neither active generation nor accumulation is indicated. Data points falling in the area below the dashed line suggest that the sediments contain migrated heavy hydrocarbons or indigenous organic matter with a high generative potential.

The pyrolysis-fluorescence values obtained at Site 397 were generally very low, rarely increasing above the background of the instrument (Figure 8). Relatively low values were obtained even for the organic-rich sediments. In Figure 8, the data points from Site 397 plot-out in the upper left portion of the diagram, close to the organic carbon axis. The absolute values of the shipboard organic carbon data may be somewhat too high (Table 7); hence, the points may need adjusting to a lower level. Even with such an adjustment, the data points fall in the region of the diagram which indicates a low generative potential and the absence of migrated heavy hydrocarbons. These results point to a low potential drilling hazard from reservoir hydrocarbons.

Organic Petrography

Reflected and transmitted light studies were undertaken on board the ship. The results of the relatively few

shipboard samples must be viewed against the detailed shore-based studies described later in this volume. From the shipboard studies, it was established that both the allochthonous and autochthonous Miocene sediments contained appreciable coaly particles such as vitrinite-humite and inertinite, indicating a higher plant (or terrestrial) input. The Hauterivian (Cretaceous) sediments contained vitrinite and inertinite particles almost exclusively, with spores being a repetitive minor component. This indicates a major higher plant (terrestrial) input to the Cretaceous organic matter (see also Arthur *et al.*, this volume, table 3). The high vitrinite content of the sediments is in agreement with the low hydrocarbon-generating potential inferred from the pyrolysis-fluorescence results.

These findings have been essentially confirmed and extended by shore-based studies (organic geochemistry shore-based reports, this volume), although higher estimates of the content of amorphous or sapropelic kerogen have been made for some of the allochthonous Miocene sediments, based on microscopy, pyrolysis, and hydrocarbon extract analysis (Cornford, this volume).

Inorganic Geochemistry

Shipboard Studies

Pore water analyses conducted on board the *Challenger* are given in Table 8. Alkalinity shows a maximum at 90 meters, with a corresponding minimum in Ca^{++} values. The trends are in agreement with those of rapidly deposited deep-sea calcareous biogenic sediments (Sayles and Manheim, 1975). Chlorinity shows a small but significant increase with depth. The observed increase is somewhat unusual, but has been found either above evaporites (not possible here) or where extensive diagenesis has occurred due to mineral hydration (F. Sayles, private communication). The sediment magnesium values must be viewed cautiously because the magnesium value for sea water (wt. magnesium/wt. of chloride), calculated from the data in Table 8, is high (0.082 as compared to the standard value of 0.067). Assuming the Mg^{++} values are internally consistent, there is a marked depletion of Mg^{++} below 150 meters, as expected for sediments of the type encountered here (Sayles and Manheim, 1975). The trend of reduction of alkalinity with depth (Table 8) has been noted in previously drilled DSDP pelagic sections (Gieskes *et al.*, 1975).

Shore-Based Studies

Eleven samples from Cores 397-2 to 397-61 were analyzed by V. Marchig (Hannover) with X-ray spectroscopy after dialyzing them to remove soluble salts. Additionally, the carbonate content was determined by means of volumetric CO_2 measurement (Scheibler method). The analyses of X-ray spectroscopy are given in Table 9; the analyses of carbonate contents in Figure 9. The samples contain high amounts of carbonate (38 to 76%; mean value of 57% CaCO_3). We could not see trends of carbonate enrichment in any direction.

TABLE 8
Summary of Shipboard Pore Water Analysis

Sample (Interval in cm)	Approximate Sub-Bottom Depth (m)	Carbonate ^a (%)	pH ^b	Alkalinity (meq/kg)	Salinity (‰) ^c	Ca ²⁺ (mmoles/liter)	Mg ²⁺ (mmoles/liter)	Cl ⁻ (‰)
Site surface sea water	—	—	8.4	2.35	36.6	10.96	67.83	20.2
2-3, 144-150	15	56.3	7.6	7.50	34.9	8.04	60.95	19.2
6-2, 144-150	50	45.7	7.6	17.70	33.0	3.52	7.44	19.5
10-5, 144-150	90	59.2	7.5	18.65	33.0	4.70	11.81	19.1
16-5, 144-150	150	37.6	7.6	15.73	32.7	5.77	34.79	19.5
21-3, 144-150	195	50.8	7.4	13.37	32.4	7.67	33.44	19.7
27-3, 144-150	250	73.5	7.6	7.12	32.7	6.59	31.23	20.2
32-3, 144-150	300	61.6	7.7	5.41	33.0	6.47	32.24	20.5
39-4, 140-150	365	75.6	7.6	4.59	33.3	8.35	32.28	20.5
44-3, 1-10	410	66.2	7.8	2.33	33.6	9.25	32.13	20.5
52-5, 140-150	500	49.7	8.1	1.22	34.4	11.72	32.61	21.1
61-3, 140-150	585	54.8	8.3	0.77	35.5	17.12	34.06	21.7
66-3, 140-150	630	nd	8.4	0.28	35.2	23.26	26.48	21.3

^aAnalysis on sediments by Marchig BGR, Hannover.

^bpH calculated from initial reading of alkalinity titration.

^cSalinity calculated from chlorinity.

From the similarities of changes with depth by contents of different elements, we concluded that the greatest part of Sr is associated with carbonate, while Si, Ti, Al, Na, K, Mg, Fe, La, V, Zn, Rb, Zr, and maybe Y, Cr, Ba, Sc, Ni, Co, Nb, and Ce correlate negatively with carbonate. The Mn, S, P, Cu, Pb, and Th variation appears independent of the carbonate content; perhaps they are distributed between different phases of the sediment, or they redistribute with diagenesis.

Sr was calculated to CaCO₃ as 100 per cent; all elements, the contents of which are more or less parallel to noncarbonate, are calculated to noncarbonate as 100 per cent. The results are given in Table 10. In the lowermost line of Table 10, mean values for each element are given. The approximate chemical compositions of carbonate and noncarbonate are derived from these mean value calculations, to facilitate comparison with other types of sediments. Carbonate, with a mean value of 0.23 per cent, shows predictable Sr content for marine

carbonates which are not under direct influence of shallow water.

Most of the mean values for the element contents in the noncarbonate are between those for deep-sea clays and clayey silts (Turekian and Wedepohl, 1961). These findings were not surprising because Site 397 (situated on the continental slope) is between areas of shallow-water clayey silts and deep-sea clays.

The elements K, Mg, V, Zr, Cr, and Nb generally are enriched in our samples, when compared with clayey silts and with deep-sea clays. Possibly, heavy minerals have caused the enrichment of these elements.

A qualitative estimate of the amounts of amorphous silica in the samples with the ratio SiO₂/TiO₂ results in a curve (Figure 9) which must be compared with microscopic analyses. Based on these calculations, samples from Cores 397-2, 397-6, 397-16, and 397-21 contain more amorphous silica than the other analyzed samples.

TABLE 9
Neutron Activation Analysis (NAA) of Cu and Mn in Pore Waters and Major and Minor Elements of the Sediments From Site 397

Core	Pore Water (NAA)		Sediments ^a (XRF)														
	Cu (ppb)	Mn (ppb)	MnO (%)	Fe ₂ O ₃ (%)	TiO ₂ (%)	CaO (%)	K ₂ O (%)	SO ₃ (%)	P ₂ O ₅ (%)	SiO ₂ (%)	Al ₂ O ₃ (%)	MgO (%)	Na ₂ O (%)	Ignit. loss (%)	Sr (ppm)	Rb (ppm)	Nb (ppm)
2	18	249	0.040	2.44	0.331	31.0	1.45	0.32	0.14	22.5	6.67	1.72	1.52	30.6	1156	52	15
6	52	24	0.049	2.95	0.403	25.5	1.77	0.43	0.13	28.7	7.93	2.07	1.63	26.4	989	64	14
10	33	42	0.054	2.29	0.338	33.3	1.48	0.26	0.13	20.2	6.77	1.88	1.08	31.4	1320	59	7
16	22	38	0.052	3.41	0.466	22.8	1.97	0.58	0.12	33.6	9.12	2.01	1.47	23.1	890	76	15
21	31	42	0.032	2.16	0.312	30.3	1.16	0.25	0.13	25.2	6.28	1.30	1.18	30.1	1212	46	13
27	31	35	0.048	1.63	0.213	40.4	0.83	0.40	0.15	12.5	4.25	1.22	0.70	36.1	1566	34	0
32	36	42	0.055	2.09	0.330	36.1	1.24	0.27	0.16	17.4	6.09	1.45	0.89	33.3	1398	47	4
39	15	27	0.051	1.61	0.224	40.8	0.87	0.28	0.14	12.5	4.23	1.02	0.76	36.3	1561	32	2
44	68	60	0.039	1.96	0.270	38.3	1.08	0.29	0.13	15.5	5.32	1.14	0.69	34.3	1515	40	5
52	65	54	0.089	3.27	0.365	31.8	1.49	0.16	0.16	21.7	7.65	1.43	0.82	30.6	1253	64	7
61	51	67	0.025	2.76	0.378	30.6	1.45	0.31	0.22	24.4	7.99	1.29	0.83	29.2	1190	67	7

Note: For details of sample depth, etc., see Table 8. Analyses by V. Marchig (BGR, Hannover).

^aSediment residues from pressed out pore waters.

In addition to chemical analyses of sediment samples, the pore waters were analyzed for Cu and Mn by means of neutron activation analysis. The results, given in Figure 9, show that Cu and Mn in pore waters are enriched in the samples from Cores 397-44, 397-52, and 397-61. That could be the result of initial diagenetic changes, although the microscopically visible diagenesis starts deeper at Site 397 (see Riech, this volume). The Cu and Mn content also could be altered by changes in mineral composition.

In addition to the enrichment of Cu and Mn, there is a strong enrichment of Mn in the pore water in Core 397-2. Such a strong enrichment of Mn can be explained only by mobilization after burial. It would be of great interest in the study of the diagenetic behavior of Mn to know if this strong enrichment is local or can be traced upward to the sediment/sea water interface.

BIOSTRATIGRAPHY

Nannoplankton

The following age determinations and zonal boundaries are based upon smear slides and SEM investigations. Graphic representation of the biostratigraphy of Holes 397 and 397A is shown in Figure 10. For a more detailed presentation and interpretation of the nannoplankton data see Čepék and Wind; Wind and Čepék; Mazzei et al. (all, this volume).

Pleistocene

Pleistocene sediments were recovered in the first 15 cores (0.0 to 136.5 m). The interval from Core 397-1 through Sample 397-2-5, 41 cm (0.0 to 15.41 m) is placed in the *Emiliana huxleyi* Zone (NN 21), on the basis of SEM identification of the first occurrence of the name species in Sample 397-2-5, 41 cm. Samples 397-2-6, 47 cm through 397-4-2, 41 cm (16.9-29.4 m) are placed in the *Gephyrocapsa oceanica* Zone (NN 20), defined as the interval from the last occurrence of *Pseudoemiliana lacunosa* to the first occurrence of *Emiliana huxleyi*.

The presence of *Pseudoemiliana lacunosa* and the absence of *Discoaster brouweri* in Samples 397-4-3, 41

cm through 397-15-3, 100 cm (31.41 to 136.5 m) place the contained interval in the *P. lacunosa* Zone (NN 19).

The last occurrence of *Discoaster brouweri* is considered to be coincident with the Pliocene/Pleistocene boundary. We place the NN 18/NN 19 boundary above the highest continuous occurrence of *D. brouweri* (at Sample 397-15-4, 41 cm; 137 m sub-bottom). No specimens of *D. brouweri* were observed in Sample 397-15-3, 100 cm. The occurrence of Miocene and Pliocene discoasters in Sample 397-15-2, 100 cm suggests that the presence of *D. brouweri* in this sample is the result of reworking. Approximately one-half of the samples studied in the Pleistocene section were found to contain reworked Tertiary and Cretaceous material.

Pliocene

Samples 397-15-4, 41 cm through 397-23-3, 35 cm (137.41 to 211.85 m) are placed in the three zones constituting the upper Pliocene: *Discoaster brouweri* Zone (NN 18), *D. pentaradiatus* Zone (NN 17), and *D. surculus* Zone (NN 16). Samples 397-15-4, 41 cm through 397-19-3, 120 cm (137.41 to 174.7 m) contain *D. brouweri* and *Coccolithus doronicoides*, which characterize the NN 18 Zone. Samples 397-19-4, 15 cm through 397-19, CC (175.15 to 180 m) contain the NN 17 nannoflora including *D. pentaradiatus*. Samples 397-20-1, 10 cm through 397-23-3, 35 cm (180.1 to 211.85 m) are placed in the NN 16 Zone. The interval includes the highest occurrence of *D. surculus*. Small specimens of *Reticulofenestra pseudoumbilica* are present in samples from the lower portion of this interval. The last occurrence of *R. pseudoumbilica* is used to mark the top of the NN 15 Zone. In this paper, we identify the top of NN 15 as the highest occurrence of large specimens of *R. pseudoumbilica*. The stratigraphic interval represented by each of the three Pliocene zones compares well with the relative thickness of the respective zones illustrated by Martini (1971).

An apparently complete record of early Pliocene sedimentation is contained in Cores 397-23 through 397-42 (213.41 to 398.5 m). Samples 397-23-4, 41 cm through 397-23, CC (213.41 to 218 m) are placed in the *R. pseudoumbilica* Zone. This zone represents the inter-

TABLE 9 - Continued

Sediments ^a (XRF)														
Zr (ppm)	Y (ppm)	Pb (ppm)	Th (ppm)	Ni (ppm)	Co (ppm)	Mn (ppm)	V (ppm)	Zn (ppm)	Cu (ppm)	Cr (ppm)	Ce (ppm)	La (ppm)	Ba (ppm)	Sc (ppm)
116	19	15	2	52	3	339	63	46	9	44	54	22	432	6
128	28	15	0	64	6	405	69	67	18	60	49	31	526	11
92	20	10	9	50	0	449	63	50	21	43	25	19	526	0
166	23	15	0	49	6	429	73	60	13	63	55	32	522	9
98	17	9	4	57	2	264	53	49	21	47	36	19	404	5
67	16	12	3	38	0	414	44	24	8	39	43	8	282	0
76	14	11	1	46	0	463	63	33	17	48	40	21	356	0
63	13	22	0	42	0	442	43	21	10	35	25	16	222	0
72	11	13	2	41	0	318	48	29	10	45	38	16	230	3
90	17	17	0	51	5	731	63	49	23	66	50	25	272	2
117	23	13	4	46	2	209	76	47	8	70	57	31	235	11

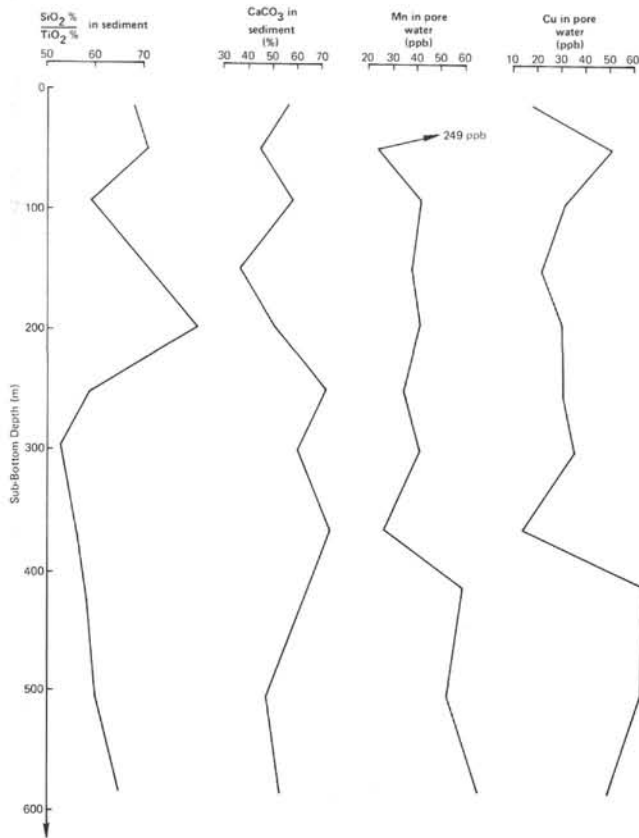


Figure 9. Carbonate analyses of $\text{SiO}_2\text{-TiO}_2$ ratios and Mn and Cu in pore water at Site 397.

val from the last occurrence of *Ceratolithus tricoraniculatus* to the last occurrence of *R. pseudoumbilica*. Zone NN 14, defined as the interval from the first occurrence of *Discoaster asymmetricus* to the last occurrence of *C. tricoraniculatus*, is represented in Cores 397-24, CC through 397-35, CC (227.5 to 332.0 m).

Samples 397-36-1, 41 cm through 397-42, CC (332.4 to 398.5) are placed in Zones NN 13 and NN 12. The division of these two zones is defined by the first occurrence of *Ceratolithus rugosus*. The inability to differentiate between these two zones is due to the extremely poor representation of *Ceratolithus*.

Miocene (Hole 397)

Samples 397-43-2, 20 cm through 397-56, CC (400.3 to 541 m) are placed in Zone NN 11, based upon the presence of *Discoaster quinqueramus*. Many of the well-preserved nannoplankton floras in Samples 397-57-1, 35 cm through 397-60-2, 21 cm (541.35 to 571.2 m) yield anomalously old ages when compared with underlying samples; this interval is regarded as being constituted largely of slumped material. Allochthonous units within this interval belong to the *Discoaster calcaris* Zone (NN 10), defined as the interval from the last occurrence of *Discoaster hamatus* to the first occurrence of *D. quin-*

queramus. Allochthonous sediments yield nannofloras containing rare specimens of *Catinaster* and are placed in the upper part of the NN 9 Zone and the NN 8 Zone.

The presence of *Discoaster hamatus*, *D. bollii*, and *D. pentaradiatus* places the interval from Samples 397-61-2, 42 cm through 397-72, CC (589.92 to 693 m) in the upper part of the NN 9 Zone. The absence of nannofloras of Zones NN 8 and the early part of NN 9 (between Cores 397-72 and 397-73) indicates the presence of a hiatus at 693 meters sub-bottom depth. Samples 397-73-1, 83 cm through 75-2, 34 cm (693.83 to 713.84 m) contain *Discoaster kugleri*, but not specimens of *Ceratolithus coalitus*; therefore, this interval is attributable to the *D. kugleri* Zone (NN 7).

The absence of *Sphenolithus heteromorphus* and *Discoaster kugleri* in Samples 397-75, CC through 397-77-3, 20 cm (721.5 to 734.2 m) suggests placement of this interval in the *Discoaster exilis* Zone (NN 6). Samples 397-77, CC through 397-80-1, 141 cm (740.5 to 760.91 m) are placed in the *Sphenolithus heteromorphus* Zone (NN 5), based on the presence of the name species and the absence of *Helicopontosphaera ampliapertura*.

Age determination for the interval from Sample 397-80-2, 41 cm through the end of the section cored at Hole 397 (761.41 to 997 m) is based upon the concurrence of *Helicopontosphaera ampliapertura* and *Sphenolithus heteromorphus*, which suggests the placement of this interval in the *H. ampliapertura* Zone (NN 4). *Sphenolithus belemnos*, whose extinction datum marks the close of the NN 3 Zone, apparently was not present in the area of Hole 397.

Miocene (Hole 397A)

Samples from Cores 1 and 2 were not analyzed.

Cores 397A-3 through Sample 397-A-16-5, 31 cm (884.0 to 1074.3 m) are considered to be NN 4 and, in part, a duplication of the section at Hole 397. The interval from Samples 397-A-16, CC through 397A-21-3, 47 cm (1077.5 to 1118.97 m) is placed in the *Sphenolithus belemnos* Zone (NN 3), based on the presence of *Helicopontosphaera ampliapertura*, *Discoaster druggi*, the occasional occurrence of *Sphenolithus belemnos*, and the absence of *Triquetrorhabdulus carinatus*. Samples 397A-21, CC through 397A-34-1, 70 cm (1134.0 to 1296.70 m) are placed in the *Discoaster druggi* Zone (NN 2). Samples from this, the oldest Tertiary zone encountered, contain *Triquetrorhabdulus carinatus*, *Helicopontosphaera kamptneri*, and *D. druggi*.

Cretaceous

The deepest sample containing Tertiary nannoplankton is 397A-34-1, 70 cm. Sample 397A-34-1, 75 cm is barren. The highest fossiliferous sample of the long Cretaceous section is in Sample 397A-34-1, 102 cm. The shallowest sample yielding sufficient numbers of specimens for precise age determination is in Sample 397A-34-1, 109 cm.

Many samples contain excellently preserved, diverse nannoplankton populations. A thorough search of the best-preserved and most productive samples has demonstrated the presence of more than 60 species, many of which are new forms, or species previously reported from only one or two sections (see Wind and Čeppek, this volume).

A significant portion of the calcareous nannoflora are holococcoliths (forms constructed of 0.1 μm calcite crystals). With the exception of *Lucianorhabdus cayeuxi* and accompanying tetraliths *Tetralithus obscuris* and *T. ovalis*, members of this lineage are only rarely preserved in Mesozoic sediments. The oldest related form previously reported, *Lucianorhabdus compactus* (Verbeek) Prins and Sissingh, is Cenomanian.

The presence of *Cruciellipsis cuvillieri* and *Speetonia colligata* in Samples 397A-52, CC through 397A-34-1, 109 cm indicates that the recovered interval is not younger than the early part of the late Hauterivian. The presence of *Nannoconus kamptneri* through to the base of the section recovered indicates that the deepest samples are late Hauterivian. Samples as deep as 397A-48, CC contain *Nannoconus bucheri* and are, therefore, younger than the earliest Hauterivian.

Rare specimens of *Lithraphidites bollii* (?) were observed in only one sample studied. However, blocky-stemmed rhabdolites common in several samples (especially in Cores 46 through 48) may represent well-preserved specimens which when modified by dissolution and reprecipitation are identifiable as *L. bollii*.

One form found in Samples 397A-46-3, 58 cm and 397A-47, CC appears to be related to *Arkhangelskiella primitiva*, which has been identified from only one sample identified as upper Hauterivian by Thierstein (1973).

Lithraphidites bollii is discounted as a diagnostic marker because of the strong suggestion that its range is largely dependent upon preservational effects. The Cretaceous sediments recovered at Hole 397A are placed, therefore, within the combined *Calcicalathina oblongata* and *Lithraphidites bollii* zones of Thierstein (1971, 1973).

Using the zonation proposed by Roth (1973), the section falls within the *Cruciellipsis cuvillieri* Zone, defined as the interval from the last occurrence of *Tubodiscus jurapelagicus* to the last occurrence of *C. cuvillieri*. The former species was not observed in any sample.

Planktonic Foraminifers

Factors Disturbing the Biostratigraphic Signal

Several factors controlled by sedimentary processes and/or by the evolution of water masses in the eastern North Atlantic affect the distribution of planktonic foraminiferal assemblages as recorded in the stratigraphic succession continuously cored at Site 397. They are considered "noise" which is superimposed on the biostratigraphic signal, i.e., on the normal evolution of foraminiferal assemblages, as a function of time. These factors will be commented upon briefly below, before discussion of the biochronology of the cored sections.

TABLE 10
X-ray Fluorescence Analysis Results for Site 397 Samples, Recalculated With Carbonates Removed

Core	Depth in Core (cm)	Carbonate (%)	Sr in Carbonate (%)	Noncarbonate (%)	SiO ₂ (%)	Al ₂ O ₃ (%)	Na ₂ O (%)	K ₂ O (%)	MgO (%)	Fe ₂ O ₃ (%)	La (ppm)	V (ppm)	Zn (ppm)	Rb (ppm)	Zr (ppm)	Y (ppm)	Cr (ppm)	Ba (ppm)	Sc (ppm)	Ni (ppm)	Co (ppm)	Nb (ppm)	Ce (ppm)	Elements Calculated on Noncarbonate as 100 Per Cent													
																								2	6	10	16	21	27	32	39	44	52	61	Mean value	43.7	54.3
2	144-150	56.3	0.21	43.7	51.5	15.3	3.48	3.32	3.94	5.58	50	144	105	119	265	43	101	989	14	119	7	34	124	124													
6	144-150	45.7	0.22	54.3	52.9	14.6	3.00	3.26	3.81	5.43	57	127	123	118	236	52	110	969	20	118	11	26	90	90													
10	144-150	59.2	0.22	40.8	49.5	16.6	2.65	3.63	4.61	5.61	47	154	122	145	225	49	105	1289	0	123	0	17	61	61													
16	144-150	37.6	0.24	62.4	53.8	14.6	2.36	3.16	3.22	5.46	51	117	96	122	266	37	101	837	14	79	10	24	88	88													
21	144-150	50.8	0.24	49.2	51.3	12.8	2.40	2.36	2.64	4.39	39	108	100	93	199	35	96	821	10	116	4	26	73	73													
27	140-150	73.5	0.21	26.5	47.3	16.0	2.64	3.13	4.60	6.15	30	166	91	128	253	60	147	1064	0	143	0	0	162	162													
32	144-150	61.6	0.23	38.4	45.3	15.9	2.32	3.23	3.78	5.44	55	164	86	122	198	36	125	927	0	120	0	10	104	104													
39	140-150	75.6	0.21	24.4	51.2	17.3	3.11	3.57	4.18	6.60	66	176	86	131	258	53	143	910	0	172	0	8	102	102													
44	1-10	66.2	0.23	33.8	45.8	15.7	2.04	3.20	3.37	5.80	47	142	86	118	213	33	133	680	9	121	0	15	112	112													
52	140-150	49.7	0.25	50.3	43.1	15.2	1.63	2.93	2.84	6.50	69	125	97	127	179	34	131	541	4	101	10	14	99	99													
61	140-150	54.8	0.22	45.2	54.0	17.7	1.84	3.21	2.85	6.11	51	168	104	148	259	51	155	520	24	102	4	15	126	126													
Mean value		57.4	0.23	42.6	49.6	15.6	2.50	3.18	3.62	5.73	51	144	99	124	231	43	122	867	9	119	4	17	103	103													

^aSr calculated on carbonate content as 100 per cent.

		Calcareous Nannoplankton Zones		m.y.B.P.			Sub-Bottom Depth (m) (base of NN Zone)
					top	base	
Quat.	NN 21	<i>Emiliana huxleyi</i> Zone		0.2	397-1-1, 0 cm	397-2-5, 40-41 cm	15.41
	NN 20	<i>Gephyrocapsa oceanica</i> Zone		0.6	397-2-6, 47 cm	397-4-2, 41 cm	29.91
	NN 19	<i>Pseudoemiliana lacunosa</i> Zone		1.8	397-4-3, 41 cm	397-15-3, 100 cm	136.50
Pliocene	Upper	NN 18 <i>Discoaster brouweri</i> Zone		2.5	397-15-4, 41 cm	397-19-3, 120 cm	174.70
		NN 17 <i>Discoaster pentaradiatus</i> Zone		2.7	397-19-4, 15 cm	397-19, CC	180.00
		NN 16 <i>Discoaster surculus</i> Zone		3.5	397-20-1, 10 cm	397-23-3, 34-35 cm	211.85
	Lower	NN 15 <i>Reticulofenestra pseudoumbilica</i> Zone		3.8	397-23-4, 40-41 cm	397-23, CC	218.00
		NN 14 <i>Discoaster asymmetricus</i> Zone		4.0	397-24, CC	397-35, CC	332.00
		NN 13 <i>Ceratolithus rugosus</i> Zone		4.6	397-36-1, 40-41 cm	397-42, CC	398.50
Miocene	Upper	NN 12 <i>Ceratolithus tricorniculatus</i> Zone		5.0			
		NN 11 <i>Discoaster quinquerramus</i> Zone			397-43-2, 20 cm	397-56, CC	
							541.00
		NN 10 <i>Discoaster calcaris</i> Zone		9.5	397-57-1, 34-35 cm	397-60-2, 21 cm	571.21
		NN 9 <i>Discoaster hamatus</i> Zone		11.0	397-61-2, 41-42 cm	397-72, CC	693.00
	Middle	NN 8 <i>Catinaster coalitus</i> Zone		12.0			Hiatus 693.83
		NN 7 <i>Discoaster kugleri</i> Zone		12.2	397-73-1, 83 cm	397-75-2, 33-34 cm	713.84
		NN 6 <i>Discoaster exilis</i> Zone		13.0	397-75, CC	397-77-3, 19-20 cm	734.20
		NN 5 <i>Sphenolithus heteromorphus</i> Zone		14.0			
					397-77, CC	397-80-1, 140-141 cm	
							760.91
Lower	NN 4 <i>Helicopontosphaera ampliaperta</i> Zone		17.0	397-80-2, 40-41 cm	397A-16-5, 30-31 cm	1074.30	
	NN 3 <i>Sphenolithus belemnos</i> Zone		18.5	397A-16, CC	397A-21-3, 46-47 cm	1118.97	
	NN 2 <i>Discoaster druggi</i> Zone		19.0	397A-21, CC	397A-34-1, 70 cm	1296.71	
	NN 1 <i>Triquetrorhabdulus carinatus</i> Zone		20.5				
Oligo.	NP 25	<i>Sphenolithus ciproensis</i> Zone		24.0			

SITE 397A

Stratigraphy		Calcar. Nanno. Zones			top	base
Cretaceous	Upper Hauterivian				397A-34-1, 102-103 cm	
					397A-34-1, 109 cm	
		<i>Calicalathina oblongata</i> and <i>Lithraphidites bollii</i> Zones (Thierstein)	<i>Crucellipsis cuvillieri</i> Zone (Roth)	<i>Cretarhabdus loriei</i> Zone (Sissingh)		52A, CC

Figure 10. Biostratigraphic zonation used at Site 397, based on calcareous nannoplankton.

Slumping

No evidence of slump phenomena is recorded above Section 397-57-3. The interval from Sections 397-57-3 to 397-61-5 is characterized by numerous slumps; whereas, the interval from Cores 397-62 to 397-72 has evidence of slumping only sporadically. Shore-based investigations support these shipboard observations. The succession of faunal assemblages in the samples examined from the "normal" hemipelagic sediments and from the slump intervals does not follow the principle of stratigraphic superposition (see Figure 11). A sharp contrast was noticed between the assemblages of planktonic foraminifers contained in autochthonous Tortonian sediments (referable to Zone N.16 of Blow, 1969) and some of the taxa from the slump intervals, which indicate ages correlatable with Zone N.14 (Serravallian or older). The latter assemblages include *Cassigerinella chipolensis*, which ranges from Zones P.18 to N.13, *Globigerinopsis aquasayensis* (N.10 to N.13), *Clavatorella bermudezi* (N.8 to N.10), *Globigerinoides subquadratus* (N.5 to N.13), *Globigerina druryi* (N.7; according to the present paper N.14), *Sphaeroidinellopsis disjuncta* (N.7 to N.13, according to Salvatorini and Cita, this volume), *Globorotalia siakensis* (N.2 to N.14), *G. praemenardii praemenardii* (N.10 to N.13), *G. peripheroronda* (N.6 to N.12), *G. peripheroacuta* (N.10 to N.13), *G. praefohsi* (N.11 to N.13), and *G. fohsi* s.l. (N.12 to N.13). It is likely, however, that at least part of the slumps contain taxa (as allochthonous elements) younger than Zone N.13 and occasionally species indicative of correlations as young as the earlier part of Zone N.16.

Reworking From Older Formations

Reworking from older formations is minor in the upper part of the section (from Core 397-54, upwards), which we consider unusual in an upper continental rise setting. Evidence of reworking from the late Pliocene has been recorded in the early Pleistocene (Core 397-12, see discussion under Submarine Erosion, below).

Reworking from the early Pliocene (M P1 3 Zone of Cita, 1975) into the late Pliocene (M P1 4 Zone) occurs in Core 397-27 (where *Globorotalia margaritae* was found in all but one section); its LAD occurs in Section 397-29-1. See Mazzei et al. (this volume) for further discussion on this topic.

Specimens reworked from pre-Neogene sediments (Upper Cretaceous Globotruncanids and Heterohelids; Paleogene Globorotalias) are rare and essentially limited to the lower part of the succession, where the presence of terrigenous components is conspicuous.

Strong reworking from Neogene sediments is recorded in the interval containing slumped beds (see above). Less obvious and occasionally confusing reworking from Neogene sediments is noted at various depths. We consider sparse specimens of *S. disjuncta* in Cores 397-57 to 397-54, an interval immediately overlying the slump phenomena, to have been reworked. *Sphaeroidinellopsis disjuncta*, which evolves into *S.*

subdehiscens at the base of Zone N.13, persists for a short interval even after this evolutionary transition was completed: indeed, we did not consistently record this taxon above Section 397-73-1, a distribution in good agreement with that recorded by Jenkins (1971) in New Zealand, where the taxon disappears along with *G. fohsi* and *G. praemenardii praemenardii*.

C. chipolensis probably also is reworked, as recorded in levels referable to Zones N.13 and N.14 where we also found evidence of terrigenous input. In Sample 397-72-1, 51-53 cm, *C. chipolensis* is associated with rare, reworked specimens of *G. fohsi robusta*. Except for a few of these reworked examples, the range of *C. chipolensis* at Site 397 is very similar to that recorded in the Mediterranean (Malta, see Giannelli and Salvatorini, 1972; DSDP Site 372, see Cita et al., 1978), ranging as high as Zone N.9.

Another example of confusing reworking is that of *G. siakensis* in Cores 397-70 to 397-68, where the taxon co-occurs with typical specimens of *G. acostaensis acostaensis*. The distinction between the latter species from immature specimens of *G. siakensis* is facilitated by differences in their coiling direction (consistently dextral = *G. acostaensis*, sinistral = *G. siakensis*). Most investigators agree that the ranges of these two taxa do not overlap (see Blow, 1969; Brönnimann and Resig, 1971; Postuma, 1971; Stainforth et al., 1975; inter alia); the biostratigraphic interval corresponding to Zone N.15 is characterized by the absence of both taxa, so that we could not identify Zone N.15 at Site 397. Specimens of *G. siakensis* in Cores 397-70 to 397-68, co-occurring with *G. acostaensis*, are interpreted here as reworked, also taking into account the occurrence of slumps in this interval (i.e., Samples 397-68-3, 49-51 cm and 397-70-1, 49-51 cm). In Samples 397-68-1, 50-52 cm and 397-69-2, 56-59 cm, we recorded other taxa reworked from older Neogene sediments; besides *G. siakensis*, these include *G. praemenardii praemenardii*, *G. praefohsi*, *G. fohsi*, *G. mayeri*, *G. subquadratus*, and *G. aquasayensis*.

Downslope Displacement

Evidence of downslope displacement is strong in the benthic assemblages (see Lutze, this volume). In our samples investigated for planktonic foraminifers, we recorded benthic forms indicating entirely different and mutually exclusive biotopes associated in the interval from Cores 397-97 to 397-83, as well as strong evidence of coarse terrigenous input. Taxa involved in displacement include the genera *Ammonia*, *Elphidium*, *Amphistegina*, *Asterigerinata*, *Cibicides*, and *Florilus*. Associated with these displaced forms are abraded fragments and/or entire specimens of mollusks, echinoids, bryozoa, ostracodes, and otoliths.

Displaced benthic populations also occur in Cores 397-77, 397-73, 397-72, and 397-56, consistently from levels rich in inorganic components.

Though downslope displacement of planktonic foraminifers also occurred, it is almost impossible to discriminate its effect from pelagic fallout.

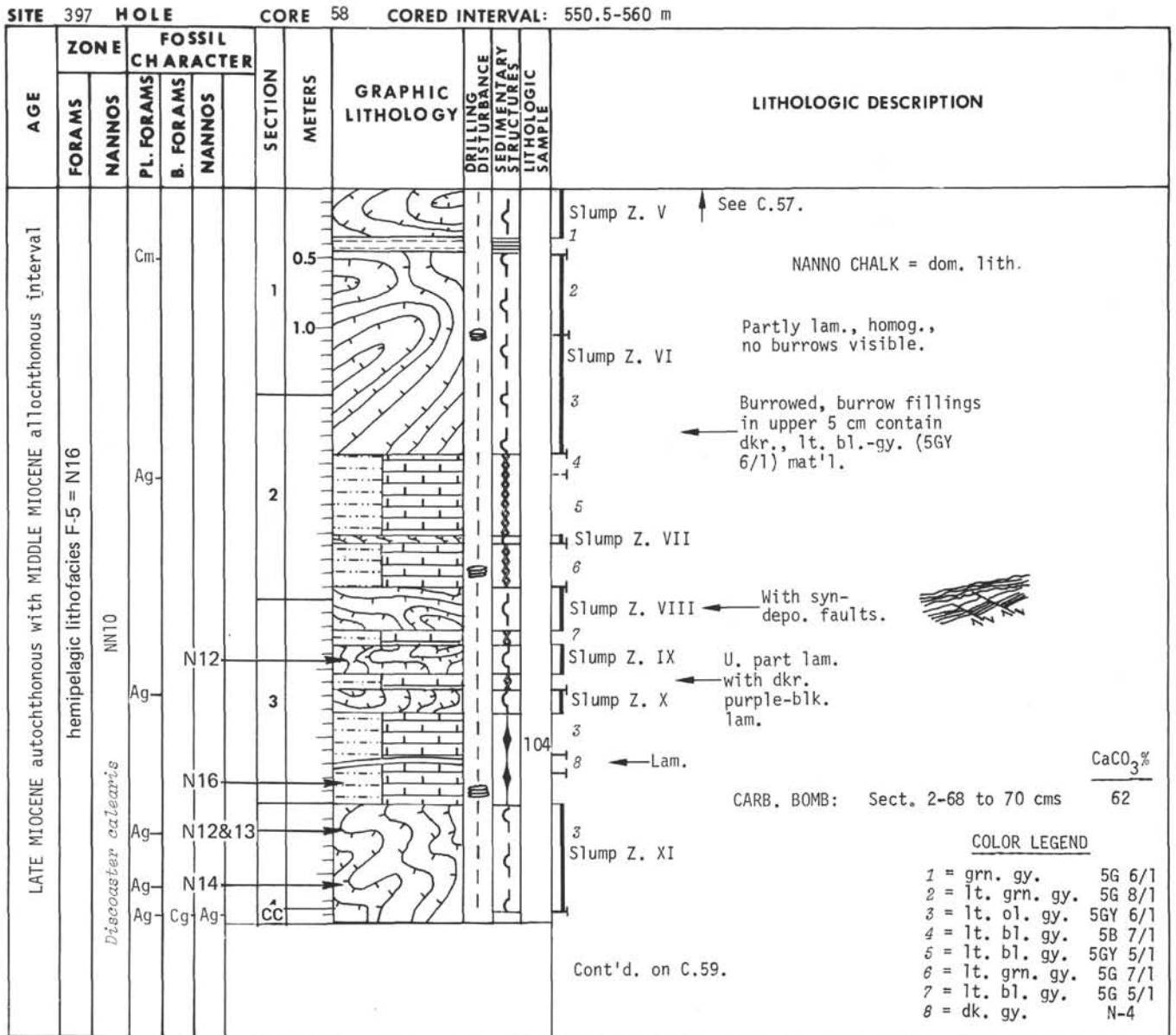


Figure 11. Columnar log of Core 397-58 (550.5 to 560 m sub-bottom), where slumped sediments are dominant. Assignments to the foraminiferal zones of Blow's "standard" zonation are shown by arrows to the left. The normal hemipelagic sediment from the undisturbed layers is referable to Zone N. 16, whereas faunal assemblages from the slumps belong to discrete biozones of the middle Miocene (Serravallian age). This time interval is only partially represented in the underlying succession (Cores 397-71 to 397-77).

Dissolution at Depth

Evidence of dissolution at depth is noted in upper Miocene and lower Pliocene intervals, from Cores 397-66 to 397-39. Dissolution is more profound in the Messinian and upper Tortonian, and is particularly evident in Cores 397-44, 397-52, 397-54 and 397-56, as shown by both the weight of the coarser sediment fraction (see Cita and Spezzibottiani, this volume) and the preservation of planktonic foraminiferal shells. In this interval, the biogenic fractions are very limited as to the

number of species and individuals; foraminiferal tests are often fragmented and dissolved.

In the lower part of the Miocene, where debris flows are present (lithologic Unit 4), no evidence of dissolution at depth is recorded. The dissolution curves constructed for the North Atlantic indicate a maximum dissolution in the middle Miocene. Consider the following observations: (1) the present-day depth of the Cape Bojador drill site is only 2900 meters; (2) there is no evidence whatsoever of uplift in the area since Miocene times; (3) the present-day CCD for the North Atlantic is

4500 meters; and (4) the estimated CCD for the late Miocene in the Atlantic was 3800 meters (Berger and von Rad, 1972). On the basis of these considerations, we tentatively conclude the following: (a) the middle Miocene dissolution cycle is only partially expressed at Site 397 because of the rapid burial of the sediments which were subtracted from the aggression of under-saturated bottom waters; and (b) the strongest dissolution recorded in the uppermost Miocene may be related to an expansion of continental glaciation in Antarctica as reported by Hays, Frakes, et al. (1974).

Preservation

Preservation of fossils is good in the upper part of the drilled interval, good to moderate relative to the intervals affected by dissolution and slumping (Cores 397-39 to 397-71). From Cores 397-73 to 397-85, the foraminiferal assemblages are fairly rich, but specimens display recrystallized tests, often encrusted and mechanically deformed. From Core 397-85 downwards, with just a few exceptions, preservation is poor and planktonic foraminifers are by far less common than in the overlying interval.

Submarine Erosion

Biostratigraphic evidence for submarine erosion is recorded between Cores 397-70 and 397-71. The latter is referable to Zone N.14 on the basis of co-occurrence of *Globigerina nepenthes* and *Globorotalia siakensis*. The former is referred to Zone N.16, because it yields typical specimens of *G. acostaensis*. The FAD³ of this taxon is considered a reliable datum plane. Because the samples were selected carefully from the interior of the cores and did not include core-catcher samples (where downhole contamination is likely to occur), we consider highly unlikely the possibility of an artificially induced lower record of the taxon. In Section 397-70-3, along with *G. acostaensis*, *Globigerina digitata praedigitata* and *G. calida praecalida* also appear (two taxa which indicate a post-Zone N.15 age); at the top of Core 397-71, we did not record specimens transitional from *G. continuosa* to *G. acostaensis*, as should be expected in an interval immediately predating the FAD of the latter taxon. Therefore, we conclude that Zone N.15 and probably also the topmost part of Zone N.14 are missing at Site 397.

We have biostratigraphic evidence of additional submarine erosion between Cores 397-78 and 397-77. The latter is referable to Zone N.11 (or to the latest part of Zone N.10); the former belongs in part to Zone N.8 (Sections 397-78-4 and 397-78-3), in part to the lowermost part of Zone N.9 (Sections 397-78-1 and 397-78-2). This hiatus is substantiated by the simultaneous disappearance of several taxa at the top of Core 397-78 (such as *Praeorbulina* spp., *Globigerinoides sicanus*, *Globorotalia praescitula*, and *G. praemenardii ar-*

chaeomenardii), and by the first occurrence of several new taxa in the lower part of Core 397-77 (*Orbulina universa*, *Globorotalia peripheroacuta*, and *G. praemenardii praemenardii*). In terms of Blow's zonation, this hiatus encompasses all or part of Zone N.10 and most of Zone N.9.

Other (minor) hiatuses occur higher in the drilled interval: one in the Quaternary (Core 397-12), another one in the upper Pliocene (Core 397-25). These hiatuses cannot be documented biostratigraphically because their duration is less than the duration of a single foraminiferal biozone. Evidence supporting a hiatus at the base of Core 397-25 comes from paleomagnetic stratigraphy analyses (see Hamilton, this volume) and from physical properties studies (Mountain, this volume). Indeed, the later part of the Gauss Normal Epoch appears unusually reduced, whereas a drastic change is recorded between Cores 397-25 and 397-26, both in shear strength and in acoustic impedance. The only foraminiferal evidence favoring such a hiatus is the short duration of Zones M P1 5 versus M P1 6 and M P1 4. In other words, the interval postdating the LAD of *Sphaeroidinellopsis* spp. and predating the LAD of *Globigerinoides obliquus extremus* appears reduced, and the missing part is likely to be the lower portion of Zone M P1 5, where *Globigerinoides obliquus extremus* is more abundant.

Indirect biostratigraphic evidence for the existence of a hiatus is found in Core 397-12: (1) the seismic profiles show an angular unconformity; (2) a sharp change in physical properties was recorded; (3) the extension of the reversed polarity interval of the Matuyama Epoch predating the Jaramillo event appears anomalously restricted in comparison with the usual record; and (4) there is extended reworking of microfossils. *Globorotalia miocenica*, whose LAD is recorded within Zone M P1 6 in Section 397-19-1, is consistently found in several sections of Core 397-12.

Biochronology

Quaternary

The Quaternary section continuously cored at Site 397 is approximately 137 meters thick.

The Pliocene/Pleistocene boundary is located between Samples 397-15-3, 50-52 cm and 397-15-4, 50-52 cm, on the basis of the first evolutionary occurrence of *Globorotalia truncatulinoides*, which defines the N.21/N.22 zonal boundary in Blow's (1969) standard zonation.

The evolution of *Globorotalia truncatulinoides* from *G. tosaensis* was poorly represented at Site 397, but could be followed step-by-step in Core 397-15 where it is abundant, as documented in Plate 1. In the upper part of the core, there is an overlap of both taxa. The FAD of *Globorotalia truncatulinoides* occurs in Section 397-15-3, and virtually coincides with a reversal in magnetic polarity which is interpreted as the base of the Olduvai event (see Hamilton, this volume), as well as coinciding with the LAD of *Discoaster brouweri* (see Čepék and Wind, this volume).

³The terms FAD and LAD are used in the present report as abbreviations for First Appearance Datum and Last Appearance Datum, respectively.

No zonal subdivision has been applied to the Quaternary section, which is referred in its entirety to the *Globorotalia truncatulinoides* total range zone, which extends to the present.

Quantitative micropaleontological analyses were conducted (see Cita and Colombo, this volume) on two test intervals, each one consisting of nine consecutive samples (one per section). The polar assemblage (left-coiling *Globigerina pachyderma*) is represented by quite low percentages in both test intervals. The sub-polar (right-coiling *G. pachyderma* + *G. bulloides* + *Globigerinita glutinata*), subtropical (*Globorotalia truncatulinoides* + *G. inflata* + *Globigerina falconensis* + *G. calida*), tropical (*Globigerinoides sacculifer* + *G. ruber* + *Hastigerina siphonifera* + *Globorotalia menardii* + *Pulleniatina obliquiloculata*) and gyre margin assemblages (*P. obliquiloculata* + *G. menardii* + *G. inflata* + *G. sacculifer* + *G. tenellus*) are present in variable amounts.⁴

Climatic fluctuations have a larger amplitude in the upper Quaternary (first test interval, encompassing Cores 397-2 and 397-3, later part of the Brunhes Epoch), than in the lower Quaternary (second test interval, Sections 397-7-6 to 397-9-2, later part of the Matuyama Epoch). In the lower Quaternary, the gyre margin assemblage constitutes an excess of 40 per cent of all assemblages, with *Globorotalia inflata* dominating. Qualitative micropaleontological investigations (carried out on 90 samples from Core 397-1 to Section 397-15-3) showed that *Globorotalia truncatulinoides* is present throughout the section and is dominantly dextral, although episodes with dominant left-coiling specimens were recorded (Cita and Colombo, this volume). *Globorotalia menardii*, recorded in 19 of the 90 samples investigated, is always accompanied by faunal assemblages indicating warm superficial water, and by δO^{18} depleted carbonates as measured on tests of benthic foraminifers (Shackleton and Cita, this volume).

Pliocene

The Pliocene section continuously cored at Site 397 consists of hemipelagic sediments yielding considerable amounts of siliceous skeletal elements down to Core 397-32. The carbonate content, which essentially consists of calcareous zooplankton and phytoplankton, increases consistently as a function of depth in the Pliocene (Cita and Spezzibottiani, this volume), with fluctuations which are interpreted as climatically modulated. The total thickness of the Pliocene, from Section 397-15-3 (~137 m sub-bottom) to the base of Core 397-42 (~398 m) is approximately 260 meters, or twice as large as that of the Quaternary. From top to bottom, the following biozones could be identified.

M P1 6 (*Globorotalia inflata* Zone of Cita, 1975): Samples 397-15-4, 50 cm to 397-20-6, 20 cm: The nominal taxon is not recorded throughout the biozone,

whose base is defined by the LAD of *Globigerinoides obliquus extremus*. Actually, the lowest record of typical specimens is recorded in Section 397-17-2 (primitive forms down to Section 397-18-2). Within this interval, the following extinction horizons previously correlated with paleomagnetic stratigraphy were recorded: LAD of *Globorotalia exilis* in Section 397-18-1; LAD of *Globorotalia miocenica* in Sample 397-18, CC. Foraminiferal assemblages are rich and highly diversified, yielding *Globigerina apertura*, *Globorotalia hirsuta*, *Globigerinoides elongatus*, *G. ruber*, *Hastigerina siphonifera*, *Globigerina eggeri*, etc.

M P1 5 (*Globigerinoides elongatus* Zone of Cita, 1975): Samples 397-21-1, 20 cm to 397-24, CC: This biozone at Site 397 appears reduced in thickness in comparison with Mediterranean sections (DSDP Site 132; Capo Rossello section, Sicily; see Cita and Gartner, 1973). Pyrite is common to abundant in the coarse sediment fraction from this interval, where the faunal diversity is large; taxa include *Globorotalia miocenica*, *G. multicamerata*, *G. crassiformis*, *G. puncticulata padana*, *Globigerina apertura*, *G. eggeri*, *Globigerinoides obliquus extremus*, *G. ruber*, *G. sacculifer*, *G. conglobatus*, etc.

M P1 4 (*Sphaeroidinellopsis subdehiscens* partial range zone of Cita, 1975): Samples 397-25-1, 50 cm to 397-28, CC: The upper boundary of this zone is defined by the LAD of the genus *Sphaeroidinellopsis*, which is consistently recorded lower in the section. We found evidence within this zone of reworking from slightly older strata, as supported by the recorded scattered occurrence of *Globorotalia margaritae* (whose LAD defines the base of the zone) and of *Globigerina nepenthes* in several sections of Core 397-27 (see above). *Globorotalia cultrata menardii*, *G. fimbriata*, *G. multicamerata*, *G. cultrata limbata*, *G. crassaformis*, *G. emiliana*, and *G. puncticulata padana* are commonly recorded within this interval. The occurrence of *Globorotalia altispira* is much more scattered than that of *Sphaeroidinellopsis*; however, the last occurrences of both taxa virtually coincide.

M P1 3 (*Globorotalia margaritae*/*G. puncticulata* concurrent-range zone of Cita, 1975): Samples 397-29-1, 50 cm, to 397-35, CC. In this interval, we noticed a strong decrease in pyrite abundance in comparison with the overlying section, whereas the (average) carbonate content steadily increases downhole (Cita and Spezzibottiani, this volume). The composition of the faunal assemblages is similar to that of Zone M P1 4, with the addition of *Globorotalia margaritae* which is represented by the subspecies *margaritae evoluta* and also *primitiva*. Its record, however, is not continuous in Core 397-30. *Globorotalia tumida* is occasionally recorded.

A detailed description of this biochronology of Cores 397-32 to 397-97, including a range chart based on a semiquantitative study of 228 samples, is presented by Salvatorini and Cita (this volume); only a few comments are included here. *Globigerina nepenthes* Zone is defined by Salvatorini and Cita as the interval with the nominal taxon from the FAD of *Globorotalia*

⁴The distinction of the faunal assemblages is after Thiede (in press).

margaritae to the FAD of *G. puncticulata*; this zone extends from Section 397-36-1 to 397-45-1. The Miocene/Pliocene boundary falls within this biozone; our best location is in Core 397-42 (see discussion in Mazzei et al., this volume).

Miocene

Sphaeroidinellopsis seminulina paenedehiscens Zone: Sections 397-45-2 to 397-52-5. Defined by Salvatorini and Cita (this volume) as the interval from the FAD of the nominal taxon to the FAD of *Globorotalia margaritae*. This zone corresponds approximately to Zone N.17 of Blow's (1969) standard zonation, whose definition of the lower boundary is highly controversial. We consider it likely that the lower boundary of the *S. seminulina paenedehiscens* Zone postdates the lower boundary of Zone N.17. The latter has been calibrated by Ryan et al. (1974) with the lower part of paleomagnetic Epoch 7. Section 397-52-5, where the zonal boundary under discussion is defined, is correlated with the later part of Epoch 7 (see Hamilton, this volume; Mazzei et al., this volume).

Globorotalia acostaensis acostaensis-G. merotumida Zone N.16: Section 397-52-6 to Sample 397-70, CC: This zone has been amended by Salvatorini and Cita (this volume) in its upper limit, which is here defined by the FAD of *G. seminulina paenedehiscens* instead of the FAD of *Globorotalia tumida plesiotumida*. Within this biozone is a 35-meter-thick interval (Sections 397-57-3 to 397-61-2) which is rich in slumps. The lower boundary of this biostratigraphic unit is interpreted as being erosional (see above, under Submarine Erosion).

Globigerina nepenthes/Globorotalia siakensis Zone N.14: Sections 397-71-1 to 397-72-2: The thickness of this biozone is limited at Site 397; Zone N.15 is missing altogether. Also the older biozones of the middle Miocene (i.e., N.13, N.12, N.11; Serravallian in age) are strongly reduced, which means that part of the sediments have been eroded. It is noteworthy that the slumped sediments encompassing Cores 397-57 to 397-61 (see Figure 11) are middle Miocene and belong to the biozones which are missing, or incompletely recorded, lower in the section (Cores 397-71 to 397-77). This is a clear indication of slope instability during middle Miocene times.

Sphaeroidinellopsis subdehiscens/Globigerina druryi Zone N.13: Sections 397-72-36 to 397-74-1: This biozone is strongly reduced, as are the preceding and following ones (see fig. 9 of Salvatorini and Cita, this volume).

Globorotalia fohsi Zone N.12: Section 397-74-2 to Sample 397-75, CC.

Globorotalia praefohsi Zone N.11: Section 397-76-1 to Sample 397-77, CC: The boundary with the underlying Zone N.10 cannot be precisely located because the lithology is highly unfavorable to the development of planktonic foraminifers, especially the *Globorotalia fohsi* group, so that it is possible that part of Zone N.10 is also present. The base of the biozone is interpreted as being erosional. See Salvatorini and Cita (this volume) for further discussion.

Orbulina suturalis/Globorotalia peripheroronda Zone N.9: Section 397-78-2: Only the earliest part of this zone is present. The evolutionary trend leading from *Globigerinoides sicanus* to *Orbulina* via *Praeorbulina glomerosa* (with subspecies) could be followed fairly well in its various steps at Site 397 (see fig. 1 of Salvatorini and Cita, this volume) notwithstanding the lithology which was not always favorable.

Globigerinoides sicanus/Globigerinatella insueta Zone N.8: Section 397-78-3 to Sample 397-89, CC: The lower boundary of Zone N.8 is defined by the FAD of *Globigerinoides sicanus*. This taxon, however, has been recorded in earlier horizons of the lower Miocene, i.e., from Zone N.6 (Brönnimann and Resig, 1971) or from levels correlated with Zone N.7. In the present report, we identify the N.8/N.7 zonal boundary with the FAD of typical specimens referable to *G. sicanus*, as illustrated in Salvatorini and Cita (this volume). The lowest recorded occurrence of these typical specimens is in Sample 397-89, CC.

Consequently, the underlying cores are referred to Zone N.7, though specimens identified as *G. cf. sicanus* are recorded as low as Sample 397A-17-3, 96-99 cm.

Globigerinatella insueta-Globigerinoides quadrilobatus trilobus Zone N.7: Section 397-90-2 to Core 397-97: Due to the scantiness and poor preservation of planktonic foraminiferal assemblages, the zonal boundaries (particularly, the lower boundary) are only tentatively identified. The lowermost part of the sequence is provisionally referred to foraminiferal Zones N.5/N.6. The scattered occurrence of *Globigerinita dissimilis* does not allow for a precise location of the N.6/N.7 zonal boundary, which is defined by the extinction horizon of the aforementioned taxon. No evidence of the lowermost Miocene biozone has been found, characterized by the concurrent range of *Globigerinoides quadrilobatus primordius* and of *Globorotalia kugleri*. Representatives of the genus *Globigerinoides* (as recorded down to Core 397A-22) include *G. quadrilobatus trilobus* and *G. quadrilobatus altiapertura*, whose first occurrence is definitely younger than the so-called *Globigerinoides* datum. The lowermost part of the lower Miocene section (Burdigalian in age) is almost barren. Several samples are semilithified, e.g., Sample 397A-11, CC, which also yields a rich population of perfectly preserved tests of benthic foraminifers (Buliminids). The nature of the early diagenesis leading to lithification of the sediments without concomitant alteration of the foraminiferal tests is unknown.

Cores 397A-16 and 397A-17 are of special interest: they essentially consist of "facies 4" brown mudstone, which is interpreted as allochthonous (mudflow) and yields abundant displaced benthic foraminifers and pelecypods, and well-preserved (empty tests) planktonic foraminifers, indicating a Burdigalian (N.6? Zone) age.

Intercalated within the brown mudstones in contorted lumps and stripes is an originally autochthonous, burrowed, pelagic, biogenic, pale gray sediment. The sand-size fraction is essentially biogenic and consists of late Oligocene planktonic foraminifers of *Globorotalia opima* Zone P.21 with *G. opima opima*, *Globigerinita*

dissimilis, *C. unicavus*, *Globigerina venezuelana* etc. Seven samples have been investigated from Cores 397A-16 and 397A-17. All those from the pale gray lithology are late Oligocene, whereas from the dark brown and green lithology (mud flows) are early Miocene. A similar finding of a pure Zone P.21 faunal assemblage was recorded in Sample 397A-10-4, 197 cm.

Early Cretaceous

A spectacular 110-m.y. hiatus occurs in Section 397A-34-1 at 1300 meters sub-bottom.

The 154-meter-thick Lower Cretaceous section penetrated consists of pale olive-gray to blue-gray mudstones and siltstones, unburrowed and showing progressively more lamination downward, followed by a blue-gray silty mudstone with sideritic intercalations (Cores 397A-51 and 397A-52). The foraminiferal content is sparse and limited to Cores 397A-39, 397A-41, 397A-46, 397A-47, and 397A-49. They are primitive, small Globigerinids referred to "*Globigerina*" *hoterivica* and to "*Globigerina*" cf. *infracretacea*. The range of both species in the Early Cretaceous is pre-Aptian (cf. also Rösler et al.; Butt; Basov et al.; all, this volume). The tests are often filled with pyrite crystals and partly broken or dissolved. They are fragile.

Benthic Foraminifers

Neogene and Quaternary⁵

Abundance and Preservation

Benthic foraminifers are generally not abundant in deep-sea sediments; they usually constitute < 1 per cent of the total foraminiferal population in well-preserved sediments. In most of the core-catcher samples of Holes 397/397A, however, the proportion was much higher for two reasons. First, selective dissolution of planktonic shells (Parker and Berger, 1971), as indicated by a comparatively high degree of fragmentation, which increases from the lower Pleistocene to the Pliocene and reaches highest values in the upper Miocene (> 50% fragments; Diester-Haass, this volume). Second, dilution by displaced shallow-water faunas, which bear higher percentages of benthic foraminifers according to their original habitat. Only a few samples from the lowermost Miocene (Samples 397A-26, CC to 397A-28, CC and 397A-31, CC to 397A-33, CC) were practically barren of benthic foraminifers. Few or no autochthonous benthic foraminifers were recorded in many samples throughout the middle-lower Miocene interval with downslope transport of sediments.

The preservation of the tests was excellent in the upper Pleistocene and deteriorated slowly down to the middle Miocene. Fossilized tests (i.e., filled chambers) were observed initially in Samples 397A-71, CC and 397A-75, CC. Reworked Eocene *Uvigerina*s were always fossilized. Compressed tests are frequent in the

lower Miocene autochthonous facies, i.e., in Samples 397A-20, CC and 397A-25, CC. However, displaced shallow-water foraminifers, which form the major proportion in the slump and mudflow sediment facies of the middle and lower Miocene, are always perfectly preserved in spite of being deeply buried as long or longer than the corroded or fossilized autochthonous foraminiferal tests. The constant alternation between well-preserved allochthonous and fossilized lower bathyal autochthonous faunas (facies 5, sedimentologically) suggests that diagenesis occurred shortly after deposition and that chemical conditions responsible for the alteration (interstitial water properties) were present only at the original depositional site. Apparently, they were not achieved after sediment transport and redeposition from shallow water. The amount of overlying sediments (total thickness exceeds 1000 m) seems to play a lesser role than anticipated (compare also Riech, in Sediment Summary Chart 1, back pocket, this volume).

Biostratigraphy

Our present knowledge on ranges and geographic distribution of Neogene deep-water benthic foraminifers is meager; therefore, biostratigraphic information supplied by benthic foraminifers is insufficient for precise age determination. One important prerequisite for their possible future utilization is a worldwide inter-ocean distribution of deep-water species. Results from Holes 397, 397A, and 369 (DSDP Leg 41: Lutze, 1978) clearly show indications for inter-ocean distribution. More than 50 per cent of the Neogene species described by Douglas (1973) from the central North Pacific (Leg 17) are also present in this part of the Atlantic. Nearly all of the typical lower-middle bathyal species mentioned by Ingle (1973) from the northwestern Pacific (Leg 18) are present at Sites 397 and 369. It is hoped that future legs may supply sufficient additional information to establish a benthic zonation for deep-sea Neogene and Quaternary sediments.

At Site 397, the Neogene-Quaternary section may be subdivided by means of benthic foraminifers into six units (see Figure 12).

Unit NB 1 is characterized by the long-ranging species *Oridorsalis umbonatus* and *Cibicidoides robertsonianus*. The base cannot be fixed for correlation purposes because of the lower Miocene/Lower Cretaceous hiatus.

The base of Unit NB 2 is defined by the first occurrence of *Bolivina multicostata*, *Rectuvigerina multicostata opima*, and *Pyrgo murrhina*. This coincides with the first appearance of volcaniclastic conglomerates and sandstones in the upper-lower Miocene (N.8/NN 4).

Unit NB 3 begins with the first occurrence of *Cibicidoides wuellerstorfi*, *Sigmoilopsis schlumbergeri*, and *Uvigerina peregrina* s.l. It corresponds roughly with nannofossil Zones NN 9 to NN 11 and planktonic foraminiferal Zones N.12 to lower N.16 (Serravallian to lower Tortonian).

The base of Unit NB 4 is marked by the disappearance of *Bolivina multicostata*, the top by the local disappearance of *Bulimina alazanensis* (as at Site 369),

⁵This study is based on core-catcher samples, with the exception of the Pleistocene (Lutze, this volume).

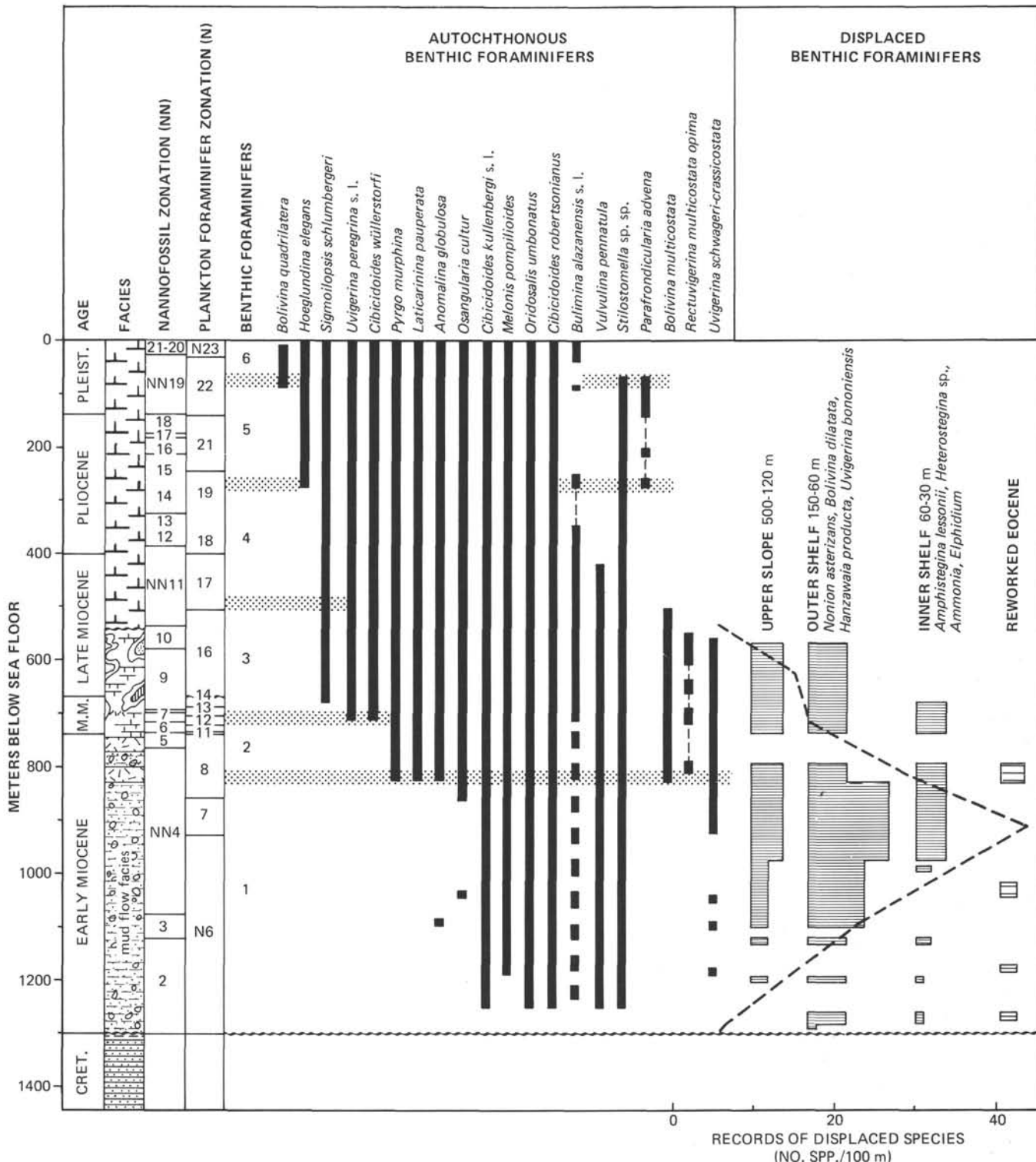


Figure 12. Neogene benthic foraminifers: autochthonous lower-middle bathyal fauna and displaced shelf fauna (cross-hatched bars). The width of the bars corresponds roughly to the number of displaced species identified. The number of recorded displaced species (broken line) reaches its maximum between 900 and 1000 meters. The study is based on the greater than 150 mm fraction of the core-catcher samples.

and the first occurrence of *Hoeglundina elegans*. This unit corresponds with nannofossil Zones NN 11 to NN 14 and planktonic foraminiferal Zones N.17 to N.19.

Unit NB 5 begins with *Hoeglundina elegans* and scattered occurrences of *Parafrondicularia advena*. It refers to the nannofossil Zones NN 15 to NN 19 and the foraminiferal Zones N.21 to N.22.

Unit NB 6 corresponds with the glacial Pleistocene and the Brunhes Magnetic Epoch. It begins with the first appearance of *Bulimina aculeata* and the disappearance of typical Pliocene species like *Stilostomella* sp. sp., *Pleurostomella acuminata*, *Parafrondicularia advena*, *Orthomorphina* 397, and *Ellipsoglandulina laevigata*.

Further subdivisions of the Pleistocene are tentatively suggested (see Lutze, this volume). The ranges used for this provisional and local zonation were compared with known ranges given in the above-cited literature. The following similarities and differences might be noted: (1) The first occurrence of *Cibicidoides wuellerstorfi* at Sites 167 and 171 of the central North Pacific (Douglas, 1973) dates middle Miocene N.12, which is exactly the time of its first appearance in the Atlantic. Also, no earlier occurrence of this species off Alaska was observed by Ingle (1973); (2) *Pyrgo murrhina* has its first occurrence in the Pacific in Zone N.9 (middle Miocene), and it appears rarely in N.8 at Site 397. However, according to Douglas, the range of this and similar miliolid species might be altered by selective dissolution of the porcellaneous chamber walls; (3) *C. robertsonianus* has its first occurrence in the Pacific in N.5/6 (lower Miocene), and is present throughout the Site 397 section which begins within this same time interval; and (4) long-ranging species in the Quaternary and Tertiary of the Pacific include abundant species like *Oridorsalis umbonatus*, which is also common throughout the entire section at Site 397.

It was not possible to apply the zonation suggested for Site 369 (1700 m water depth), which was drilled close to the present site but in much shallower water (Lutze, 1978). The boundaries of NB 1/NB 2 and NB 2/NB 3 correlate quite well, but "index species" for Units 4 and 5 are either absent (e.g., the slope species *Uvigerina auberiana*) or show different ranges (like *Bolivina multicostata* and *Rectuvigerina multicostata opima*, which persist up to the *margaritae* Zone at Site 369). Such restricted ranges might reflect a response to the cooling of bottom water in the late Miocene (Shackleton and Kennett, 1974, p. 748). This cooling resulted in an upward shift of the lower depth limits of slope species.

A broad species concept had to be applied in this study. The usage of "stage restricted" species names was avoided.

Paleobathymetry

Introduction: The distribution of benthic foraminifers reflects water-mass distribution rather than absolute depth. Off western Africa, several dominant

species (e.g., *Uvigerina peregrina* and *Cibicidoides kullenbergi*) show even, vertical distribution boundaries instead of horizontal ones (Lutze, this volume). It is not possible, therefore, to explain temporary disappearances of lower bathyal species (e.g., *Melonis pompilioides*) by epeirogenetic uplift and subsidence. Nevertheless, well-known differences between shelf and lower-middle bathyal (LMB) faunas allow a clear definition of displaced shelf material, at least down to the Pliocene. This approach was tentatively extended in this study to interpret the displaced Miocene sediments of the lower part of the section at Hole 397 (see Table 11).

Autochthonous: The depth classification used in this study is taken from Ingle (1973). Species indicative of LMB to LB environments (i.e., 1500-4000 m water depth) are: *Melonis pompilioides*, *Osangularia cultur*, *Cibicidoides robertsonianus*, *Gyroidina orbicularis*, *Cibicidoides kullenbergi*, *Pyrgo murrhina*, *C. wuellerstorfi*, *Bulimina alazanensis*, *Pullenia bulloides*, *Laticarinina pauperata*, *Anomalina globulosa*, *Gyroidina lamarciana*.

Most of these species occur throughout the autochthonous parts of the section at Site 397. They indicate water paleodepths similar to those at present, or at least not shallower than 1500 meters. In facies 5, as defined by the sedimentologist group, these and related species form the entire benthic foraminiferal population. In the slump and mudflow facies of the middle and lower Miocene, however, they are mixed with displaced shelf and upper slope faunas.

Allochthonous: In the upper part of the section, only minor indications were detected in the larger grain-size fractions. However, in the fraction <125 μ m, certain shelf Bolivinas were found to form major proportions of the benthic assemblage (e.g., *Bolivina pseudoplicata*: up to 14% during cool intervals of the Pleistocene). This indicates significant downslope particle transport affecting the silt fraction.

In the upper Miocene part of the section, scattered occurrences of *Bolivina dilatata* also were observed in the larger fractions (e.g., Sample 397-53, CC), indicating increased transport from the shelf. In addition, Sample 397-56, CC yielded specimens of *Dorothyia rudis* and *Bigennerina nodosaria*, which are upper-bathyal to outer-shelf species.

TABLE 11
Depth Classification of Marine Benthic Environments
Utilized in Leg 47 Foraminiferal Reports

Benthic Zone	Abbr.	Depth Range (m)
Supralittoral		Splash zone to HHW
Littoral (intertidal)		HHW to LLW
Inner shelf (inner sublittoral)		LLW to 50 m
Outer shelf (outer sublittoral)		50 m to 150 m
Upper bathyal	UB	150 m to 500 m
Upper middle bathyal	UMB	500 m to 1500 m
Lower middle bathyal	LMB	1500 m to 2500 m
Lower bathyal	LB	2500 m to 4000 m
Abyssal		4000 m to 6500 m
Hadal (trenches)		6500 m +

An entirely different picture was found in the middle and lower Miocene. Nearly all of the core-catcher samples referable to facies 4, 3, and 2 yielded large quantities of displaced shelf foraminifers. Two main groups were distinguished:

1) Outer-shelf species: *Nonion asterizans*, *Bolivina dilatata*, *Hanzawaia producta*, *Uvigerina bononiensis* group, *Heterolepa praecinctus* group, *Trifarina angulosa*.

2) Inner-shelf species: *Amphistegina lessonii*, *Heterostegina* sp., *Elphidium complanatum/fichtelianum*, *E. crispum* group, *Textularia sagittula*.

The number of occurrences of these species per 100-meter interval gives an approximate estimation of the degree of shelf material displacement (see Figure 12). Highest numbers were recorded in the interval between Cores 397-82 and 397A-20 in the upper part of the lower Miocene debris flow section. Reworked Eocene *Uvigerinas* and other species were also frequently found there. The majority of allochthonous species are clearly indicative of outer-shelf conditions, that is, to water depths between 150 and 50 meters. Whereas these species occur from the base of the Miocene up to the top of the allochthonous part of the section (Sample 397-57, CC), the inner shelf group of species was only found up to Sample 397-71, CC (in turbidites, close to the D₂ reflector). Since seismic profiles indicate this part to be a distinctive member of the debris and slump cover on the continental slope, different erosional source areas might be suggested as follows: (1) intermittent displacement activity from about 20 to 18 m.y.B.P. (NN 2 absolute time scale according to Berggren and Van Couvering [1974]) affected both the outer and inner shelf; (2) maximum and continuous displacement occurred from 17 to 12.5 m.y.B.P. (NN 3 to NN 7). At that time, the entire shelf and upper slope was affected, the latter partially stripped, thus yielding Eocene reworked faunas. Maximum amount of inner-shelf input was provided by turbidity current transport as indicated in Sections 397-71-1 and 397-71-2 (*Amphistegina* sands); and (3) decreasing displacement activity from 11 to about 10 m.y.B.P. (NN 9), affected only the outer shelf and upper slope. At that time, complete masses of older slope sediments slumped down.

This picture requires refinement by more detailed core studies. It was outlined, however, to demonstrate the general frame of environmental information obtainable from benthic foraminifers. Additional information might be applied to determining the dominant sediment type that was eroded on the outer shelf. The dominant species are buliminids, such as *Bolivina dilatata*, *Buliminella tenuata*, *Fursenkoina* sp., *Bolivina* sp. sp., *Uvigerina* sp., and only a few *Ammonia*, *Cancris*, *Miliolids*, etc. Assemblages of this type today inhabit soft-bottom sediments, e.g., mud pillows accumulating near river mouths.

Table 12 is added to demonstrate the relation between foraminiferal information and sediment facies. It shows that some types of allochthonous sediments (F-4A₂) contain no LMB deep-water foraminifers, whereas others are always (F-2, F-4A₁), or sometimes

TABLE 12
Foraminiferal Analysis of Core-Catcher Samples

	Facies Designations							
	F1	F2	F3	A1	B	F4 A2	C	F5
Inner shelf								
Inner shelf and outer shelf				•				
Outer shelf		•						
Shelf and upper slope								
No autochthonous LMB forams present								
Autochthonous LMB present		•						
Only autochthonous, no displaced material								••
Reworked Eocene Cretaceous				•				

Note: Facies designations according to the sedimentology group (Michael A. Arthur, Oscar E. Weser). Black dots refer to special test samples taken from reference Core 397-87. Bars indicate relative frequencies with which various foraminiferal environments occur in the different sediment facies.

(F-4C₃) mixtures of both, the autochthonous and allochthonous components.

Early Cretaceous

Benthic foraminifers are rare in the Early Cretaceous sediments recovered from Site 397. A total of nine species was found; none are age diagnostic based on information presently available.

The preservation is moderate, but most of the tests are fragile. This applies in particular to the *Epistominas*. Their structures are perfectly preserved (peripheral apertures, toothplates), but might collapse when touched with the wet brush.

Summing up the analysis of all 53 specimens, a clear dominance of one species of *Lenticulina* and a small "*Miliolina*" is shown (together >55%). Whether this low diversity is caused by an originally shallow habitat remains an open question; selective dissolution and sorting cannot be excluded.

Mollusks

Miocene

Several remains of displaced mollusks (gastropods, pelecypods) and corals were found in the allochthonous lower Miocene part of the drilled interval (i.e., lithostratigraphic Unit 4), and kindly identified by W. Hinsch, Kiel, Germany. He contributed the following list. The identifications confirm the foraminiferal and nannoplankton ages.

397-93-1, 68 cm	<i>Turritella pseudogradata</i> Cossman and Peyrot, 1922. Occurrence: Aquitanian/Burdigalian (early Miocene).
397-92-2, 75 cm	<i>Ceratocyathus</i> sp.
397-92-4, 32 cm	<i>Flabellum</i> sp.

397-93-2, 23 cm	<i>Gryphostrea ricardi</i> (Cossman and Peyrot, 1914), 1 right-hand shell. Occurrence: early Burdigalian (upper early Miocene).
397-95-1, 15-50 cm	<i>Acanthocyathus</i> cf. <i>laterocristatus</i> (Milne-Edwards and Haime, 1848). Occurrence: ? Oligocene, Burdigalian to Tortonian (Miocene). <i>Anadara diluvii</i> (Lamarck, 1805). Occurrence: late Oligocene to Recent.
397-95-4, 45-46 cm	<i>Turricula</i> (<i>Surcula</i>) cf. <i>regularis</i> (Koninck, 1837). Occurrence: middle Oligocene to ? early Miocene.
397-96-1, 63 cm	<i>Ficus conditus</i> (Brongnart, 1823). Occurrence: late Oligocene to Pliocene.
397A-4-3, 39-40 cm	<i>Glycymeris bimaculata saucatsensis</i> (Mayer, 1868). Occurrence: Burdigalian to Helvetian (Miocene).

Cretaceous

Three ammonites and one bivalve were identified by J. Wiedmann (this volume). Both ammonites belong to long-ranging, conservative groups of species: (1) *Proteragonites* cf. *crebriculatus* (Uhlig), to the group of *P. quadrisulatus* (d'Orbigny); and (2) *Phylloceras* cf. *thetys diegoi*, Boule, Lemoine, and Thevenin, to the group of *P. thetys* (d'Orbigny). The most appropriate age for both specimens is Barremian. (3) A *Neocomites* gr. *N. neocomiensis* (d'Orb.) supports a Valanginian to early Hauterivian age. This age does not contradict the nannofossil age (late Hauterivian), considering the limited knowledge of ranges, poor preservation, and taxonomic difficulties.

NEOGENE SEDIMENTATION RATES AT SITE 397

The accumulation rates of the Neogene sediments cored continuously at Holes 397 and 397A are extremely high for a section dominated by pelagic biogenic components.

Detailed sedimentation rate curves have been constructed on the basis of nannofossil zonal boundaries (Figure 13) and planktonic foraminifers (Figure 14) in the samples examined. Biostratigraphic data at Site 397 are given in these figures. The late Neogene sedimentation rates based on both approaches are consistent.

Neogene Sedimentation Rates Based on Nannoplankton

The chronostratigraphic scale used for the respective zonal boundaries is taken from Martini (1976, table 1).

Early Miocene sediments (Cores 397A-21 to 397-80), from *Sphenolithus belemnoides* Zone (NN 3) to *Helicopontosphaera ampliapertura* Zone (NN 4), accumulated extremely rapidly (approximately 180 m/m.y.; see Figure 13). Probably the same rate of sedimentation also occurred during what is recognized as the *Discoaster druggi* Zone (NN 2; Samples 397A-52, CC to 397A-21, CC).

During the late part of early Miocene to the middle part of middle Miocene, represented by Section 397-77-3 to Core 397-73 and including *Sphenolithus heteromorphus* Zone (NN 5) to *Discoaster kugleri* Zone (NN 7), the average rate slowed to 15 m/m.y.

In the middle Miocene, there is a stratigraphic gap which, according to the sedimentation rate curves, has a duration of approximately 1.5 m.y.

Slumps are a major component of late Miocene sedimentation (Cores 397-72 to 397-43), from *Discoaster hamatus* Zone (NN 9) to *Discoaster quinqueramus* Zone (NN 11). The rate was approximately 50 m/m.y., but it is very difficult to determine the accumulation rate for this part of the hole.

After the early Miocene (Cores 397-42 to 397-15), the average rate in the Pliocene, from *Ceratolithus tricoroniculatus* Zone (NN 12) to *Discoaster brouveri* Zone (NN 18), increased to approximately 82 m/m.y.

During the Quaternary (Cores 397-15 to 397-1; *Pseudomemiliana lacunosa* Zone, NN 19, to *Emiliania huxleyi* Zone, NN 21), the rate of accumulation increased at the base to 89 m/m.y.; in the last 0.6 m.y.B.P., it dropped to 50 m/m.y.

These rates discussed above are very similar to those found using the planktonic foraminifer zonation from Site 397 (Figure 14).

Neogene Sedimentation Rates Based on Planktonic Foraminifers

The chronostratigraphic scale used for the respective zonal boundaries is taken from the paleomagnetic calibration of Ryan et al. (1974) with a modification of Martini for the boundary of the base of Zone NN 14 (personal communication to P. Čepik

The extremely rapid rates in the early Miocene (120 m/m.y.) result from the interaction of (a) volcanogenic debris flows derived from the Canaries, (2) accumulation of turbidity current transported sand and silts from Africa, and (3) subaqueous debris flows from the continental slope.

A late Miocene debris flow (Section 57-3 to Core 61) is located at approximately 8 m.y. by its position near the *Globorotalia merotumida*/*G. plesiotumida* evolutionary change. The slump deposits associated with the debris flow may have been emplaced instantaneously in a geological sense.

A stratigraphic gap is placed in the middle Miocene and according to the sedimentation rate curves, it has a duration of approximately 2 m.y.

The rate of accumulation of the preserved middle Miocene ranges from 20 to 30 m/m.y. with an uncertainty depending upon the duration of the stratigraphic gap.

A marked change in sedimentation rates is observed around 16 m.y. which may be related to (1) eustatic sea level rises accompanying early-middle Miocene warming and deglaciation of parts of the Antarctic ice caps; (2) the rise of the CCD in middle Miocene times recorded in all the other oceans (i.e., the so-called middle Miocene environmental crisis); and (3) the strong winnowing of sediments by geostrophic boundary currents whose acme is probably related to the D₂ erosional surface.

The Plio/Quaternary rate is approximately 80 m/m.y. dropping to 50 m/m.y. for the late Miocene. The pre-D₂ early Miocene sedimentation rates are extremely fast and range from 120 to 145 m/m.y.

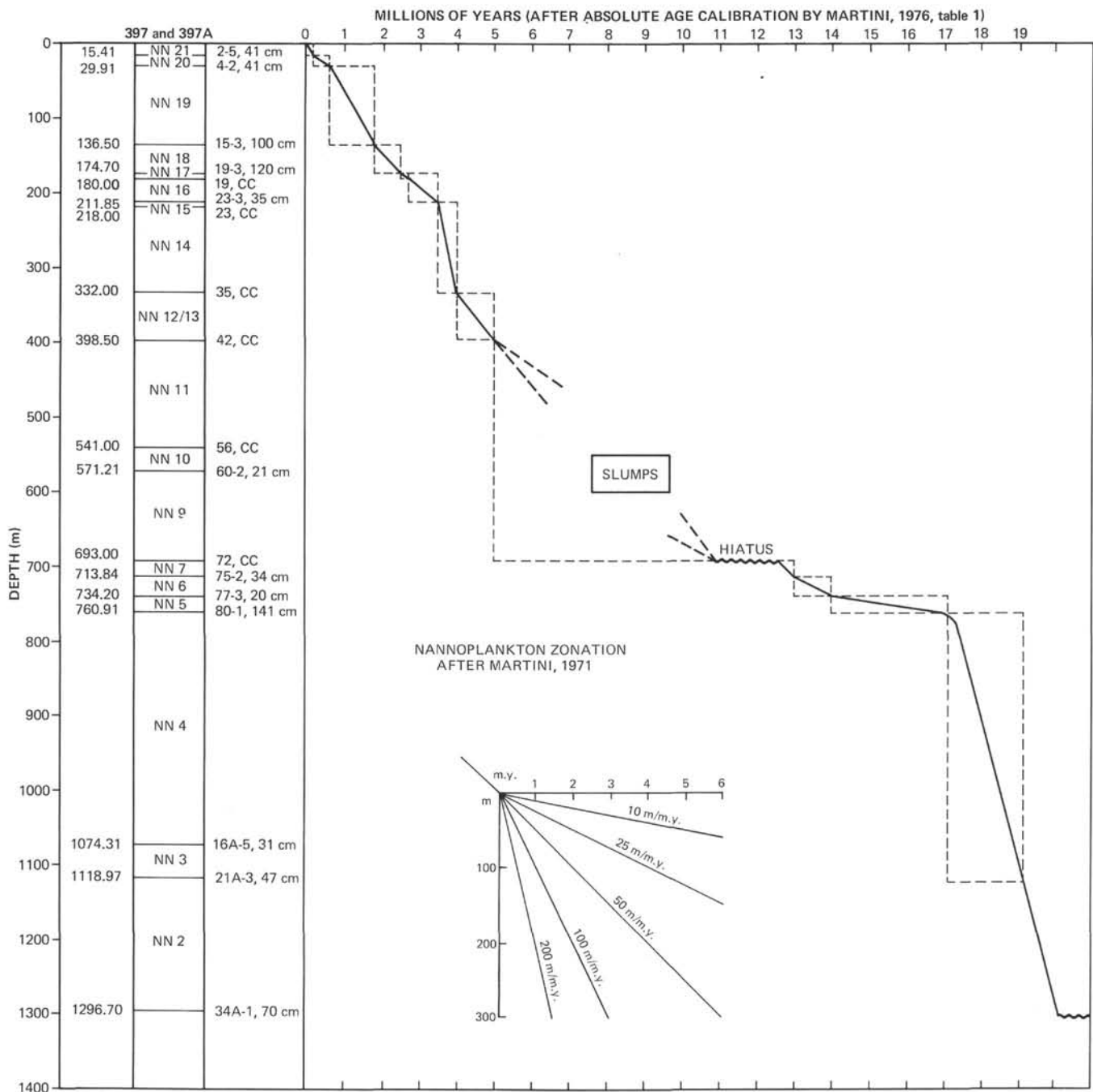


Figure 13. Sedimentation rates in the Neogene Section at Site 397.

The more or less uniform rates for lithologic Unit 1 at this site, consisting of nannofossil oozes and marls, are attributed to a high productivity in an area of upwelling. If we do not take into account differences due to terrigenous dilution, the biogenic production could exceed that of the equatorial Pacific Site 62.1 by three times! This difference might be accounted for by a concentration through winnowing of the biogenic components and terrigenous clays at Site 397 by bottom currents at the base of the continental slope. The more modest rates recorded for the deeper part of the late Miocene are at-

tributed, in part, to dissolution observed in the foraminiferal tests and in part due to compaction.

Cretaceous Sedimentation Rates

The Cretaceous sedimentation rates are more uncertain than those of the Neogene due to the lack of a precise stratigraphic zonation. Four approaches are considered:

1) **Geophysical:** The sediments directly beneath the unconformity at 1300 meters sub-bottom are considered to be Hauterivian in age (< 126 m.y.) and the lowermost

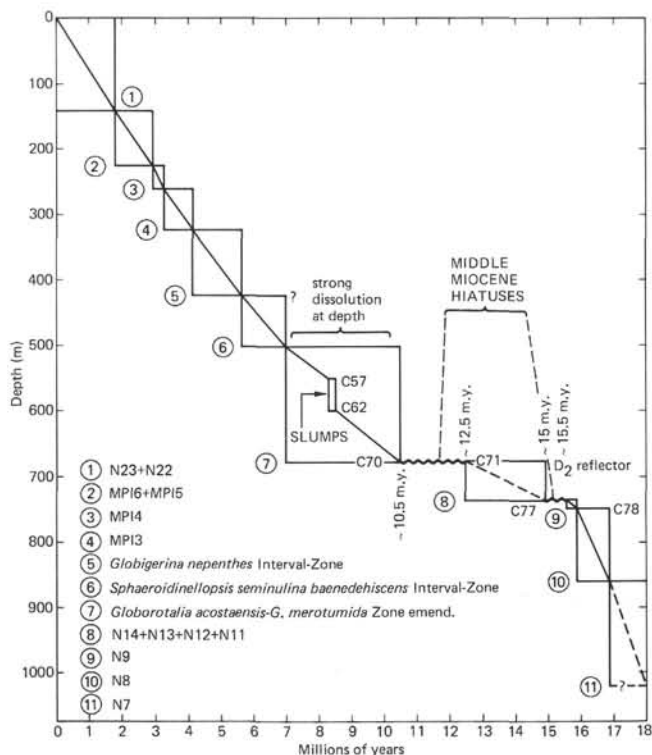


Figure 14. Sedimentation rates at Site 397, based on planktonic foraminifers.

strata at Site 369 are late Aptian in age (>108 m.y.). The immediate pre-unconformity layer can be traced landward beneath the slope and occurs at Site 369 approximately 1.9 seconds (= 3 km at 3.2 km/s interval velocity) below the Aptian horizon. If we assume a uniform sedimentation rate, the average for this Early Cretaceous interval is 166 m/m.y.

2) **Sedimentological:** The Early Cretaceous has a varve-like appearance. Some alternating laminae are 0.1-0.5 mm in thickness and if we assume them to be annual varves we get accumulation rates >100 m/m.y.

3) **Magnetostratigraphical:** The pre-Albian Cretaceous and Late Jurassic contains numerous magnetic polarity changes mapped within the Atlantic and Pacific oceans as the Mesozoic lineations *M-0* to *M-25*. On the average the frequency of magnetic reversals was greater than one every million years. The longest normal interval is approximately 1.5 m.y. in duration. Only one interval of unambiguous negative polarity was observed in Cores 397A-34 to 52 in an otherwise normal sequence with the possibility of a second interval of low inclination being misidentified as normally magnetized due to deviation of the hole from vertical. If Unit 5 is correlated with the interval between anomalies *M-3* and *M-5* and if the large interval of normal polarity is not produced by secondary overprint, the 150-meter Early Cretaceous sequence is not likely to exceed 2 m.y. in duration, giving a predicted sedimentation rate of >75 m/m.y.

4) **Biostratigraphical:** Due to the scantiness of foraminifers, only calcareous nannofossils will be used

for documenting the Early Cretaceous age of Cores 397A-34 to 52. The nannofossil assemblage can be entirely assigned to the *Calcicalathina oblongata* or *Lithraphidites bollii* Zone (Wind and Čepék this volume). The presence of *Cruciallopsis cuvillieri* with an extinction level within the late Hauterivian might indicate a minimum age. If we assume that the cored interval represents approximately 1 to 2 m.y. (after the van Hinte, 1976, time scale), an accumulation rate of >75 (~ 150) m/m.y. results.

STRATIGRAPHIC HIATUSES

Three stratigraphic gaps have been provisionally detected on the practically continuously cored sections from Holes 397 and 397A. Their recognition is based partly on the absence of certain evolutionary sequences in the microfossil groups, partly on abrupt changes in lithofacies, and to some extent on criteria thought to be indicative of sea-floor erosion or extended periods of non-deposition.

The youngest gap is thought to exist in the late Pliocene. It was first suggested by depositional and/or erosional bed forms in the subsurface illustrated on the *Glomar Challenger* reflection profile (Figure 23). These features are distributed across reflector R-2 (β) and appear as large undulating sediment waves. They correlate in depth with an interval near Cores 25 and 26 of Hole 397 where a noticeable degree of fragmentation and corrosion of the sand-sized calcareous tests was first recorded. Although this fragmentation might be related to laboratory disturbance during washing, the coarse portion contained a slightly unusual amount of large detrital grains. The interval under discussion falls between the extinction horizons of *Sphaeroidinellopsis* (above) and of *Globorotalia margaritae* (below). When analyzing the sedimentation rates, this interval appears as somewhat reduced in thickness if uniform accumulation is assumed. Some additional evidence of something amiss is provided by the shipboard paleomagnetic stratigraphy where a slightly abbreviated Gauss Epoch was discerned which lacked one of its two reversal events. The gap, if it exists, is perhaps only 0.1 m.y. in duration. Its biostratigraphic position would place it approximate to 3 m.y.B.P. more or less coincidental with the abrupt glacial cooling seen at Site 112 in the Labrador Sea and within the interval of cutting of marine terraces around the Canary Islands. The gap may, in fact, not be a true hiatus in the sense of an omission surface, but may simply reflect either a much reduced rate of accumulation or short episodes of winnowing accompanied by partial fragmentation and dissolution of exposed calcareous tests.

The 3 m.y.B.P. level has been discussed by Schlanger and Douglas (1974) as one of the significant oceanographic changes leading to incipient diagenesis in carbonate sediments and the formation of an oceanwide reflecting horizon labeled by them as reflector "a" (see also Cita and Ryan, this volume).

The next older gap is considerably more distinct and falls between the late and middle Miocene. It is assigned

to a position between Cores 397-70 (foraminiferal evidence, Figure 14) and 73 (nannoplankton evidence; Figures 10, 13). No discrete lithologic change was detected according to the visual core descriptions. The gap lies in the close vicinity to the extinction horizon of *Globorotalia mayeri* and between the upwardmost occurrence of *Discoaster exilis* and the lowermost record of *Discoaster hamatus*. By a combination of extrapolation of sedimentation rates downwards through the late Miocene and upwards through the middle Miocene, the late to middle Miocene hiatus extends from approximately 10.5 to 12.5 m.y.B.P. according to the foraminiferal biozonation and 11.0 to 12.5 m.y.B.P. according to the nannofossil zonation.

The approximate 2 m.y. duration of this gap is more or less in agreement with the thickness interval between reflectors R-6 (β) to D₂ noted on the seismic profile along the initial approach to the drill site.

The late/middle Miocene hiatus is probably a true "omission" surface, induced by ocean-floor erosion. A significant lithologic change is also noticed from Cores 69 to 73 where the carbonate content versus detrital minerals changes very rapidly, unlike the overlying and underlying intervals. The diachronous downcutting is illustrated by seismic horizon D₂ in the lower slope/upper rise region off Cape Bojador. A gap at a similar stratigraphic position occurs at Site 369 at a sub-bottom depth of 80 meters. An additional short mid-Miocene hiatus between 15 and 15.5 m.y. is only evident from the foraminiferal record (see Figure 14).

The next stratigraphic gap discussed is a true chasm with a hiatus representing 100 m.y. In less than 20 cm of Section 1 of Core 397A-34, the lithology changes from a semi-indurated radiolarian-bearing, nannofossil mudstone of early Miocene age to a tightly compacted non-bioturbated shale deposited during the Early Cretaceous. The actual discontinuity has probably been mechanically distorted by the coring operations.

The oldest sediment recovered directly above the visually abrupt change in facies belongs to foraminiferal Zone N.5-N.6 and to nannofossil Zone NN 2. The oldest sediment with an intact lithology in the entire overlying sequence is late Oligocene belonging to the *Globorotalia opima opima* foraminiferal zone (P.21) and the *Sphenolithus distentus* nannofossil zone (NP 24). The Oligocene sediment is an original biogenic hemipelagic deposit now found only as thin lenses intercalated within large lower Miocene slump masses belonging to lithologic Unit 3. The Oligocene sediment is especially prevalent in Cores 397A-15, 16, and 17 and indicates that the first recorded deposition above the large discontinuity in Core 397A-34 began somewhat prior to 25 m.y.B.P. (with a probable position at 30 to 27 m.y.). The youngest sediment below the discontinuity is assigned to a late Hauterivian age. For a detailed discussion of the age and causes of this huge gap see Arthur et al. (this volume).

DISCUSSION OF THE AGE OF THE LOWER CRETACEOUS LITHOSTRATIGRAPHIC UNIT 5

A variety of conflicting ages (ranging from Valanginian to Aptian) has been determined for Lower Cretaceous lithostratigraphic Unit 5 (Cores 397A-34 to 397A-52) by different shipboard and shore-based paleontologists (see Wind and Čepek Basov et al.; Roesler et al.; Butt; Wiedmann; all, this volume). In the framework of the sedimentary synthesis (Arthur et al., this volume), sedimentology (Einsele and von Rad, this volume), magnetostratigraphy (Hamilton, this volume), and seismic stratigraphy (Hinz, this volume), the age of Unit 5 has been assumed to be Hauterivian. Therefore, a short summary of the evidence and arguments of all groups working or commenting on Unit 5 might be useful for the reader, as given below.

Biostratigraphy

Nannofossils

Seventy-eight samples (one sample per section) containing calcareous nannoplankton were investigated both at Hannover, Germany (P. Čepek and at Tallahassee, Florida (F. Wind). A few samples were also examined by H. Thierstein (La Jolla, California). In Samples 397A-38, CC to 397A-52, CC, no nannofossils younger than late Hauterivian occur. They contain *Crucellipsis cuvillieri* (known range: Berriasian to Hauterivian, i.e., not younger than late Hauterivian), *Calicalathina oblongata* (not younger than early Barremian), and *Nannoconus kampteri* (not older than late Hauterivian?). Therefore, the nannofossils suggest an age of early-late Hauterivian (see Wind and Čepek this volume). Based on the occurrence of *Diadorhombus erectus* (middle Valanginian), H. Thierstein suggests a Valanginian to early Hauterivian age.

Foraminifers

Roesler, Lutze, and Pflaumann (Kiel University) found a sparse small microfauna in Cores 397A-34 to 397A-52, containing the planktonic foraminiferal genus *Favusella*, from which they described eight specimens by SEM as *Favusella stiftia* n. sp. An age determination based on these favusellas still has to remain open (Roesler et al., this volume). Favusellas from the Albian/Cenomanian are found only in neritic facies. Further investigations are needed to demonstrate whether this paleoecological aspect is applicable also to the pre-Albian precursors which these favusellas might represent.

Basov et al. (Research Institute of the Geology of the Arctic, Leningrad) describe a number of species which are common with those from the upper Barremian to lower Aptian of the North Caucasus, with the middle Barremian of western Austria, and with the middle to upper Barremian of Trinidad (Basov et al., this

volume). They state that all known pre-Barremian faunas are less variable than that found in Section 397A-47-4. They therefore suggest Barremian or Barremian to early Aptian as the most probable age for the upper part of Unit 5 (Cores 397A-41 to 397A-47), whereas Hauterivian age cannot be excluded for the lowermost part of the section.

Butt (Tübingen University) compares the Lower Cretaceous biostratigraphy of Site 397 with that of the Aaiun Basin and Agadir section (Morocco). He found *Hedbergella hoterivica* (which he believes to be the same as *Favusella* sp. of the Kiel group), and several species of *Epistomina*. Butt believes the lower part of Unit 5 (Cores 397A-50 to 397A-52) is late Hauterivian/early Barremian. The middle part (Cores 397A-43 to 397A-50) is Barremian, and the upper part (Cores 397A-42 to 397A-35) is Barremian/Aptian (with a relatively abundant and diverse post-Hauterivian planktonic fauna; see Butt, this volume).

Ammonites

A few fragmented ammonites in aragonitic preservation were found, especially a *Neocomites* ex. gr., *N. neocomiensis*, which supports a Hauterivian interpretation. The other specimens belong to long-ranging species, but are presumed to be Barremian due to their degree of evolution (see Wiedmann, this volume).

Magnetostratigraphic Evidence

Hamilton (this volume) suggests that the dominantly normal polarity of the Cretaceous portion of the sequence in Hole 397A might correlate well with the interval between anomalies *M-3* and *M-5* which are early Hauterivian. This correlation was suggested with knowledge of the information on the nannofossil ages. However, the dominant normal polarity could also represent any interval within the range of Albian through Santonian.

Seismic Evidence

A pre-Aptian age for strata below the major pre-early Miocene unconformity at Site 397 is supported by seismic evidence. Site 369, located higher on the slope, bottomed in upper Aptian strata which appear to be 1 to 2 km stratigraphically higher than the sediments of Unit 5 in Site 397 (Hinz; Wissmann; Arthur et al.; all, this volume).

Sedimentological Evidence

Sedimentological evidence (especially the varve-like laminations in a distal prodelta setting, almost complete lack of sand layers) suggests a comparatively tranquil setting without strong currents, which might have winnowed the entire "autochthonous" nannoflora. However, downslope reworking of more or less contemporaneous coarse-grained and fine-grained components is very conspicuous (prodelta mud environment). There is not evidence for deposition below a CCD (in general, good preservation of nannoflora, some ammonites, calcite-cemented sand layers, etc.; see Einsele and von Rad, this volume).

Conclusion

Weighing all this evidence, the editors and Co-Chief Scientists of Leg 47A recommend usage of late Hauterivian as the official age for all site and synthesis reports, tables, and figures. One should, however, keep in mind that the nannofossil age is not confirmed by the foraminiferal determinations of the group working in Leningrad, which suggests a probable Barremian/Aptian age for this unit.

PALEOMAGNETICS

During Leg 47A, we undertook the first on-board paleomagnetic study of a continuously cored sediment sequence. The advantage of sedimentary paleomagnetic study is well known, since good biostratigraphic control on the same sediments is often possible. This gives an opportunity, dependent on sedimentation rates, to record a downhole magnetic stratigraphy that can be compared to an established geomagnetic time scale.

Paleomagnetic study of sediments is more difficult than a comparable study of igneous rocks. The intensities of natural remnant magnetization (NRM) of pelagic (biogenic) and hemipelagic sediments are several orders of magnitude less. Thus, a measuring system of high sensitivity is required. To meet this objective, a sophisticated computerized spinner magnetometer (Digico magnetometer system) was installed onboard *Glomar Challenger* at the commencement of Leg 47. The principles of operation of this system are described by Molyneux (1971).

Demagnetization studies are a necessary adjunct to any comprehensive paleomagnetic study. We accomplished this on board in a preliminary way, by using a newly designed alternating field demagnetizer (Molyneux, personal communication). A major advantage offered by this unit over those employed on previous legs is two-axis as opposed to single-axis tumbling. The demagnetizer appears to be reliable for peak fields up to 600 Oe without introducing any appreciable anhysteritic magnetization in the samples.

To monitor the downhole magnetic stratigraphy, the sampling frequency should be such that resolution of all epochs (and ideally all events) recorded within the penetrated section is achieved. This is dependent on sedimentation rates and is constrained by the need to avoid disturbed intervals whether caused by drilling artifacts or by natural phenomena, such as slumping. Another limitation relates to reliable remanence measurement of weakly magnetized sediments. Onboard *Glomar Challenger*, as a compromise between expediency and reliability, we used a signal integration time of 2⁶ spins for NRM measurement of some 178 samples with subsequent measurement on 2⁷ spins after AF demagnetization at 50 Oe. Post-cruise shore-based studies on the entire Quaternary/Neogene paleomagnetic sample collection employed a longer signal integration time corresponding to 2⁹ spins; this improved measurement precision after further demagnetization at high peak fields of 150 to 300 Oe in an effort to isolate stable remanence directions. A more detailed account of

these stability studies, together with the full paleomagnetic results, are contained in Hamilton (this volume).

We encountered predominantly low NRM intensities in the range of 0.1 to 0.7×10^{-6} G for the Quaternary and upper Neogene part of the drilled interval down to a sub-bottom depth of 450 meters. Variable intensity values, normally within the range of 0.5 to 20×10^{-6} G, typify the remainder of the Neogene section (down to 1300 m). Some higher intensities, up to 420×10^{-6} G, are associated with the volcanoclastic sandstones and conglomerates. The Cretaceous sediments have a mean NRM intensity of $15.83 \pm 15.44 \times 10^{-6}$ G.

We measured volume susceptibility of all samples used for paleomagnetic studies with a Highmoor inductance bridge system. The bridge was calibrated using salts of known susceptibility and igneous rock standards whose susceptibility are well established.

Volume susceptibilities at Site 397 are in the range 10^{-3} to 10^{-6} G/Oe. Lowest susceptibility values are found for the nannofossil marl oozes of the Quaternary; the highest values as associated with the volcanoclastic conglomerates and sandstones of the middle Miocene. Table 13 gives a summary of the mean susceptibilities of the principal lithologic units; complete magnetic susceptibility results for Site 397 samples are presented by Hamilton (this volume).

The quality of the paleomagnetic data is such as to justify an attempt to define a tentative magnetic polarity stratigraphy for Site 397. An outline of this is given here (for details, see Hamilton, this volume). Between the sea bottom and the occurrence of slumps in Core 397-57, the interval is assigned on the magnetic polarity time scale from the Brunhes Epoch through Epoch 7 times. Within the upper Matuyama Epoch, a possible condensed sediment sequence or hiatus may be present between the base of the Jaramillo (103 m sub-bottom) and the Olduvai events, if the magnetic polarity assignment is correct. Below the Olduvai, a long reversed interval (represented by 60 m of sediments) records a high sedimentation rate within lower Matuyama Epoch times. The underlying Gauss Epoch recorded at this site is not as straightforward as that normally recognized. The normal intervals within this epoch are much shorter than expected, perhaps again reflecting possible hiatuses. Likewise, only two of the few normal events

within the Gilbert Epoch are recognized. Nevertheless, we located the Gilbert/Epoch 5 boundary at a sub-bottom depth of 398 meters, i.e., between Cores 397-42 and 397-43. This correlates well with the biostratigraphic placement of this boundary. The slump horizons occur below a reversed interval, possibly in Epoch 7 times.

Gaps in the sampling, particularly where the debris flows occur, make difficult an unambiguous correlation to the geomagnetic polarity time scale below Core 397-57. Tentatively, we can assign the fragmentary polarity record by using the biostratigraphic control. Thus, the magnetic stratigraphy between Cores 397-57 and 397-72 indicates Epochs 9/10 and possibly Epoch 11. From 700 to 1300 meters, the lower Neogene section is referred to Epochs 16 through 19.

The 153 meters of Lower Cretaceous sediments reveal a sequence of dominantly normal polarity; only a single thin reversed zone is encountered in Core 397A-35. This may be correlated with the long normal epoch of the M5 marine magnetic anomaly sequence (123-124 m.y.B.P. after van Hinte, 1976, time scale).

DOWNHOLE TEMPERATURE MEASUREMENTS

Two downhole temperature measurements were made in Hole 397 and two in Hole 397A. Of four successful runs, only two gave data which were considered to be reliable in calculating *in-situ* thermal gradients. The temperatures were obtained using an entirely self-contained temperature recorder (see Site Chapter Introduction and Explanatory Notes), which was inserted into a core barrel with a thermistor probe protruding about 50 cm through the center of the core catcher. Upon drilling to the depth where a temperature measurement was desired, the core barrel was lowered on the sand line to the bottom of the drill string. Once the core barrel was locked into the bottom-hole assembly, the drill string was gradually lowered to the bottom of the hole. Lowering pushed the thermistor probe into the undrilled sediment in front of the bit, where it remained for approximately 20 minutes with about 8 to 10 thousand pounds of weight on the drill bit. Calm seas and an alert and skilled drilling team and electronics technician were major assets to the collection of high-quality data.

Measurements 1-3 showed that the thermistor came more or less into thermal equilibrium with the adjacent sediment. However, measurement 2 (Figure 16) was considered unreasonably low, possibly due to excessive cooling of the bottom-hole sediments (dense shales) by vigorous circulation of drilling fluids. This measurement was discarded, although the plateau looks similar to that of measurement 2.

Measurements 1 and 3 (Figures 15, 17) in plastic oozes and marls were judged to be satisfactory, and both indicated little disturbance from frictional heating or thermal convection during the actual measurement interval.

The sea-floor water temperature is estimated at about 4.75°C based on data from the thermistor probe as it passed the mudline during its descent to the bottom of the hole and its ascent back to the drill floor.

TABLE 13
Summary of Magnetic Susceptibility, Site 397

Lithologic Unit	Number of Samples	Mean Susceptibility $\times 10^{-6}$ G/Oe (\pm sd)
Sub-unit 1A	17	6.57 ± 12.11
Sub-unit 1A	15 ^a	2.86 ± 1.10
Sub-unit 1B	27	3.96 ± 1.26
Unit 1	44	4.92 ± 7.58
Unit 2	23	7.23 ± 5.95
Unit 3	27	21.93 ± 18.79
Unit 4	50	127.70 ± 282.67
Unit 5	21	28.28 ± 13.18

^aExcluding uppermost two samples (397-1-1, 16-18 cm and 397-2-1, 61-63 cm).

The thermal measurements are listed below; the continuously recorded temperature data for each station are illustrated in Figures 15, 16, 17, and 18.

Two further measurements were attempted at the bottom of Hole 397A: neither was wholly successful. A six-hour measurement was attempted at 1429 meters, but electrical problems (a loose soldered joint in the thermistor leads) meant that no data were recorded. It appeared that the medium-length thermistor probe had penetrated the Cretaceous shales, so another measurement (20 minutes duration) was attempted. This measurement (no. 5, Figure 18) gave a mean downhole temperature of 23 °C at 1438 meters rising to about 27 ° at end of the 20 minutes measuring time. It was felt that due to the high pumping rates necessary to drill through these compacted shales, a high degree of sediment cooling had occurred, even 30 cm ahead of the bit. This interpretation is confirmed by the temperature rise observed over the measuring period.

Hole	Temperature Measurement	Sub-Bottom Depth (m)	Sediment Temperature (°C)	Figure
397	1	360.5	19.5 ± 0.5	15
397	2	579.0	18.1 ± 0.25 (?)	16
397A	3	447.5	22.5 ± 0.25	17
397A	5	1438	?21 - 27(?)	18

The thermal gradients for Hole 397 is plotted in Figure 19. A single straight line will fit both of the reliable downhole temperature determinations (no. 1 and 3) and the sea-floor estimate, giving an overall mean gradient of 4.2 °C/100 meters. If the measurements are taken separately, the gradient from 0 to 360.5 meters is 4.4 °C/100 meters; from 360.5 to 447.5 meters, the gradient is 3.5 °C/100 meters. However, it is questionable whether a linear extrapolation of the tempera-

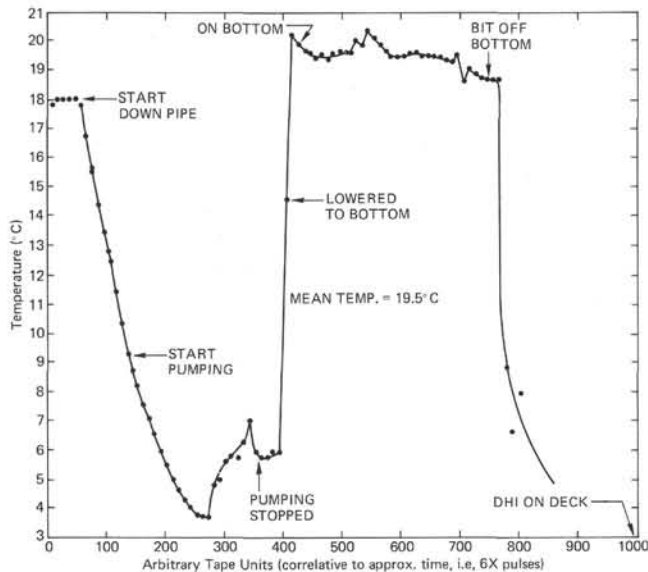


Figure 15. Downhole temperature measurement 1 at 360.5 meters sub-bottom at Site 397.

ture values of the uppermost 450 meters to a total depth of 1450 meters (and below) is possible.

The change in gradient at depth to a lesser value is consistent with relatively higher thermal conductivities in the more compacted and lithified sediments. Conductivities were measured in recovered core samples with a needle probe technique, but the data must be reduced because of the lack of thermistor calibrations aboard ship. Rough estimates (Ryan, personal communication) range from 3.0 to 3.5 mcal/cm s °C.

Multiplication of the mean thermal gradient of 4.2 °C/100 meters by the estimated conductivity values gives a thermal heat flow of 1.3 to 1.5 × 10⁻⁶ cal/cm² at the drillsite location. The calculations bracket the worldwide average value of 1.35 HFU and do not differ greatly from other measurements made on passive-type margins by 10-meter to 15-meter long thermoprobes.

We conclude that the northwestern Africa margin has an adequate thermal gradient such that organic-rich sediments buried at sub-bottom depths exceeding 1.5 to 2 km will reach temperatures sufficient for the initiation of the process of thermal chemical maturation of the sedimentary organic matter, leading to the generation of potentially mobile hydrocarbons.

A thermal gradient of 4.2 °/100 m might be explained as a regional anomaly produced by the mid-Tertiary evolution of the Canary Island volcanism (Arthur et al., this volume). Temperature gradients in the nearby shelf well Spansah 51A-1 (outer Aaiun Basin) are considerably lower (2-3 °C/100 m). For example, the offshore well Alisio 15A-1 (N of Cape Bojador) has a temperature of 119 °C at 34-82 m total penetration, corresponding to a thermal gradient of approximately 3 °C/100 m (Connan, 1974).

CORRELATION OF SEISMIC REFLECTION PROFILES WITH DRILLING RESULTS

Introduction

Prior to Leg 47A, the Bundesanstalt für Geowissenschaften und Rohstoffe (BGR, Hannover) had proposed five drill sites at the Cape Bojador continental slope and rise. These sites were selected on the basis of detailed presite survey by R/V *Meteor* and R/V *Valdivia* (Hinz et al., 1974; Seibold and Hinz, 1976; von Rad et al., 1979). A 24-fold stacked profile (A1L), supplied by Geophysical Service International, Ltd. (GSI), provided one additional drill-site proposal (47A-3, see Figure 20). From these six proposed sites, three (47A-1 to 47A-3) were approved by the JOIDES Safety Panel. Site 397 is located close to the proposed (but undrilled) Site 47A-3,⁶ between *Meteor* Profile M-25 A2 (Figure 21) and the GSI line (Figure 22). The airgun profile shot by *Glomar Challenger* during the site approach (Figure 23) proved very useful for the identification of intra-Neogene acoustic horizons, but did not penetrate be-

⁶Because reflectors D₁ (R-9) and D₂ (R-7) converge near proposed Site 47A-3 (pinch-out situation), Site 397 had to be moved about 5 nautical miles seaward (see Figures 20 and 23a).

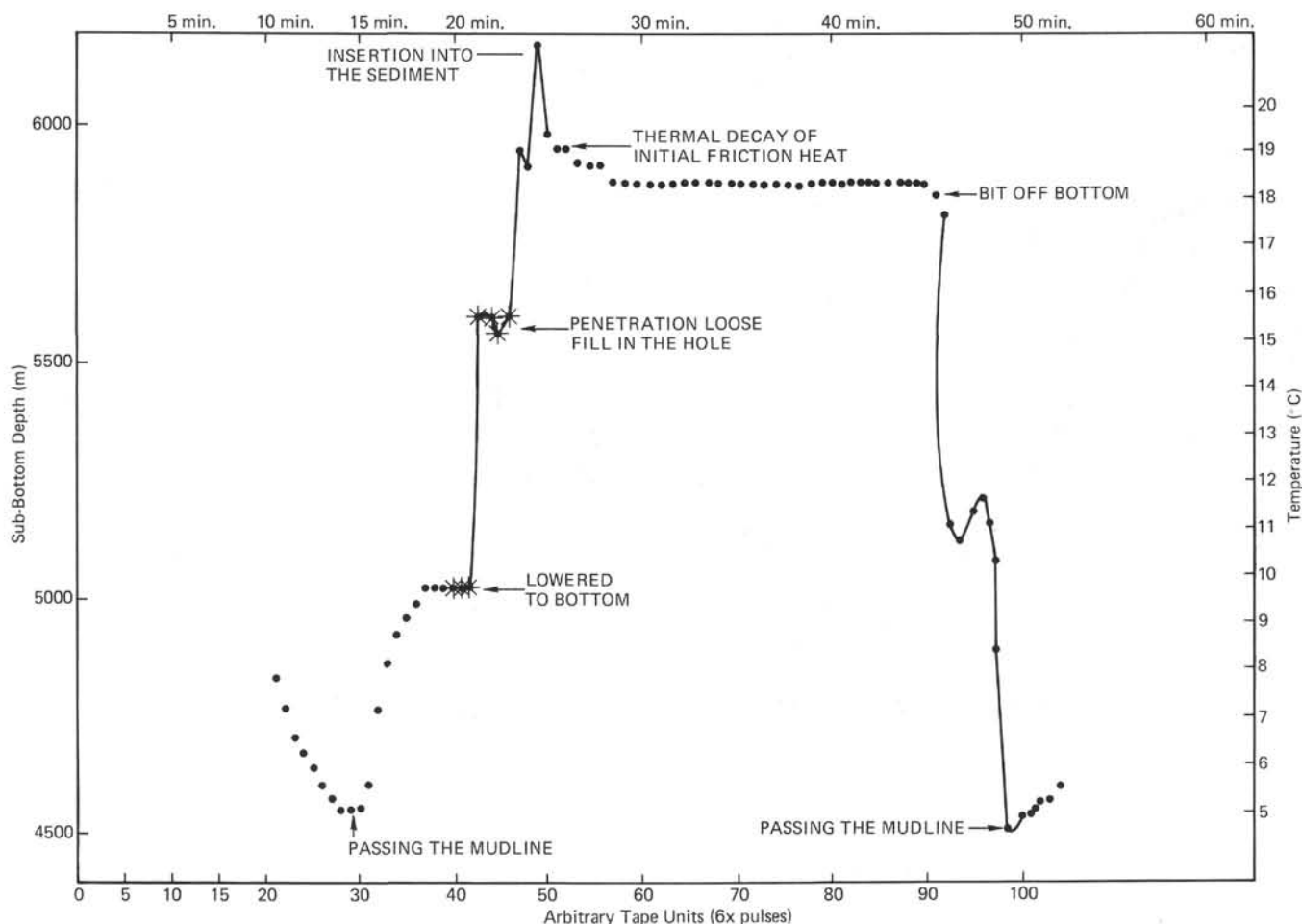


Figure 16. Downhole temperature measurement 2 at 579.0 meters sub-bottom at Site 397.

yond about 1-s two-way travel time below the sea floor. Additional seismic data, which were used for correlation purposes during and after the drilling of Site 397, include a single-channel profile from Lamont-Doherty Geological Observatory (*Vema* 30-05), a new single-channel airgun profile by R/V *Meteor* (M46-37) connecting DSDP Sites 369 and 397 (Figure 24; see also Wissmann, this volume), and commercial multichannel profiles (see Hinz, this volume).

Wissmann (this volume) discusses in detail the differences between pre-site and post-site interpretation of the Cape Bojador slope, as well as the potential pitfalls which await the seismic interpreter in the lower slope region, where many unconformable reflectors merge and meet with the seemingly simple, conformably bedded horizons of the upper rise. There the seismic stratigraphy should be checked by drilling and refined by logging which, unfortunately, was not available during Leg 47A. Hinz (this volume) stresses that a regional acoustostratigraphy should be based on seismically detectable depositional sequences, rather than on the correlation of individual reflectors.

Seismic Reflectors

The following discussion is mainly based on the shipboard report and on information from the drilling record and the GSI-A1L, M25-A2, and *Glomar Challenger* lines. For the immediate vicinity of Site 397, the reflector tags R-1 to R-10 are used (see Table 14) to avoid confusion with the ambiguous and obsolete reflector nomenclature of the literature.

Several erosional horizons are acoustic reflectors on both the *Glomar Challenger* (Figure 23) and *Meteor* seismic profiles (Figure 21) which cross Site 397. A relatively shallow reflector at about 125 meters below the intermediate slope has been referred to as D₂ ("Oligocene to early Miocene") by Hinz et al. (1974) and Seibold and Hinz (1974). This reflector was later dated at Site 369 as early Miocene, where a small diagenetic change observed between calcareous marls and underlying siliceous nannofossil marls (Lancelot, Seibold, et al., 1978). In 1974, Hinz et al. traced this reflector "D₂" downslope to a level at 0.820 s below sea floor in the area where the M-25 A2 profile is proximal to Site

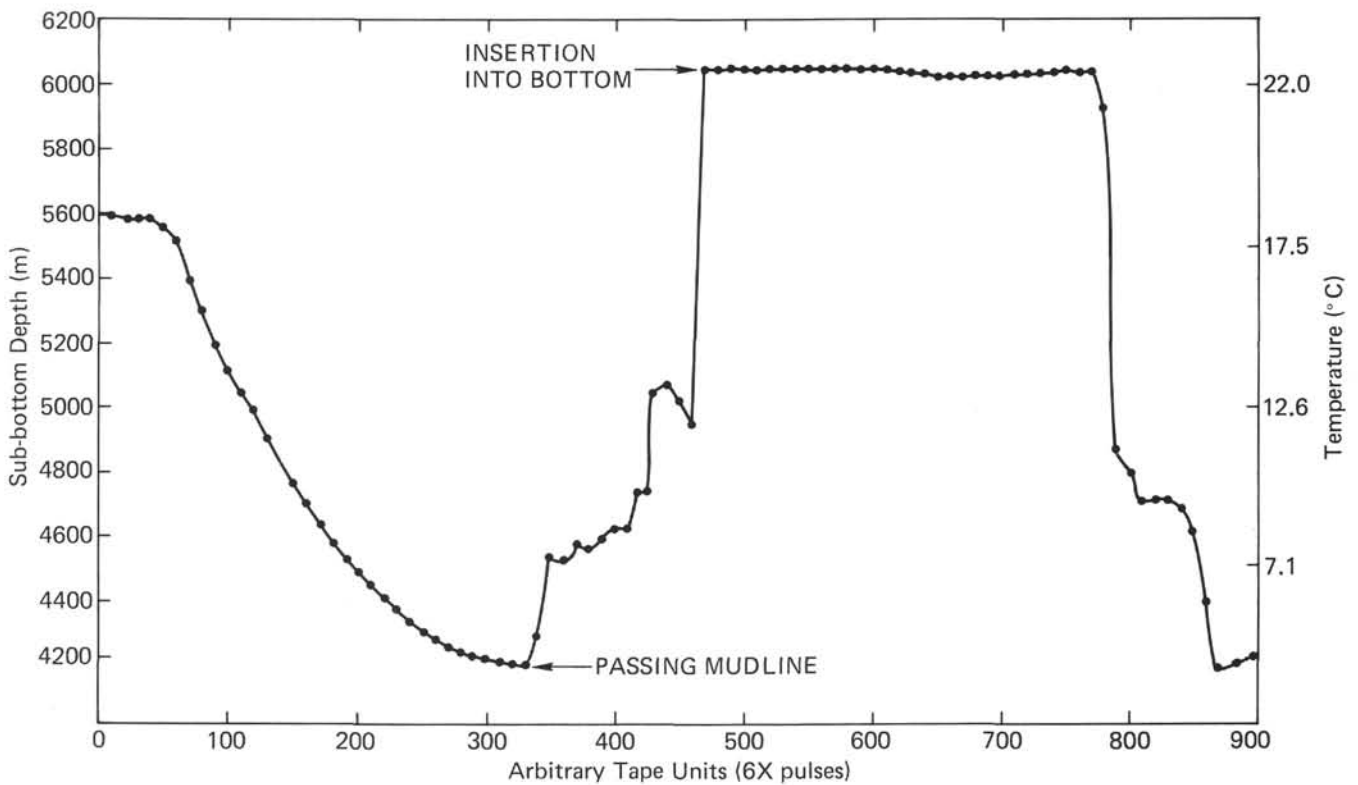


Figure 17. Downhole temperature measurement 3 at 447.5 meters sub-bottom Hole 397A.

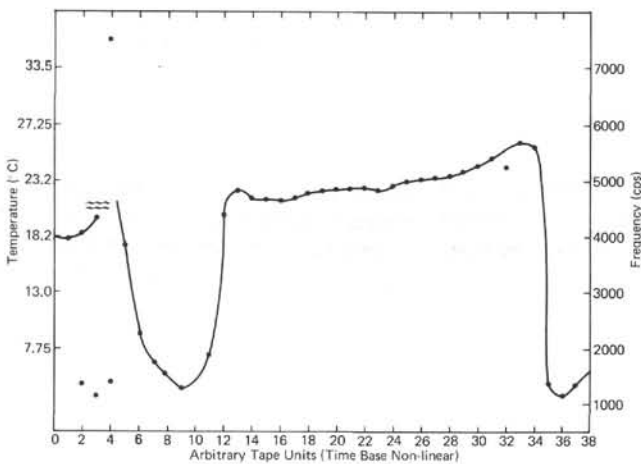


Figure 18. Approximate thermal gradients at Site 397 calculated using downhole temperature measurements 1 through 3.

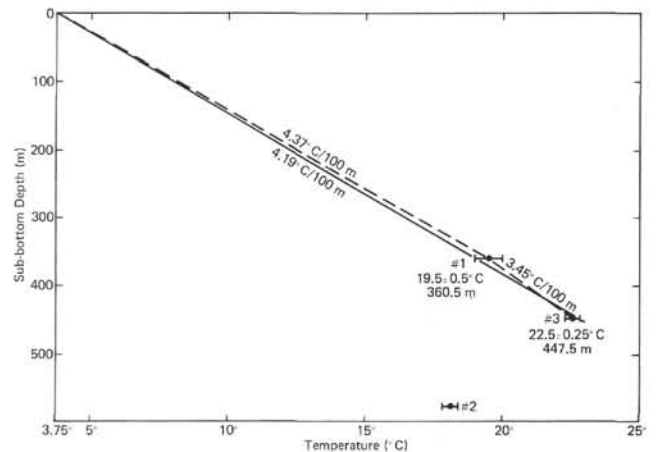


Figure 19. Downhole temperature measurement 5; anomalous sediment cooling (see text).

397. Leg 47A drilling, however, proved that this “rise-D₂” is much younger than “D₂” at Site 369 (see Figure 21).

A deeper reflector at 0.995 s (1.03 s in M25-A2), labeled D₁ (“Cenomanian”) by Hinz et al. (1974). In 1974, this reflector was correlated upslope to a level at about 370 meters, which at Site 369 is equivalent to a 10-meter-thick middle Eocene limestone or to Maestrichtian chalks and porcellanites underlying a 17-m.y.

Eocene hiatus (Figure 21). Along a lengthy stretch of the upper slope of the African margin from Cape Bojador south to Cape Blanc, the deeper so-called D₁ reflector (i.e., R-10 or “rise-D₁”) truncates successively more ancient strata as it descends down the continental slope. Along the lowermost slope just south of Site 397, the younger D₂ horizon (i.e., R-7) cuts deep enough to penetrate to the upslope D₁ horizon. In fact, at one time in the past, the lower slope-D₂ surface created a window into the formerly extensively buried sedimentary layers

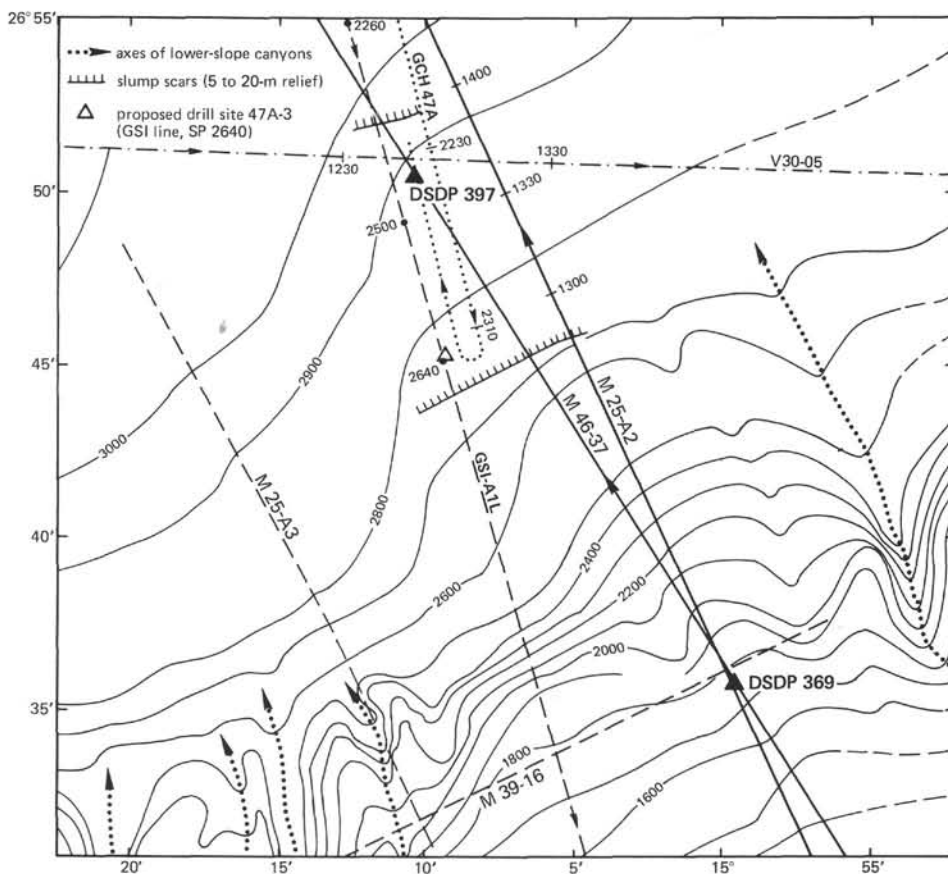


Figure 20. Location sketch of DSDP Sites 397 and 369 and selected seismic profiles: Meteor Profiles M-25, A2, M-39 16, and M-46 37 (all from BGR, Hannover), GSI-line A1L (multichannel), and Glomar Challenger 47A. Bathymetry (depth contours in m) modified after von Rad et al. (1978).

(Hinz et al., 1974, their fig. 2; von Rad et al., 1979, their fig. 4).

The "rise- D_2 (R-7) surface has been contoured on Figure 25 and displays a trough-like configuration whose axis plunges to the southwest. Subsurface channels are depicted by arrows; they reflect conduits into the trough from the Canary Islands at the north and northwest and from the African slope situated to the east and southeast.

In addition to reflectors " D_2 " and " D_1 ," (*sensu* Hinz et al., 1974), five acoustic horizons could be identified on the *Glomar Challenger* and *Meteor* M25-A2 profiles between the sea floor and reflector R-7 (i.e., rise- D_2). They are labeled on Figures 23 and 26, and listed in Table 14 as reflectors R-1 (α), R-2 (β), R-3 (γ), R-4 (δ), and R-5 (ϵ). They are all parallel-bedded and indicate a relatively uniform depositional realm (acoustic Units 1 and 2). The interval between R-5 (δ) and R-6 (ϵ) wedges out against the base of the continental slope. It passes in a landward direction from an acoustically transparent unit (acoustic Sub-unit 3A) with faint internal, non-coherent diffractors to a stratified sequence (acoustic Sub-unit 3b), whose seaward edges have been truncated by erosion. The interval between R-6 (ζ) and R-7 (D_2) is

variable in thickness and ranges from 0.1 s in the approach track to completely absent at the drill site.

In general, the seismic reflectors have been assigned to levels where major lithologic and stratigraphic events have been observed. The independent correlations by Mountain (this volume), placing the reflectors R-1 (α), R-2 (β), and R-7 (δ) at levels of abrupt changes in acoustic impedance, are basically the same as ours (see Table 14 and Figure 27).

The interval from reflectors R-7 (D_2) to R-8 (D_{2a}), i.e. acoustic Unit 4, is highly stratified on the *Glomar Challenger* profile (not on the *Meteor* M25-A2 profile) and its upper surface is somewhat bevelled at the base of the continental slope. The interval from R-8 (D_{2a}) to R-9 (D_1), i.e., acoustic Unit 5, is transparent and exhibits a differential type of deposition, namely, thinner on highs and thicker in depressions. The base of this unit directly overlies the R-9 horizon, which was labeled D_1 in the site prospectus (according to Hinz et al., 1974, their fig. 2).

Stratigraphic Correlation of Reflectors

The correlation of the cores to the reflectors is given in Figures 26 and 27. The correlations are ambigu-

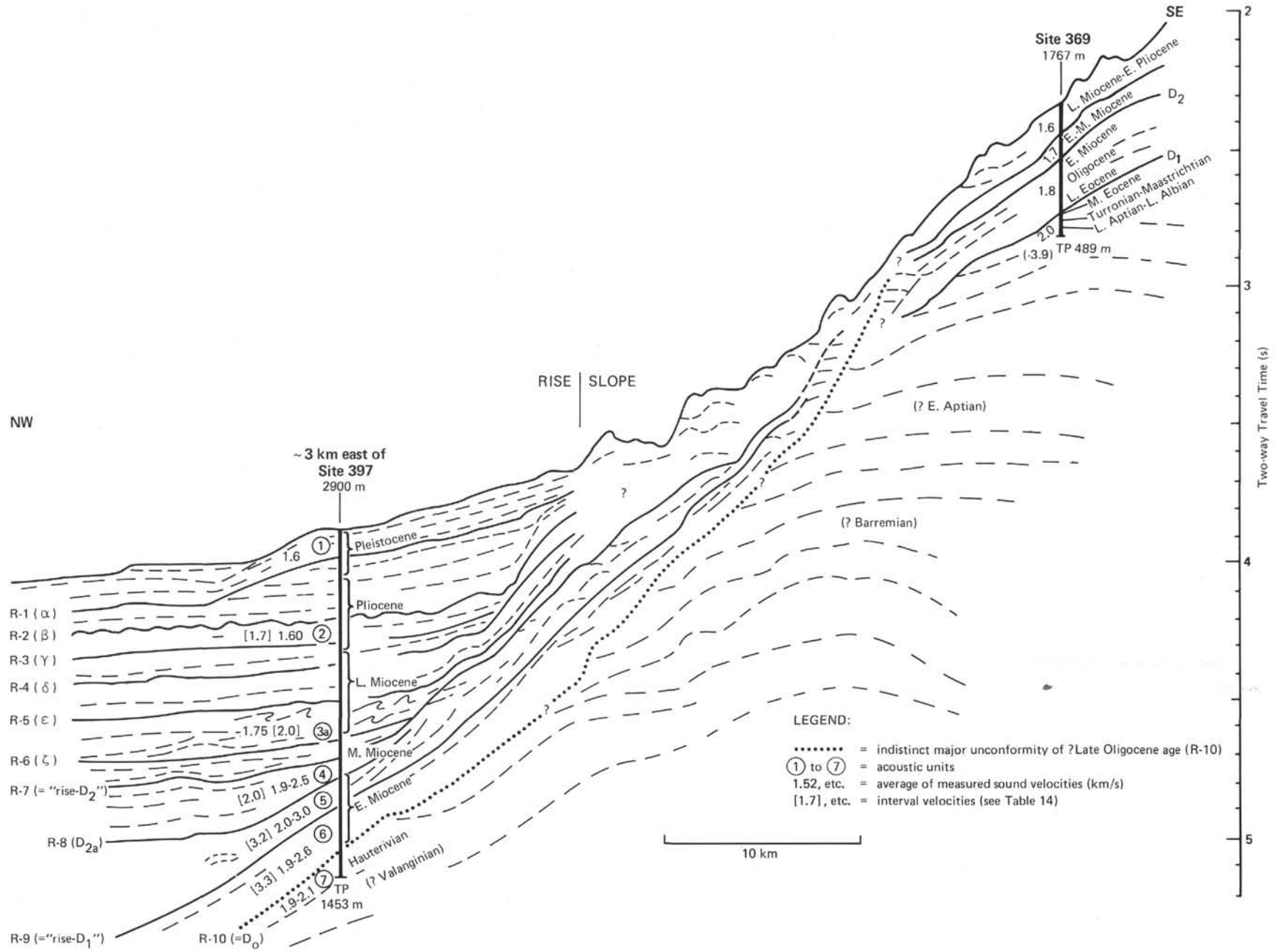


Figure 21. Line drawing of single-channel Meteor Profile M-25 A2 (BGR, Hannover, 1971). Original profile: see Wissmann (this volume, his fig. 1) and Hinze (this volume, his fig. 1).

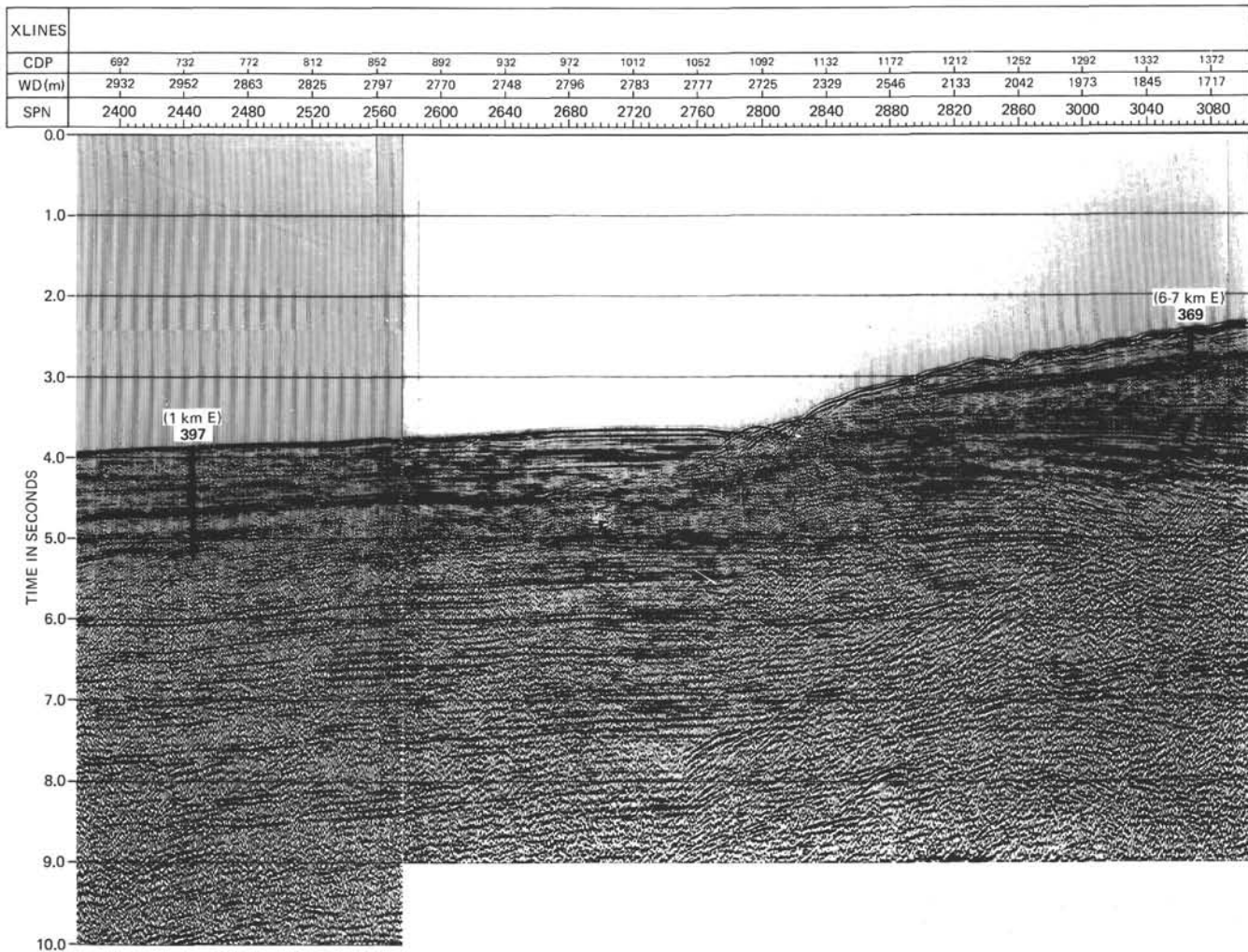


Figure 22a. *Nonexclusive African marine reconnaissance survey line AIL (shotpoints 2400 to 3102; filtered, 24-fold stacked), released for publication by Geophysical Service International, Ltd. (GSI).*

ous; interval velocities calculated by reflector matching with core lithologies have some discrepancies with the velocities measured on the sediments by the Hamilton Frame velocimeter (see Figure 27). The interval velocities (see Table 14) are consistently higher than the measured values in the deeper section. This difference in velocity is tentatively ascribed to the development of minute cracks in the sediment samples, a sort of dilatancy produced by decompression and gas expansion.

The highly stratified acoustic Unit 1 represents well-bedded calcareous oozes of Cores 397-1 to 397-10, which exhibit fluctuating amounts of carbonate and terrigenous minerals. This unit has been dated as belonging to the glacial Pleistocene (0 to 1.1 m.y.B.P.). Its base coincides with a possible minor erosional hiatus at about 100 meters sub-bottom.

Acoustic Unit 2 includes biogenic oozes and marls of the pre-glacial Pleistocene, Pliocene, and late Miocene. Reflector R-2 (β) is tentatively matched with a small increase in the velocity gradient and a discrete bulk density change observed at a short hiatus occurring in Cores 397-25 and 397-26. The first appearance of radiolarians

and diatoms in the coarse fraction is observed above this level. Reflector R-4 (δ) can be placed either at Core 397-50 (450 m) or at Core 397-42 (400 m, top Messinian; Sarnthein, personal communication).

Reflector R-5 (ϵ) coincides with the top of the slump units and breccias of the upper Miocene recorded in Core 397-57. Some of the breccia components may be derived locally from the upslope region of acoustic Subunit 3b which might be equivalent to the interval between reflectors R-6 (ζ) and R-7 (D_2) on the approach profile.

The seismic record on the site approach (left and central part of Figure 23b) shows a layer between reflectors R-6 (ζ) and R-7 (D_2) which pinches out against the slope and is absent on the drill site. A detectable stratigraphic gap (10.5 to 12.5 m.y.B.P.) has been provisionally located between Cores 397-70 and 397-73. Tentatively, we correlate R-7 (D_2) with Core 397-73, and R-6 (ζ) with Core 397-71. Where the missing layer at Site 397 is present at the left of the profile (NNW of Site 397, Figure 23b), it accounts for about 12 per cent of the post-R-7 (D_2) section; thus, the gap may indeed be approximately

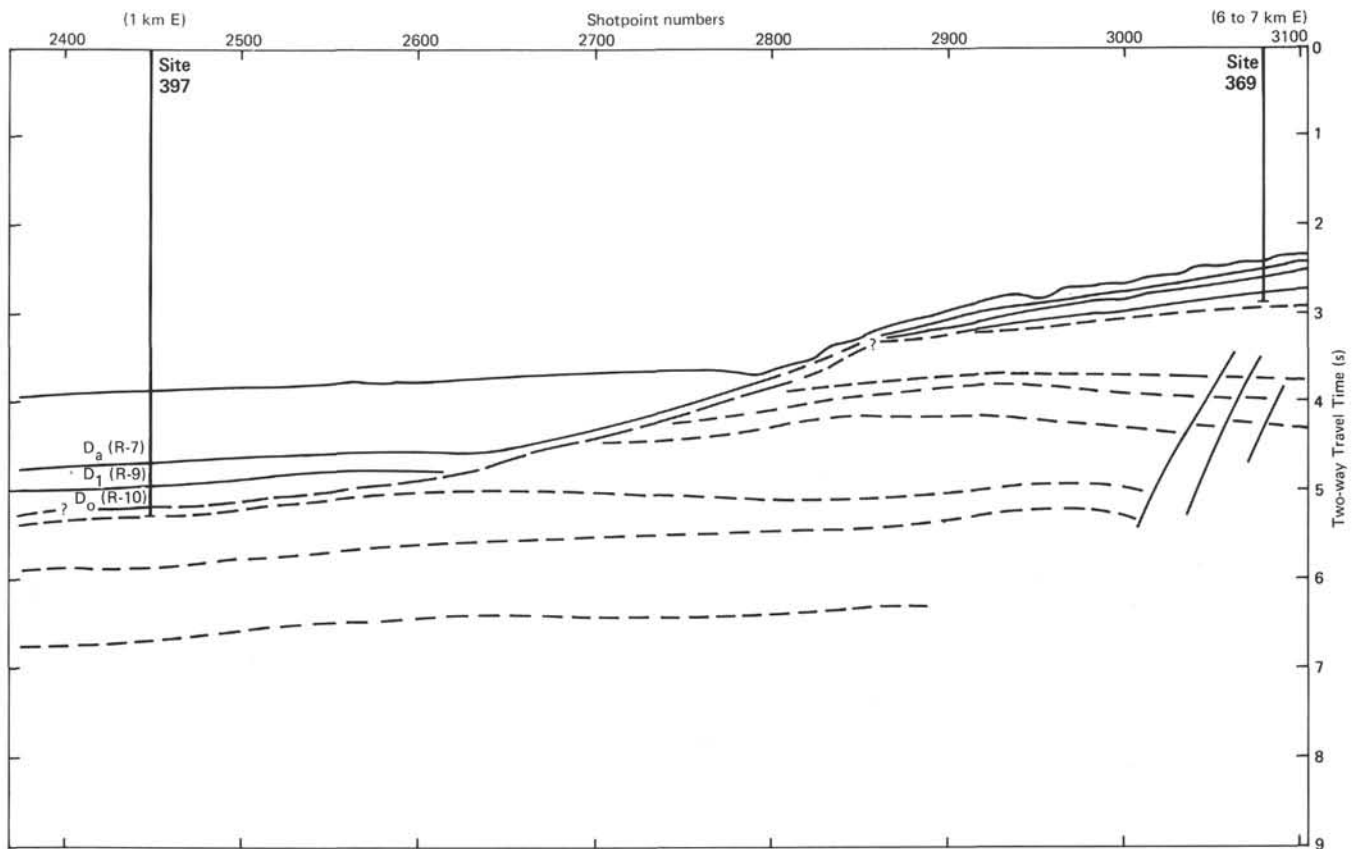


Figure 22b. Line drawing of GSI line A1L showing a modified interpretation by Brown (GSI).

two million years in duration. Another possibility would be to correlate R-7 (D_2) with the top of the uppermost volcanoclastic debris flow V-1 in Core 397-79 (approximately 750 m; see Wissmann, this volume).

Reflector R-8 (D_{2a}) is correlated to Cores 397-85 and 397-86, and marks either the base of the volcanoclastic sandstones derived from Fuerteventura (Cores 397-78 to 397-86; Schmincke and von Rad, this volume) or the top of the thick debris flow V-3 in Core 397-85.

Tentatively, reflector R-9 ("rise- D_1 ") can be assigned to the level of Cores 397A-6 and 397A-7 at 960 to 990 meters sub-bottom, where we penetrated a 20 to 30 meter thick, partly graded, mixed clayey, quartzose, volcanoclastic sandstone (hyaloclastite, V-4, Arthur and von Rad, this volume). The early Miocene age assignment to reflector R-9 (rise- D_1) in the vicinity of the drill site suggests that this horizon beneath the lowermost slope and upper rise is not the same as that originally referred to as D_1 in the intermediate slope region of Site 369 (see Wissmann, this volume). Preliminary results suggest that the upper-rise D_1 reflector (R-9) is isochronous with the intermediate-slope D_2 reflector at Site 369 (early Miocene, Zone NN 4/5, about 17 m.y.B.P.). The upper-rise D_2 reflector (R-7) is time equivalent to an upslope reflector located at 0.1 s sub-bottom at Site 369. This corresponds to a sub-bottom depth of about 80 meters, below which extensive reworking of middle Miocene faunas was observed along with the mixing of nannoplanktons from the NN

9 to the NN 7 zones. A marked change in sedimentation rate is observed at 75 to 80 meters at Site 369 and is considered likely to be the same kind of stratigraphic disturbance located between Cores 397-70 and 397-73. Newer data by Wissmann (this volume) and Hinz (this volume), however, suggest that none of the slope reflectors can be continued onto the upper rise.

The major discontinuity (R-10 or " D_0 ") was eventually discovered at 1300 meters sub-bottom in Hole 397A and separates the early Miocene pebbly mudstone lithologic Unit 4 from the Lower Cretaceous laminated mudstone of Unit 5. It is expressed very vaguely on the Meteor M25-A2 seismic profile at 5.09 s below sea level (about 1.15 to 1.20 s below sea floor) at 1350 hours on 29 October, 1971, and on the GSI A1L line at SP 2500 (2445) at about 1.25 (1.30) s below sea floor (see Figures 21, 22, and 26). The gradient of the erosional escarpment which truncates Paleogene to Lower Cretaceous strata along the lower slope decreases gradually to the uppermost rise. Due to the lack of a large impedance contrast and differences in internal configuration (proximal onlap or concordant relationship between the Lower Miocene and Hauterivian strata) across the 100-m.y. hiatus at Site 397, this unconformity does not produce a significant reflector which can be areally mapped (Hinz; Wissmann; both, this volume). Therefore, the early Miocene/Early Cretaceous unconformity is not recognized on most single-channel reflection profiles, such as the *Glomar Challenger* profile (Figure 23).

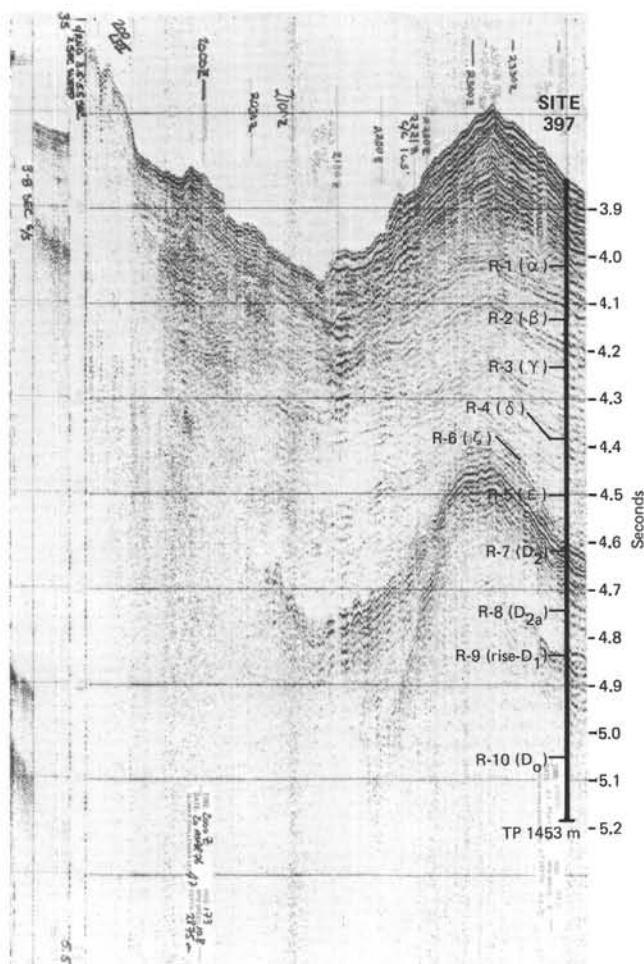


Figure 23a. Glomar Challenger seismic profile on site approach (20 March 1976, 20:00 to 21 March, 00:10). Note the good resolution of Neogene reflectors between sea floor and 1 s sub-bottom (4.9 s below sea level); 3.5- to 5.5-s sweep.

The travel time between the R-9 (rise-D₁) reflector at Site 397 (early Miocene) and the early Miocene/Hauterivian unconformity (tentatively called R-10 or D₀ reflector) is about 0.20 s (profile M-25 A2, see Table 14). With the R-9 reflector assigned to a downhole depth of 970 meters, the calculated interval compressional wave velocity for R-9 to R-10 is about 3.3 km/s.

Measured Sonic and Interval Velocities

Figure 27 and Table 14 show the depth of reflectors, interval compressional wave velocities, and measured sound velocities for Site 397. Between R-1 and R-7 (0 to 700 m sub-bottom), the shipboard velocities are slightly smaller than the computed average "in-situ" compressional wave interval velocities. This systematic difference increases considerably between reflectors R-7 (700 m) and R-10 (1300 m), where the interval velocities are 3.2 or 3.3 km/s, as compared to shipboard average velocities of only 2.47 or 2.3 km/s (see also the Physical Properties sections of this Site Report). The apparent velocity inversion across the major unconformity (2.3

km/s above, 1.9 km/s below R-10) is probably not representative of the earliest Cretaceous sediments, because only the uppermost 153 meters (which showed a downhole velocity increase) were penetrated.

SUMMARY AND CONCLUSIONS

Introduction

Holes 397 and 397A are located on the uppermost continental rise, west-northwest of Cape Bojador (northwestern Africa) at 26°50.7'N, 15°10.8'W, in a water depth of 2900 meters. The thick sequence of Neogene rise sediments and the underlying Early Cretaceous strata were almost continuously cored down to a single-bit record depth of 1453 meters sub-bottom. In Hole 397, 1000 meters were penetrated, 981 meters cored, and 584.83 meters recovered (60%). Because of a plugged drill bit, a second hole (397A) was drilled at the same site. Hole 397A yielded 52 cores, penetrated 467 meters, and recovered 242.66 meters (52%). Extremely slow penetration rates (1 to 2 m/hr) in high-sedimentation-rate Lower Cretaceous mudstones, as well as time constraints forced us to terminate this hole at 1453 meters, although the bit was still in satisfactory condition.

The major objective of Leg 47A, the first IPOD continental margin leg, was to decipher the complex Cretaceous and Tertiary history of a tectonically stable, "flexured," mature passive margin; such a setting (see Uchupi et al., 1976) is provided by the West Saharan margin between the Precambrian to Paleozoic Requibat Uplift (Cape Blanc) and the AntiAtlas Uplift/South Atlas Fault (Cape Juby). The subsiding edge of this marginal basin has experienced major episodes of erosion, non-deposition, and redeposition, especially during the widespread mid-Cretaceous and mid-Tertiary regressive events. Thus, Site 397 was expected to allow a better reconstruction of the history of uplift and subsidence; paleoenvironment evolution; and erosional, depositional, and diagenetic processes from the Early Cretaceous to Neogene. DSDP Site 369 on the continental slope nearby (Lancelot, Seibold, et al., 1978), dredging and coring of the continental slope (von Rad et al., 1979), seismic information (Hinze; Wissmann; both, this volume) and onshore and offshore commercial wells from the Aaiun Basin (von Rad and Einsele, in press) should allow sedimentological, paleontological, and geodynamic rise-slope-shelf comparisons and the evaluation of vertical gradients of water properties through time.

The anticipated stratigraphy of Site 397 was based on the interpretation of reflectors D₁ (R-9) as being mid-Cretaceous to Eocene and D₂ (R-7) as being Oligocene to early Miocene (Figures 21, 23; Table 14). This interpretation was based on the literature (Seibold and Hinze, 1974; Uchupi et al., 1976), and on subsequent drilling (Site 369) and presite surveys. The presence of 1300 meters of Neogene strata proved that this interpretation was wrong and showed that it is almost impossible to trace reflectors across the lower slope, where older layers pinch out and younger ones are onlapping farther

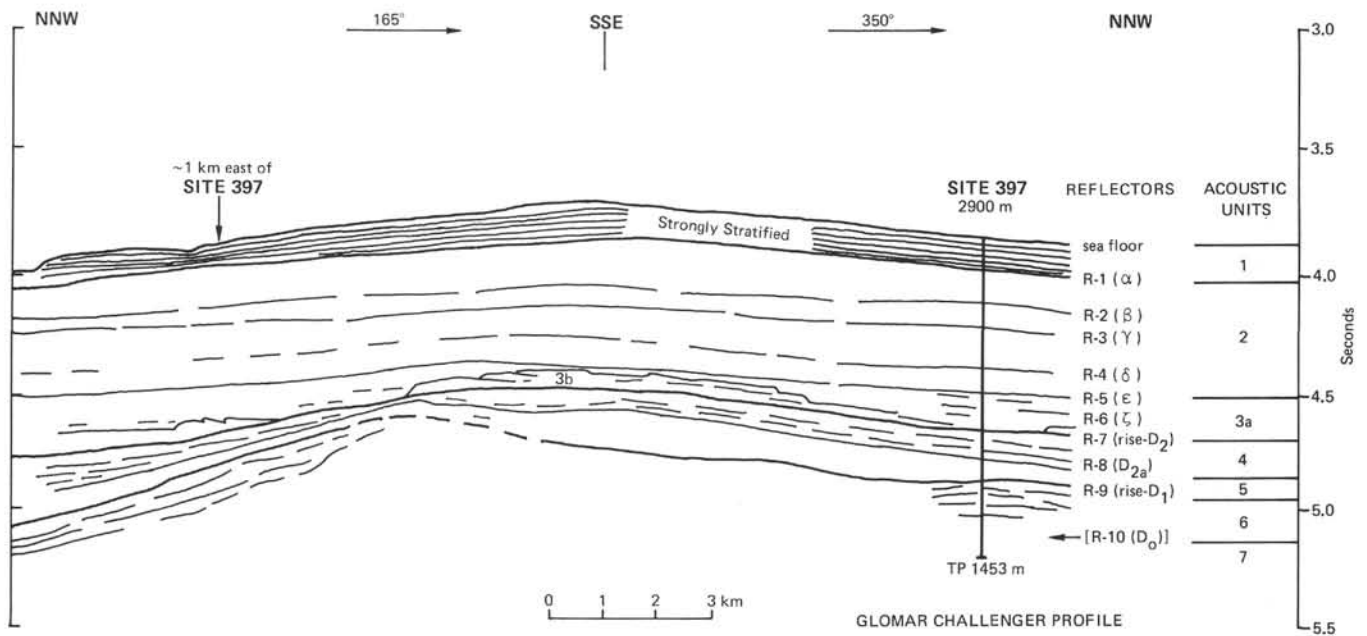


Figure 23b. Line drawing with reflector interpretation (from 10-s sweep) by Ryan. Note progressive erosional truncation of acoustic Unit 3b, south-southeast at Site 397.

downslope. Apparently, the major 100-m.y. unconformity is not evident on most single-channel seismic records, whereas strong reflectors may depict facies changes within lithostratigraphic units.

While these considerations changed our original objectives, the continuously cored, very deep Hole 397 provided a number of unexpected and exciting discoveries: (a) a well-developed, complete, undisturbed, expanded hemipelagic late Miocene to Quaternary section of the eastern North Atlantic with optimal resolution for nannofossil and foraminiferal biostratigraphy, magnetostratigraphy, and paleoenvironment studies; (b) rapidly deposited allochthonous lower Miocene mass flow deposits and slumps, allowing the study of the evolution of "flysch sedimentation" in an atectonic passive margin setting; (c) enigmatic 100-m.y. hiatus between lower Miocene strata and upper Hauterivian prodelta muds (correlative with shallow-water and sub-aerial deltaic subenvironments of the Aaiun/Tarfaya Basin); and (d) ideal site to study the petroleum potential of the northwestern African margin, the diagenetic evolution of organic matter and gasses, silica, and carbonate in a high-fertility, high-sedimentation rate, relatively high-heat-flow continental margin setting.

This section attempts to summarize the major results of the Site 397 contributions by the shipboard scientific party (see also Sediment Summary Chart 1, back pocket, this volume) and also quotes selected highlights from shore-based researchers. For a more interpretative sedimentary synthesis of the Leg 47A results ("Evolution and sedimentary history of the Cape Bojador continental margin"), see Arthur et al. (this volume); for a synthesis of the late Neogene paleoenvironment, see Cita and Ryan (this volume); for a synthesis of the Early Creta-

ceous paleoenvironment, see Einsele and von Rad (this volume).

Paleoenvironment and Sedimentary Processes

Jurassic to Hauterivian (the undrilled Mesozoic and basement)

According to seismic and magnetic data (Wissmann, this volume; Hayes and Rabinowitz, 1975, their fig. 2 and 3), transitional (to oceanic?) crust, possibly Early Jurassic ("Quiet Zone" 170 to 190 m.y.B.P.), underlies Site 397 at a depth of about 9 to 10 s below sea level. Thus, about 7 to 8 km of shallow-water carbonates (?) and clastics were deposited at extremely high sedimentation and subsidence rates (?70 to 140 m/m.y.) within the unpenetrated Early Jurassic to late Hauterivian interval during the early rift, drift, and subsidence stages of this divergent passive margin (von Rad and Einsele, in press).

Late Hauterivian Facies and Paleoenvironment (lithostratigraphic Unit 5; approximately 117 to 118 m.y.B.P.)

This interval, of which 153 meters were penetrated, is characterized by monotonous, finely laminated, dark gray, silty claystones rich in terrigenous components (quartz, mica, plant debris), fish remains, and organic matter, but poor in carbonate (10%) and microfossils. Only primitive, small-sized globigerinids and a sparse, moderately preserved, low-diversity benthic foraminiferal fauna were found. Because of the excellent preservation of some aragonitic tests of *Epistomina* and a few ammonites and pelecypods, the general low carbonate content is explained by low productivity and a low evolutionary level and dilution, rather than by dissolu-

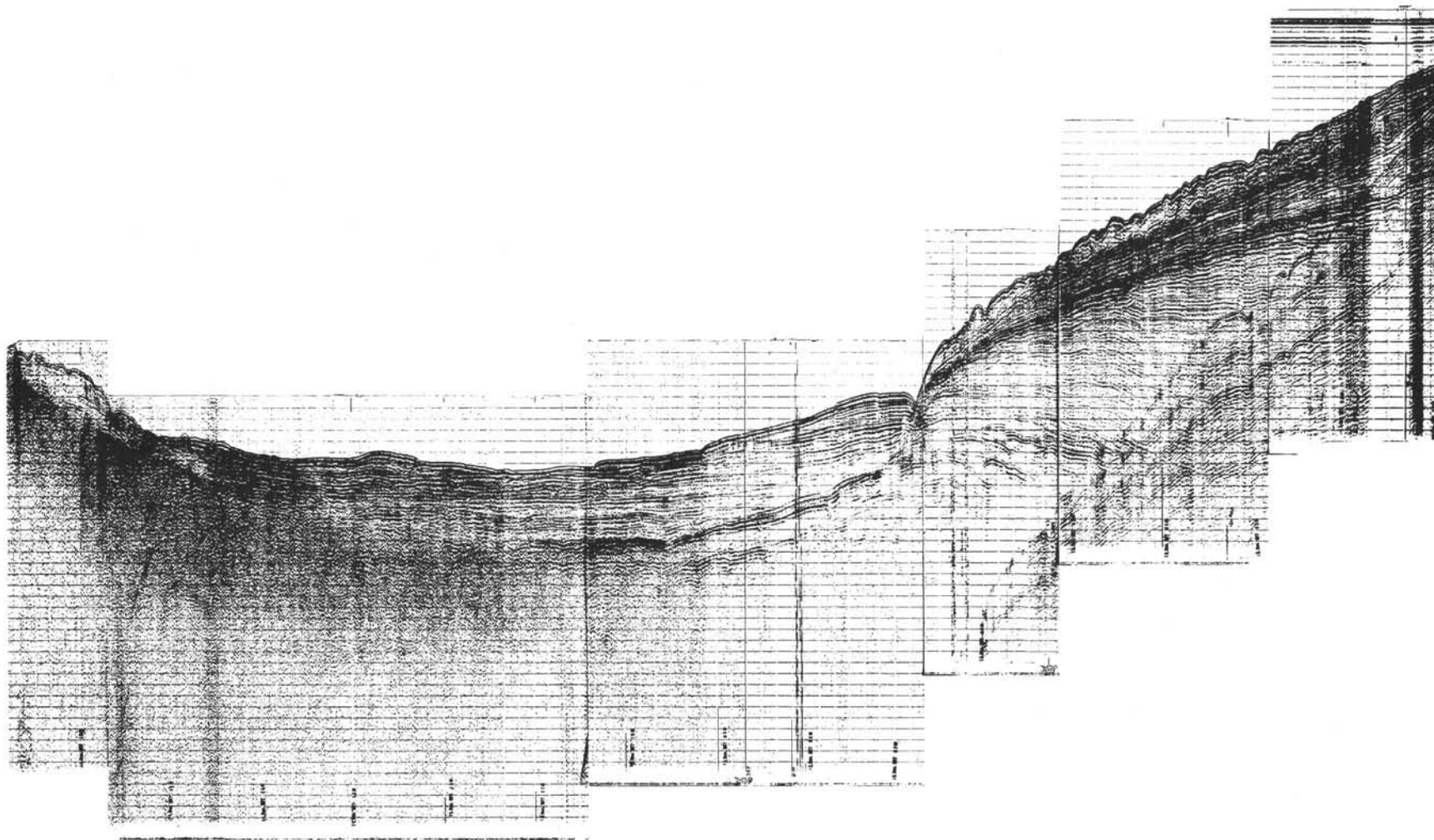


Figure 24. Single-channel seismic reflection profile Meteor M-46 37 across the outer Cape Bojador continental margin connecting DSDP Sites 369 and 397 (digital single-trace recording processed by BGR, Hannover; seismic source: 3 × 5 liter airguns). Interpretation and correlation with Sites 369 and 397 by Wissmann (this volume).

TABLE 14
Correlation of Acoustic Reflectors (*Glomar Challenger* Profile) With Shipboard Sonic Velocity Measurements at Site 397

Reflector Designation	Acoustic Unit	Two-Way Travel Time (s) Below Sea Level	Two-way Travel Time (s) Below Sea Floor	Sub-Bottom Depth (m) ^a	Interval Velocity (km/s)	Typical Shipboard Sonic Velocity Measurements	Hamilton Frame Velocimeter Averages (no. of meas. in brackets)	Comments
Sea floor	Unit 1	3.86	0.000		1.60	1.50 1.52	1.515 ±0.03 (43)	(Quaternary)
R-1 (α)	b	4.02	0.125	100				Brief hiatus with small increase of velocity gradient
R-2 (β)	b	4.15	0.280	230				Brief hiatus with small increase in velocity gradient
R-3 (γ)	Unit 2	4.23	0.360	320	1.74		1.60 ±0.12 (84)	(? top Messinian)
R-4 (δ)		4.39	0.525	450 ±20 (or 400)				First chalks slumps
R-5 (ε)		4.5	0.643	550				First limestones (2-m.y. hiatus)
R-6 (ζ)	b Unit 3a	4.64	0.770	680 ±10	2.04		1.75 ±0.25 (16)	
R-7 ("rise-D-2")	Unit 4	4.66	0.790	700 ± 20	2.0	2.9 ± 0.4 Volcaniclastic Sandstone (F-4B)	2.2 ± 0.3 (20)	Thick volcaniclastic debris flows (V-1 and V-3)
R-8 ("D-2a")	Unit 5	4.77	0.900	810 ± 20	3.2	2.3 ± 0.3 pebbly mudstone (F-4A)	2.47 ± 0.5 (21)	
R-9 ("rise-D-1")	Unit 6	?4.86	?1.00	970 ± 20		2.2 ± 0.3 allochthonous mudstone (F-2/3)		Clayey-quartzose volcaniclastic sandstone (Early Miocene)
R-10 (major unconf.)	b Unit 7	?5.06	?1.200 (1.150)	1300	3.3	2.1 ± 0.2 autochthonous mudstone (F-5)	2.3 ± 0.3 (28)	(100-m.y. hiatus)
						1.85-2.10 (mudstone) 3.5-4.8 (siderite layers)	1.9 ± 0.2 (16)	Small velocity inversion (Hauterivian)

^aDistance between sea floor and correlated lithologic or impedance change.

^bSee comments column.

tion (Butt; Roesler et al.; Basov et al.; all, this volume). Locally, there are marlstones and surprisingly well-preserved and diverse nannoflora. Numerous thin siderite layers alternate with the mudstones.

The depositional environment was probably a distal prodelta slope at a water depth of a few hundred to a thousand meters and comparable to the Recent Niger prodelta (Einsele and von Rad, this volume). Oxygen depletion is suggested by an abundance of organic matter, paucity of benthic invertebrates, almost complete lack of bioturbation, a distal setting by the dominance of the clay fraction, the abundance of mica and plant fragments, and the paucity and thinness of well-sorted silt and very fine and layers. These were deposited by intermittent, low-velocity, bottom-seeking currents. A downslope gradient and slope instability is indicated by local slumps, contorted bedding, and consistently high dipping laminations. The spectacular mm-thick, varve-like lamination is due to annual or longer term climatic variations, storm periods, etc., under conditions of oxygen depletion and very high sedimentation rates (75 to 150 m/m.y.). Coeval sediments of the Aaiun coastal basin represent the landward neritic, intertidal, lagoonal, and alluvial plain subenvironments of a widespread "Wealden-type" prograding delta system which was fed by rivers draining the crystalline Precambrian Requibat Massif and the Paleozoic rocks of the Mauretanes and/or AntiAtlas Mountains (Einsele and von Rad, this volume). Most of the organic matter consists of woody and coaly substances, derived from higher

land plants (Cornford, this volume). The plant fragments and the detrital clay mineral association (abundant, well-crystallized illite, common kaolinite, and chlorite) suggest a temperate, humid climate, and erosion of crystalline rocks, more or less weathered by pedogenesis (Chamley and d'Argoud, this volume).

The 100-m.y. Hiatus (Hauterivian to early Miocene)

This stratigraphic gap is a true chasm. The lithology changes at 1300 meters sub-bottom from a compacted upper Hauterivian unburrowed shale to a semi-indurated radiolarian-nannofossil mudstone that was deposited during the early Miocene. Because of the large gap in the fossil record, it is difficult to date more accurately the pre-early Miocene destruction of the continental slope and rise. However, reworked fossils and lithologies help to bridge the missing record (Arthur and von Rad, this volume); these include: (1) upper Aptian to Albian nannofossils in a mid-Miocene slump (Core 397-57); (2) a pot-middle Albian limestone in a lower Miocene pebbly mudstone (Core 397-89); (3) a Turonian to lower Coniacian mudstone (Core 397-89); (4) reworked Cretaceous and Eocene benthic foraminifers in allochthonous sediments of Unit 4; (5)? Eocene porcelanites and cherts; and (6) upper Oligocene (P. 21, NP24) hemipelagic sediments found as thin stringers in lower Miocene debris flow deposits. This proves that a more or less complete Middle Cretaceous to Oligocene sedimentary record did exist on the uppermost rise at the end of the Paleogene. Tentatively, we suggest a

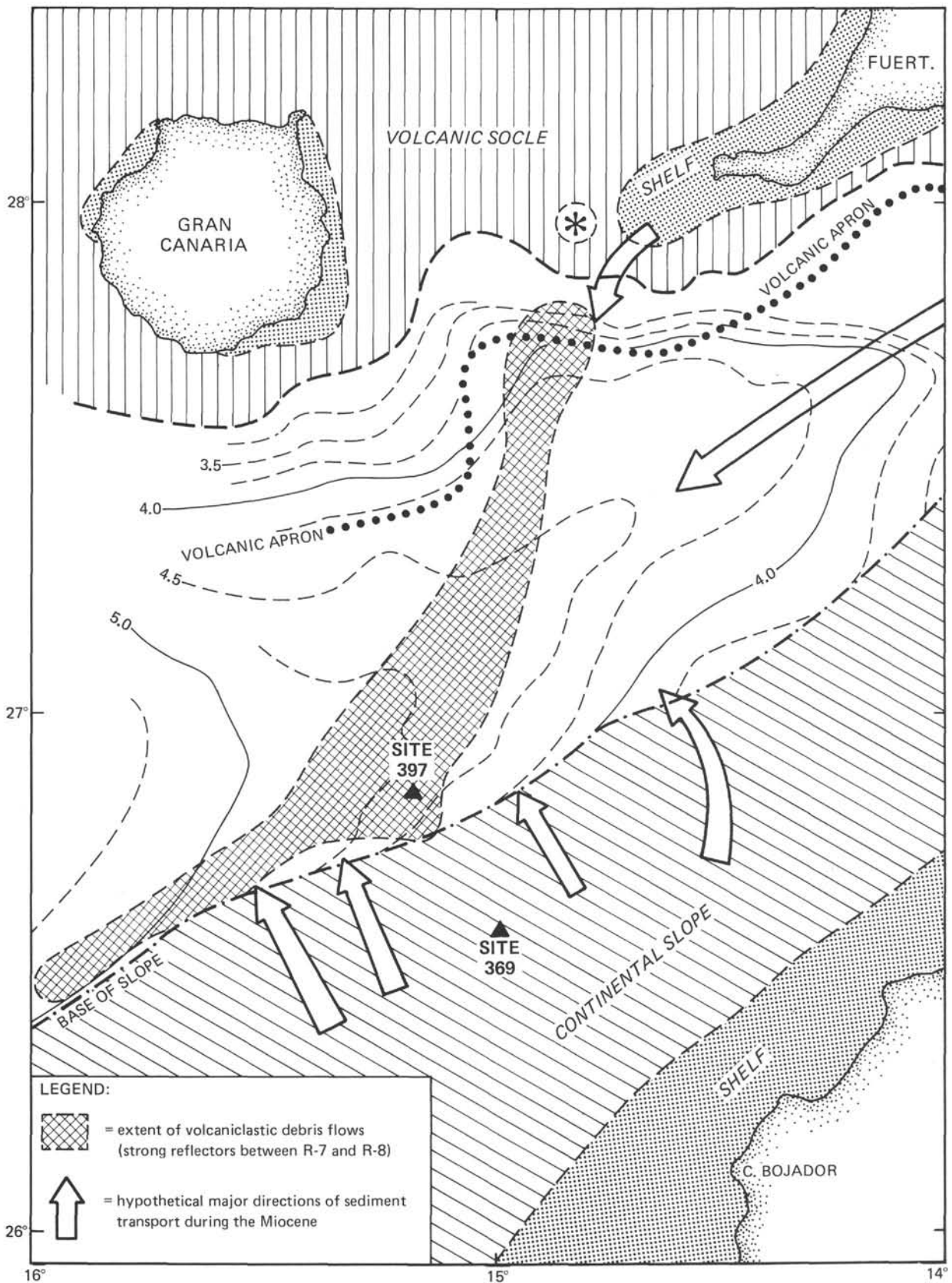


Figure 25. Depth contours of "rise-D₂" (i.e., R-7; about the top of middle Miocene volcanoclastic debris flows) between the base-of-slope and the volcanic socle of the Canary Islands (in seconds of two-way travel time). Seismic interpretation by Wissmann (modified from Schmincke and von Rad, this volume, their fig. 1).

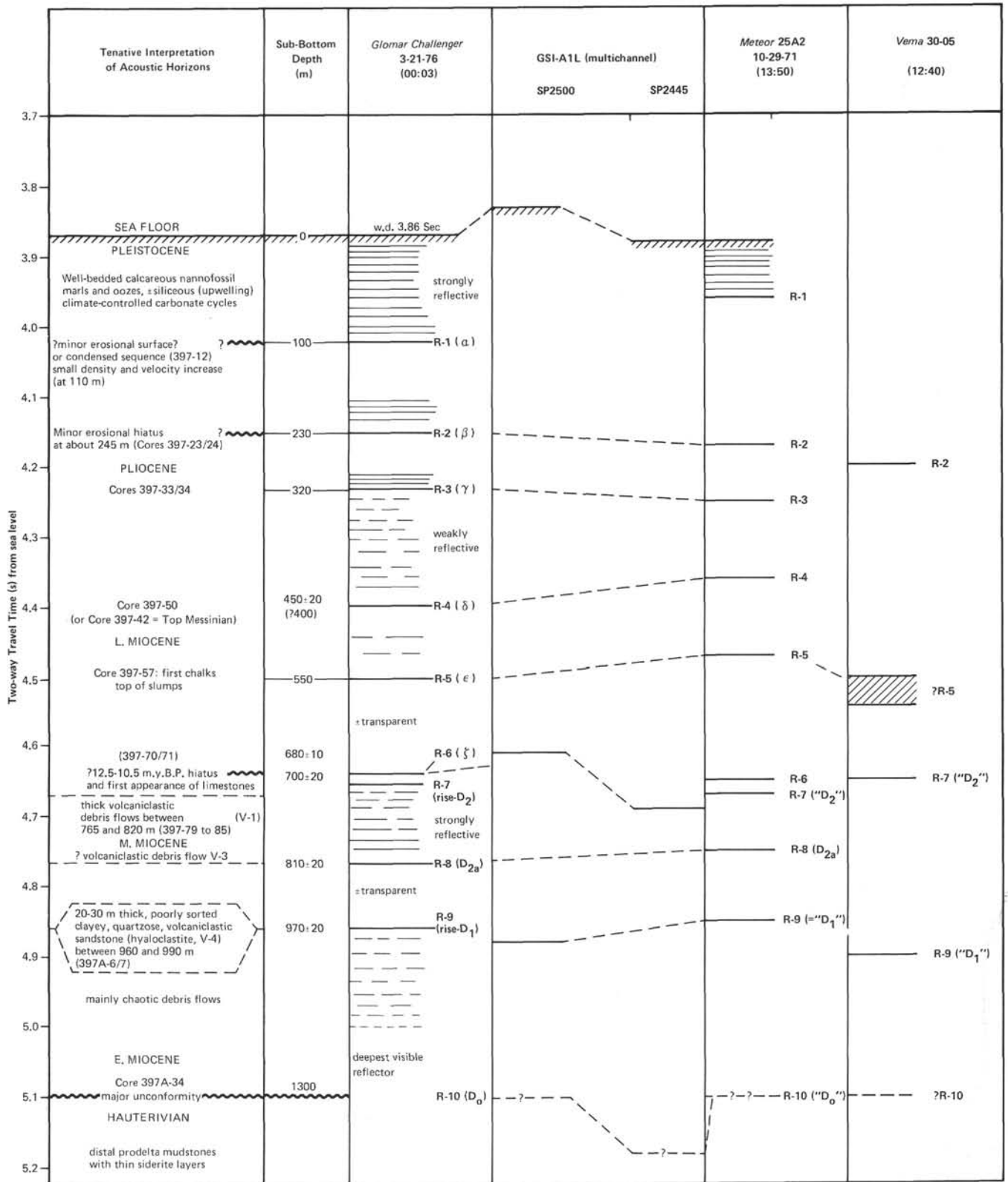


Figure 26. Correlation of acoustic reflectors from seismic profiles near Site 397 and tentative interpretation of acoustic horizons at Site 397.

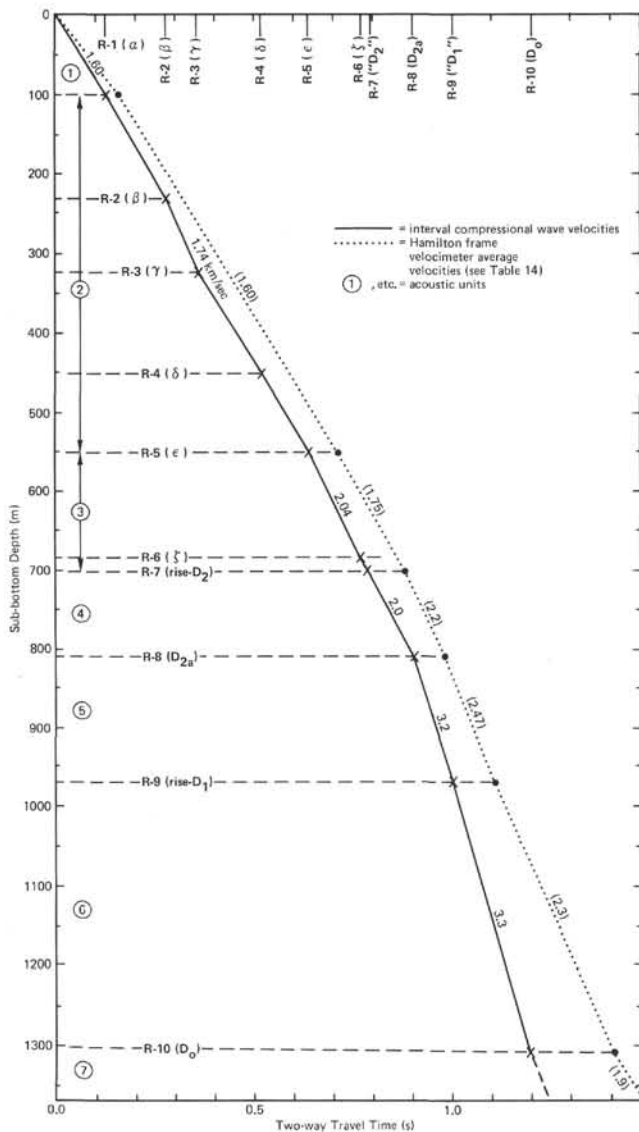


Figure 27. Depth of acoustic reflectors, interval compressional wave velocities, and Hamilton Frame velocimeter average velocities at Site 397. Note that the Hamilton Frame average velocities line does not fit the travel time assumed for acoustic reflectors from seismic evidence (horizontal axis of diagram).

middle Oligocene to earliest Miocene age for this large-scale erosional event, more or less coinciding with the initiation of a deep-seated circum-Antarctic flow at 30 to 25 m.y.B.P. after the onset of substantial Antarctic glaciation near the Eocene/Oligocene boundary (Kennett, 1977). Additional earlier hiatuses of shorter duration, e.g., during the Paleocene to early Miocene and during parts of the "Middle" Cretaceous, might be inferred from the record of DSDP Site 369 and from the Aaiun Basin (Arthur et al., this volume).

Although the major upper rise unconformity may be the result of the superposition of several hiatuses, the

large-scale erosion of the outer continental margin beyond a water depth of 2500 meters was probably accomplished during a relatively brief interval of a few to 10 million years in the late Paleogene (?middle to late Oligocene). This erosion may have been caused by geostrophic contour-following eastern boundary currents intensified by the late Oligocene initiation of the strong circum-Antarctic bottom-water circulation after the separation of Australia from Antarctica (Kennett et al., 1975), coinciding with the major late Oligocene regression.

Study of seismic records (Hinz; Wissmann; both, this volume) revealed that 1 to 2 km of sediment were definitely eroded along extensive parts of the lowermost slope and uppermost rise off northwestern Africa. Inferences from the degree of maturation of organic matter (Cornford et al., this volume) suggest a maximum removal of 1.3 km of pre-Miocene sediments and do not contradict the seismic interpretations. A vast amount of sediment, conceivably 7,500 to 15,000 km³, was probably eroded from an ancient prograding slope by steady geostrophic currents. This resulted in erosion from an inclined surface of >10,000 km² and in the back-cutting of an exaggerated escarpment into the Mesozoic to Paleogene margin. It probably also caused isostatic readjustment of the unloaded portion of the margin forming the "slope anticline" and further increasing the gradient and instability of the slope. It is unknown where this huge volume of eroded Lower Cretaceous to Oligocene sediments came to rest. It is not found on the upper rise, the repository typically proposed for such talus material.

Lower to Middle Miocene Gravitational Deposition of Allochthonous Sediments (lithostratigraphic Units 3 and 4; 22 to 9 m.y.B.P.)

Erosion of the upper continental rise ceased abruptly during the earliest Miocene (about 20 to 22 m.y.B.P.), when cascades of debris slumped down the oversteepened lower continental slope and accumulated rapidly (110 to 140 m/m.y.) on the erosion surface at the lower slope/upper rise boundary (Arthur and von Rad, this volume). Units 3 and 4 consist of a 650-meter-thick "flyschoid" sequence with a preponderance of allochthonous sediment types, such as graded and ungraded sandstones, sandy mudstones, volcanoclastic sandstones, and amalgamated pebbly mudstones. A wide variety of composition, texture and sedimentary structures was encountered and a confusing juxtaposition of "gravitational" or allochthonous (80 to 90% of sediment section!) and "autochthonous" hemipelagic lithotypes. By a careful study of sediment color, composition, structures, and bioturbation, six distinctive allochthonous facies (F1 to 4C), and one hemipelagic ("autochthonous") facies type (F-5) were differentiated and inferences on their provenance and transport mechanisms were defined by the shipboard sedimentologists (see Arthur et al., this volume). The following

evolutionary sequence of gravitational mass transporting processes is proposed (Arthur and von Rad, this volume):

1) At about 20 to 18 m.y.B.P., transverse debris flows, derived from the (upper) slope, rapidly deposited chaotic pebbly mudstones with plastically deformed (sheared and stretched) mudstone clasts (F-4A₂). Towards the top of this section, mudstone clasts are rounded and not deformed by syndepositional shear (F-4A₁). The clasts include hemipelagic and upper slope carbonaceous lower Miocene mudstones and a few fragments from Aptian to Oligocene strata outcropping along the erosional scarp. The pebbly mudstones are interbedded with dark olive-gray, carbonaceous fine-grained turbidites or turbid layer sediments (F-2 and F-3).

2) About 18 to 17 m.y.B.P., poorly sorted debris or grain flow deposits with abundant pebbly quartz and shallow-water calcareous skeletal material (solitary corals, pelecypods, gastropods, worm tubes) and only a few mudstone clasts (F-4C) reached the area of Site 397. They might be derived from the periodic flushing of canyon head reservoirs near the shelf edge.

3) Fewer debris flows, but more graded turbiditic sandstones (F-1) and more hemipelagic sediments (F-5) have been deposited since 17 m.y.B.P., signaling a further diminishment of the slope-rise gradient. However, most turbidites still bypassed Site 397 on their way to the lower rise. Well-sorted, quartzose, calcareous sandstones (F-1A) are possibly turbidites, funneled longitudinally into the elongated southern Canary Island Channel from a nearshore source along the south Moroccan coast. About 17 to 16.5 m.y.B.P., several meter-thick volcanoclastic sandstones (F-4B) were deposited by turbidity currents or grain flows draining the emerging volcanic Canary Islands situated to the north and northeast.

4) Finally, downslope creep and slumping of hemipelagic sediments stabilized the slope (between 12 and 9 m.y.B.P.), the gradient of which no longer was steep enough for the detachment of debris flows and turbidity currents. A 50-meter-thick interval consists of about 20 individual decimeter to meter-thick intraformational slump zones of laminated chalks of only slightly younger age (middle Miocene, N.12-14) than the associated autochthonous sediments (early late Miocene, N.16). At the same time, only a few very thin distal turbidites and/or contourites were deposited on a stabilized upper rise which, since 9 m.y.B.P., received almost solely autochthonous, hemipelagic marly sediments.

During the middle Miocene, sedimentation rates decreased drastically (20 to 50 m/m.y.). Also, two hiatuses were recognized on the basis of nannoplankton and/or foraminiferal biostratigraphy: one about 15 m.y.B.P. and a longer one from 12.5 to 10.5 m.y.B.P. The former possibly can be correlated with the beginning of oceanic circulation related to the development of the Antarctic Convergence (Kennett, 1977). This se-

quence is characterized by a great variety of downslope transport mechanisms, including debris and grain flows, turbidity currents, turbid layer transport, (?) contour currents, slumping, and slow downslope creep. Surprisingly, no active tectonism is necessary to generate such chaotic sediment sequences, which strikingly resemble flysch and "wildflysch" assemblages from elongate troughs and trenches along consuming plate boundaries (active margins), such as the Cretaceous-Paleogene Carpathian flysch and the Recent Puerto Rico Trench. Apparently, "passive" margins are subject to a remarkable vertical (isostatic) adjustment after unloading by erosion. The rapid gravitational sedimentation is only the compensation of an oversteepened scarp which was sculptured by intensified geostrophic currents, until an equilibrium gradient is re-established (Arthur and von Rad, this volume).

The coarse-fraction of the lowermost Miocene consists of fine-grained quartz, mica, and plant material, thus suggesting phases of wet climate (Sarnthein, this volume). Fish debris and echinoderm remains might indicate enhanced fertility on the shelf (? early Miocene delta; Sarnthein, this volume). Radiolarians suggest upwelling conditions (? related to Southern Hemisphere glaciation) in the earliest Miocene (20 to 17 m.y.B.P.). Coarse frosted-quartz grains might indicate dune formation and more arid climate in the late-early and middle Miocene. In the allochthonous sediments, both benthic and planktonic foraminifers are much better preserved than in the autochthonous facies. Benthic foraminifers indicate bathyal (>1500 m) water depth for the hemipelagic sediments. The benthic foraminifers give valuable clues to the source environment of the allochthonous sediment types: about 20 to 18 m.y.B.P., intermittent sediment displacement affected mostly the outer and inner shelf; 18 to 12.5 m.y.B.P., maximum and continuous sediment displacement occurred which affected the entire shelf and upper slope (including outer-shelf faunas of Eocene to early Oligocene). Coarse-shelled fragments of calcareous algae, solitary corals, bryozoans, barnacles, decapods, serpulids, mollusks, phosphorite, ooides, and glauconite indicate maximum shallow-water input about 18 to 17 m.y.B.P. This association suggests a warm, temperate, shallow-water environment. The slumps, deposited about 10-9 m.y.B.P., are only derived from the outer shelf and upper slope.

The sediment material from the upper slope is a dark olive-green to brown-black mudstone which is not burrowed and is rich in organic carbon (3 to 4%). The benthic populations have a low species diversity, possibly pointing to an expanded oxygen-minimum layer. Apparently, these sediments were derived from the oxygen-depleted upper-slope regime. Preservation of calcitic and aragonitic tests is much better in the gravitational mudstone pebbles than in the bioturbated hemipelagic sediments. Smectite is the most abundant clay mineral of Unit 4; it is probably derived from the erosion of

montmorillonite-rich soils under warm conditions with seasonal contrasts in humidity (Chamley and d'Argoud, this volume).

Neogene Evolution of Canary Island Volcanism

Several volcanoclastic sandstones and conglomerates (lithofacies F-4B) were deposited as mass-flow deposits in the southern Canary Island Channel. In particular, these include a 7.8-meter-thick, indistinctly graded, altered palagonite tuff (hyaloclastite, flow "V-3," Cores 397-84 and 397-85) and a 4.5-meter-thick tuffaceous sandstone to conglomerate (flow V-1, Cores 397-79 and 397-80) with subaerial detritus (basalt to "microgabbro") and tachylite from lavas advancing into the sea. The stratigraphic distribution of the different types of volcanoclastics reflects the early to middle Miocene uplift and emergence of the Canary Islands, in general, and that of Fuerteventura, the probable source area for the volcanoclastic flows, in particular. Volcanic activity was most intense during the shield-building stage producing mass-flow deposits (a) during a submarine stage (flow V-3), about 17 m.y. B.P., and (b) during a subaerial shield stage (flow V-1), about 16.5 m.y. B.P. (Schmincke and von Rad, this volume). Approximately 19 m.y. B.P., ash falls derived from trachytic volcanic eruptions were deposited in the lower-most Miocene and might be the earliest datable record of volcanic activity after the formation of the "basement-complex" at Fuerteventura. Fifteen Eolian vitreous (to zeolitized) ash layers are present in the mid-Miocene to Quaternary sediment and indicate less voluminous, but highly differentiated volcanic events from 14 to 9 m.y. B.P. (rhyolitic eruptions on Gran Canaria?), about 4 m.y. B.P., and from 3.3 to 0.3 m.y. B.P. (trachytic to phonolitic eruptions on Tenerife?).

Upper Neogene Autochthonous Hemipelagic Sediments (lithostratigraphic Units 1 and 2; late Miocene to Quaternary, 9 m.y. B.P. to present)

The more or less siliceous, nannofossil oozes, marls, and chalks of this 550-meter-thick, undisturbed, hemipelagic section were rapidly deposited (60 to 80 m/m.y.) under conditions of upwelling, high fertility and good ventilation. Average carbonate content is 55 per cent (marl) and organic carbon content is low (<0.5%; up to 1.2% in Unit 1). Bioturbation is commonly observed. Some well-bedded and finely laminated intervals are indicative of winnowing tractive (?contour-following) currents or turbid layer transport. The uniformity of this biogenic hemipelagic carbonate ooze sedimentation was surprising, when one considers its proximity to the African continent (which received little coarse-grained terrigenous input over a period of 9 m.y.). Dissolution pulses are recorded by a maximum of fragmented foraminifers and comparatively low CaCO₃ percentages in the uppermost Miocene (about 6 to 8 m.y. B.P.) and might reflect a rise of the CCD during the Messinian "salinity crisis" (Cita and Ryan, this volume).

A detailed investigation of the wide-ranged detrital clay mineral assemblage and of the coarse fraction allowed the following inferences on the development of the paleoclimate and paleoceanography (see Diester-Haass; Chamley and d'Argoud; Chamley and Diester-Haass; all, this volume).

According to these authors, an arid climate is indicated by low terrigenous input, high content of wind-transported red-stained "desert quartz," chlorite, and detrital (wind-blown) palygorskite. Humid conditions are inferred from a high input of river-transported terrigenous components (e.g., plant fibers, mica, feldspar), irregular mixed-layer clay minerals, and shallow-water particles due to lowered sea level; during those periods, a degradation of clay minerals by soil formation was noted. Strong Quaternary to late Pliocene upwelling is suggested by a high content of siliceous organisms, and increased percentages of benthic foraminifers, echinoderms, and ostracodes; upwelling appears to correlate with a humid climate. According to Diester-Haass (this volume), humid intervals with high shallow-water input (e.g., the late Miocene) correlate positively with cold climatic phases and high (i.e., heavier) $\delta^{18}\text{O}$ values (Shackleton and Cita, this volume).

Sarnthein (in Arthur et al. this volume) and Lutze et al. point out that increased input of terrigenous sediment and presence of red-stained quartz is not related to either humid or arid climate in northwestern Africa. Stained quartz is also characteristic of lateritic weathering; coarse silt and fine sand grain sizes are typical of lowland rivers and wind-transported dust. According to Sarnthein, additional coarse terrigenous sediment is supplied by downslope particle-by-particle transport from the shelf, mainly controlled by sea-level and swell changes.

The rapid upbuilding of a hemipelagic sediment wedge was only briefly interrupted by minor hiatuses or condensed sequences, about 3 and 0.9 m.y. B.P. (based on foraminiferal biostratigraphy and magnetostratigraphy). The 3-m.y. B.P. hiatus tentatively might be correlated with the cutting of marine terraces on Gran Canaria due to glacioeustatic regression (erosional interval II, Lietz and Schmincke, 1975) and the start of the Northern Hemisphere ice-sheet development. Probably not only high fertility and upwelling, but also contour-parallel geostrophic currents were responsible for the concentration of the fine-grained hemipelagic drape along the foot of the continental slope.

The late Pleistocene record of the last 90,000 years was studied in detail in a 9.4 meter long section in two *Meteor* cores. Lutze et al (this volume) used these cores as a reference section for the climatological and sedimentary interpretation of the Neogene of Site 397. They derived sedimentation rates of 7-9 cm/1000 years for the warm and 15-20 cm/1000 years for the cold stages.

Biostratigraphy and Magnetostratigraphy

The continuously cored, undisturbed, high-sedimentation-rate, hemipelagic, upper Miocene to Quaternary section (Units 1 and 2) is ideal for a refinement of the

planktonic foraminiferal (Salvatorini and Cita, this volume) and nannoplankton stratigraphy (Čepek and Wind; Mazzei et al.; both this volume), as well as of a local Neogene benthic foraminiferal stratigraphy (Lutze, in Site Chapter, this volume) and magnetostratigraphy (Hamilton, this volume). Thus, Site 397 is a valuable reference section for correlations with other eastern Atlantic and Mediterranean onshore and offshore upper Neogene sequences. The biostratigraphic "signal" is not disturbed by slumping, reworking from older formations, or downslope displacement of coeval benthic organisms. Only minimal CaCO_3 dissolution and minor hiatuses or condensed series were noted (Cita and Ryan, this volume; Salvatorini and Cita, this volume). During the Quaternary and most of the Pliocene, abundance and diversity of calcareous plankton is high and preservation excellent. Dissolution increases toward the late Miocene, where preservation is good to moderate.

Below 550 meters (Units 3 and 4), preservation decreases and the disturbance of the biostratigraphic record by slumping, reworking, downslope displacement, and erosional hiatuses increases continuously down to the base of the lower Miocene. Few autochthonous corroded benthic foraminifers are present in Unit 4, whereas the better-preserved, displaced, shallow water forms allows the detection of the source environments which were actively eroded (Lutze, this volume).

The first on-board paleomagnetic study of a continuously cored sediment sequence established a magnetic polarity stratigraphy from the Brunhes down to Epoch 7 (Cores 397-1 to 397-57), although the intensities of natural remanent magnetization are very low (0.1 to 0.7×10^6 G). This magnetostratigraphy is controlled by the detailed biostratigraphy and allows tentative inferences about short-term hiatuses or condensed sequences in the Pliocene-Pleistocene which could not be resolved by the nannoplankton or foraminiferal zonation.

In general, the upper Hauterivian mudstones contained only a sparse, low-diversity foraminiferal fauna and nannoflora. The benthic foraminifers are neither age-diagnostic, nor do they provide unambiguous clues to paleodepth and ecology (Rösler et al.; Butt; Basov et al.; all, this volume). Locally, nannofossil marls are present with a surprisingly well-preserved ammonite fauna (Wiedmann, this volume) and diverse nannoflora, consisting of >60 (partly new) species (Wind and Čepek this volume). For Hauterivian nannofossils, this is one of the best DSDP sections drilled thus far.

Diagenesis of Organic Matter, Carbonate, and Silica

Organic Matter and Hydrocarbon Gases

Within the uppermost 200 meters, the organic carbon percentages fluctuate considerably (0.1 to 1.0%). Local high values are due to high late Pliocene-Quaternary bioproduction (upwelling). The autochthonous, hemipelagic carbonate-rich oozes, marls, and chalks between 200 and 1300 meters contain <0.5% C_{org} , whereas the

allochthonous middle to lower Miocene turbidites and debris flows are much richer in organic matter (1 to 4%); vitrinite-huminite and inertinite are prominent, all from higher plants or terrestrial input (Cornford et al., this volume). Organic-rich sediments, derived from the oxygen-depleted upper-slope regime, seemingly were emplaced and preserved by the mass transport and thereby evaded biochemical degradation in the oxygenated deeper waters. This is an important aspect when prospecting for hydrocarbons in the rapidly deposited flyschoid sediments of the upper continental rises. The organic matter of the upper Hauterivian sediments (0.4 to 0.8% C_{org}) is exclusively vitrinitic and inertinitic, pointing to an input by higher terrestrial plants.

The increase of reflectivity of small dispersed vitrinite-huminite particles indicates maturation of organic matter (Cornford et al., this volume). Because no significant break in maturity across the 100-m.y. unconformity was recognized, the inferred present *in-situ* temperatures (about 65 °C) at 1450 meters are probably the highest yet generated in these sediments. This suggests that less than 1300 meters of sediments were eroded between the late Hauterivian and early Miocene. Slightly higher than normal temperatures and vitrinite reflectances are probably due to short-duration heating by rapidly deposited Neogene sediments and/or the middle Miocene emergence of Canary Island volcanoes (10 °C/4m.y.).

In terms of petroleum generation, the sediments are immature. Given enough suitable source material, the onset of petroleum genesis would start slightly below the base of the hole (>65 °C); but no migratory gas was encountered below 1300 meters (see discussion in Arthur et al., this volume).

Methane and trace quantities of C_2 to C_5 hydrocarbons, generated by poorly understood low-temperature diagenetic processes, were continuously monitored as a safety measure (Whelan, this volume). Methane and successively higher hydrocarbon gasses are present between 196 and 1450 meters. No evidence of potentially hazardous hydrocarbon accumulations or source beds was found. The "in-phase behavior" of C_2 to C_5 hydrocarbon gasses in fine-grained sediments proved their nonmigratory character. Lateral preferential movement and entrapment of the lighter C_1 and C_2 hydrocarbons with respect to the C_3 , C_4 , and C_5 gasses occurred in a stratigraphic pinch-out zone with porous coarse-grained sediments between reflectors R-7 (D_2) and R-8 (D_{2a}), between about 700 and 800 meters. Trace C_2 to C_5 gas patterns correlate surprisingly well with the seismic and lithologic horizons, as well as with the physical properties of the strata. Isotopic data ($\delta^{13}\text{C}$ values between -60 and -80) indicate that all the methane is of biogenic, rather than petrogenic origin (Whelan, this volume).

Carbonate Diagenesis

The transition of calcareous oozes to chalks occurs between 380 and 490 meters; that of chalk to limestone, below about 700 meters. The CaCO_3 cementation of autochthonous calcareous and allochthonous silty-

sandy sediments increases discontinuously with increasing burial depth, and produces major seismic reflectors at 700 to 850 meters. The change to a dominantly clayey facies at the middle/lower Miocene boundary is responsible for the paucity of calcite cement in Unit 4. According to Riech (personal communication, see also Sediment Summary Chart 1, back pocket, this volume), composition of the original sediment ("diagenetic potential"), burial depth (pressure, temperature), and carbonate nucleation conditions are the major factors influencing the processes of early carbonate diagenesis.

Micritic dolomites and individual rhombs of dolomite (and siderite) occur in lower Miocene mudstones between 850 and 1300 meters. These dolomites are probably of diagenetic origin, although reworking from the shelf cannot be completely excluded (Riech, personal communication). Numerous thin siderite layers and some nodules are interbedded with the Hauterivian silty claystones. Most of this micritic siderite appears to be of diagenetic origin; it was formed *in situ* after the precipitation of pyrite, and possibly replaces earlier calcite (Einsele and von Rad, this volume).

Silica Diagenesis

The formation of zeolites is clearly dependent on the facies of the host sediments and burial depth (Riech, this volume); phillipsite is always associated with diagenetically altered volcanic glass and forms in Pliocene to middle Miocene sediments below 300 meters burial depth. Clinoptilolite, derived from dissolved opaline organisms at burial depths between 700 and 1300 meters, mostly fills foraminiferal pore space. It is often associated with opal-CT (i.e., disordered low-temperature cristobalite-tridymite) and is always precipitated after calcite cement. Significant amounts of opal-CT are found only in a few silicified mudstones and porcellanites of earliest Miocene age. The *in-situ* transformation of amorphous skeletal opal into opal-CT occurs at about the same burial depth (700 m) below which silica or clinoptilolite starts to be precipitated from interstitial solutions.

Physical Properties and Seismic Stratigraphy

The uniform, undisturbed sediment character of this continuously cored, deep hole also proved ideal for a study of the change of physical properties with depth (Williams and Mountain, Part 2 of this volume). Units 1 and 2 (0 to 686 m) have uniform gradients with a continuous increase of sonic velocity (1.51 to 1.70 km/s) and wet density (1.55 to 1.97), and a decrease of porosity (69 to 41%) and water content (45 to 21 %). Two small hiatuses might be present at 100 and 230 meters, as suggested by an abnormal increase of density and velocity below these depths. Because of the wide range of lithologies, Units 3 and 4 (686 to 1300 m) show scattered values. The velocity for autochthonous sediments (F-5) is 2.09 ± 0.21 km/s; for volcanoclastic debris flows (F-4B), 2.73 ± 0.41 km/s; for chalks, 1.53 to 2.06 (depending on compaction); and for calcareous sandstones (F-16), even 3.53 km/s.

Surprisingly, a slight velocity inversion is seen at 1300 meters with 1.93 km/s above and 1.85 km/s below the 100-m.y. hiatus. The mudstones of the bottom of the hole have densities of 2.3 and maximum velocities of 2.1 km/s (compared with maximum velocities in thin siderite layers of 3.5 to 4.8 km/s). These values are similar to those extrapolated from the nearly continuous Neogene curve downward, suggesting that the late Hauterivian was buried by about 1300 meters of strata prior to pre-Miocene large-scale erosion. This agrees with inferences from the maturation of organic matter.

The temperature gradient derived from two reliable *in-situ* measurements of the upper 450 meters is about $4^\circ/100$ m. This is a comparatively high value for a continental margin setting (only $1^\circ/100$ m at Site 398) and was possibly influenced by the Canary Island volcanism since the middle Miocene. Thermal conductivities permit a rough calculation of heat flow at 1.3 to 1.5 $\mu\text{m cal/cm}^2$.

Seismic reflectors are correlated with lithostratigraphic, organic geochemical, and bulk property variations. Certain acoustic horizons (e.g., R-7, R-10) correspond to biostratigraphically recognized hiatuses. Other horizons (e.g., R-8, R-9) reflect only acoustic impedance variations due to rapid facies changes (e.g., volcanoclastic sandstones; thick amalgamated debris flows, sequences of limestones, etc.) within stratigraphically complete units.

Acoustic stratification in the Quaternary is strong and probably a climatic signature caused by changes in the "diagenetic potential" of calcareous components (carbonate cycles), related to climate-induced oceanographic events. Reflector R-2 is tentatively correlated with a minor hiatus at about 3 m.y.B.P.; reflector R-5 (550 m) marks the top of the lower-upper Miocene slump deposits; reflector R-6 correlates with the 12.5 to 10.5 m.y. hiatus; and reflector R-7 ("D₂") surface (see Figure 25; Wissmann; Schmincke and von Rad; all, this volume) display a trough-like configuration with southwestward-plunging axis. The interval between R-7 and R-8 (825 m) is highly stratified, probably due to the very dense volcanoclastic sandstones, whereas the section between R-8 and R-9 ("D₁") is transparent (pebbly mudstones). Reflector R-9 can be tentatively assigned to a thick, partly graded, volcanoclastic pebbly mudstone between 960 and 985 meters (Core 397A-6). The major unconformity at 1300 meters sub-bottom (R-10; "D₀") is only vaguely expressed on some of the seismic profiles.

According to Seibold and Hinz (1974), the key features of the investigated area are two major unconformities and an "anticlinal" structure ("slope anticline") underneath the lower continental slope. These features were detected by shallow-penetration seismic records. Subsequent multichannel seismic profiles revealed a sequence of horizontal to landward dipping layers underneath the anticlinal structure (Wissmann; Hinz; both, this volume). Present information points to a 3 to 5 km-thick deltaic Early Cretaceous basin fill overlying a thick pile of Jurassic carbonates under the

present upper slope (see Frontispiece). Surprising was the absence of Upper Cretaceous and Paleogene sediments known from Site 369 and predicted from geophysical and dredge surveys to be present under reflector R-7 (D₂). Additional seismic profiles, inspection of commercial multichannel lines, and correlation with DSDP sites (139, 367 to 369, and 397) allowed a tentative re-evaluation: the uppermost major unconformity under the present upper continental rise is of Oligocene-early Miocene age, whereas older (Paleogene and mid-Cretaceous) unconformities are present under the slope. The surprising results from DSDP sites and the commercial onshore and offshore wells of the Aaiun Basin provide us with the opportunity to test and revise the models for the interpretation of seismic sequences on the continental margin off northwestern Africa (Hinz; Wissmann; both, this volume).

REFERENCES

- Bandy, O. L. and Chierici, M. A., 1966. Depth-temperature evaluation of selected California and Mediterranean bathyal foraminifera, *Marine Geol.* v. 4, p. 259.
- Beck, R. H. and Lehner, P., 1974. Oceans, new frontier in exploration, *Am. Assoc. Petrol. Geol. Bull.*, v. 58, p. 376-395.
- Berger, W. H. and Soutar, A., 1970. Preservation of plankton shells in an anaerobic basin off California, *Geol. Soc. Am. Bull.*, v. 81, p. 275-282.
- Berger, W. and von Rad, U., 1972. Cretaceous and Cenozoic sediments from the Atlantic Ocean. In Hayes, D. E., Pimm, A. C., et al., *Initial Reports of the Deep Sea Drilling Project*, v. 14: Washington (U.S. Government Printing Office), p. 787-954.
- Berger, W. H. and Winterer, E. L., 1975. Plate stratigraphy and the fluctuating carbonate line. In Hsü, K. J. and Jenkins, H. C. (Eds.), *Pelagic sediments on land and under the sea: Inter. Assoc. Sediment. Spec. Publ. 1*, p. 59-96.
- Berggren, W. A. and Van Couvering, J. A., 1974. The Late Neogene, *Paleogeogr., Paleoclimatol., Paleoecol.*, v. 16, p. 1-216.
- Blow, W. H., 1969. Late middle Eocene to Recent planktonic foraminiferal biostratigraphy, *First Plankt. Conf. Proc.*, Geneva, 1967: Brill (Leiden), v. 1, p. 199-422.
- Brönnimann, P. and Resig, J., 1971. A Neogene globigerinacean biochronologic time-scale of the southwestern Pacific. In Winterer, E. L., Riedel, W. R., et al., *Initial Reports of the Deep Sea Drilling Project*, v. 7, Part 2: Washington (U.S. Government Printing Office), p. 1235-1470.
- Cita, M. B., 1975. Planktonic foraminiferal biozonation of the Mediterranean Pliocene deep sea record. A revision. *Riv. Ital. Paleontol. Strat.*, v. 81, p. 527-544.
- Cita, M. B., and Gartner, S., 1973. The stratotype Zanclean: foraminiferal and nannofossil biostratigraphy, *Riv. Ital. Paleontol. Strat.*, v. 79, p. 503-558.
- Cita, M. B., Colalongo, M. L., D'Onofrio, S., Iaccarino, S., and Salvatorini, G., 1977. Biostratigraphy of Miocene deep sea sediments from the Mediterranean DSDP Sites 372 and 375, with special reference to the Messinian pre-Messinian interval. In Hsü, K. J., Montadert, L., et al., *Initial Reports of the Deep Sea Drilling Project*, v. 42, Part 1: Washington (U.S. Government Printing Office), p. 671-686.
- Connan, J., 1974. Time-temperature relation in oil genesis, *Am. Assoc. Petrol. Geol. Bull.*, v. 58, p. 2516.
- Douglas, R. C., 1973. Benthonic foraminiferal biostratigraphy in the Central North Pacific, Leg 17. In Winterer, E. L., Ewing, J. I., et al., *Initial Reports of the Deep Sea Drilling Project*, v. 17: Washington (U.S. Government Printing Office), p. 607-672.
- Embley, R. W., 1976. New evidence for occurrence of debris flow deposits in the deep sea, *Geology*, v. 4, p. 371-374.
- Giannelli, L. and Salvatorini, G., 1972. I foraminiferi planctonici dei sedimenti terziari dell'arcipelago maltese. I. Biostratigrafia del "Globigerina Limestone," *Atti Soc. Tosc. Sci. Nat. Mem.*, v. 79, p. 49-74.
- Gieskes, J. M., Kastner, M., and Warner, T. B., 1975. Evidence for extensive diagenesis, Madagascar Basin, Deep Sea Drilling Site 245, *Geochim. Cosmochim. Acta*, v. 39, p. 1385-1393.
- Hayes, D. E., Frakes, L. A., et al., 1974. *Initial Reports of the Deep Sea Drilling Project*, v. 28: Washington (U.S. Government Printing Office).
- Hayes, D. E. and Rabinowitz, P. D., 1975. Mesozoic magnetic lineations and the magnetic quiet zone off northwest Africa, *Earth Planet. Sci. Lett.*, v. 28, p. 105-115.
- Heacock, R. L. and Hood, A., 1970. Process for measuring the live carbon content of organic samples, U.S. Patent 3,508,877.
- Hinz, K., Seibold, E., and Wissmann, G., 1974. Continental slope anticline and unconformities off West Africa, "Meteor" *Forsch.-Ergebn. C*, no. 17, p. 67-73.
- Houtz, R. E., 1974. *Physics of sound in marine sediments*, Loyd Hampton (Ed.): New York (Plenum Publishing Corp.).
- Hunt, J. M., 1975. Origin of gasoline range alkanes in the deep sea, *Nature*, v. 254, p. 411-413.
- Hunt, J. M. and Whelan, J. K., 1978. Dissolved gases in Black Sea sediments. In Ross, D. A., Neprochnov, Y. P., et al. *Initial Reports of the Deep Sea Drilling Project*, v. 42, Part 2: Washington (U.S. Government Printing Office), p. 661-666.
- Ingle, J. C., Jr., 1973. Neogene foraminifera from the northeastern Pacific Ocean, Leg 18, Deep Sea Drilling Project. In Kulm, L. D., von Huene, R., et al., *Initial Reports of the Deep Sea Drilling Project*, v. 18: Washington (U.S. Government Printing Office), p. 517-567.
- Jacobi, R. D., Rabinowitz, P. D., and Embley, R. W., 1975. Sediment waves on the Moroccan continental rise, *Marine Geol.*, v. 19, p. M61-67.
- Jenkins, D. G., 1971. New Zealand Cenozoic planktonic foraminifera, *New Zealand Geol. Survey Paleontol. Bull.*, v. 42, p. 1-278.
- Kennett, J. P., 1977. Cenozoic evolution of Antarctic glaciation, the circum-Antarctic Ocean, and their impact on global paleoceanography, *J. Geophys. Res.*, v. 82, p. 3843-3860.
- Kennett, J. P., Burns, R. E., Andrews, J. E., et al., 1975. Australian-Antarctic continental drift, paleocirculation changes and Oligocene deep-sea erosion, *Nature, Phys. Sci.*, v. 239, p. 51-55.
- Lancelot, Y., Seibold, E., et al., 1978. *Initial Reports of the Deep Sea Drilling Project*, v. 41: Washington (U.S. Government Printing Office).
- Laughton, A. S., 1954. Laboratory measurements of seismic velocities in ocean sediments, *Royal Soc. Proc.*, v. 222, p. 336-341.
- Lees A., 1975. Possible influence of salinity and temperature on modern shelf carbonate sedimentation, *Marine Geol.*, v. 19, p. 159-198.
- Lietz, J. and Schmincke, H. U., 1975. Miocene-Pliocene sea level changes and volcanic phases on Gran Canaria (Canary Islands) in the light of new K-Ar ages, *Palaogeogr., Palaoclimatol., Paleoecol.*, v. 18, p. 213-239.

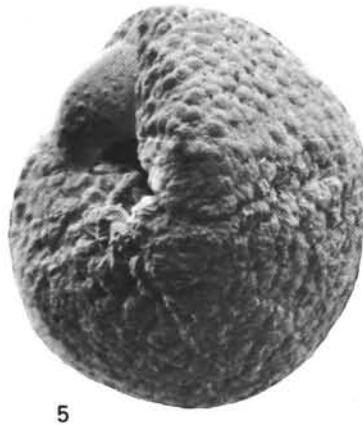
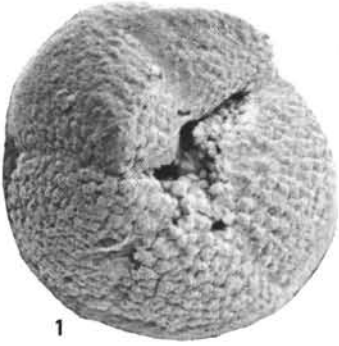
- Lutze, G. F., 1978. Neogene benthonic foraminifera from Site 369, Leg 41, Deep Sea Drilling Project. In Lancelot, Y., Seibold, E., et al., *Initial Reports of the Deep Sea Drilling Project*, v. 41: Washington (U.S. Government Printing Office), p. 659-666.
- Martini, E., 1971. Standard Tertiary and Quaternary calcareous nannoplankton zonation, *Second Plankt. Conf. Proc.*, Rome, 1970, p. 739-785.
- _____, 1976. Cretaceous to Recent calcareous nannoplankton from the Central Pacific Ocean (DSDP Leg 33). In Schlanger, S. O., Jackson, E. D., et al., *Initial Reports of the Deep Sea Drilling Project*, v. 33: Washington (U.S. Government Printing Office), p. 383-423.
- McIver, R., 1975. Hydrocarbon occurrences from JOIDES deep-sea drilling project, *World Petroleum Congr., Panel Disc.*, v. 5(1), p. 1.
- Molyneux, L., 1972. A complete results magnetometer for measuring the remanent magnetization of rocks, *Geophys. J.*, v. 24, p. 429, 435.
- Parker, F. L. and Berger, W. H., 1971. Faunal and solution patterns of planktonic foraminifera in surface sediments of the South Pacific, *Deep-Sea Res.*, v. 18, p. 73-107.
- Postuma, J. A., 1971. *Manual of planktonic foraminifera*: Amsterdam (Elsevier Publishing Company).
- Ratschiller, L. K., 1970. Lithostratigraphy of the Northern Spanish Sahara, *Mem. Museo Tridentino Sci. Nat.*, v. 18, p. 9-84.
- Roth, P., 1973. Calcareous nanofossils — Leg 17, Deep Sea Drilling Project. In Winterer, E. L., Ewing, J. I., et al., *Initial Reports of the Deep Sea Drilling Project*, v. 17: Washington (U.S. Government Printing Office), p. 695-795.
- Ryan, W. B. F., Cita, M. B., Dreyfus Rawson, M., Burckle, L. H., and Saito, T., 1974. A paleomagnetic assignment of Neogene stage boundaries and the development of isochronous datum planes between the Mediterranean, the Pacific and Indian Oceans in order to investigate the response of the world ocean to the Mediterranean "salinity crisis," *Riv. Ital. Paleontol.*, v. 80, p. 631-688.
- Sarnthein, M., 1978. Neogene sand layers off northwest Africa: composition and source environment. In Lancelot, Y., Seibold, E., et al., *Initial Reports of the Deep Sea Drilling Project*, Supplement to Volumes 38, 39, 40, and 41: Washington (U.S. Government Printing Office), p. 939-960.
- Sarnthein, M. and Diester-Haass, L., 1977. Eolian sand turbidites, *J. Sediment. Petrol.*, v. 47, p. 868-890.
- Sayles, F. L. and Manheim, F. T., 1975. Interstitial solutions and diagenesis in deeply buried marine sediments: results from the Deep Sea Drilling Project, *Geochim. Cosmochim. Acta*, v. 39, p. 103-127.
- Schlanger, S. O. and Douglas, R. G., 1974. Pelagic ooze-chalk-limestone transition and its implications for marine stratigraphy. In Hsü, K. J. and Jenkyns, H. C. (Eds.), *Pelagic sediments on land and under the sea: Inter. Assoc. Sedim. Spec. Publ. 1*, p. 117-148.
- Seibold, E. and Hinz, K., 1974. Continental slope construction and destruction, West Africa. In Burk, C. A. and Drake, C. L. (Eds.), *The geology of continental margins*: New York (Springer), p. 179-196.
- Seibold, E. and Hinz, K., 1976. German cruises to the continental margin of North West Africa in 1975. General reports and preliminary results from "Valdivia" 10 and "Meteor" 39, "Meteor" *Forsch. Ergebnisse*, Reihe C, no. 25, p. 47-80.
- Shackleton, N. J. and Kennett, J. P., 1974. Paleotemperature history of the Cenozoic and the initiation of Antarctic glaciation: oxygen and carbon isotope analyses in DSDP Sites 277, 279, and 281. In Kennett, J. P., Houtz, R. E., et al., *Initial Reports of the Deep Sea Drilling Project*, v. 29: Washington (U.S. Government Printing Office), p. 743-755.
- Stainforth, R. M., Lamb, J. L., Luterbacher, H., Beard, J. H., and Jeffords, R. M., 1975. Cenozoic planktonic foraminiferal zonation and characteristic index forms, *The Univ. Kansas Contrib. Article 60*, p. 1-425.
- Stanley, D. J. and Unrug, R., 1972. Submarine channel deposits, fluxoturbidites and other indicators of base-of-slope environments in modern and ancient marine basins. In Rigby, J. K. and Hamblin, W. K. (Eds.), *Soc. Econ. Paleontol. Mineral. Spec. Publ. 16*, p. 387-340.
- Thiede, J., in press. The North Atlantic eastern boundary current system during Glacials and Interglacials (last 150,000 yr), preprint.
- Thierstein, H., 1971. Tentative Lower Cretaceous calcareous nannoplankton zonation, *Eclog. Geol. Helv.*, v. 64, p. 459-488.
- _____, 1973. Lower Cretaceous calcareous nannoplankton biostratigraphy, *Abhandl. Geol. Bundesanst.*, v. 29, p. 1-52.
- Turekian, K. K. and Wedepohl, K. H., 1961. Distribution of the elements in some major units of the Earth's crust, *Geol. Soc. Am. Bull.*, v. 72, p. 175-192.
- Uchupi, E., Emery, K. O., Bowin, C. O., and Phillips, J. D., 1976. Continental margin off Western Africa: Senegal to Portugal, *Am. Assoc. Petrol. Geol. Bull.*, v. 60, p. 809-878.
- van Hinte, J. E., 1976. A Cretaceous time scale, *Am. Assoc. Petrol. Geol. Bull.*, v. 60, p. 498-516.
- von Rad, U. and Einsele, G., in press. Mesozoic-Cenozoic subsidence history and paleobathymetry of the Northwest African Continental margin (Aaiun Basin to DSDP Site 397), *Phil. Trans. Roy. Soc. London*.
- von Rad, U., Čepek, P., von Stackelberg, U., Wissmann, G., and Zobel, B., 1979. Cretaceous and Tertiary sediments from the Northwest African slope (dredges and cores supplementing DSDP results), *Marine Geol.*, v. 29, p. 273-312.

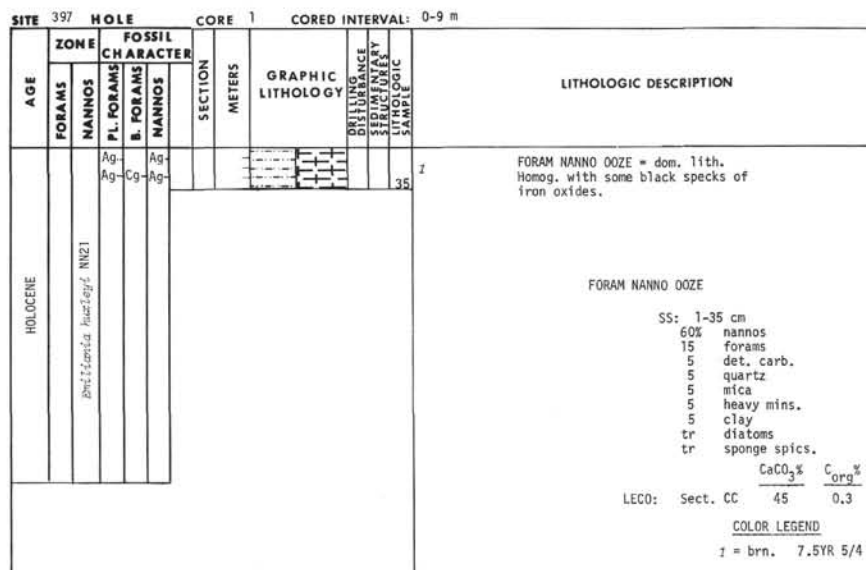
PLATE 1

Evolutionary transition from *Globorotalia tosaensis* to
G. truncatulinoides as recorded in Core 397-15 (200).

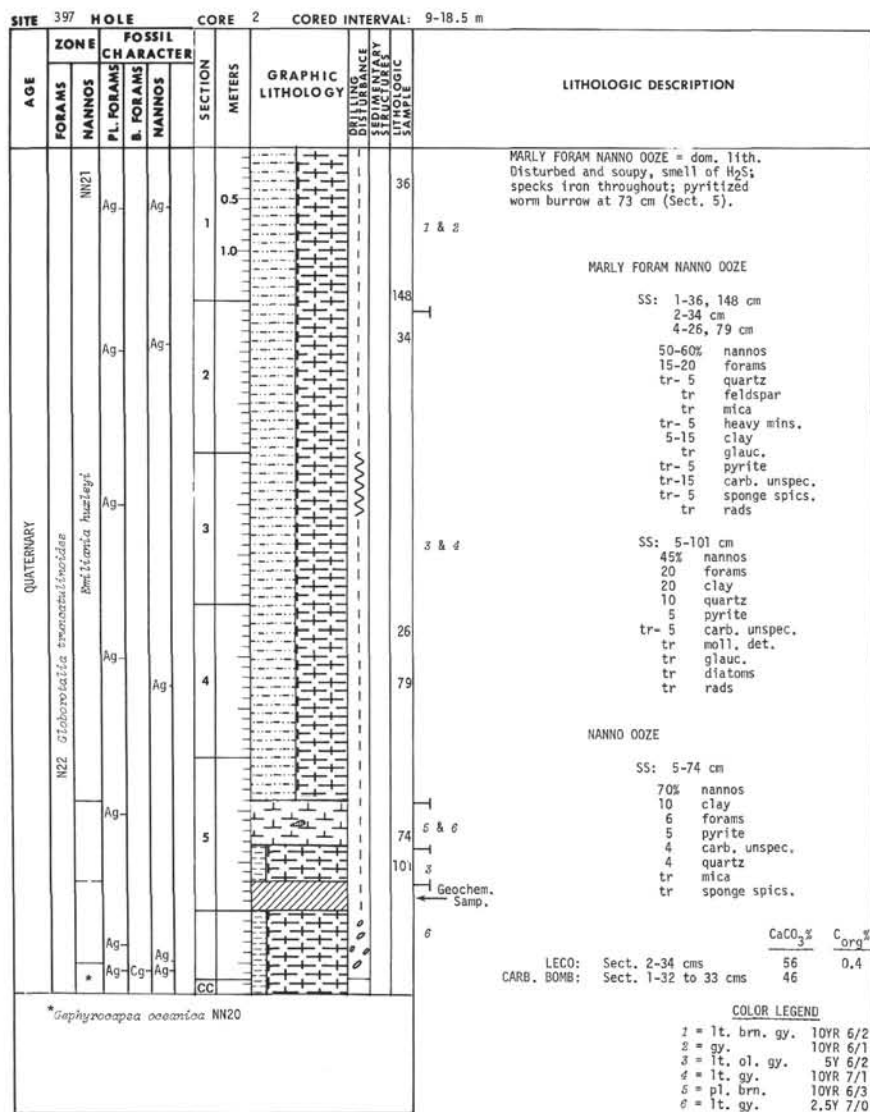
- Figures 1-3 Umbilical views of *Globorotalia tosaensis* Takayanagi and Saito from (respectively) Samples 397-15-1, 50-52 cm; 397-15-2, 50-52 cm; and 397-15-3, 50-52 cm.
- Figure 4 Side view of *G. tosaensis* from Sample 397-15-5, 50-52 cm.
- Figure 5 Umbilical view of *G. tosaensis* from Sample 397-15-6, 50-52 cm.
- Figure 6 Spiral view of a specimen transitional to *G. truncatulinoides*, with a faint, imperforate peripheral keel in the last formed chamber.
- Figure 7 Side view of a primitive form of *G. truncatulinoides* recorded in Sample 397-15-2, 50-52 cm.
- Figure 8 Umbilical view of *G. truncatulinoides* from Sample 397-15-3, 50-52 cm.
- Figure 9 Spiral view of a fully keeled specimen of *G. truncatulinoides* from Sample 397-15-1, 50-52 cm. The FAD of *G. truncatulinoides* is located in Section 3, where the first fully keeled forms are recorded. It occurs at the base of an interval with normal remanent magnetization, interpreted as the Olduvai event (Hamilton, this volume).

PLATE 1

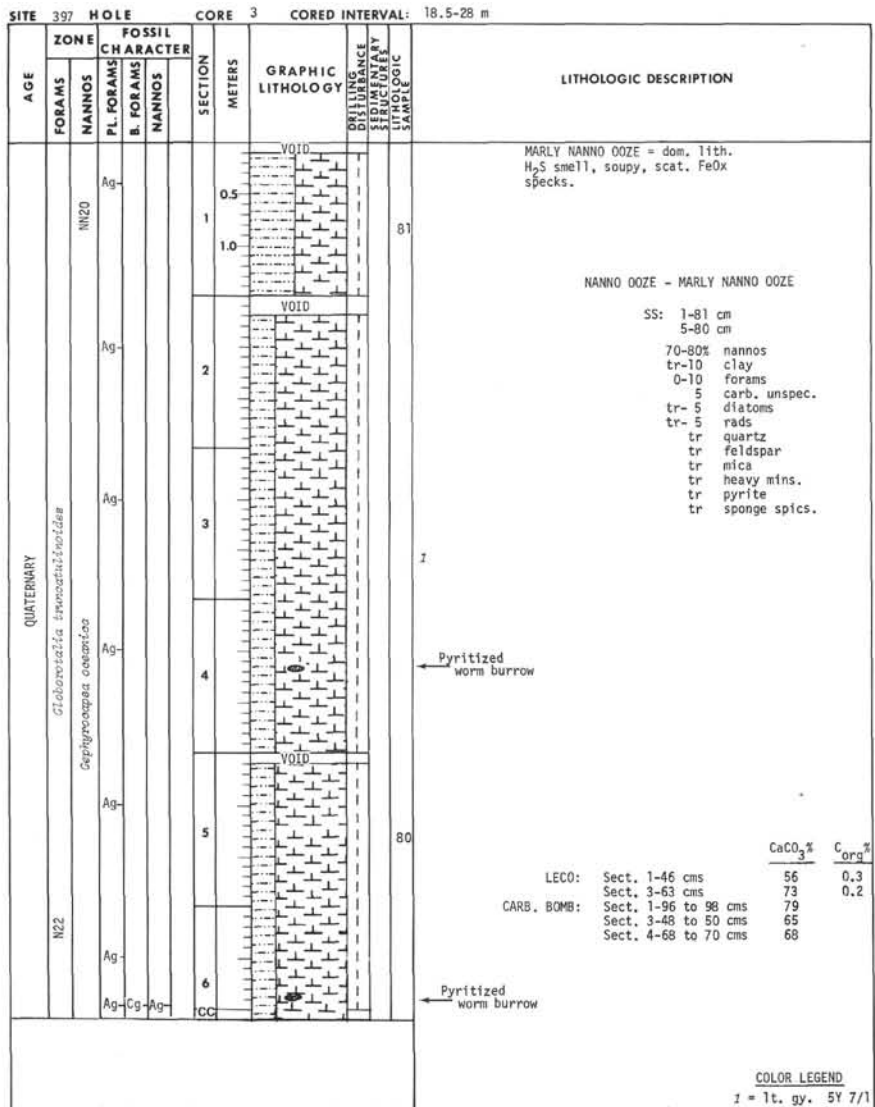


CORE DESCRIPTIONS, SITE 397¹

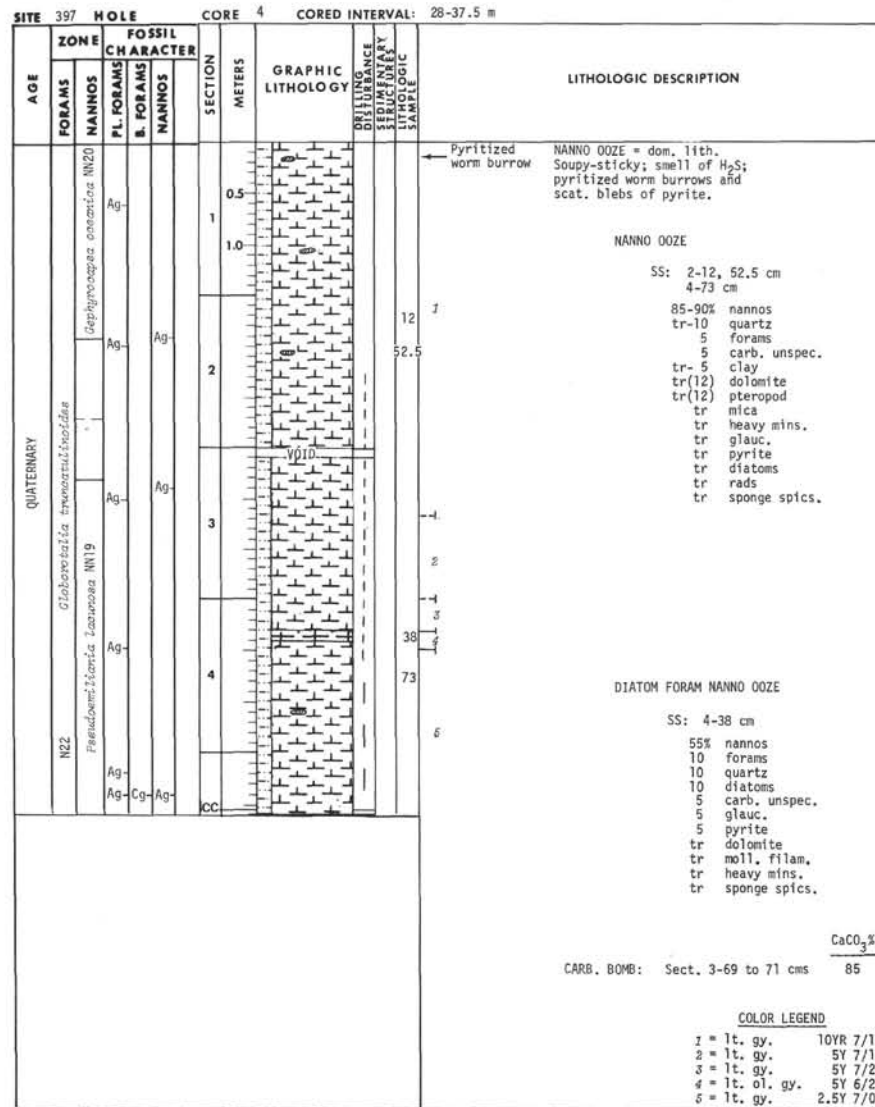
Explanatory notes in Chapter 1

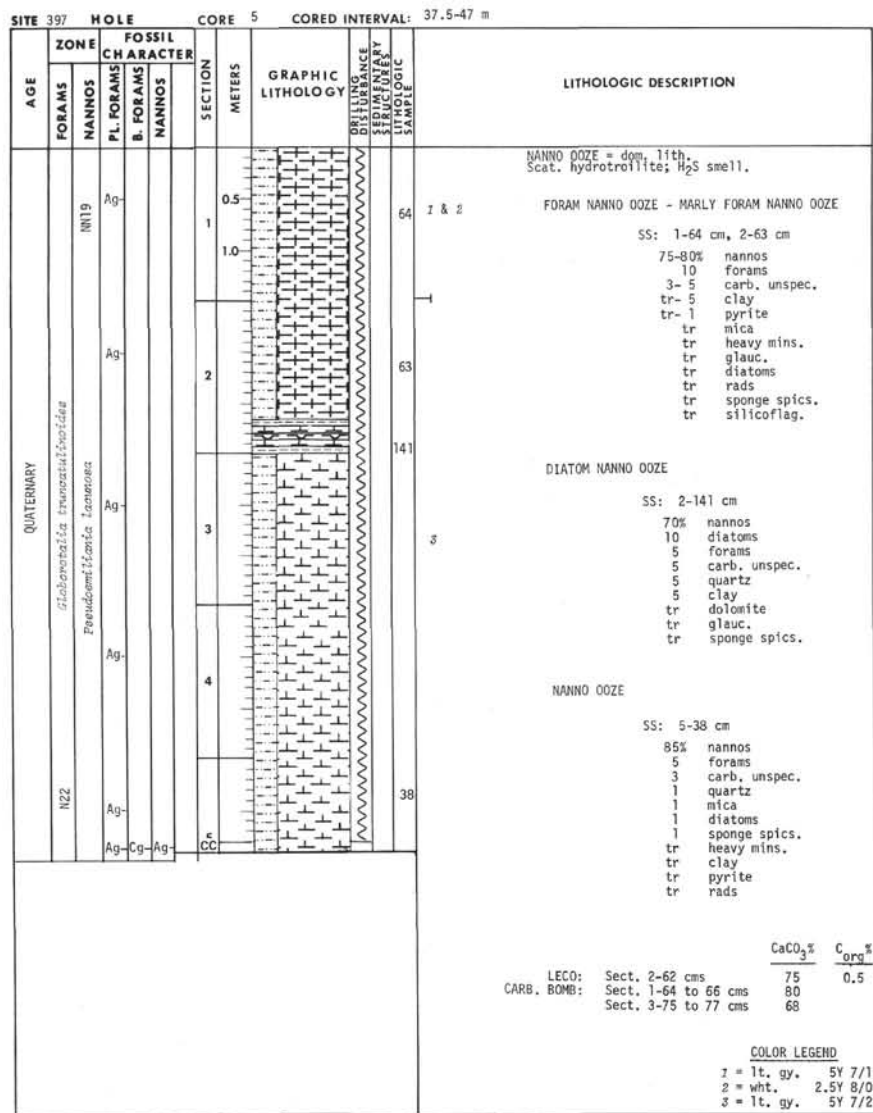
* *Serpilobospora oceanica* NN20

¹ Information on core description sheets represents field notes taken aboard ship under time pressure. Some of this information has been refined in accord with postcruise findings, but production schedules prohibit definitive correlation of these sheets with subsequent findings. Thus the reader should be alerted to the occasional ambiguity or discrepancy.

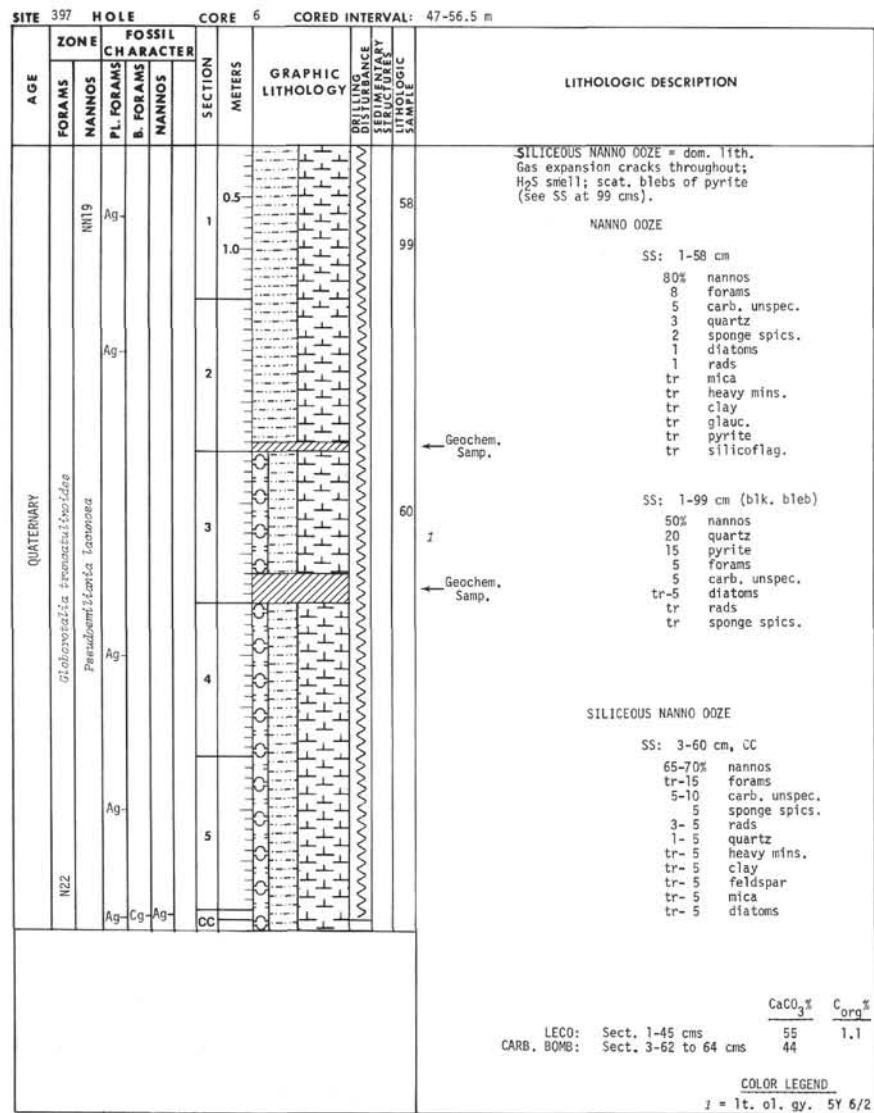


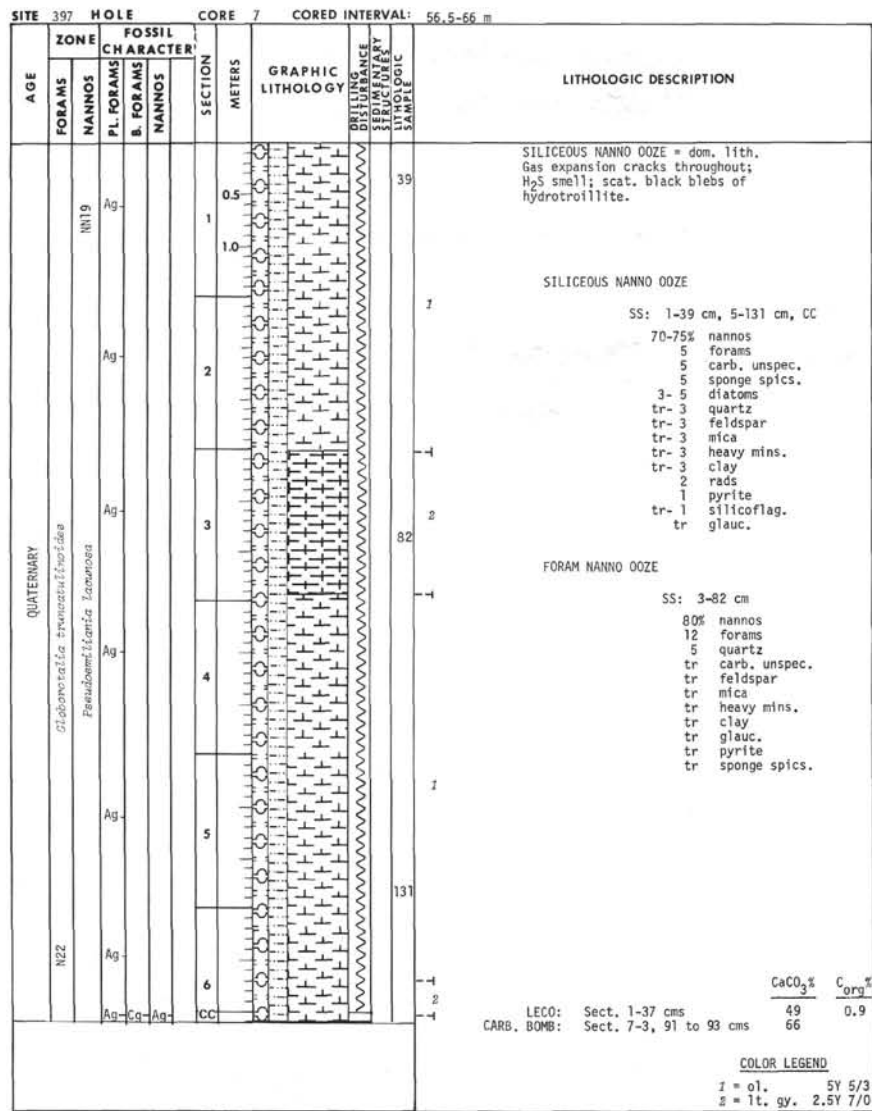
Explanatory notes in Chapter 1



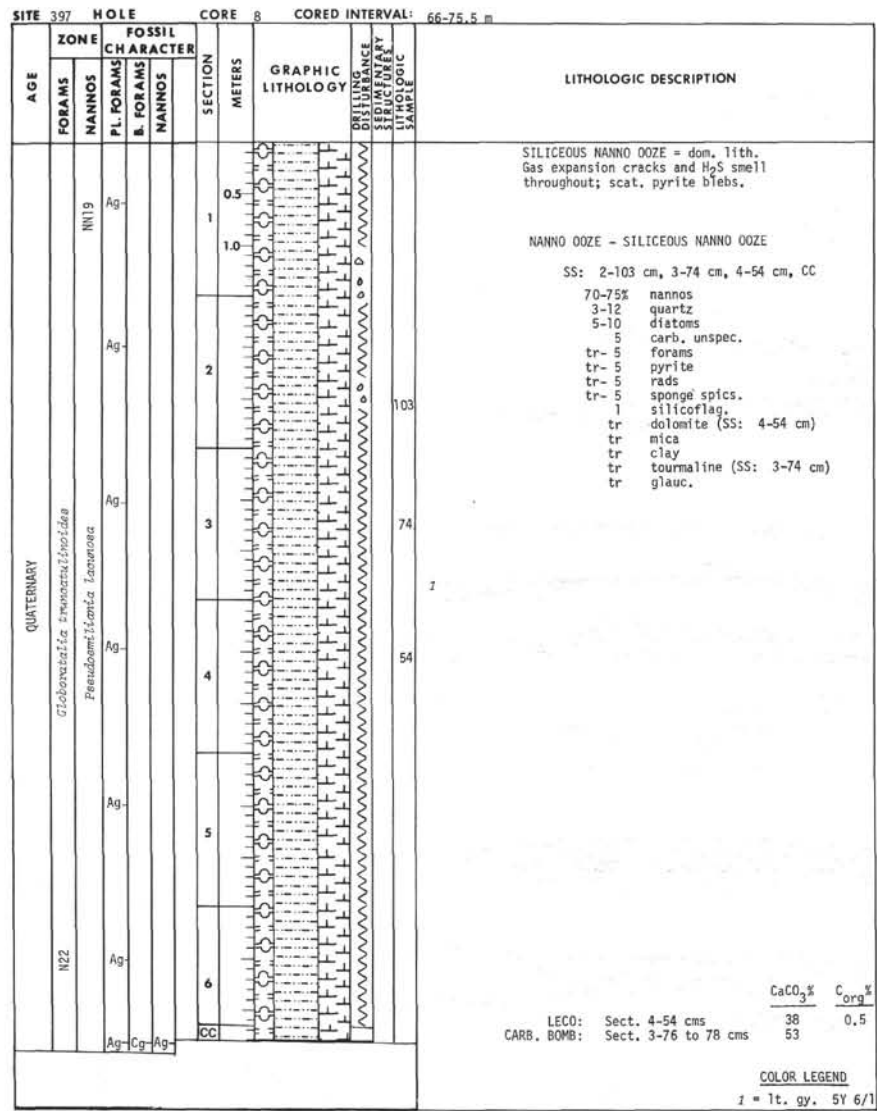


Explanatory notes in Chapter 1





Explanatory notes in Chapter 1



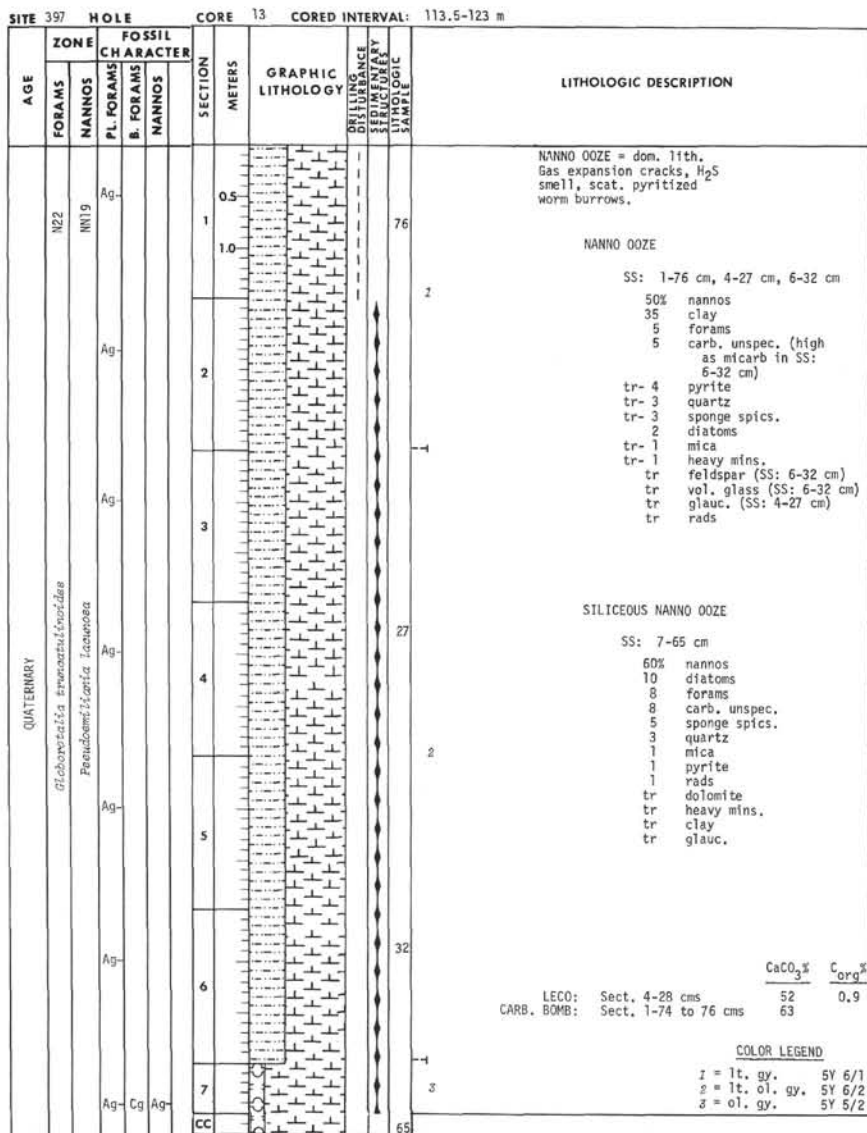
SITE 397 HOLE CORE 11 CORED INTERVAL: 94.5-104 m

AGE	FOSSIL CHARACTER			SECTION METERS	GRAPHIC LITHOLOGY	DRILLING DISTURBANCE STRUCTURE LITHOLOGIC SAMPLE	LITHOLOGIC DESCRIPTION									
	FORAMS	NANNOS	P.L. FORAMS													
QUATERNARY	N22	NN19	Ag	0.5			SILICEOUS NANNO OOZE = dom. lith. Gas expansion cracks; H ₂ S smell; numerous pyritized worm burrows esp. in lt. gy. interval.									
			Ag	1.0			SILICEOUS NANNO OOZE SS: 1-42 cm 65% nannos 10 diatoms 5 sponge spics. 5 mica 5 quartz tr-5 forams 3 glauc. tr carb. unspec., feldspar, heavy mins., rads, plant debris.									
		Ag	2	NANNO OOZE SS: 4-81 cm 80% nannos 5 forams 5 carb. unspec. 5 diatoms 3 sponge spics. 2 quartz tr dolomite, mica, heavy mins., clay, pyrite, glauc., rads.												
		Ag	3	SANDY-SILTY FORAM NANNO OOZE SS: 5-34 cm 40% nannos 25 forams 20 quartz 10 carb. unspec. 2 pyrite tr clay, vol. glass, glauc., sponge spics., ostracods.												
		Ag-Cg	5													
			CC													
							<table border="0"> <tr> <td></td> <td>CaCO₃%</td> <td>C_{org}%</td> </tr> <tr> <td>LECO: Sect. 4-79 cms</td> <td>48</td> <td>0.4</td> </tr> <tr> <td>CARB. BOMB: Sect. 1-40 to 42 cms</td> <td>56</td> <td></td> </tr> </table> <p>COLOR LEGEND 1 = lt. ol. gy. 5Y 6/2 2 = lt. gy. 5Y 6/1 3 = ol. gy. 5Y 5/2</p>		CaCO ₃ %	C _{org} %	LECO: Sect. 4-79 cms	48	0.4	CARB. BOMB: Sect. 1-40 to 42 cms	56	
	CaCO ₃ %	C _{org} %														
LECO: Sect. 4-79 cms	48	0.4														
CARB. BOMB: Sect. 1-40 to 42 cms	56															

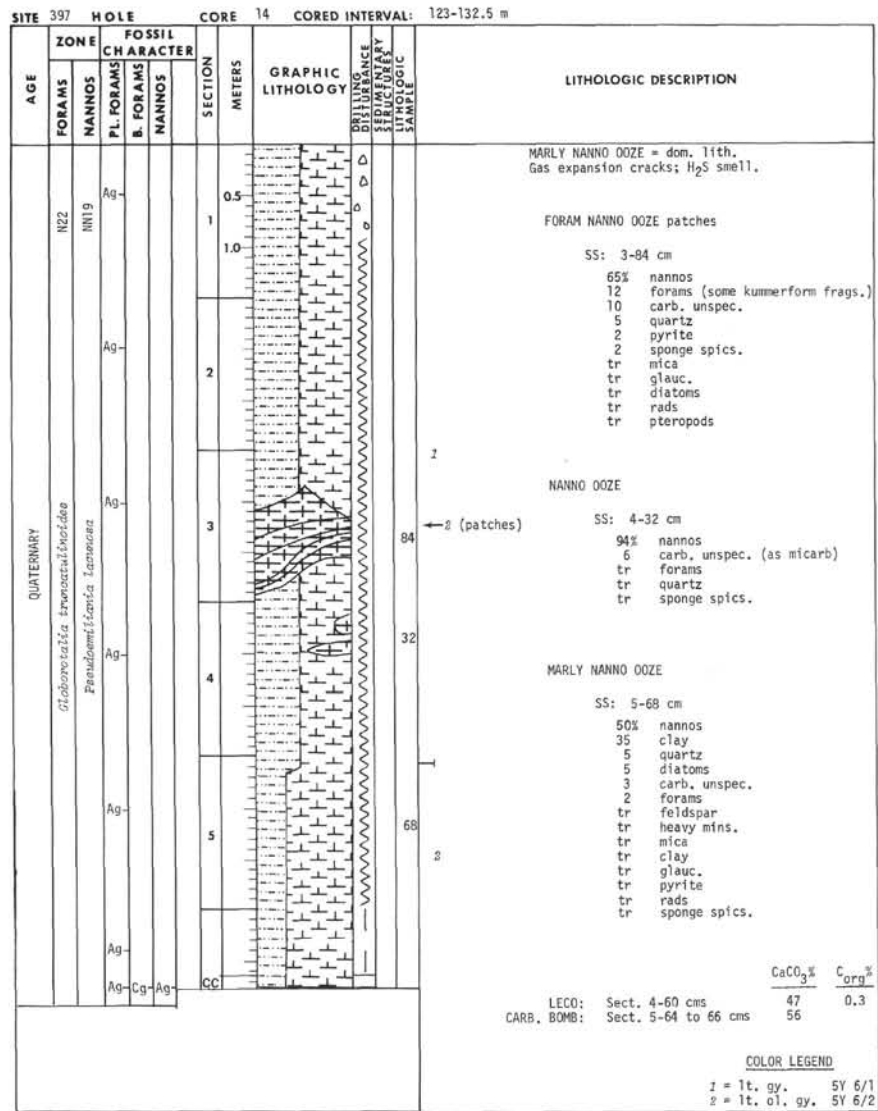
Explanatory notes in Chapter 1

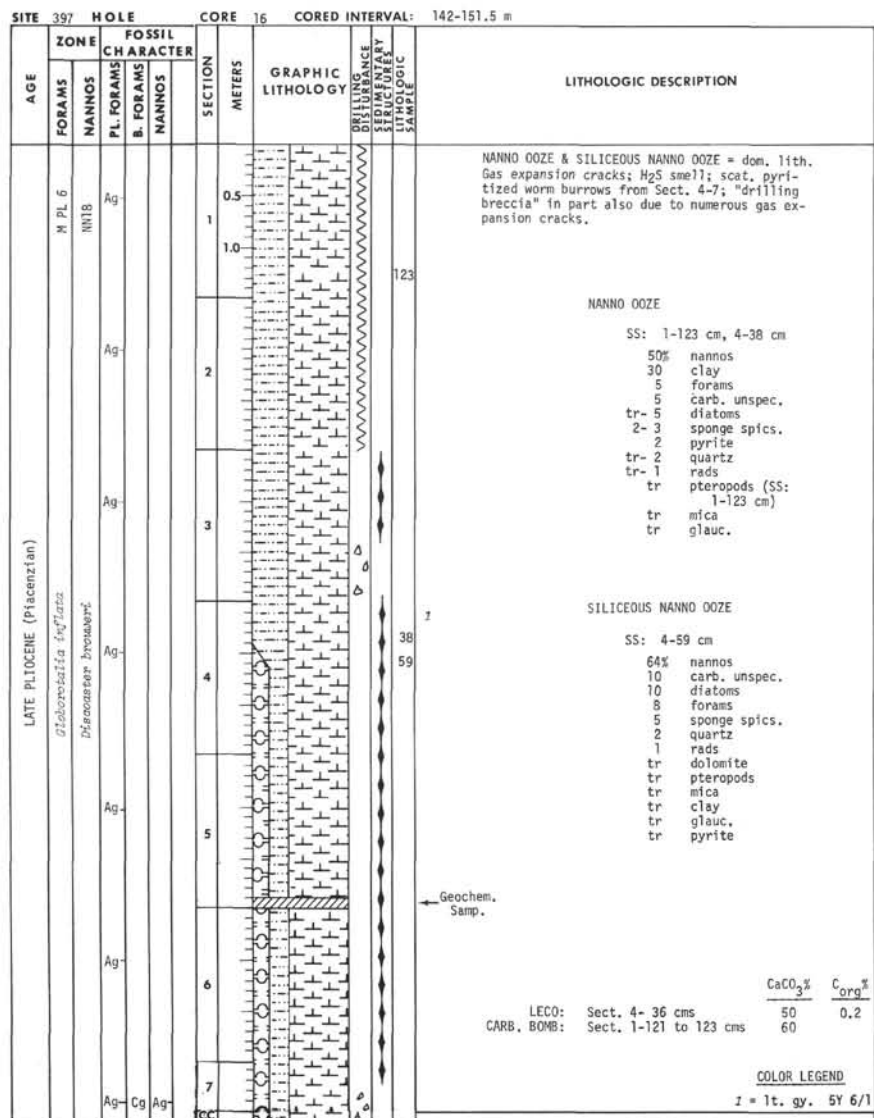
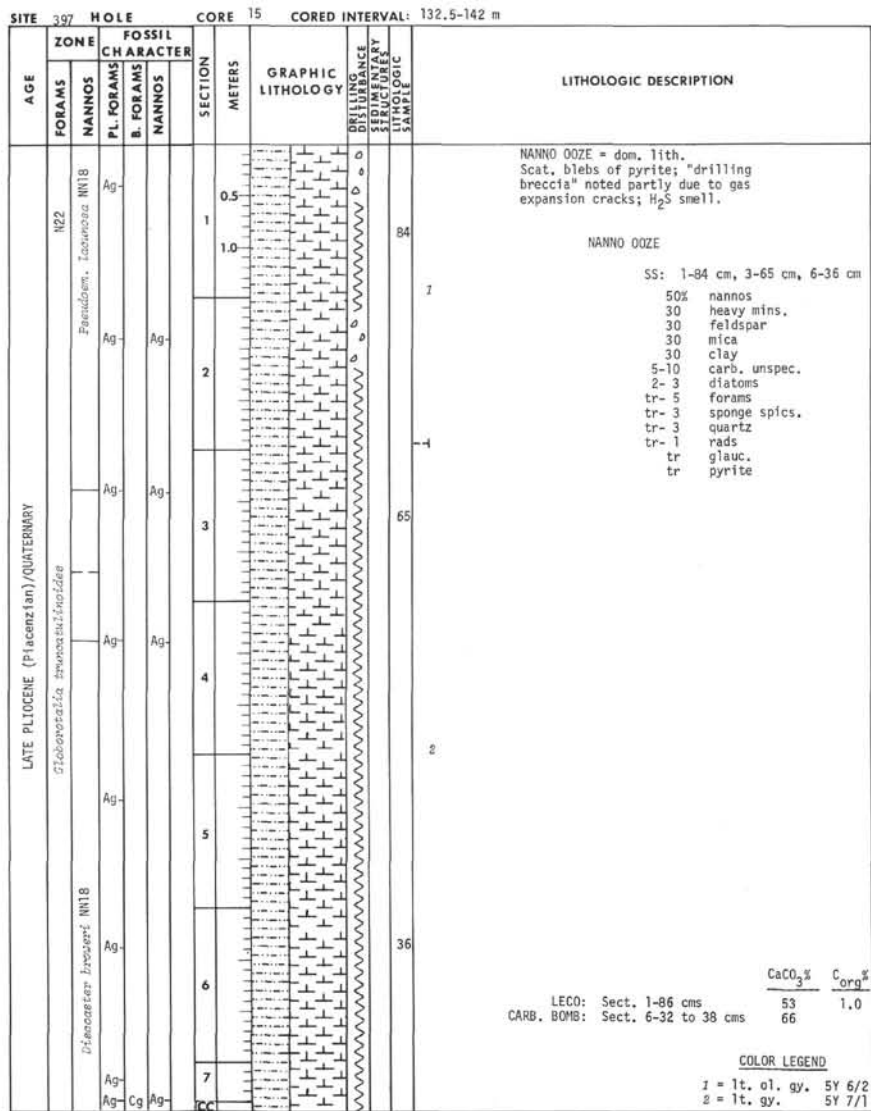
SITE 397 HOLE CORE 12 CORED INTERVAL: 104-113.5 m

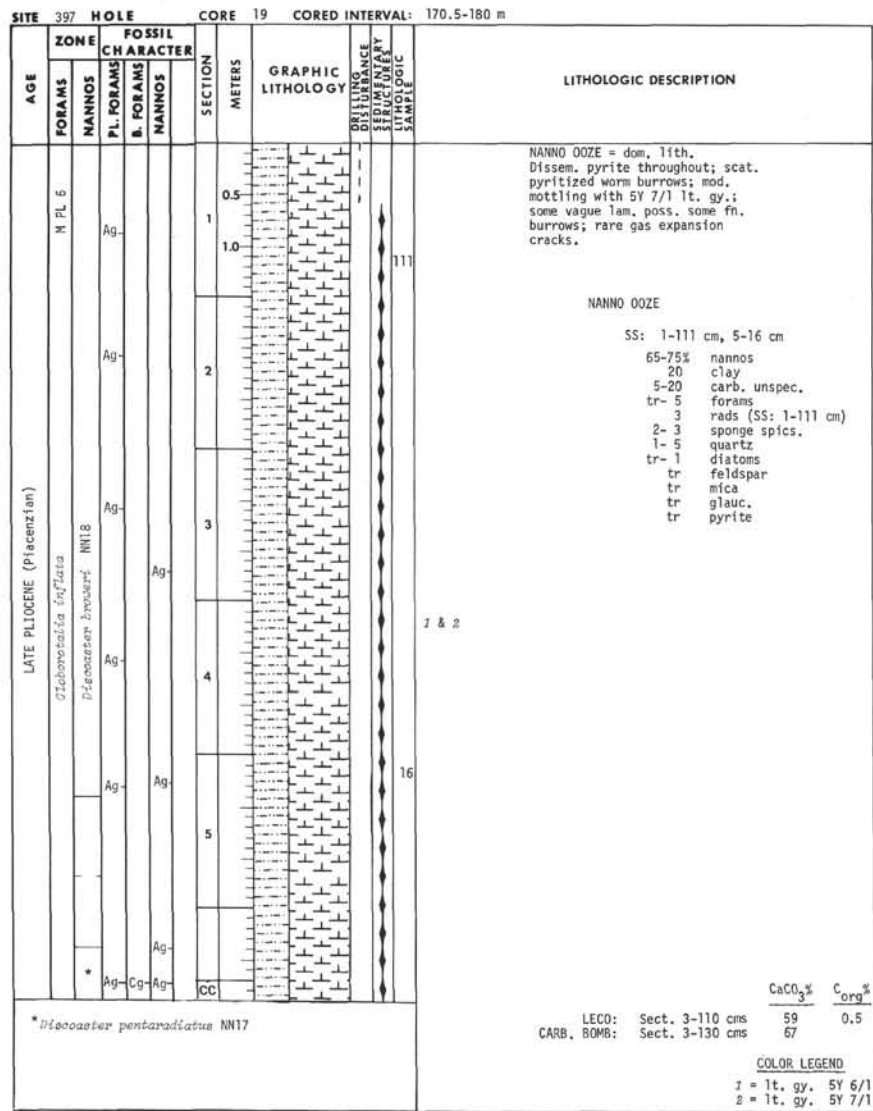
AGE	FOSSIL CHARACTER			SECTION METERS	GRAPHIC LITHOLOGY	DRILLING DISTURBANCE STRUCTURE LITHOLOGIC SAMPLE	LITHOLOGIC DESCRIPTION									
	FORAMS	NANNOS	P.L. FORAMS													
QUATERNARY	N22	NN19	Ag	0.5			MARLY FORAM NANNO OOZE = dom. lith. Numerous gas expansion cracks; H ₂ S smell; otoliths at 4-80 cm, 7-10 cm; scaphopod frag. ~5 mm long at 6-30 cm.									
			Ag	1.0			MARLY FORAM NANNO OOZE SS: 1-19 cm ~45% clay nannos 5 quartz 5 sponge spics. 3 forams 2 carb. unspec. tr dolomite tr mica tr glauc. tr pyrite tr diatoms tr rads									
		Ag	2	MARLY NANNO OOZE SS: 5-98 cm 65% nannos 15 clay 10 quartz 5 carb. unspec. 3 forams 1 mica 1 sponge spics. tr dolomite tr feldspar tr glauc. tr pyrite tr diatoms												
		Ag	3													
		Ag	4													
		Ag	5													
		Ag	6													
			CC													
			Ag-Cg													
							<table border="0"> <tr> <td></td> <td>CaCO₃%</td> <td>C_{org}%</td> </tr> <tr> <td>LECO: Sect. 5-87 cms</td> <td>58</td> <td>0.6</td> </tr> <tr> <td>CARB. BOMB: Sect. 1-15 to 17 cms</td> <td>58</td> <td></td> </tr> </table> <p>COLOR LEGEND 1 = lt. ol. gy. 5Y 6/2 2 = gy. 5Y 5/1</p>		CaCO ₃ %	C _{org} %	LECO: Sect. 5-87 cms	58	0.6	CARB. BOMB: Sect. 1-15 to 17 cms	58	
	CaCO ₃ %	C _{org} %														
LECO: Sect. 5-87 cms	58	0.6														
CARB. BOMB: Sect. 1-15 to 17 cms	58															



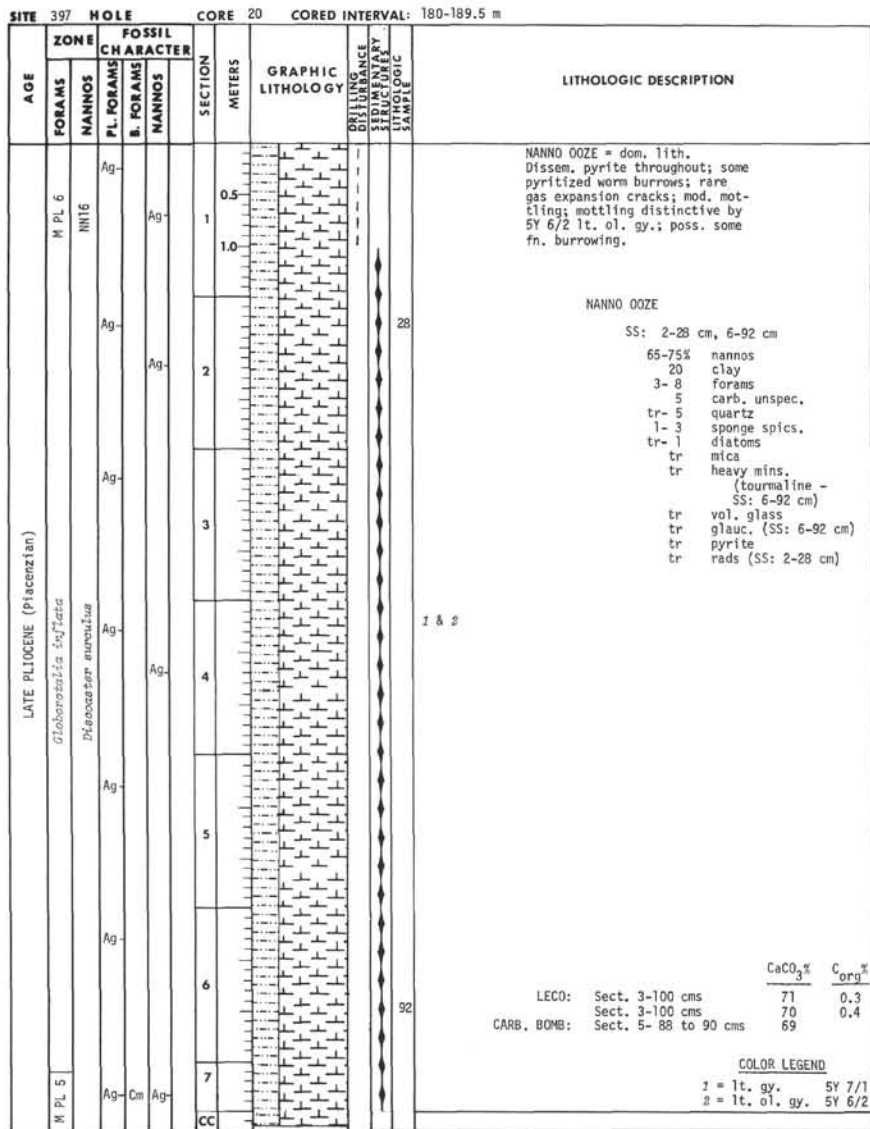
Explanatory notes in Chapter 1







Explanatory notes in Chapter 1



SITE 397 HOLE CORE 17 CORED INTERVAL: 151.5-161 m

AGE	ZONE		FOSSIL CHARACTER		SECTION METERS	GRAPHIC LITHOLOGY	DRILLING FLUID SEEDING STRUCTURE SAMPLE	LITHOLOGIC DESCRIPTION
	FORAMS	NANNOS	P. FORAMS	NANNOS				
LATE PLIOGENE (Pliocenzian)	M PL 6	NN1B	Ag-		0.5	VOID		<p>MARLY FORAM NANNO OOZE = dom. lith. Homogeneous with scat. mottling, pyritized worm burrows, & dissem. pyrite.</p> <p>MARLY FORAM NANNO OOZE</p> <p>SS: 2-21 cm, 3-57 cm</p> <p>50% nannos 30 clay 5-7 quartz 5 forams 5 unspec. carb. tr-3 pyrite tr-3 diatoms tr-2 sponge spics. 1 dolomite (SS: 2-21 cm) 1 feldspar (SS: 2-21 cm) 1 rads (SS: 2-21 cm) tr mica; tr vol. glass tr glauc. (SS: 2-21 cm)</p> <p>LECO: Sect. 6-55 cms $\text{CaCO}_3\%$ 57 $\text{C}_{org}\%$ 0.3 CARB. BOMB: Sect. 2-20 to 22 cms 63</p> <p>COLOR LEGEND 1 = 1t. ol. gy. 5Y 6/2</p>
			Ag-		1.0			
			Ag-		2			
			Ag-		3			
			Ag-		4			
			Ag-		5			
			Ag-		6			
		Ag-Cg Ag-		7				

Explanatory notes in Chapter 1

SITE 397 HOLE CORE 18 CORED INTERVAL: 161-170.5 m

AGE	ZONE		FOSSIL CHARACTER		SECTION METERS	GRAPHIC LITHOLOGY	DRILLING FLUID SEEDING STRUCTURE SAMPLE	LITHOLOGIC DESCRIPTION
	FORAMS	NANNOS	P. FORAMS	NANNOS				
LATE PLIOGENE (Pliocenzian)	M PL 6	NN1B	Ag-		0.5			<p>MARLY NANNO OOZE = dom. lith. Scat. otoliths, pyritized worm burrows, and dissem. pyrite; mod. mottling from Sect. 2 on; vague lam. throughout; rare <i>Pyrgo</i> large forams; rare gas expansion cracks.</p> <p>MARLY NANNO OOZE</p> <p>SS: 1-41 cm, 3-40 cm</p> <p>68% nannos 30 clay 5-15 carb. unspec. 7-8 forams tr-3 quartz 2 diatoms (SS: 1-41 cm) 2 sponge spics. tr-2 mica tr-1 pyrite tr dolomite (SS: 1-41 cm) tr glauc. (SS: 1-41 cm) tr rads</p> <p>LECO: Sect. 1-31 cms $\text{CaCO}_3\%$ 58 $\text{C}_{org}\%$ 0.4 Sect. 3-76 cms 61 0.4 CARB. BOMB: Sect. 3-44 to 46 cms 65 Sect. 3-65 cms 63</p> <p>COLOR LEGEND 1 = 1t. gy. 5Y 6/1</p>
			Ag-		1.0			
			Ag-		2			
			Ag-		3			
			Ag-		4			
			Ag-		5			
			Ag-		6			
		Ag-Cg Ag-		7				

SITE 397 HOLE		CORE 21		CORED INTERVAL: 189.5-199 m					
AGE	ZONE	FOSSIL CHARACTER		SECTION	METERS	GRAPHIC LITHOLOGY	DRILLING DISTURBANCE	SEDIMENTARY STRUCTURES	LITHOLOGIC DESCRIPTION
		P. FORAMS	NANNOS						
	M. PL. 5		Ag-		0.5				NANNO OOZE = dom. lith. Mottled; Sect. 4 distinctively darker in color; extensive fn. burrows; dissem. pyrite throughout; apparently in some of worm burrows; rare gas expansion cracks.
	NN16				1.0				
			Ag-		2				NANNO OOZE SS: 4-80 cm, 5-71 cm 55-65% nannos 20 clay 5-10 carb. unspec. 5-6 diatoms 1-5 forams 3-4 quartz 2 sponge spics. 2 pyrite tr-2 mica 1 sil. unspec. (SS: 5-71 cm) tr dolomite (SS: 5-71 cm) tr glauc. (SS: 5-71 cm) tr rads
			Ag-		3				
			Ag-		4				
			Ag-		5				
			Ag-		6				LECO: Sect. 3-90 cms 56 0.5 Sect. 4-76 cms 50 0.9 CORG: Sect. 5-71 to 73 cms 70
			Ag-Cm Ag-		7				COLOR LEGEND 1 = lt. ol. gy. SY 6/2 2 = pl. ol. SY 6/3
					CC				

Explanatory notes in Chapter 1

SITE 397 HOLE		CORE 22		CORED INTERVAL: 199-208.5 m					
AGE	ZONE	FOSSIL CHARACTER		SECTION	METERS	GRAPHIC LITHOLOGY	DRILLING DISTURBANCE	SEDIMENTARY STRUCTURES	LITHOLOGIC DESCRIPTION
		P. FORAMS	NANNOS						
	M. PL. 5		Ag-		0.5				NANNO OOZE = dom. lith. Numerous fn. burrows; dissem. pyrite throughout; no gas expansion cracks; some mottling (slight) particularly from Sect. 4 down (with apparent concomitant decrease in fn. burrows).
	NN16				1.0				
			Ag-		2				Sequences noted in Sect. 3 (only 2 noted, possibly 3)
			Ag-		3				~15-20 cm Numerous fn., hor. burrows, decreasing down. Sharp contact
			Ag-		4				NANNO OOZE SS: 1-49 cm, 3-46 cm 60-70% nannos 15-20 clay 2-8 forams 5 carb. unspec. 2-5 diatoms 2 sponge spics. 1 sil. unspec. (SS: 3-46 cm) 1 quartz tr dol. (SS: 3-46 cm) tr feldspar (SS: 3-46 cm) tr mica tr heavy mins. (SS: 3-46 cm)
			Ag-		5				
			Ag-		6				
			Ag-Cm Ag-		7				COLOR LEGEND 1 = lt. ol. gy. SY 6/2 2 = lt. gy. SY 7/1
					CC				ASH LAYER (50% volcanic glass)

SITE 397 HOLE CORE 23 CORED INTERVAL: 208.5-218 m

AGE	FOSSIL CHARACTER		SECTION	METERS	GRAPHIC LITHOLOGY	DRILLING DISTURBANCE STRUCTURE LITHOLOGIC SAMPLE	LITHOLOGIC DESCRIPTION
	FORAMS	NANNOS					
LATE PLIOCENE (Piacenzian)	M PL 5	NN16	1	0.5			<p>SILICEOUS FORAM NANNO OOZE = dom. lith. In gen., sed. becoming more sticky; some gas expansion cracks (more than in prev. core); pyrite dissem. throughout; scat. pyritized worm burrows.</p> <p>SILICEOUS FORAM NANNO OOZE</p> <p>SS: 1-30 cm</p> <p>50% nannos 15-20 clay 12 forams 10 diatoms 8 carb. unspc. 2 quartz 2 sponge spics. 1 mica 1 rads tr pyrite</p> <p>Numerous fn. hor. burrows, suggestion of sequences noted in C.22; becoming mottled in Sect. 5 (coring disturb. in Sects. 1-3 prohibit any distinction of these struc.).</p> <p>MARLY NANNO OOZE</p> <p>SS: 5-48 cm</p> <p>45% nannos 40 clay 4 forams 2 mica (muscovite?) 2 diatoms 1 carb. unspc. 1 quartz 1 heavy mins. 1 sponge spics. tr dolomite tr feldspar tr Fe Ox tr vol. glass (w/opaque inclusions) tr rads</p> <p>LECO: Sect. 2-54 cms $\frac{CaCO_3\%}{67}$ $\frac{C_{org}\%}{0.3}$ CARB. BOMB: Sect. 5-42 to 44 cms $\frac{CaCO_3\%}{52}$</p> <p>COLOR LEGEND 1 = lt. gy. 5Y 6/1</p>
			2	1.0			
			3				
			4				
			5				
				48			

Explanatory notes in Chapter 1

SITE 397 HOLE CORE 24 CORED INTERVAL: 218-227.5 m

AGE	FOSSIL CHARACTER		SECTION	METERS	GRAPHIC LITHOLOGY	DRILLING DISTURBANCE STRUCTURE LITHOLOGIC SAMPLE	LITHOLOGIC DESCRIPTION
	FORAMS	NANNOS					
LATE PLIOCENE (Piacenzian)	M PL 5		1	0.5			<p>MARLY NANNO OOZE = dom. lith. Some small hor. burrows; dissem. pyrite throughout; rare gas expansion cracks.</p> <p>NANNO OOZE</p> <p>SS: 1-73 cm</p> <p>55% nannos 15-20 clay 10 carb. unspc. 5 forams 5 diatoms 2 quartz 2 sponge spics. 1 pyrite 1 sil. unspc. tr mica tr glauc.</p> <p>Some mottling; fewer burrows; this gray interval more homog. and sticky.</p> <p>MARLY NANNO OOZE</p> <p>SS: 4-63 cm</p> <p>45% nannos 30 clay 5 forams 5 diatoms 4 sponge spics. 3 pyrite 2 carb. unspc. 1 quartz 1 mica 1 heavy mins. 1 rads tr feldspar tr dolomite tr glauc.</p> <p>LECO: Sect. 1-73 cms $\frac{CaCO_3\%}{55}$ $\frac{C_{org}\%}{0.3}$ CARB. BOMB: Sect. 4-71 to 73 cms $\frac{CaCO_3\%}{49}$</p> <p>COLOR LEGEND 1 = lt. gy. 5Y 6/1 2 = gy. 5Y 5/1</p>
			2	1.0			
			3				
			4				
			5				
			6				
			7				
				73			

SITE 397		HOLE		CORE 25		CORED INTERVAL: 227.5-237 m				
AGE	ZONE		FOSSIL CHARACTER			SECTION METERS	GRAPHIC LITHOLOGY	DISTURBANCE SEDIMENTARY STRUCTURES	LITHOLOGIC SAMPLE	LITHOLOGIC DESCRIPTION
	FORAMS	NANNOS	PL. FORAMS	B. FORAMS	NANNOS					
LATE PLEISTOCENE (Piacenzian)	M PL 4	NN14	Ag			0.5				NANNO OOZE = dom. lith. Dissem. pyrite throughout; some vague lam. in Sects. 4 and 5 where disturb. are less.
						1.0				
						2	VOID			
						3				
						4				NANNO OOZE SS: 5-62 cm 45% nannos 25 clay 5 forams 5 carb. unspec. (bryozoan frag.) 4 diatoms 3 feldspar (altered) 3 vol. glass 2 dolomite 2 mica 2 heavy mins. (tourmaline) 1 pyrite 1 sponge spics. tr glauc.(?)
					5					
					CC					
										CaCO ₃ %
										CARB. BOMB: Sect. 5-51 to 53 cms 72
										COLOR LEGEND z = lt. gy. 5Y 6/1

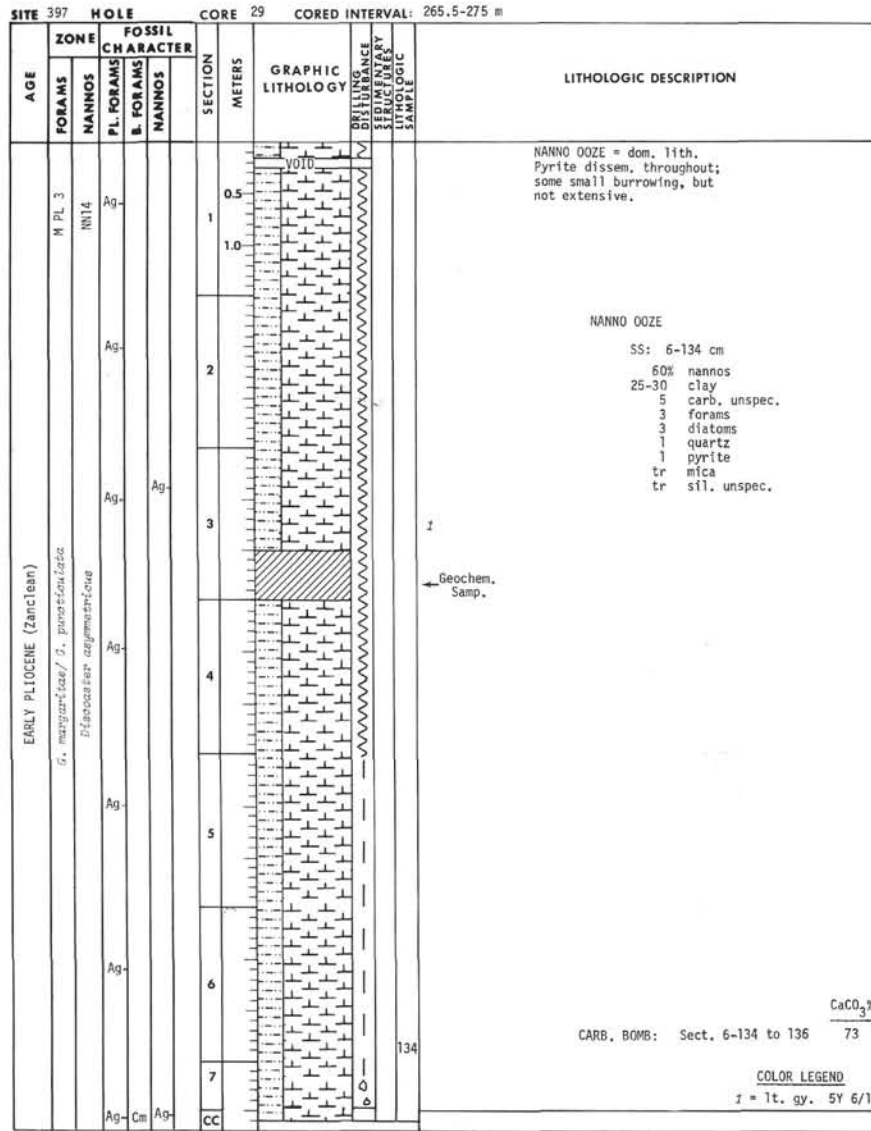
Explanatory notes in Chapter 1

SITE 397		HOLE		CORE 26		CORED INTERVAL: 237-246.5 m				
AGE	ZONE		FOSSIL CHARACTER			SECTION METERS	GRAPHIC LITHOLOGY	DISTURBANCE SEDIMENTARY STRUCTURES	LITHOLOGIC SAMPLE	LITHOLOGIC DESCRIPTION
	FORAMS	NANNOS	PL. FORAMS	B. FORAMS	NANNOS					
LATE PLEISTOCENE (Piacenzian)	M PL 4	NN14	Ag			0.5				NANNO OOZE = dom. lith. Dissem. pyrite; numerous gas expansion cracks only in Sect. 3 and decreasing in Sect. 4, rare in other sections.
						1.0				
						2				
						3				
						4				
						5				
						6				
					7					
					CC					
										COLOR LEGEND z = lt. gy. 5Y 6/1 z = lt. gy. 5Y 7/1

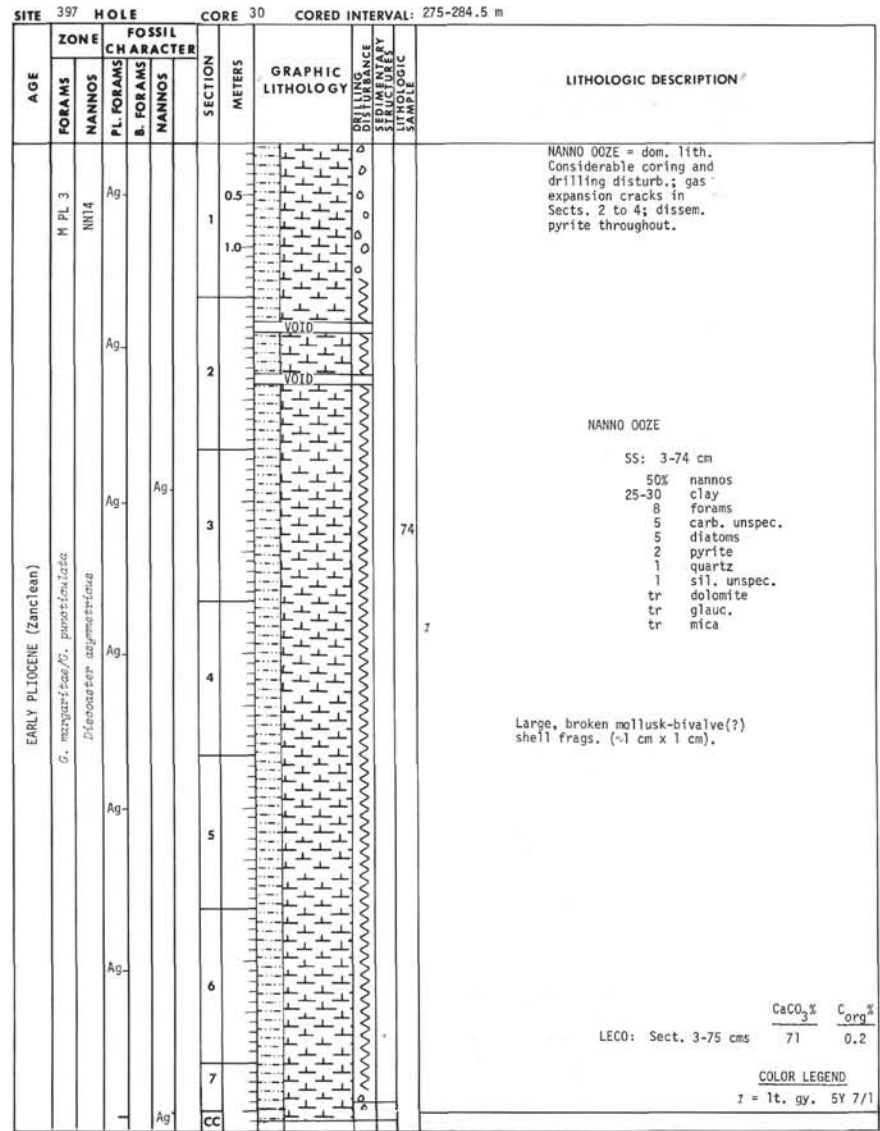
SITE 397		HOLE		CORE 27		CORED INTERVAL: 246.5-256 m	
AGE	FOSSIL CHARACTER		SECTION METERS	GRAPHIC LITHOLOGY	DRILLING MUD STRUCTURE BY STANDARD METHODS	LITHOLOGIC DESCRIPTION	
	FORAMS	NANNOS					
LATE PLIOCENE (Piacenzian)	M PL 4		0.5			<p>NANNO OOZE = dom. lith. Dissem. pyrite throughout; rare pyritized worm burrows.</p> <p>NANNO OOZE</p> <p>SS: 1-51 cm</p> <p>60% nannos 15-20 clay 10 diatoms 5 forams 5 carb. unspec. 2 quartz tr mica tr glauc. tr pyrite tr sponge spics.</p> <p>NANNO OOZE</p> <p>SS: 3-105 cm</p> <p>65% nannos 20 clay 5 forams 5 carb. unspec. 2 diatoms 1 dolomite 1 pyrite tr quartz tr mica</p> <p>Smear slide of pyrite-filled worm burrow:</p> <p>PYRITIZED MARLY OOZE</p> <p>SS: 3-50 cm</p> <p>45-50% nannos 30-35 clay 5 carb. unspec. 3 forams 2 diatoms tr dolomite tr quartz tr mica</p>	51
	M PL 4		1.0				
			2				
			3				
			4				
		5					
		CC					
						<p>LECO: Sect. 3- 58 cms $\frac{\text{CaCO}_3\%}{3}$ $\frac{\text{C}_{org}\%}{0.2}$</p> <p>CARB. BOMB: Sect. 3-111 to 113 cms 83</p>	
						COLOR LEGEND	
						1 = 1t. gy. 5Y 7/1	

Explanatory notes in Chapter 1

SITE 397		HOLE		CORE 28		CORED INTERVAL: 256-265.5 m	
AGE	FOSSIL CHARACTER		SECTION METERS	GRAPHIC LITHOLOGY	DRILLING MUD STRUCTURE BY STANDARD METHODS	LITHOLOGIC DESCRIPTION	
	FORAMS	NANNOS					
LATE PLIOCENE (Piacenzian)	M PL 4		0.5			<p>NANNO OOZE = dom. lith. Dissem. pyrite; no gas expansion cracks; homog. (except for drilling disturb.).</p> <p>NANNO OOZE</p> <p>SS: 3-75 cm</p> <p>60% nannos 25-30 clay 3 forams 3 carb. unspec. 3 diatoms 1 pyrite 1 sil. unspec. tr quartz tr mica</p>	75
	M PL 4		1.0				
			2				
			3				
			4				
		5					
		6					
		7					
		CC					
						<p>LECO: Sect. 2-77 cms $\frac{\text{CaCO}_3\%}{54}$ $\frac{\text{C}_{org}\%}{0.3}$</p>	
						COLOR LEGEND	
						1 = 1t. gy. 5Y 6/1	



Explanatory notes in Chapter 1

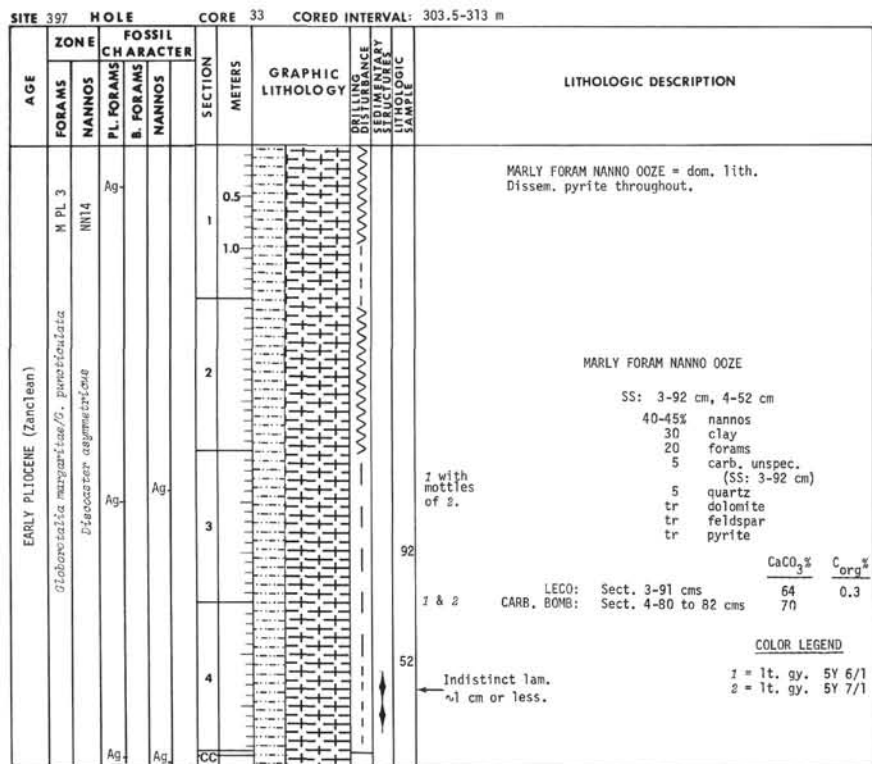


SITE 397 HOLE		CORE 31		CORED INTERVAL: 284.5-294 m		
AGE	FOSSIL CHARACTER			SECTION METERS	GRAPHIC LITHOLOGY	LITHOLOGIC DESCRIPTION
	FORAMS	NANNOS	B. FORAMS			
EARLY PLIOCENE (Zanclean)	M PL 3			0.5	VOID	MARLY NANNO OOZE = dom. lith. Pyrite dissem. throughout; considerable drilling disturb.
	NIN14			1.0		
				2.0		MARLY NANNO OOZE SS: 2-106 cm 55% nannos 30 clay 5 forams 3 carb. unsp. 3 diatoms 1 quartz 1 pyrite 1 sil. unsp. tr dolomite tr mica tr glauc. tr heavy mins. (tourmaline)
			Ag	3.0		LECO: Sect. 3-32 cms $\frac{\text{CaCO}_3\%}{41}$ $\frac{\text{C}_{org}\%}{0.3}$ COLOR LEGEND z = 1t. gy. 5Y 6/1
			4.0			
			CC			

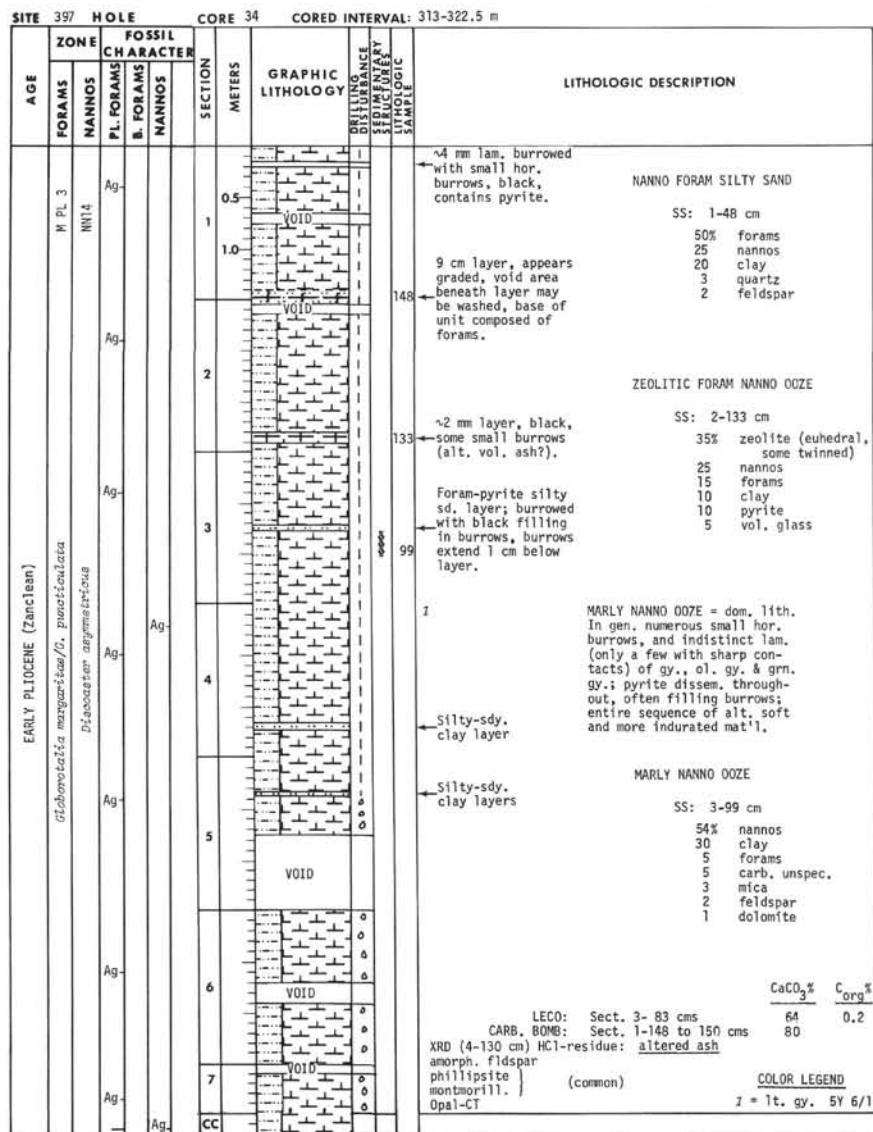
Explanatory notes in Chapter 1

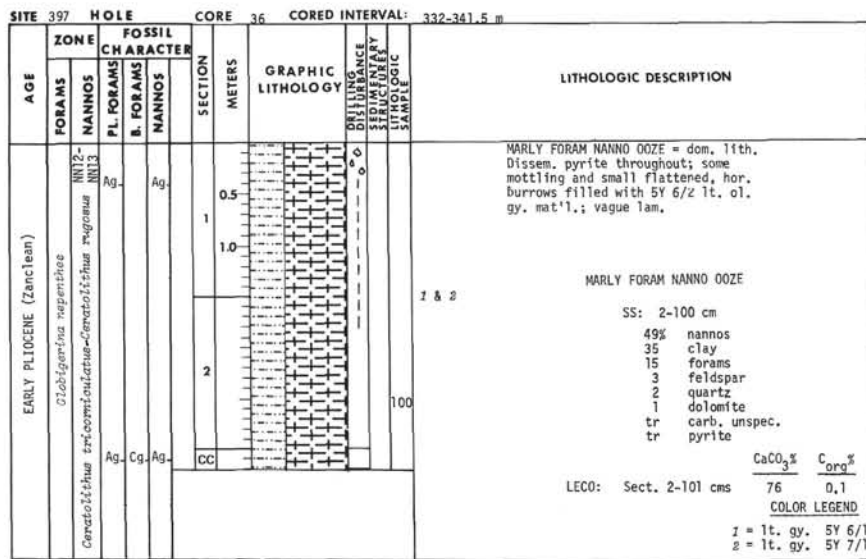
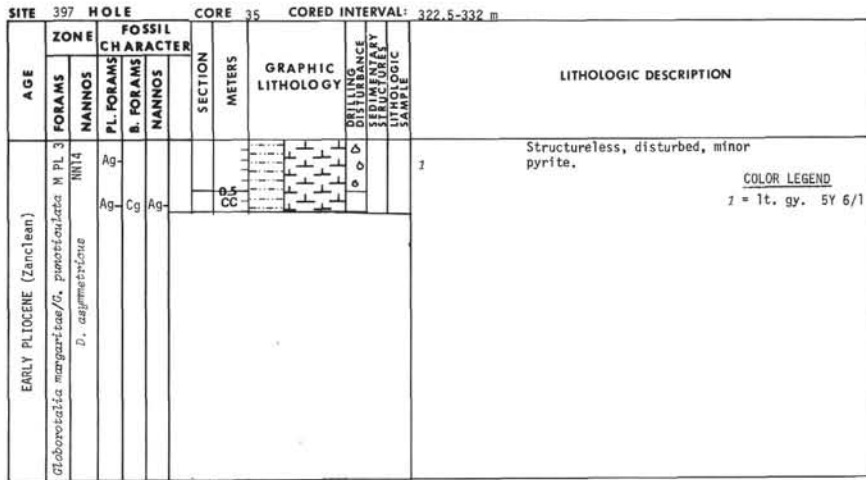
SITE 397 HOLE		CORE 32		CORED INTERVAL: 294-303.5 m		
AGE	FOSSIL CHARACTER			SECTION METERS	GRAPHIC LITHOLOGY	LITHOLOGIC DESCRIPTION
	FORAMS	NANNOS	B. FORAMS			
EARLY PLIOCENE (Zanclean)	M PL 3			0.5		MARLY NANNO OOZE = dom. lith. Dissem. pyrite throughout; coring disturb.
	NIN14			1.0		
				2.0		MARLY NANNO OOZE SS: 3-131 cm 60% nannos 30 clay 3 forams 3 carb. unsp. 3 diatoms 1 sil. unsp. tr quartz tr mica tr pyrite tr sponge spics.
			Ag	3.0		MARLY FORAM NANNO OOZE in small bleb. SS: 4-48 cm 35% clay 32 nannos 20 forams 10 carb. unsp. 5 quartz 2 pyrite 1 dolomite tr feldspar tr heavy mins.
			4.0			
			CC			

COLOR LEGEND
z = 1t. gy. 5Y 6/1

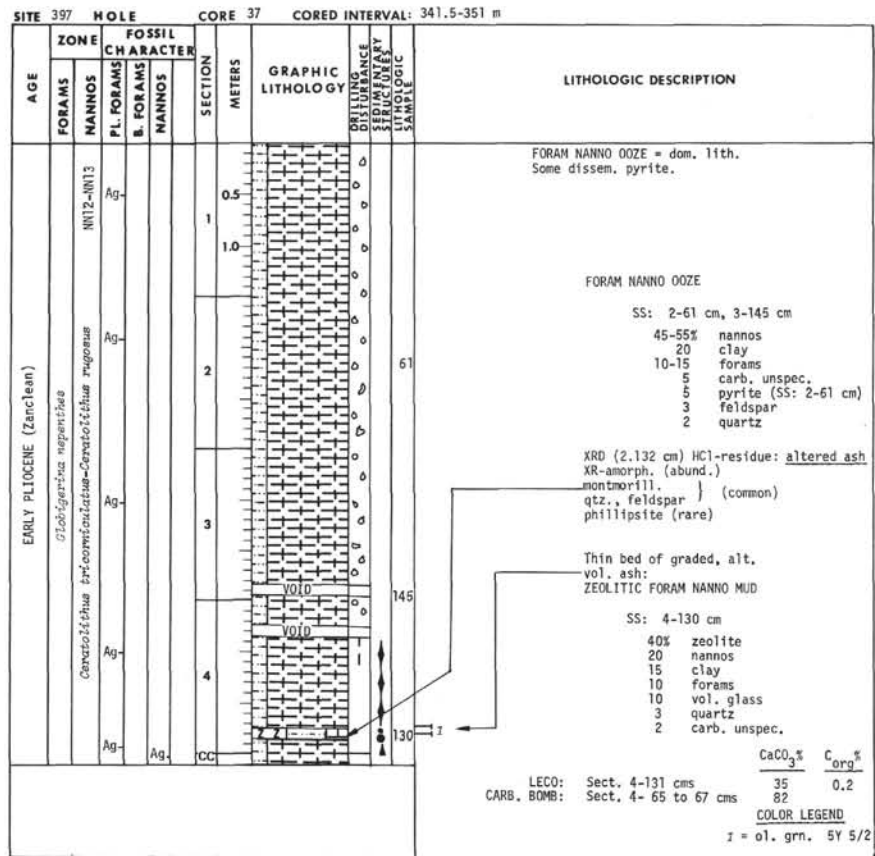


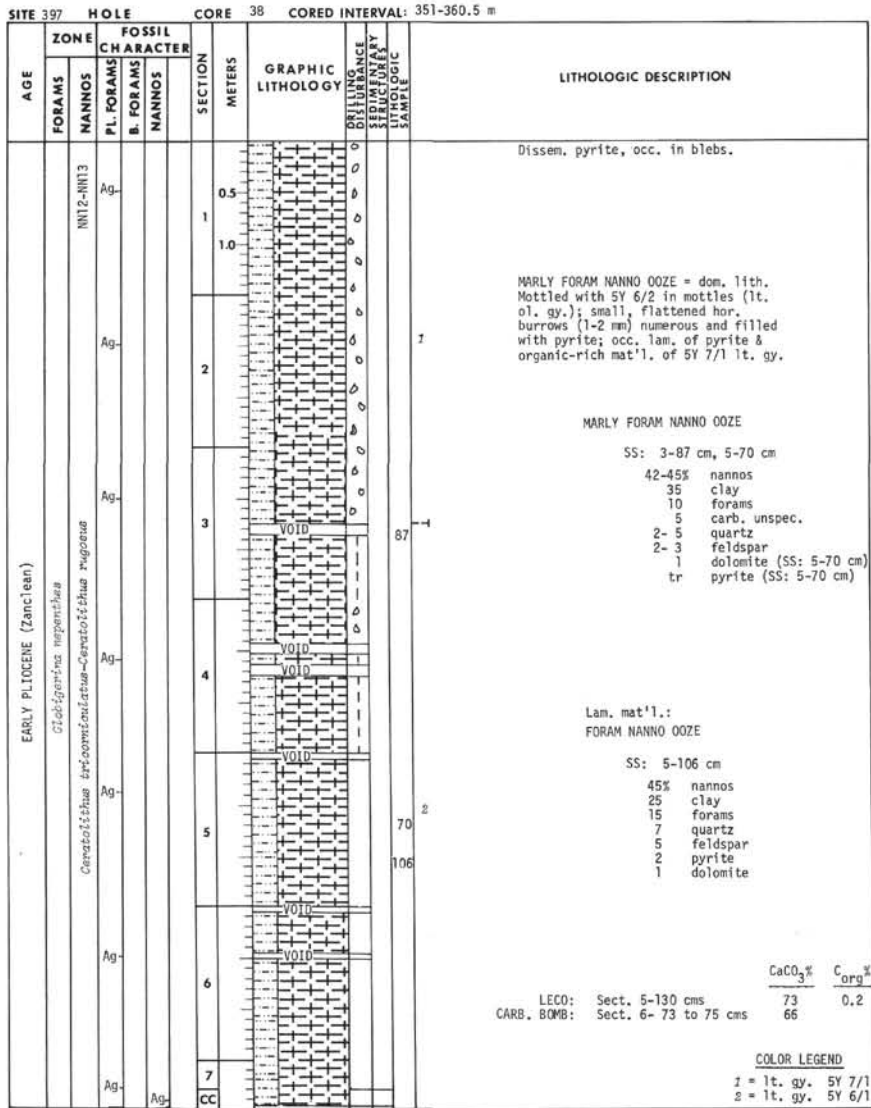
Explanatory notes in Chapter 1



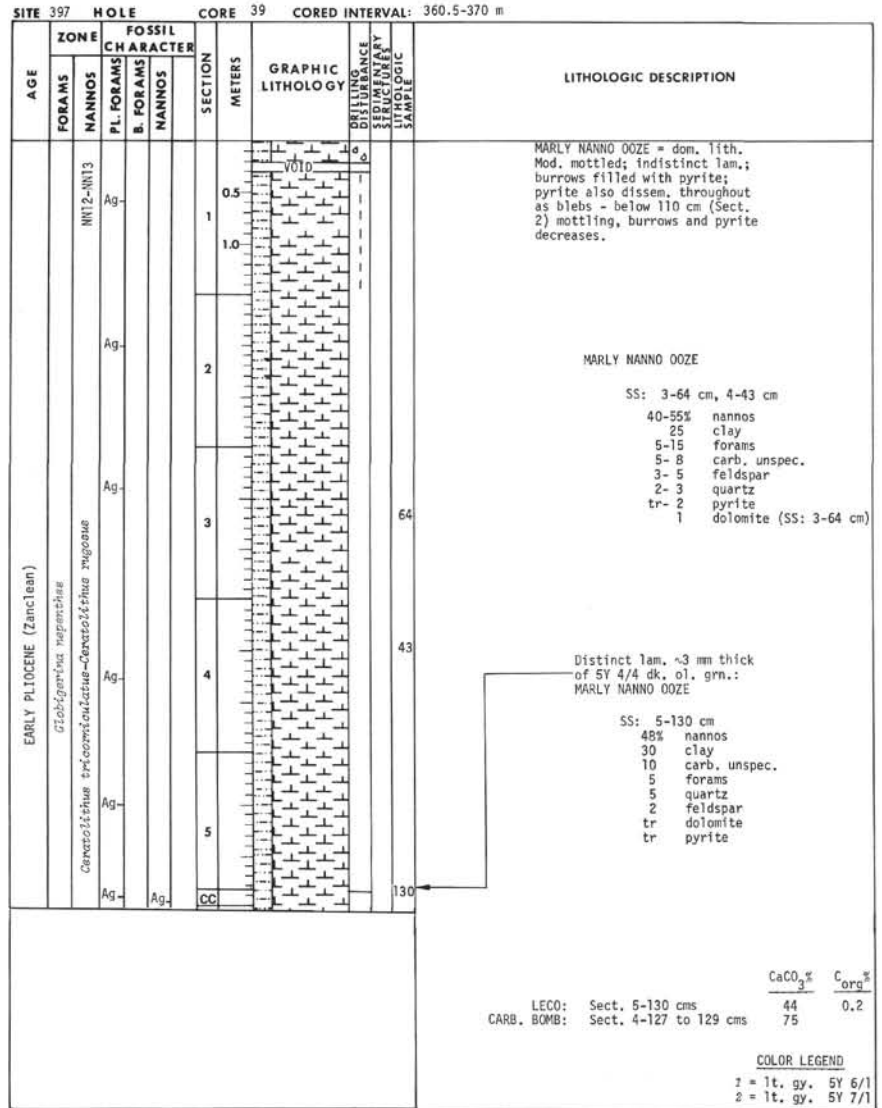


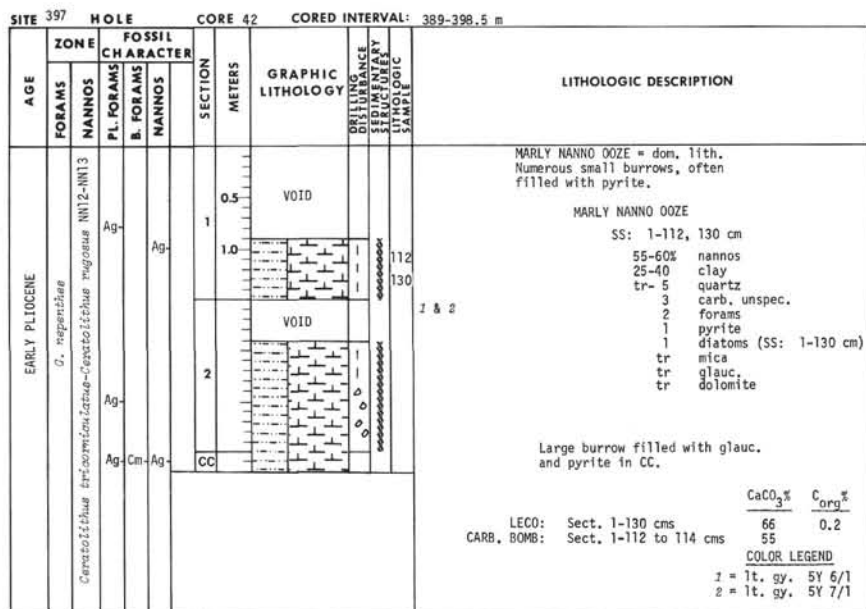
Explanatory notes in Chapter 1



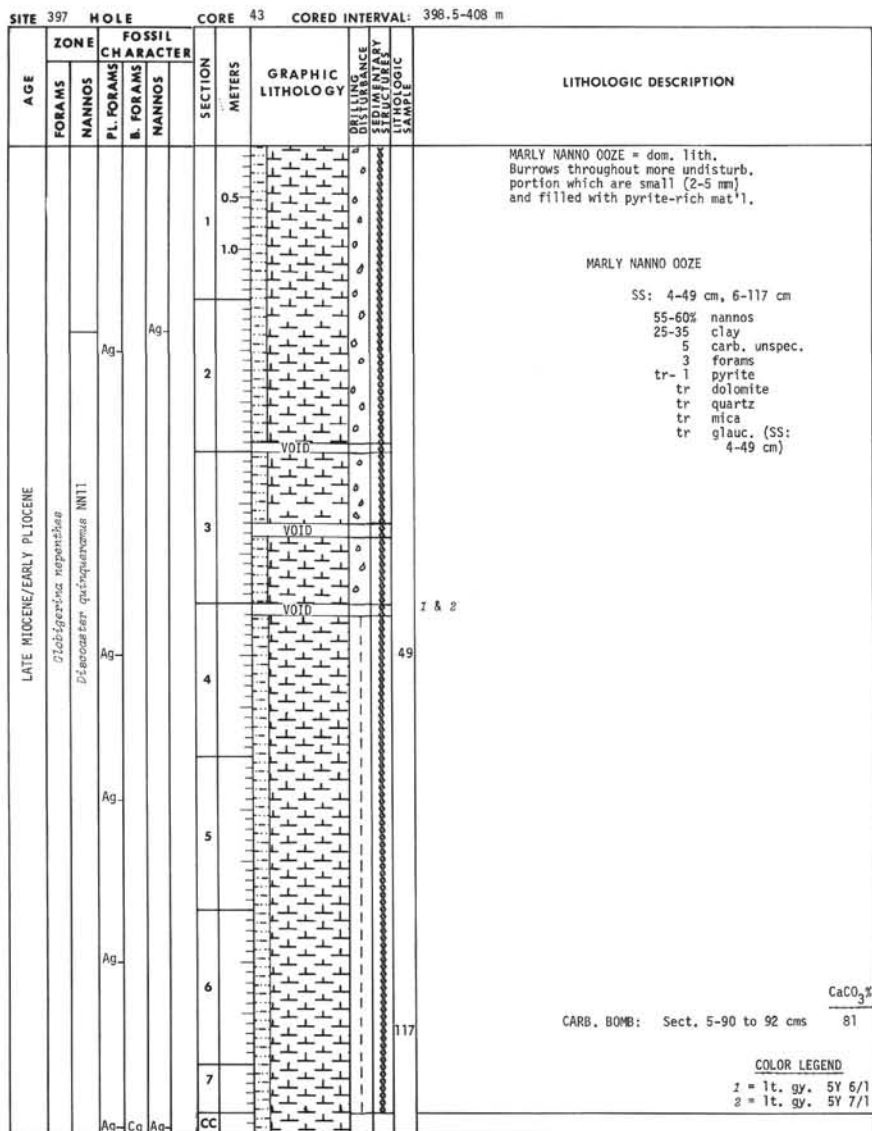


Explanatory notes in Chapter 1



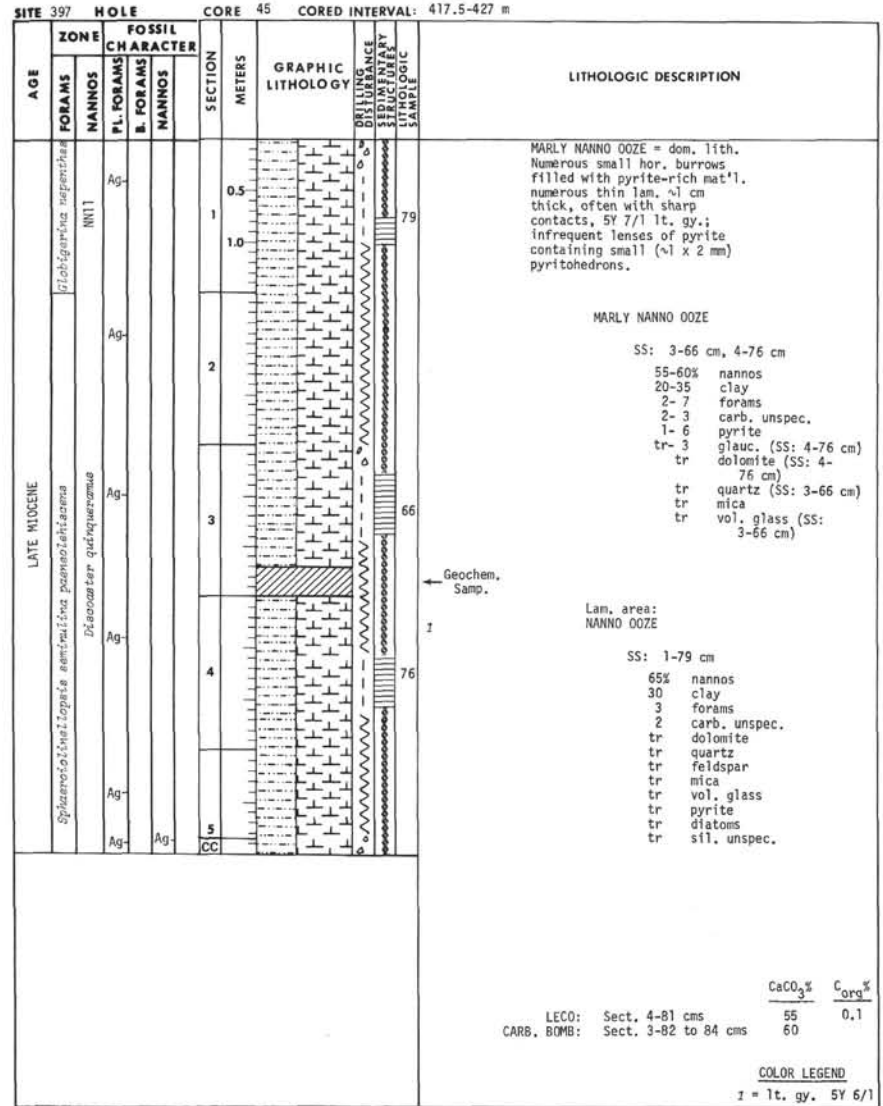
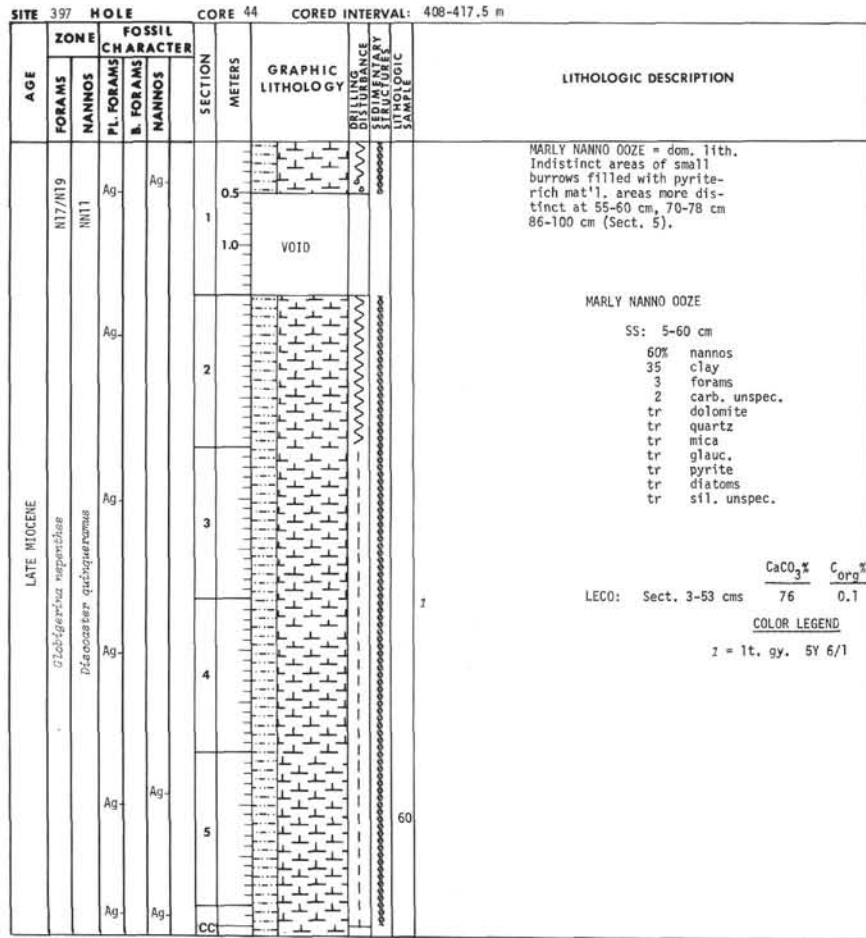


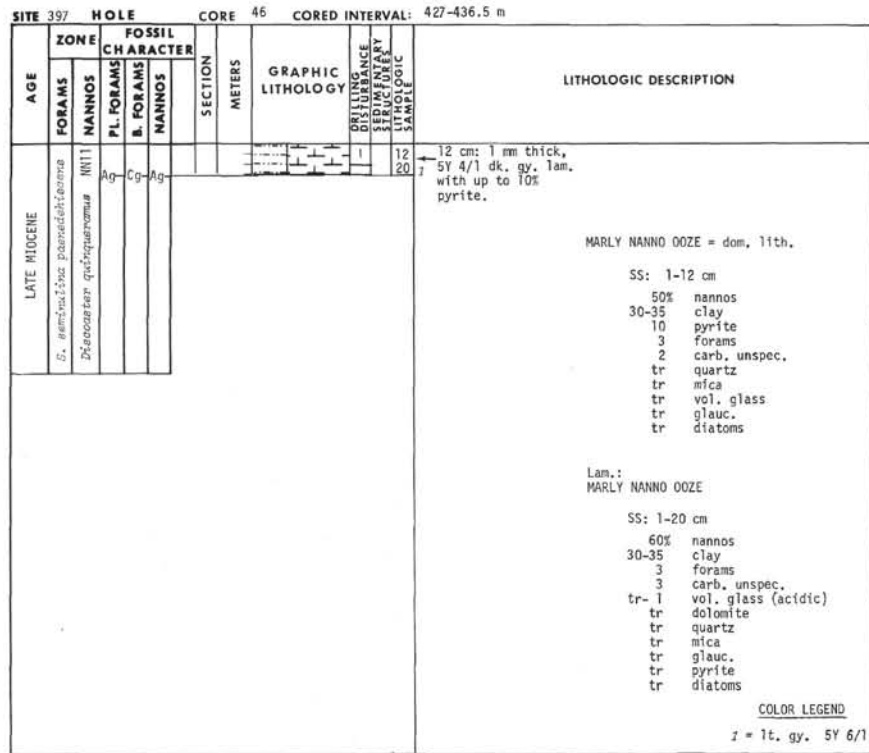
Explanatory notes in Chapter 1



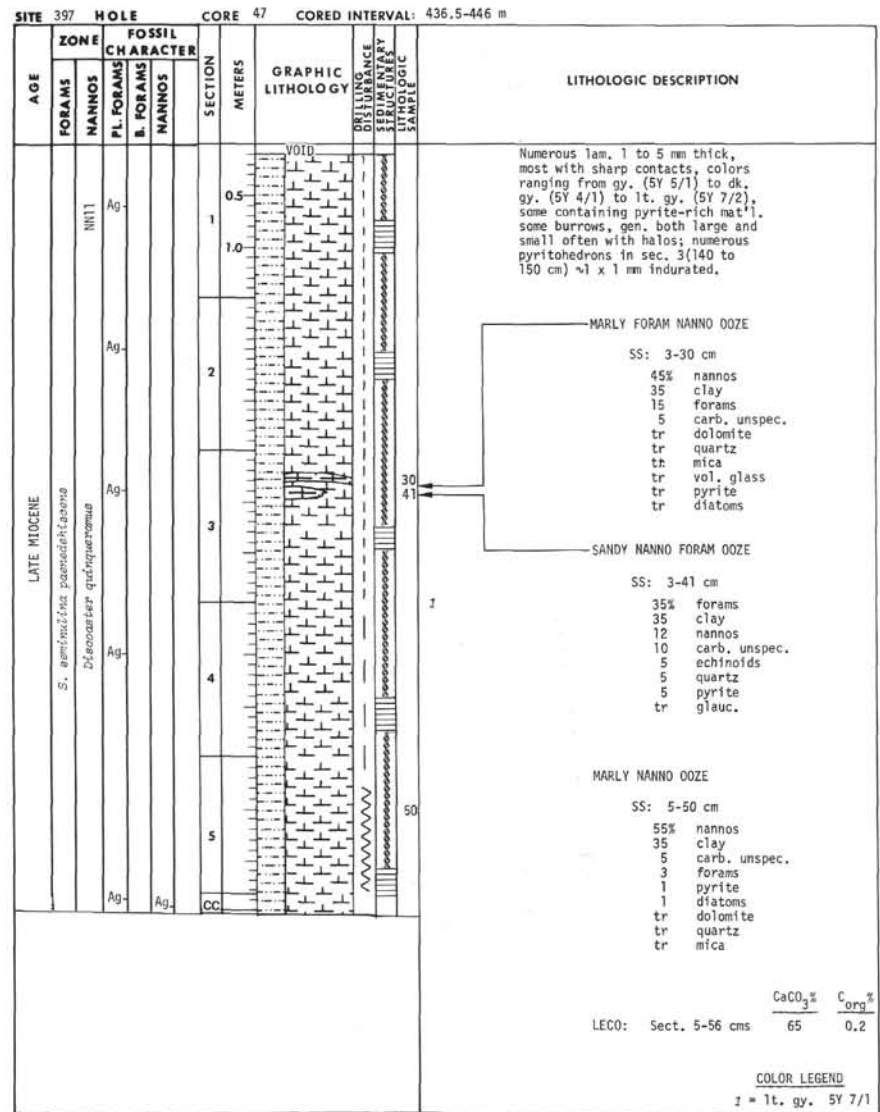
CaCO₃%
 CARB. BOMB: Sect. 5-90 to 92 cms 81

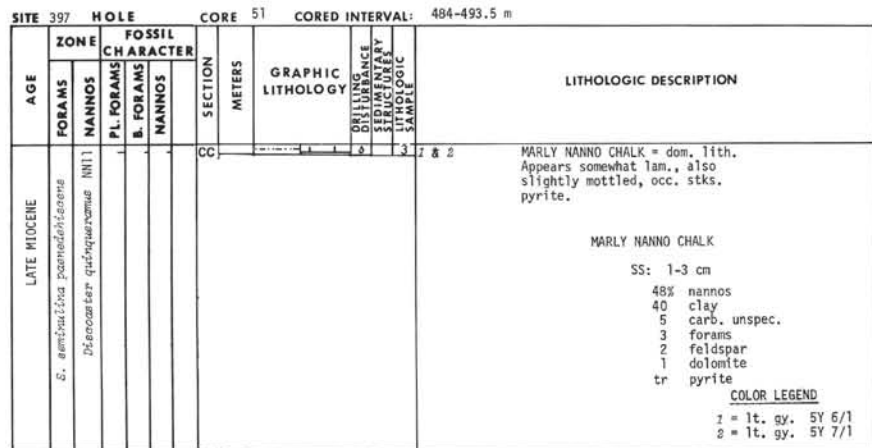
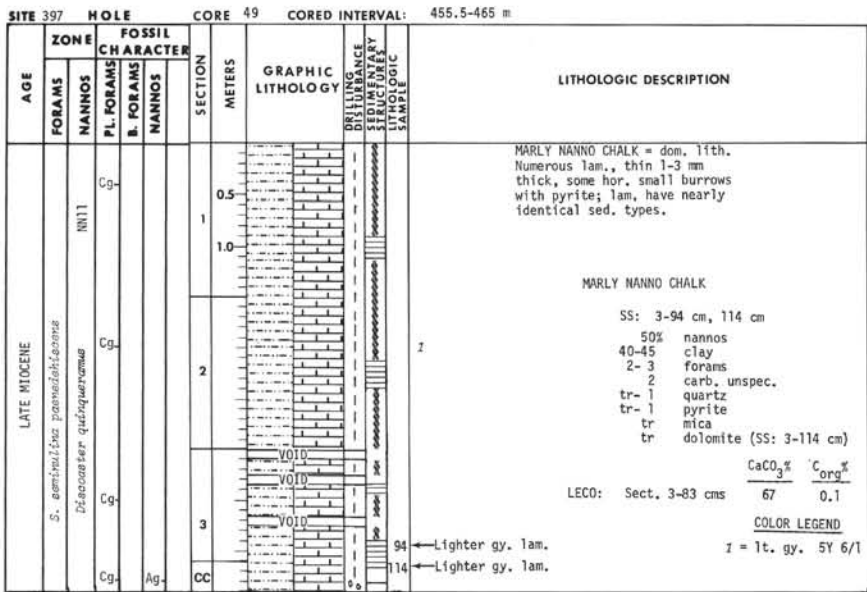
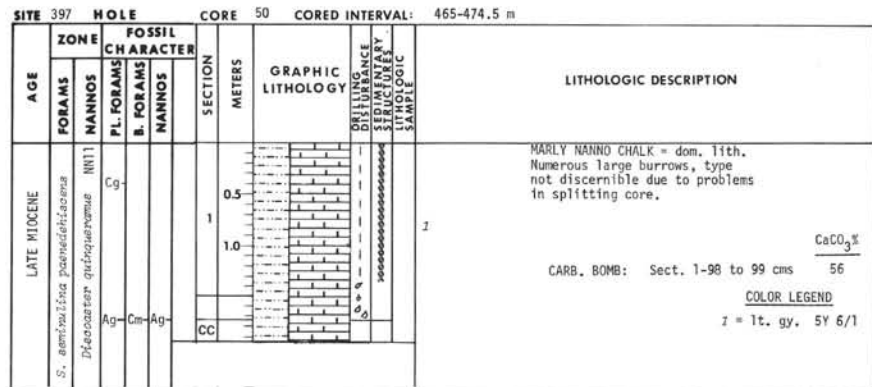
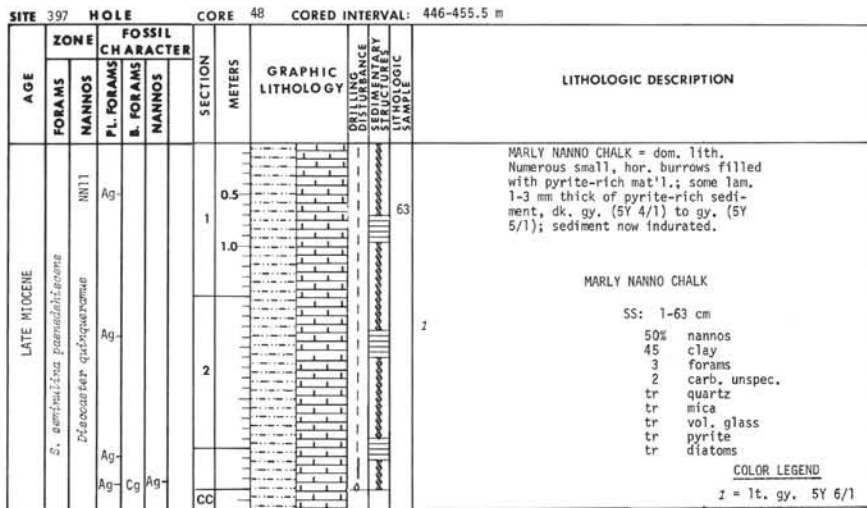
COLOR LEGEND
 1 = lt. gy. 5Y 6/1
 2 = lt. gy. 5Y 7/1



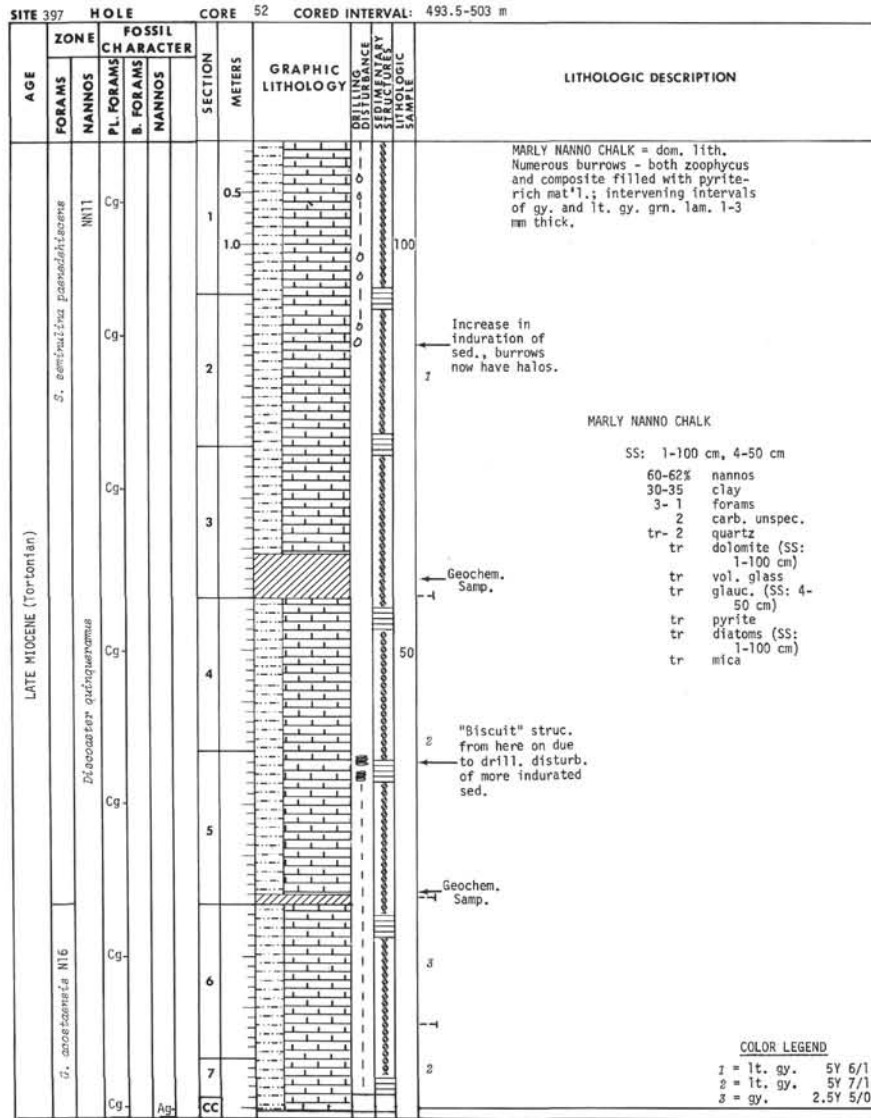


Explanatory notes in Chapter 1

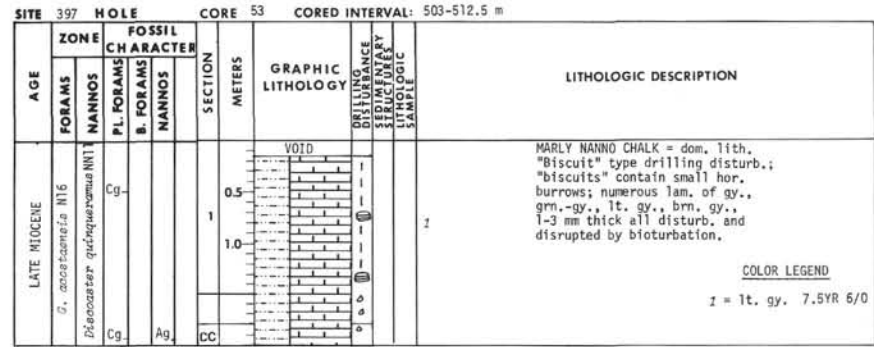




Explanatory notes in Chapter 1



Explanatory notes in Chapter 1



SITE 397 HOLE		CORE 54		CORED INTERVAL: 512.5-522 m								
AGE	ZONE	FOSSIL CHARACTER			SECTION METERS	GRAPHIC LITHOLOGY	DRILLING DISTURBANCE STRUCTURE LITHOLOGIC SAMPLE	LITHOLOGIC DESCRIPTION				
		FORAMS	NANNOS	PL. FORAMS					B. FORAMS	NANNOS		
LATE MIOCENE (Tortonian)	N16	NNT1	Cg				27	<p>MARLY NANNO CHALK = dom. lith. "Biscuit" type drill. disturb.; numerous burrows (zoophycus and composite mainly with some chondrites); burrows disrupt numerous vague lam. which are gy., dk. gy. and grn.-gy.; lam. of diff. colors are identical in composition (smear slide).</p>				
									MARLY NANNO CHALK	SS: 1-27 cms, 3-110 cms 55% nannos 35-40 clay 1-2 carb. unspec. tr-2 quartz tr-1 pyrite tr Forams tr dolomite (SS: 3-110 cm) tr feldspar tr mica tr vol. glass (SS: 1-27 cm) tr glauc. tr diatoms tr sil. unspec. (SS: 1-27 cm)		
											LECO: Sect. 2-133 cms	$\frac{\text{CaCO}_3\%}{51}$ $\frac{\text{C}_{org}\%}{0.2}$ CARB. BOMB: Sect. 2-34 to 36 cms
											Cg	2
Cg	3											
			Cg	4								
Cg	5											
			Ag	CC								

Explanatory notes in Chapter 1

SITE 397 HOLE		CORE 55		CORED INTERVAL: 522-531.5 m								
AGE	ZONE	FOSSIL CHARACTER			SECTION METERS	GRAPHIC LITHOLOGY	DRILLING DISTURBANCE STRUCTURE LITHOLOGIC SAMPLE	LITHOLOGIC DESCRIPTION				
		FORAMS	NANNOS	PL. FORAMS					B. FORAMS	NANNOS		
LATE MIOCENE (Tortonian)	N16	NNT1	Cg				10	<p>MARLY NANNO CHALK = dom. lith. Numerous burrows, mainly zoophycus and composite, many with halo's; disrupted lam. of gy., dk. gy., grn.-gy. and brn.-gy. numerous with vague contacts; pyrite in burrow fillings, some with larger pyritohedrons up to 1 x 1 mm.</p>				
									MARLY NANNO CHALK	SS: 1-10 cm, 4-22 cm 40-70% nannos 20-40 clay 3-5 quartz 5 carb. unspec. 3 forams (SS: 4-22 cm) tr-3 feldspar tr dolomite (SS: 4-22 cm) tr mica (SS: 1-10 cm) tr glauc. tr pyrite tr heavy mtns. (SS: 1-10 cm, epidote).		
											LECO: Sect. 3-60 cms	$\frac{\text{CaCO}_3\%}{55}$ $\frac{\text{C}_{org}\%}{0.2}$ COLOR LEGEND I = lt. gy. 2.5Y 6/0
											Cg	2
Cg	3											
			Cg	4								
Cg	5											
			Ag	CC								

SITE 397 HOLE		CORE 56		CORED INTERVAL: 531.5-541 m								
AGE	ZONE	FOSSIL CHARACTER			SECTION	METERS	GRAPHIC LITHOLOGY	DRILLING DISTURBANCE STRUCTURE LITHOLOGIC SAMPLE	LITHOLOGIC DESCRIPTION			
		FORAMS	NANNOS	P.L. FORAMS						B. FORAMS	NANNOS	
LATE MIOCENE (Tortonian)			NN11			0.5 1.0			MARLY NANNO CHALK = dom. lith. Numerous burrows, mainly multiple type with some zoophycus, most with halos, lam. considerably disrupted by bioturbation, lam. are gy., grn.-gy. and gy. brn.			
										2		z

Explanatory notes in Chapter 1

COLOR LEGEND
z = gy. 2.5Y 5/0

SITE 397 HOLE		CORE 57		CORED INTERVAL: 541-550.5 m								
AGE	ZONE	FOSSIL CHARACTER			SECTION	METERS	GRAPHIC LITHOLOGY	DRILLING DISTURBANCE STRUCTURE LITHOLOGIC SAMPLE	LITHOLOGIC DESCRIPTION			
		FORAMS	NANNOS	P.L. FORAMS						B. FORAMS	NANNOS	
LATE MIOCENE autochthonous with MIDDLE MIOCENE allochthonous interval (Tortonian)	NN10			Ag		0.5 1.0			NANNO CHALK = dom. lith. Extensively bioturbated. Burrows are predom. a composite-type or oval types with halos (ovals 5 mm to 8 mm long along minor axis), some chondrites; "biscuit" type drill. disturb.			
										2		z
										4		z

SS: 2-36 cm
 60% nannos
 20 clay
 5 forams
 5 carb. unspec.
 4 feldspar
 3 quartz
 3 pyrite
 1 dolomite

Alt. vol. ash
ZEOLITIC FORAM NANNO CHALK

SS: 3-90 cm
 35% zeolite
 30 nannos
 15 clay
 10 forams
 5 carb. unspec.
 4 feldspar
 1 quartz

Black pyrite layer with hollow pyrite-hedron ~2 mm.

VOLCANIC ASH

SS: 4-140 cm
 58% vol. glass
 20 feldspar
 20 pyrite
 2 nannos

CLAYSTONE

SS: 5-8 cm
 88% clay
 5 nannos
 5 feldspar
 2 quartz

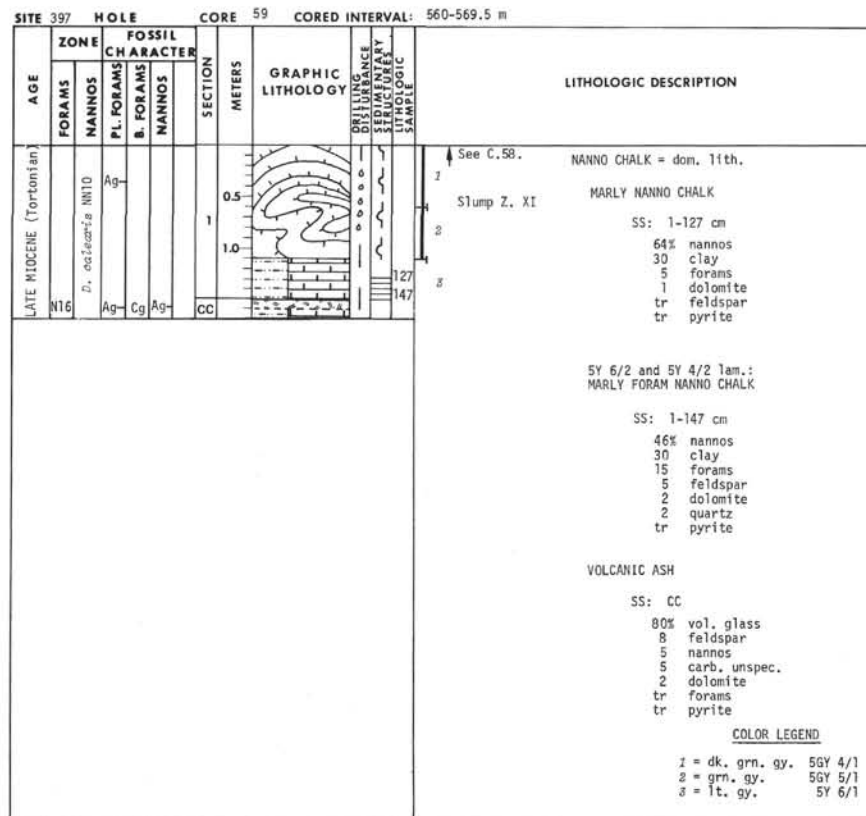
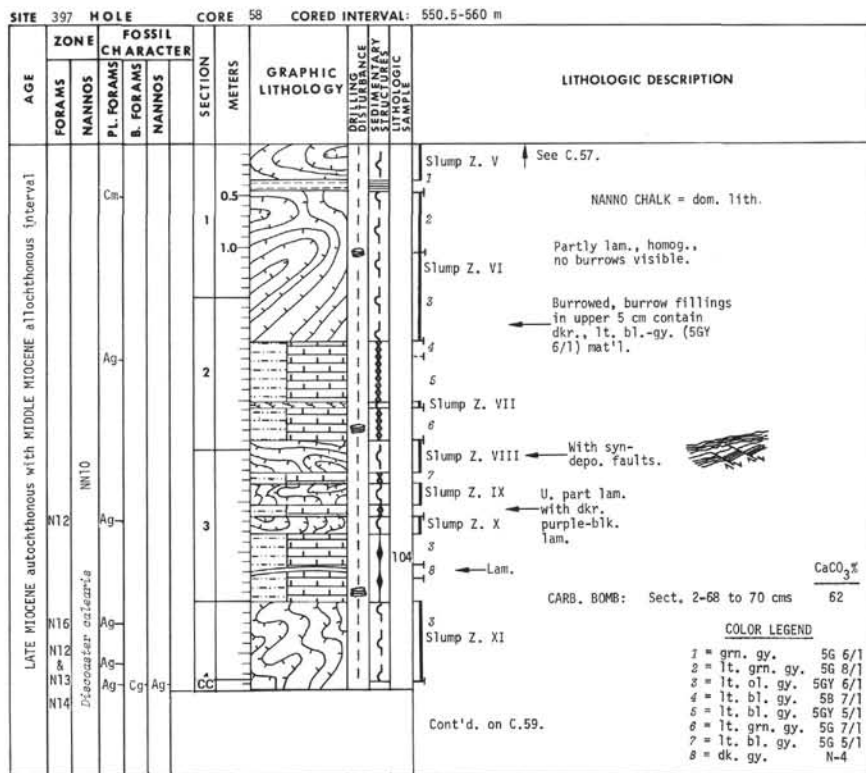
Cont'd. on C.58

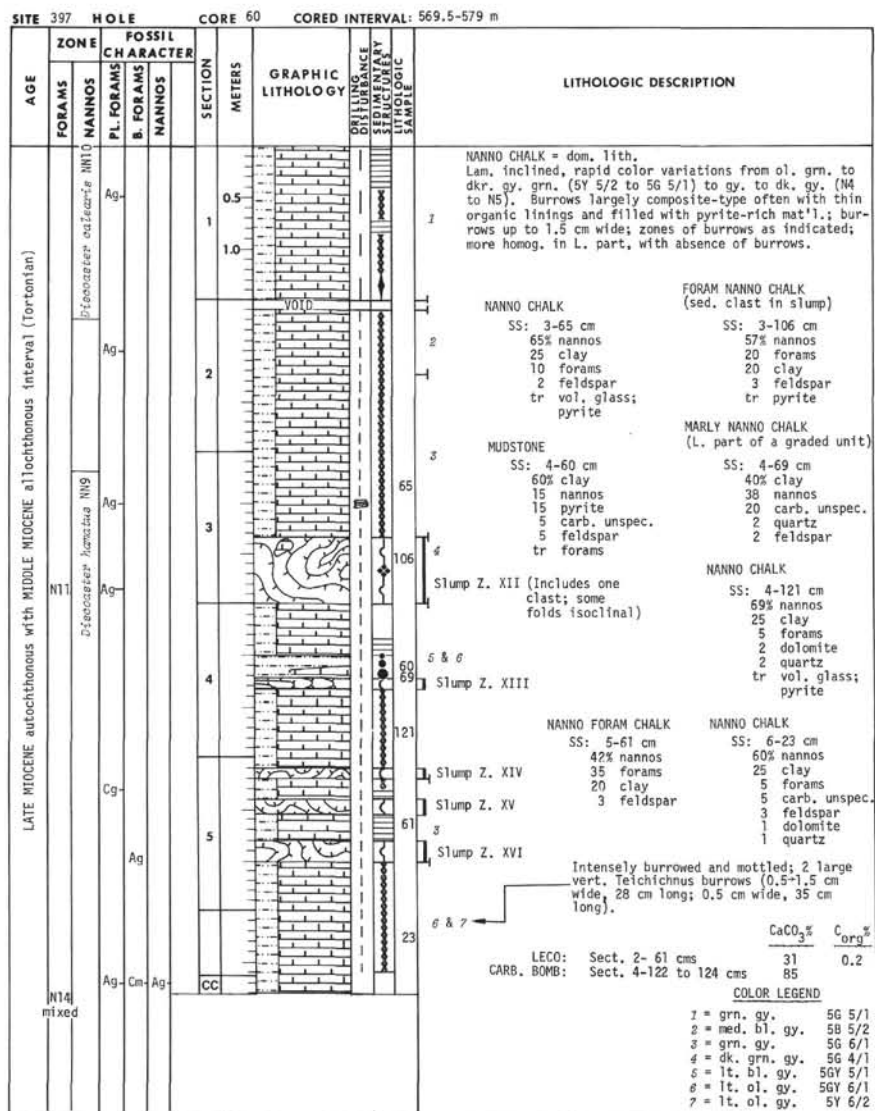
NANNO FORAM CHALK

SS: 5-34 cm
 43% nannos
 20 forams
 20 clay
 5 carb. unspec.
 2 feldspar

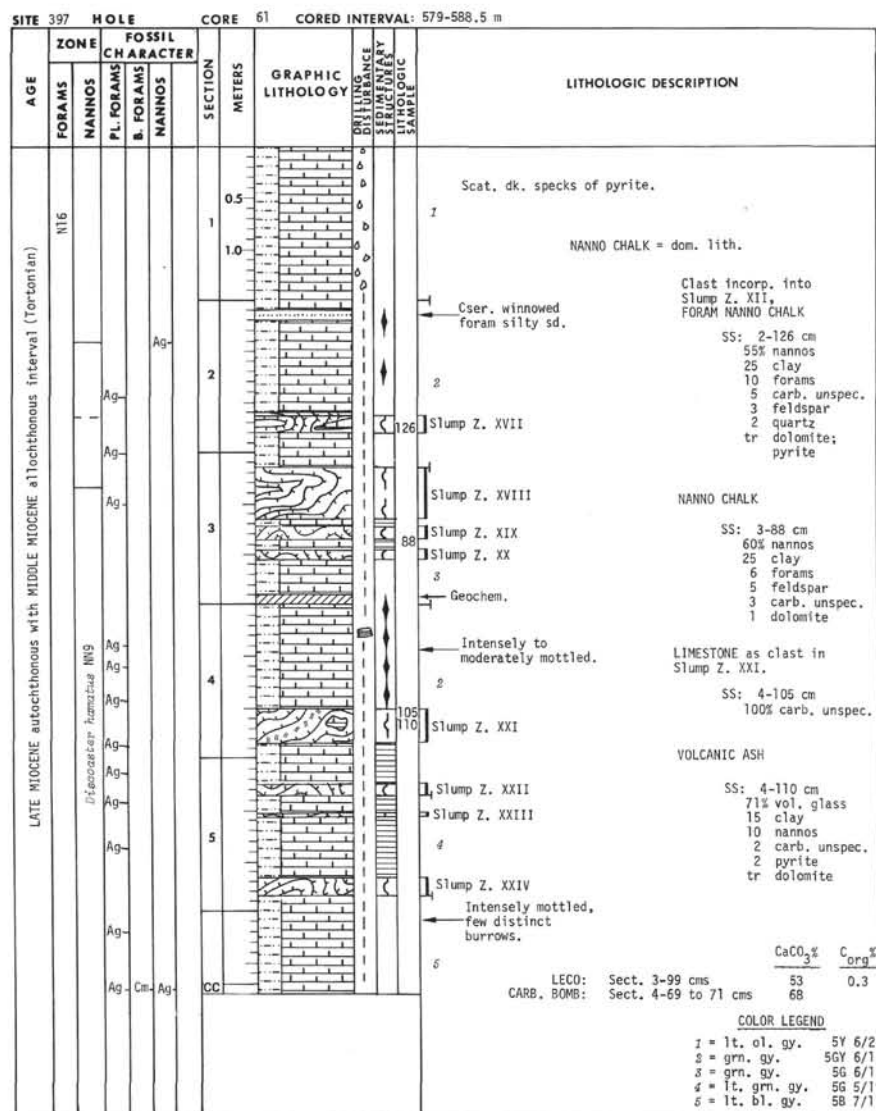
XRD (3,86-88 cm)
 XR-amorph. (abund.)
 calcite
 feldspar } (common)
 quartz
 phillipsite (rare)
 opal-CT

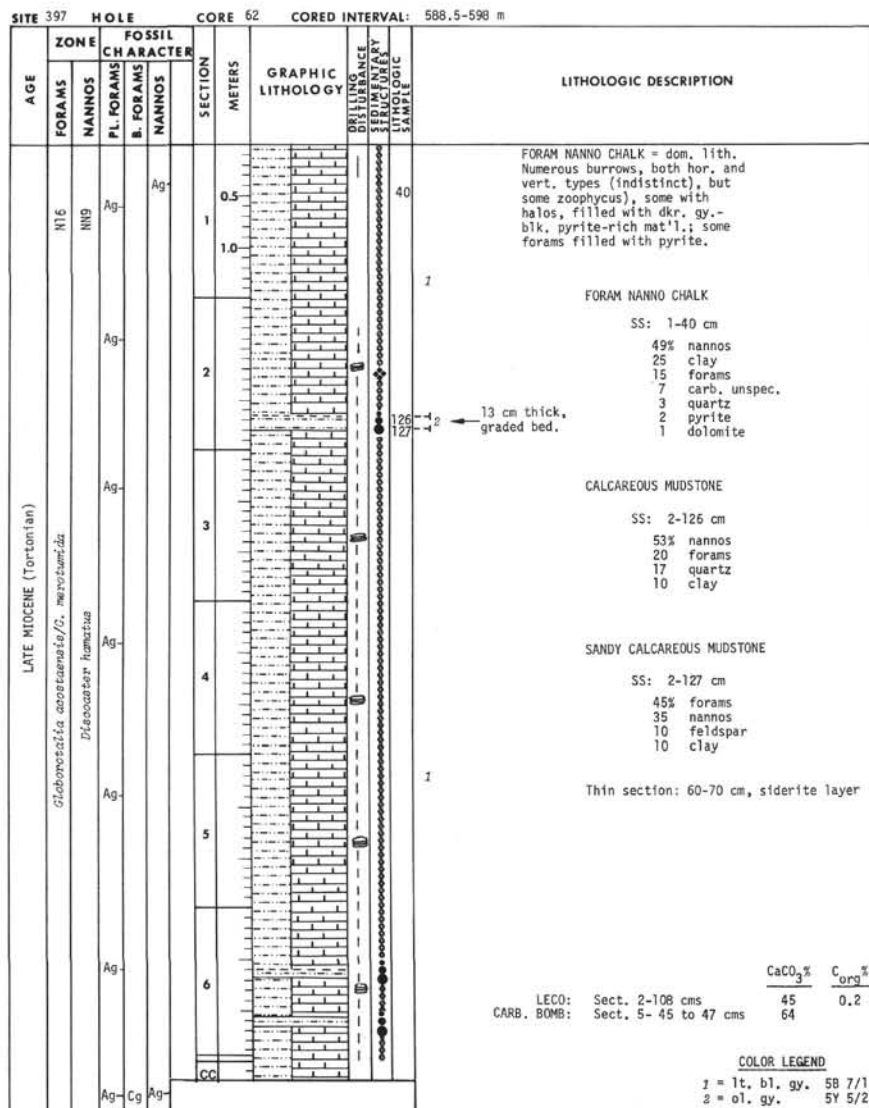
COLOR LEGEND
z = lt. gy. 2.5Y 6/0
z = grn. gy. 5G 6/1



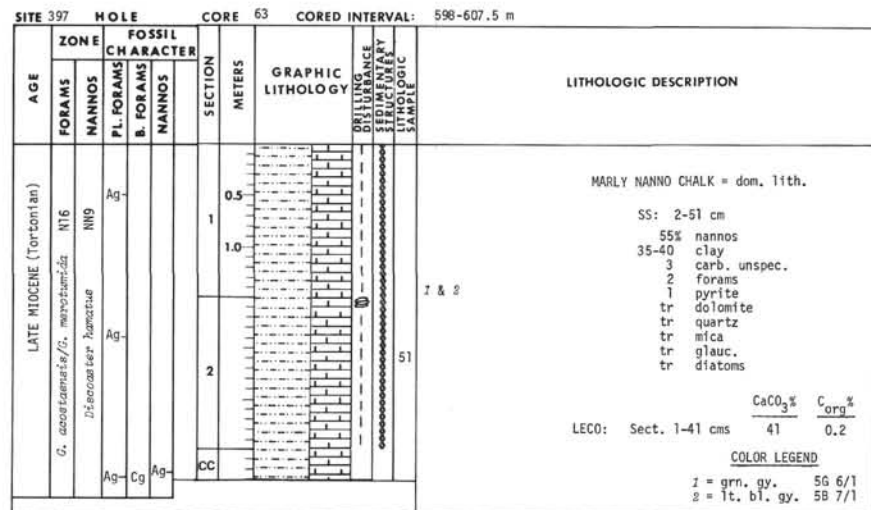


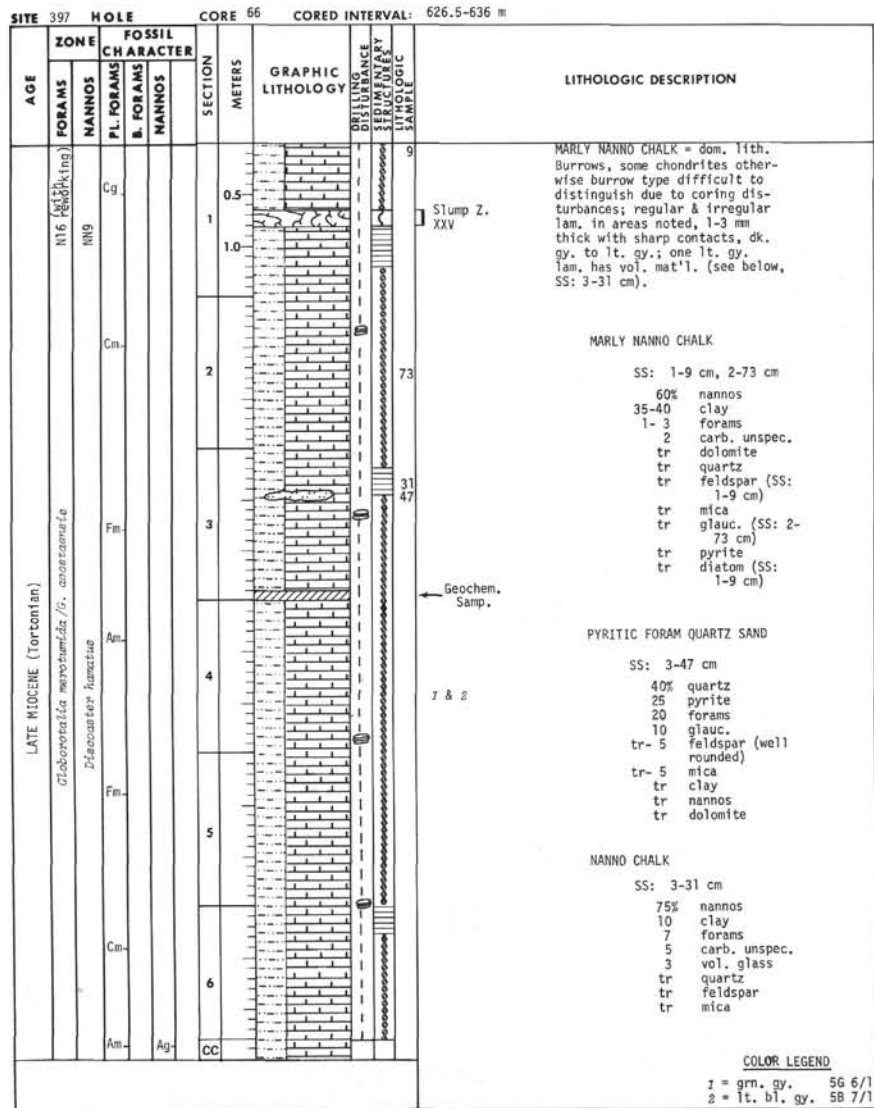
Explanatory notes in Chapter 1



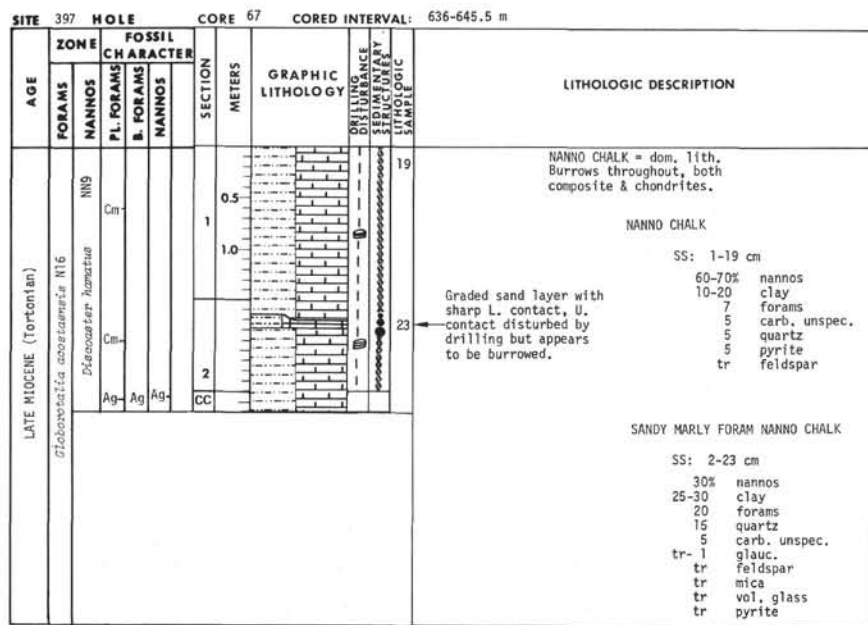


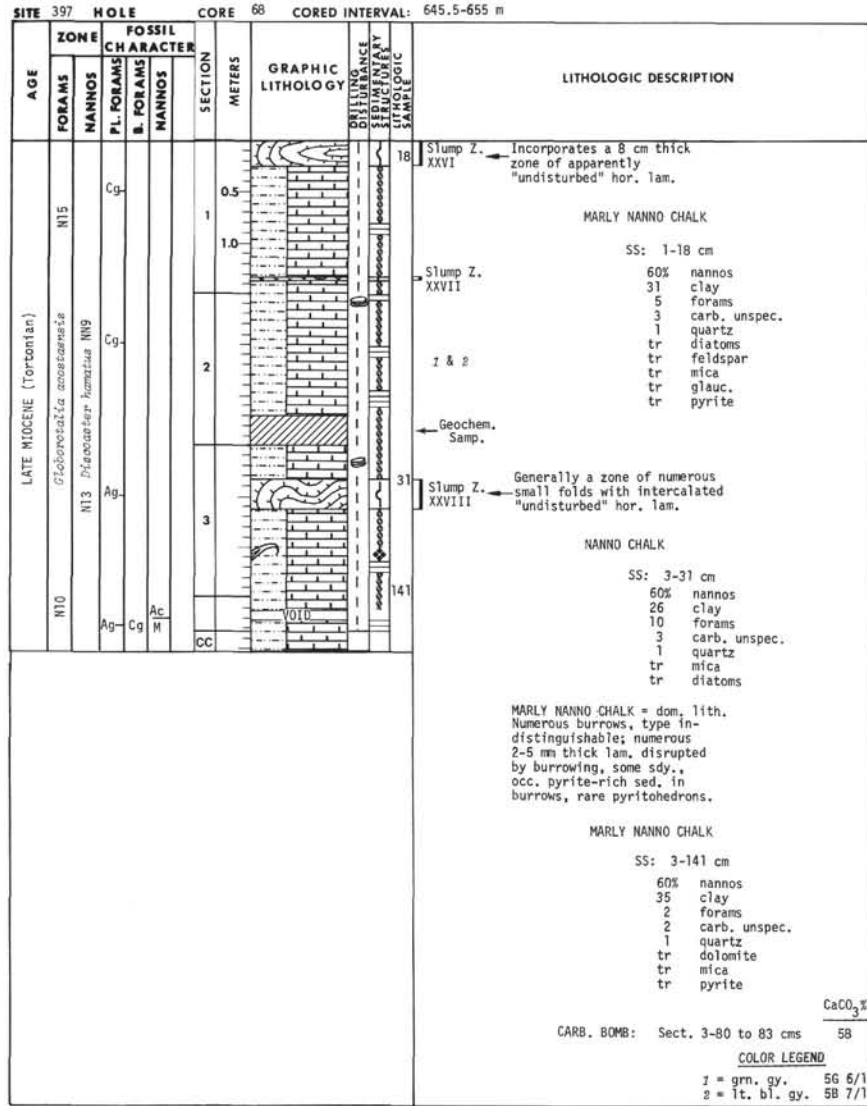
Explanatory notes in Chapter 1



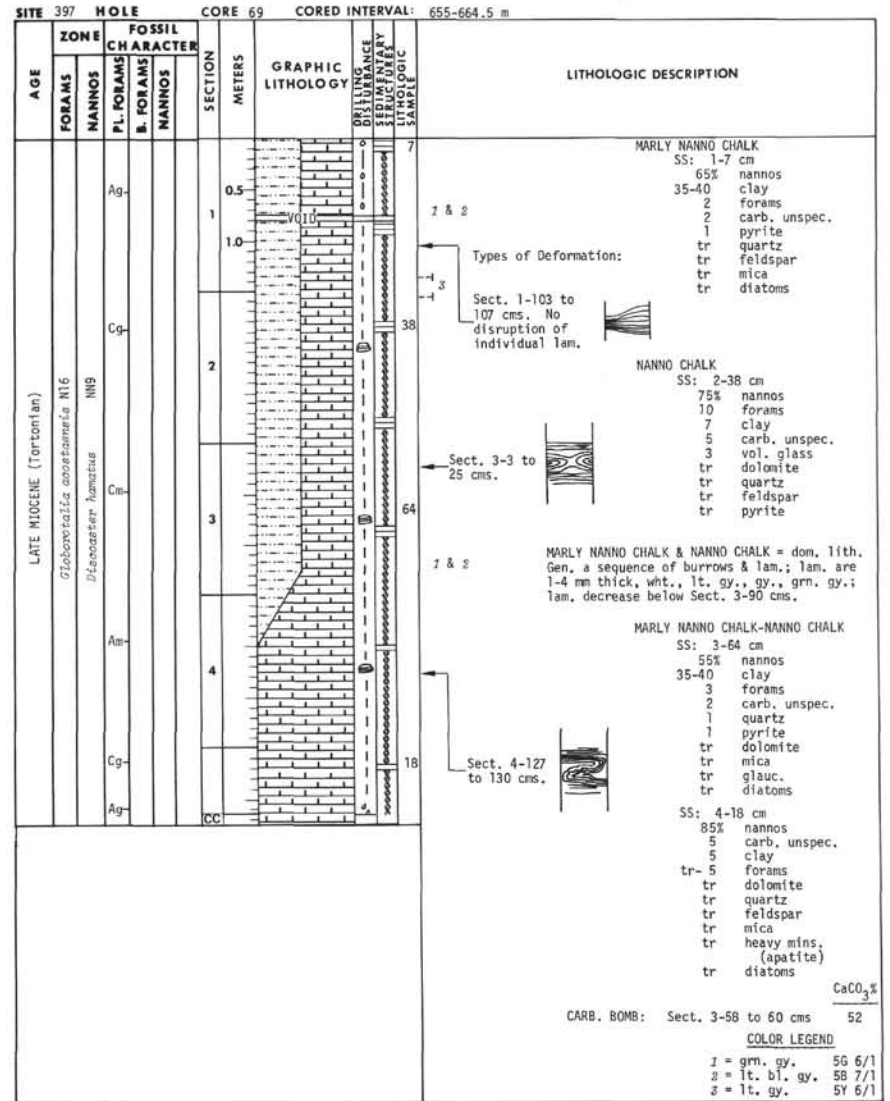


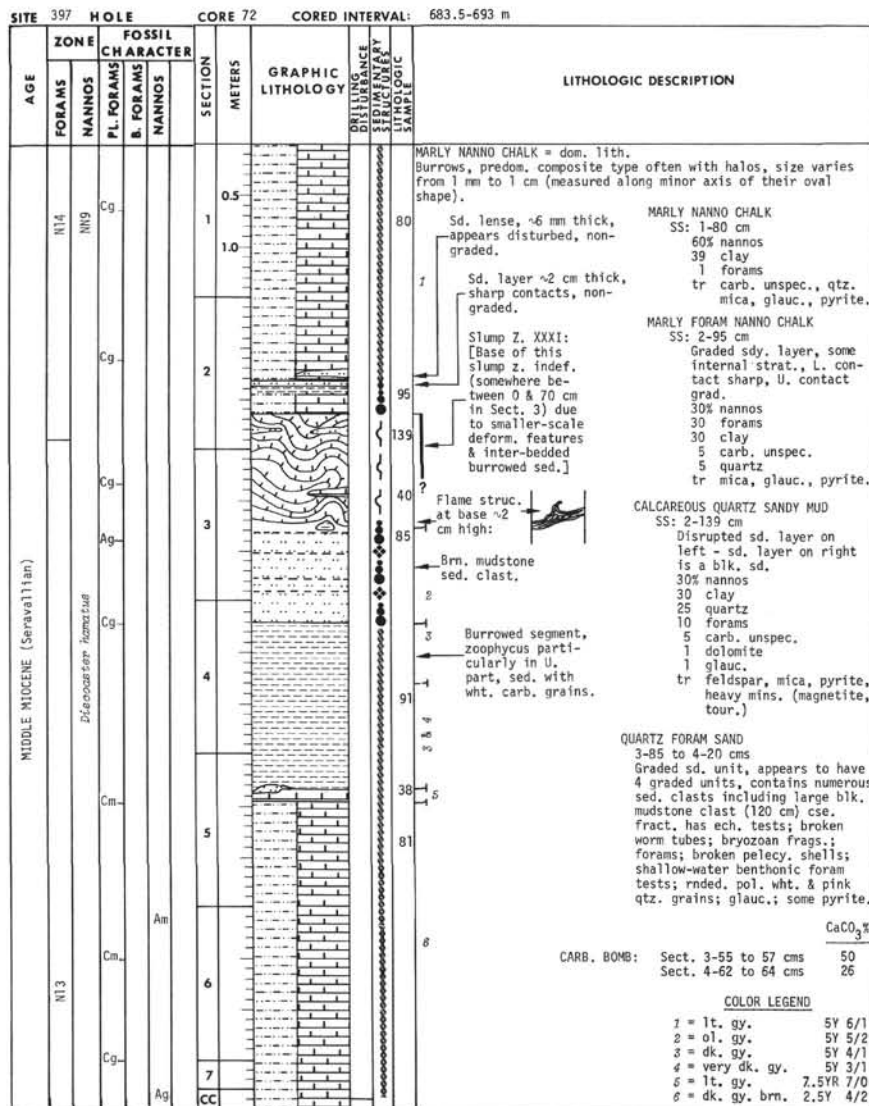
Explanatory notes in Chapter 1



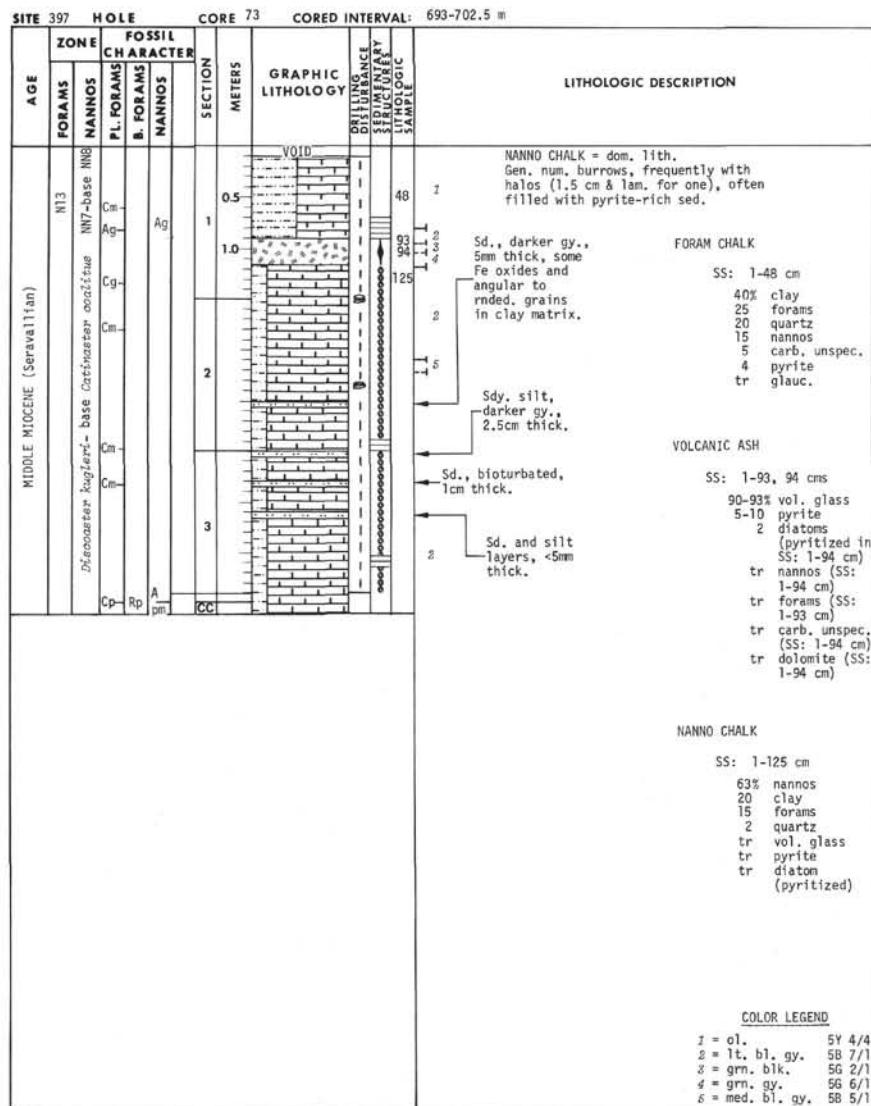


Explanatory notes in Chapter 1





Explanatory notes in Chapter 1



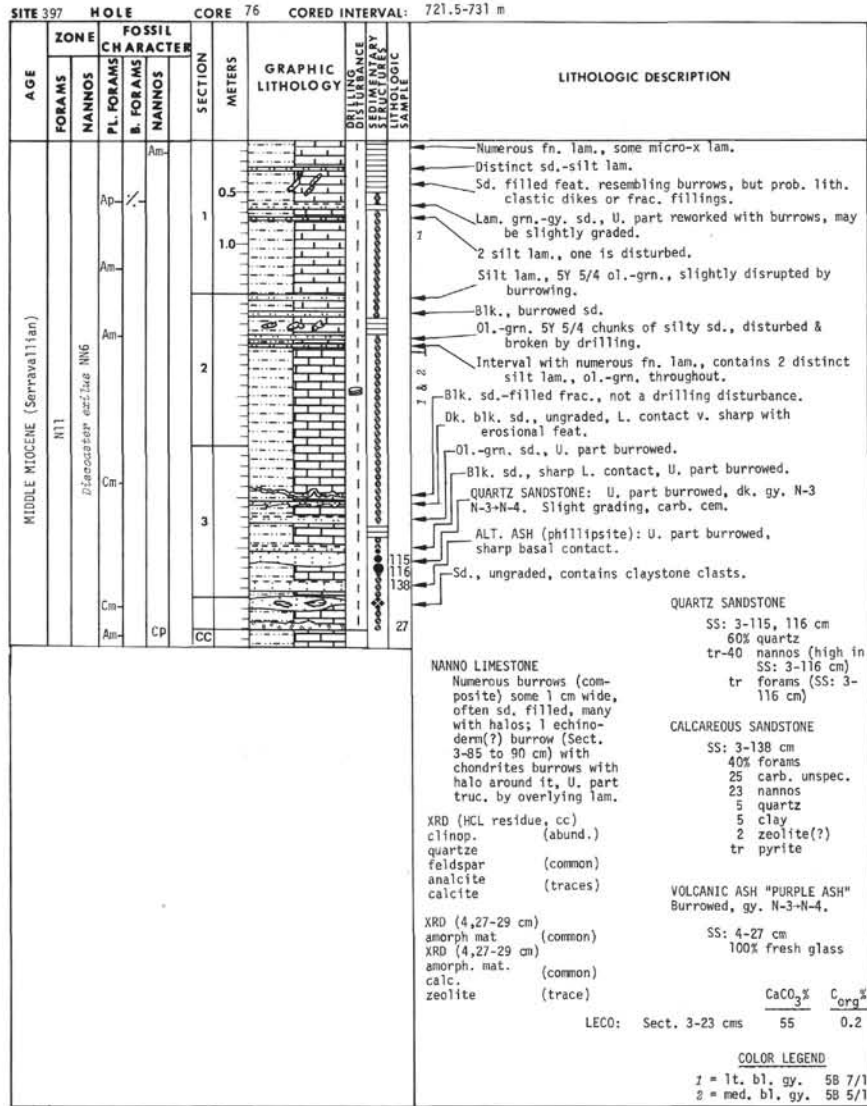
SITE 397 HOLE CORE 74 CORED INTERVAL: 702.5-712 m

AGE	ZONE		FOSSIL CHARACTER		SECTION	METERS	GRAPHIC LITHOLOGY	DRILLING SAMPLING SCHEDULE	LITHOLOGIC SAMPLE	LITHOLOGIC DESCRIPTION
	FORAMS	NANNOS	P.L. FORAMS	B. NANNOS						
MIDDLE MIOCENE (Serravallian)	N12				1	0.5	VOID		1	<p>NANNO CHALK = dom. lith. Numerous burrows, some Teichichnus(?), other burrows up to 2 cm in size, often filled with organic or pyritic mat'l. Upper 2 cm of this portion beneath the sd. bed is a dker. grn. Sed. clast is a cse. sd. Numerous faint lam. strong calc. cement. in foram chambers.</p> <p>CALCAREOUS QUARTZ SAND</p> <p>SS: 1-1 cm</p> <p>2.5 cm thick, well indurated, ungraded, dk. gy.</p> <p>40% quartz</p> <p>30 nannos</p> <p>20 carb. unspec.</p> <p>10 cclay</p> <p>tr forams</p> <p>CaCO₃% 65</p> <p>C_{org}% 0.1</p> <p>LECO: Sect. 2-76 cms</p> <p>CARB. BOMB: Sect. 1-70 to 72 cms</p> <p>CARBON BOMB: Sect. 1-70 to 72 cms</p> <p>62</p> <p>COLOR LEGEND</p> <p>1 = lt. bl. gy. 5B 7/1</p> <p>2 = grn. gy. 5G 5/1</p>
	N13				2	1.0				

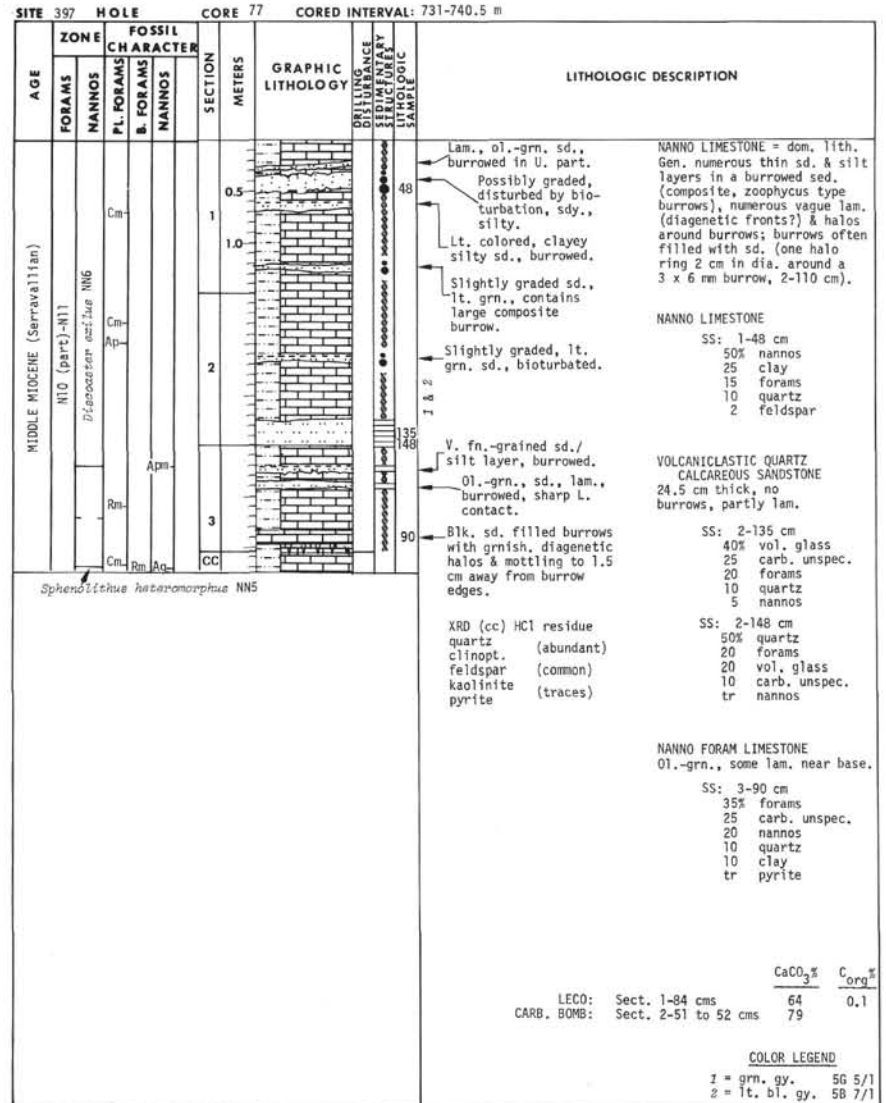
Explanatory notes in Chapter 1

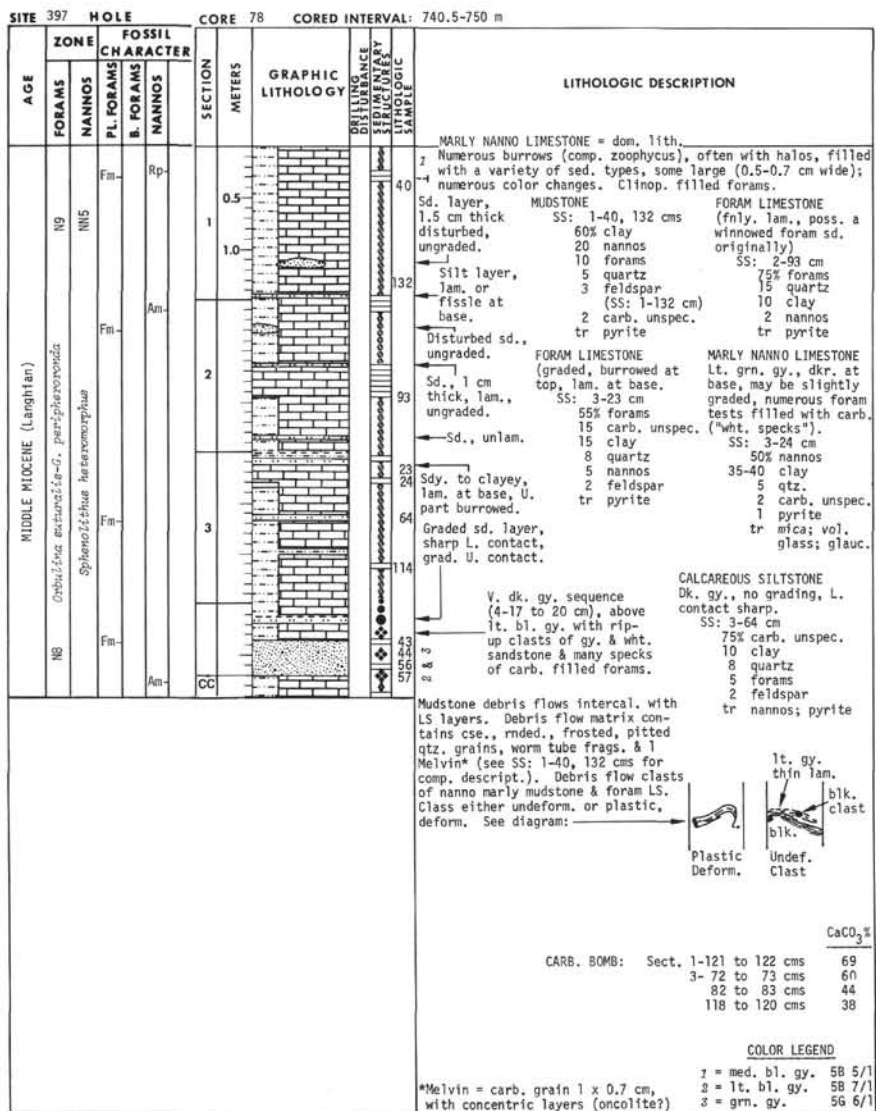
SITE 397 HOLE CORE 75 CORED INTERVAL: 712-721.5 m

AGE	ZONE		FOSSIL CHARACTER		SECTION	METERS	GRAPHIC LITHOLOGY	DRILLING SAMPLING SCHEDULE	LITHOLOGIC SAMPLE	LITHOLOGIC DESCRIPTION
	FORAMS	NANNOS	P.L. FORAMS	B. NANNOS						
MIDDLE MIOCENE (Serravallian)	N12				1	0.5			1	<p>NANNO CHALK = dom. lith. Numerous burrows, often with halos (one is up to 0.5 cm in dia.).</p> <p>CALC. CEMENT. SANDSTONE-SILTSTONE NANNO CHALK</p> <p>SS: 1-38 cm</p> <p>31.5 cm thick, ungraded burrowed, forams and nannos rexlized.</p> <p>75% carb. unspec.</p> <p>10 forams</p> <p>10 quartz</p> <p>5 nannos</p> <p>21.5 cm thick, ungraded sandstone-siltstone, burrowed similar to appearance to above unit; nanno chalk ~5 cm separates both clastic units.</p> <p>11.5 cm thick, ungraded sandstone dker. in color, ungraded.</p> <p>CALCAREOUS SANDSTONE-SILTSTONE</p> <p>15 cm thick, some evidence of micro-x lam.; nannos & forams rexlized.</p> <p>80% carb. unspec.</p> <p>15 quartz</p> <p>5 forams</p> <p>tr nannos</p> <p>XRD (1-88-91 cm): altered ash</p> <p>XR-amorph. (abund.)</p> <p>calcite (common)</p> <p>phillipsite</p> <p>NOTE: Marked increase in induration of chalks from C.74->76, now they will be specified as limestones (LS).</p> <p>CaCO₃% 67</p> <p>C_{org}% 0.2</p> <p>LECO: Sect. 2-51 cms</p> <p>COLOR LEGEND</p> <p>1 = lt. bl. gy. 5B 7/1</p> <p>2 = grn. gy. 5G 6/1</p>
					2	1.0				

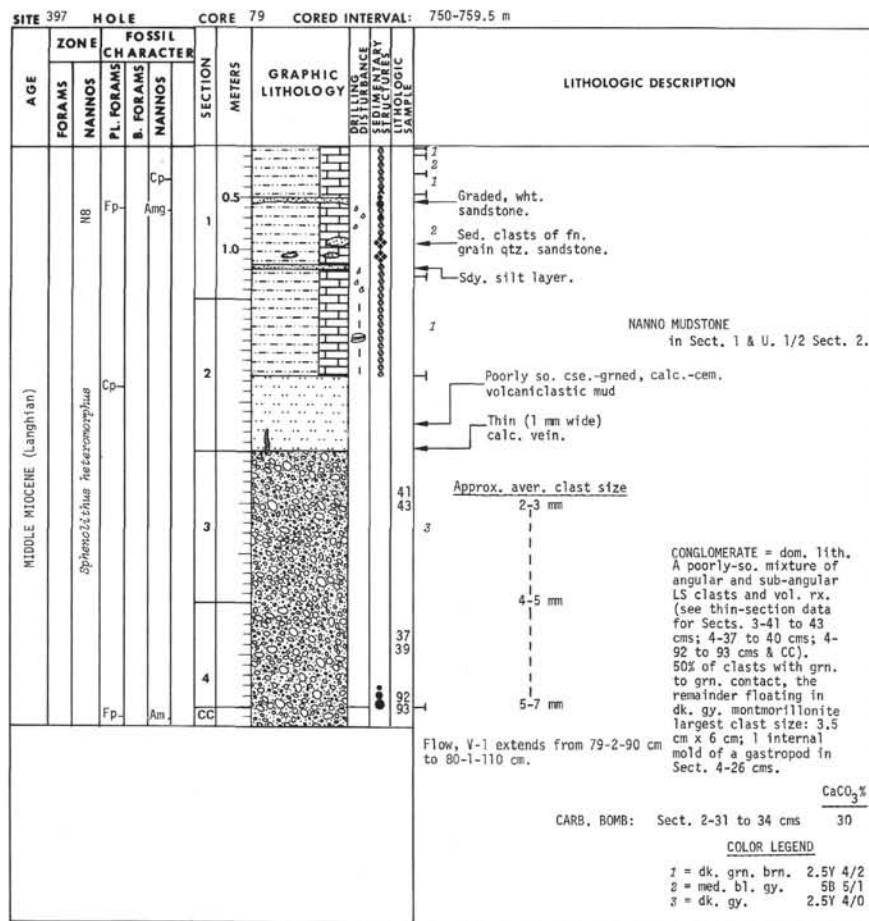


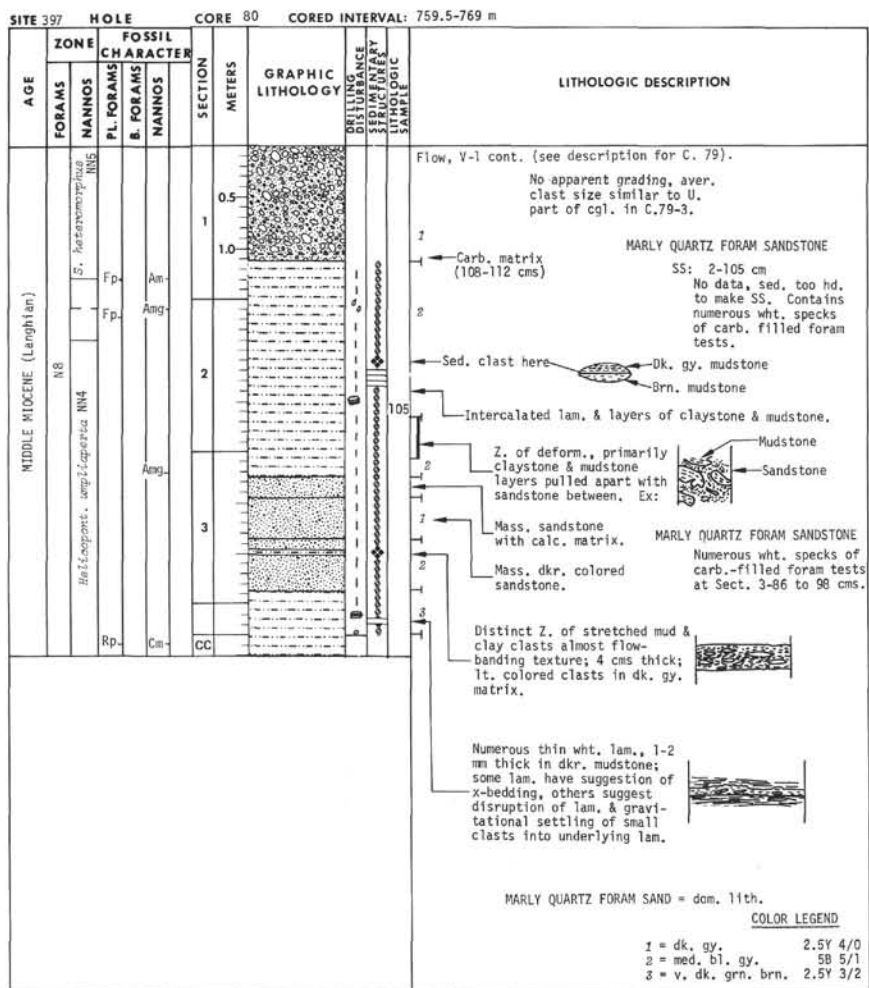
Explanatory notes in Chapter 1



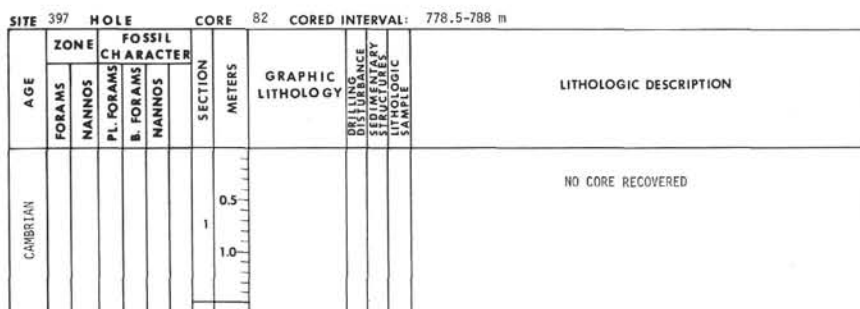
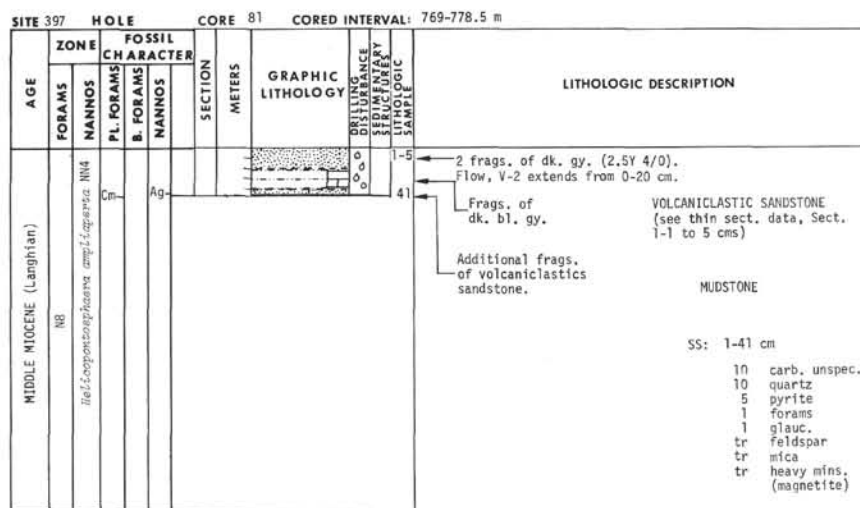


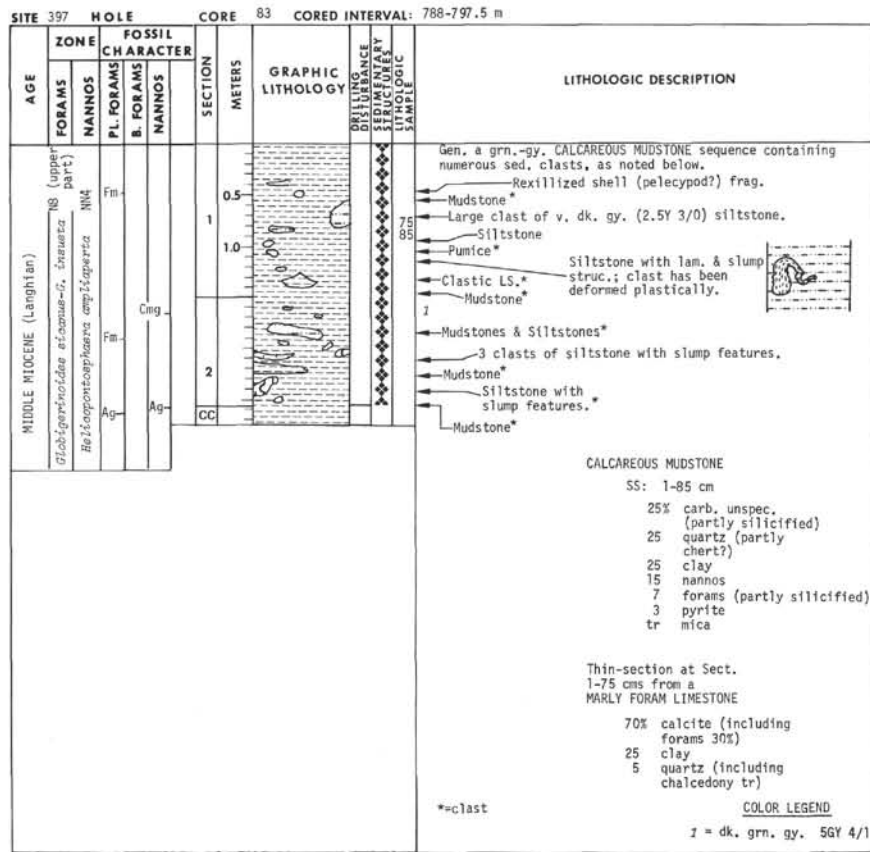
Explanatory notes in Chapter 1



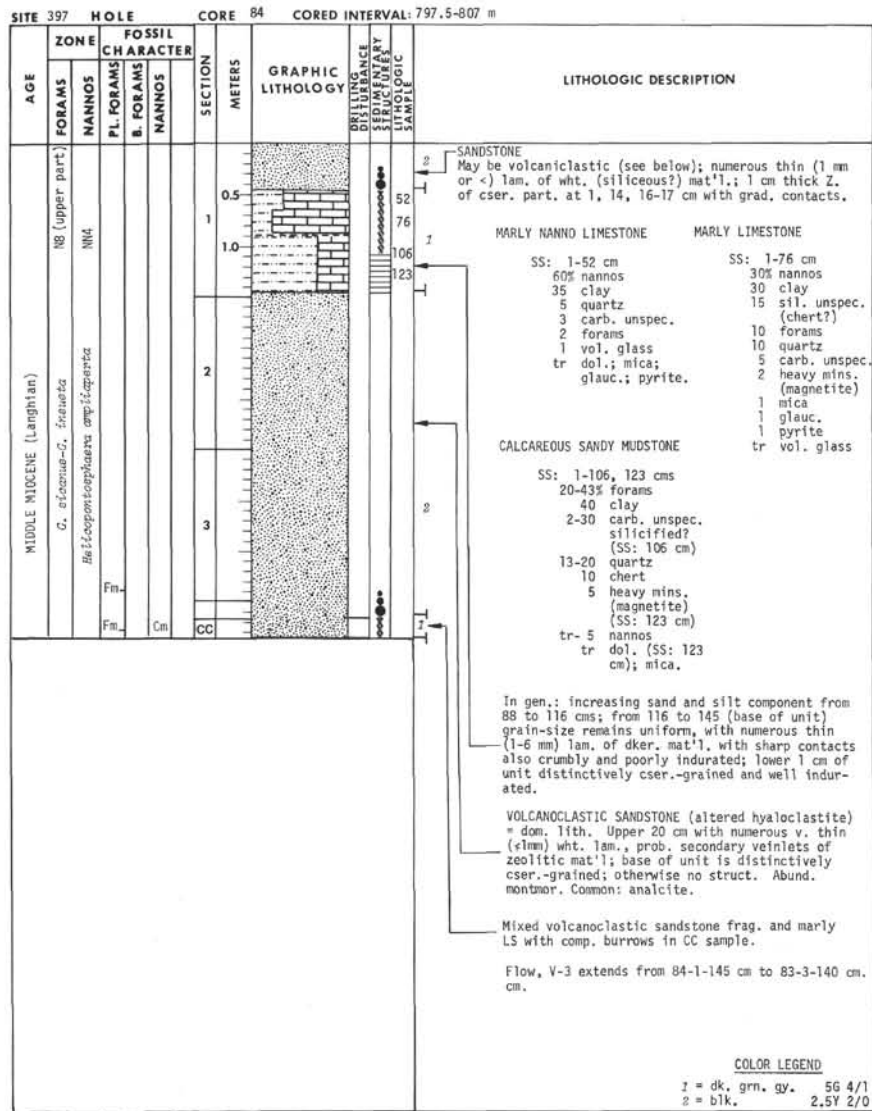


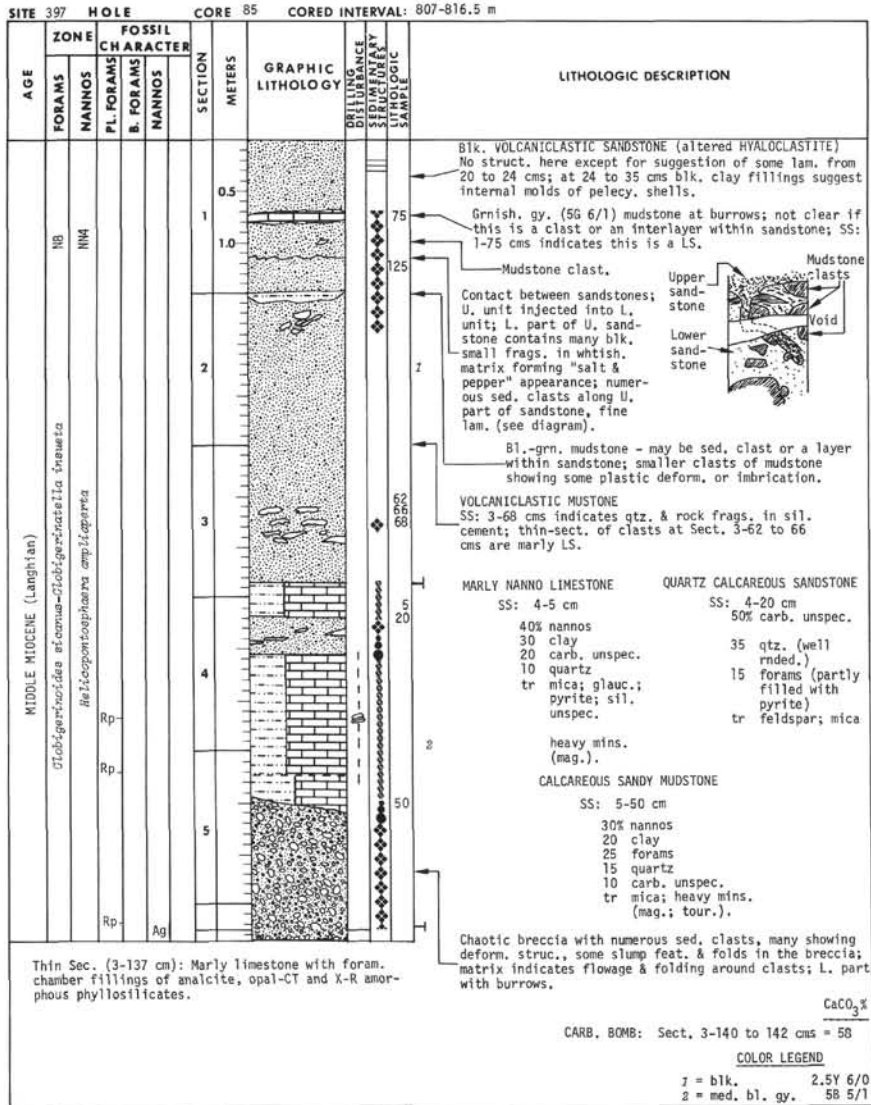
Explanatory notes in Chapter 1



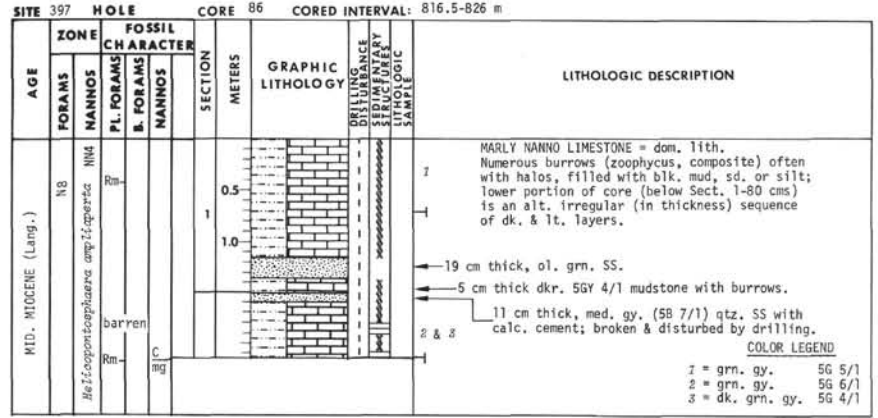


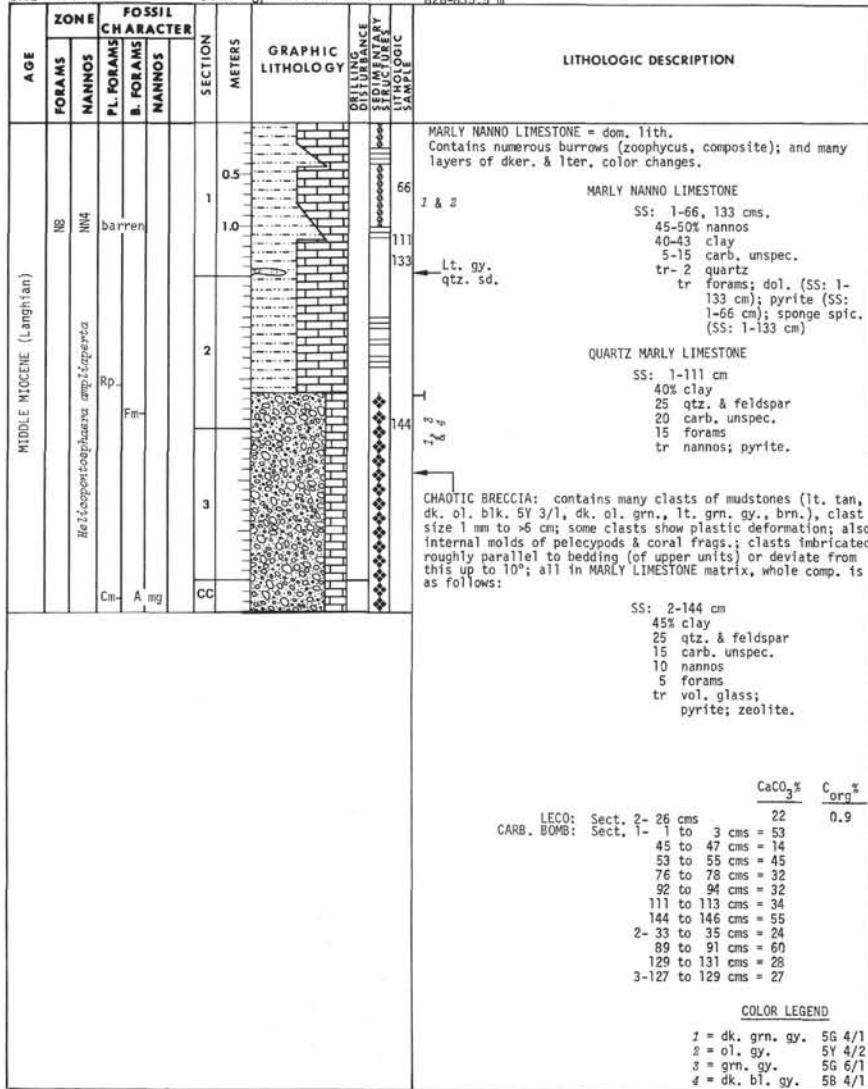
Explanatory notes in Chapter 1



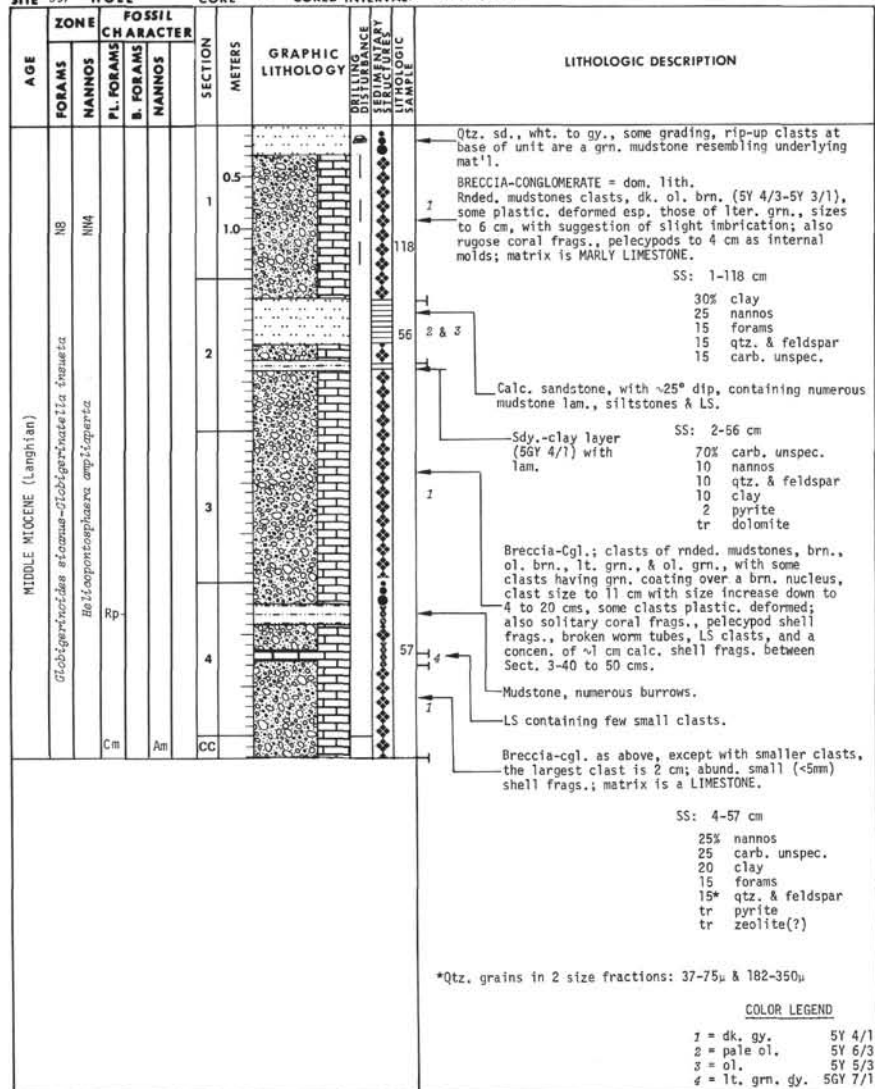


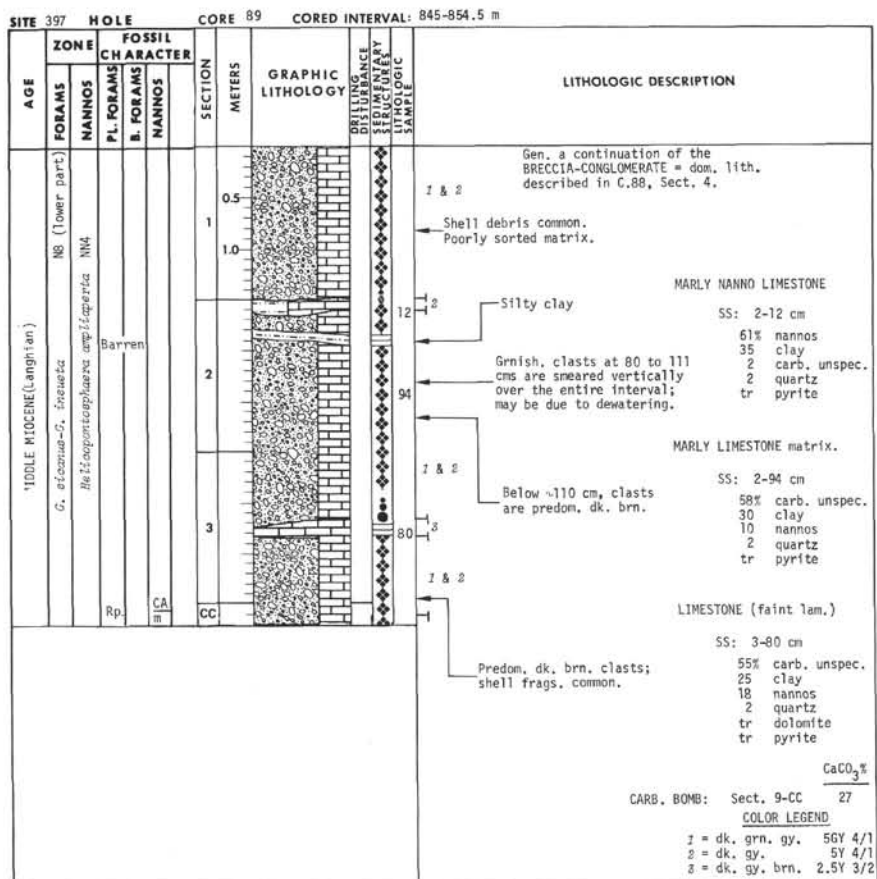
Explanatory notes in Chapter 1



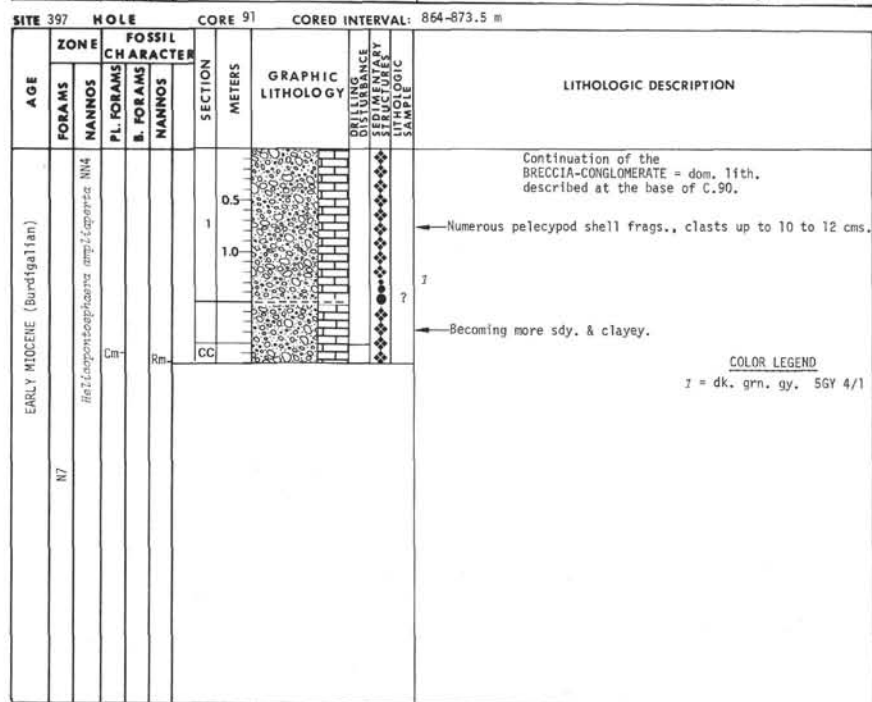
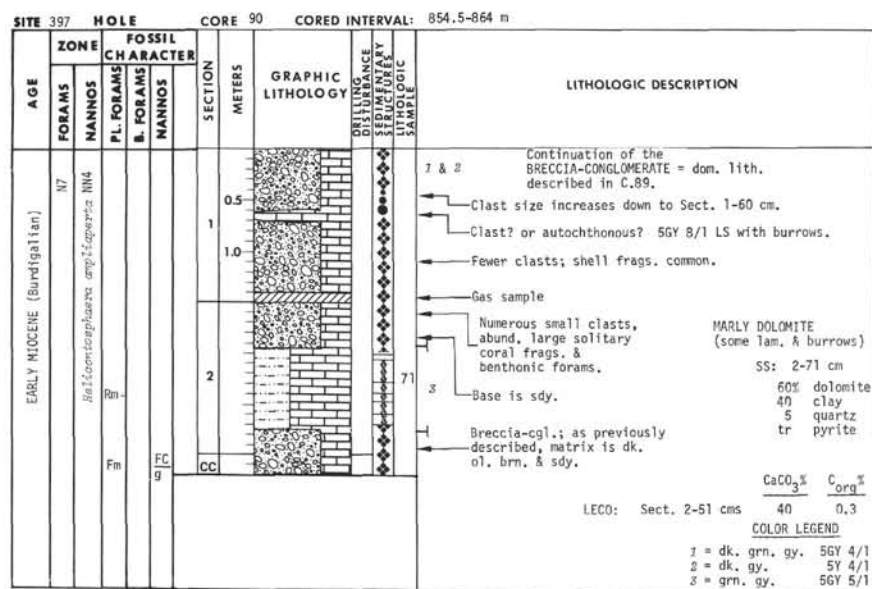


Explanatory notes in Chapter 1





Explanatory notes in Chapter 1



SITE 397		HOLE		CORE 92		CORED INTERVAL: 873.5-883 m	
AGE	ZONE		FOSSIL CHARACTER		SECTION METERS	GRAPHIC LITHOLOGY	LITHOLOGIC DESCRIPTION
	FORAMS	NANNOS	P.L. FORAMS	B. FORAMS			
EARLY MIOCENE (Burdigalian)	N7		P.L. FORAMS	NANNOS	1		<p>←Shell hash</p> <p>SANDY PEBBLY MUDSTONE = dom. 11th. Continuation of breccia-cgl. described at base of C.91. Breccia-cgl. here more a pebbly sdy. mudstone or a sdy. pebbly mudstone. Fewer large clasts & numerous rnded., clear qtz. granules & pebs. & shell frags. of pelecypods & gastropods (one gastropod whole until Mike Arthur broke it); some solitary corals; chert pebs. increase in size & quantity down core, up to 2 cm in dia. in sec. 4.</p> <p>Matrix: CALCAREOUS SANDY MUDSTONE</p> <p>SS: 3-25 cm</p> <p>35% clay 20 nannos 15 quartz 10 forams 5 dolomite carb. unspec. feldspar pyrite heavy mins. (apatite; magnetite)</p> <p>COLOR LEGEND I = grn. blk. 5G 2/1</p>
					2		
					3		
					RF		
					CC		

Explanatory notes in Chapter 1

SITE 397		HOLE		CORE 93		CORED INTERVAL: 883-892.5 m	
AGE	ZONE		FOSSIL CHARACTER		SECTION METERS	GRAPHIC LITHOLOGY	LITHOLOGIC DESCRIPTION
	FORAMS	NANNOS	P.L. FORAMS	B. FORAMS			
EARLY MIOCENE (Burdigalian)	N7		P.L. FORAMS	NANNOS	1		<p>Continuation of SANDY PEBBLY MUDSTONE = dom. 11th. described in C.92 here predom. rnded. & subrnded. qtz. granules; rare blk. qtzite. or chert granules & tan mudstone; qtz. pebs. at B. of core 1.5 x 2 cm.</p> <p>Matrix: CALCAREOUS SANDY MUDSTONE</p> <p>SS: 2-103 cm</p> <p>60% clay & chert 15 quartz 10 nannos 10 forams 5 pyrite tr dolomite tr sponge spics.</p>
					2		
					3		
					CC		
					Fc g		

←Yellowish peb. qtzite. or chert (100% clay-sized qtz.).

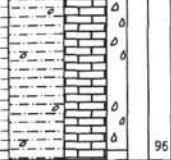
COLOR LEGEND

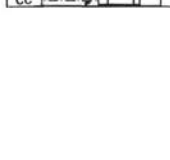
I = grn. blk. 5G 2/1

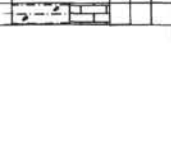
SITE 397 HOLE		CORE 94		CORED INTERVAL: 892.5-902 m			
AGE	ZONE	FOSSIL CHARACTER			SECTION METERS	GRAPHIC LITHOLOGY	LITHOLOGIC DESCRIPTION
		FORAMS	NANNOS	P.L. FORAMS			
EARLY MIOCENE (Burdigalian)	N7	G. <i>insuetudo</i> , <i>trilobus</i>	Heticopontopora <i>ampliceras</i> NN4	Fm	1		Continuation of SANDY PEBBLY MUDSTONE = dom. lith. described in C.93; here, however, there is decreasing amt. of qtz. granules but numerous broken frags. of pelecypod shells; matrix also less sdy. Matrix: CALCAREOUS MUDSTONE SS: 1-12 cm 75% carb. unspec. (silicified?) 15 quartz 5 nannos (silicified?) 5 forams (silicified?) tr feldspar tr vol. glass tr pyrite Some indistinct layers of more brownish sed. CALCAREOUS SANDY MUDSTONE SS: 1-28 cm 45% carb. unspec. (partly silicified) 35 quartz 6 forams 5 nannos 2 feldspar 2 pyrite tr dolomite tr glauc. tr fish debris tr mollusk frags. tr heavy mins. (monazite) COLOR LEGEND 1 = grn. blk. 5G 2/1
					2		

Explanatory notes in Chapter 1

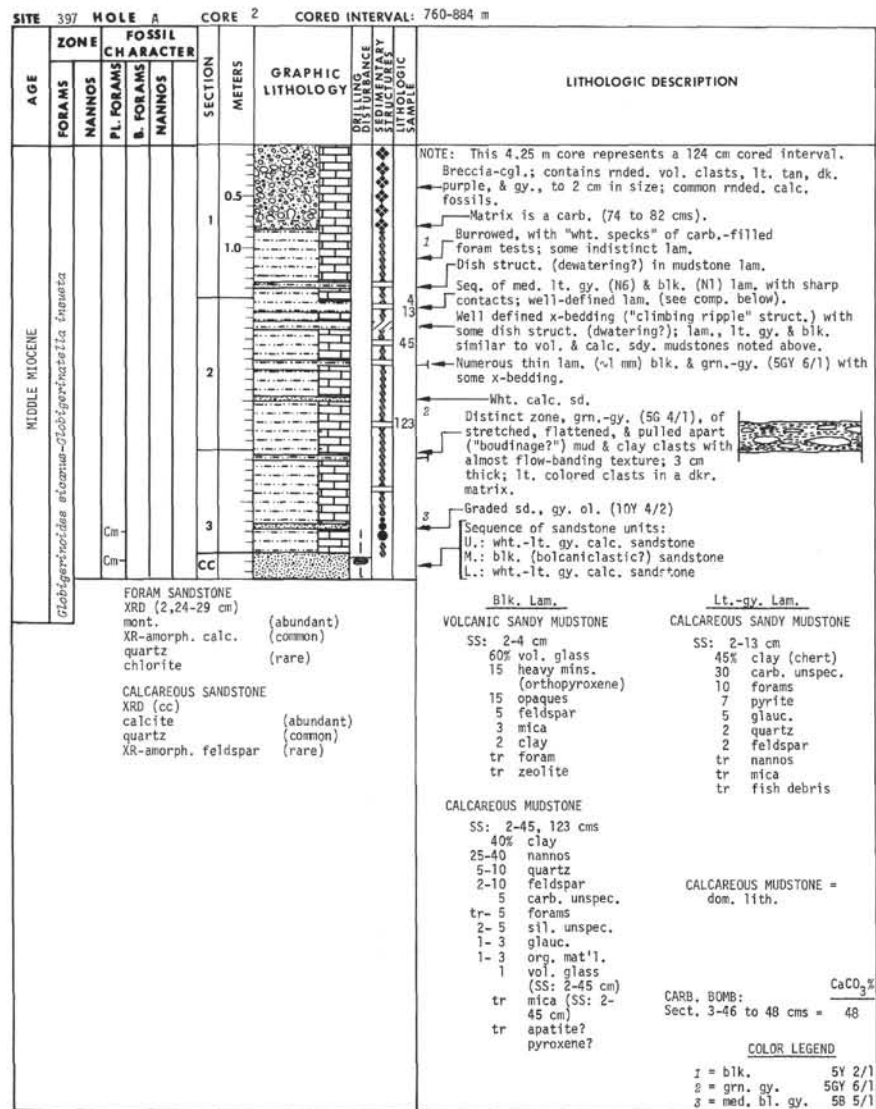
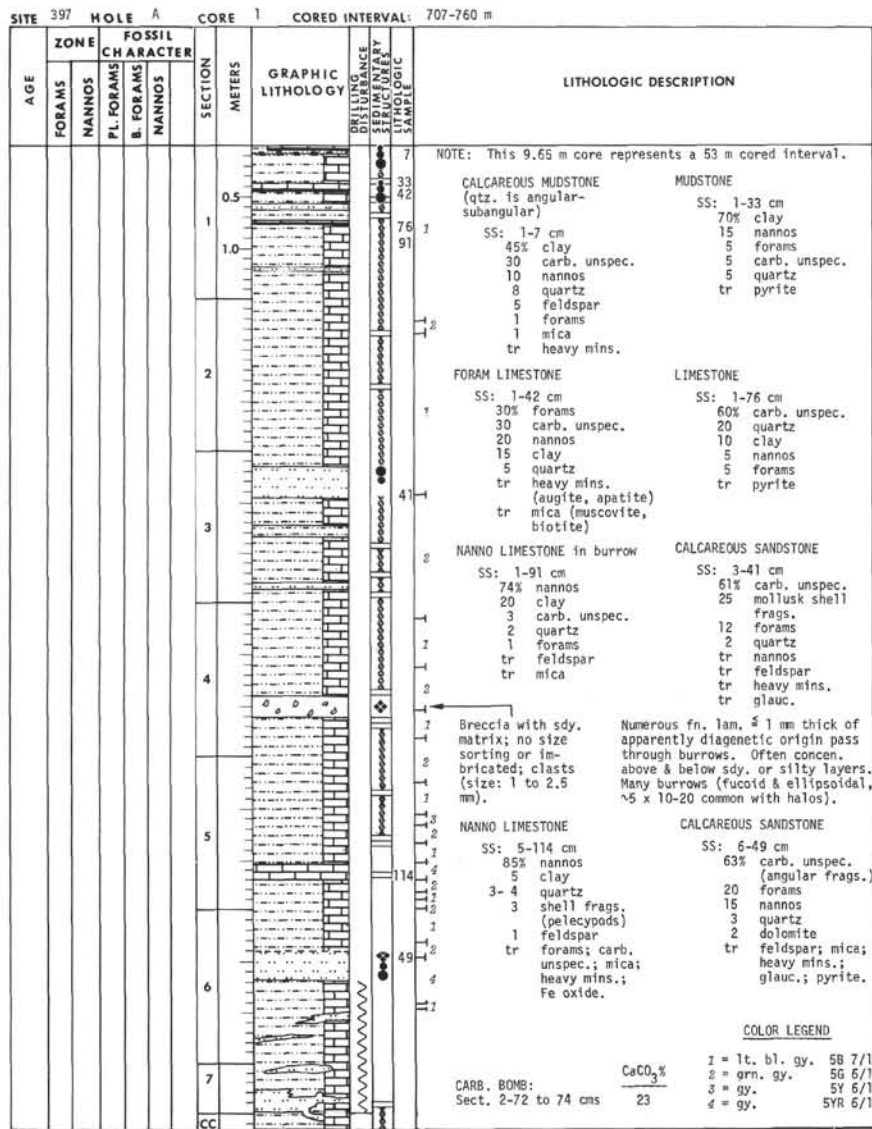
SITE 397 HOLE		CORE 95		CORED INTERVAL: 902-911.5 m			
AGE	ZONE	FOSSIL CHARACTER			SECTION METERS	GRAPHIC LITHOLOGY	LITHOLOGIC DESCRIPTION
		FORAMS	NANNOS	P.L. FORAMS			
EARLY MIOCENE (Burdigalian)	N7	G. <i>insuetudo</i> , <i>trilobus</i>	Heticopontopora <i>ampliceras</i> NN4	Fm	1		Continuation of SANDY PEBBLY MUDSTONE = dom. lith. described in C.94; here also with a decreasing qtz. granule content & with numerous broken pelecypod shell frags.; one scaphopod frag. at Sect. 1-25 cms. Sed. filling shell frag.: SANDY CALCAREOUS MUDSTONE SS: 1-38 cm 40% quartz 20-30 clay 20-30 carb. unspec. (silicified?) 10 shell frags. tr nannos tr feldspar tr mica tr glauc. tr pyrite Matrix: SANDY CALCAREOUS MUDSTONE SS: 2-51 cm, 3-19 cm 60% carb. unspec. 55-40 quartz tr nannos tr forams tr feldspar Indistinct dk. brn. layer: CALCAREOUS SILICIFIED MUDSTONE SS: 4-99 cm 30-40% chert 15-25 clay 15 quartz 10 carb. unspec. 5-10 nannos tr-5 forams tr dolomite COLOR LEGEND 1 = grn. blk. 5G 2/1 2 = dk. grn. gy. 5G 4/1
					2		
					3	19	
					4	99	← Geochem. Samp.
					5		

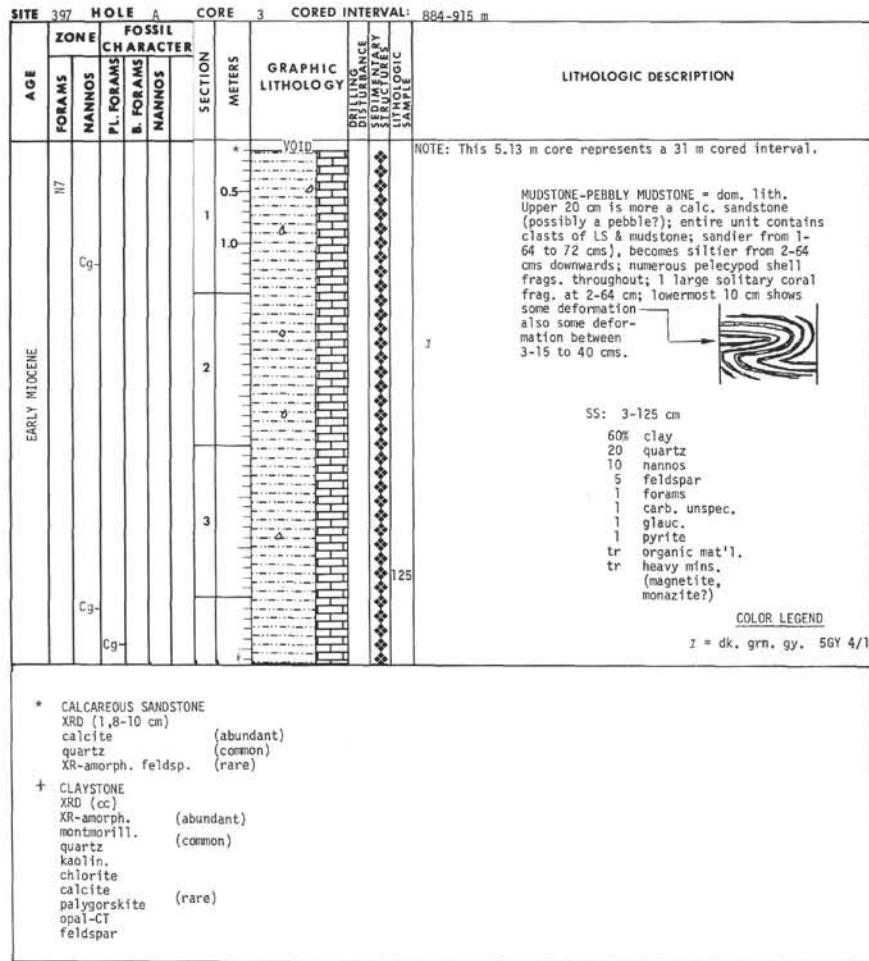
SITE 397		HOLE		CORE 101		CORED INTERVAL: 968.5-978 m		
AGE	ZONE		FOSSIL CHARACTER		SECTION	METERS	GRAPHIC LITHOLOGY	LITHOLOGIC DESCRIPTION
	FORAMS	NANNOS	PL. FORAMS	B. FORAMS				
EARLY MIOCENE (Burdigalian)								Continuation of SANDY PEBBLY MUDSTONE = dom. lith. described in C.97 Matrix: MUDSTONE SS: 1-96 cm 65% feldspar & qtz. 35 clay tr nannos tr carb. unspec.
							96	

SITE 397		HOLE		CORE 103		CORED INTERVAL: 967.5-997 m		
AGE	ZONE		FOSSIL CHARACTER		SECTION	METERS	GRAPHIC LITHOLOGY	LITHOLOGIC DESCRIPTION
	FORAMS	NANNOS	PL. FORAMS	B. FORAMS				
EARLY MIOCENE (Burdigalian)								Only CC recovered. Continuation of SANDY PEBBLY MUDSTONE = dom. lith. described in prev. cores. Matrix: MUDSTONE SS: CC 65% clay 30 feldspar & qtz. 5 carb. unspec. tr nannos tr dolomite
								Site 397, Core 104, 997-1000 m: NO CORE RECOVERED

SITE 397		HOLE		CORE 102		CORED INTERVAL: 978-987.5 m		
AGE	ZONE		FOSSIL CHARACTER		SECTION	METERS	GRAPHIC LITHOLOGY	LITHOLOGIC DESCRIPTION
	FORAMS	NANNOS	PL. FORAMS	B. FORAMS				
EARLY MIOCENE (Burdigalian)								Continuation of SANDY PEBBLY MUDSTONE = dom. lith. described in C.101. Matrix: MUDSTONE SS: CC 70% clay 25 feldspar & qtz. 5 pyrite tr nannos tr forams tr carb. unspec. tr dolomite

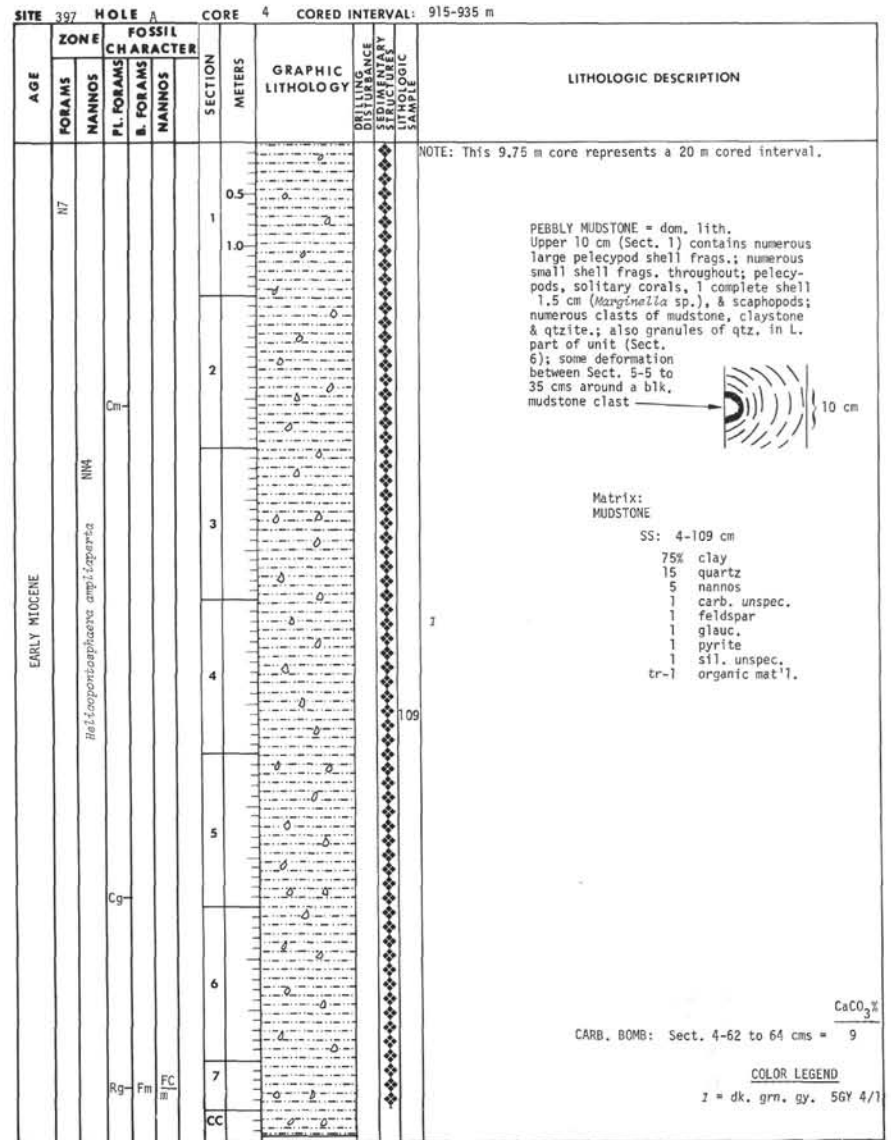
Explanatory notes in Chapter 1





- * CALCAREOUS SANDSTONE
XRD (1.8-10 cm)
calcite (abundant)
quartz (common)
XR-amorph. feldsp. (rare)
- + CLAYSTONE
XRD (cc)
XR-amorph. montmorill. (abundant)
quartz (common)
kaolin
chlorite
calcite
palygorskite (rare)
opal-CT
feldspar

Explanatory notes in Chapter 1

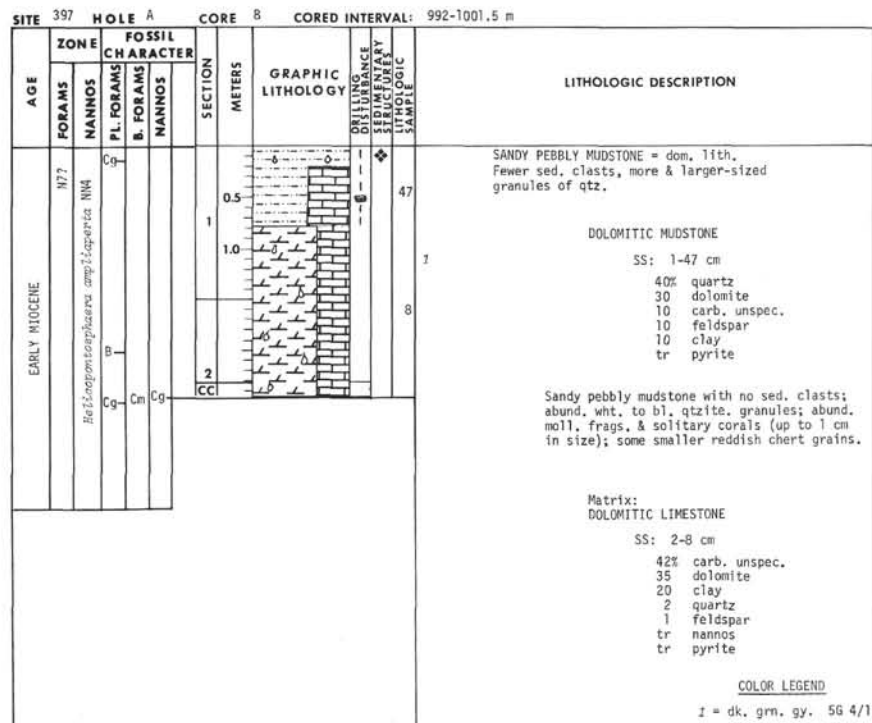
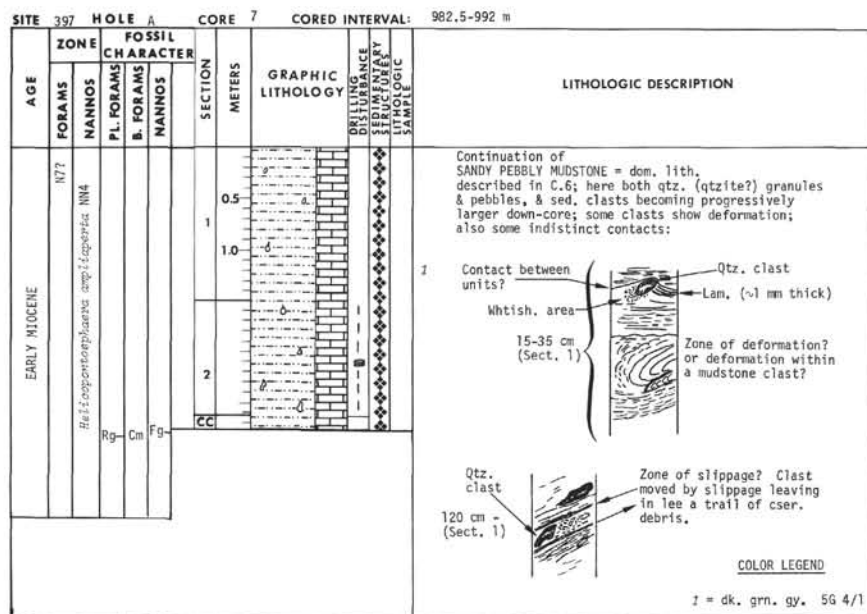


SITE 397 HOLE A CORE 5 CORED INTERVAL: 935-963.5 m		AGE		ZONE		FOSSIL CHARACTER		SECTION METERS	GRAPHIC LITHOLOGY	DRILLING LOG TEMPERATURE STRUCTURE LITHOLOGIC SAMPLE	LITHOLOGIC DESCRIPTION
FORAMS	NANNOS	PL. FORAMS	B. FORAMS	NANNOS	FORAMS	NANNOS	SECTION METERS				
EARLY MIOCENE	N7	NM						0.5	VOID		NOTE: This 3.3 m core represents a 28.5 m cored interval.
	<i>H. amplicapervoz</i>	NM						1.0			DOLOMITE (Sect. 1-0 to 65 cm)
								1.0			SS: 1-30 cm
								1.0			70% dolomite
								1.0			15 clay
								1.0			5 nannos
								1.0			5 carb. unspec.
								1.0			3 quartz
								1.0			3 forams
								1.0			tr pyrite
								1.0			Homog., no granules or shell frags.
								1.0			PEBBLY MUDSTONE = dom. lith. Containing pelecypod shell frags., scaphopod shell frags. & granules of qtz., some sed. clasts a few show deformation (folds) struct.
								1.0			Matrix: SANDY MUDSTONE
								1.0			SS: 2-61 cm
								1.0			40% quartz
								1.0			35 clay
								1.0			10 forams
								1.0			5 nannos
								1.0			5 feldspar
								1.0			5 carb. unspec.
								1.0			1 heavy mins. (magnetite)
								1.0			tr glauc.
								1.0			tr pyrite
								1.0			tr organic mat'l.
								1.0			MUDSTONE [tr. ol. gy. (SY 6/1) area (matrix)]
								1.0			SS: 2-90 cm
								1.0			60% clay
								1.0			20 carb. unspec.
								1.0			10 quartz
								1.0			6 nannos
								1.0			3 feldspar
								1.0			tr mica
								1.0			tr pyrite
								1.0			COLOR LEGEND
								1.0			1 = very dk. brn. 2.SY 3/2
								1.0			2 = dk. grn. gy. 5GY 4/1
								1.0			3 = lt. gy. SY 6/1
								1.0			4 = blk. SY 2/1

Explanatory notes in Chapter 1

SITE 397 HOLE A CORE 6 CORED INTERVAL: 963.5-982 m		AGE		ZONE		FOSSIL CHARACTER		SECTION METERS	GRAPHIC LITHOLOGY	DRILLING LOG TEMPERATURE STRUCTURE LITHOLOGIC SAMPLE	LITHOLOGIC DESCRIPTION
FORAMS	NANNOS	PL. FORAMS	B. FORAMS	NANNOS	FORAMS	NANNOS	SECTION METERS				
EARLY MIOCENE	N7	NM						0.5			NOTE: This 3.7 m core represents a 18.5 cored interval. SANDY PEBBLY MUDSTONE = dom. lith.
								0.5			MUDDY LIMESTONE
								0.5			SS: 1-15 cm
								0.5			70% clay
								0.5			12 quartz
								0.5			5 carb. unspec. (chert)
								0.5			5 silt. unspec.
								0.5			3 nannos
								0.5			3 feldspar
								0.5			2 forams
								0.5			1 dolomite
								0.5			1 pyrite
								0.5			1 heavy mins. (magnetite, monazite)
								0.5			tr glauc.
								0.5			tr organic mat'l.
								0.5			MUDDY LIMESTONE (with a small recrystallized pelecypod shell; lt. ol. gy. (SY 6/1); containing:
								0.5			SS: 1-50 cm
								0.5			55% carb. unspec.
								0.5			20 quartz (well rnded.)
								0.5			15 clay
								0.5			5 forams
								0.5			3 nannos
								0.5			2 pyrite
								0.5			SANDY PEBBLY MUDSTONE [with numerous well-rnded. qtz. or qtzite, granules (including some "blue qtz."; rnded. sed. clasts of dk. gy. mudstones & some LS; rare clasts of vol. rx. (with a strongly foliated texture.)]
								0.5			SS: 1-95 cm
								0.5			30% quartz
								0.5			30 clay
								0.5			10 nannos
								0.5			10 feldspar
								0.5			8 forams
								0.5			5 carb. unspec.
								0.5			2 organic mat'l.
								0.5			1 glauc.
								0.5			1 pyrite
								0.5			1 heavy mins. (amphibole)
								0.5			COLOR LEGEND
								0.5			1 = dk. grn. gy. 5GY 4/1

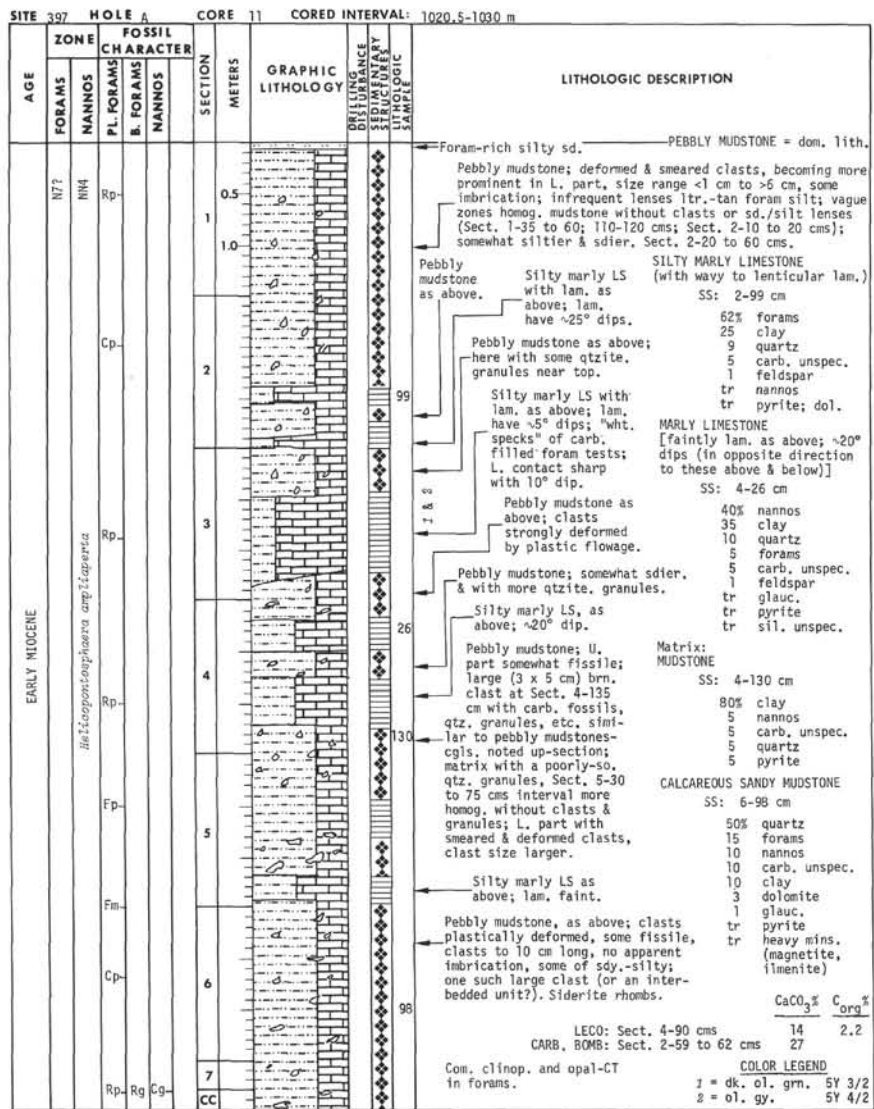
1 = dk. grn. gy. 5GY 4/1



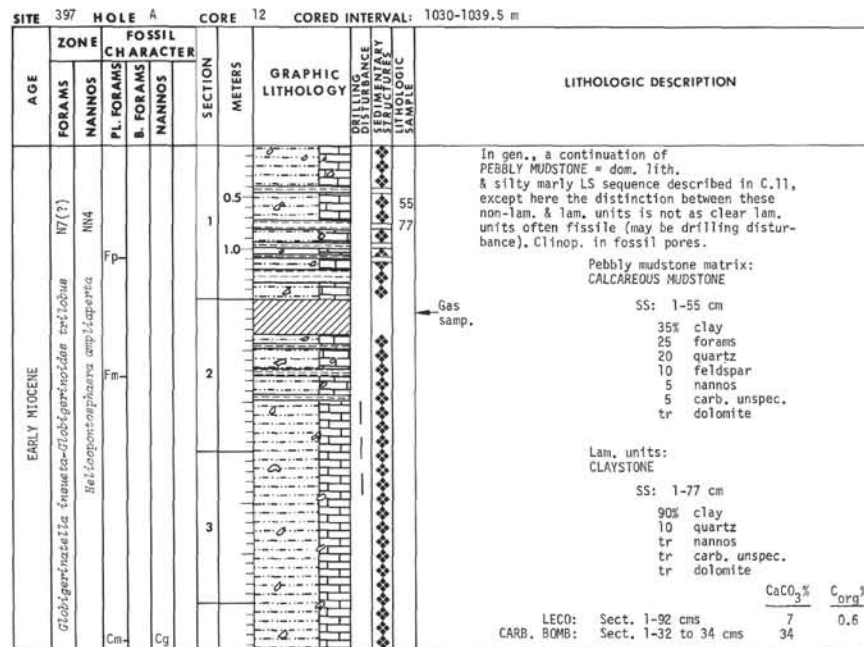
SITE 397		HOLE A		CORE 9		CORED INTERVAL: 1001.5-1011 m	
AGE	ZONE		FOSSIL CHARACTER		SECTION METERS	GRAPHIC LITHOLOGY	LITHOLOGIC DESCRIPTION
	FORAMS	NANNOS	P.L. FORAMS	B. FORAMS			
EARLY MIOCENE	N7?	NN4	Cg	Ag	CC		Continuation of SANDY PEBBLY MUDSTONE = dom. lith. see C.8. Qtzite, pebbles here to 3 cm.
							<p>Calcareous mudstone</p> <p>SS: 1-20 cm</p> <p>45% clay 20 nannos 15 quartz 5 forams 5 carb. unspec. 5 feldspar 3 sil. unspec. 1 mica 1 pyrite tr-1 dolomite tr-1 diatoms tr heavy mins. (pyroxene?)</p> <p>Becoming more sil. at base of core; also decrease in terrig. component:</p> <p>NANNO LIMESTONE</p> <p>SS: cc</p> <p>60% nannos 10 carb. unspec. 5-10 diatoms 5 quartz 5 clay 5 sponge spics. tr-5 forams 2 rads tr dolomite tr mica tr pyrite</p> <p>COLOR LEGEND 1 = dk. gm. gy. 5GY 4/1</p>

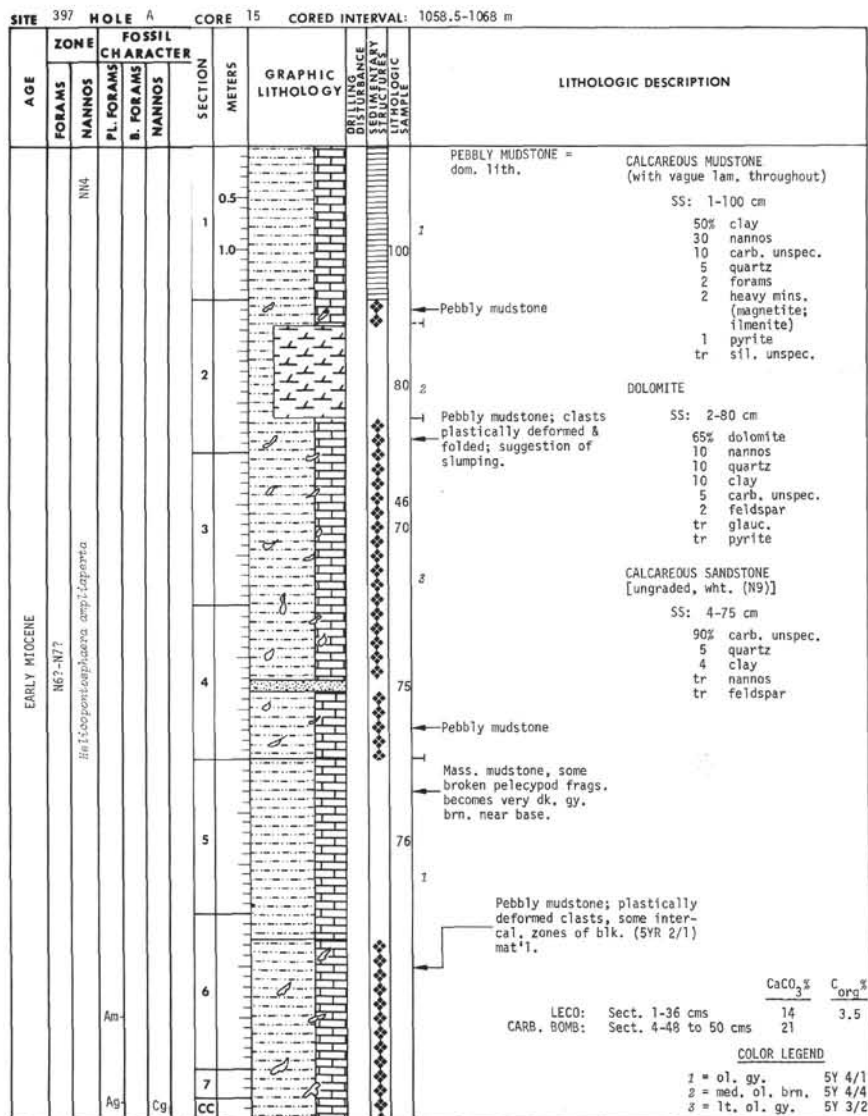
Explanatory notes in Chapter 1

SITE 397		HOLE A		CORE 10		CORED INTERVAL: 1011-1020.5 m	
AGE	ZONE		FOSSIL CHARACTER		SECTION METERS	GRAPHIC LITHOLOGY	LITHOLOGIC DESCRIPTION
	FORAMS	NANNOS	P.L. FORAMS	B. FORAMS			
EARLY MIOCENE	N7?	NN4	Cg	Ag	CC		<p>PEBBLY MUDSTONE CONGLOMERATE = dom. lith. rich in zeolite.</p> <p>SS: 1-7 cm</p> <p>50% clay 20 nannos 15 quartz 5 forams 5 carb. unspec. 5 feldspar tr-1 organic mat'l. tr-1 dolomite tr heavy mins. (magnetite) tr pyrite tr diatoms</p> <p>MARLY LIMESTONE, ± dolo. Gassy odor; some occ. peb.-sized clasts, some deformed & smeared to bedding; seds. gen. dip 10°, locally to 30° (Sect. 1-40 to 50 cms); scat. tests of benthic forams & small gastropods:</p> <p>SS: 1-83 cm</p> <p>35% clay 25 carb. unspec. 20 quartz 15 forams 5 feldspar tr nannos</p> <p>Thin-Sec. (CC), opal-CT replaced rads. CaCO₃% C_{org}% LECO: Sect. 4-65 cms 18 2.9 CARR. BOMB: Sect. 1-82 to 84 cms 27</p> <p>COLOR LEGEND 1 = dk. ol. gm. 5Y 3/2 2 = ol. gy. 5Y 5/2</p>
							<p>Sequence of foran-rich (ltr. SY 3/2) & clay-rich (dkr. SY 4/2, dk. ol. gy.) lam.; all with 18 to 20° dip; some burrowing although no evid. of dep. break to allow burrowing; contacts grad.</p> <p>Pebbly mudstone-cgl.; trans. upwards into overlying lam. unit; numerous clasts, to 4 cm, some plastically deformed; slight imbrication, non-deformed clasts rned. becomes silty in lower 15 cms.</p> <p>Sequence of claystone & marly siltstone lam.; ~10° dip.</p> <p>Pebbly mudstone-cgl. (see above).</p> <p>Sequence of claystone & marly LS lam.; L. contact sharp & angular.</p> <p>Pebbly mudstone-cgl. again (see above).</p>

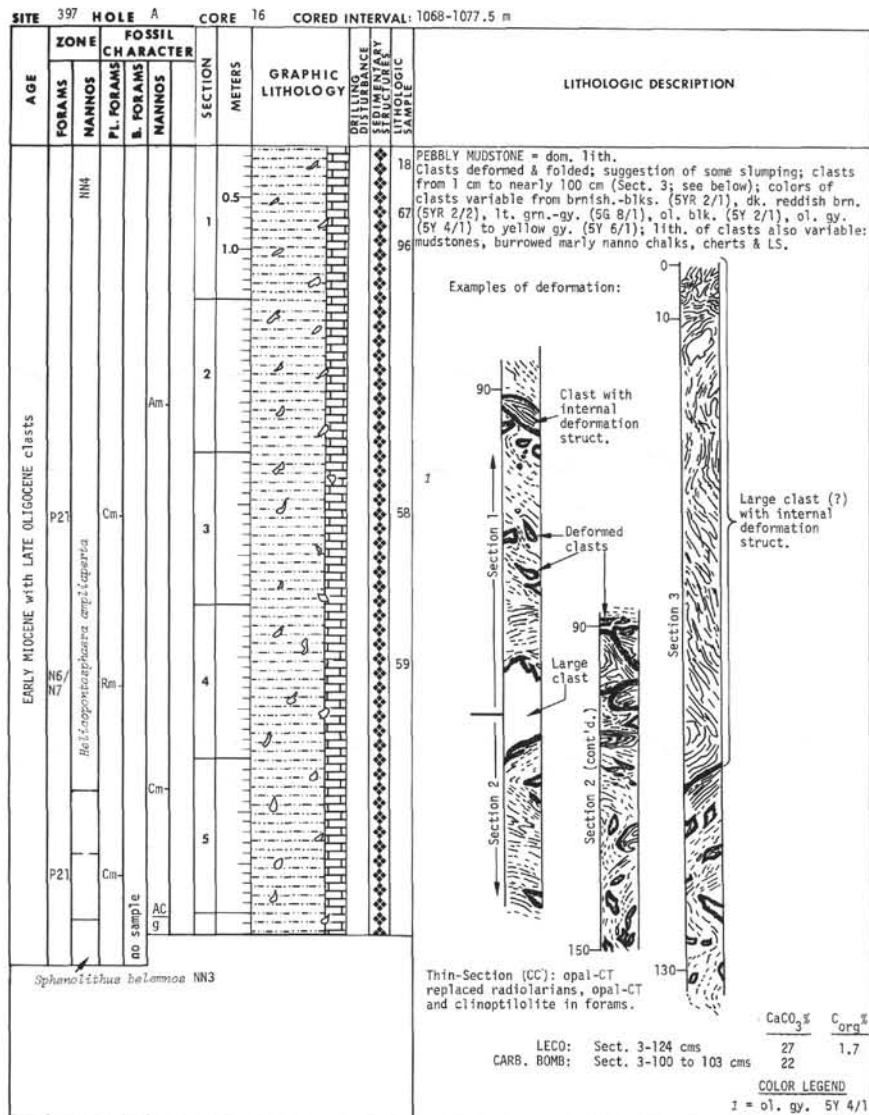


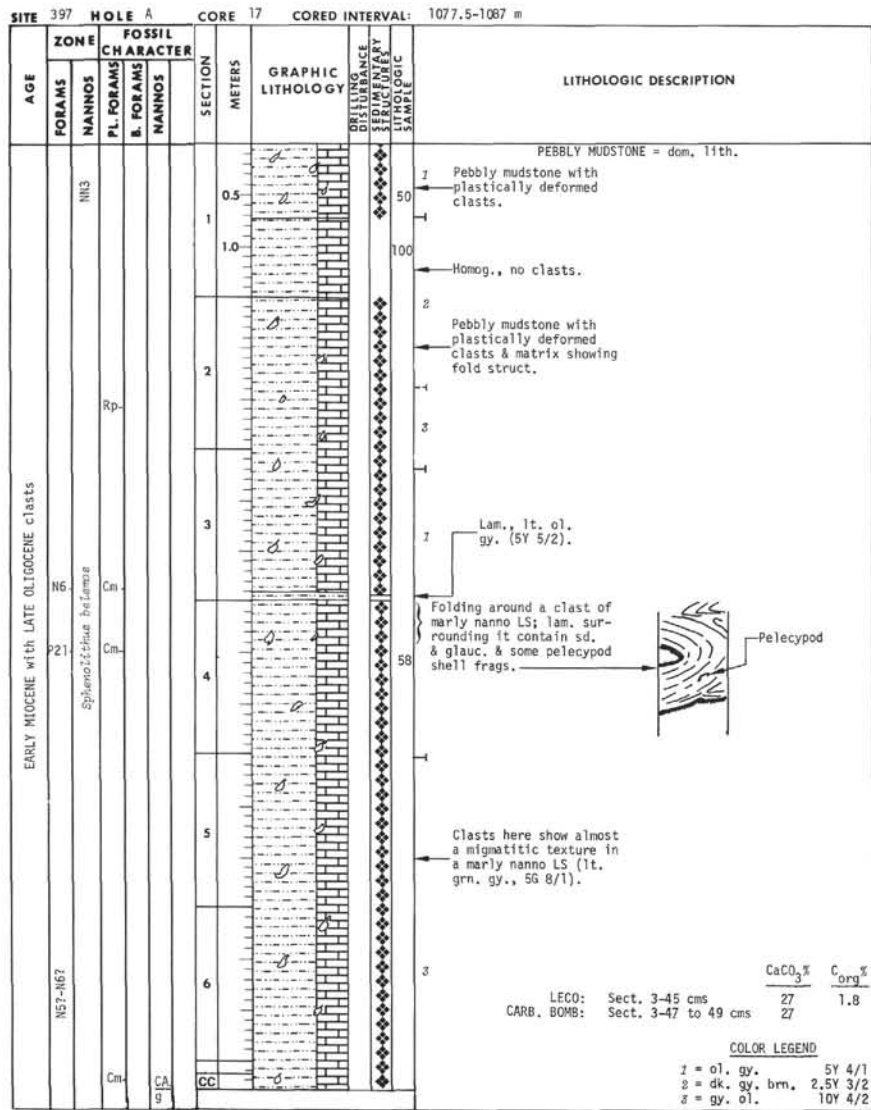
Explanatory notes in Chapter 1



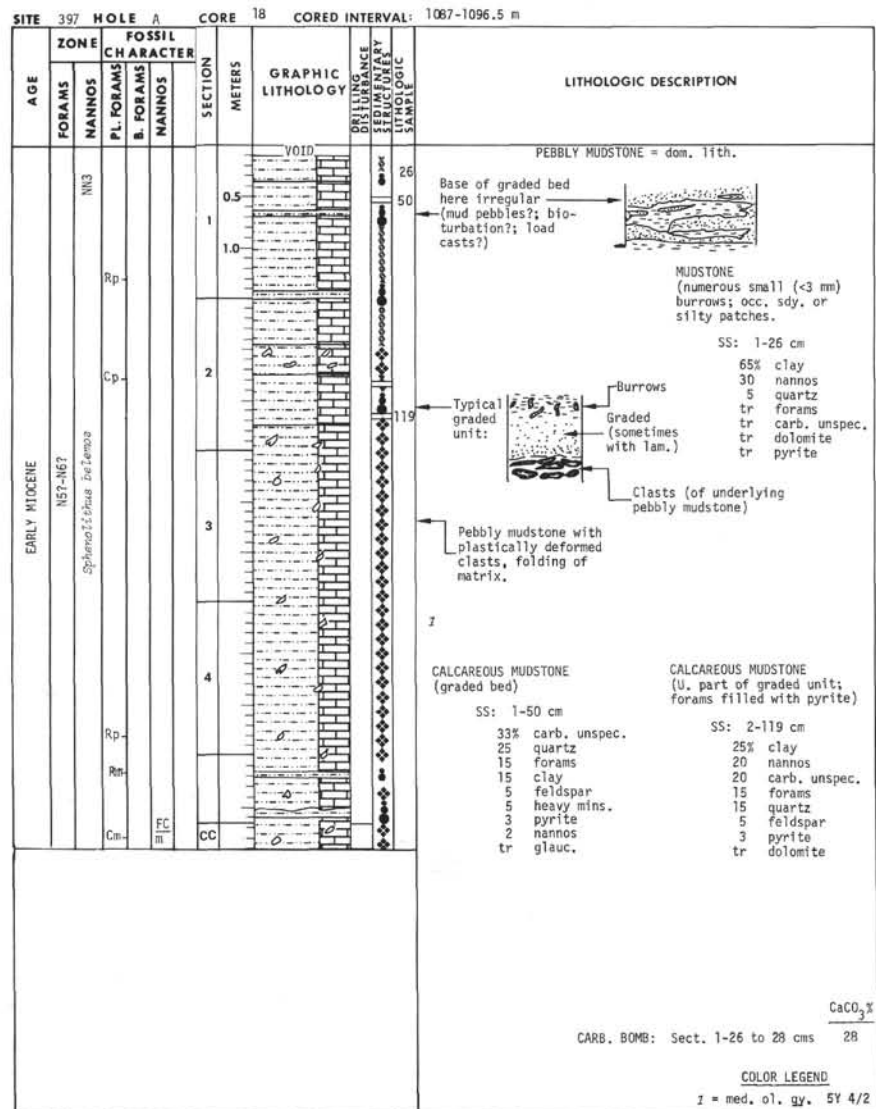


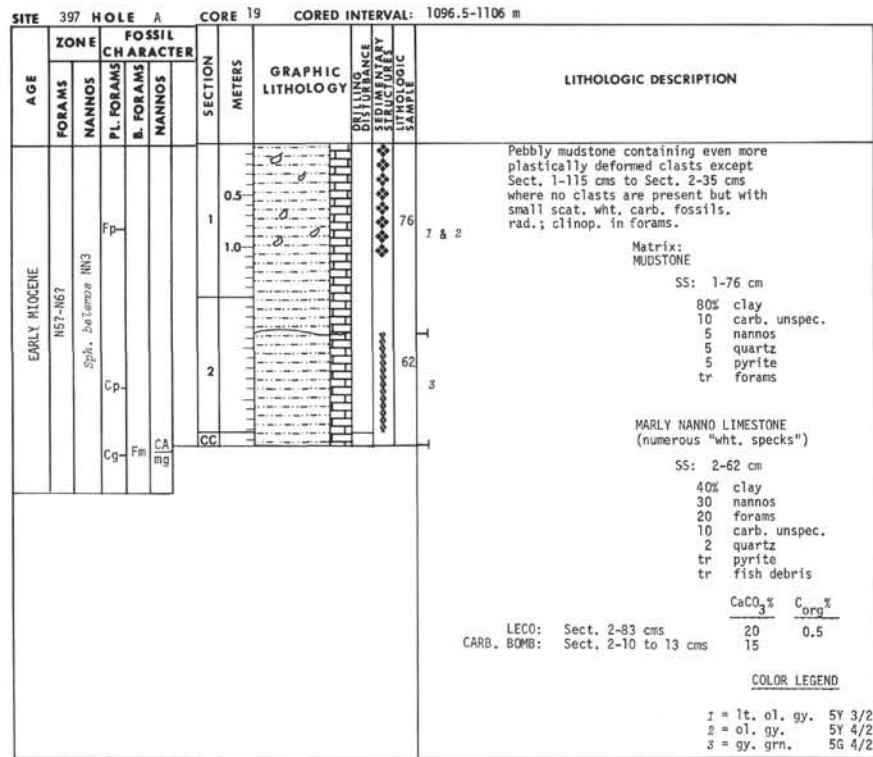
Explanatory notes in Chapter 1



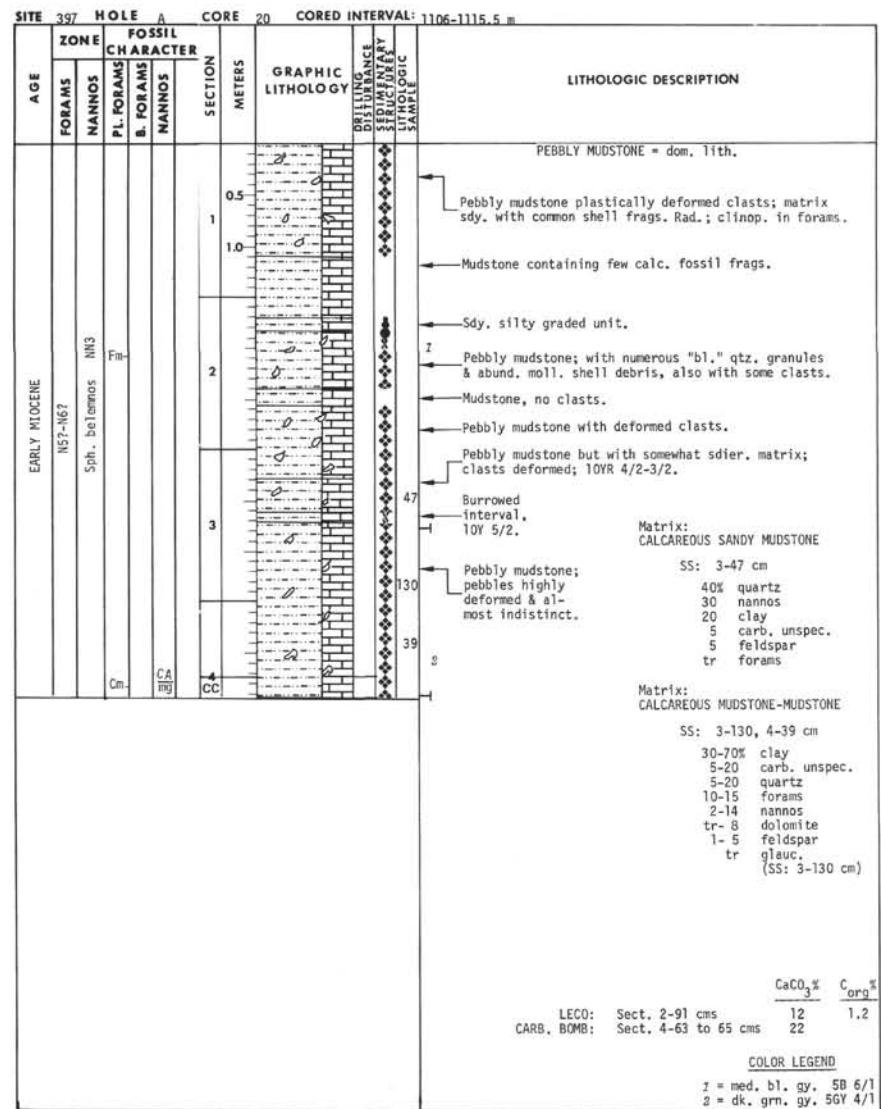


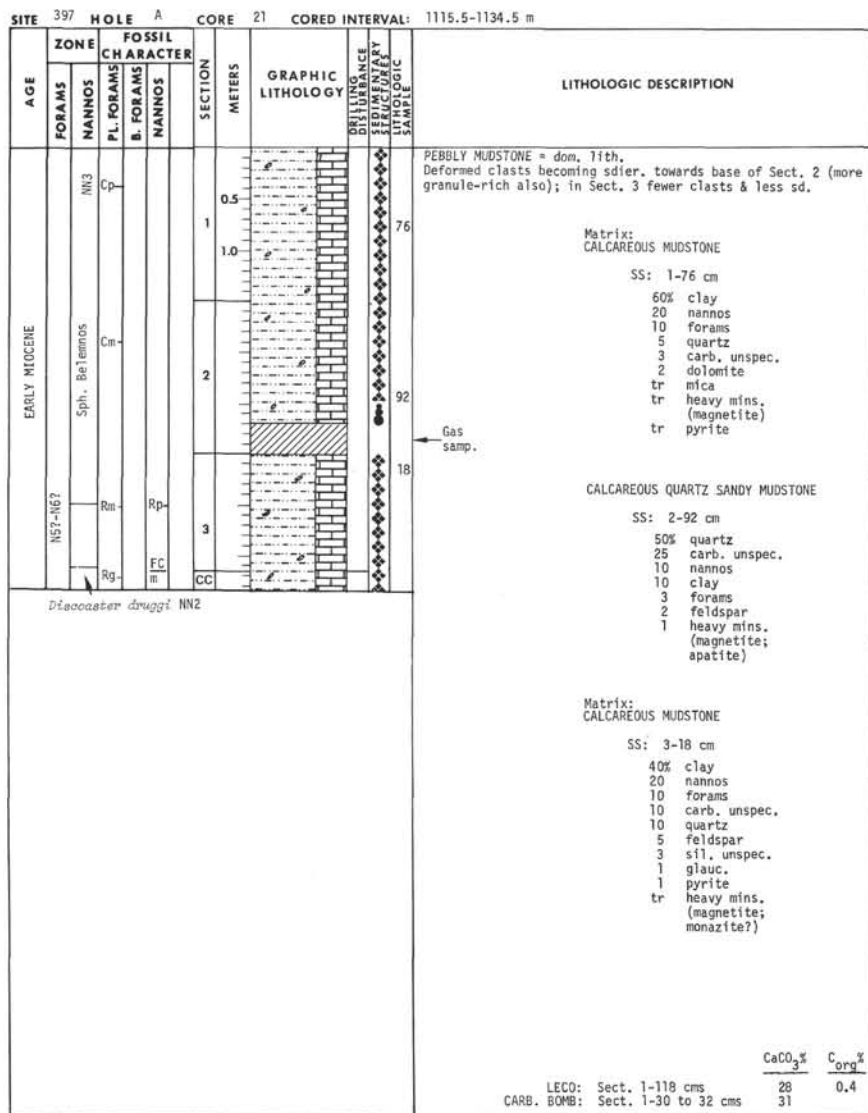
Explanatory notes in Chapter 1

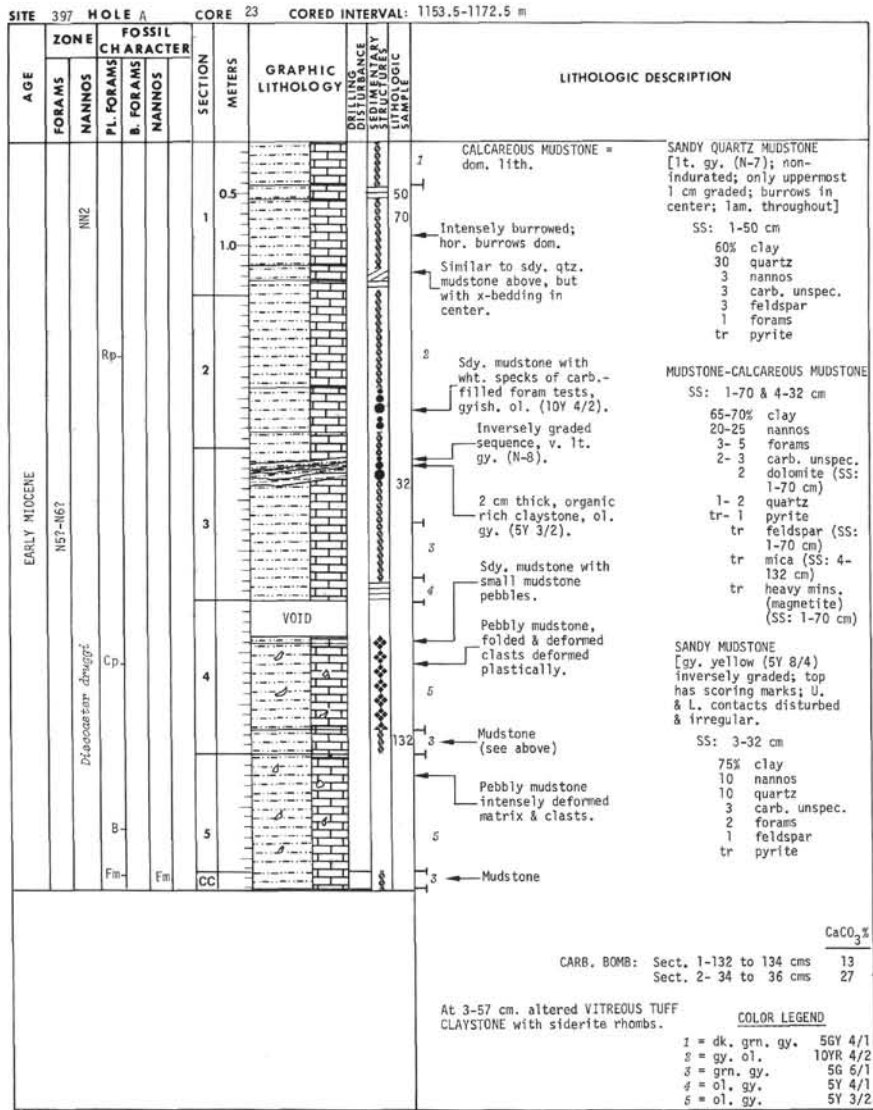




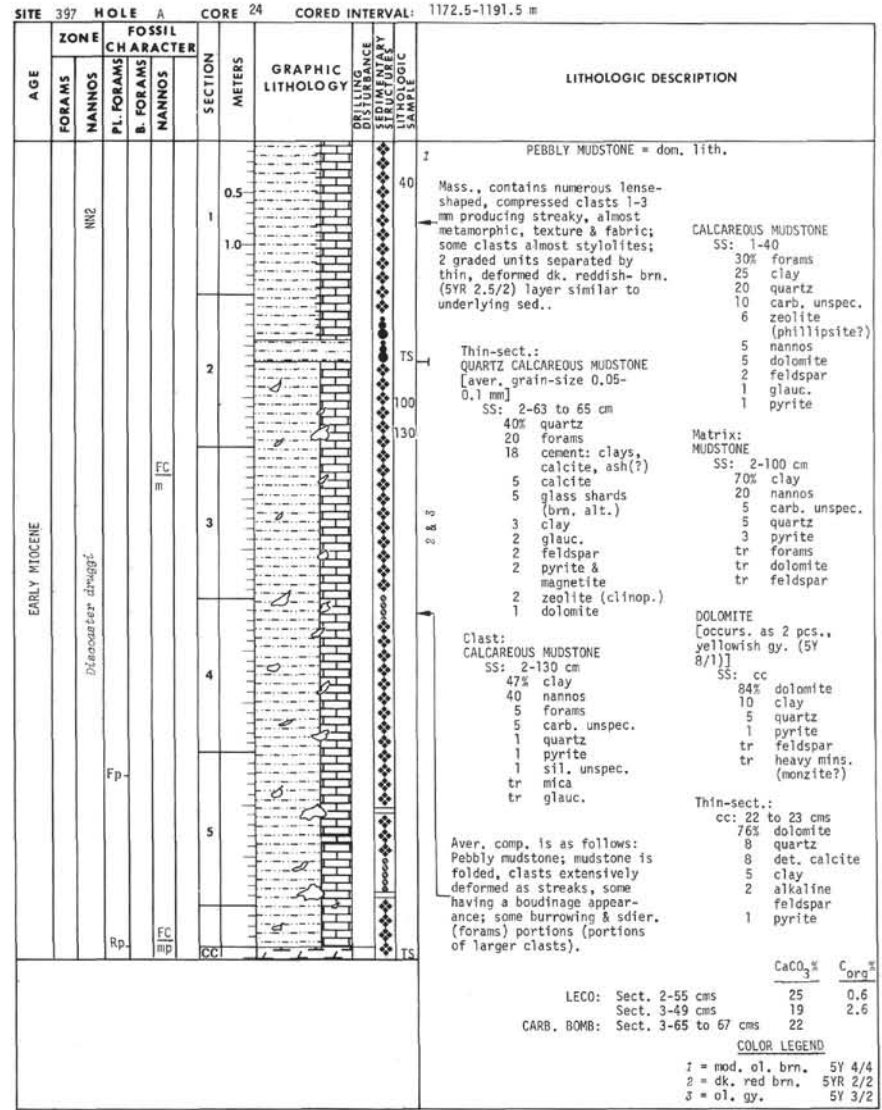
Explanatory notes in Chapter 1







Explanatory notes in Chapter 1



SITE 397		HOLE A		CORE 25		CORED INTERVAL: 1191.5-1210.5 m	
AGE	ZONE		FOSSIL CHARACTER		SECTION METERS	GRAPHIC LITHOLOGY	LITHOLOGIC DESCRIPTION
	FORAMS	NANNOS	PL. FORAMS	B. FORAMS			
EARLY MIOCENE	N57 - N67	Diacocarter druggi	Fp	FC	1		DOLOMITE (pebbly mudstone, med. lt. gy.) SS: 1-5 cm 53% dolomite 30 carb. unspec. 10 clay 2 quartz 1 forams Matrix: MUDSTONE SS: 1-115; 2-97 cms 65% clay 10-15 quartz 6-10 carb. unspec. 5-10 nannos 8-9 dolomite 1-5 sil. unspec. tr- 5 mica (authigenic?) tr- 3 forams tr- 1 pyrite tr plauc. (SS: 1-115 cms) tr heavy mins. (zircon? in SS: 1-115 cm) CaCO ₃ % Sect. 2-92 to 94 cms 24 Sect. cc 15 CARB. BOMB: Sect. 2-92 to 94 cms 24 Sect. cc 15 COLOR LEGEND 1 = dk. grn. gy. 5Y 6/1
					2		

Explanatory notes in Chapter 1

SITE 397		HOLE A		CORE 26		CORED INTERVAL: 1210.5-1229.5 m	
AGE	ZONE		FOSSIL CHARACTER		SECTION METERS	GRAPHIC LITHOLOGY	LITHOLOGIC DESCRIPTION
	FORAMS	NANNOS	PL. FORAMS	B. FORAMS			
EARLY MIOCENE	N67 - N67	Diacocarter druggi	Rp	FC	1		MUDSTONE SS: 1-30, 45 cms 40-45% clay 20-25 quartz 10-20 forams 10 sil. unspec. (chert?) (SS: 1-30 cm) 3-10 nannos 5 carb. unspec. tr- 3 pyrite 2 feldspar tr dol. (SS: 1-45 cm) tr mica tr coltophane(?) (SS: 1-30 cm)
					2		
					3		MUDSTONE SS: 2-96 cm 80% clay 10 nannos 4 quartz 3 carb. unspec. 2 forams 1 mica *Thin-Section (1, 13-15 cm): Silicified claystone with (XRD) common opal-CT, XR-amorphous matter, calcite, and quartz.
							CaCO ₃ % C _{org} % LECO: Sect. 1- 36 cms 23 2.3 CARB. BOMB: Sect. 1- 37 to 39 cms 22 Sect. 2-103 to 105 cms 15
							COLOR LEGEND 1 = very dk. gy. brn. 10YR 3/2 2 = dk. gy. brn. 10YR 4/2 3 = gy. brn. 10YR 5/2

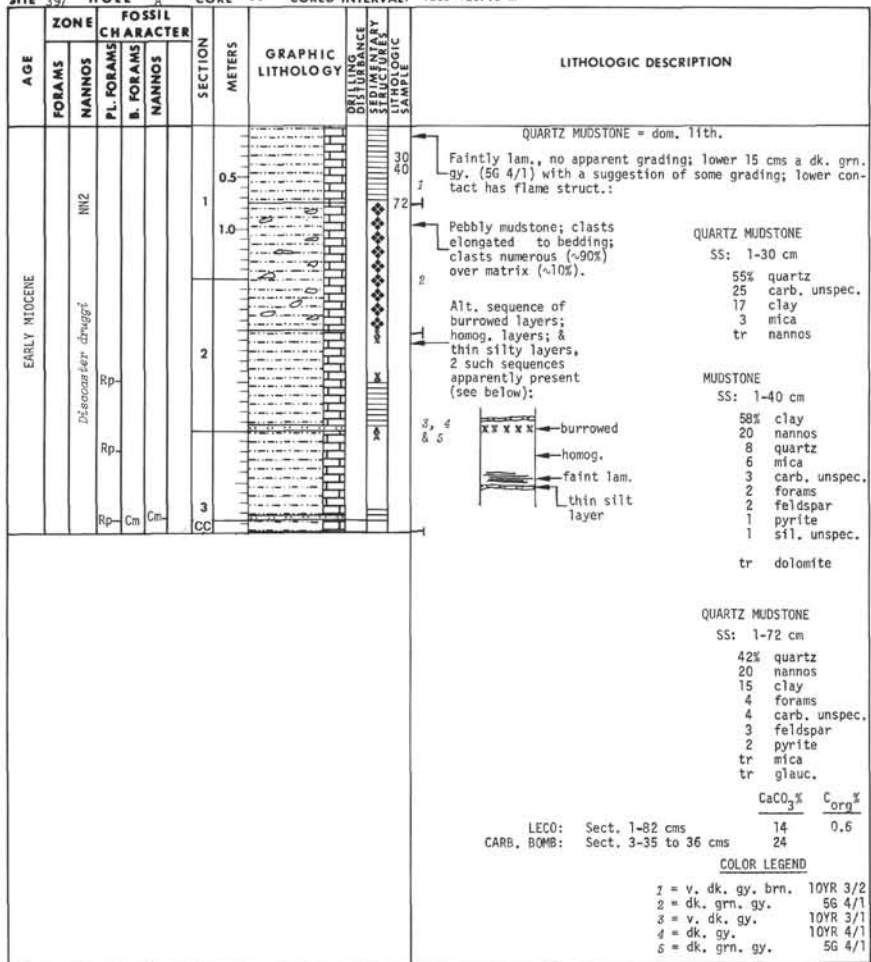
SITE 397 HOLE A CORE 27 CORED INTERVAL: 1229.5-1239 m								
AGE	ZONE		FOSSIL CHARACTER		SECTION METERS	GRAPHIC LITHOLOGY	DRILLING LOG	LITHOLOGIC DESCRIPTION
	FORAMS	NANNOS	PL. FORAMS	B. FORAMS				
EARLY MIOCENE	Dienocaster druggi	NN2	Rp	Rp	1		61	<p>PEBBLY MUDSTONE = dom. lith. Clasts def. - lenticular stretched, often to produce a migmatitic texture; sdier. portions (Sect. 1-15 to 20 cms, 64 & 78 cms), dips of vague lam. 18 to 25°.</p> <p>Matrix: CLAYSTONE</p> <p>SS: 1-61</p> <p>75% clay 15 nannos 9 carb. unspec. 4 quartz 1 pyrite tr mica</p> <p>CaCO₃% C_{org}% 15 0.7</p> <p>LECO: Sect. 1-89 cms CARB. BOMB: Sect. 2-33 to 35 cms</p> <p>COLOR LEGEND</p> <p>1 = grn. blk. 5G 2/1 2 = lt. bl. gy. 5B 7/1 3 = dk. gy. brn. 10YR 4/2 4 = dk. gy. 5Y 4/1</p>
					CC			

SITE 397 HOLE A CORE 29 CORED INTERVAL: 1248.5-1258 m								
AGE	ZONE		FOSSIL CHARACTER		SECTION METERS	GRAPHIC LITHOLOGY	DRILLING LOG	LITHOLOGIC DESCRIPTION
	FORAMS	NANNOS	PL. FORAMS	B. FORAMS				
EARLY MIOCENE	Dienocaster druggi	NN2	Rp	Rp	17		27	<p>PEBBLY MUDSTONE = dom. lith. Clasts completely streaked & distorted, clast's size range from 0.5 to 1.5 cms; opal-CT replaced rads.</p> <p>MUDSTONE (taken from both matrix & clast-SS: 1-17 & 27 cms, respectively)</p> <p>SS: 1-17, 27 cm</p> <p>64-74% clay 15-20 nannos 4-6 sil. unspec. (chert? or v. fn.-grained metaqtzite frags.) 3-6 quartz 2-4 carb. unspec. 1 pyrite (SS: 1-17 cm) 1 mica (SS: 1-17 cm) tr forams (SS: 1-27 cm) tr dolomite (SS: 1-17 cm)</p> <p>CaCO₃% 19</p> <p>CARB. BOMB: Sect. 1-40 to 42 cms 19 Sect. 1-68 to 70 cms 14</p>
					CC			

SITE 397 HOLE A CORE 28 CORED INTERVAL: 1239-1248.5 m								
AGE	ZONE		FOSSIL CHARACTER		SECTION METERS	GRAPHIC LITHOLOGY	DRILLING LOG	LITHOLOGIC DESCRIPTION
	FORAMS	NANNOS	PL. FORAMS	B. FORAMS				
EARLY MIOCENE	Dienocaster druggi	NN2	B-Rm	Rm	4		16	<p>Alt. sequence of burrowed sed. with lam. & homog. mat'l. often burrowed only in its upper portion; numerous intercalated silt & sandstone layers; dips of 22-24° in Sect. 2; silt & sd. layers 1 to 10 cms thick; colors variable: burrowed mat'l. dk. grn. gy. (5G 4/1), v. dk. gy. (10YR 3/1) wht. more homog. non-burrowed portions dk. brn. (10YR 3/3) to v. dk. gy. (10YR 3/1); in gen. the sed. is a:</p> <p>CLAYSTONE CALCAREOUS MUDSTONE (homog. sequence)</p> <p>SS: 1-4 cm SS: 2-116 cm</p> <p>88% clay 28% clay 10 nannos 18 quartz 2 quartz 10 nannos tr carb. unspec. 10 dolomite tr mica 10 carb. unspec. tr pyrite 3 feldspar tr sponge spics. 1 mica tr pyrite</p> <p>CaCO₃% C_{org}% 10 0.3</p> <p>LECO: Sect. 1-137 cms CARB. BOMB: Sect. 1- 80 to 82 cms</p>
					CC			

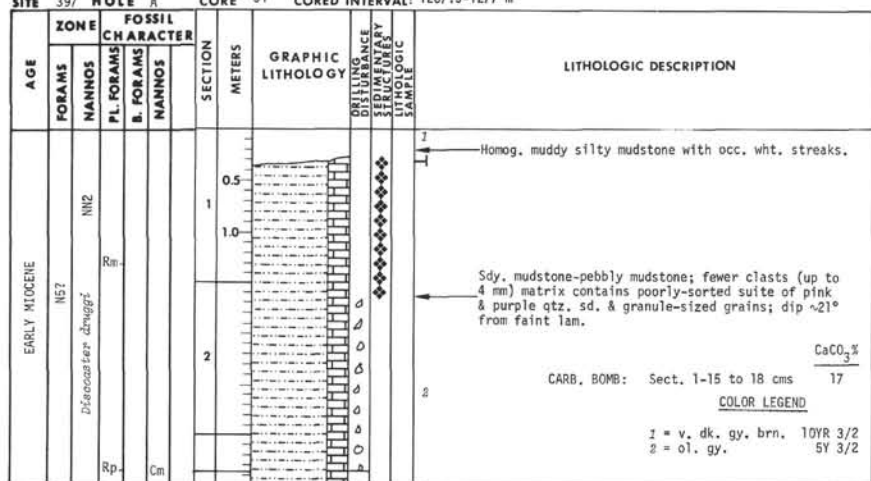
Explanatory notes in Chapter 1

SITE 397 HOLE A CORE 30 CORED INTERVAL: 1258-1267.5 m



Explanatory notes in Chapter 1

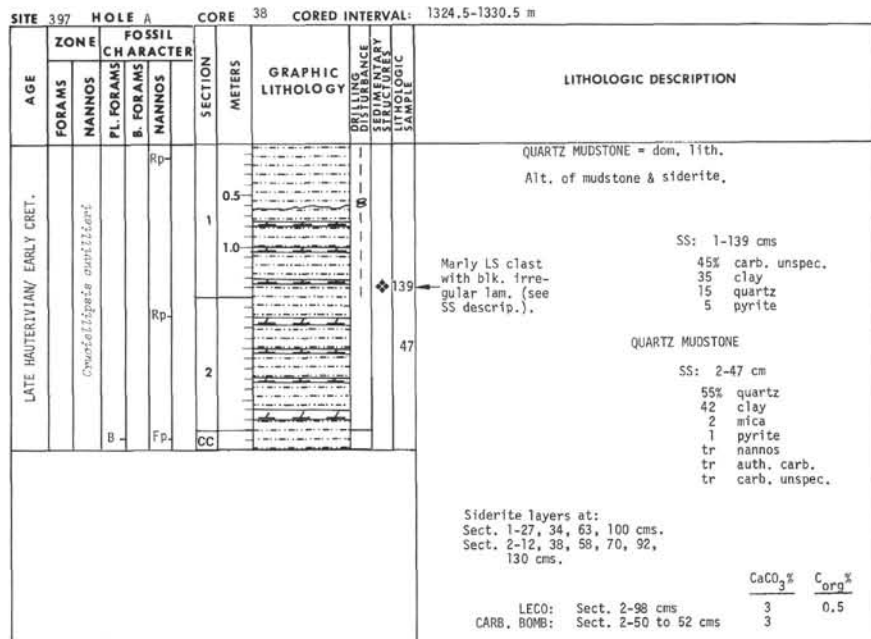
SITE 397 HOLE A CORE 31 CORED INTERVAL: 1267.5-1277 m



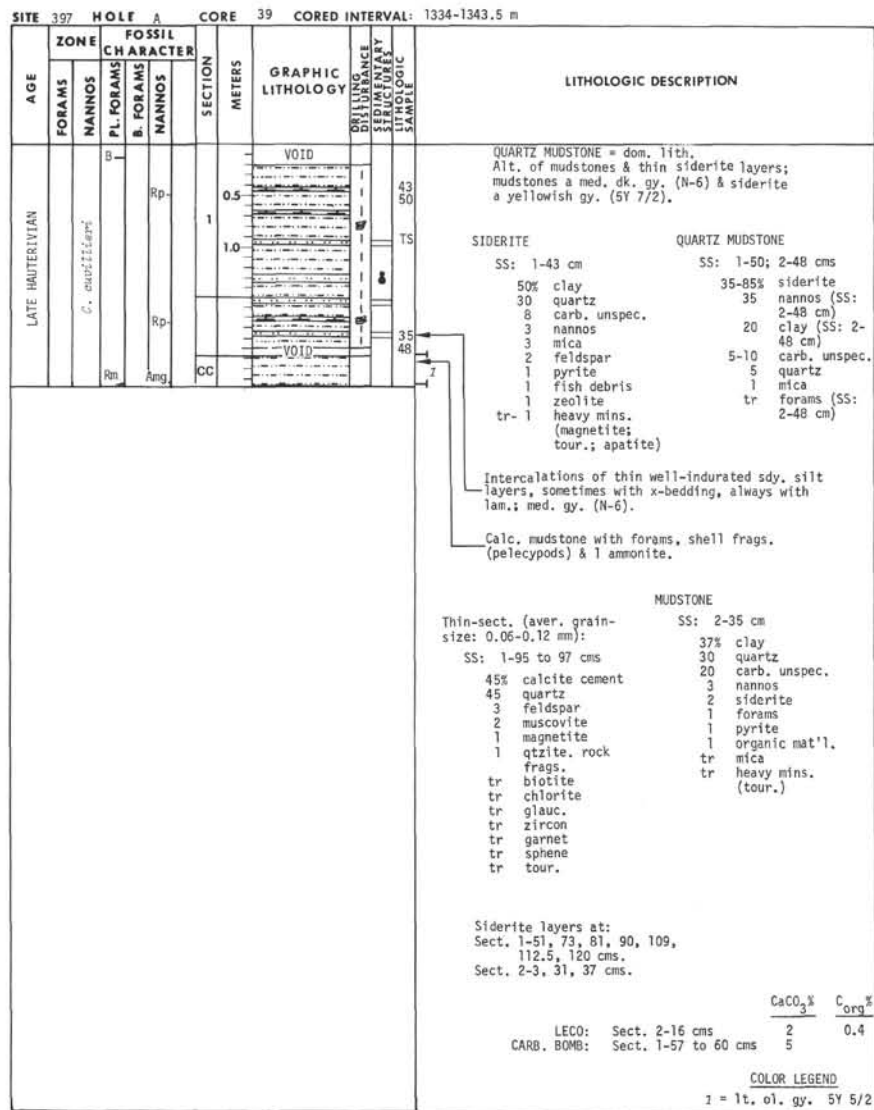
SITE 397		HOLE A		CORE 32		CORED INTERVAL: 1277-1286.5 m		
AGE	ZONE		FOSSIL CHARACTER		SECTION	METERS	GRAPHIC LITHOLOGY	LITHOLOGIC DESCRIPTION
	FORAMS	NANNOS	PL. FORAMS	B. NANNOS				
EARLY MIOCENE						0.5	VOID	PEBBLY MUDSTONE = dom. lith. Clasts of shale & mudstone; numerous qtz. granules; no apparent dip.
						1.0		
						2		Calc. mudstone
						CC		Mudstone; lam.; upper portion a ol. gy. (5Y 3/2); 27° dip; lower 25 cm inversely then normally graded with opal-CT replaced rads and clinoptilolite-filled forams.
								<p>DRILLING DISTURBANCE</p> <p>SEDIMENTARY LITHOLOGIC SAMPLE</p> <p>70</p> <p>103</p>
								<p>CALCAREOUS MUDSTONE</p> <p>SS: cc</p> <p>22% clay</p> <p>20 forams</p> <p>20 quartz</p> <p>15 nannos</p> <p>15 carb. unspec.</p> <p>3 glauc.</p> <p>3 pyrite</p> <p>1 zeolite</p> <p>1 heavy mins. (magnetite; tour.)</p> <p>CaCO₃% C_{org}%</p> <p>LECO: Sect. 2- 55 cms 5 0.7</p> <p>CARB. BOMB: Sect. 1-100 to 102 cms 4</p> <p>Sect. 2- 65 to 67 cms 6</p> <p>COLOR LEGEND</p> <p>1 = grn. blk. 5G 2/1</p> <p>2 = dk. grn. gy. 5G 4/1</p> <p>3 = grn. ol. 10Y 4/2</p>

Explanatory notes in Chapter 1

SITE 397		HOLE A		CORE 33		CORED INTERVAL: 1286.5-1296 m		
AGE	ZONE		FOSSIL CHARACTER		SECTION	METERS	GRAPHIC LITHOLOGY	LITHOLOGIC DESCRIPTION
	FORAMS	NANNOS	PL. FORAMS	B. NANNOS				
EARLY MIOCENE						0.5		PEBBLY MUDSTONE = dom. lith. Clasts stretched, streaked, smeared, pulled apart (boudinage), imbrication suggests 20° dip; 110-120 cms (Sect. 1) burrowed (part of a large clast?).
						1.0		
						CC		<p>Matrix: MUDSTONE</p> <p>SS: 1-70, 103 cms</p> <p>40-55% clay</p> <p>30-40 quartz</p> <p>5 nannos</p> <p>5 carb. unspec.</p> <p>2-3 forams</p> <p>2 opal(?) SS: 1-103 cm</p> <p>tr-2 feldspar</p> <p>1 pyrite</p> <p>tr-1 dolomite</p> <p>tr-1 glauc.</p> <p>tr heavy mins. (magnetite; zircon - SS: 1-70 cm - tour.)</p> <p>COLOR LEGEND</p> <p>1 = med. bl. gy. 5B 5/1</p>



Explanatory notes in Chapter 1



SITE 397 HOLE A		CORE 40		CORED INTERVAL: 1343.5-1353 m		
AGE	FOSSIL CHARACTER		SECTION	METERS	GRAPHIC LITHOLOGY	LITHOLOGIC DESCRIPTION
	FORAMS	NANNOS				
LATE HAUTERIVIAN	C. <i>Quartzifera</i>	Fcp	1	0.5		QUARTZ MUDSTONE = dom. lith. Alt. series of mudstones & siderites, the ol. gy. (5Y 3/2) to brn. gy. (5YR 4/1) mudstone contain numerous mm thick lam. of clay & silt-sized sed., the latter have sharp contacts; lam. are the same color; the dolomites also contain numerous 1 mm thick lam., which are also the same yellowish gy. color (5Y 7/2) as the siderites.
			2	1.0		QUARTZ MUDSTONE SS: 1-19; 2-32; 3-13 cms 38-50% clay 30-40 quartz 5-8 mica 3-5 carb. unspec. 1-5 fish debris 1-5 organic mat'l. 3 nannos (SS: 1-19; 3-13 cm) 2 feldspar (SS: 1-19; 3-13 cm) 1 forams (SS: 3-13 cm) 1 heavy mins. (tour.) 1 magnetite 1 glauc. (SS: 2-32; 3-13 cm) 1 pyrite (SS: 2-32; 3-13 cm) tr zeolite (SS: 1-19; 3-13 cm)
		B. Rp.	CC			SIDERITE SS: 2-18, 102 cms 83-87% siderite 10 clay 3-5 quartz 1 mica (SS: 2-18 cm)
						Siderite layers at: Sect. 1-28, 47, 72, 83, 108, 119 cms. Sect. 2-5, 19, 22, 67, 102, 103, 114, 117, 123, 139, 147 cms. Sect. 3-3, 6 cms.
						CaCO ₃ % C _{org} % LECO: Sect. 2-59 cms 4 0.6 CARB. BOMB: Sect. 2-42 to 44 cms 6

Explanatory notes in Chapter 1

SITE 397 HOLE A		CORE 41		CORED INTERVAL: 1353-1362.5 m		
AGE	FOSSIL CHARACTER		SECTION	METERS	GRAPHIC LITHOLOGY	LITHOLOGIC DESCRIPTION
	FORAMS	NANNOS				
LATE HAUTERIVIAN	C. <i>Quartzifera</i>	FC	1	0.5		CLAYSTONE = dom. lith. As described in prev. core - alt. sequence of claystones & siderites (sideritic claystone) both with numerous small lam.; portions here are burrowed, burrows are flattened.
			2	1.0		CLAYSTONE SS: 2-108; 3-15 cms 90-92% clay 3-5 carb. unspec. 2-5 pyrite 2 quartz tr-1 nannos tr dolomite (SS: 3-15 cm) tr vol. glass (SS: 3-15 cm) tr fish debris
		Rm CA	CC			SIDERITIC MUDSTONE SS: 2-97 cm 59% clay 40 siderite 1 quartz tr carb. unspec. tr pyrite
						Siderite layers (sideritic mudstone) at: Sect. 1-11, 35, 56, 95, 121 cms. Sect. 2-10, 64-66, 93-98 cms.
						CaCO ₃ % C _{org} % LECO: Sect. 2-81 cms 8 0.4 CARB. BOMB: Sect. 2-48 to 50 cms 5
						COLOR LEGEND 1 = grn. gy. 5GY 5/1 2 = grn. gy. 5GY 6/1

SITE 397 HOLE A CORE 42 CORED INTERVAL: 1362.5-1372 m											
AGE	ZONE CHARACTER				SECTION	METERS	GRAPHIC LITHOLOGY	DRILLING DISTURBANCE	SEDIMENTARY STRUCTURE	LITHOLOGIC SAMPLE	LITHOLOGIC DESCRIPTION
	FORAMS	NANNOS	PL. FORAMS	B. FORAMS							
LATE HAUTERIVIAN				Fp	1	0.5					QUARTZ MUDSTONE = dom. lith. Alt. sequence prev. described; siderite & mudstones both containing numerous v. thin (<1 mm) lam.:
				Fcm	1	1.0					QUARTZ MUDSTONE
				Rp	2					88	SS: 2-88, 110 cms 45-75% clay 20-50 quartz 4 siderite (SS: 2-88 cm) tr- 3 carb. unspec. 1- 2 pyrite tr nannos tr fish debris
				Rp	CC					110	Siderite layers at: Sect. 1-87, 88 cms. Sect. 2-44, 114 cms.
											CaCO ₃ % 45 C _{org} % 0.5
											LECO: Sect. 2-114 cms CARB. BOMB: Sect. 1- 27 to 30 cms

SITE 397 HOLE A CORE 44 CORED INTERVAL: 1381.5-1384.5 m											
AGE	ZONE CHARACTER				SECTION	METERS	GRAPHIC LITHOLOGY	DRILLING DISTURBANCE	SEDIMENTARY STRUCTURE	LITHOLOGIC SAMPLE	LITHOLOGIC DESCRIPTION
	FORAMS	NANNOS	PL. FORAMS	B. FORAMS							
LATE HAUTERIVIAN				Rp	1	0.5					QUARTZ MUDSTONE = dom. lith. Alt. mudstones & siderites.
				Rp	1	1.0					QUARTZ MUDSTONE
				Rp	2					60	SS: 1-60; 2-24 cms 53-69% clay 30-45 quartz 1 pyrite (SS: 2-24 cm) tr- 1 carb. unspec. tr- 1 fish debris tr nannos tr siderite tr plant debris (SS: 2-24 cm)
				Rp	CC					24	Siderite layers at: Sect. 2-34, 43 cms.
											CaCO ₃ % 1 C _{org} % 0.7
											LECO: Sect. 2-65 cms CARB. BOMB: Sect. 1-24 to 27 cms
											COLOR LEGEND 1 = med. gy. brn. 5Y 4/2 2 = med. gy. brn. 5Y 3/2

SITE 397 HOLE A CORE 43 CORED INTERVAL: 1372-1381.5 m											
AGE	ZONE CHARACTER				SECTION	METERS	GRAPHIC LITHOLOGY	DRILLING DISTURBANCE	SEDIMENTARY STRUCTURE	LITHOLOGIC SAMPLE	LITHOLOGIC DESCRIPTION
	FORAMS	NANNOS	PL. FORAMS	B. FORAMS							
LATE HAUTERIVIAN				Rp	1	0.5					1 & 2 QUARTZ MUDSTONE = dom. lith. Alt. sequence of mudstones & siderites. Only occ. lam.
				Rp	1	1.0				70	DOLOMITE
				Rp	2					75	QUARTZ MUDSTONE
				Rp	2						VOID
				Rp	CC					20	SS: 1-70 cm 90% siderite 10 clay tr pyrite tr fish debris
											SS: 1-75; 2-20 cms 55-59% clay 30-35 quartz 3 mica (SS: 3-20 cm) tr- 2 nannos tr- 2 carb. unspec. 1 feldspar (SS: 3-20 cm) 1 pyrite tr- 1 fish debris tr glauc. (SS: 3-20 cm) tr organic mat'l. (SS: 3-20 cm) tr zeolite (SS: 3-20 cm) tr heavy mins. (SS: 3-20 cm) tour.; apatite; zircon.
											Siderite layers at: Sect. 1-11, 26, 70 cms. Sect. 2-16, 54, 75, 120 cms.
											COLOR LEGEND 1 = wht. 5Y 8/1 2 = dk. ol. gy. 5Y 3/2

Explanatory notes in Chapter 1

SITE 397 HOLE A		CORE 45		CORED INTERVAL: 1384.5-1391 m		
AGE	FOSSIL CHARACTER		SECTION	METERS	GRAPHIC LITHOLOGY	LITHOLOGIC DESCRIPTION
	FORAMS	MANNOS				
LATE HAUTERIVIAN						MUDSTONE = dom. lith. Alt. of mudstones & siderites, except once again both contain numerous thin lam.
				0.5		
				1.0		MUDSTONE SS: 1-40; 2-26 cms 60-68% clay 25-30 quartz 3-5 mica tr-3 fish debris tr-3 organic mat'l. 1 nannos tr-1 carb. unspec. tr-1 siderite tr-1 glauc. tr-1 pyrite tr forams (SS: 2-26 cm) tr heavy mins. (apatite; tour.) tr zeolite (SS: 1-40 cm)
				2		
						Siderite layers at: Sect. 1-13, 29, 37, 52, 56, 61, 71, 90, 125, 136 cms. Sect. 2-7, 8, 18, 25, 43, 78, 101, 126, 131 cms. Sect. 3-9, 14, 21, 33, 43, 53, 60 cms.
						CaCO ₃ % C _{org} % LECO: Sect. 1-72 cms 2 0.7 Sect. 2-45 cms 1 0.7
						COLOR LEGEND 1 = lt. gy. 5Y 7/2 2 = gy. N-5

Explanatory notes in Chapter 1

SITE 397 HOLE A		CORE 46		CORED INTERVAL: 1391-1400.5 m		
AGE	FOSSIL CHARACTER		SECTION	METERS	GRAPHIC LITHOLOGY	LITHOLOGIC DESCRIPTION
	FORAMS	MANNOS				
LATE HAUTERIVIAN						MUDSTONE & NANNO MARLSTONE = dom. lith. Alt. sequence of mudstone & siderite, siderite layers 2-10 mm thick with one (Sect. 1-74 cms) having graded siderite clasts (?); both sed. types have numerous lam.
				0.5		
				1.0		SIDERITE SS: 1-67 cm 95% siderite 3 quartz 1 carb. unspec. 1 fish debris
				2		MUDSTONE SS: 2-59 cm 55% clay 25 quartz 5 mica 5 fish debris 3 carb. unspec. 3 organic mat'l. 2 pyrite 1 nannos 1 feldspar 1 heavy mins. (magnetite; tour.)
						Changing to a mudstone with more dolomite; also with 1 ammonite: MUDSTONE SS: 2-60 cm 57% clay 25 siderite 10 nannos 3 quartz 2 carb. unspec. 1 pyrite 1 fish debris 1 organic mat'l. tr mica tr heavy mins. (tour.)
						Then changing to a sequence of 0.5-2 cms thick claystone layers in a: CALCAREOUS MUDSTONE SS: 3-20 cm 55% clay 30 nannos 5 siderite 3 carb. unspec. 3 mica 3 pyrite 1 quartz tr fish debris
						Then becoming more calc. with "specks" of Nannococcus, more x-bedding Sect. 4-2 to 4 cms. NANNO MARLSTONE SS: 4-85 cm 45% clay 25 nannos 20 dolomite 5 mica 3 carb. unspec. 1 quartz 1 pyrite tr fish debris
						Thin-sect.: SS: 1-7 to 10 cms 76% siderite (avg. grain-size <5µm) 16 clay mins. 5 quartz (avg. grain-size ~0.05 mm) 3 calcite tr muscovite tr magnetite tr fish debris
						Yellow-gy. calc. mudstone layers at: Sect. 4-43 & 75 cms. Siderite layers at: Sect. 1-23, 28, 30, 39, 57, 68, 74, 88, 99, 108, 112 cms. Claystone layers at: Sect. 3-13 to 15; 32 to 34; 53; 78 to 81 cms. Sect. 2-22, 27, 36, 42, 61, 71, 85, 122 cms. Sect. 4-75 cms.
						X-bedding between: Sect. 3-86 to 90 cms. CaCO ₃ % C _{org} % LECO: Sect. 3-100 cms 12 0.5 CARB. BOMB: Sect. 3- 83 to 85 cms 22
						COLOR LEGEND 1 = med. bl. gy. 5B 5/1 2 = dk. gm. gy. 6GY 4/1

SITE 397 HOLE A		CORE 47		CORED INTERVAL: 1400.5-1410 m	
AGE	FOSSIL CHARACTER		SECTION METERS	GRAPHIC LITHOLOGY	LITHOLOGIC DESCRIPTION
	FORAMS	NANNOS			
LATE HAUTERIVIAN			0.5		MUDSTONE = dom. lith. Alt. of mudstone, nanno marlstone, & siderite; numerous v. fn. lam., varve-like (e. g. 1-12 cms, 2, has 9 varve couplets) with individual Sect. lam. 40.25-0.50 cm thick; small Helminthoid burrows mainly in more clay-rich lam. so that lam. texture is not disturbed; some siltier intervals.
			1		
			2		
			3		
			46		LIMESTONE SS: 4-46 cm 85% carb. unspec. 10 clay 4 siderite 1 pyrite tr mica
					Siderite layers at: Sect. 1-142 cms. Sect. 2-12, 40, 55, 68, 81, 84, 95, 149 cms. Sect. 3-51, 52, 53, 74, 86, 94, 95, 96, 126, 127, 128 cms.
					LECO: Sect. 1-54 cms 44 0.4 CARB. BOMB: Sect. 1-22 to 24 cms 6

Explanatory notes in Chapter 1

i = dk. grn. gy. 56 4/1

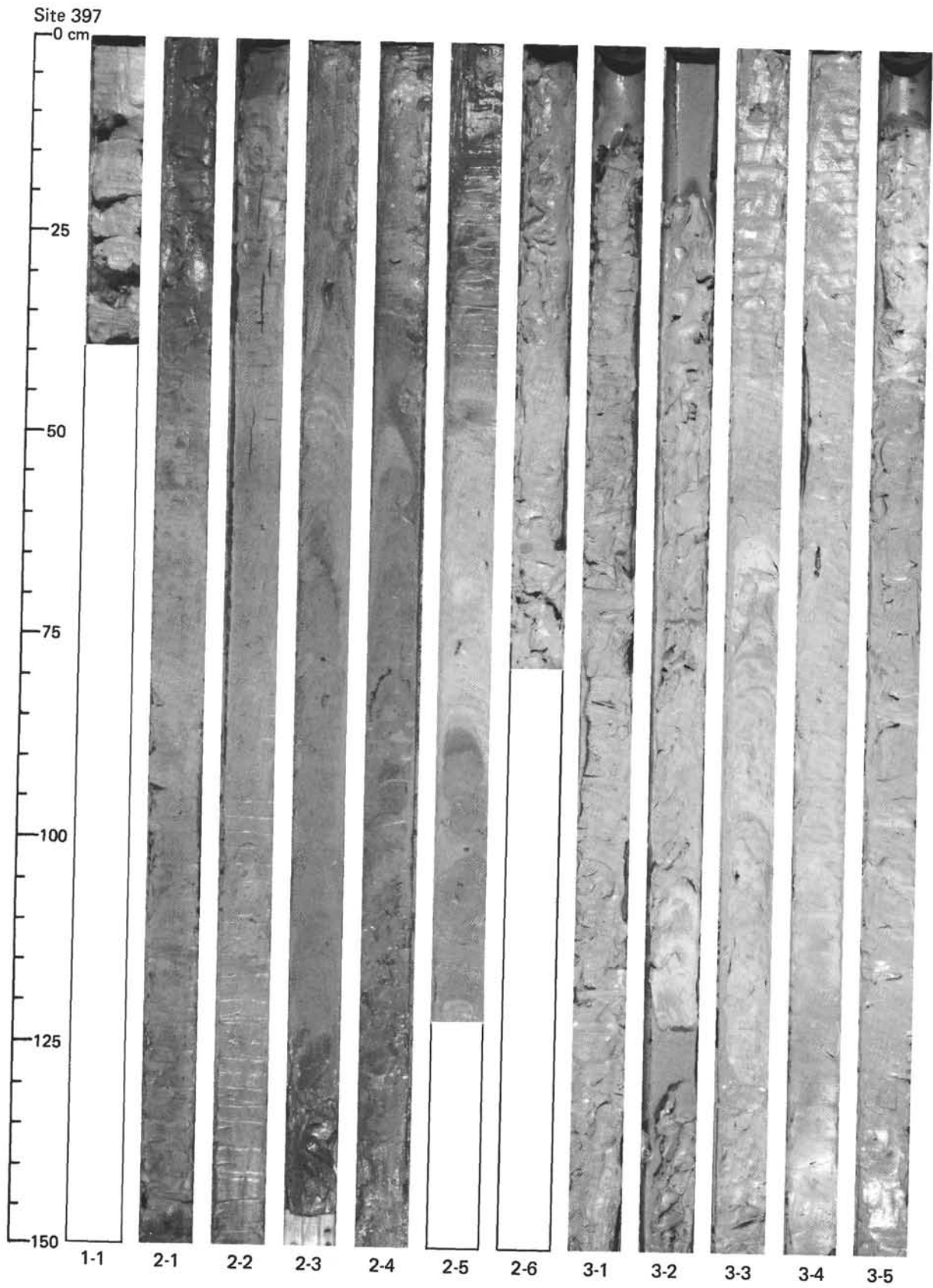
SITE 397 HOLE A		CORE 48		CORED INTERVAL: 1410-1419.5 m	
AGE	FOSSIL CHARACTER		SECTION METERS	GRAPHIC LITHOLOGY	LITHOLOGIC DESCRIPTION
	FORAMS	NANNOS			
LATE HAUTERIVIAN			0.5		MUDSTONE = dom. lith. Mudstones & siderite sequences; lam. as described for C.47, but here with less intense burrowing; siltier layers Sect. 1-24 to 26, 49, 89, 114 cms; Sect. 2-24 to 26, 56 to 58, 85 to 88 cms. Entire sequence is bioturbated.
			1		
			2		
			CC		
					Siderite layers at: Sect. 1-24, 25, 26, 49, 89, 114 cms. Sect. 2-24, 25, 26, 56, 57, 58, 85, 86, 87, 88 cms.
					LECO: Sect. 2- 4 cms 3 CARB. BOMB: Sect. 1-101 to 103 cms 7

CaCO₃% C_{org}%

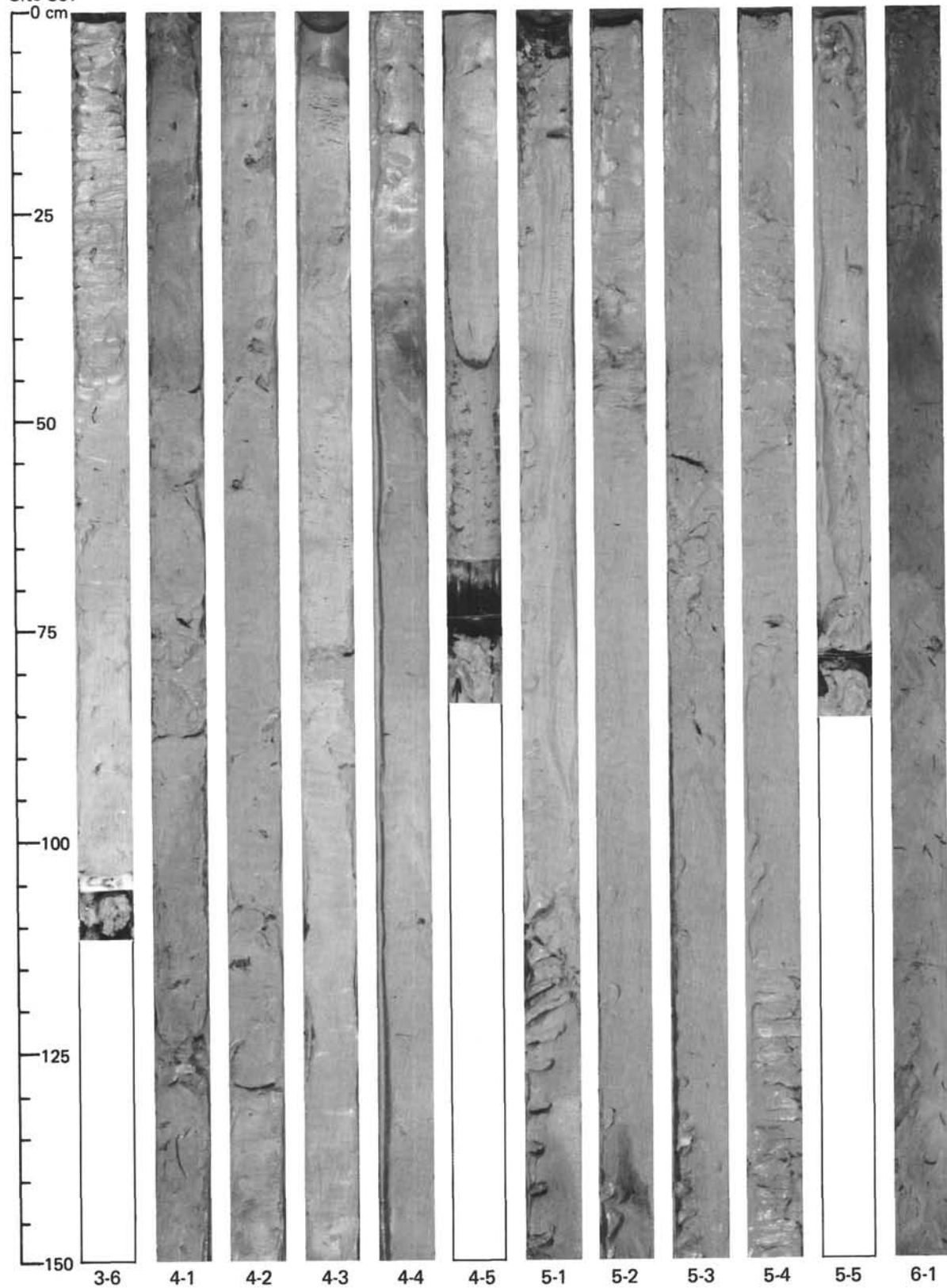
SITE 397		HOLE A		CORE 49		CORED INTERVAL: 1419.5-1429 m		
AGE	ZONE		FOSSIL CHARACTER		SECTION	METERS	GRAPHIC LITHOLOGY	LITHOLOGIC DESCRIPTION
	FORAMS	NANNOS	PL. FORAMS	B. FORAMS				
LATE HAUTERIVIAN			<i>Chuaritesipate nobilitiensis</i>			0.5 1.0	Fm Cm	MUDSTONE = dom. lith. Alt. sequence of mudstone (med. dk. gy., N-6) & siderites (lt. brn. gy., 5YR 6/1); siderite sequences occur as thin layers (mm-thick); mudstones are also lam. with lam. thicknesses to 3 mm often containing yellowish spots of siderite; siderite lam. at Sect. 1-37, 89, 117 cms; Sect. 2-9, 18, 46, 68, 76 to 84, 91, 101, 109 cms; blk. lam. 0.5 mm thick occur in Sect. 1-121 and 135 cms; piece of wood debris found in Sect. 2-53 cms.
								2
								Lt. brn.-gy.: SIDERITE SS: 2-19 cm 96% siderite 3 quartz tr-1 fish debris tr heavy mins. (magnetite)
								Yellowish speck: SIDERITE SS: 2-62 cm 70% siderite 20 clay 5 nannos 3 mica 2 carb. unspec. 1 quartz 1 fish debris tr heavy mins. (tour.) CaCO ₃ % 8 C _{org} % 0.6 LECO: Sect. 2-87 cms
								VOID

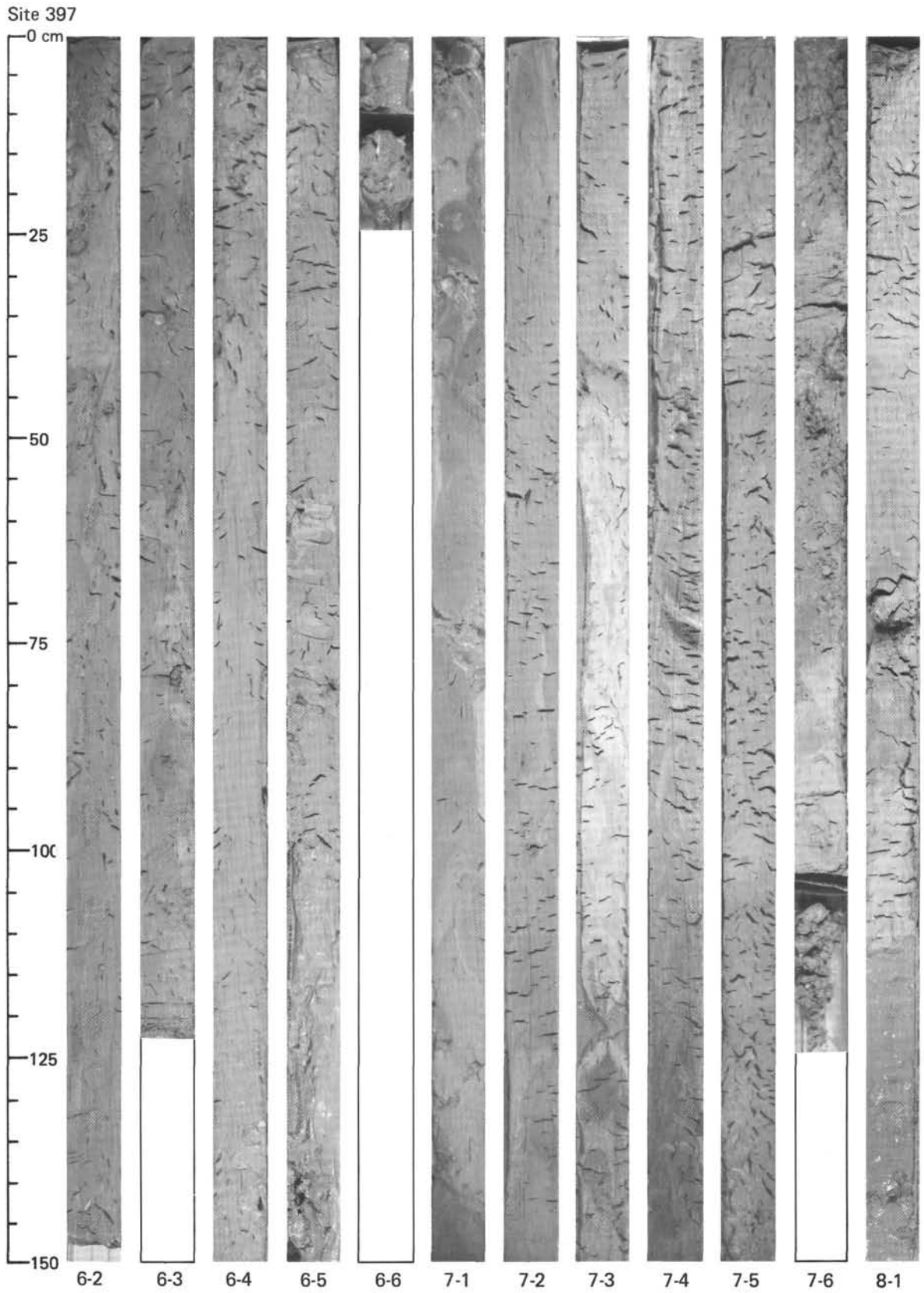
Explanatory notes in Chapter 1

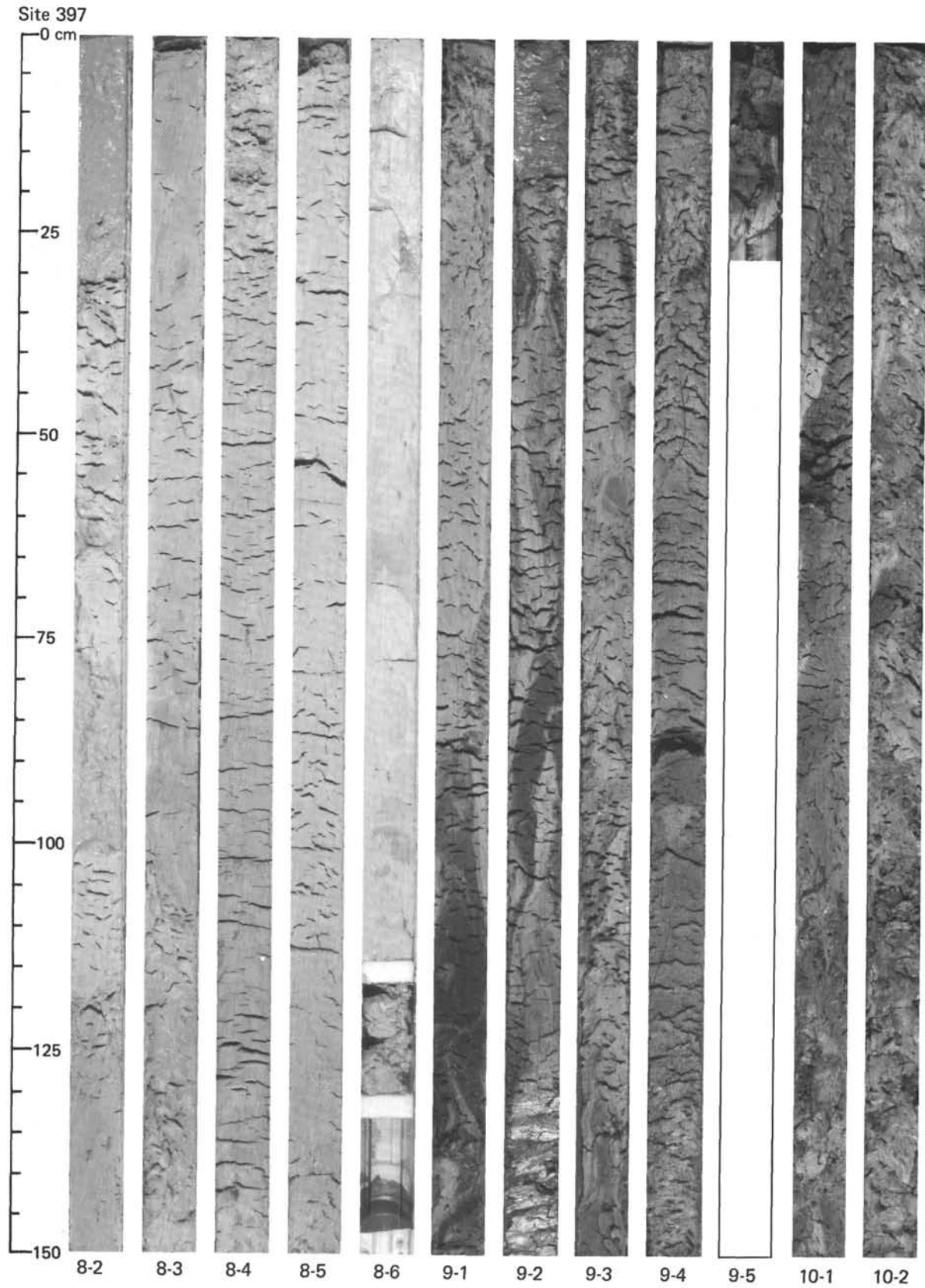
SITE 397		HOLE A		CORE 50		CORED INTERVAL: 1429-1438.5 m		
AGE	ZONE		FOSSIL CHARACTER		SECTION	METERS	GRAPHIC LITHOLOGY	LITHOLOGIC DESCRIPTION
	FORAMS	NANNOS	PL. FORAMS	B. FORAMS				
LATE HAUTERIVIAN			<i>Chuaritesipate nobilitiensis</i>			0.5 1.0	Rp Rp	QUARTZ MUDSTONE = dom. lith. Gen. a mudstone with deformation struct. (slumps, folds) and isolated clasts of sed.; parts are lam.
								2
								Large nodule: SIDERITE SS: 1-34 cm 97% siderite 2 quartz 1 plant debris tr pyrite
								Homog. portion: SIDERITIC QUARTZ MUDSTONE SS: 5-10 cm 37% clay 30 dolomite 30 quartz 1 mica 1 pyrite 1 fish debris tr heavy mins. (tour.; zircon)
								CaCO ₃ % 13 C _{org} % 0.6 LECO: Sect. 5-11 cms CARB. BOMB: Sect. 2-29 to 31 cms
								COLOR LEGEND 1 = ol. blk. 5Y 3/1 2 = dk. ol. gy. 5Y 4/1 3 = gy. ol. 10YR 7/4 4 = dk. gy. N-3

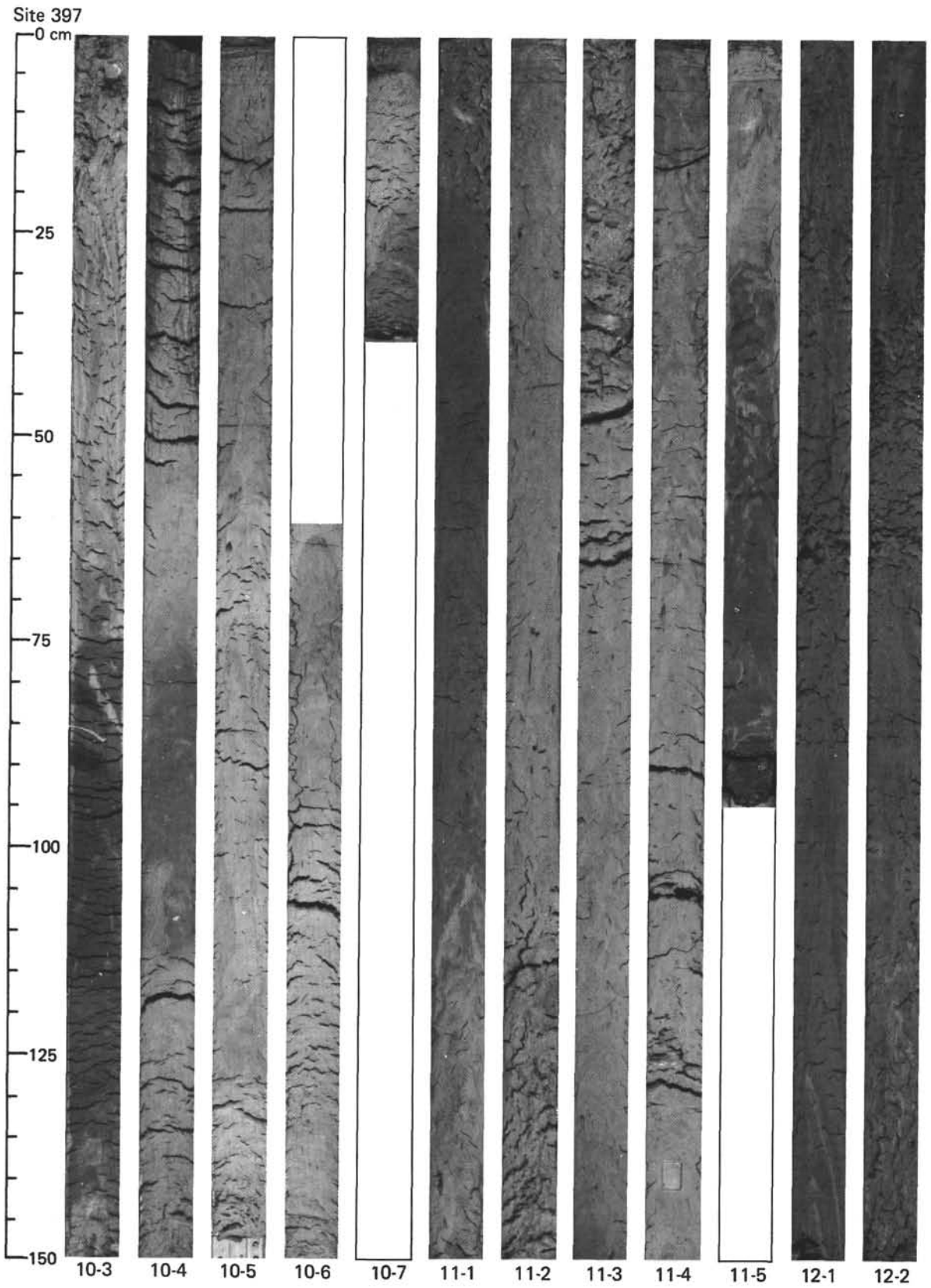


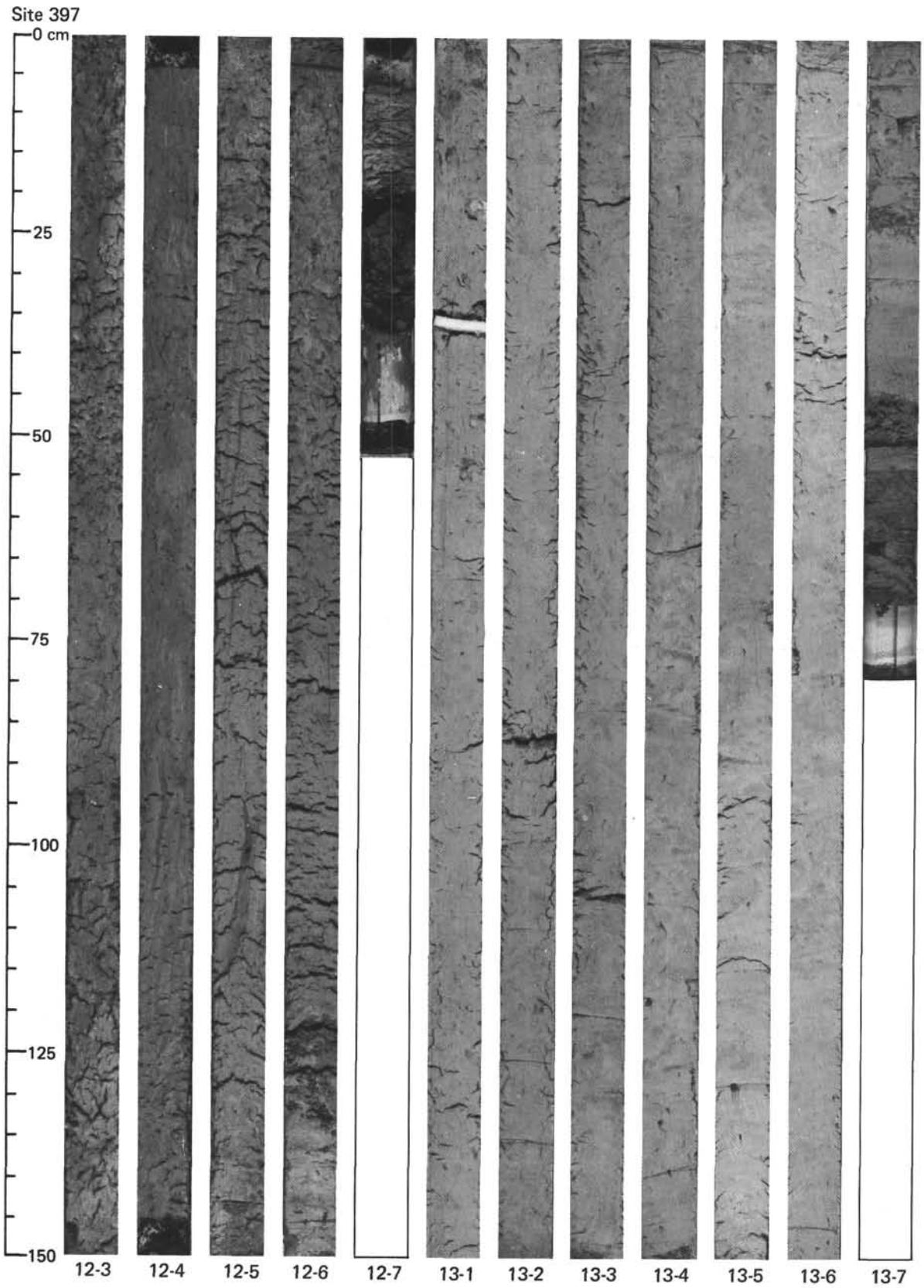
Site 397

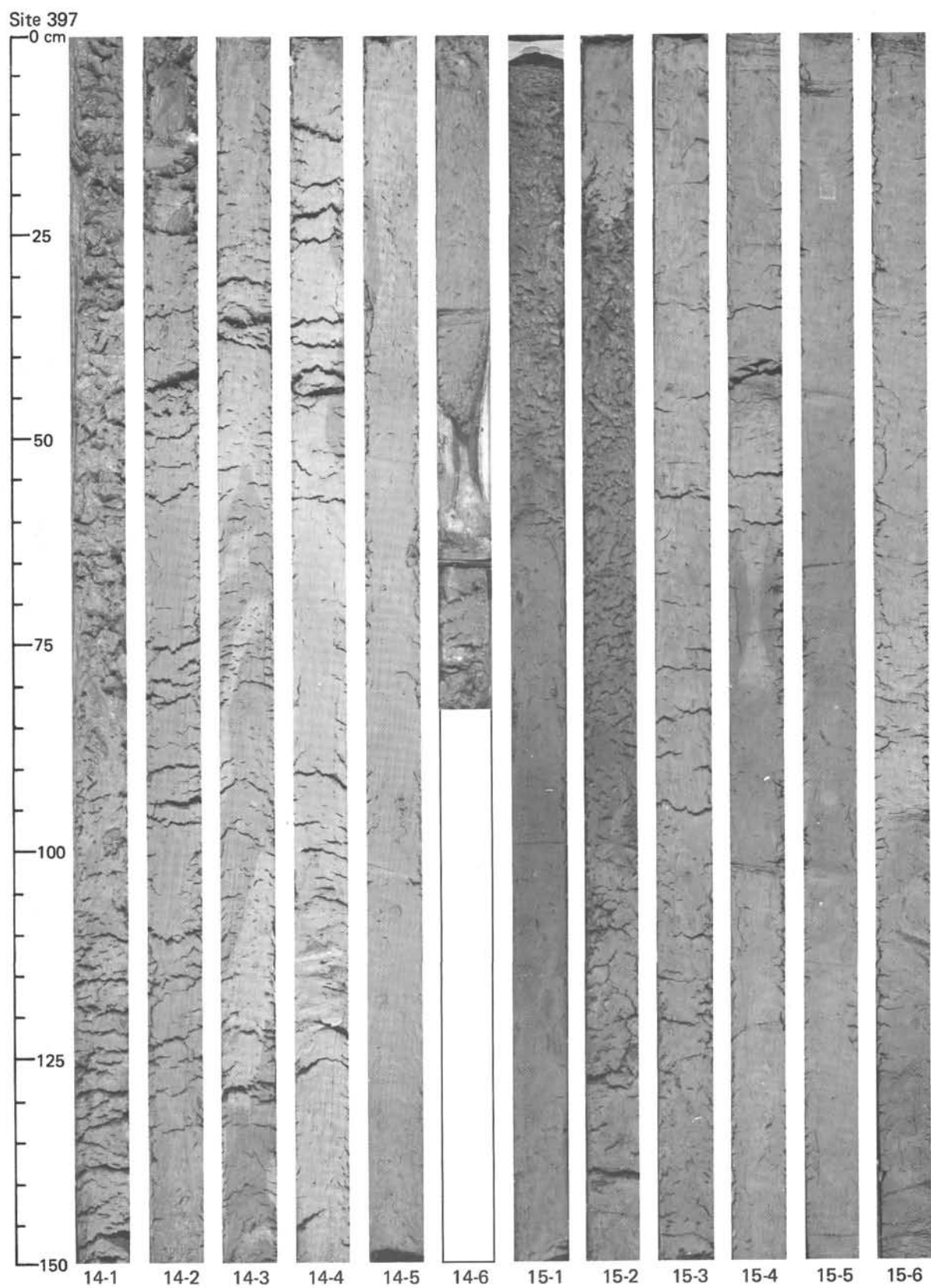




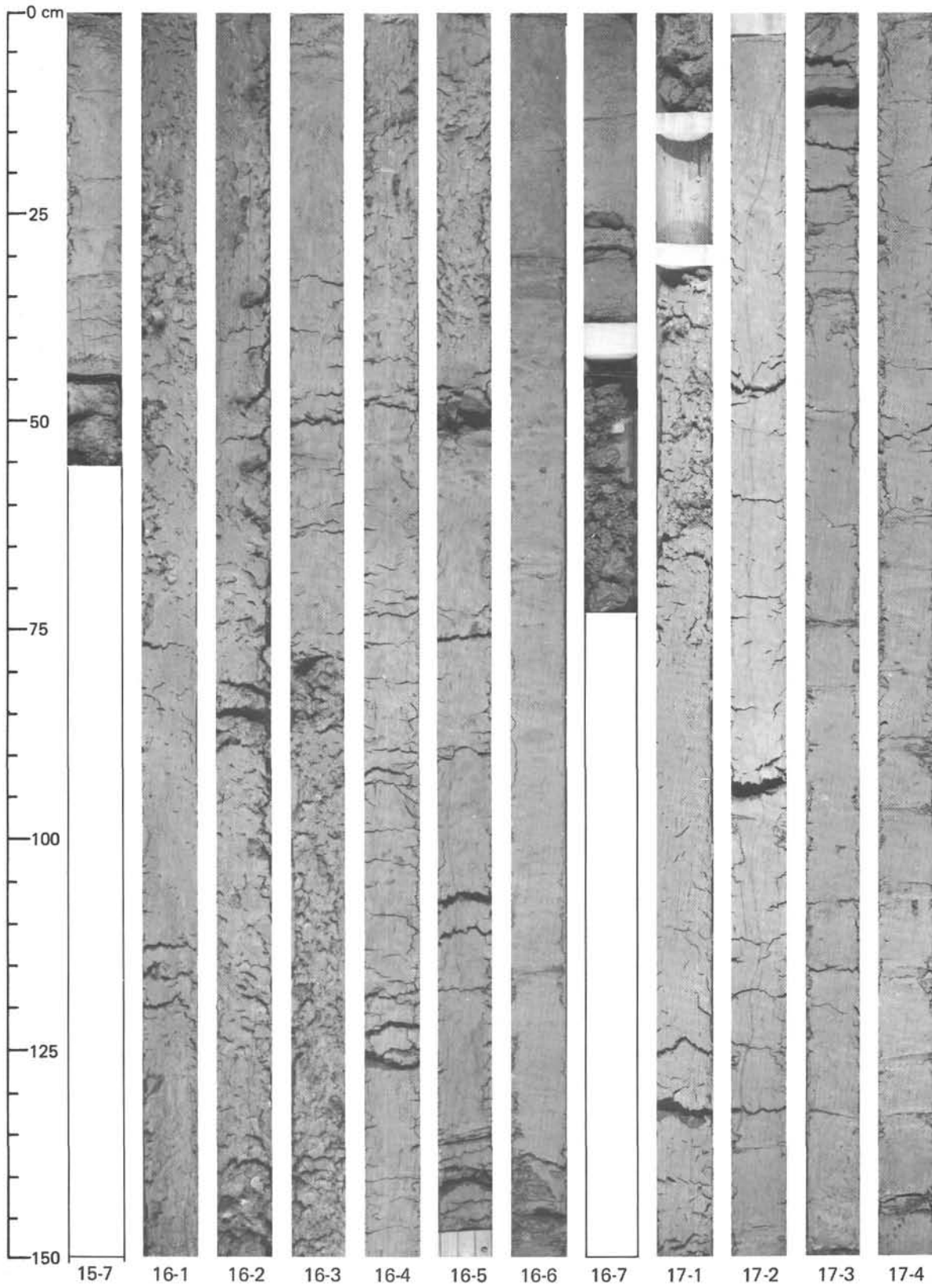


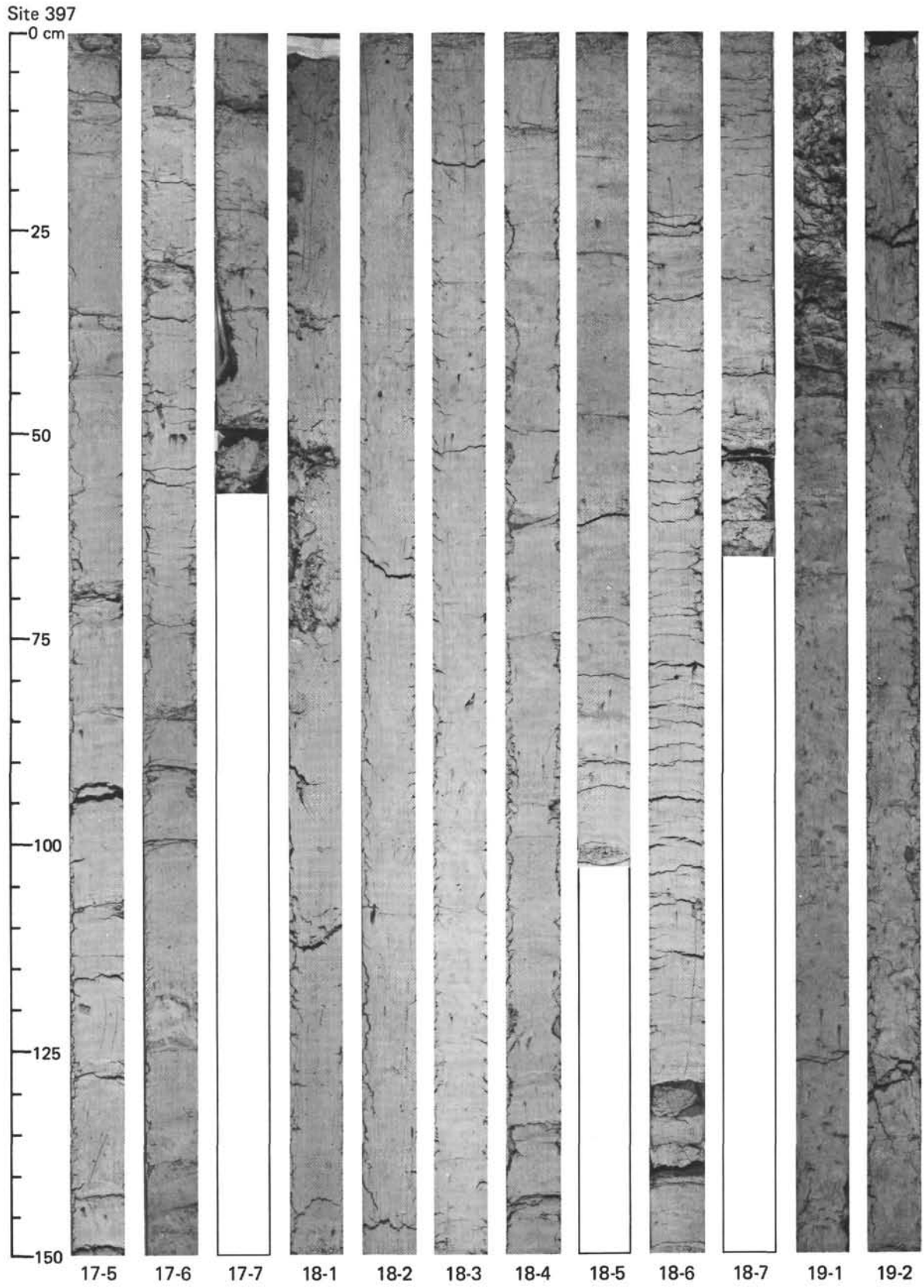


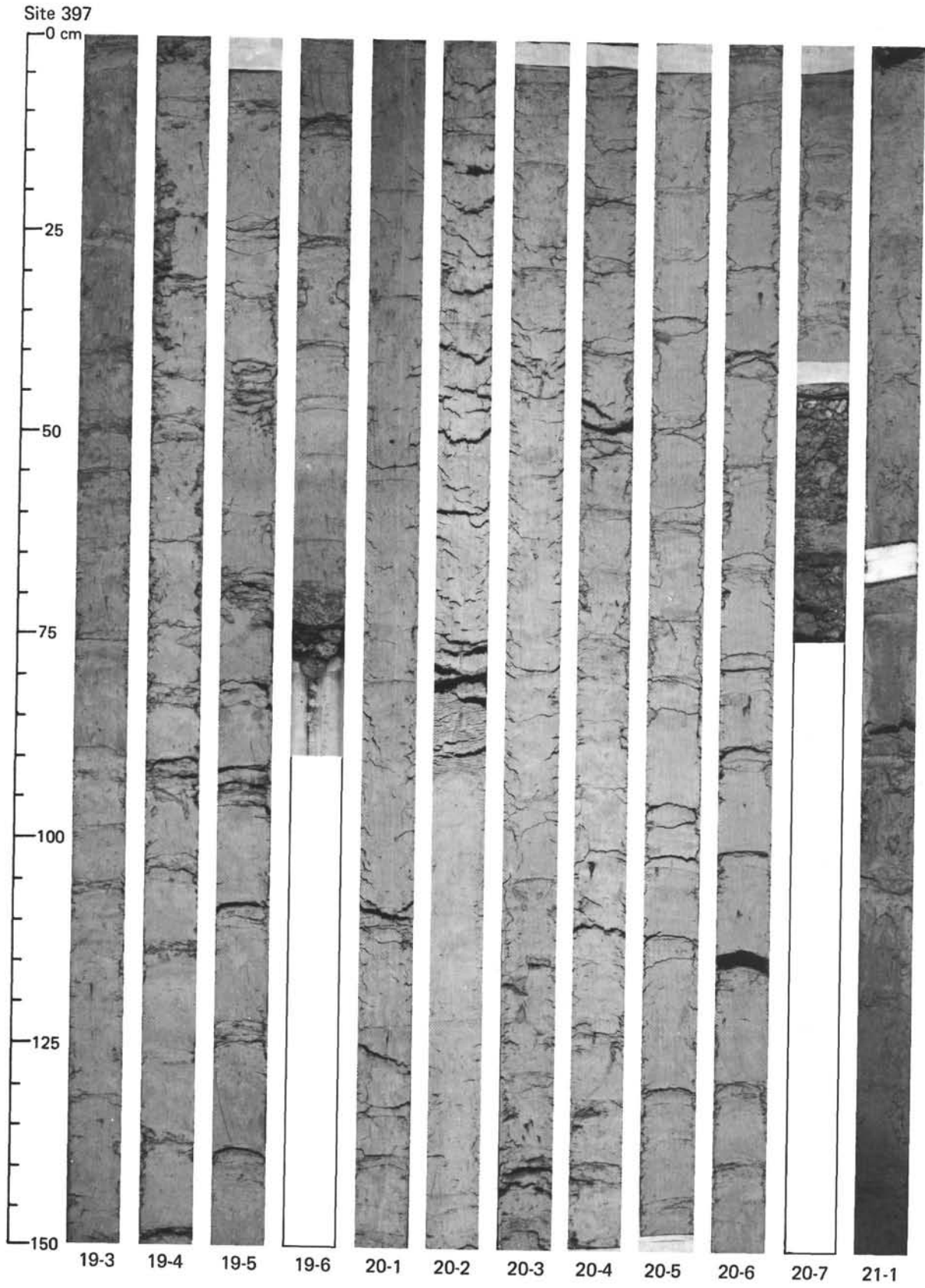


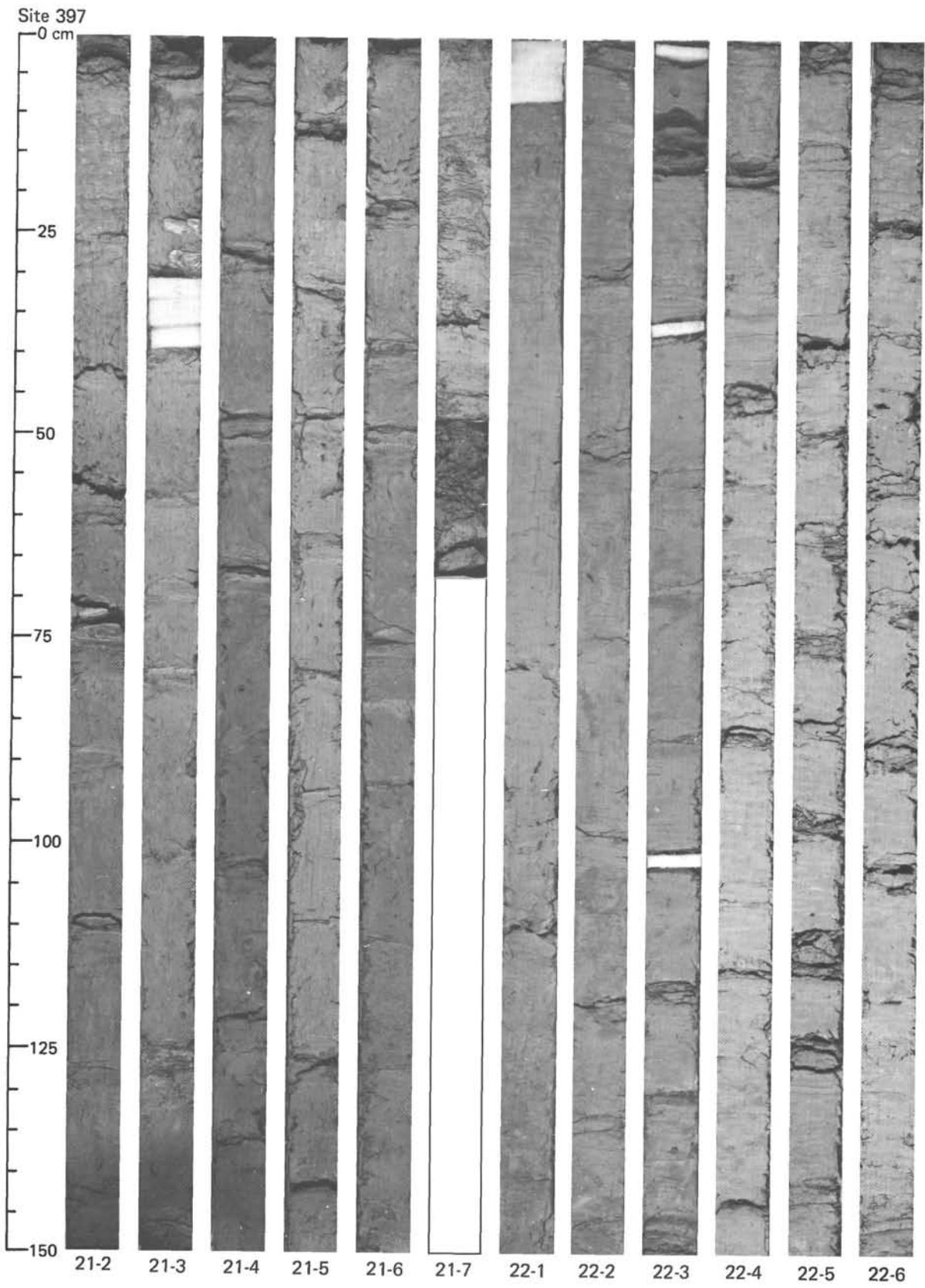


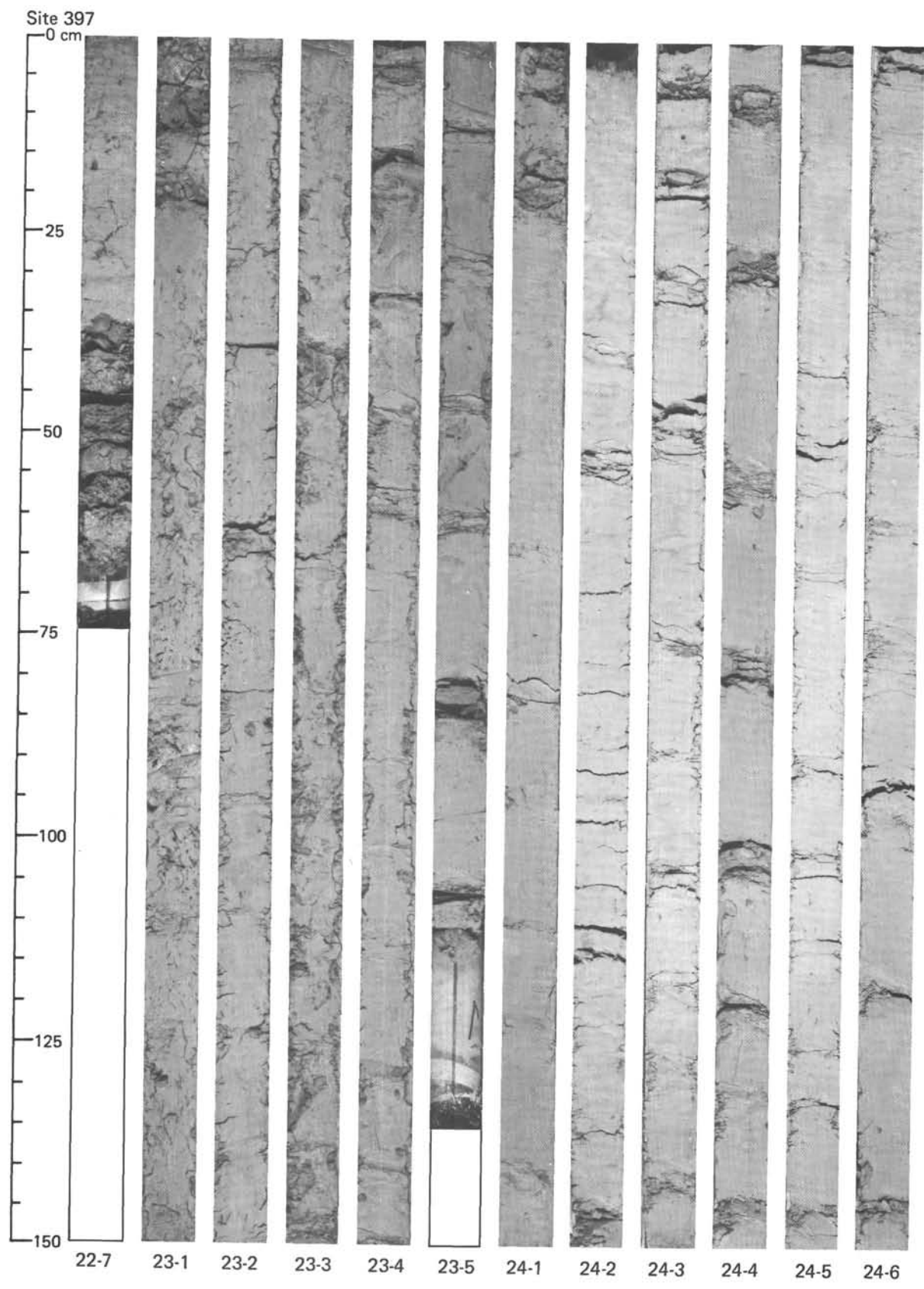
Site 397

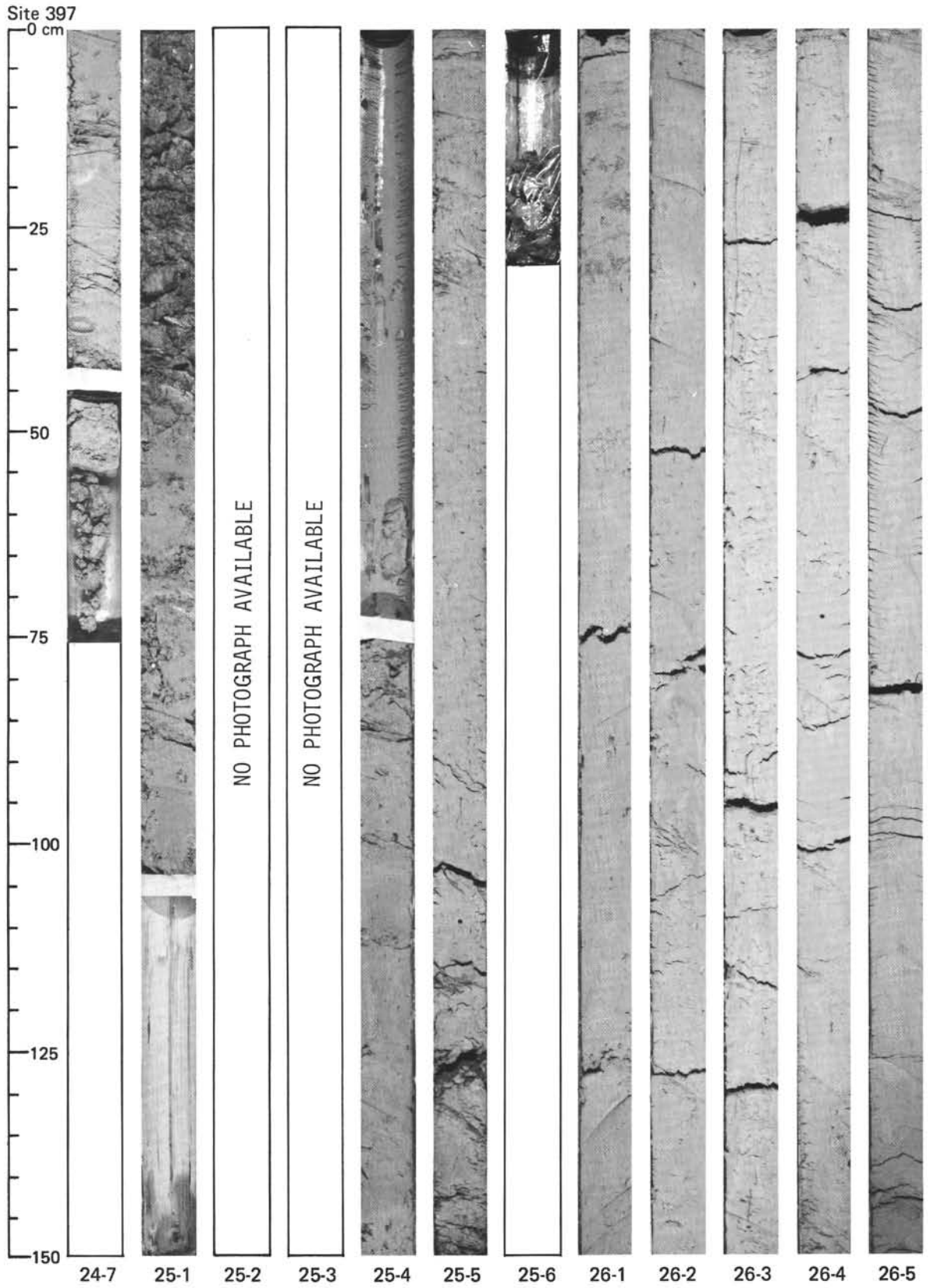


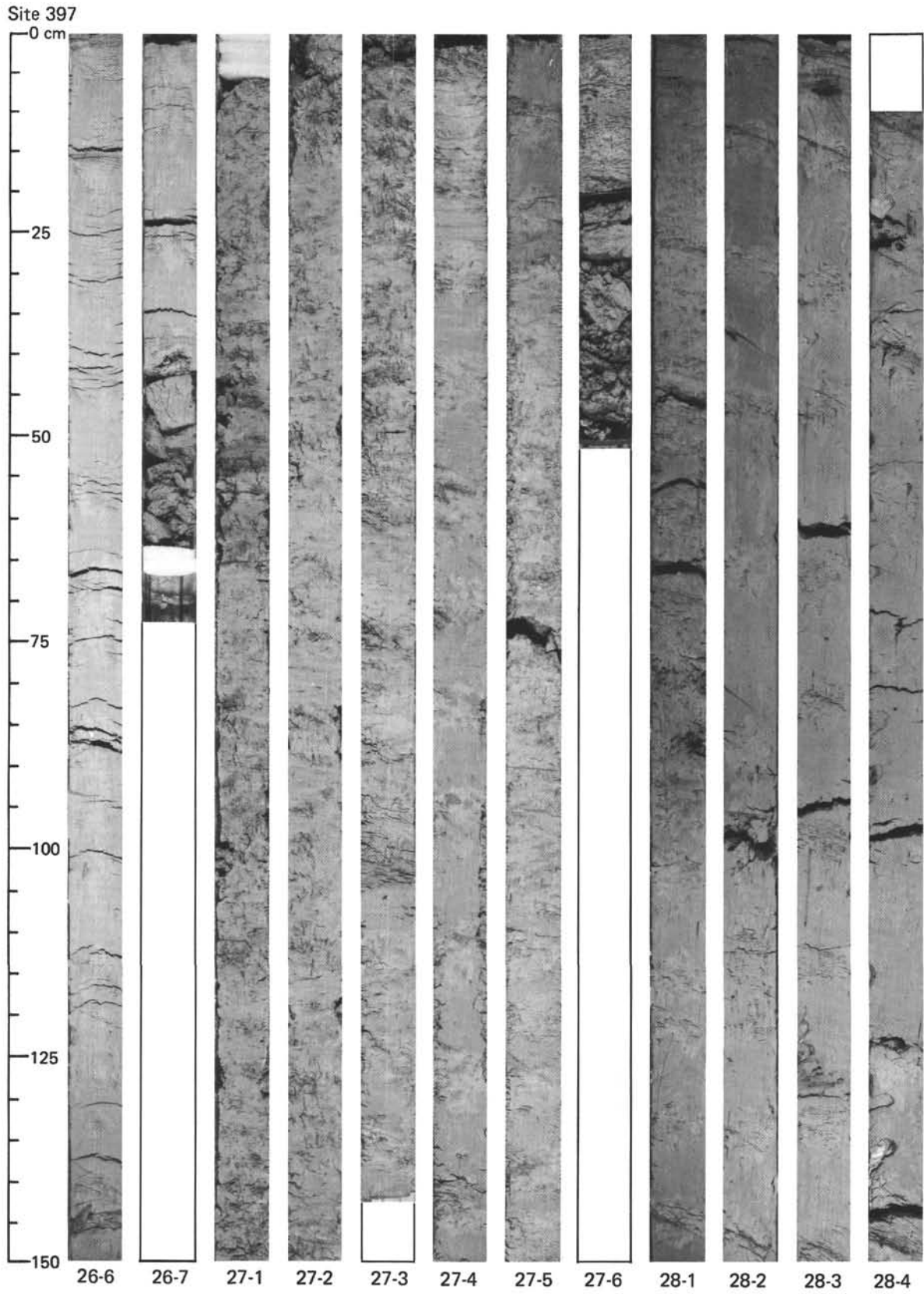


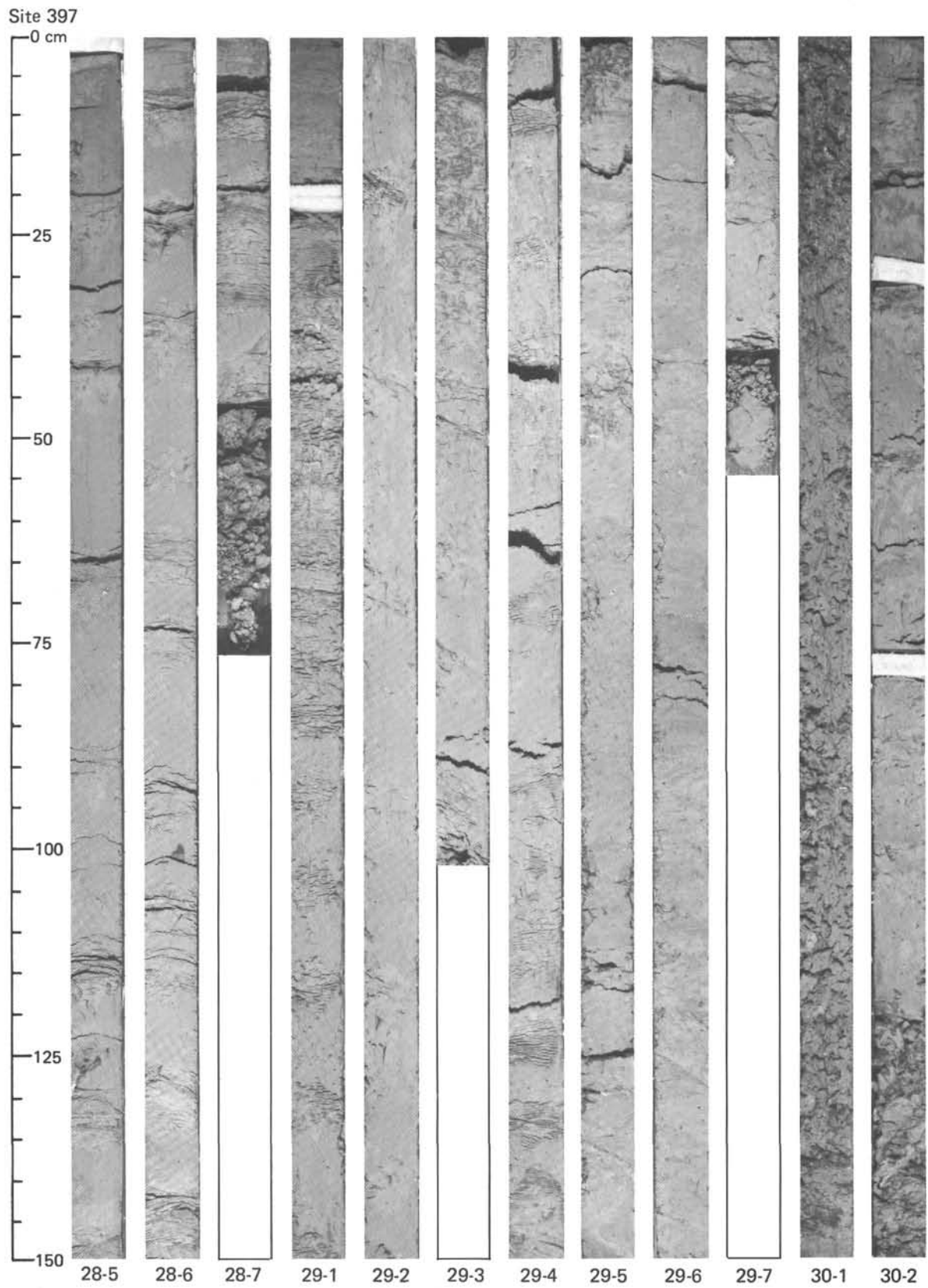


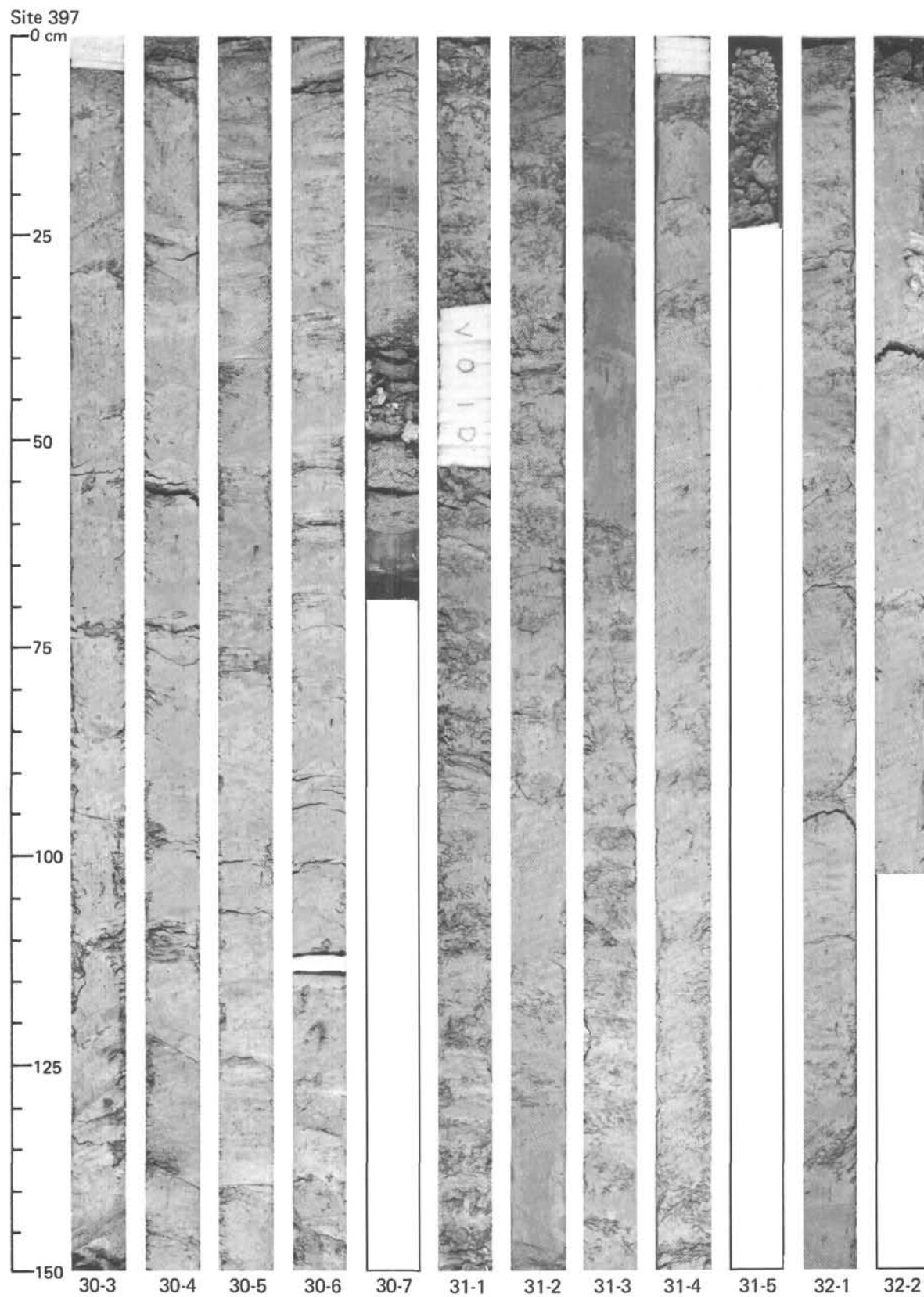


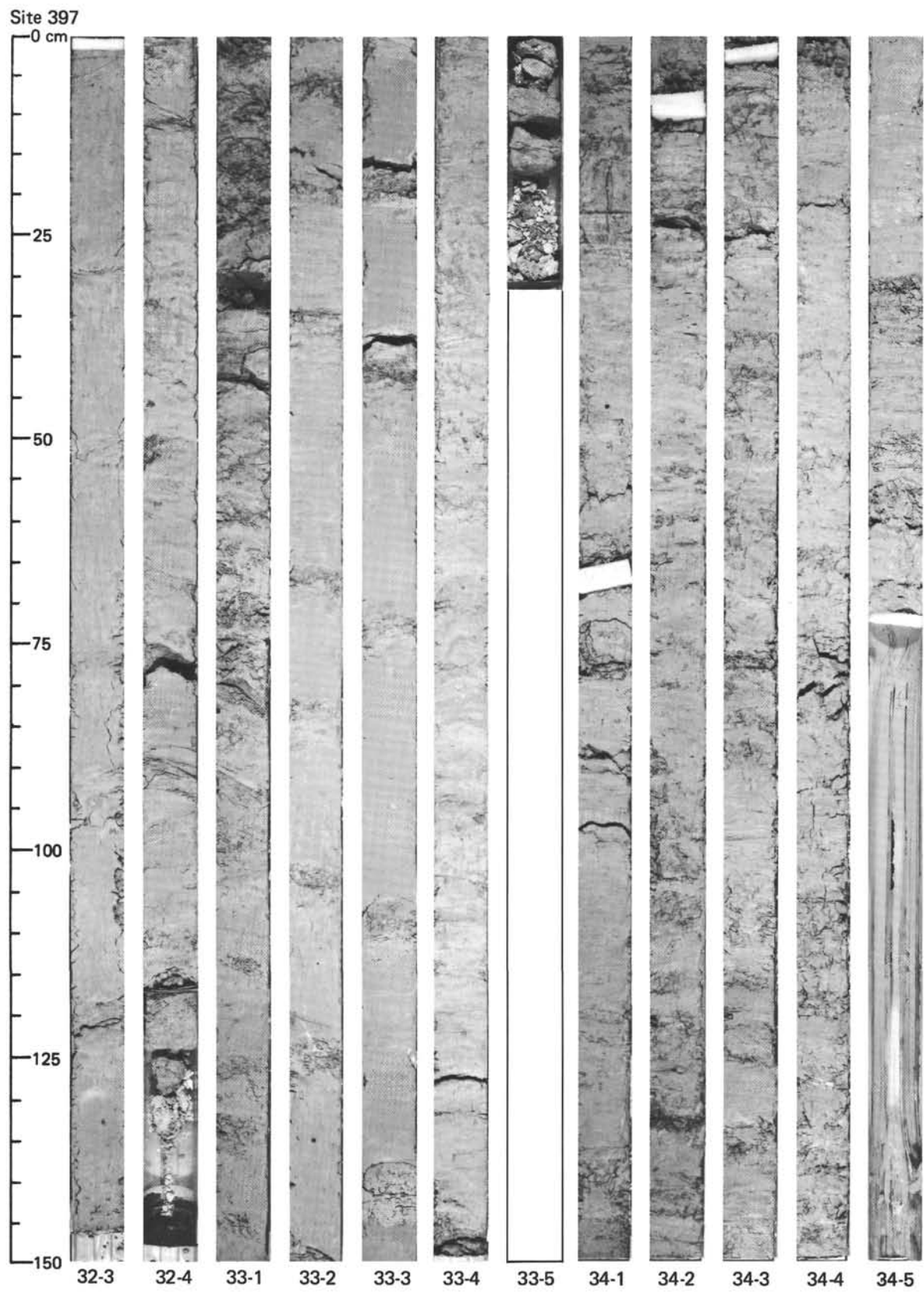


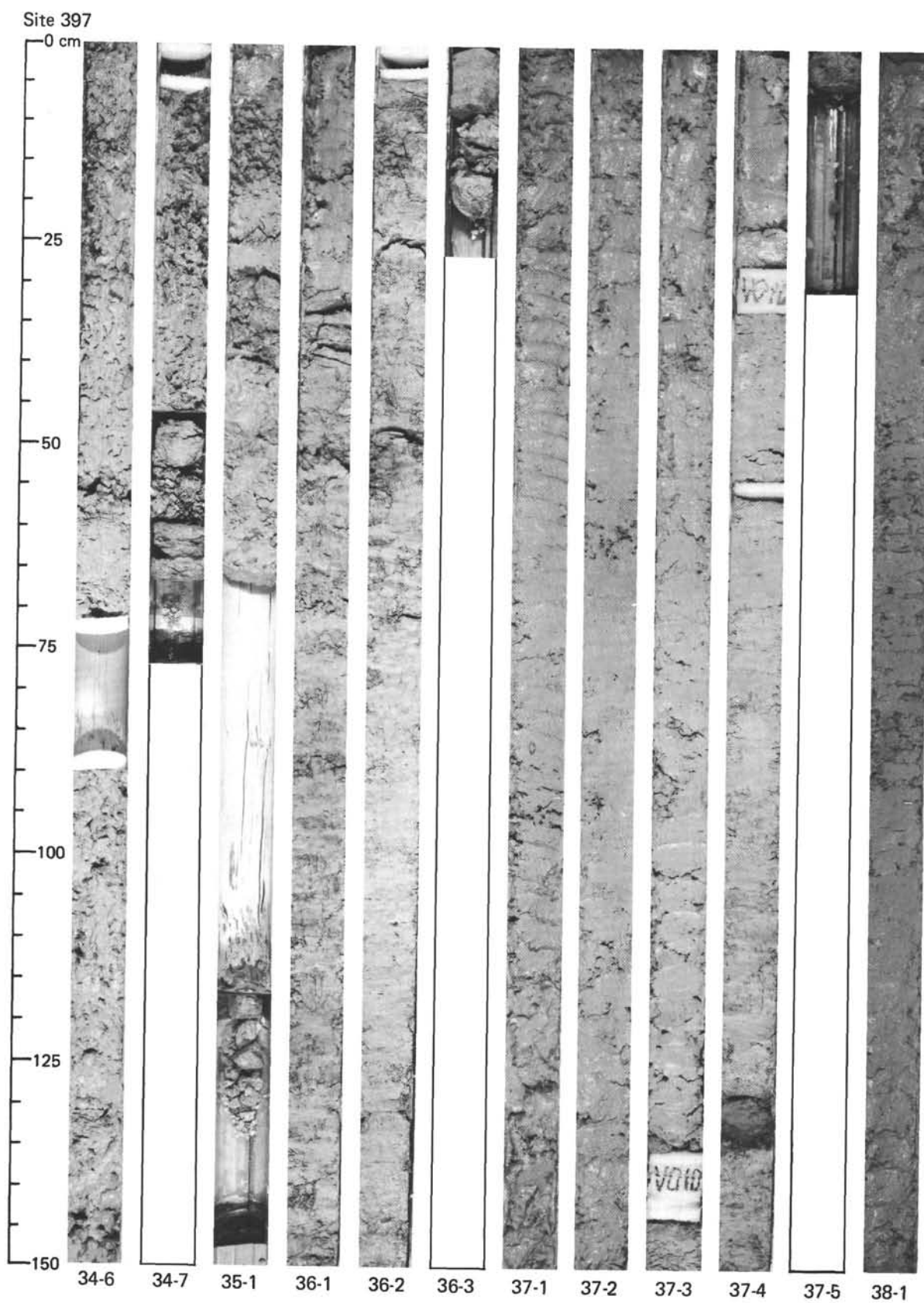


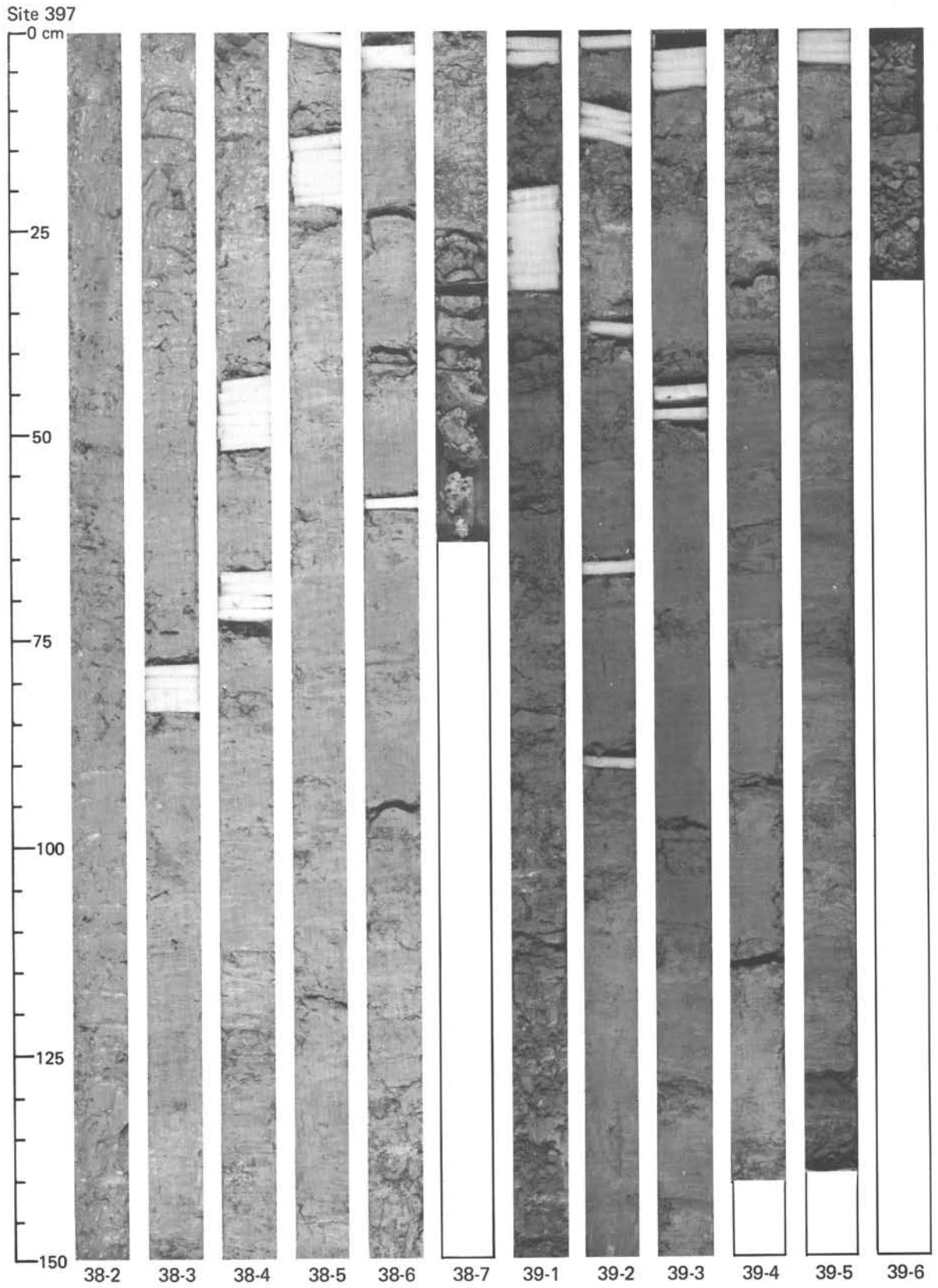




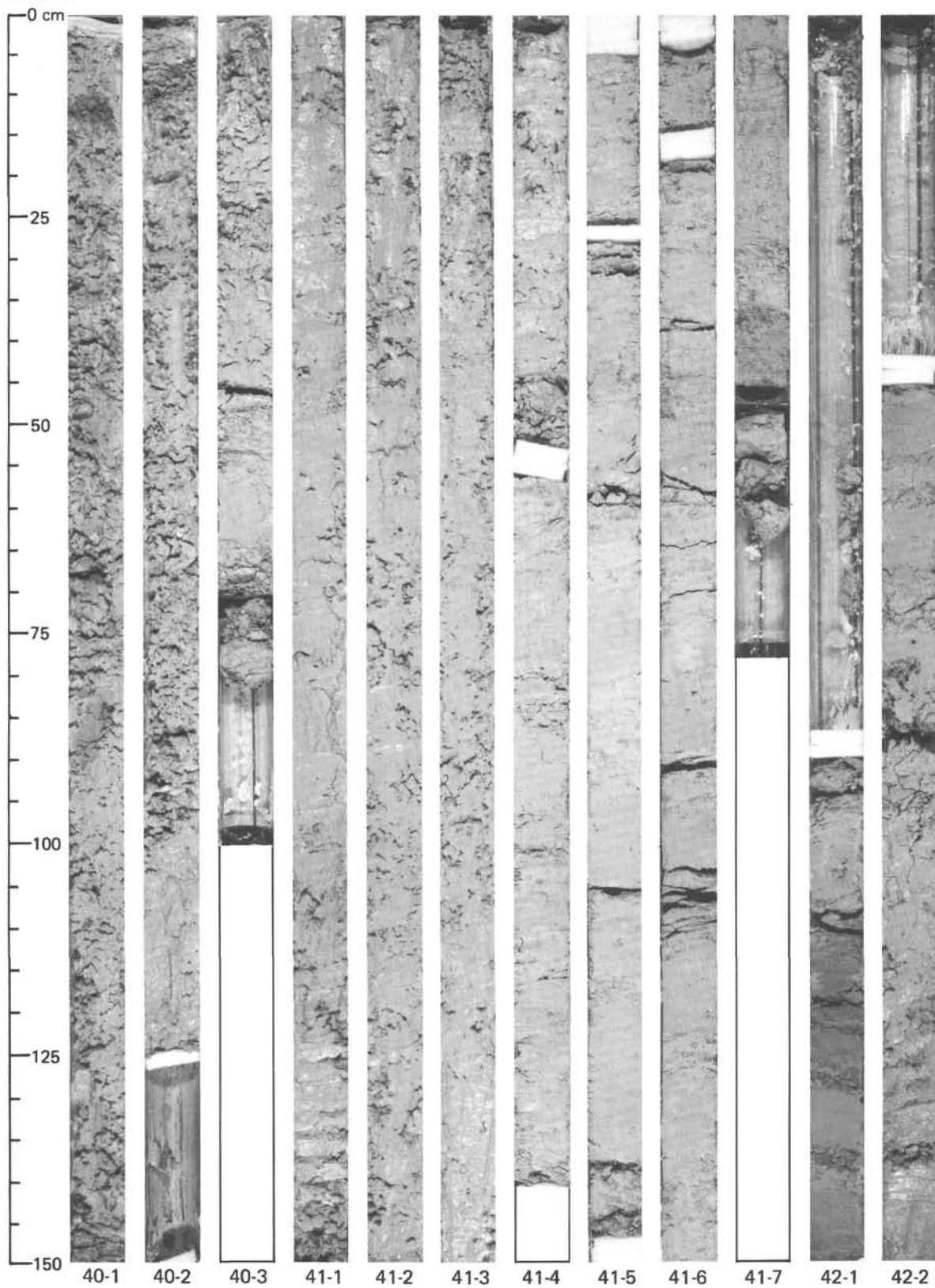


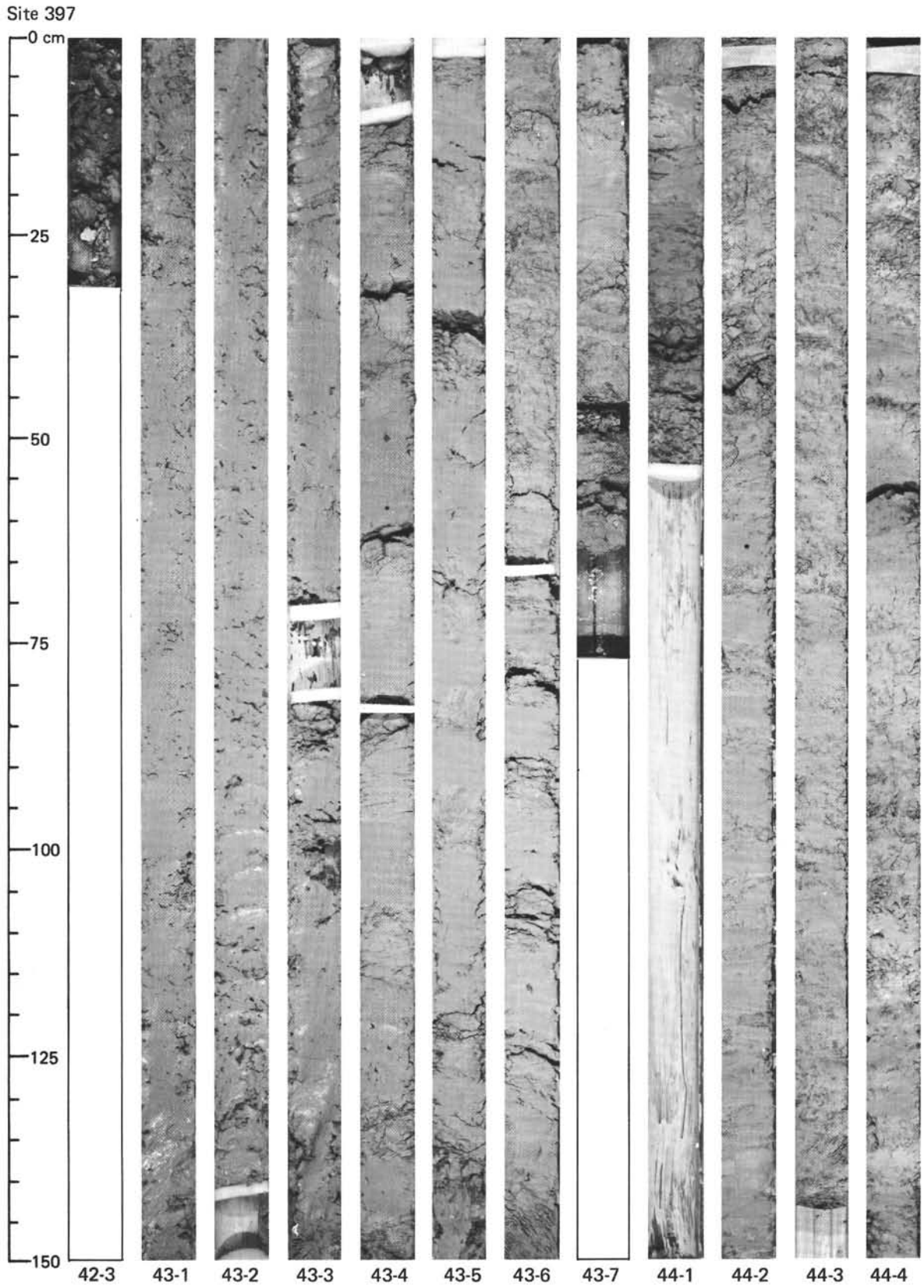




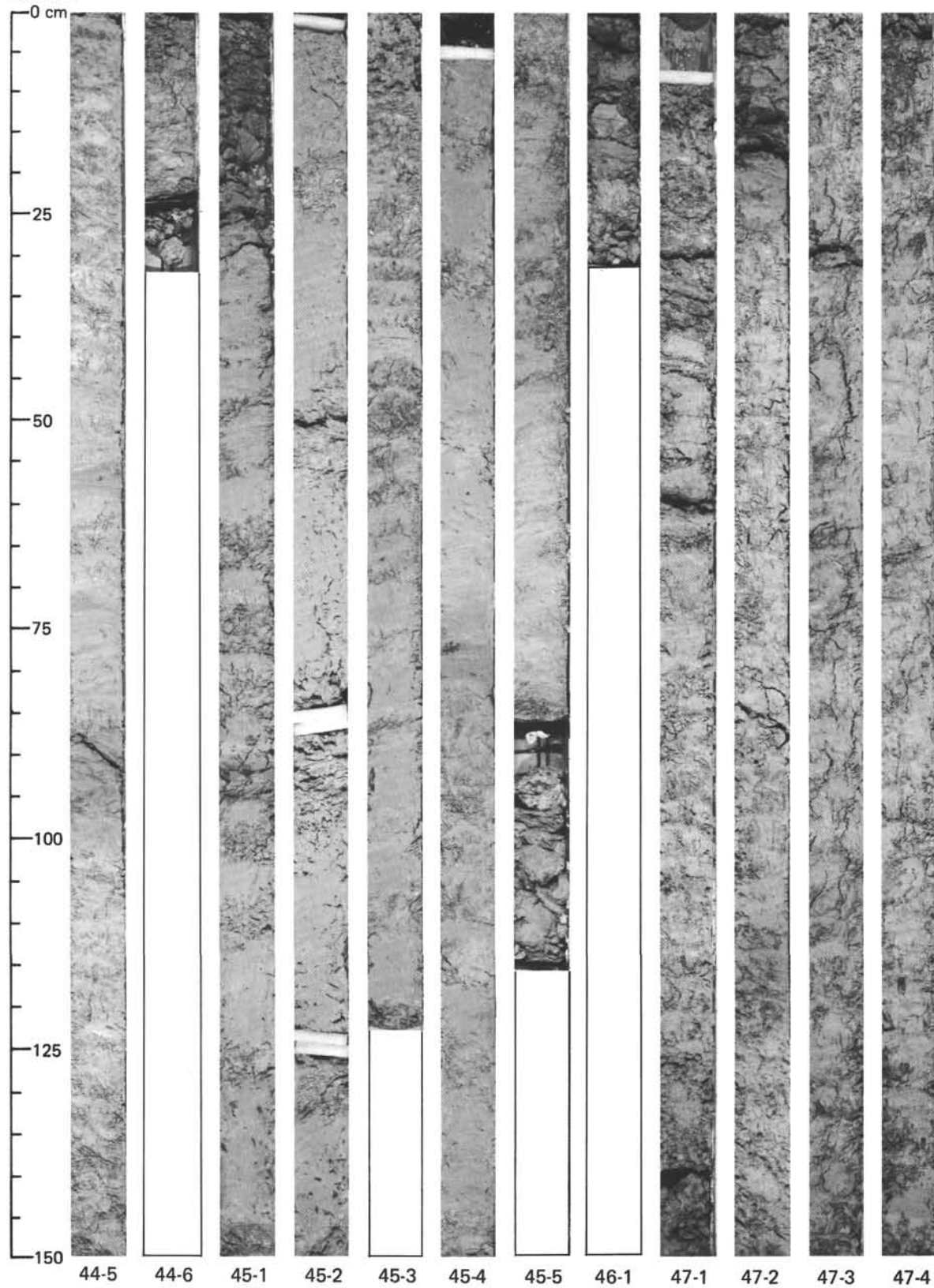


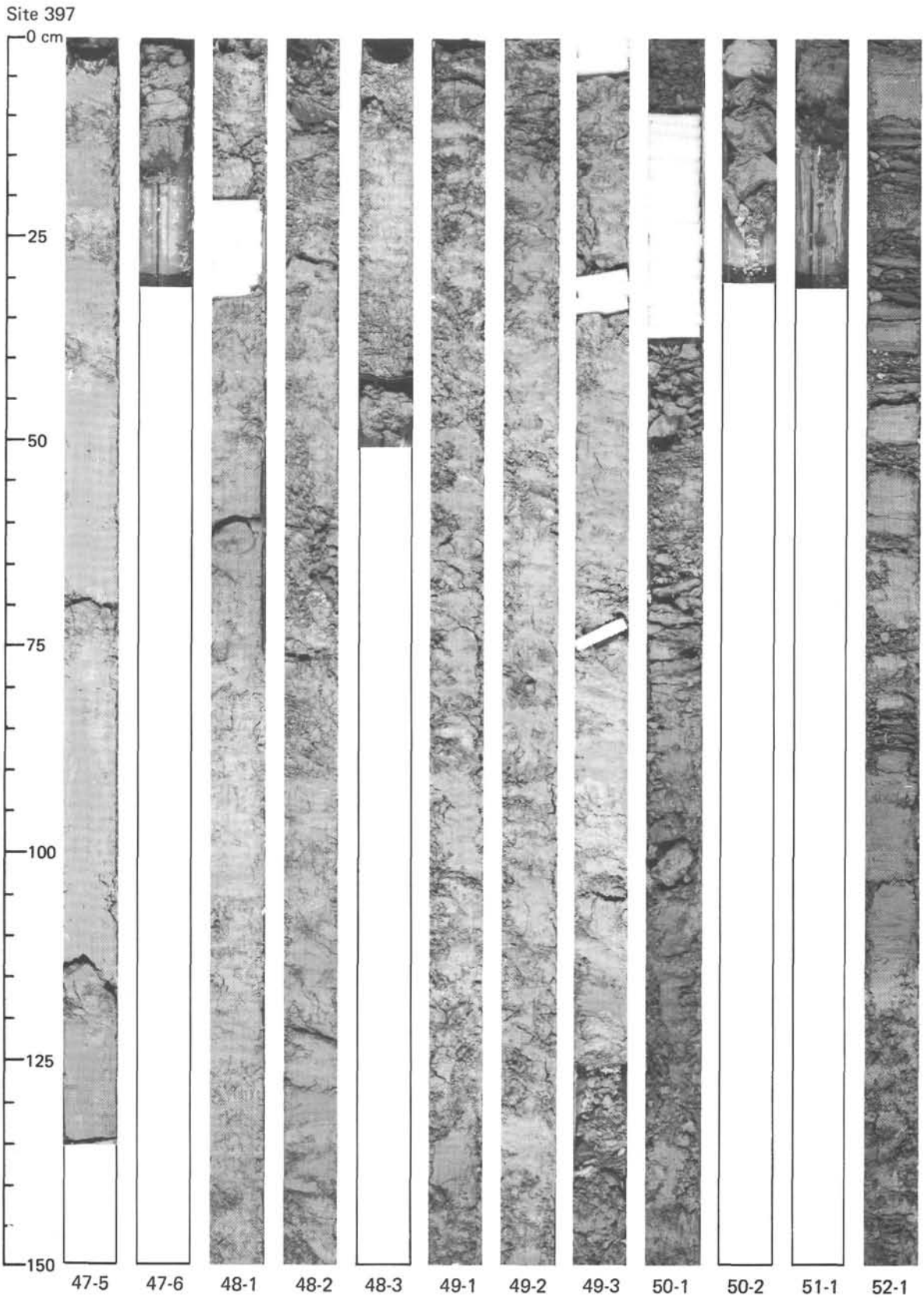
Site 397



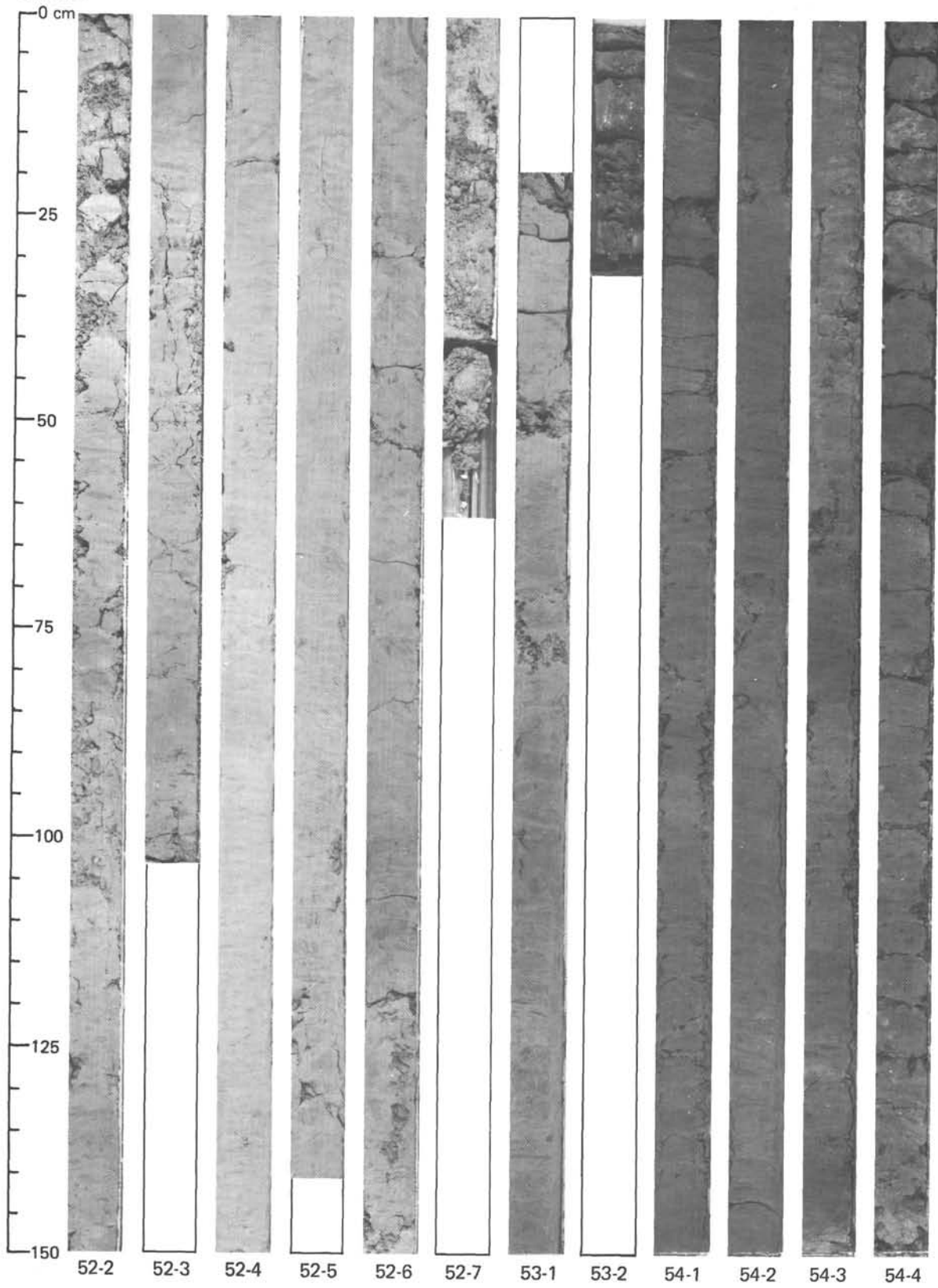


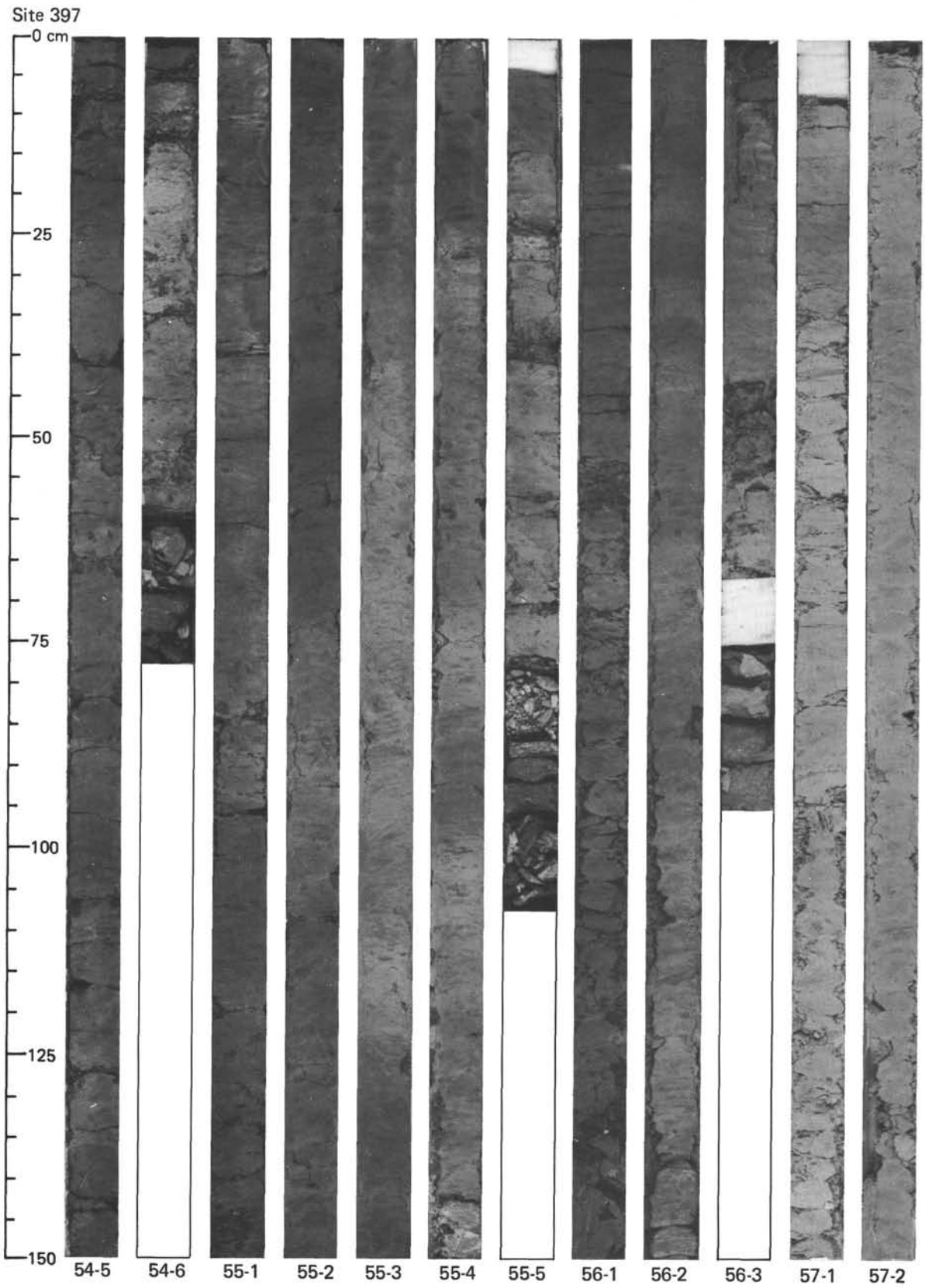
Site 397



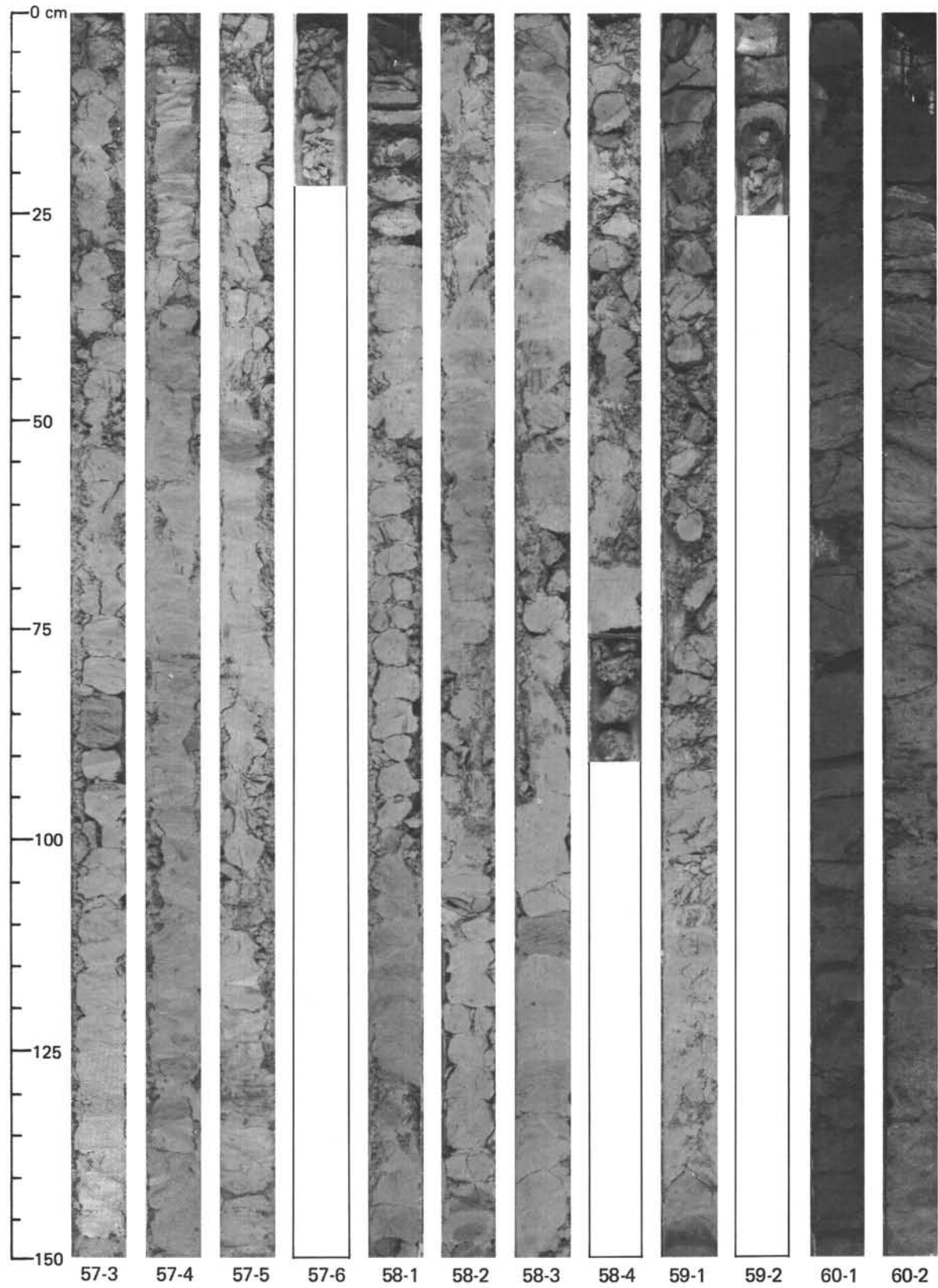


Site 397

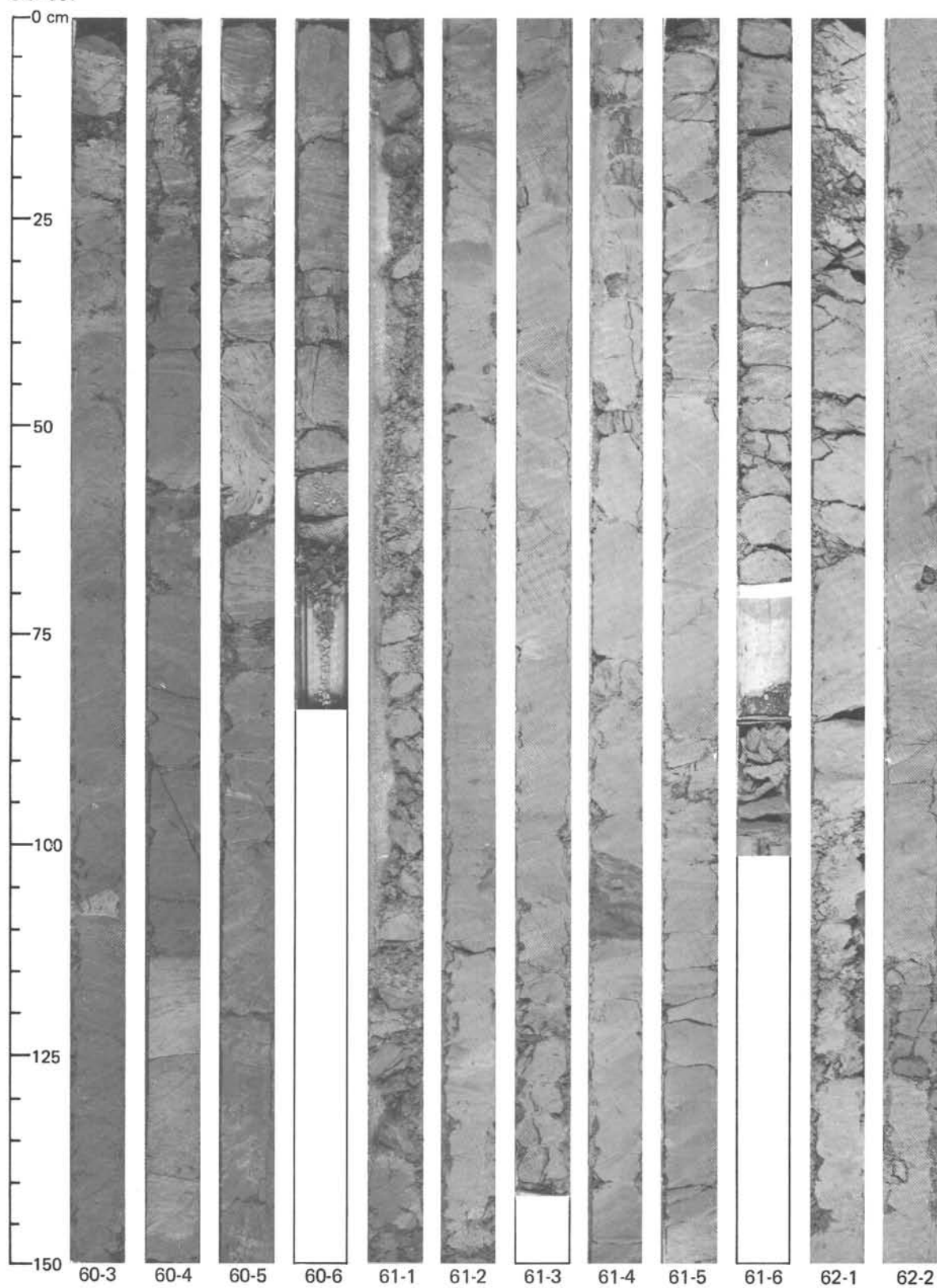


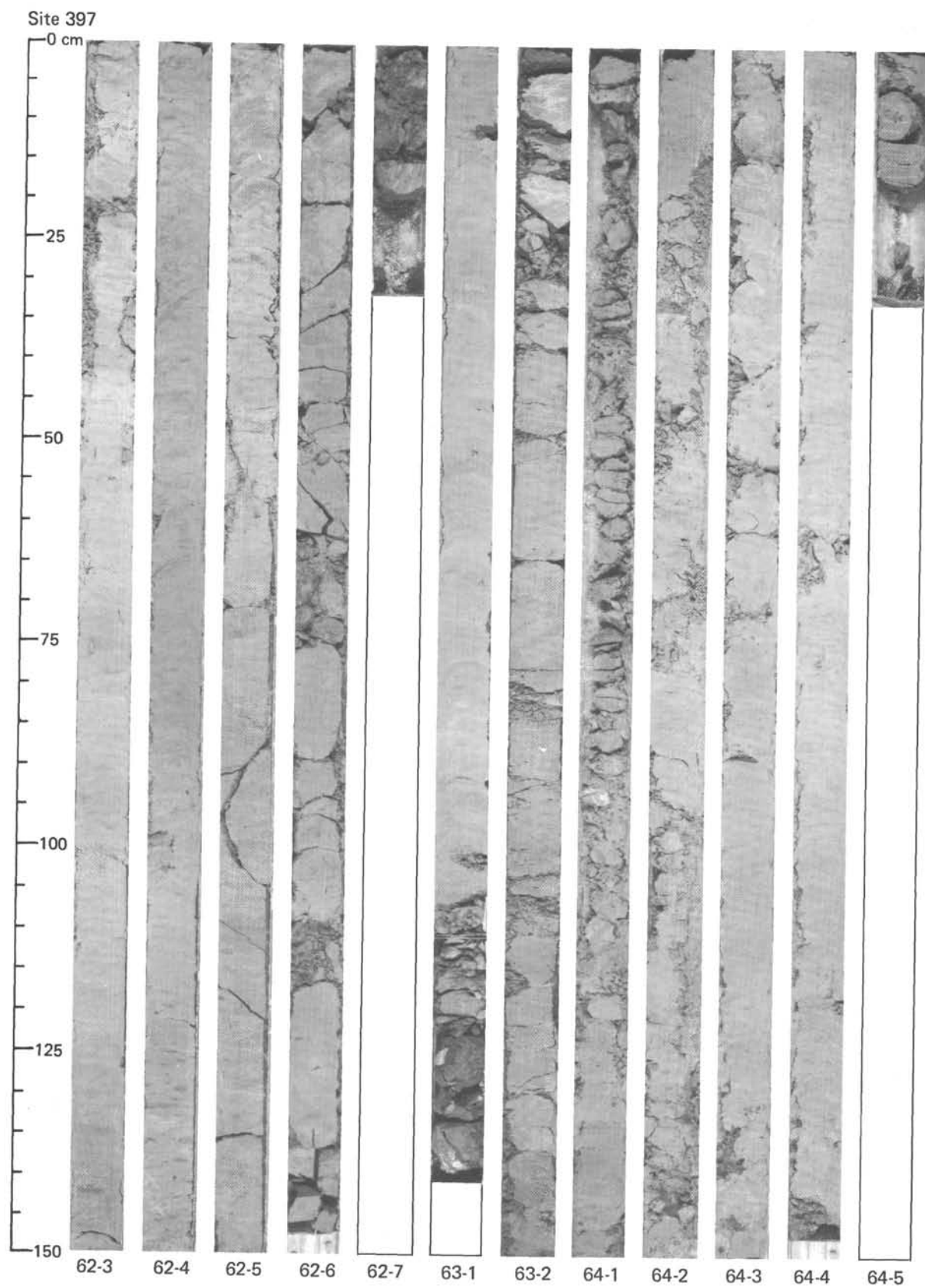


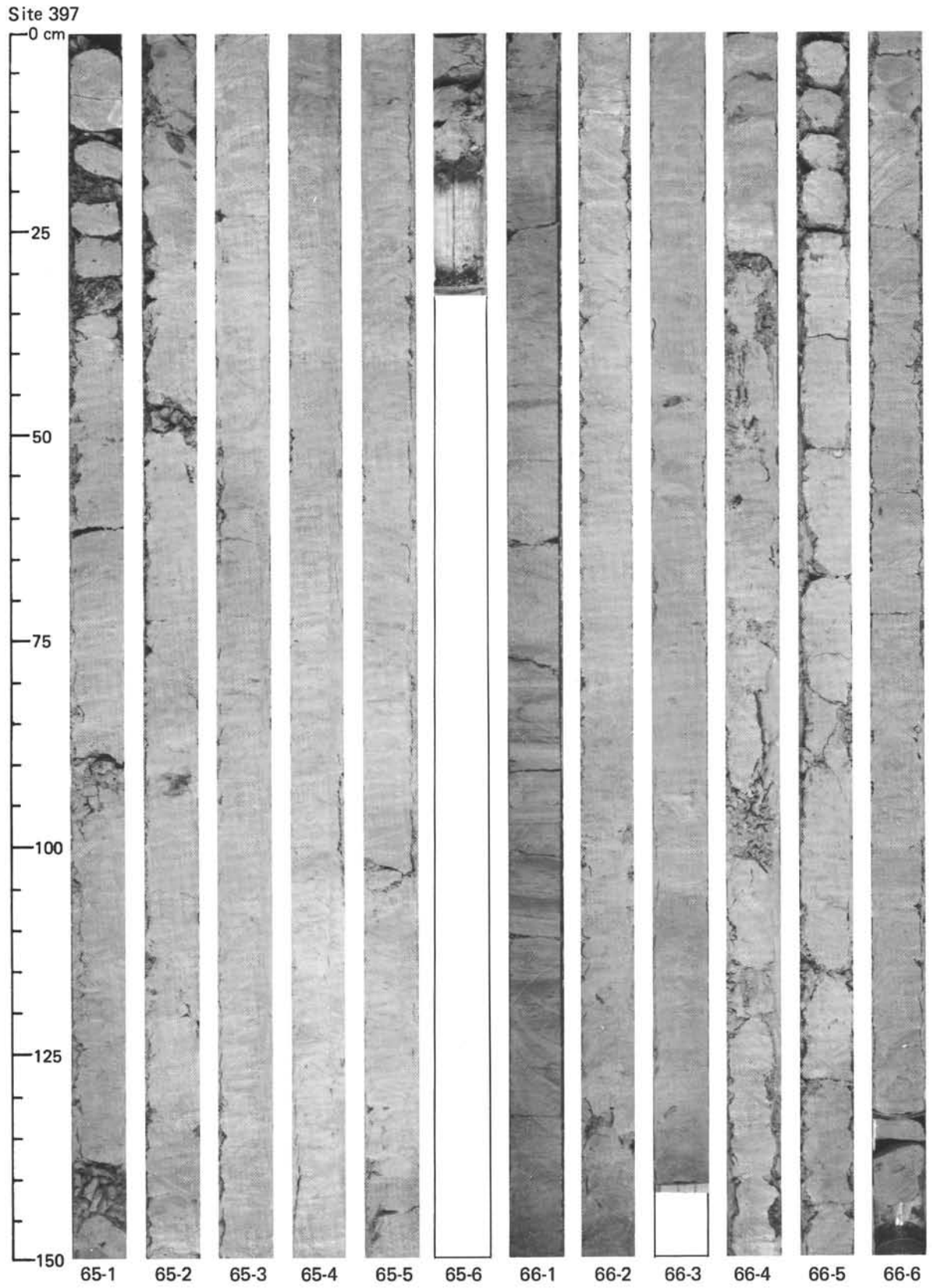
Site 397



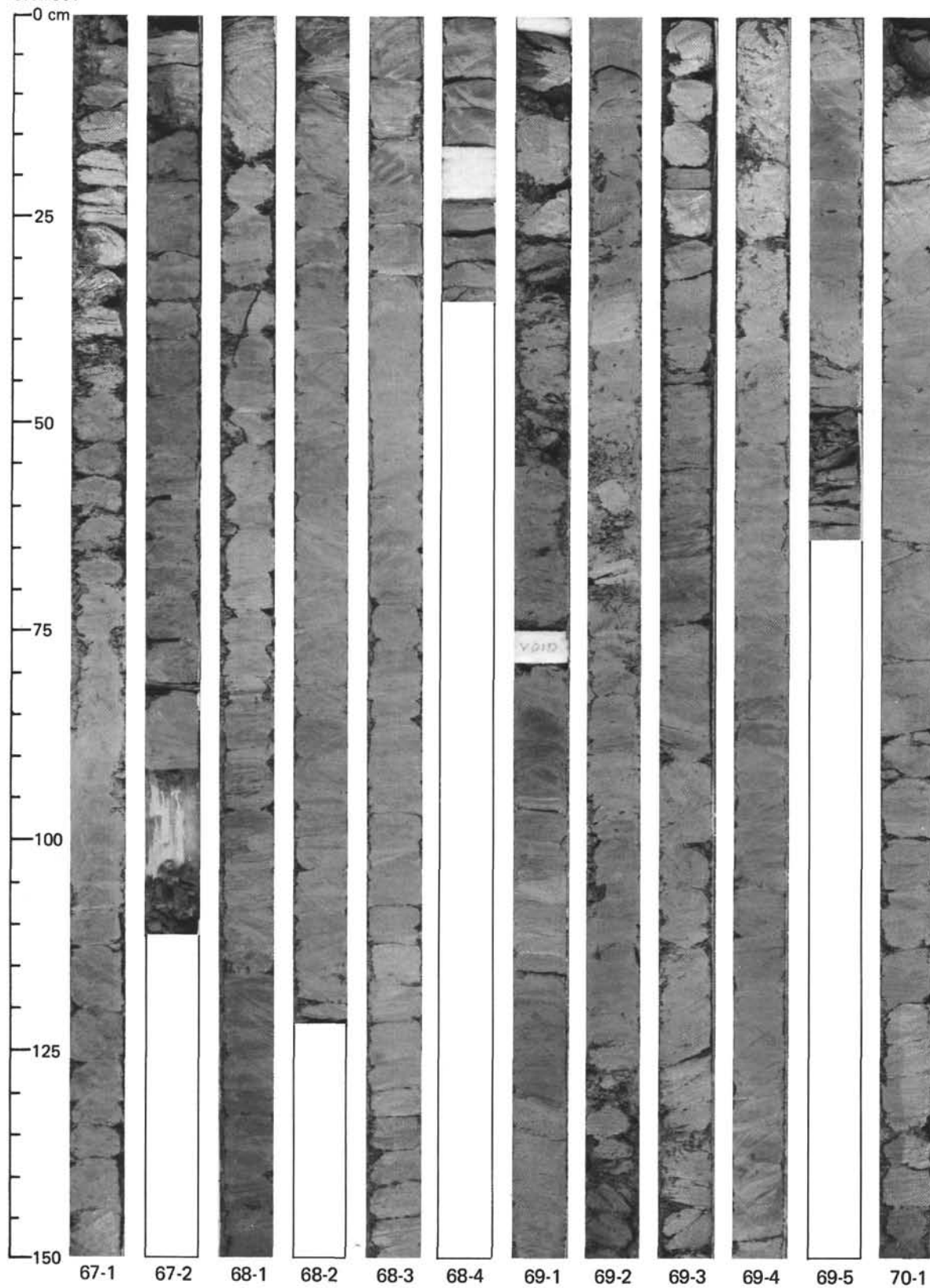
Site 397

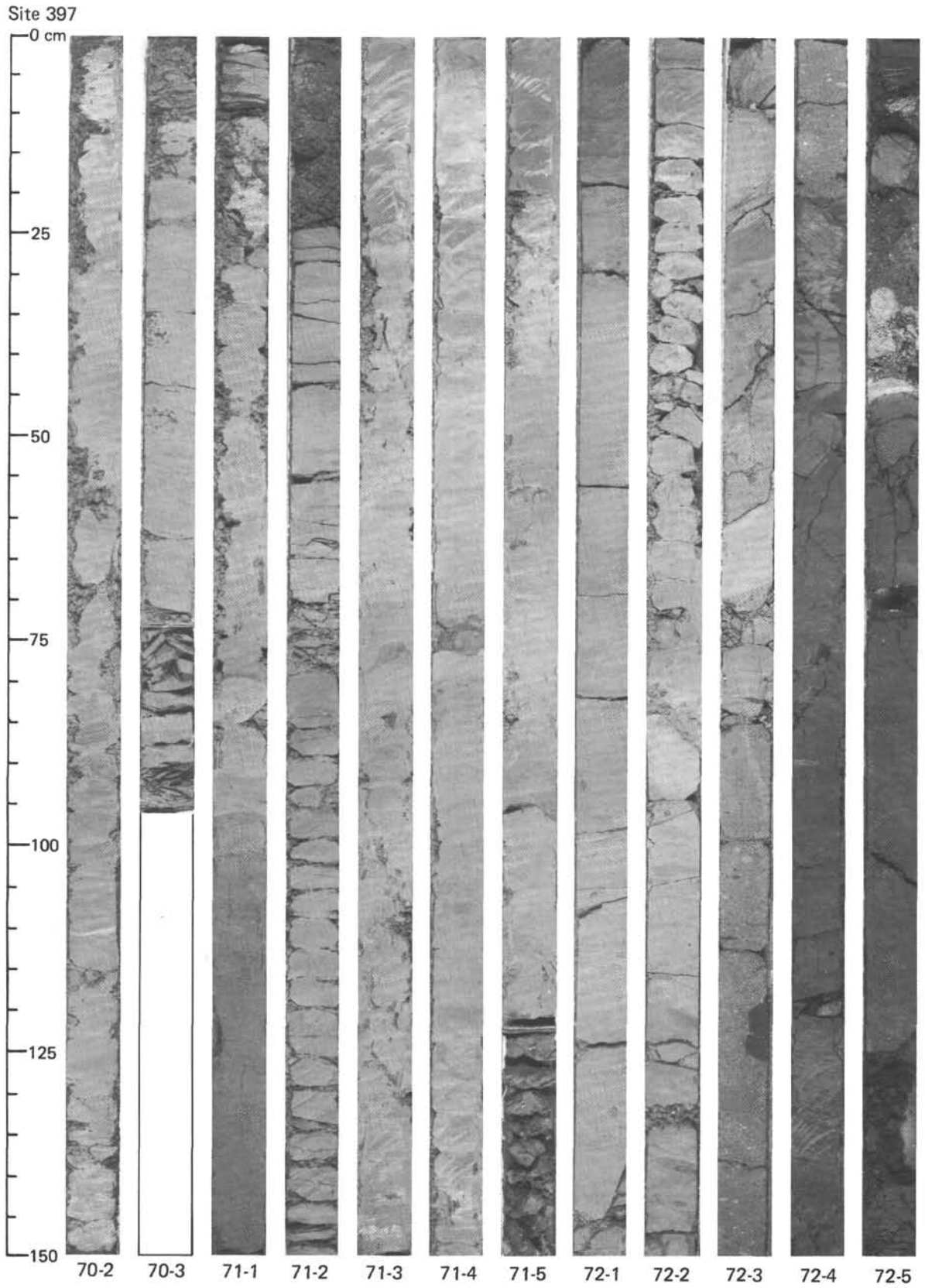




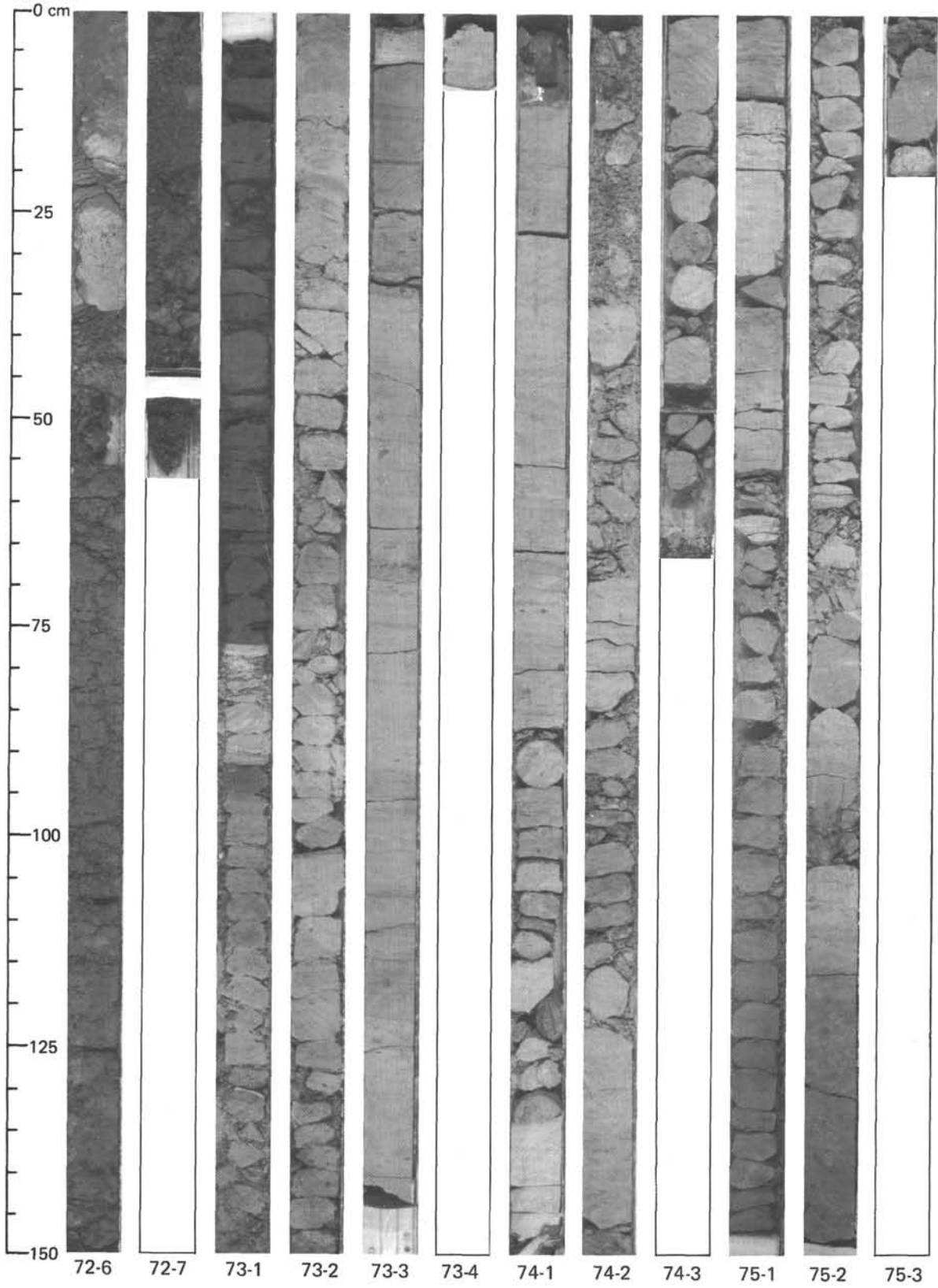


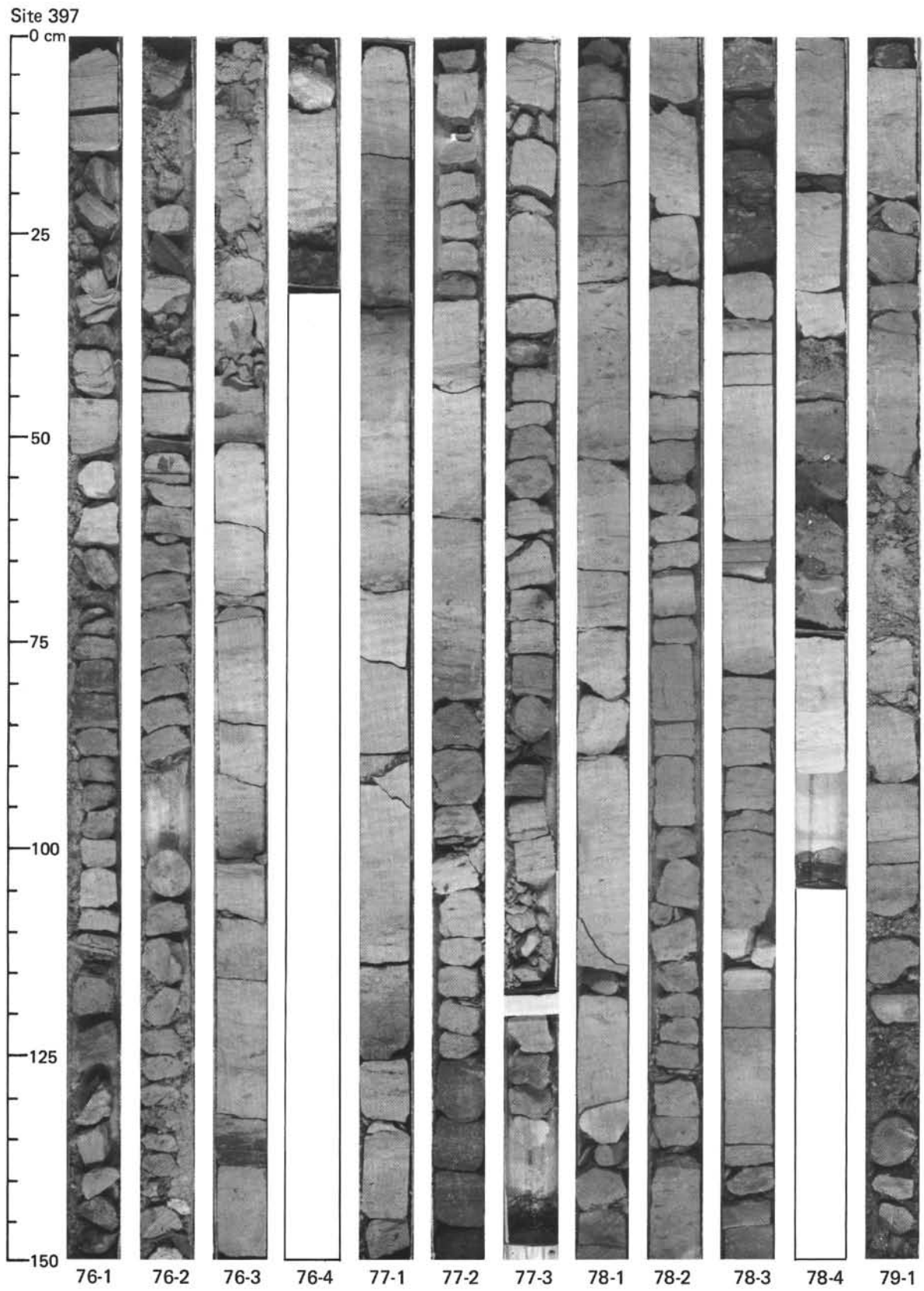
Site 397



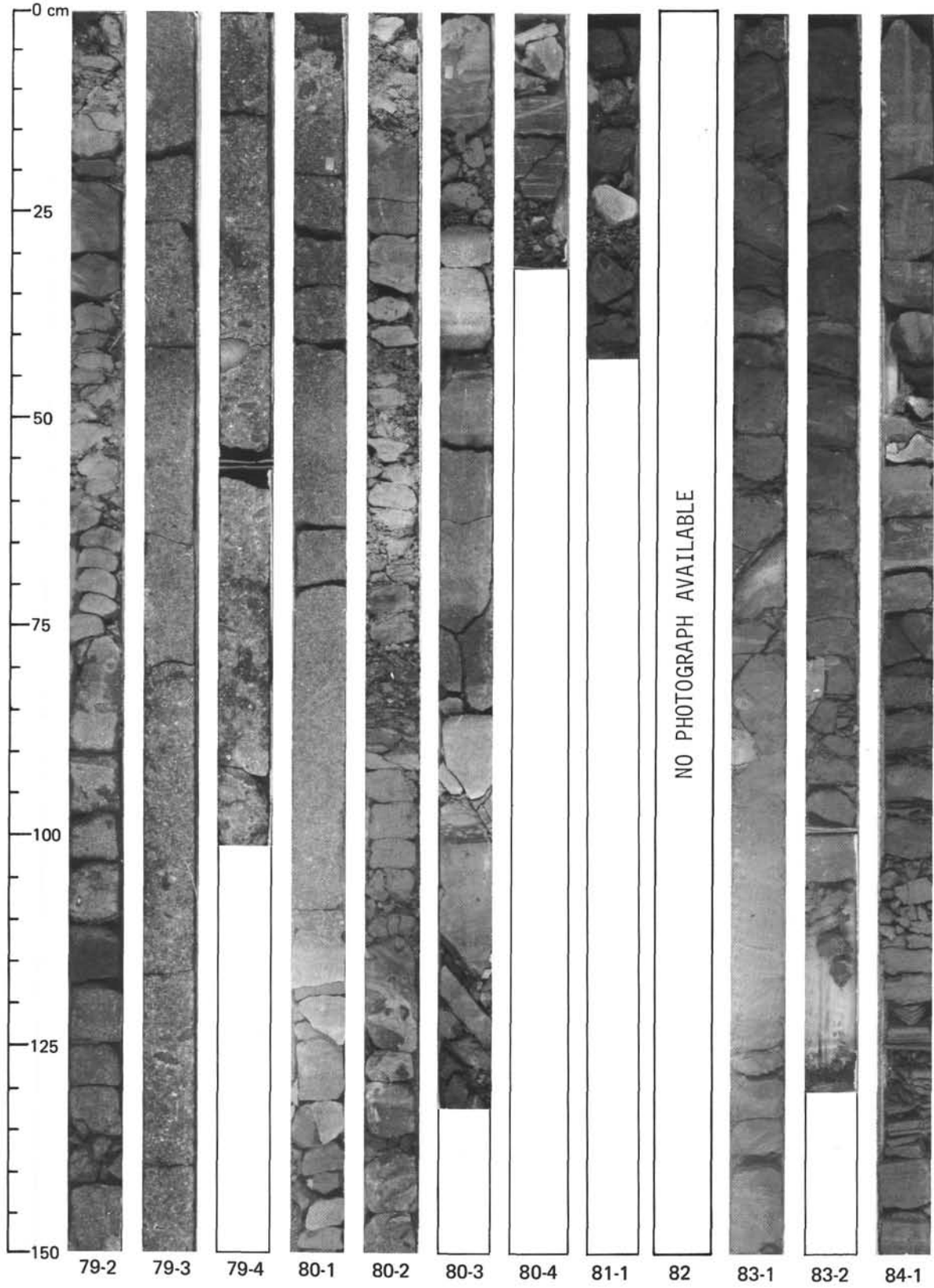


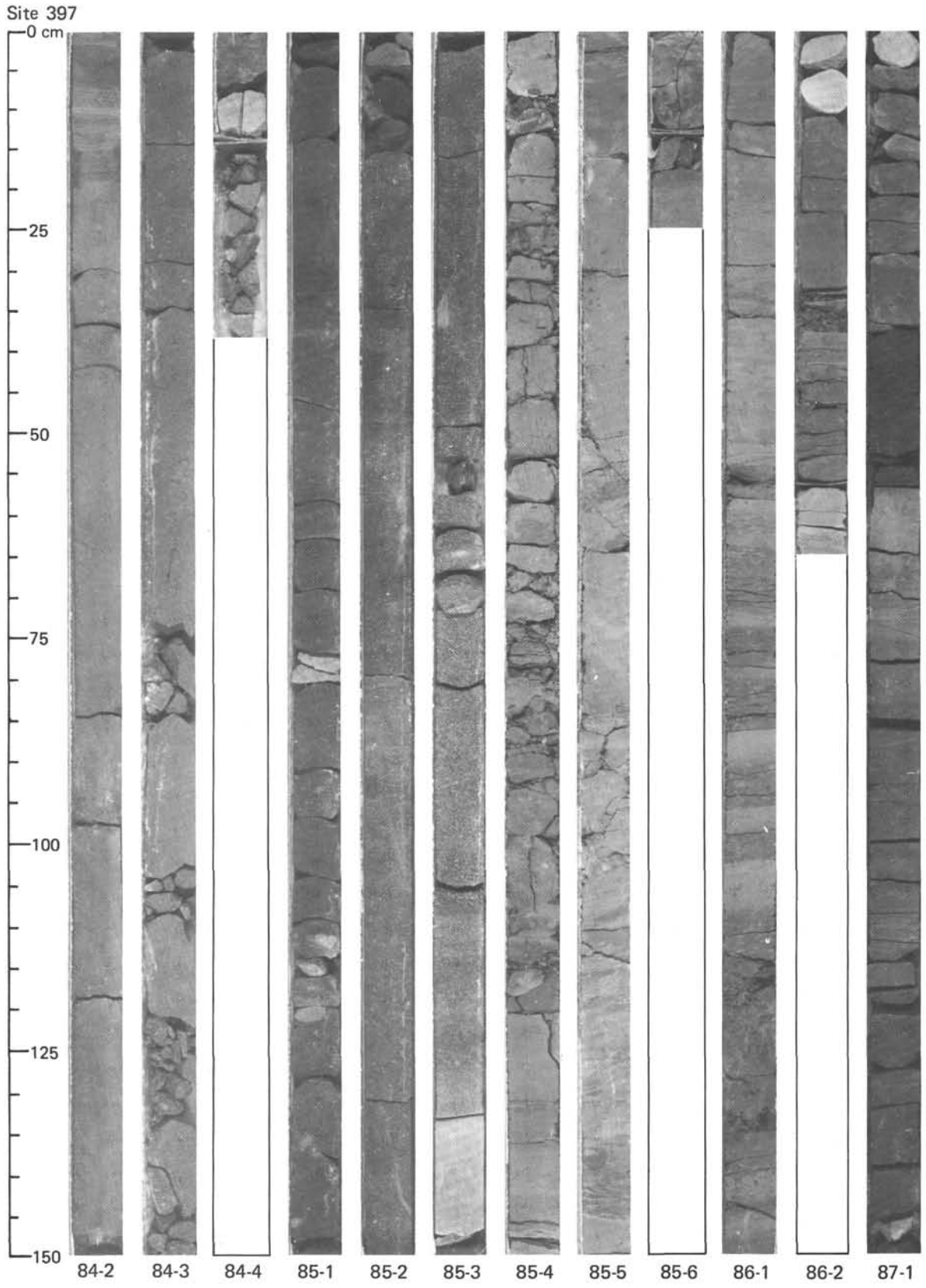
Site 397

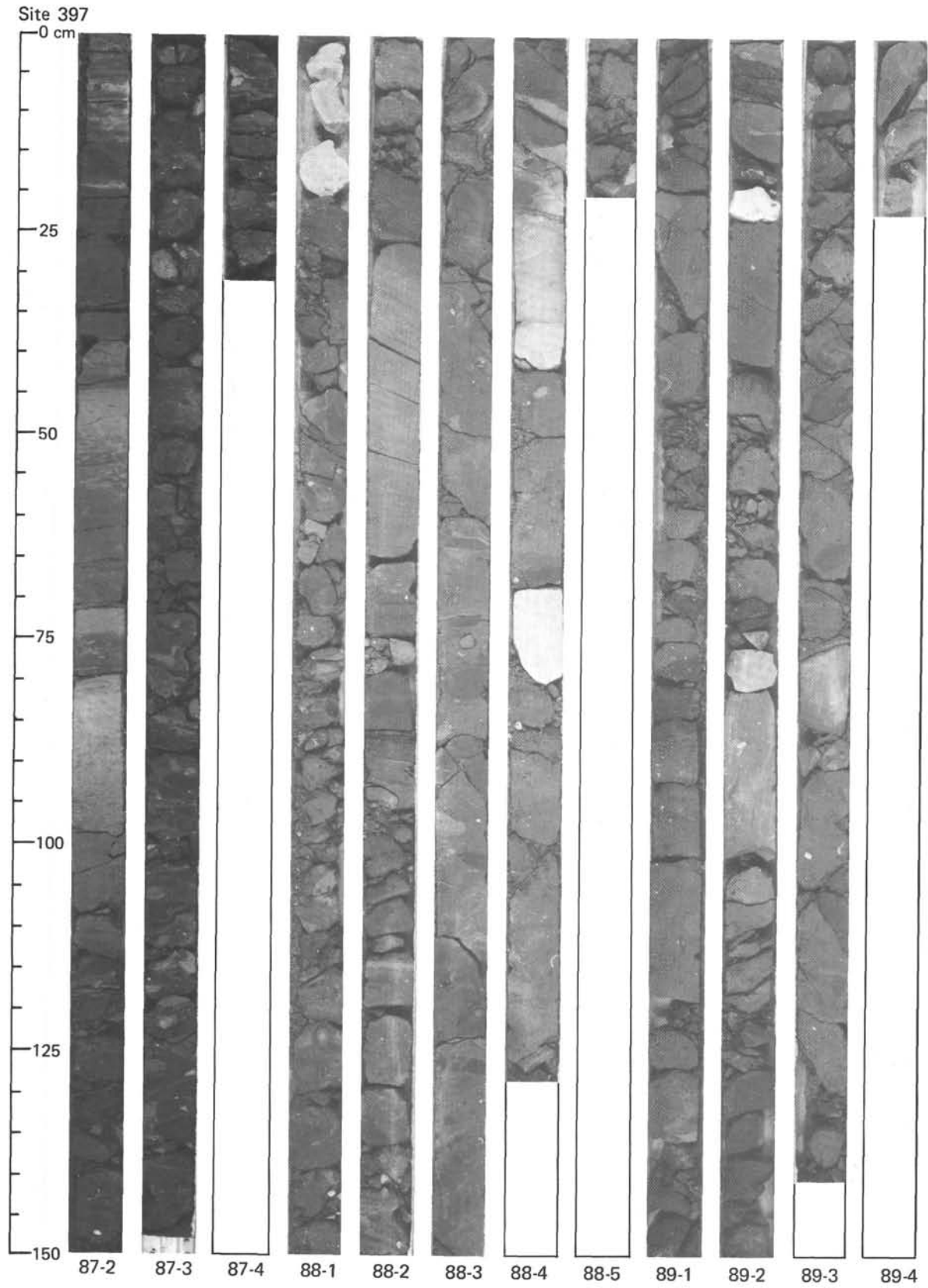


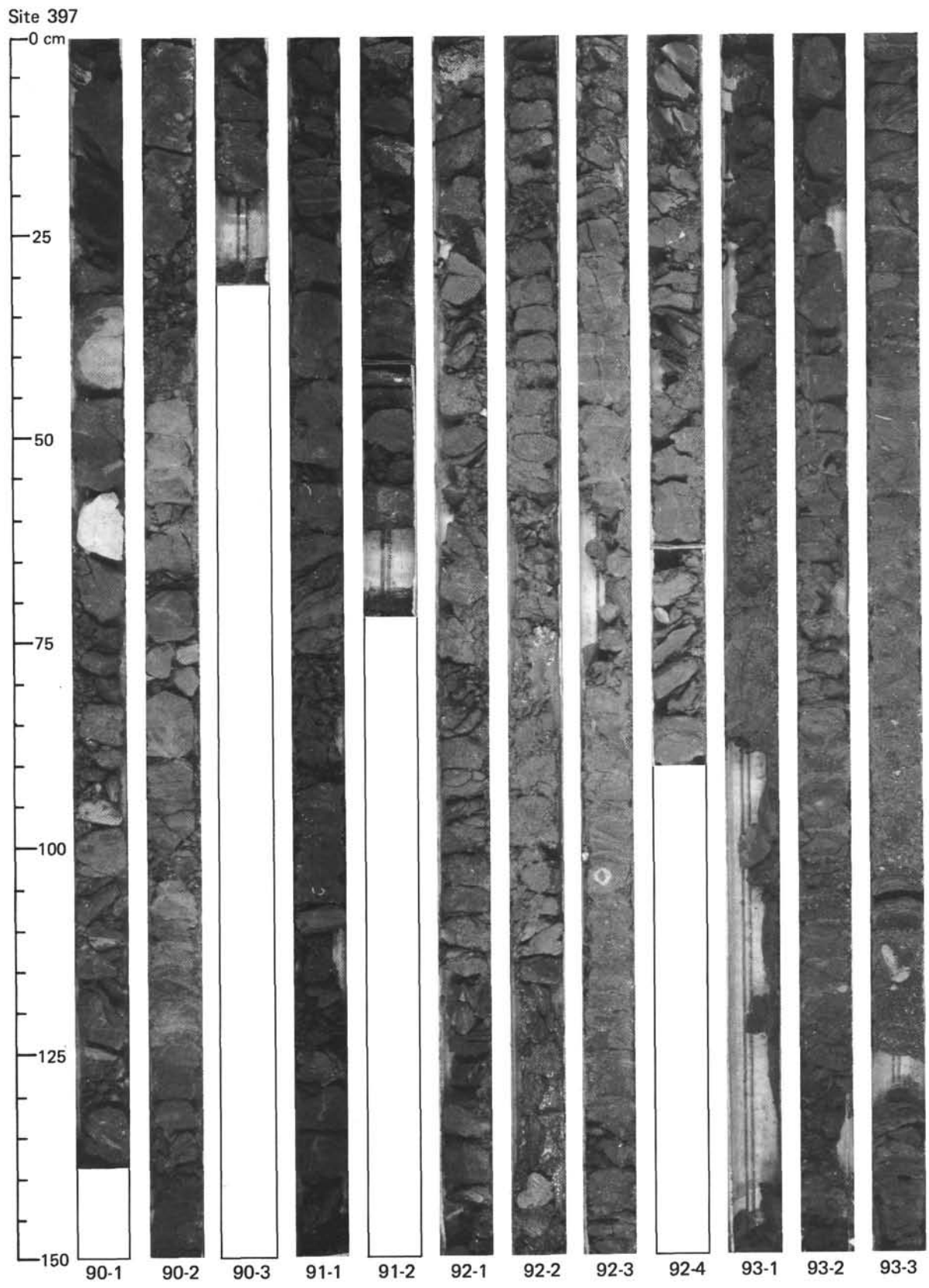


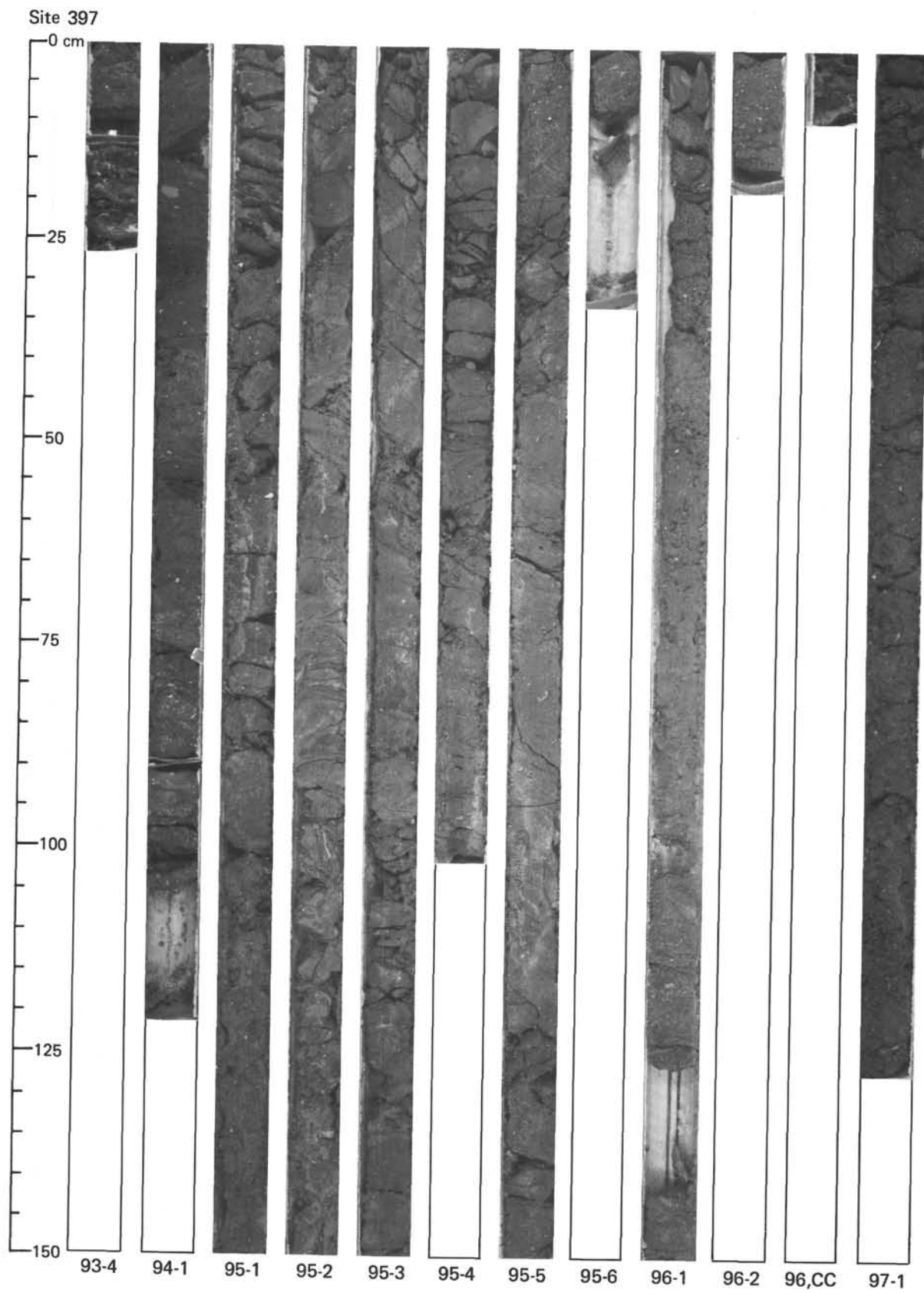
Site 397

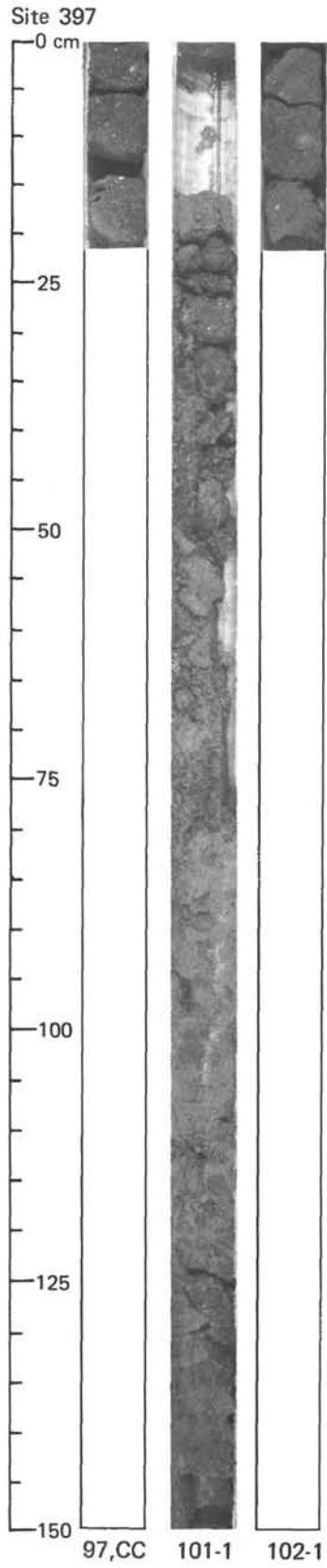


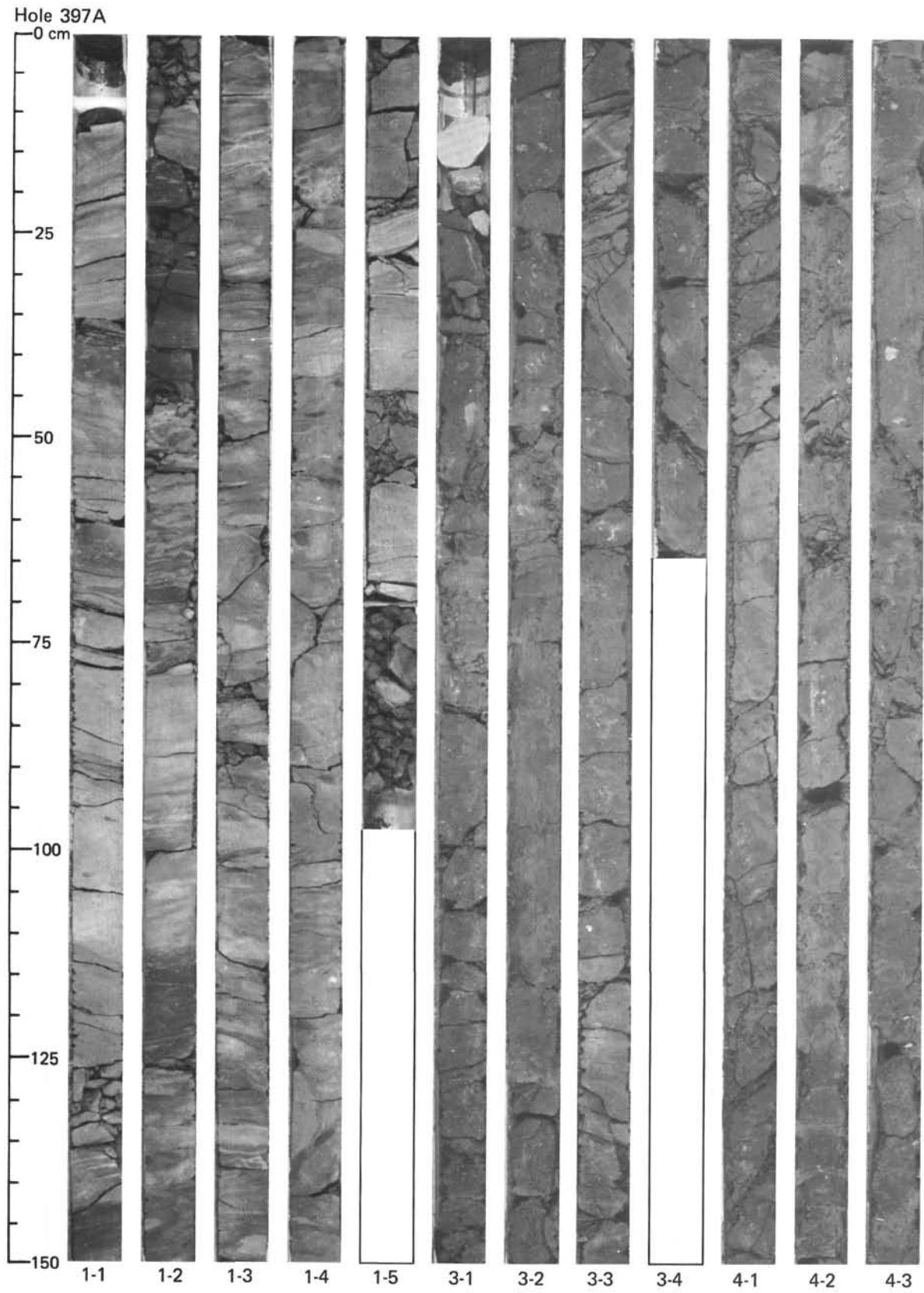


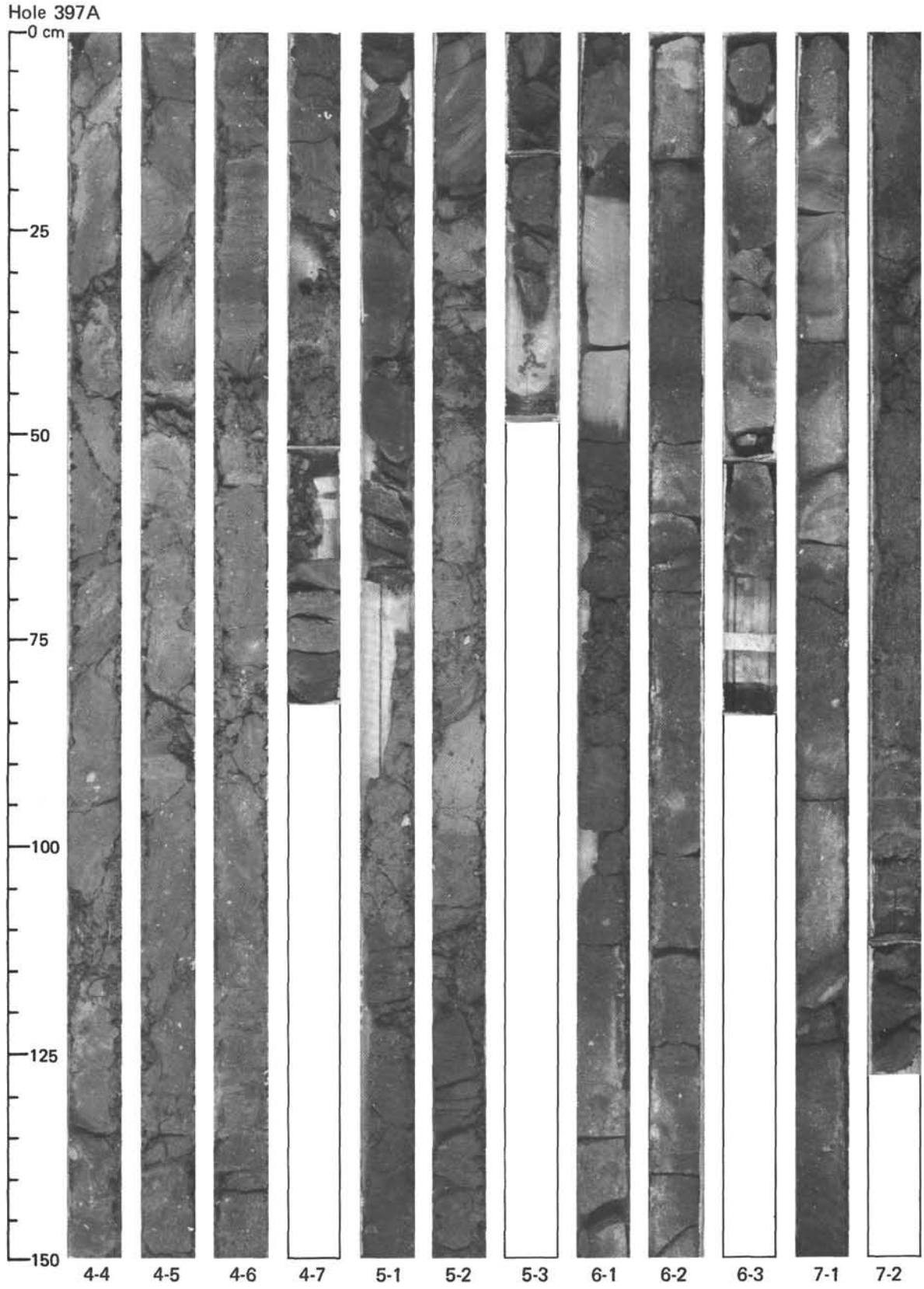


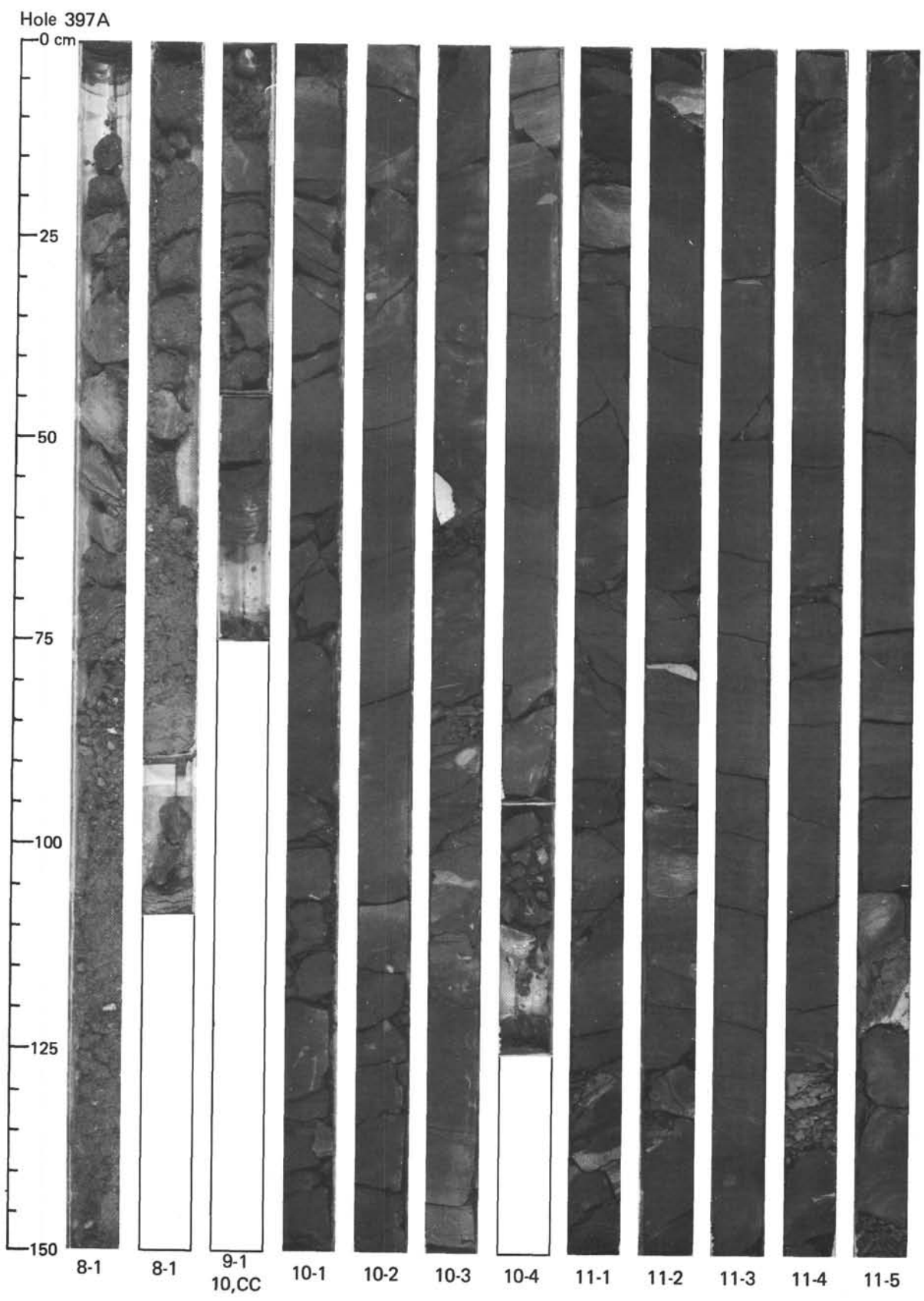




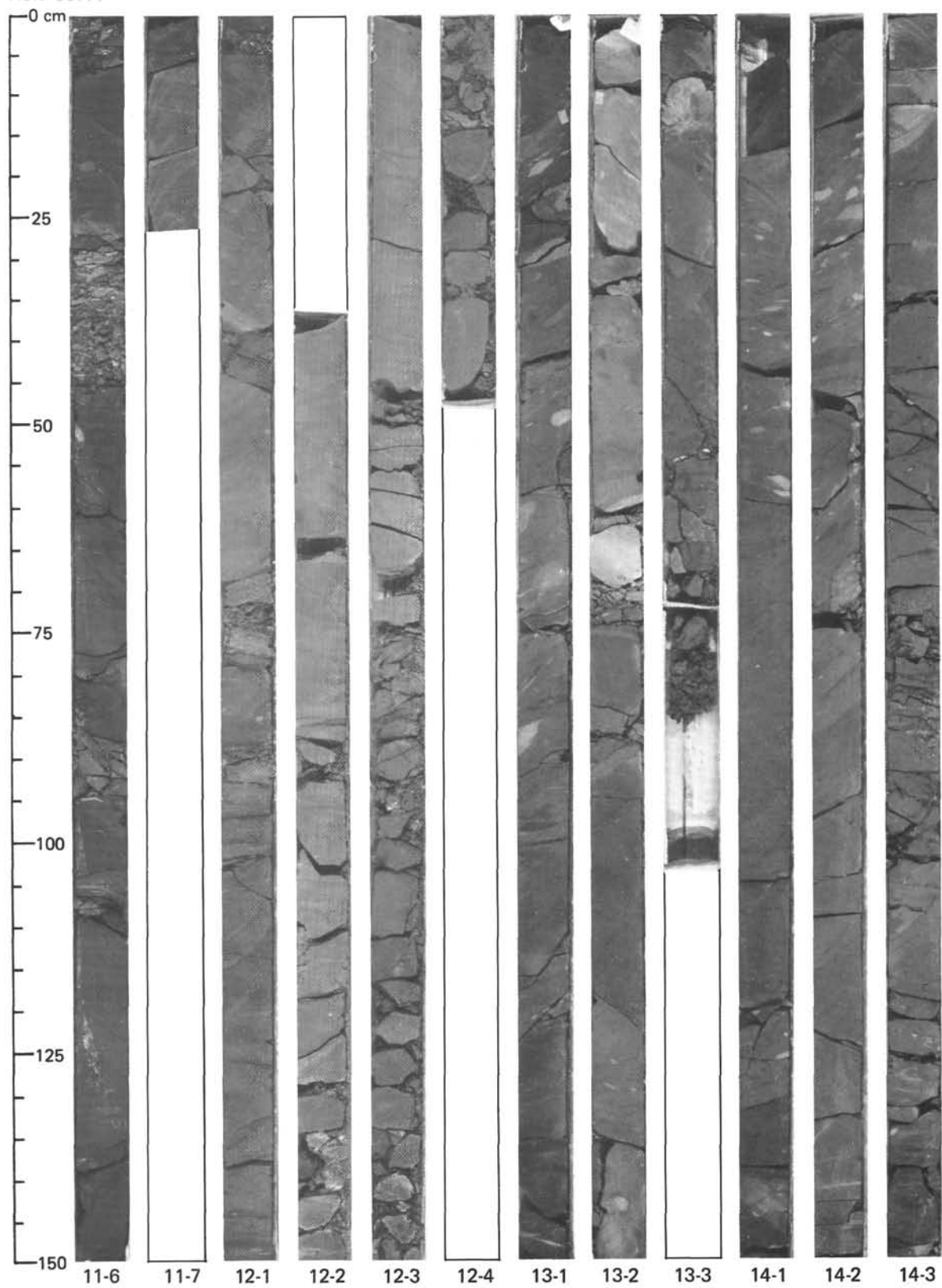


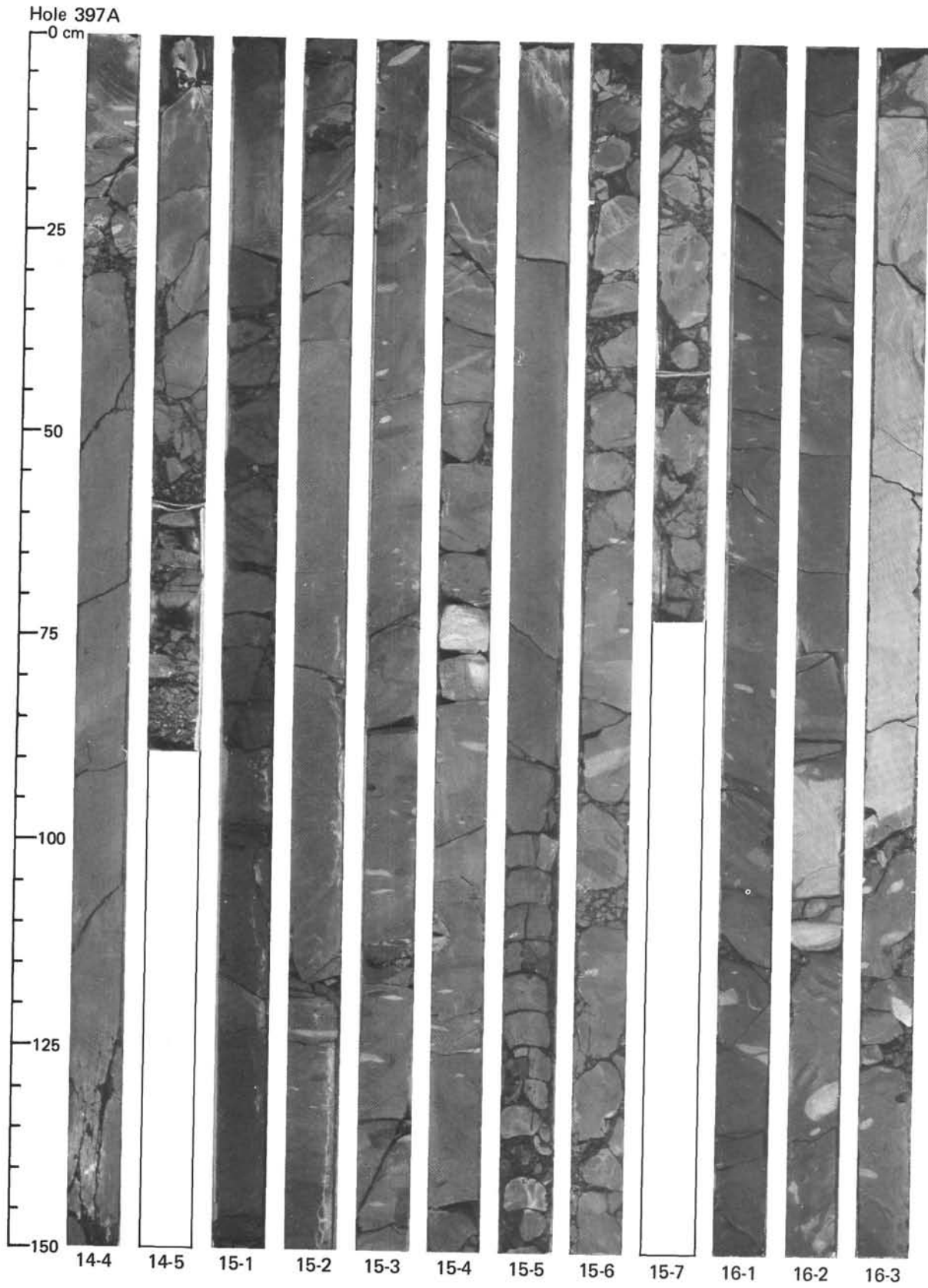




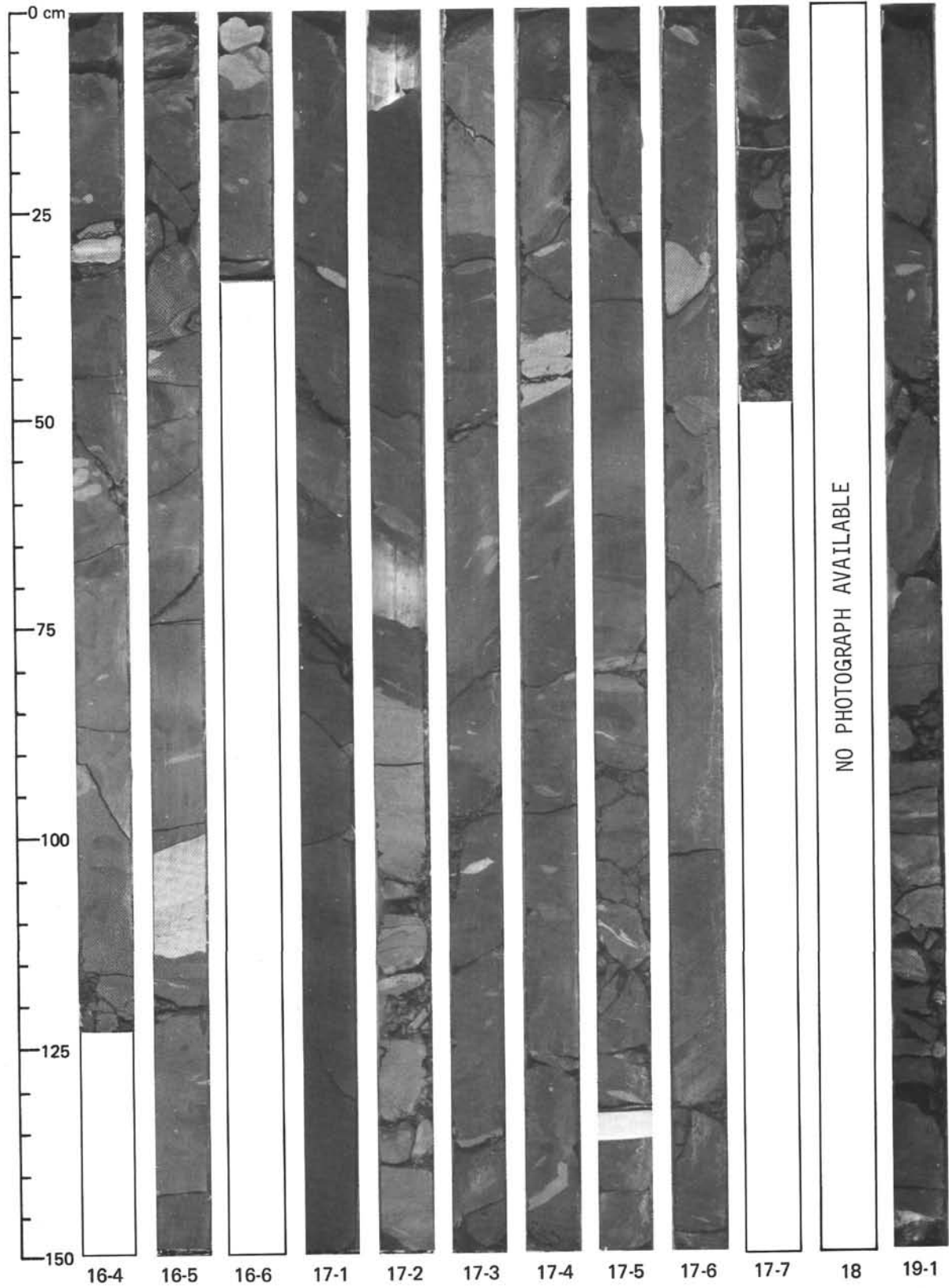


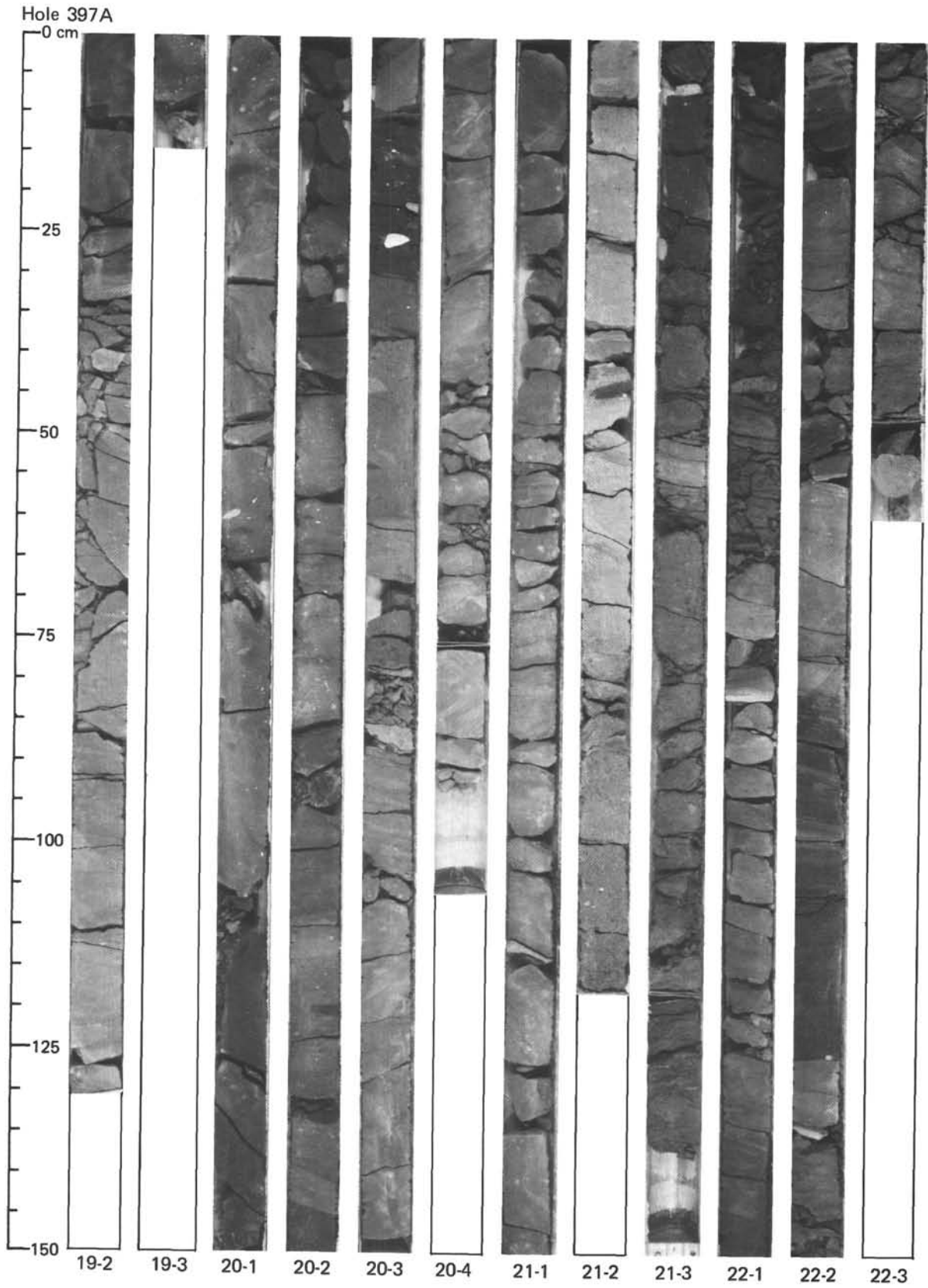
Hole 397A

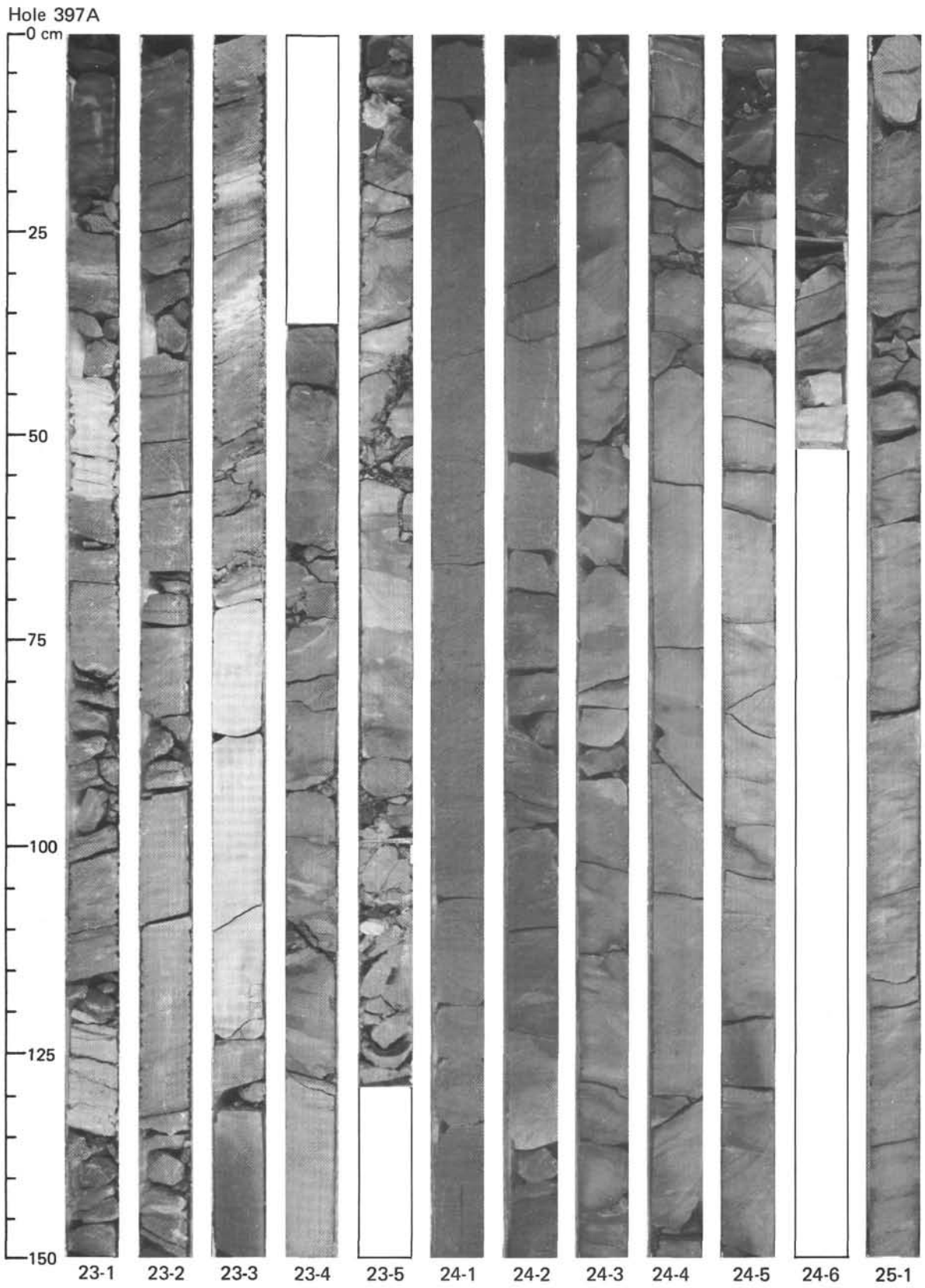




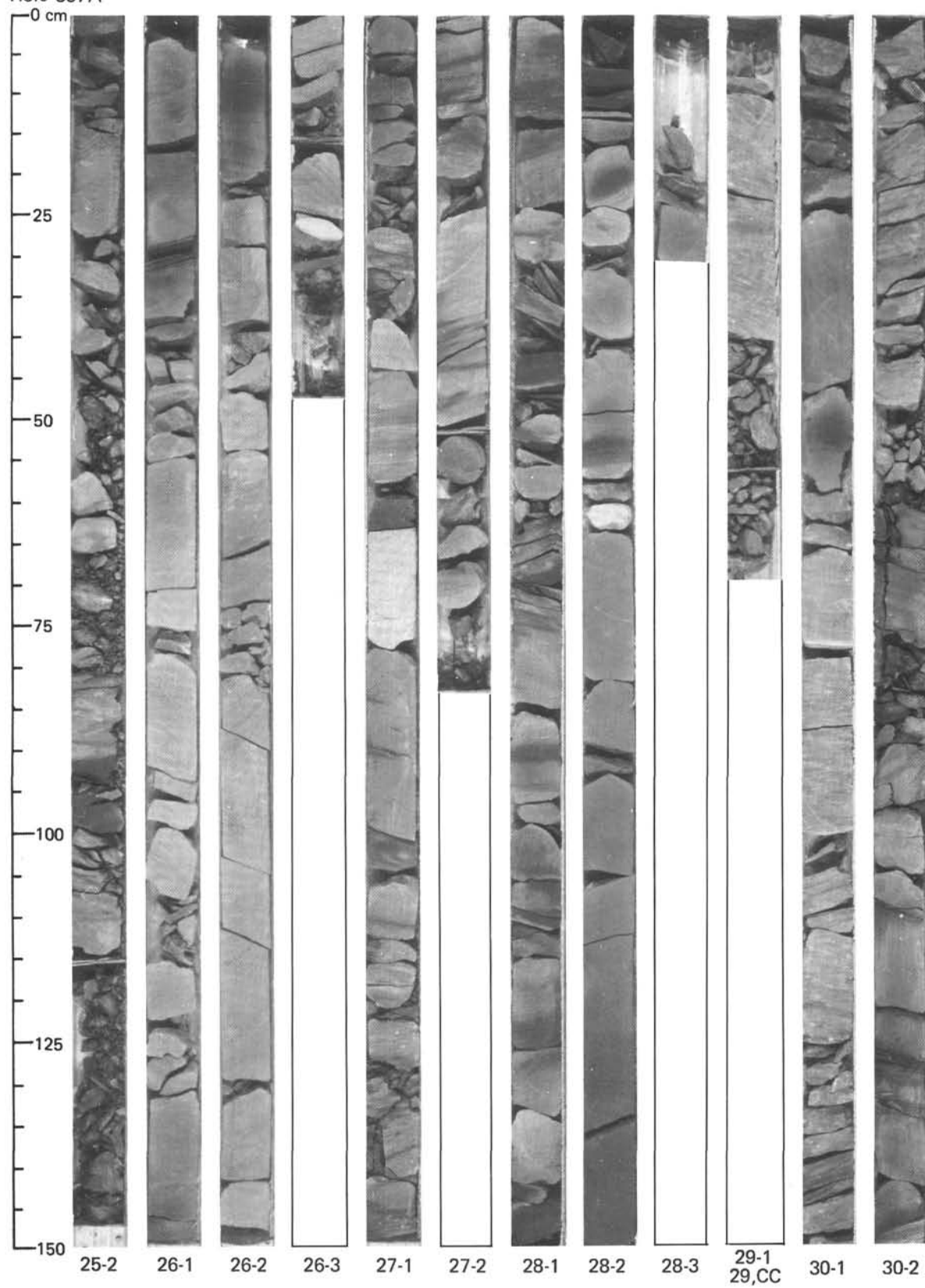
Hole 397A

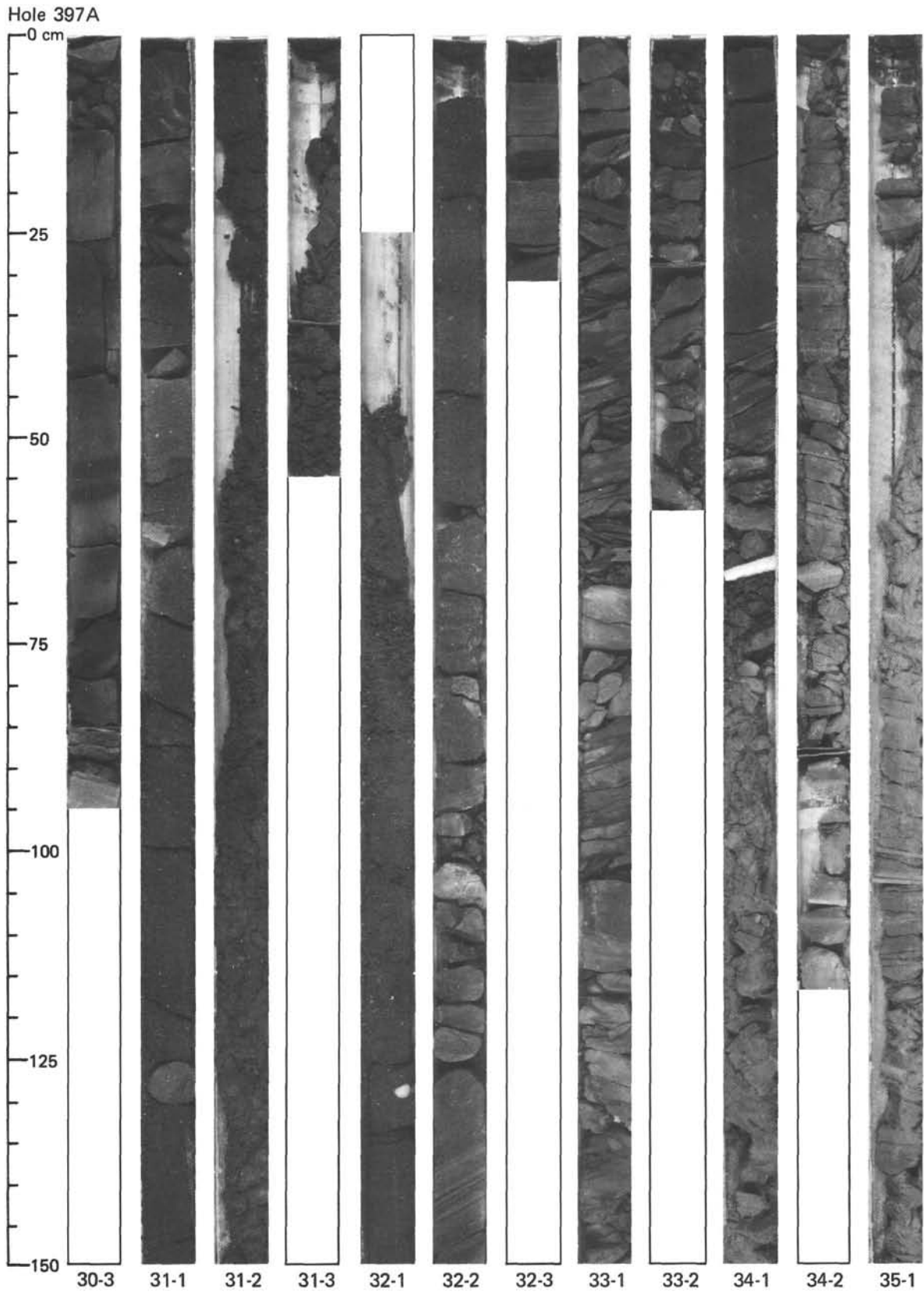




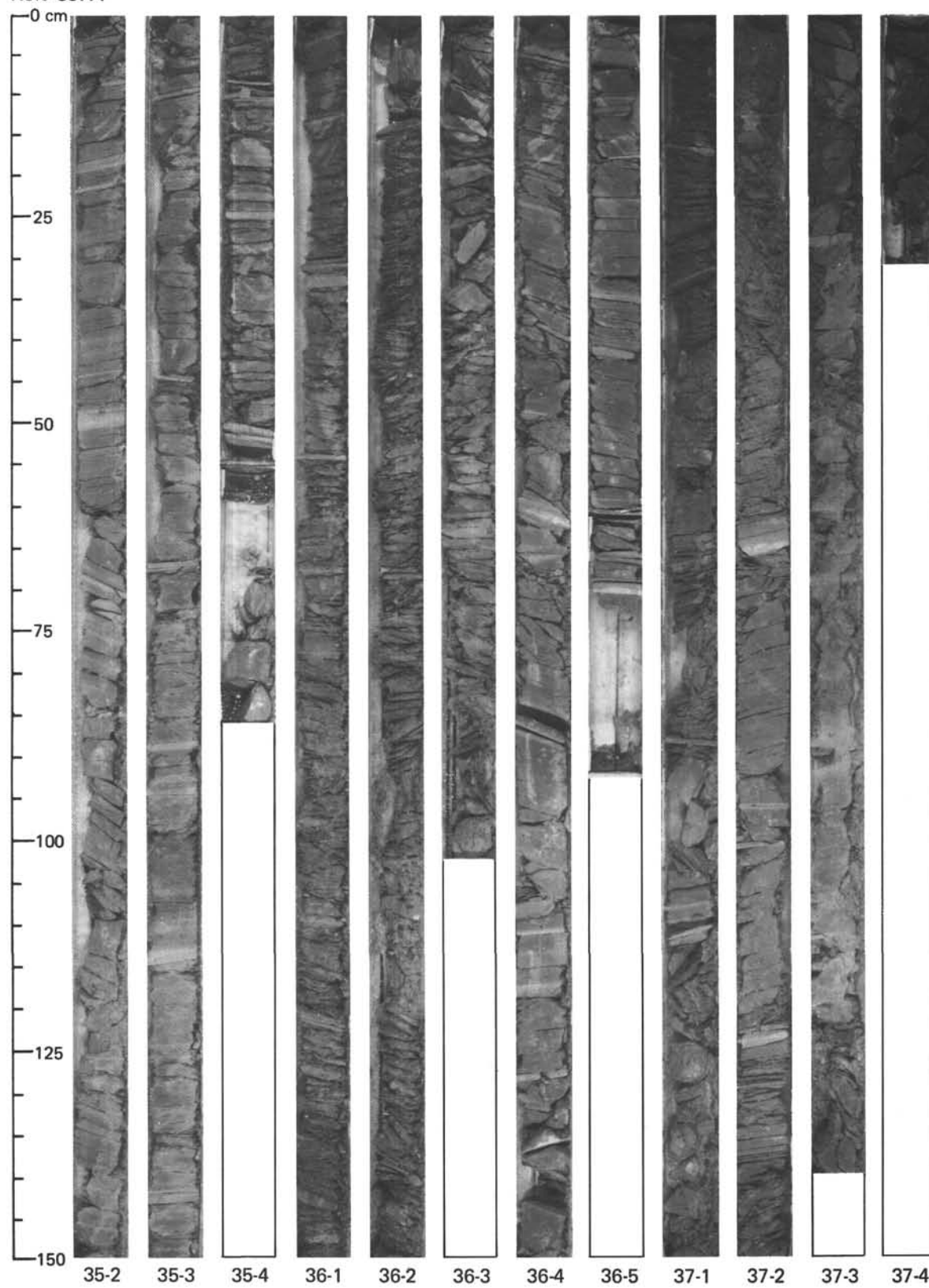


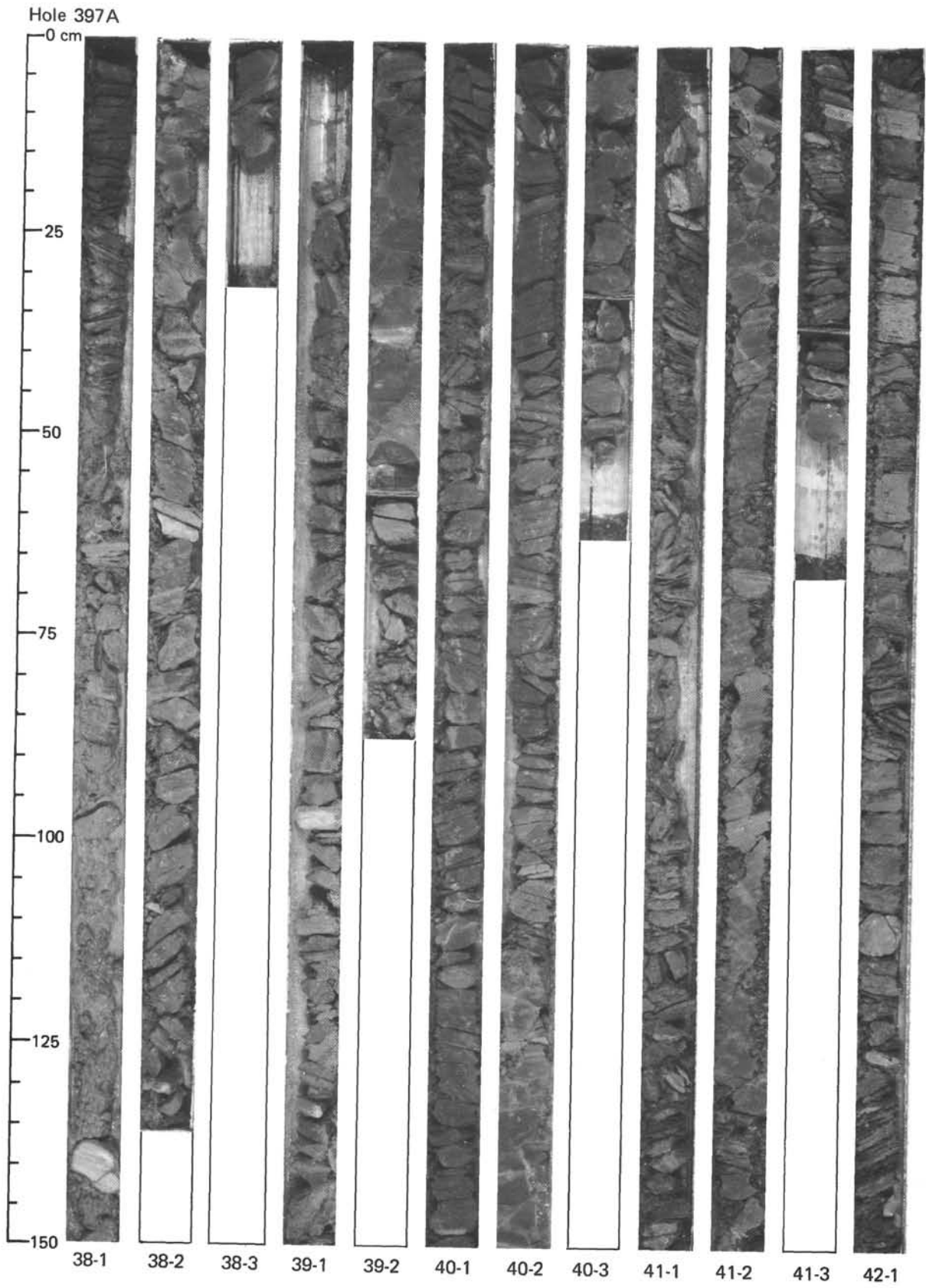
Hole 397A

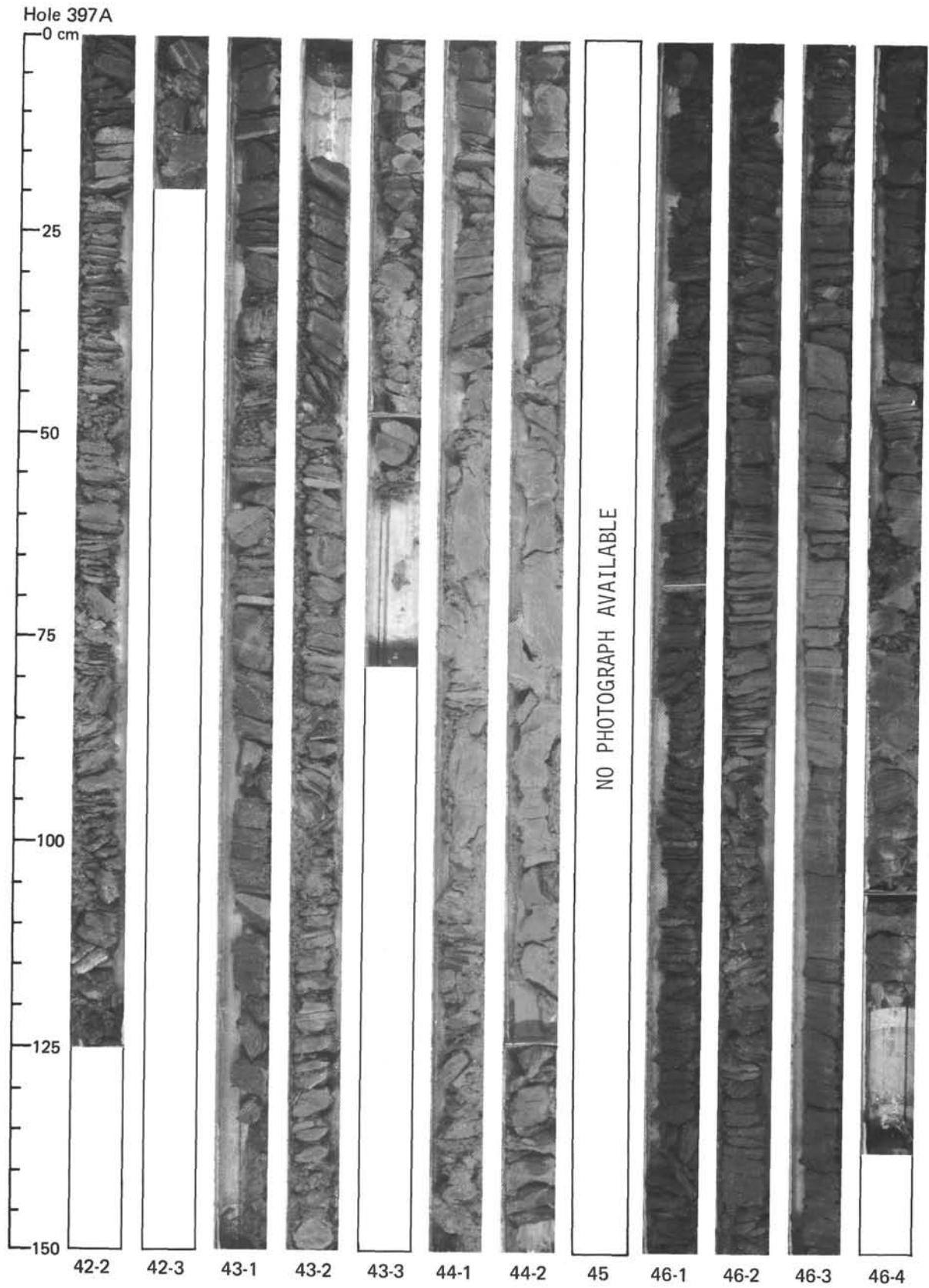




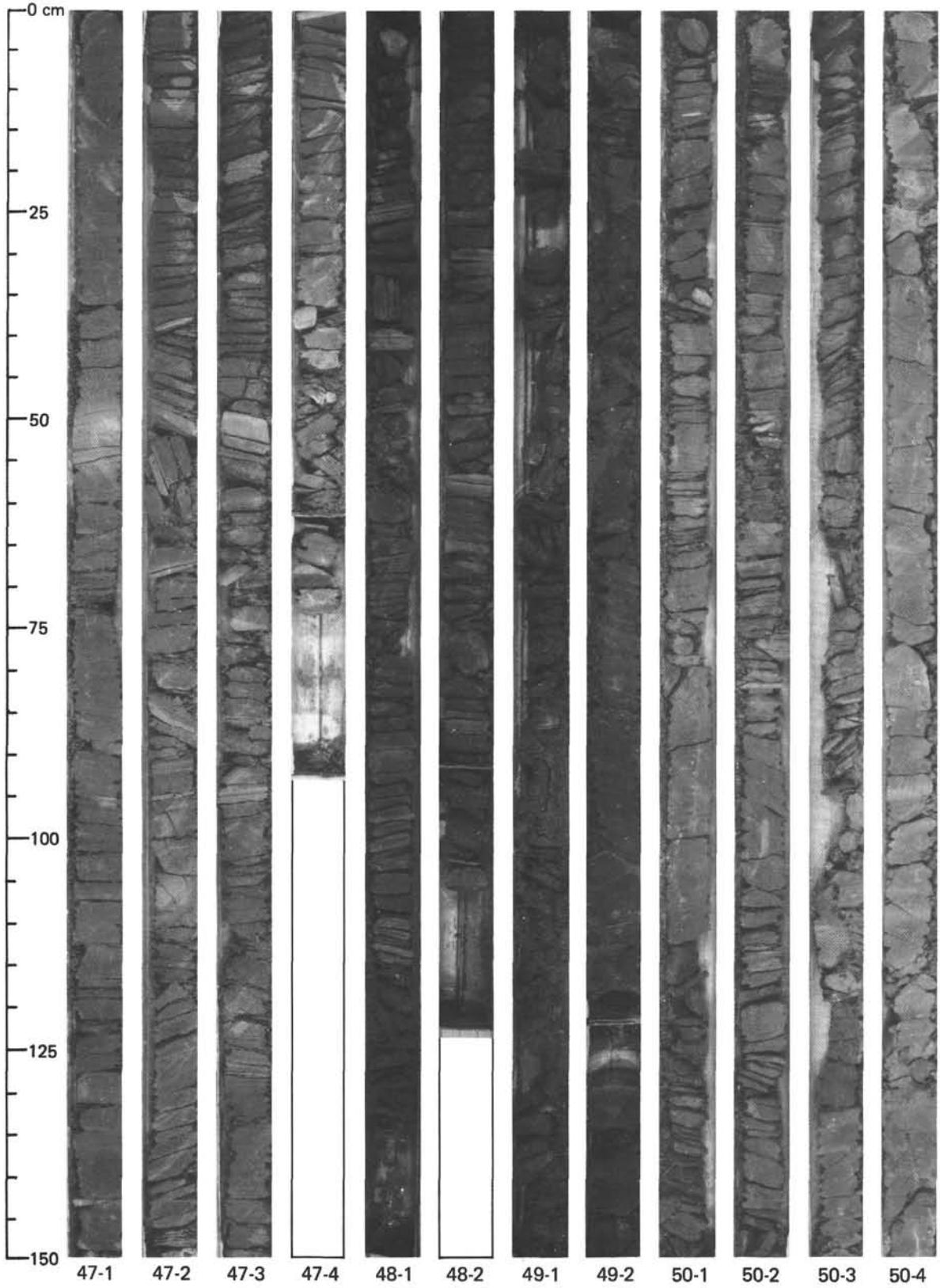
Hole 397A







Hole 397A



Hole 397A

